



MRMS Applications Handbook

- Cutting-Edge Research in MALDI Imaging, Metabolomics/Phenomics, Native MS and Petroleomics

Dear Mass Spec Customer,

Thank you for your interest in Bruker's scimaX[®] and solariX-series instruments. Powered by MRMS (Magnetic Resonance Mass Spectrometry), this leading technology represents the next evolutionary step in mass spectrometry. Cutting-edge research in MALDI Imaging, Metabolomics/Phenomics, Native MS and Petroleomics is easily accessible to researchers across the globe.

Continuing with a tradition of record setting magnet designs (1.2 GHz NMR, 18T MRI and 21T ICR), Bruker's novel Maxwell magnet technology enters a new era of innovation. The conduction-cooled system means no liquid cryogen fills are ever required and allows for placement into any standard lab. The 2xR detection capabilities enable high-field performance at 7T, providing unmatched eXtreme Resolution and mass accuracy. Routine Isotopic Fine Structure (IFS) analysis across a broad mass range results in unmatched confidence for compound identification across any application.

We are happy to provide this synopsis of our technologies and examples of chemical excellence that can be achieved in a manner never experienced before. With instruments in 37 countries, our global MRMS team members are there for you. Please reach out to your local representative to learn how we can integrate this technology into your lab.



Christopher J. Thompson, Ph.D.
Business Manager MRMS
Bruker Scientific LLC



Countries with scimaX and solariX-series instruments

• Table of Content

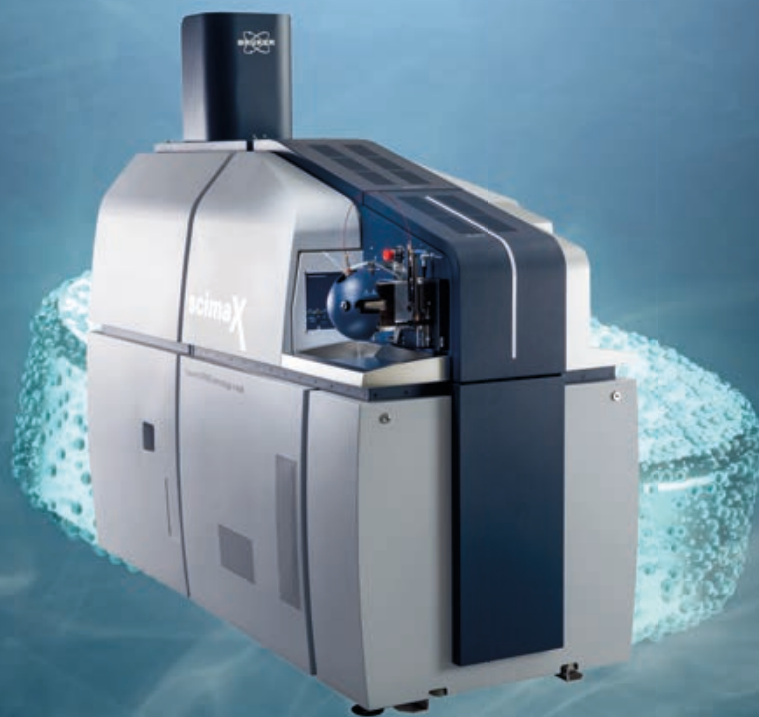
scimaX	05
---------------------	-----------

Applications

<i>MALDI Imaging</i>	<i>08</i>
<i>Metabolomics and Phenomics</i>	<i>98</i>
<i>Native Proteomics</i>	<i>172</i>
<i>Petroleomics and Complex Mixtures</i>	<i>223</i>
<i>Isotopic Fine Structure</i>	<i>263</i>

• **scimaX**

Identify with Confidence



●

User Testimonials: scimaX



"The development of the scimaX® will surely be a game-changer for ultra-high resolving power mass spectrometry."

Professor Joe Loo, University of California, Los Angeles, USA



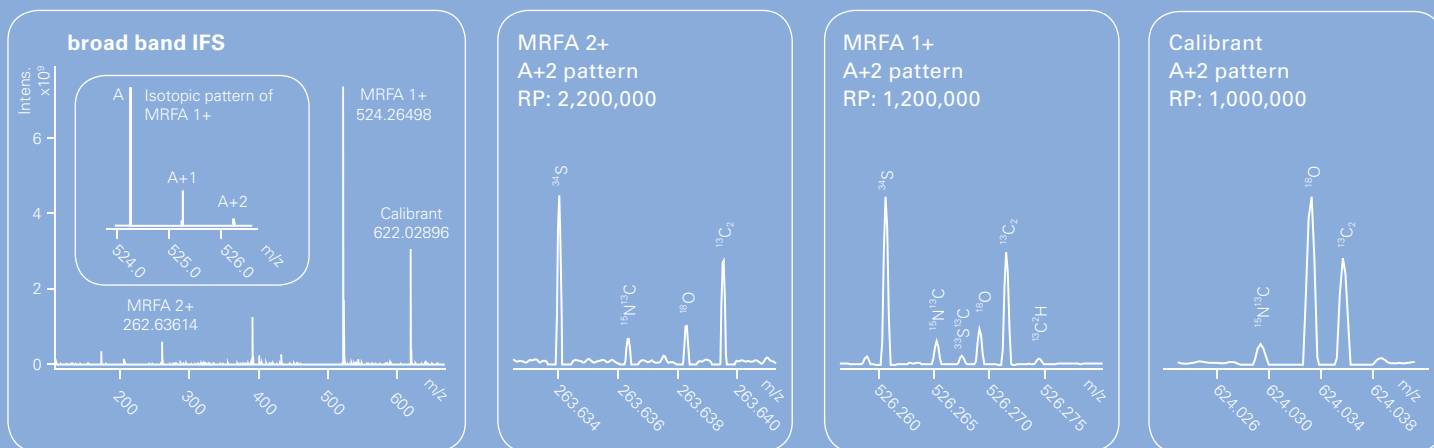
"Continuing the tradition of Bruker innovation, the ParaCell™ is a new enabling technology for solariX XR. This radical concept is a departure from traditional ICR cell strategies and provides uncommon broadband ion stability resulting in resolution order of magnitude above other detection schemes. This power enables the user to effortlessly obtain the extreme resolving power needed to probe isotopic fine structure or highly complex mixtures."

Professor Eugene Nikolaev, ParaCell Inventor, Russian Academy of Sciences, Moscow

Taking Science to the Max

Remarkable advances have been made in life sciences research using the advanced capabilities of the versatile solarix platform. Now imagine if this enabling technology was made smaller and maintenance-free when it came to liquid cryogenes, so that it could fit in a standard laboratory.

scimaX allows you to dramatically improve your productivity by operating around the clock by doing your ESI experiments during the day and acquiring MALDI Imaging data when you go home. Take on projects that demand exceptional scientific insight and breakthrough with scimaX.

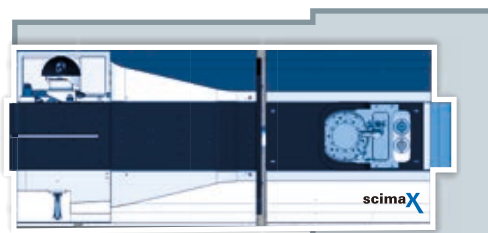


A maximum resolving power of > 20,000,000 without the need for operational cryogen fills, ever!

Solve difficult problems in science and capture the “high hanging fruit.” When you want the ultimate extreme performance, with advanced versatility, the only choice is scimaX.

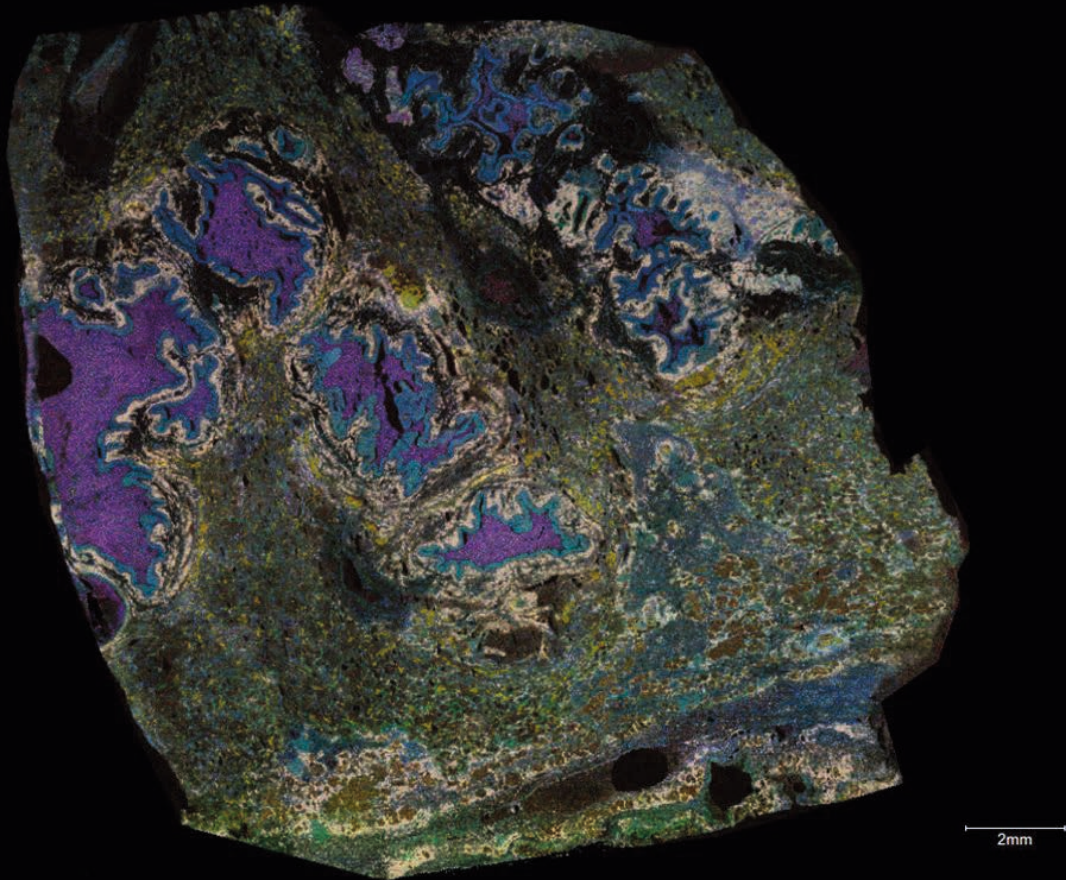
- Featuring an integrated 7T conduction cooled magnet, scimaX is small and fits in a standard lab
- Liquid helium filling and quench line not required
- Includes MALDI and ESI with no switching required
- Continuous Accumulation of Selected Ions (CASI) for enhanced sensitivity
- Choice of 8 fragmentation techniques

Footprint: scimaX and solarix



solarix

• MALDI Imaging



Brochure

- Label-Free Molecular Imaging

Customer Insights

- How Mass Spectrometry Techniques are Propelling the Advancements of Single Cell Biology
- MALDI Imaging in Neuroscience: Revealing the Biomolecular Map of the Brain
- Translating Cancer Biomarkers into the Clinic with MALDI Mass Spectrometry Imaging

Application Notes

- High-Resolution Climate Reconstruction Using MRMS MALDI Imaging
- Designer Drug Analysis by Forensic MALDI Techniques
- Interrogation of the Spatial Metabolome of Ginkgo Biloba with High-Resolution MALDI Imaging
- Integrating Ultra-High Speed MALDI-TOF and MALDI MRMS Imaging for Spatial Proteomics
- Single Cell Lipid Analysis using the Bruker ultrafleXtreme TOF/TOF and the 7T solariX MRMS
- MALDI FTMS Imaging Mass Spectrometry of N-glycans as Tissue Biomarkers of Cancer
- MALDI Imaging Success Stories in Clinical Research –Mini Review
- Microbial Imaging Mass Spectrometry with Fourier Transform Ionization Mass Spectrometry
- High-Performance MALDI Imaging Analysis of on-Tissue Digested Proteins in Mammalian FFPE Tissues

User Testimonials: MALDI Imaging



"If I had to pick one instrument to save in a fire (and did not have to worry about its size or weight), it would be the solariX XR™..."

Prof. Jonathan Sweedler, James R. Eiszner Family Endowed Chair in Chemistry, University of Illinois at Urbana Champaign (UIUC)



"We have developed and continue to evolve new glycan and glycoprotein methods for MALDI imaging. Bruker has been a strong partner in facilitating and supporting these efforts with their innovative instrumentation and software solutions."

Richard R. Drake, Professor & Director of MUSC Proteomics Center.

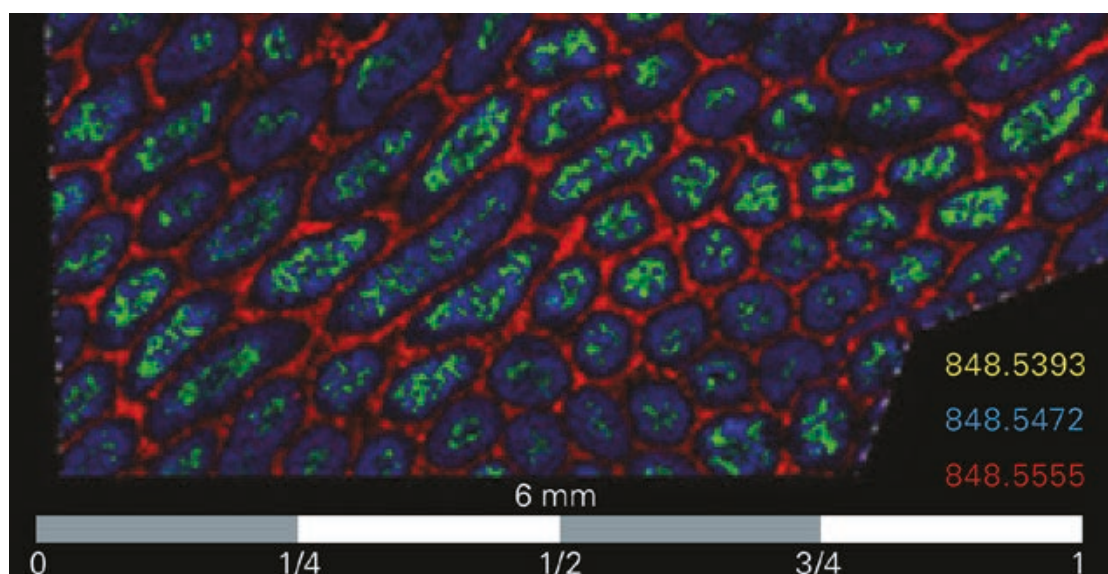


"The solariX is never resting. This is why I am so eager to buy a second one. If I had two, I could obtain my data a lot faster, and also complete more collaborations."

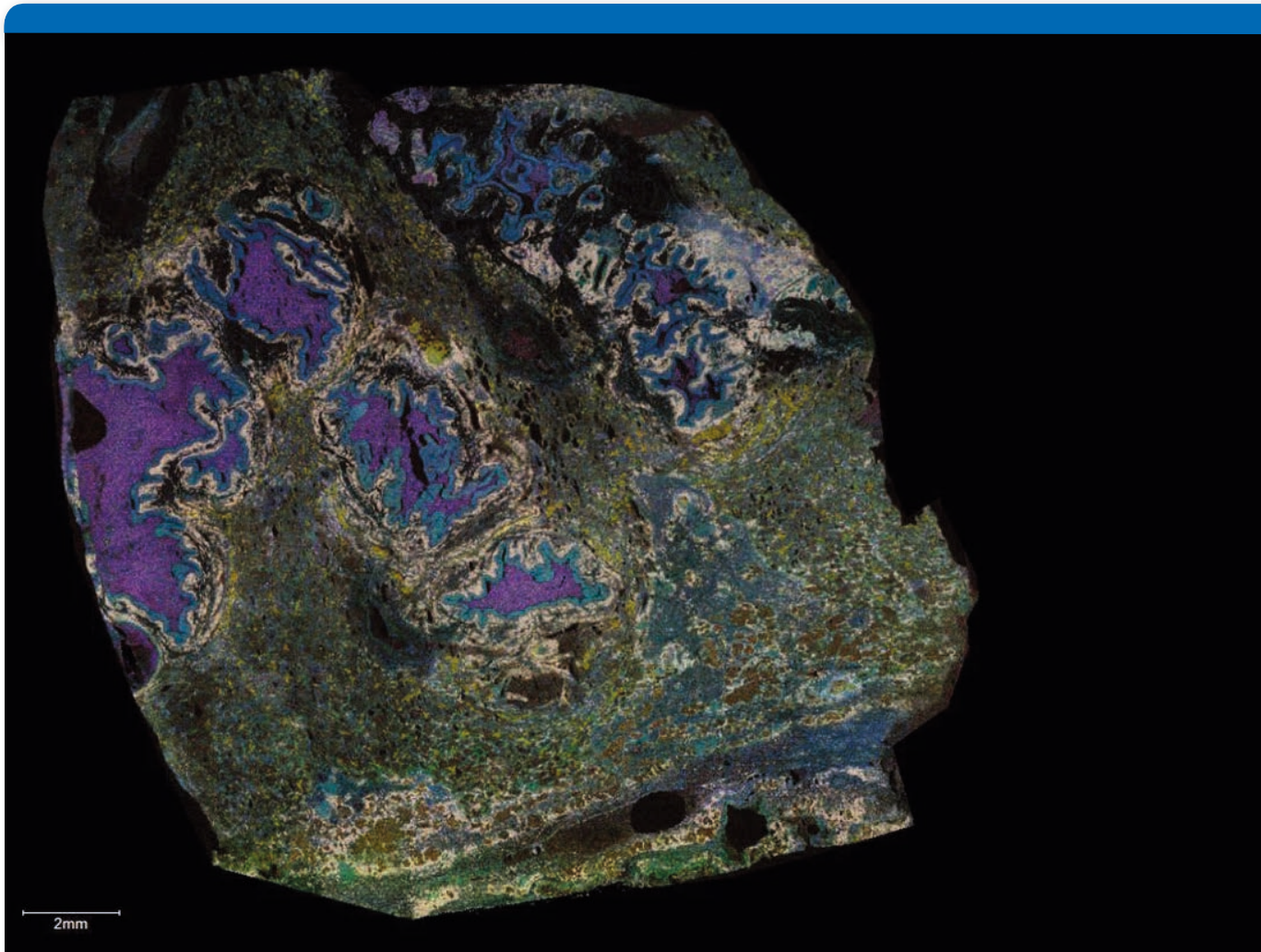
Dr. Per Andrén, Professor of Mass Spectrometry Imaging at the Department of Pharmaceutical Biosciences at Uppsala University and Director of the National Resource for Mass Spectrometry Imaging (NRMSI).

Benefits for MALDI Imaging

scimaX is the ultimate MALDI Imaging system for analyzing small to medium molecules, m/z 100-1500. Its unrivaled eXtreme Resolution capability and sub-ppm mass accuracy, over a wide mass range, can differentiate images that are only mDa apart and are a prerequisite for Isotopic Fine Structure (IFS) analysis and molecular formula confirmation.



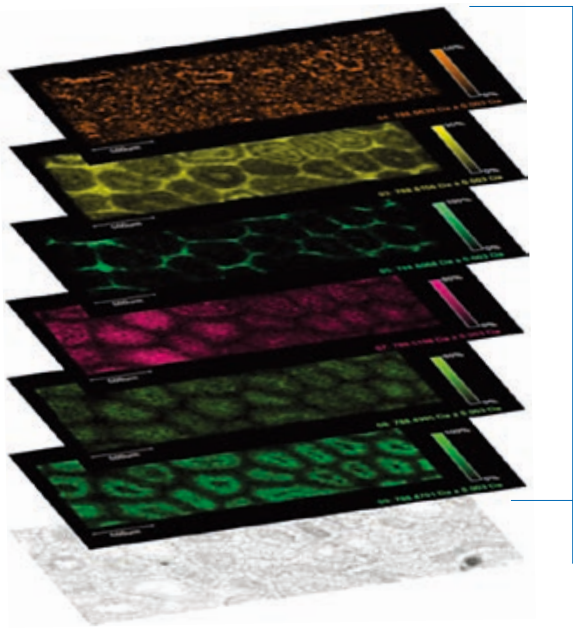
Realize the full benefit of eXtreme Resolution. Above, a 3-color image from rat testis showing distributions of three ions at nominal m/z 848 and differing only by less than 20 mDa.



Label-Free Molecular Imaging

- Discover, localize and quantify biochemical changes and molecular markers

Bruker, the global leader in MALDI-MS technology, is also your partner for label-free molecular MALDI Imaging



MALDI is the most robust ion desorption technology for analyzing many different classes of analyte molecules from many types of samples. When MALDI spectra are collected in a spatially orientated pattern, each spectrum represents a molecular fingerprint of a specific and unique region of the sample being analyzed.

Any detected ion can be projected into a 2 dimensional map of sample location and intensity – an ion image. From a single dataset, hundreds to thousands of unique, label-free ion images may be generated and used for mapping targeted compounds or untargeted discovery of molecular markers which have a specific regional localization.

MALDI Imaging ion images of six uniquely distributed phospholipids from the below rat testis section

Whether you discover, classify or monitor, it is all about location, location, location

MALDI Imaging is a powerful label-free molecular imaging tool for biomarker discovery or targeted monitoring. This revolutionary technique reveals molecular distributions on a cellular scale and can be a key problem-solver in many different fields of research:

Lipidomics

Proteomics

Drug discovery

Cellular disease

Infectious disease

Plant metabolism

Entomology

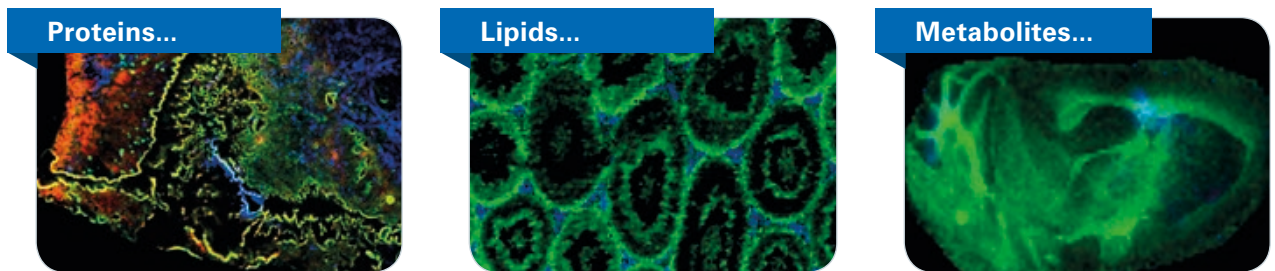
Inorganic surfaces

Benefits:

- + Add a spatial component to LC-based 'omics' studies
- + Discover regionally specific biochemical changes and molecular markers
- + Localize and quantify for drug discovery
- + Add molecular specificity to other imaging techniques
- + Correlate protein glycosylations to disease
- + Visually explore metabolic pathways

It is no longer enough to find molecular differences. You also need to precisely map their origin and MALDI guided SpatialOMx enhances the discovery workflow

Homogenized samples analyzed by LC-MS/MS present no localization information and the process may dilute highly localized compounds below limit of detection. Analyze samples by MALDI Imaging and capture compound distributions, even when localized to very small compartments.

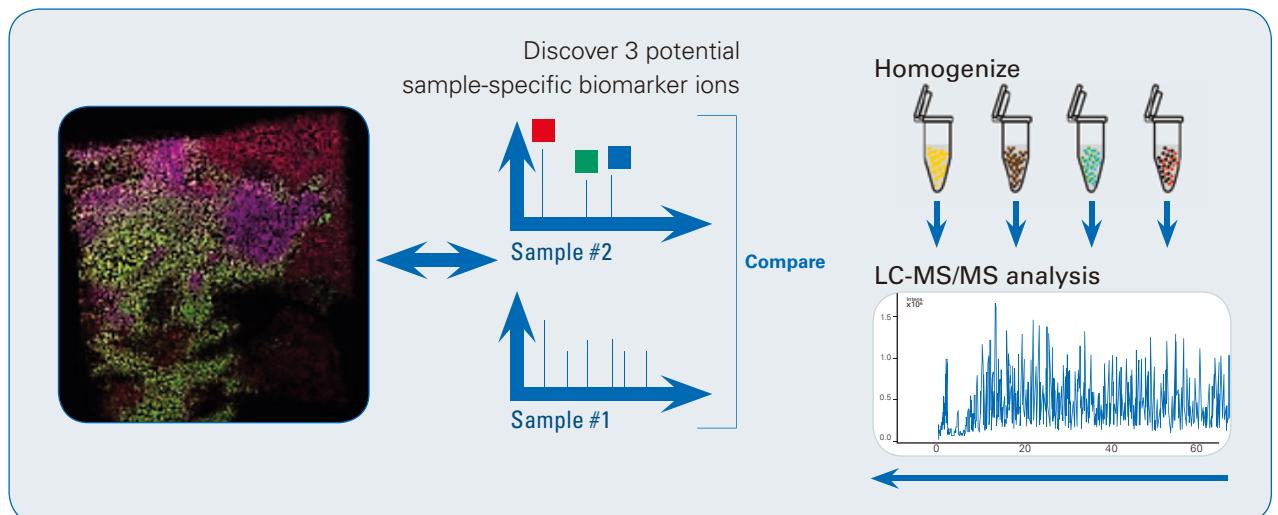


MALDI Imaging can simultaneously map hundreds of different compounds within a small region or across large cohorts of samples.

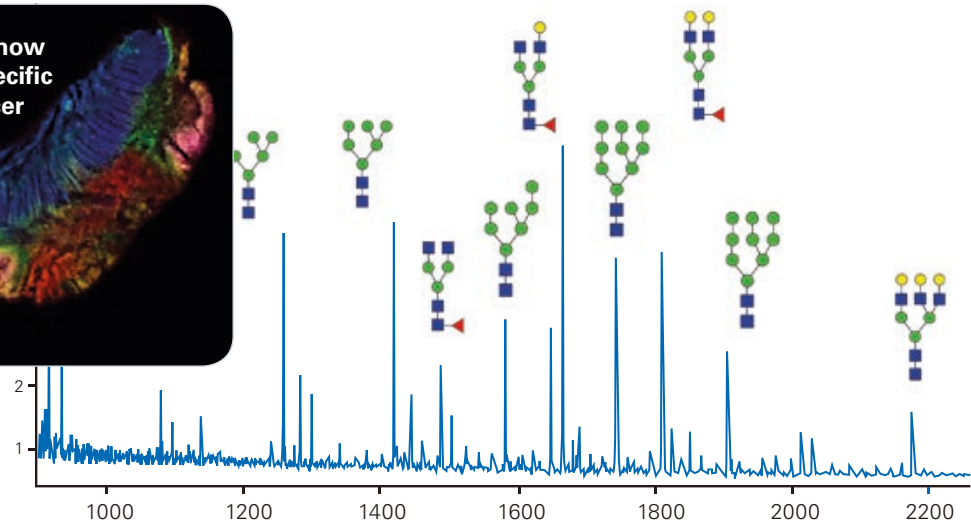
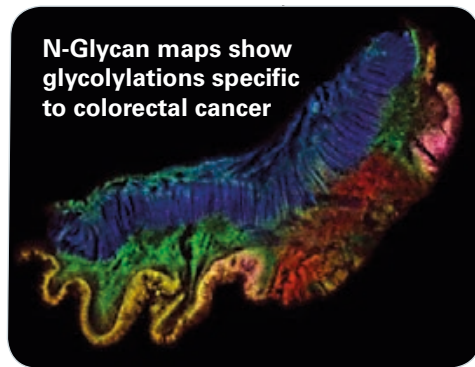
Locate, Discover, Identify ...

- Analyze many samples by MALDI Imaging to identify regionally-specific molecular changes. Match these molecules against LC-MS/MS data from the same samples for confirmation and identification.
- Analyze many samples by LC-MS/MS to identify sample-specific molecular changes. Map these molecules in the samples using MALDI Imaging to confirm that they have proper regional specificity.

Locate 3 potential biomarkers and correlate with pathology



Correlate protein glycosylation to disease

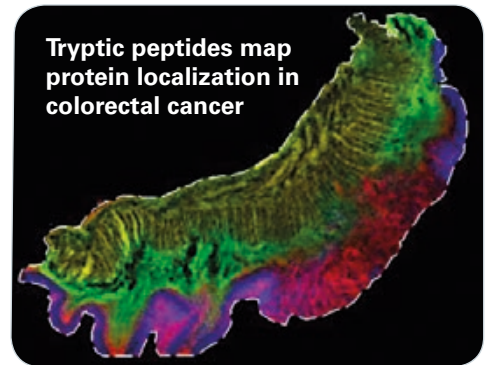


PNGase F treatment liberates N-linked glycans

- Visualize patterns of glycosylation
- Identify N-glycans using MS/MS
- Correlate glycosylation patterns to pathology

Trypsin cleaves intractable proteins into detectable peptides

- Tryptic peptides reveal distribution of larger proteins in fresh frozen and FFPE tissues
- Identify protein from peptide MS/MS
- Access insoluble proteins

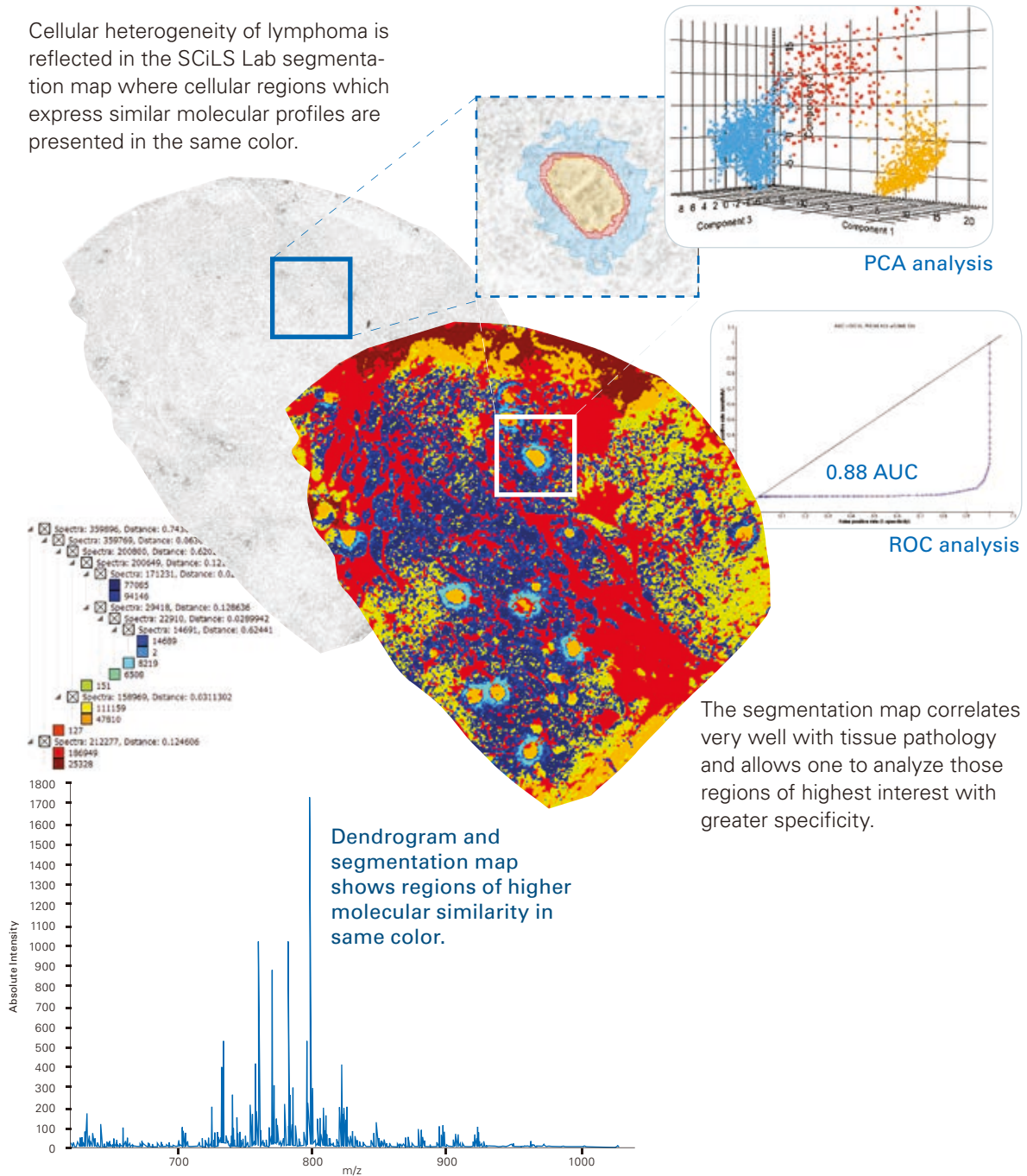


Richard R. Drake
Professor and Director of MUSC Proteomics Center,
Medical University of South Carolina, Charleston, SC

"We have developed and continue to evolve new glycan and glycoprotein methods for MALDI imaging. Bruker has been a strong partner in facilitating and supporting these efforts with their innovative instrumentation and software solutions."

The complete solution to discover regionally specific biochemical differences and molecular markers

Cellular heterogeneity of lymphoma is reflected in the SCiLS Lab segmentation map where cellular regions which express similar molecular profiles are presented in the same color.



The segmentation map correlates very well with tissue pathology and allows one to analyze those regions of highest interest with greater specificity.

Systems for highest sample throughput

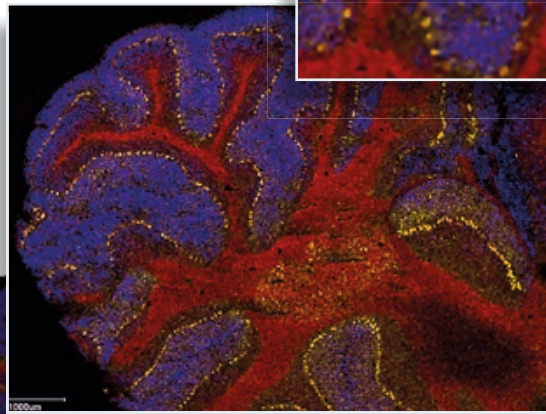
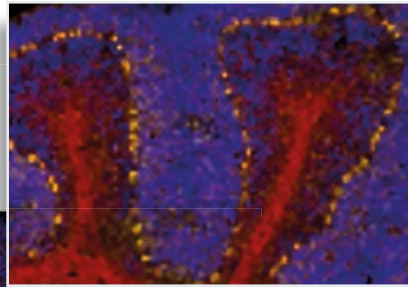
Flex MALDI-TOF systems offer the most versatile analytical range and speed while producing hundreds of ion images per sample.



autoflex maX:
outstanding entry-level MALDI system for Imaging and much more. TOF/TOF is available.

rapifleX:
novel laser optics designed specifically for highest performance and highest speed for MALDI Imaging. TOF/TOF is available.

Layer of purkinje cells visible



3 phospholipids mapped from rat brain section

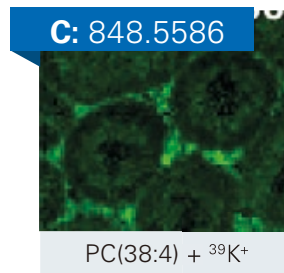
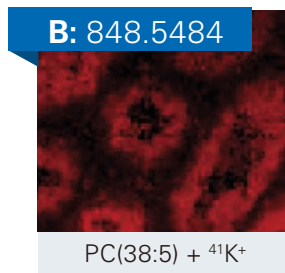
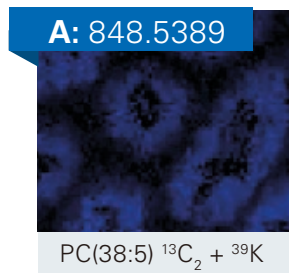
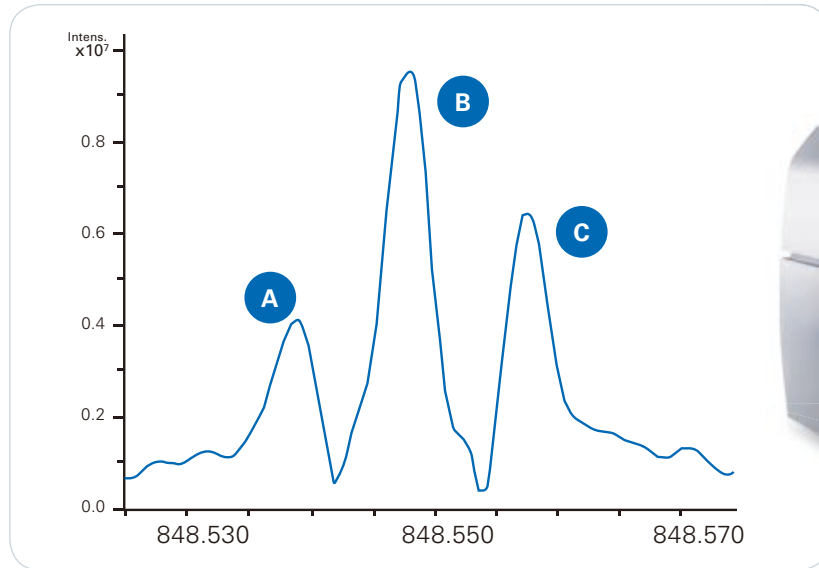


ulfleXtreme:
high performance TOF/TOF imaging system

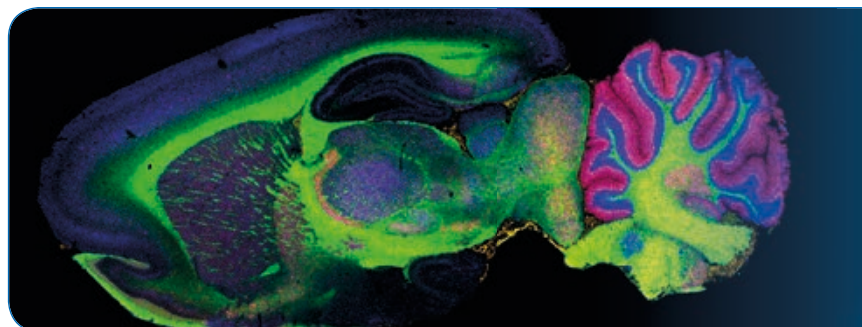


Systems for highest information content

scimaX and 2xR MRMS systems offer the highest mass resolving power of any commercial MALDI system and are the ultimate systems for imaging drugs, metabolites and lipids.



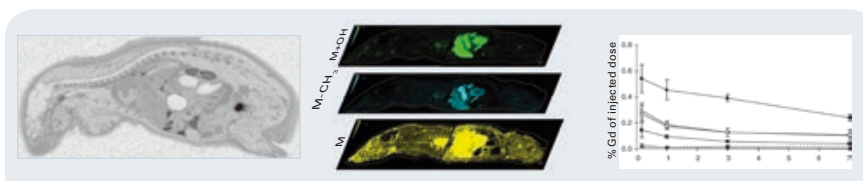
timsTOF fleX combines the best proteomics platform and MALDI Imaging. Discover MALDI guided SpatialOMx for the most complete discovery workflow



Localize and quantify for drug discovery

Make critical decisions earlier: The low operational cost of MALDI Imaging allows it to be deployed very early in the discovery pipeline to help make decisions faster and bridges the gap between traditional LC-MS and Quantitative Whole Body Autoradiography (QWBA) for distribution and metabolism studies.

Whether part of dosing and PK studies or for ADME/Tox studies, MALDI Imaging offers high sensitivity, multiple target localization, and simultaneous discovery of toxicity markers – all integrated with histology.



Benefit/Technique	QWBA	MALDI Imaging	LC-MS/MS
Spatial distribution	✓	✓	X
Drug/metabolite differentiation	X	✓	✓
Quantitative	✓	✓	✓
Integrate with histology	✓	✓	X
Label free	X	✓	✓



Steve Castellino
 Director, Imaging MS and DMPK GlaxoSmithKline,
 Raleigh-Durham, NC

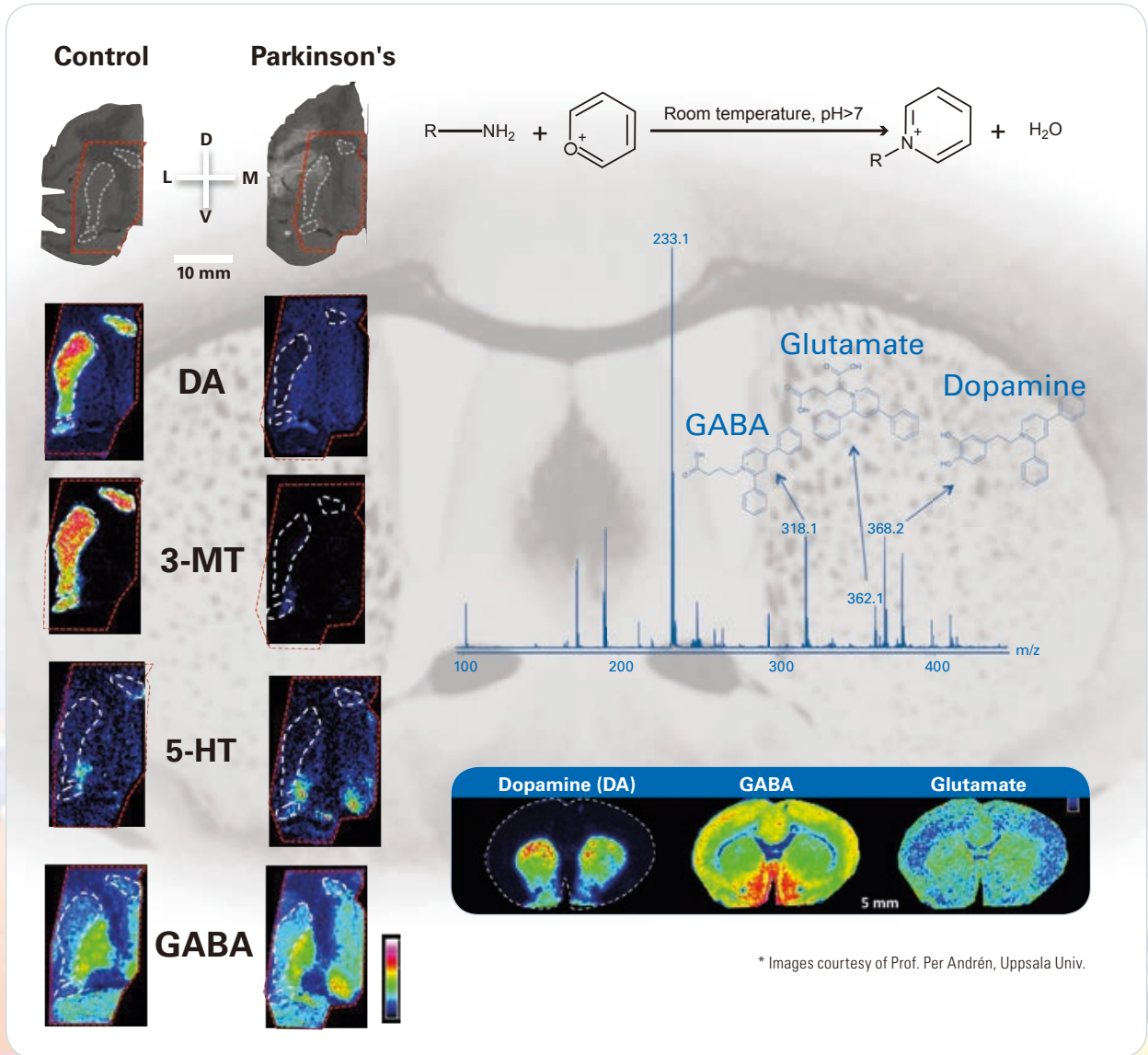
"We have been able to achieve the spatial and spectral resolution required to examine sub-compartment tissue distributions and correlate them with histology in the preclinical setting. This ability to link chemistry and biology is permitting us to more closely examine the basis of drug toxicity and pharmacology as well as refine our understanding of pharmacokinetics and drug transport."



Dr. Jonathan Stauber
 CEO imaBiotech, Billerica, MA

"ImaBiotech purchased several Bruker instruments because their devices' high performance fit perfectly with our MALDI Imaging technology platform to provide superior services to the pharmaceutical and biomedical industries. Our extensive research made possible by integrating Bruker into our repertoire is proof of the unparalleled quality and robustness of Bruker technology."

Visually explore biochemical pathways

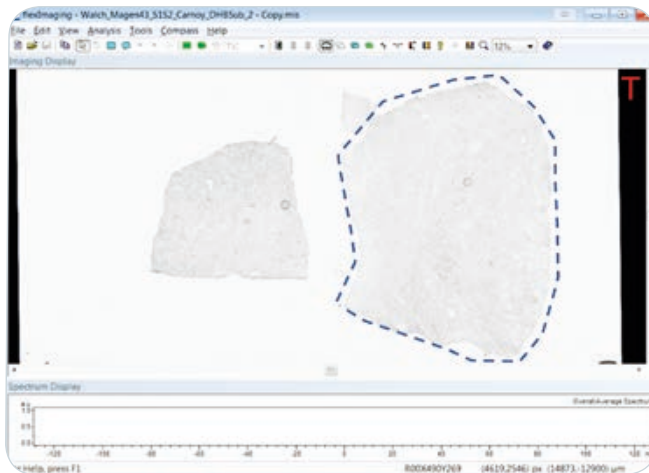


Prof. Per Andréén
Uppsala University, Sweden

"Mass spectrometry imaging enables us to simultaneously map and quantitate multiple neurotransmitters, their precursors and metabolites directly in tissue sections. That is, almost the complete dopaminergic and serotonergic neurotransmitter networks."

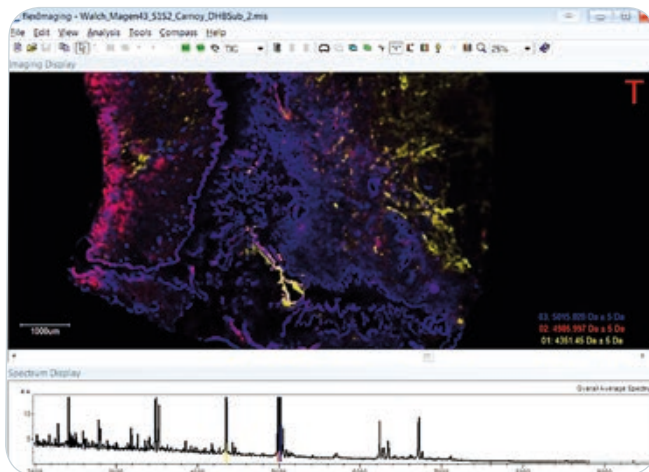
Complete software toolkit

Acquire + Visualize + Analyze → Information



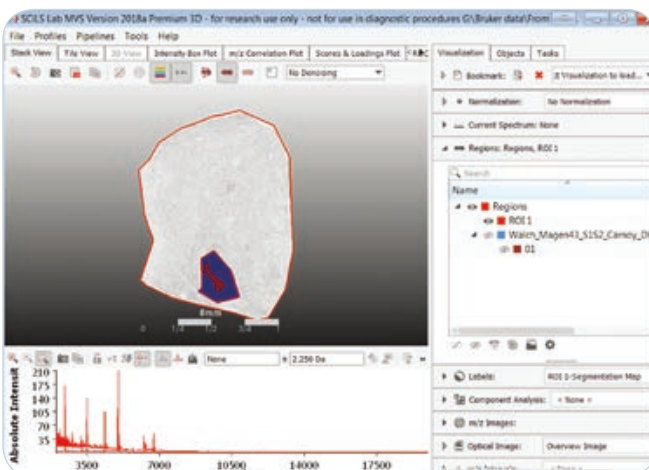
Acquire

- Method driven image acquisition
- Define measurement areas from microscopic image
- Image all of the sample or just regions of interest



Visualize

- Multiple ion overlays
- ROI segmentation
- Save targeted ions for instant visualization or explore interactively



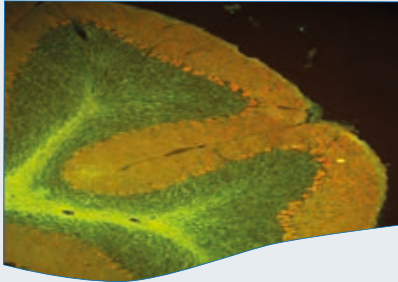
Analyze

- SCiLS Lab Core: auto-segmentation and co-localization
- SCiLS Cloud: integrates remote teams
- SCiLS Lab Pro: full analyses of large sample cohorts
- SCiLS Lab Premium 3D: full analyses of 2- and 3-dimensional images

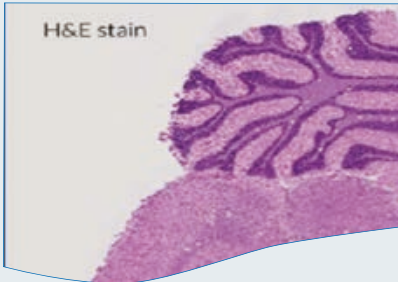


Add molecular specificity to other imaging techniques

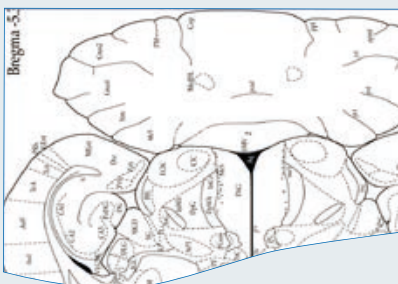
Fluorescence



Histology



Atlas Reference



IHC

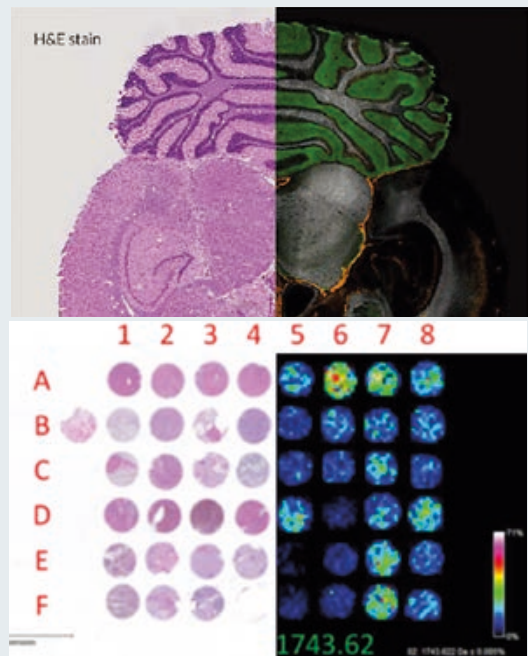


Look beyond optical morphology. Import many other imaging modalities to examine your MSI data in the most relevant context and boost confidence in your analyses.

Histology*

MALDI Imaging*

Whole Tissue



Tissue microarrays (TMA)

Bruker pioneered the integration of MALDI Imaging data with other imaging modalities to provide you with the most biologically relevant information. Bruker's imaging software allows co-registration and overlays of multiple images with full user control.

* Image courtesy of Dr. Jeff Spraggins, Mass Spectrometry Research Center at Vanderbilt, USA

Contact your local Bruker representative to learn more about our MALDI products and how they can expand your research into the visual world of MALDI Imaging



scimaX & 2XR



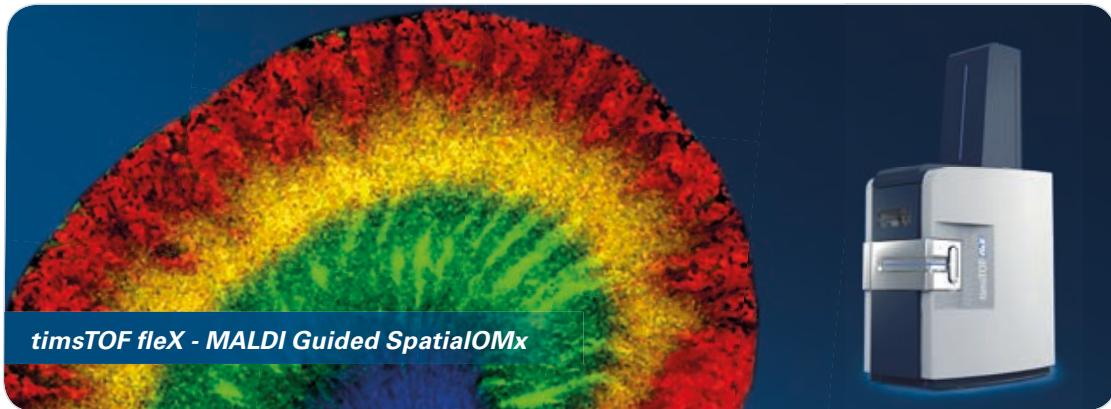
rapifleX



ultrafleXtreme



autoflex maX



For research use only. Not for use in clinical diagnostic procedures.



Customer Insights

- How Mass Spectrometry Techniques are Propelling the Advancements of Single Cell Biology

How Mass Spectrometry Techniques are Propelling the Advancements of Single Cell Biology

Bruker's range of high-spec mass spectrometry instruments enable the Sweedler group at the University of Illinois at Urbana Champaign (UIUC) to take the lead in analytical discovery



Working with Bruker

Prof. Jonathan Sweedler's research group at UIUC benefits from a broad range of analytical equipment chosen for its optimal performance for his specific applications.

"For mass spectrometry imaging, Bruker's technology leads the way. In particular, their MALDI imaging instruments have incredible figures of merit that other vendors don't come close to."

The Department of Chemistry at UIUC

The Department of Chemistry has been a part of the University of Illinois at Urbana Champaign (UIUC) since its establishment in 1868 and supports a range of research areas from chemical biology to analytical, inorganic, materials, organic, physical and theoretical chemistry. Consistently placed in the top of national chemistry department rankings, UIUC is in a prime position for innovative chemical discovery.

Professor Jonathan V. Sweedler, a faculty member of the department for almost 26 years, conducts bioanalytical chemistry research at the intersection of analytical chemistry, bioengineering, neuroscience, and physiology. With over 365 peer-reviewed publications to his name, Professor Sweedler is a leader in the field; his group currently consists of two research scientists, 7 postdoctoral associates, 12 graduate students, two visiting scholars and 11 undergraduate students. With a research focus

on single cell biology, his group relies on robust instrumentation to make ever-increasingly detailed measurements of small biological samples, such as individual cells, related to a broad range of fundamental and applied studies.

The Research

The work done by the Sweedler research group can be broadly categorized as measurement science and technology, with a focus on the development of analytical methods for investigation of complex biological specimens. The Sweedler lab is renowned for developing, optimizing, and using highly sensitive methodologies to study a wide range of model organisms, spanning many phyla, with an overarching goal of gaining a better understanding of known neurochemical pathways and discovering new and unusual pathways. Sweedler is especially interested in discovering and annotating novel neuropeptides involved in mechanisms of behavior, memory and learning. By using microscopy-guided MALDI (matrix-assisted laser desorption/ionization) mass spectrometry

and capillary electrophoresis-coupled electrospray mass spectrometry, cells can be probed for cell-to-cell signaling molecules to map the chemical bases of connectivity within well-defined neuronal networks.

The Sweedler group has chemically characterized thousands of neuropeptides across a wide range of animal models, through a combination of analytical approaches.

"It is a rather bold statement, but we have discovered and reported more novel brain peptides across the animal kingdom than any other group. This extends to discovering novel neuropeptide genes as well," comments Professor Sweedler.

An increasingly important area of research is that of single cell measurements. By developing and using sensitive and low sample-volume methods, the genes expressed by an individual cell type can be elucidated, and the dynamic phenotypes of seemingly homogenous cells under different external situations can be characterized and classified. Professor Sweedler describes the nature of his groups' neurobiology research with mass spectrometry imaging:

"We want to know what compounds are in the brain, where they are and when they were at particular location, as well as how they change based on behavior, learning and environment. Mass spectrometry shows you what compounds are present in the brain, for example, by removing a brain region and assaying it with liquid chromatography mass spectrometry. We also want to know where the compounds are, and so we can take a tissue slice from the brain, conduct mass spectrometry imaging, and figure out the localization of different chemicals. For example, we can ask what happens in distinct brain regions of rats when you alter their diet, or induce learning with a learning task. We perform the mass spectrometry imaging measurements with a Bruker ultrafleXtreme™ and our new solariX XR™. These instruments allow us to probe what's in a particular location, for example within a layer of the hippocampus, and characterize the changes in neurotransmitters, neuropeptides, and lipids"



What the Group works on

"Single cell measurements are an exciting area. In the last few years, there has been an increase in interest and government funding channeled towards this technology, and therefore it is a hot area that scientists – undergraduates, graduate students and post docs – want to work in. ...

... Because of this interest, around half of my group is now working in single cell biology, using some of the newest equipment we have, such as the solariX XR™."

Sweedler's group is constantly striving to improve the sensitivity and information content of their measurements, which goes hand-in-hand with access to the best instrumentation. The solariX XR™ provides this level of information through extremely high mass resolution detection.

One challenge in academics that is not found in industry is the need for continuous training. In any academic setting, the rate of staff turnover is faster than in industry as the undergraduate, graduate and postdoctoral associates move on to other positions every few years. Although this is a constraint on

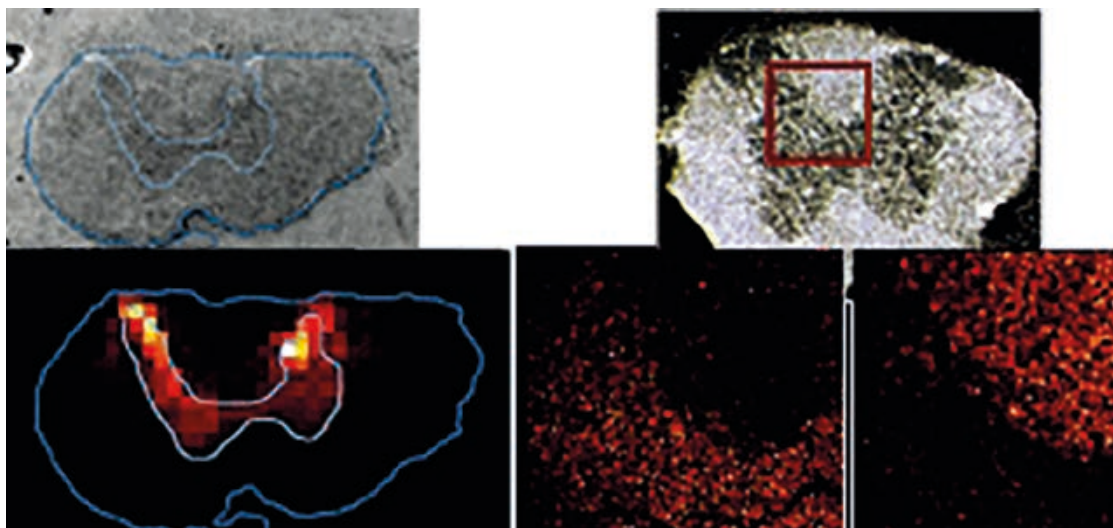
the level of expertise that can build up within the Sweedler group over time, this certainly helps the field in general. For example, perhaps 50 percent of Professor Sweedler's students move into the pharmaceutical industry, bringing their expertise to many other teams. A benefit to a steady influx of students and postdoctoral associates is that *"new people tend to be fairly fearless and want to try new things,"* according to Professor Sweedler.

While there is a steady turnover, he has been fortunate to have two senior scientists, Dr. Stanislav Rubakhin and Dr. Elena Romanova, who have been in the group for about 20 years.

"One of our goals is to carry out complex measurements on cell-to-cell signaling, for example, on neurotransmitters and neuromodulators across the brain. It has been enabling to have these two expert senior scientists with broad expertise in sample preparation, LC mass spectrometry, mass spectrometry imaging, and a myriad of other related areas work on these projects. They contribute to the long-term group knowledge of instrumentation and procedures and enable a number of projects to succeed."

Training

The level of training provided to students and staff in the group is vital for excellence in research done inside of the group and in multiple collaborative projects, as well as future contributions from





group members who move into science and industry. Members enter the lab begin with varying degrees of knowledge and experience with mass spectrometry, so the training requirements vary. Professor Sweedler explains,

“Single cell measurements with mass spectrometry require a steady hand, and potentially someone who doesn’t drink much coffee! We have found it best to train undergraduate students on equipment like the MALDI mass spectrometer where small samples can be used and the instrument is robust. For example, the ultrafleXtreme™ can handle a large number of sample plates, and so is great for training. If students want to progress to capillary electrophoresis - mass spectrometry, this makes a good transition for more experienced users as more attention to detail and greater potential for complications exist.”

As well as receiving training from higher level staff and academics, Bruker has provided multiple training events and continuous support for the Sweedler group, enabling them to sustain a high degree of knowledge on the latest equipment required for cutting-edge research.

“Continuous training is one of the beneficial elements of collaborating with Bruker,” ...

... says Professor Sweedler, adding that *“they supply an incredible amount of expertise – that’s worth a lot!”*

Bruker also benefits from this relationship; of the scientists that come from Sweedler lab, around 50 percent head towards the pharmaceutical industry, bringing with them their affinity for Bruker instruments.

A Challenge for the Group

When conducting research at the individual cell level, there are certainly many challenges to overcome. Professor Sweedler identified several hurdles to cross before single cell measurements

become robust: more universal sampling protocols, increasing analyte detectability, and improving the throughput of mass spectrometry.

“My group is continually fighting against detectability, attempting to achieve progressively lower detection limits. We have pushed creating better sampling approaches and we are using instruments where we can work at the single cell level and have the best detection limits – ...

... in practice this has always tended to be with Bruker, because of their increasingly sophisticated mass spectrometry technologies.”

There are a number of unusual physical constraints that they face. Professor Sweedler explains how his team overcame one such challenge:

“Studying brain chemistry involves sacrificing animals and removing brain tissue. If someone has a genetically modified mouse that they want us to take measurements on, it is difficult to send cells that stay intact overseas. We have a room on our campus that can be sterilized, where we can complete the dissection and run samples without having to quarantine the animals. In another recent example, we were collaborating with someone in the UK who was researching salt loading in animals and how this affects a certain brain region. His work was mostly conducted on rodents, but he also had a partnership with scientists in the Middle East completing similar studies on camels. The first set of samples had too high a measurement variability and so one of my senior scientists went to the Middle East to help them collect more rigorous and quantifiable samples. We find we often have to work with those collecting the samples and train them to obtain the best quality data.”

The Takeover of the Sweedler Group by Mass Spectrometry

At the start of Professor Sweedler's career at UIUC, there were a number of analytical techniques used to conduct measurements on samples, of which mass spectrometry was one. However, mass spectrometry methods and equipment have sustained significant improvement and growth, and this is taking over other areas. Mass spectrometry is becoming an even more potent tool in the hands of scientists when combined with other techniques such as transcript measurements, electrophysiology and fluorescent microscopy. Professor Sweedler described how analytical measurements have changed over the 25+ years since he began at the university:

"My initial research proposal was on how to measure cell-to-cell signaling, in the brain. I proposed working with sea slugs, a simple organism with 10,000 neurons that can learn to find food and avoid being eaten, which we still work on today. We also now work on both simpler and more complex animal models, the more complex being rodents and sometimes primates. Twenty-five years on, we're more capable of getting information out of our samples and conducting measurements, and equipment has entirely changed. Back then I proposed to use capillary electrophoresis with fluorescent detection, in addition to radioactivity detection and NMR. Now almost all measurements involve mass spectrometry. ...*

... Somewhere along the way we started working with Bruker and as mass spectrometry improved, other methods have been used much less often."

New Instruments for new Measurements

The world of single cell biology is rapidly gaining traction and will continue to do so in the coming years. This alone will help facilitate advancements in the technology required to make these

measurements. As one recent development, the Sweedler group has devised a high throughput approach where they disperse thousands of cells on a microscope slide, make them fluorescent, and use optical microscopy to identify cell locations. The information on the specific locations guides the Bruker ultrafleXtreme™ and the solariX XR™ to acquire mass spectra from only the cells and not the empty spaces between them. This enables them to obtain lipid and peptide profiles from tens of thousands of cells.

As another area of research, the Sweedler group is working to combine mass spectrometry with other chemically information-rich approaches:

"We're working with a couple of groups where we can image a brain slice with vibrational spectroscopy such as infrared and Raman. Light is non-destructive, so once we get that chemical information, we can then carry out mass spectrometry imaging. We are currently working on how to combine the different datasets."

In addition to this, the group is also developing an approach for sampling brain slice content after mass spectrometry imaging at select locations, and then performing capillary electrophoresis mass spectrometry analyses of collected analytes.

*For more details visit:
www.nsf.gov/news/special_reports/science_nation/sluggishthoughts.jsp

How has Bruker's Technology helped to solve these Challenges? Future

When assessing which instrumentation should be used for a particular experiment, there is not always a clear-cut answer.

"Sometimes one instrument will excel, and another will not," explains Professor Sweedler. "There are several flavors of instruments, but when it comes to mass spectrometry imaging with MALDI MS, Bruker has very strong platform performance."

Bruker also provides an abundance of expertise, from software update assistance to on-site training at UIUC, and *"offers a partnership which is worth a lot!"* – adds Professor Sweedler. Bruker also facilitates the way in which Professor Sweedler pushes their instruments to higher and higher limits:

"We often use the instruments slightly differently than most users, which can be tricky, but Bruker has always helped us."

"One job of an academic analytical chemist is to push the measurement science beyond what it can easily do. A frequent question we ask ourselves is 'we want to make this measurement, but how can we make the instrument do it?' – working with Bruker enables us to collect such data."

Professor Sweedler's lab recently acquired Bruker's solariX XR™:

"If I had to pick one instrument to save in a fire (and did not have to worry about its size or weight), it would be the solariX XR™. ...

... It's a lower throughput instrument than the ultrafleXtreme™, but it provides great chemical information with the added capability of electrospray."

Solutions to the challenge of single cell measurements have shifted over the past two decades. Professor Sweedler explains that:

"Companies like Bruker are enabling for single cell measurements because they are producing increasingly high quality mass spectrometers. ...

... It's kind of a fun evolution! The last two years have been especially exciting with the combination of mass spectrometry with other approaches."

"In the next decade, I would like to see more robust methods of data integration with other non-mass spectrometry based platforms. We can currently acquire a large amount of data, but the ability to integrate data not just with Bruker instruments but with other instrumental platforms as well, really needs to be improved. Data integration tools need to become more universal."

The longevity of the Sweedlers group collaboration with Bruker is a testimonial to Bruker's high specification equipment, which allows labs like Professor Sweedler's continue to make revolutionary discoveries, through pushing the instrumentation to its limits.

References:

1. National Science Foundation, 2016. Sea slug brain chemistry reveals a lot about human memory, learning www.nsf.gov/news/special_reports/science_nation/sluggishthoughts.jsp [Accessed 16/01/2017]



Customer Insights

- MALDI Imaging in Neuroscience:
Revealing the Biomolecular Map of the Brain

MALDI Imaging in Neuroscience: Revealing the Biomolecular Map of the Brain

From understanding Parkinson's Disease progression to drug behavior across the blood-brain barrier, Bruker's sophisticated mass spectrometry solutions enable researchers at Uppsala University to break new ground in neuroscience.



Working with Bruker

Dr. Per Andrén, Professor of Mass Spectrometry Imaging at the Department of Pharmaceutical Biosciences at Uppsala University and Director of the National Resource for Mass Spectrometry Imaging (NRMSI), has accelerated the adoption of MALDI-MSI technology in the medical research field.

"Our use of Bruker's MS instruments provides the medical research community with the tools to visualize exactly what is going on in diseased tissue, particularly in the brain. MS imaging is now also vital in our drug discovery and development work."

Department of Pharmaceutical Biosciences, Uppsala Biomedical Centre, Uppsala University

Uppsala Biomedical Centre (BMC) at Uppsala University, Sweden, is one of the largest centers for life sciences in Europe. Research and education encompass a number of fields, from small molecules to whole organisms. The Department of Pharmaceutical Biosciences within the BMC is at the forefront of pharmaceutical, biological and medical research at the university, and contains a specialist mass spectrometry (MS) laboratory, founded in 2003.

The Medical Mass Spectrometry Imaging research group is led by Dr. Per Andrén, who is Professor of Mass Spectrometry Imaging at the Department of Pharmaceutical Biosciences. The research group conducts prominent research in the fields of neuroscience and medicine, to uncover the behavior of molecules in

certain disease states, such as Parkinson's Disease, as well as how drugs localize within the brain. The research group currently consists of three researchers, two postdocs, two PhD students and two Master's students.

Dr. Andrén is also the Director of the National Resource for Mass Spectrometry Imaging (NRMSI) infrastructure at Uppsala University, which was founded in 2010. The NRMSI aims to provide a better understanding of health and disease at the molecular level, using cutting-edge mass spectrometry imaging (MSI) technology. A key focus for the Resource is the sharing of knowledge between experts in the field of MSI and the wider scientific community, to communicate the technology's benefits in biological research. The laboratory at Uppsala University was one of the first established in Europe dedicated to MSI, and was the first in Scandinavia. The NRMSI also aims to provide collaboration resources to other academic research groups, pharmaceutical biotech and big pharma companies.

Bringing mass spectrometry imaging to Uppsala

One mission of the NRMSI is to accelerate the use of matrix-assisted laser desorption/ionization (MALDI) imaging technology in biomedical research. The Resource uses this technology to advance projects in the fields of drug discovery and development, neuroscience, oncology and pathology. As one of the most modern MALDI imaging laboratories in Europe, the NRMSI invests in cutting-edge equipment, as Dr. Andrén explains:

“I probably have the most modern mass spectrometry imaging technology in the world.”

The oldest instrument I currently have in my laboratory is Bruker’s ultrafleXtreme, from 2014. My other instruments include a MALDI tandem time-of-flight (TOF)/TOF (rapifleX) and a magnetic resonance mass spectrometry (MRMS) system, a 7T solariX XR, both from Bruker and installed in 2017. The solariX is the Premier League of MSI.”

Funding imaging innovation

Dr. Andrén explains how he was able to bring such modern equipment to the university:

“In 2015 and 2016 I received a rather large research infrastructure fellow grants from the Swedish Foundation for Strategic Research and Science for Life Laboratory (SciLifeLab). The university also installed a professorial chair in 2016, the first one in MS imaging, through which I received funding. It is through these funding streams that I am able to purchase the Bruker instruments and continually update my laboratory’s MS capabilities.”

Core research

The activity of Dr. Andrén’s research group is divided into two parts. The first is commissioned activity, which takes place at the NRMSI core facility, where researchers from

outside the department present new imaging needs to the laboratory, such as visualizing a certain drug. This activity is funded by the Swedish Foundation for Strategic Research and the SciLifeLab infrastructure. The second part is the group’s own research, which encompasses two focus areas covered by grants from the Swedish Research Council: one for neuroscience, focusing on Parkinson’s Disease research, and the second for drug discovery and development.

Parkinson’s Disease – imaging neurotransmitter

The neuroscience program is currently researching a specific stage of Parkinson’s Disease, called levodopa (L-DOPA)-induced dyskinesia (LID), which develops in approximately 50 percent of patients after five to six years of L-DOPA treatment. Dr. Andrén describes the work that his group is carrying out:

“At the moment, little is known why LID occurs. Parkinson’s is characterized by a lack of dopamine in certain regions of the brain (caused by cell death), and the symptoms are often treated with a drug called L-DOPA, the precursor molecule to dopamine. However, altered response to L-DOPA treatment can lead to dyskinesia – a form of involuntary movement which can be extremely debilitating for patients.”

My group is focused on imaging the spatial distribution of neurotransmitters (signaling molecules in the brain) that are known to be affected in Parkinson’s Disease.”

The group has developed a method to image most of the neurotransmitters in a specific brain region, at the same time, providing a new view of the brain and the transmitters involved in current Parkinson’s Disease models. This method, using MALDI imaging, has enabled researchers to measure and quantify different neurotransmitters, and their metabolites and precursors, simultaneously.

The group has published data on the simultaneous measurement of neurotransmitter levels, including tyrosine, tryptamine, tyramine, phenethylamine, dopa-

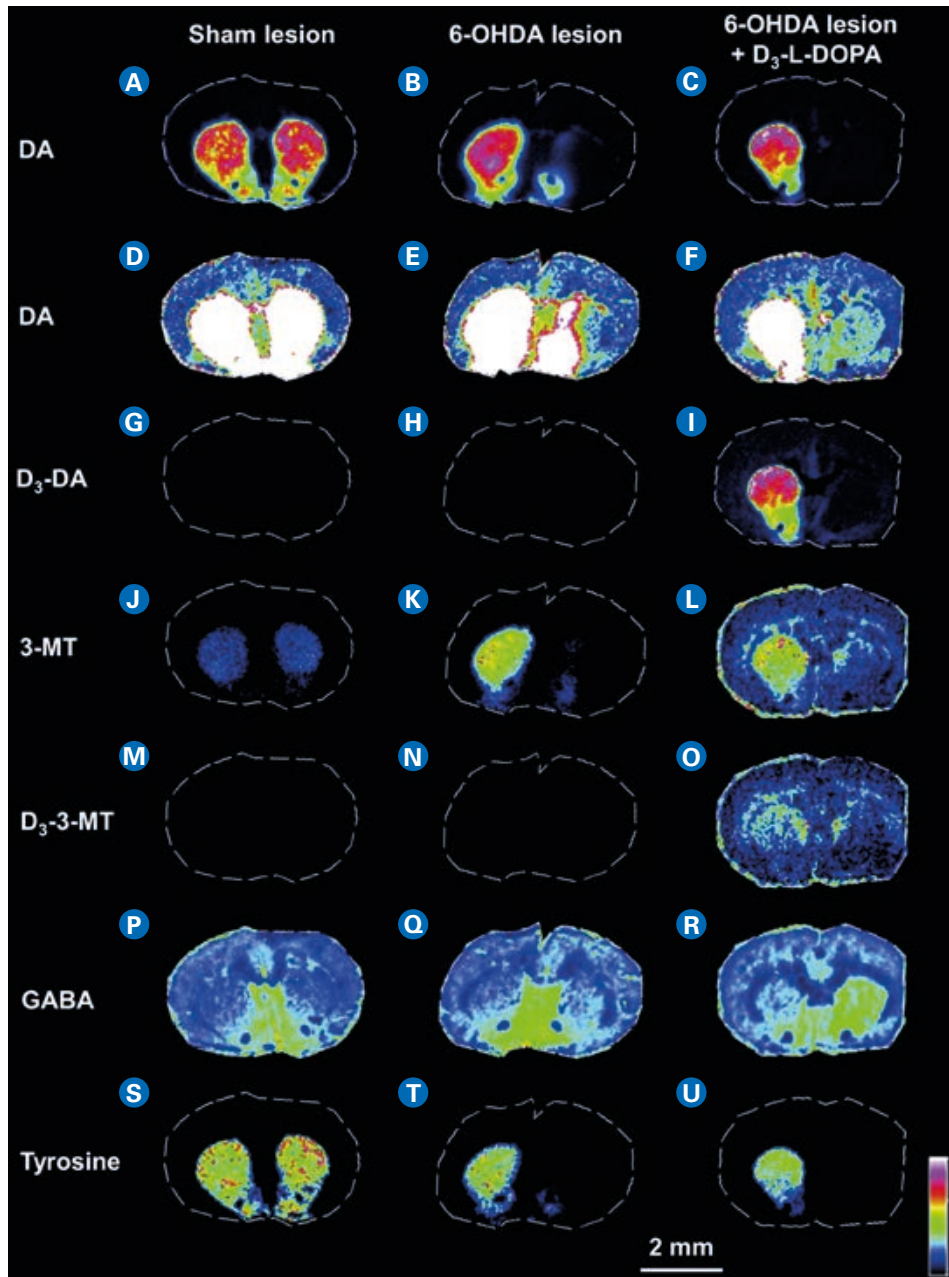


Figure 1. MALDI-MSI images of neurotransmitters in coronal rat Parkinson's Disease model tissue sections. (A-U) Imaging experiments were conducted on brain tissue sections from unilateral sham-lesioned, unilateral 6-hydroxydopamine (6-OHDA)-lesioned animals treated with subchronic L-DOPA for 4 weeks, with the final dose being given as deuterated (D₃)-L-DOPA. The images show the distributions of dopamine (A-F) in sham-lesioned (A), 6-OHDA-lesioned (B), and 6-OHDA-lesioned L-DOPA-treated animals. Rescaling images (A-C D-F) made it possible to determine the distribution of dopamine in the 6-OHDA-lesioned side of the brain, and in structures with low dopamine concentrations, such as the cortex. Distribution of D₃-dopamine (formed by the *in vivo* breakdown of D₃-L-DOPA) is imaged in sham-lesioned (G), 6-OHDA-lesioned (H), and 6-OHDA-lesioned L-DOPA-treated animals (I). Distribution of endogenous 3-MT is imaged in sham-lesioned (J), 6-OHDA-lesioned (K), and 6-OHDA-lesioned L-DOPA-treated animals (L). Distribution of D₃-3-MT (derived from D₃-L-DOPA) is imaged in sham-lesioned (M), 6-OHDA-lesioned (N), and 6-OHDA-lesioned L-DOPA-treated animals (O). Distribution of GABA (P-R) is imaged in sham-lesioned (P), 6-OHDA-lesioned (Q), and 6-OHDA-lesioned L-DOPA-treated animals (R). Tyrosine is imaged in sham-lesioned (S), 6-OHDA-lesioned (T), and 6-OHDA-lesioned L-DOPA-treated animals (U). Figure from reference [1].

mine, 3-methoxytyramine (3-MT), serotonin (5-HT), GABA, and glutamate, in specific brain structures of animal models with and without dopamine depletion and L-DOPA treatment [1]. Figure 1 shows clear differences in the concentrations of the neurotransmitters studied, in different regions of the brain and between treatments. MALDI imaging experiments were carried out using the solariX XR system. As well as simultaneously determining the spatial distributions of multiple known species, the results also potentially enable the group to gain information on yet-to-be-identified molecular species.

“Over the past two years we have been developing an improvement on that technology” comments Dr. Andrén, continuing: “These neurotransmitters are usually difficult to ionize with MS (with both electrospray ionization (ESI) and MALDI methods), so we have developed a derivatization strategy. We spray a compound on top of the tissue, to derivatize the neurotransmitters. We have also developed a new and improved strategy, meaning that we can study almost all catecholamines, for example.”

Using this new strategy, the group has made novel findings in Parkinson’s Disease, particularly the LID stage (unpublished data). For the first time, L-DOPA, dopamine and almost all the metabolites, can be imaged at the same time. Most current imaging techniques for neurotransmitters are indirect, meaning that a marker is measured rather than the neurotransmitter itself. For example, an enzyme called tyrosine hydroxylase, which catalyzes the synthesis of catecholamines such as dopamine, is commonly measured. Dr. Andrén explains his alternative method:

“With MSI, we can do things that are not possible with any other technique. Rather than indirect measurements, we can measure dopamine itself directly (and other catecholamines).”

We need the high mass resolution of the solariX XR to resolve molecules in the surface of the tissue. Currently, many other researchers rely on indirect histochemical, immunohistochemical and ligand-based assays to image small molecule transmitter systems.”

Drug discovery and development

The second element of Dr. Andrén’s research efforts is focused on developing MSI as a tool for drug imaging and studying drug metabolism. Working in all different areas of drug discovery and development, the Biomolecular MSI laboratory conducts experiments in ADME (absorption, distribution, metabolism and excretion), toxicology and, most recently, studying drug penetration of the blood-brain barrier (BBB). Dr. Andrén’s describes the nature of this work:

“We carry out a lot of our drug discovery and development work together with pharmaceutical companies. For example, we work closely with both small and big Pharma companies.

I believe we have imaged over 100 different pharmaceutical compounds, and almost 40 potential drugs, which are in the pipeline with pharmaceutical companies. We can provide a lot of information about those drugs, which are difficult to obtain with other techniques.”

The group is particularly interested in where drugs move over time in the body after administration. For example, the route of an inhaled drug, after it reaches the lung, is complex and often unclear. Finding out where these drugs localize and quantifying them is an important factor in the laboratory’s research, so much so that they have developed their own software for quantification.

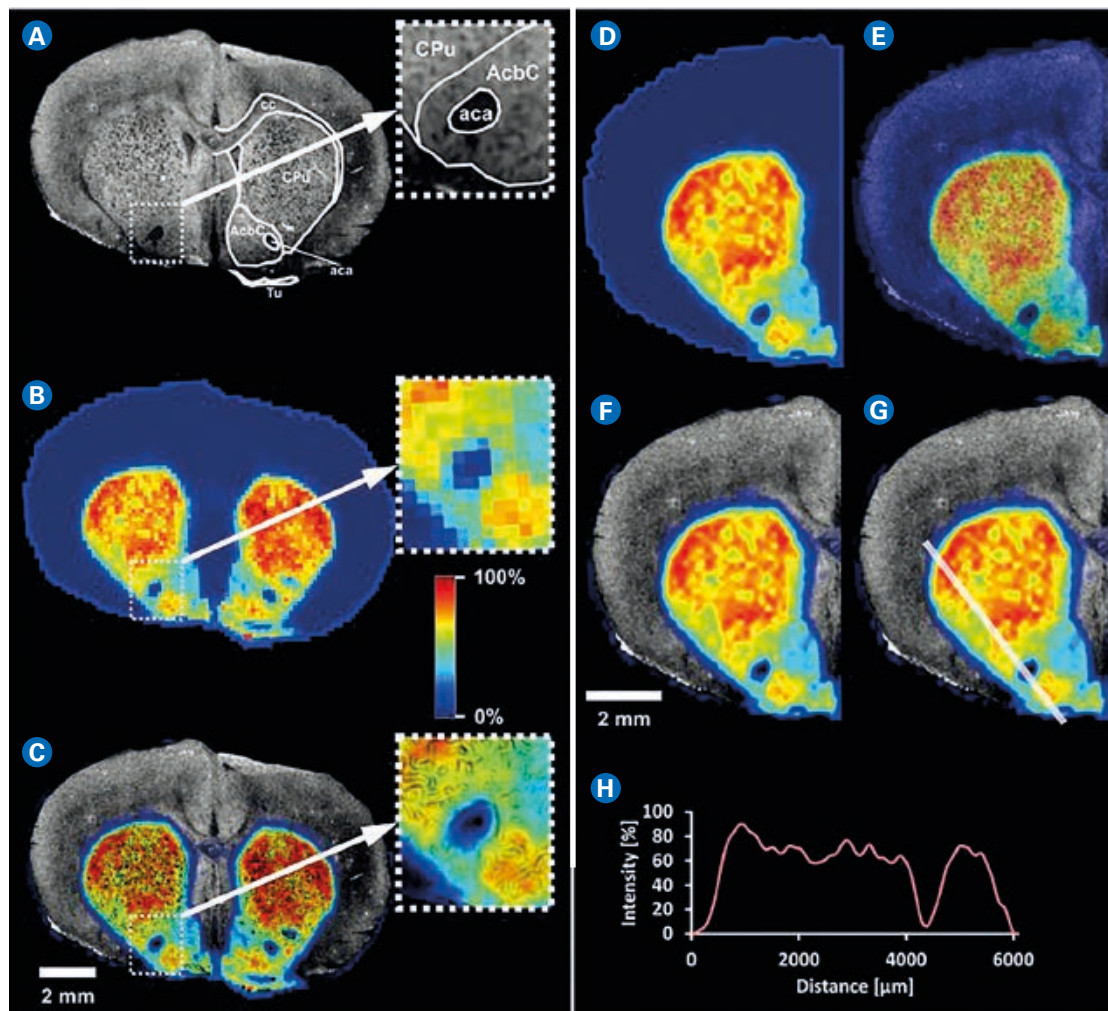


Figure 2. Low intensity transparency, profile intensity, and image fusion using mslQuant. **A** Optical image of a coronal rat brain tissue section displaying brain structures such as the corpus callosum (cc), striatum (caudate-putamen, CPu), nucleus accumbens, core (AcbC), anterior part of anterior commissure (aca), and olfactory tubercle (Tu) at 15 μm resolution. The magnified inset shows the aca, AcbC, and CPu. **B** Ion image of dopamine (m/z 368.165, derivatized dopamine with 2,4-diphenylpyranilium tetrafluoroborate (DPP-TFB)) with nearest neighbor interpolation at 150 μm spatial resolution. **C** The dopamine image was sharpened with the image fusion function of mslQuant by using the optical image to display ion distribution at a spatial resolution smaller than that of the measured ion image. **D** An ion image showing the distribution of dopamine (derivatized dopamine with DPP-TFB) with bicubic interpolation at a spatial resolution of 150 μm . **E** The optical image is shown as the bottom layer, and the dopamine distribution is shown at 50% opacity in the top layer. **F** The optical image is shown in the bottom layer, and the dopamine ion distribution with low intensity transparency is shown on the top layer. The low intensity transparency makes it possible to preserve the brightness and contrast of both image layers. **G** The profile ion intensity of dopamine is selected from a defined area (width 200 μm and length 6082 μm), and **H** is displayed as a graph with the relative intensity of DA on the y-axis and the tissue length (μm) on the x-axis. The MS images were generated using a MALDI MRMS instrument (Bruker Daltonics). From reference [2].

This software, called mslQuant, is the first of its kind to be integrated into this workflow. It converts and imports data, and creates standard curves to automatically calculate the concentration of drugs in regions of interest in tissue [2]. Figure 2 shows the image sharpening process

and fusion function, for more detailed visualization of data. It also highlights low intensity transparency, which enables better visualization of a fused image's intensity dynamics (Figures 2D-F). Regions of high intensity are completely opaque, while regions with intensities below 15% of the maximum are increasingly transparent.

This enhances the visibility of the underlying histological and/or optical image. Without the low intensity transparency function, it is difficult to differentiate intensities close to zero.

MS imaging of the blood-brain barrier

Currently, one of the PhD students in Dr. Andrén's group is studying drug transport over the BBB, with the overall goal of using this information, as well as distribution properties of drug compounds, to develop new, safe and efficacious neuroactive compounds. One recently published set of experiments shows how MSI techniques can elucidate the localization of compounds in specific brain structures, such as the choroid plexus – a section of tissue that forms one of the BBB interfaces [3].

MSI experiments using MALDI-MSI investigated the effects of a multidrug resistance 1 protein (MDR1) inhibitor, elacridar, on the BBB permeability of two well-characterized drugs, propranolol and loperamide. Propranolol is not an MDR1 substrate and has high BBB permeability, whereas loperamide is a substrate of MDR1 and therefore has limited permeability. The study found that loperamide was highly retained by the choroid plexus, a result that was further supported by the spatial correlation between loperamide and endogenous ions. These ions correspond to protonated sphingomyelin (SM) (d18:1/22:0) and its sodium and potassium adducts, which were shown in this experiment to localize in the choroid plexus by MALDI-MSI (Figure 3) and MALDI MS/MS (Figure 4). Sphingomyelin is a type of lipid found in the membranous myelin sheath surrounding certain nerve cell axons, and the spatial correlation found between SM(d18:1/22:0) and loperamide indicates that this lipid could play an important role in choroid plexus function.

MSI technology can provide sophisticated spatial information that may reveal unknown drug-target interactions and/or highlight pharmacokinetic prop-

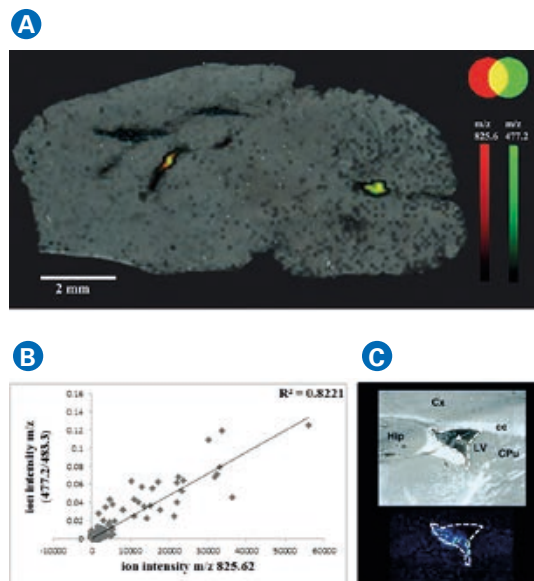


Figure 3. High spatial resolution (20 μm) matrix-assisted laser desorption/ionization (MALDI)-MSI of the potassium adduct of SM(d18:1/22:0) (m/z 825.6) in the lateral ventricle (highlighted in dashed lines) of a sagittal mouse brain section. The structures of interest are highlighted in dashed line in the corresponding optical image. The choroid plexus is annotated by white arrows. Abbreviations: LV; lateral ventricles, Cx; cerebral cortex, Hip; hippocampus, CPU; caudate putamen, cc; corpus callosum. From reference [3] supplementary material.

erties, such as tissue binding. These new understandings can be used to improve drug efficacy or influence further research.

Collaboration

The NRMSI collaborates with a wide network of scientists, including those in private industry, universities, and research institutes around the world. For example, the European Cooperation in Science and Technology (COST) funded a collaborative research MSI project involving 24 European countries during 2011-2015. It involved major European pharmaceutical companies and was supported by the MS vendors and the European Proteomics Association. The aim behind the COST Action was information exchange and training, including data acquisition, data analysis, and to provide this knowledge as a public resource. This research Action strengthened the development of MSI. Another European initiative (Innovative Training Networks) sponsors an interdis-

disciplinary training program in drug discovery and development called ARIADME, where MSI plays an important role.

The Medical MSI laboratory collaborates with a number of research institutes and companies across its various project areas. Key relationships exist with different neuroscience groups in France and Stockholm, both of which provide the animal models required for the group to carry out its research. Dr. Andrén describes these relationships:

“We are working with very talented groups of researchers at Karolinska Institute in Stockholm, led by the neurologist Prof. Per Svenningsson, and in France with Prof. Erwan Bezard at the University of Bordeaux.

Both of these researchers have state-of-the-art animal models for Parkinson’s Disease. We have a fantastic biobank of tissue from these research groups and the solariX is running day and night, analyzing those tissues.”

The laboratory collaborates on projects outside its usual areas of Parkinson’s and drug discovery and development. Joining with the Pharmacy Faculty at Uppsala University, Dr. Andrén’s group completed imaging experiments on a neurotoxin found in a species of water snake,

which lives off the west coast of Sweden [4]. Dr. Andrén comments:

“They came to us to find out exactly where this neurotoxin is located. We conducted some imaging experiments and tracked it down nicely. The goal is to use this knowledge to understand the toxin’s mechanism of action and ultimately, to develop new drugs.”

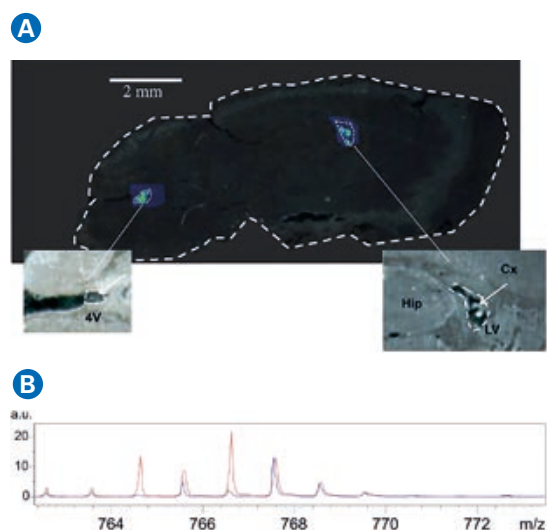


Figure 4. (A) MALDI-MS/MSI of the potassium adduct of sphingomyelin species SM (d18:1/22:0) (product ion m/z 766.6) in the lateral and fourth ventricle of a sagittal mouse brain section at high spatial resolution (20 μm). The structures of interest are highlighted (dashed line) in the corresponding optical image. The choroid plexus is annotated by white arrows. (B) Overlaid spectra of the following ROIs: part of the choroid plexus in the lateral ventricle (red), ventricular interior including the ependymal (blue). The detected product ion was confirmed by the literature (Sugimoto et al., 2016). Abbreviations: LV; lateral ventricles, 4V; fourth ventricle, Cx; cerebral cortex, Hip; hippocampus. From reference [3] supplementary material.

●

Working with Bruker

Since purchasing his first Bruker instrument in 2003, Dr. Andr n has continuously updated his repertoire of MS equipment as his requirements have expanded. He most recently purchased Bruker's solariX XR in 2017, and explains the decision behind this acquisition:

"Before investing in MALDI imaging, I used liquid chromatography mass spectrometry (LC-MS) techniques for identifying and quantifying neuropeptides from different brain regions. Using LC-MS, I identified many novel peptides which no one else had before.

But when the new imaging technology became available, having the spatial distribution of the neuroactive compounds was such an advantage that I completely switched to this method."

The solariX's ease of use, 24/7 running time and high mass resolution were key selling points of the instrument.



●

“The solariX is never resting. This is why I am so eager to buy a second one. If I had two, I could obtain my data a lot faster, and also complete more collaborations.”

At the moment I have to delay many opportunities – I have had all kinds of requests because my laboratory does not have enough capacity on one instrument.”

Dr. Andr n was a postdoc in the group of Professor Richard Caprioli, a renowned researcher in the field, who has a number of Bruker MS systems in his laboratory. He describes the benefits of using Bruker instruments, especially the solariX XR:

“Once you have learned how to use one Bruker instrument, it is very easy to transfer this knowledge to the others. Everyone in my lab can use them, even the master’s students. The solariX opens up a lot of doors.”

You can decipher what is in the complex area of the brain tissue, for example, which you cannot do with other instruments. You need this kind of high mass resolution for MSI.”



Future

“I believe that our new technology for imaging neurotransmitters will open up the neuroscience field for MSI. We will not only research Parkinson’s Disease, but drugs of abuse, Alzheimer’s Disease, pretty much any application where neurotransmitters are involved.”

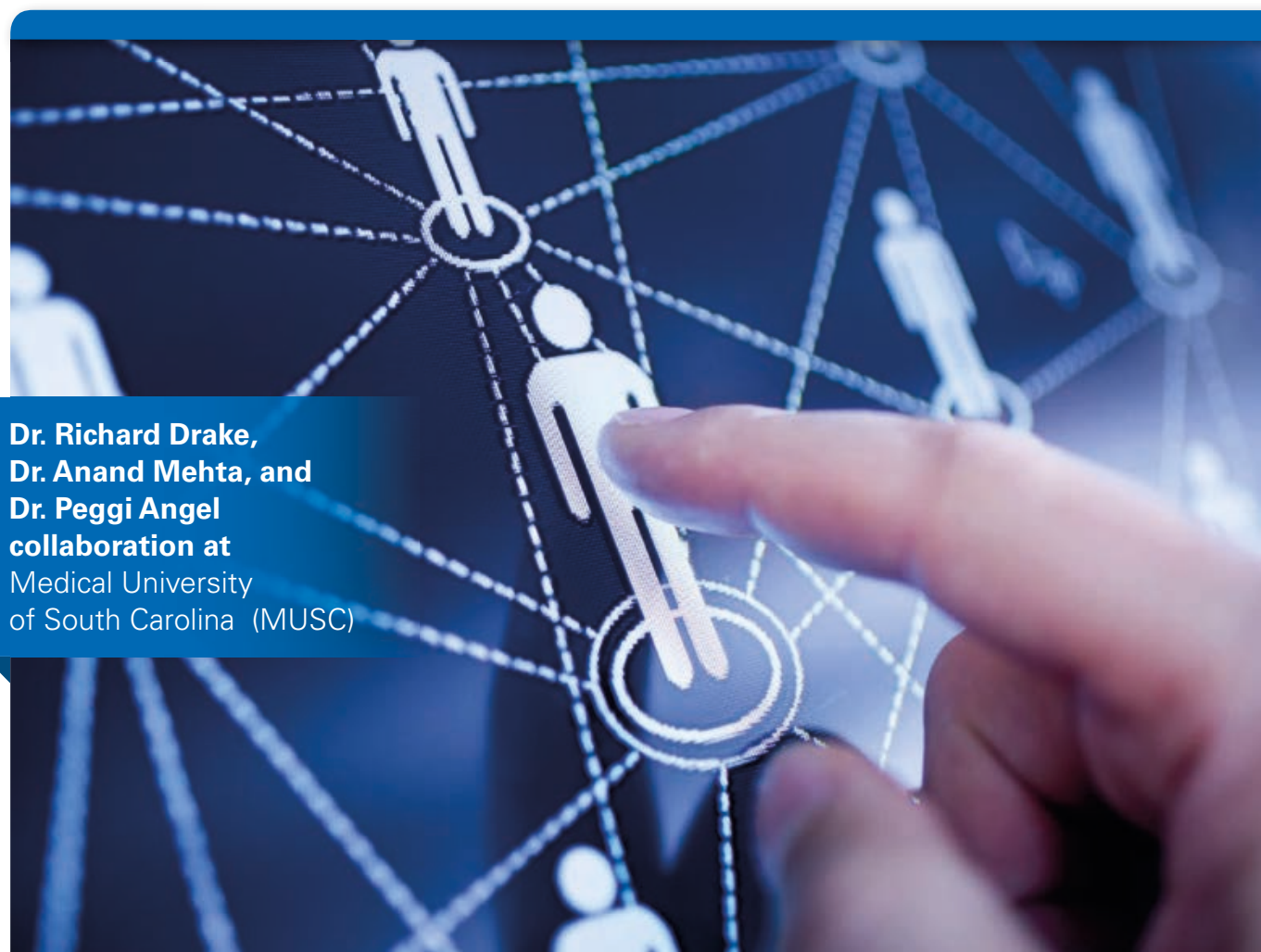
Dr. Andrén has submitted an abstract to the Society of Neuroscience in 2018 on MSI of neurotransmitters, in the hope that it will inspire new debate in this area. This is still a relatively new technology in the neuroscience field.

For more information on the Uppsala Biomedical Centre, please visit <http://www.bmc.uu.se/>, and for more on the National Resource for Mass Spectrometry Imaging, please visit <http://www.farmbio.uu.se/Plattformar/NCMSI/>.

For more information on Bruker’s solariX XR, please visit <https://www.bruker.com/products/mass-spectrometry-and-separations/ftms/solarix/overview.html>.

References

- [1] Shariatgorji M, Nilsson A, Goodwin RJA, Källback P, Schintu N, Zhang X, Crossman AR, Bezard E, Svenningsson P and Andrén PE (2014) *Direct Targeted Quantitative Molecular Imaging of Neurotransmitters in Brain Tissue Sections*, *Neuron*, **84**, 697-707 <http://dx.doi.org/10.1016/j.neuron.2014.10.011>
- [2] Källback P, Nilsson A, Shariatgorji M and Andrén PE (2016) *msIQuant – Quantitation Software for Mass Spectrometry Imaging Enabling Fast Access, Visualization, and Analysis of Large Data Sets*, *Analytical Chemistry*, **88**, No. 8, 4346-4353 <https://pubs.acs.org/doi/pdf/10.1021/acs.analchem.5b04603>
- [3] Vallianatou T, Strittmatter N, Nilsson A, Shariatgorji M, Hamm G, Pereira M, Källback P, Svenningsson P, Karlgren M, Goodwin RJA and Andrén PE (2018) *A mass spectrometry imaging approach for investigating how drug-drug interactions influence drug blood-brain barrier permeability*, *NeuroImage*, **172**, 808-816 <https://doi.org/10.1016/j.neuroimage.2018.01.013>
- [4] Jacobsson E, Andersson HS, Strand M, Peigneur S, Eriksson C, Lodén H, Shariatgorji M, Andrén PE, Lebbe EKM, Rosengren KJ, Tytgat J, Göransson U (2018) *Peptide ion channel toxins from the bootlace worm, the longest animal on Earth*. *Scientific Reports*, **8**, 4596 <http://doi.org/10.1038/s41598-018-22305-w>



**Dr. Richard Drake,
Dr. Anand Mehta, and
Dr. Peggi Angel
collaboration at
Medical University
of South Carolina (MUSC)**

Customer Insights

- Translating Cancer Biomarkers into the Clinic with MALDI Mass Spectrometry Imaging

Translating Cancer Biomarkers into the Clinic with MALDI Mass Spectrometry Imaging

Researchers at the Medical University of South Carolina are breaking new ground in cancer biomarker development with high-end MALDI Imaging technology.



Working with Bruker

The collaborative work at Medical University of South Carolina (MUSC), led by Dr. Richard Drake, Dr. Anand Mehta and Dr. Peggi Angel, is fueled by advanced MALDI Imaging instrumentation:

“The unparalleled speed of Bruker’s rapifleX MALDI TissueTyper and the sensitivity of the solariX MRMS allow us to develop our imaging methods, to better understand disease progression and improve treatments.”

Department of Cell and Molecular Pharmacology and Experimental Therapeutics, Medical University of South Carolina

The Department of Cell and Molecular Pharmacology & Experimental Therapeutics at the Medical University of South Carolina (MUSC), Charleston, SC, is home to cutting-edge facilities including the MUSC Proteomics Center, which is comprised of two core laboratories – the Mass Spectrometry Facility and the MS Imaging Research Center. The Department is ranked within the 30th percentile of national Medical School Pharmacology Departments, according to National Institute of Health (NIH) ranking, and collaborates with the Hollings Cancer Center at MUSC to broaden research scope and offer interdisciplinary educational opportunities. The department includes a total staff of 30, ten students and 20 faculty members (with 15 on the tenure track and five on the research track). The collaboration between three principal investigators (PIs), Dr. Richard Drake, Dr. Anand Mehta and Dr. Peggi Angel, is

centered around their research focus on biomarker discovery, mass spectrometry (MS)-based imaging, and cancer therapeutics. The group has individual research interests spanning the study of various cancers and other diseases, with a common link of glycobiology.

Richard Drake is Professor and Director of the MUSC Proteomics Center, with a background in protein biochemistry and glycosylation. His post-doctoral studies focused on the mechanisms of N-linked glycan synthesis, later establishing their potential as biomarkers. In 2005, Dr. Drake began working with Dr. Mehta as part of the Early Detection Research Network (EDRN). The EDRN is an initiative of the National Cancer Institute (NCI), which aims to accelerate the translation of biomarker information into clinical applications and allowed Dr. Drake and Dr. Mehta to collaborate on various aspects of biomarker development, while maintaining individual projects on prostate cancer and liver cancer, respectively. This has evolved into current funded projects supported by the NCI Alliance of Glycobiologists for Cancer Research, a consortium of nine Tumor Glycomics Laboratories. Dr. Drake moved to MUSC in 2011, bringing expertise in

MS that developed from his work on serum proteomics as biomarkers, which would be crucial for the collective work of the group. Dr. Mehta and Dr. Drake share a common interest in developing biomarkers that are linked with glycosylation changes in cancer, and since 2012 have been working together on tissue imaging of N-linked glycans. Dr. Angel joined the group at MUSC in 2015 as Assistant Professor at the Department of Pharmacology and Director of the MS Imaging Research Center, with an established background in analytical chemistry and matrix-assisted laser desorption/ionization (MALDI) imaging of biological and engineered tissues.

Dr. Angel researched glycan site mapping of protein structure at graduate school and completed two post-doctoral positions, one researching alcoholism in the development of liver disease, and one in the laboratory of Professor Richard Caprioli, the pioneer of MALDI Imaging. It was during the second post-doc that Dr. Angel became interested in lipids, particularly in the context of cardiovascular disease.

"MALDI Imaging is very important in advancing the study of lipids"

explains Dr. Angel, adding:

"Lipids have no useful antibodies, so by using MS we can see very distinct structural conformations. It is a unique way to study, at one time, thousands of different lipids in tissue."

Dr. Mehta is Professor and Smart State Chair in Proteomic Biomarkers at MUSC. His background in viral hepatitis has paved the way for his research interest in liver cancer, leveraging his experience in glycobiology to develop biomarkers. His laboratory currently studies liver disease, often caused by a virus such as hepatitis B or C. Dr. Mehta also investigates liver disease caused by excess fat consumption, which is the number one cause of liver disease in the US and is often referred to as non-alcoholic fatty liver disease. Such disease eventually leads to fibrosis and cirrhosis, which is the major risk factor for liver cancer. Dr. Mehta's laboratory focuses on developing methods of detecting liver cancer, to eventually treat it.



"I had been working with several people at MUSC before I moved here in 2016, particularly Dr. Drake" explains Dr. Mehta, adding: "I knew of his work in the MS and proteomics fields through the EDRN program, and knew his group was very strong in glycomics and proteomics and, more recently, in imaging. This was the main reason I joined MUSC."

Current collaborative research

There are many benefits to the three-way synergy of the research laboratories at MUSC. Dr. Drake, Dr. Mehta and Dr. Angel's individual research backgrounds have brought new expertise and insight to achieve the common goal of biomarker development. The three PIs can co-mentor

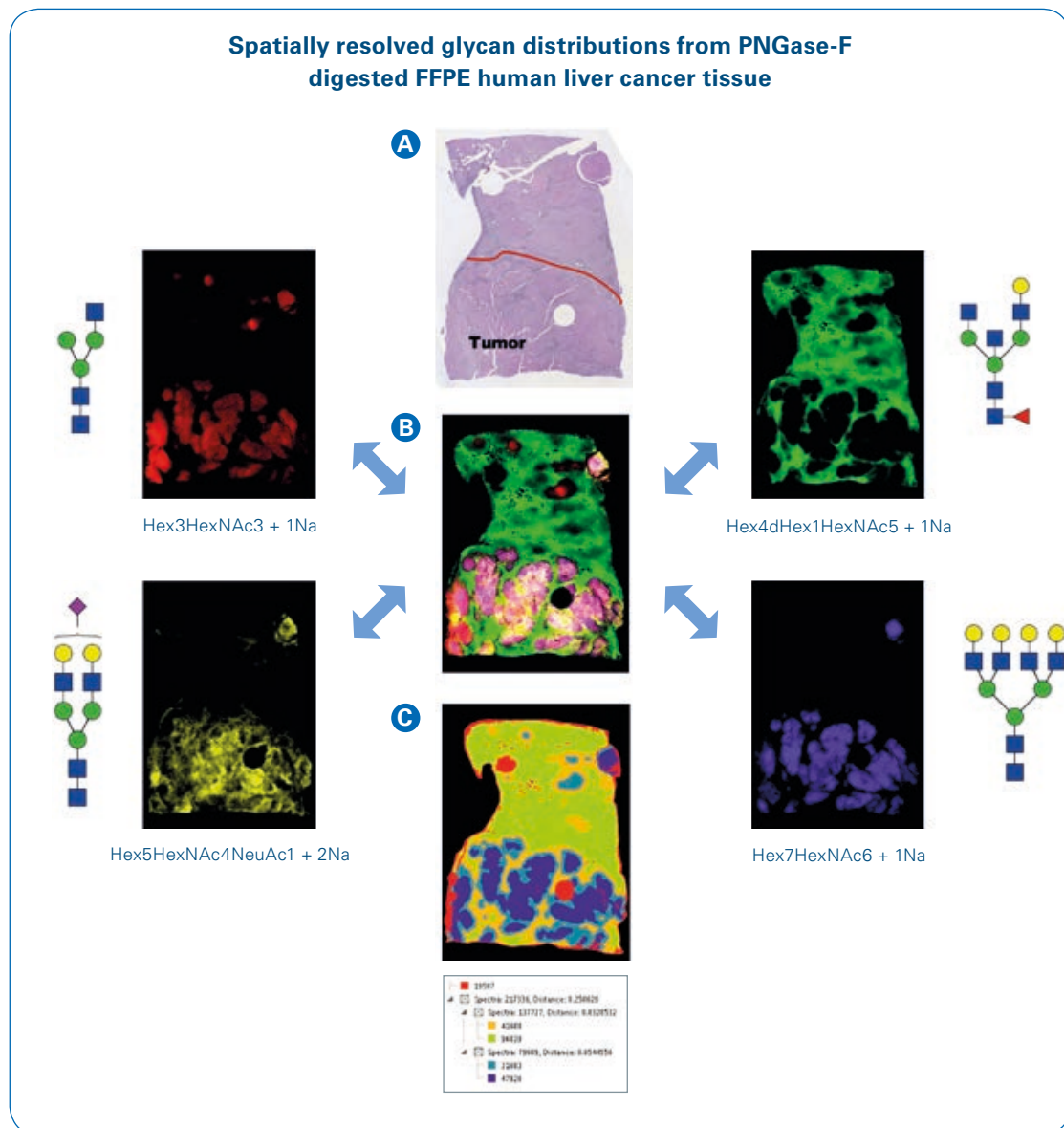


Figure 1: Spatially resolved glycan distributions from PNGase-F digested FFPE human liver cancer tissue. **(A)** An H&E stain of a hepatocellular carcinoma tissue. The bottom half of the tissue below the red line represents the region of tumor. **(B)** A glycan image overlay of four m/z values corresponding to sodium adducts of the N-glycan species shown on the right and left side panels. The major tumor glycan is the Hex7HexNAc6 glycan in blue, and also reported in ref. [1] **(C)** A segmentation analysis of 5 partitions of 44 N-glycans was done in SCiLS Lab software from Bruker. The distribution patterns of the 5 nodes is shown in the image. Tumor glycans were localized in the blue regions

students and post-docs, providing them with a flexible learning environment. The group has found that the collaboration is also a successful and unique way to be competitive for grant funding.

Since 2012, Dr. Drake has been developing new methods to analyze biomolecules within tissues using MALDI Imaging, focusing on N-linked glycosylation, which is important in tumor development and progression. He brought with him to MUSC a new method to analyze fixed tissue, allowing the spatial localization of differences in samples. At the time, he was focusing on lipids and proteins as there was no viable method for visualizing glycans. The enzymes required were expensive, costing approximately \$1000 for 40 μ L of enzyme, and were unsuitable for spraying onto tissue. Dr. Mehta explains how his group helped solve this challenge:

"Prior to moving to MUSC, my research group developed an enzyme that would allow imaging of tissue with glycans for the first time. This ended up being very powerful and we went on to develop this as a new platform technology to base subsequent research on."

When MALDI Imaging was growing as a technique, it was primarily used to visualize lipids or proteins using a trypsin digest. The development by Dr. Mehta of a highly active and stable recombinant version of peptide N-glycosidase (PNGaseF Prime™), which cleaves sugars off proteins – enabled glycan imaging on tissues for the first time. The enzyme is now commercially available, at a much lower price than those previously used, and is validated for use on MALDI Imaging.

In one study, the group assessed the PNGaseF method for MALDI Imaging on archived pathology formalin-fixed paraffin-embedded (FFPE) tissue blocks for liver cancer [1]. An example of liver cancer glycan imaging is shown in Figure 1, as different N-glycans were detected that could distinguish between non-tumor and tumor regions. Four different glycan species were detected, as well as an overlay image and segmentation analysis image done in SCiLS Lab software. The shown tissue was analyzed using Bruker's timsTOF fleX MALDI-Q-TOF mass spectrometry system.



The breakthrough development of the PNGaseF enzyme also synergized with the work of Dr. Angel, whose research focus on collagen imaging and the glycosylation of extracellular matrix (ECM) glycoproteins. Dr. Drake describes the group's typical workflow:

"In a typical experiment with tumor tissue, my laboratory will prepare a sample and run the N-linked glycans analysis and generate that image. The sample is then rinsed and Dr. Angel completes the collagenase treatment and obtains that imaging data, which can then be correlated with other liquid chromatography mass spectrometry (LC-MS) data from her database. None of this would be possible without the PNGaseF and collagenase enzyme prepared by Dr. Mehta's group."

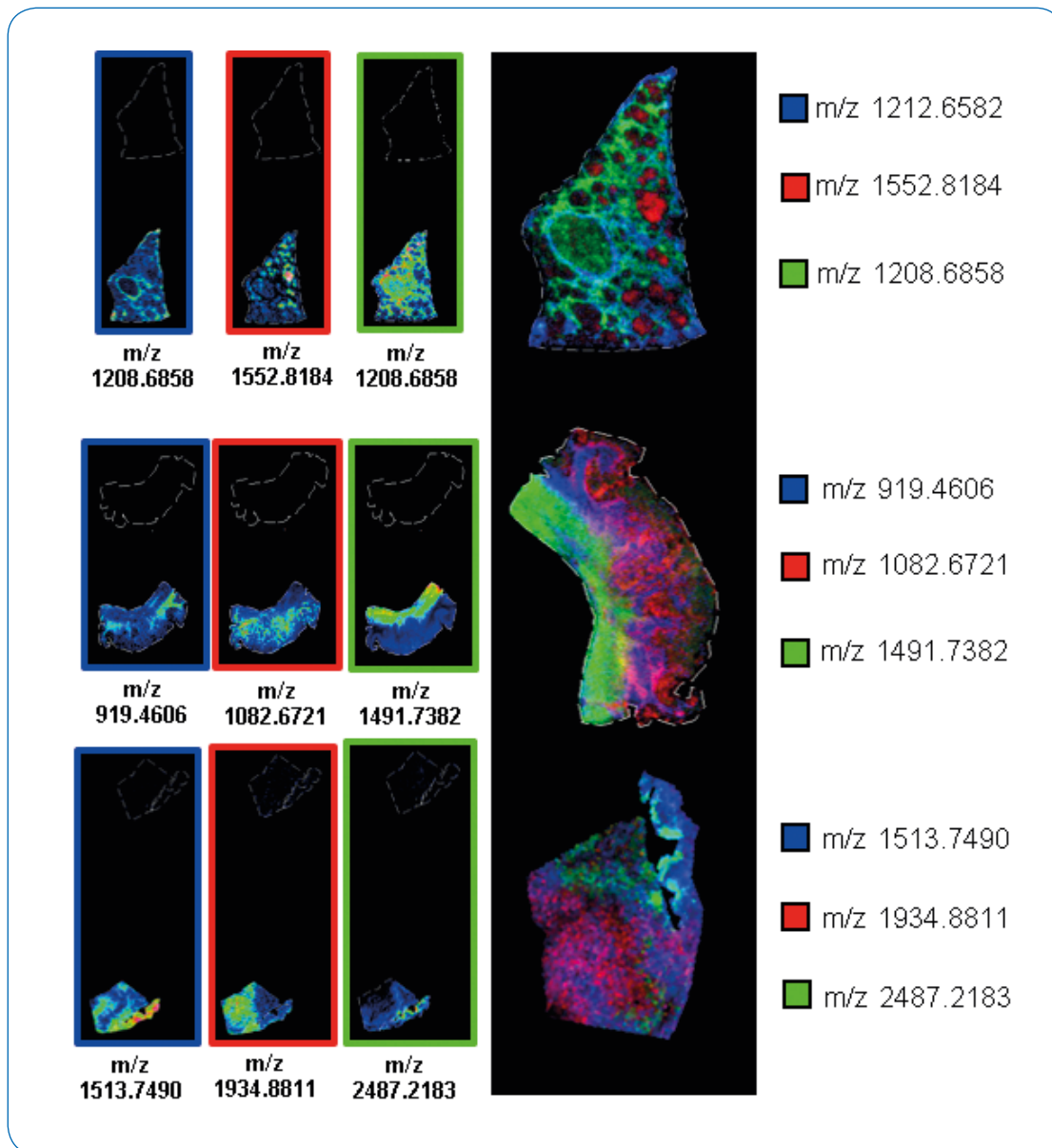


Figure 2: Examples of collagenase type III image data across tissue types. Combined images illustrating distinct localization of collagenase type III produced peptides across tissue types (solarix MRMS MALDI Imaging data). Reprinted with permission from Angel PM, Comte-Walters S, Ball LE, et al. J Proteome Res. 2018;17(1):635–646. Copyright 2019 American Chemical Society

Initially, ECM peptides were being removed from tissue to increase detection of glycans. As part of her research at MUSC, Dr. Angel developed a strategy to detect the ECM peptides from fixed tissue sections instead of removing them. *"This has opened up a whole new field for imaging mass spectrometry"* comments Dr. Angel, adding: *"It's really due to this synergy with Dr. Drake and Dr. Mehta that we are able to do this. I have a couple of projects with Dr. Mehta to improve enzymes for*

accessing ECM glycoproteins, and Dr. Drake is continually working on novel methods to look at glycosylation."

Figure 2 shows how the group used MALDI Imaging to localize collagen and elastin peptides within the tissue microenvironment using bacterial matrix metalloproteinase (MMP) enzyme (Collagenase types; COLases), enabling them to directly detect localized biochemical information related to ECM collagens and elastin proteoforms [2].

The importance of glycans

All cells are surrounded by a coating of glycans, called the glycocalyx and ECM proteins outside of the cell are also glycosylated. Glycosylation is an important process, as it defines intercellular interactions – how cells 'talk' to and 'see' each other, but it is still an emerging field. For example, glycosylation determines blood groups, and what the body recognizes as 'self' and 'non-self', playing an important role in the immune response. The glycosylation on the cell surface is recognized by the immune system, and facilitates immune cell binding, particularly in cancer.

In a disease state, changes in glycosylation can be crucial, and the group at MUSC is researching how glycans change on the surface of cells in response to different disease processes. At the pathological level, changes in glycosylation and their importance in tumor progression have been well documented over time, but until now have not been effectively demonstrated and localization has not been achieved. Using MALDI Imaging for N-linked glycans, these processes can be directly localized in the tissue, to assign different glycans with different tissue features.

"It quickly became apparent, with the powerful spatial localization of MALDI Imaging, that very specific biological changes were occurring that we hadn't been able to detect before"

comments Dr. Drake.

The composition of the ECM is critical to understanding disease progression, as it contains many proteins and small molecules which contribute to cell communication and influences how drugs diffuse between cells during treatment. One of the key challenges of imaging the ECM is that it consists of compact, highly organized 'bundles' of proteins which, until now, have been difficult to access analytically. Dr. Angel uses ECM degradation enzymes like collagenase to access these proteins and report on proteins present in the ECM. Glycan imaging

is a crucial part of understanding the ECM, as over 90% of ECM proteins are glycosylated. After Dr. Drake's laboratory has studied the glycosylation of a specific tissue, it is passed to Dr. Angel's laboratory to map the changes occurring in the ECM.

"Using these recombinant enzymes allows us to target ECM proteins in clinical specimens, which had never been done before because at the time, there were no tools to report the changes in these proteins during disease progression" comments Dr. Angel, adding: "We've seen many new, interesting changes that are relevant to disease status."

One application involves examining the ECM of patients with breast cancer, which has a distinct organization through progression and propels the disease in early stages but is poorly understood. Dr. Angel's laboratory has used MALDI Imaging to find specific peptides that are modified in the disease state, which could potentially become biomarkers for early stage breast cancer [3]. The group has recently found that hydroxylation of proline may be a contributor to cancer progression [2], and because this is a nutrient-sensitive pathway, the data could be correlated with socioeconomic status.

MALDI Imaging at MUSC

At the start of their working relationship, Dr. Mehta and Dr. Drake primarily conducted serum-based analysis. At that point, there was no method for two-dimensional (2D) tissue analysis for glycomic changes, so the 'grind and find' approach was used, where a tumor tissue sample is homogenized and the glycans extracted for analysis. However, this method loses the spatial resolution required to establish where the glycans originated from in the tissue. MALDI Imaging of glycans leaves tissues intact, and also allows findings in tissue to be translated to glycan changes occurring in blood. Dr. Mehta explains the significance of this:

"If you can see what you see in cancer tissue in the blood, you can find a biomarker. So glycan imaging has really transformed our biomarker discovery, which can now start directly in the tissue and will really drive biomarker development at a much faster pace."

Dr. Drake has a background in serum protein profiling using MALDI-TOF instruments, and has been carrying out MALDI Imaging on tumor tissues since 2006, initially on peptides in prostate cancer tissues. His move to MUSC in 2011 opened up new instrumentation and research options. Dr. Drake explains how he came to use Bruker's solariX MRMS instrument: "Moving to MUSC provided me with a great opportunity to try new instrumentation. Coming from a background in MALDI Imaging with Bruker systems, there was only one instrument I wanted – the solariX MRMS. It gave me the opportunity to develop new methods and has been a very flexible workhorse instrument. We have been able to look at almost any biomolecule of interest, and it was key to developing the N-linked glycan workflows. We continue to use it in novel ways."

One advantage of using MALDI Imaging to analyze glycans is that their defined masses can be obtained and assessed reproducibly. Dr. Drake's laboratory has found that glycans in formalin-fixed tissues make excellent targets due to their well-defined structures and the lack of background. The signal is reproducible as it is generated from the activity of the PNGase F enzyme sprayed onto the tissue.

The ease of use of MALDI front-end technology is of great benefit to the field. Enzymes and matrices are rapidly sprayed onto the sample and users receive an answer within one to two hours. Dr. Mehta describes the advantages of

this: "The solariX has been absolutely essential to our work. It has unparalleled sensitivity, which is a great benefit when you are conducting a new experiment, because often you are looking for a needle in a haystack. You need an instrument that is extremely sensitive to that needle, and the solariX is that instrument."

The MUSC group's long-term goal of biomarker development requires the analysis of vast numbers of tissues. A robust platform is needed to handle, visualize and extract large amounts of data for further analysis. "Bruker's SCiLS Lab MS imaging software and flexImaging package have always been ideal for this purpose" comments Dr. Drake, continuing:

"When you combine Bruker's long history of excellent MALDI MS instrumentation with sophisticated software, it has allowed us achieve our goals of moving these assays toward clinical applications."

The sensitivity of the solariX 7T MRMS enables the group to analyze incredibly small amounts of starting material, to see attomolar (10⁻¹⁸) or femtomolar (10⁻¹⁵) levels of sugar, with ease. It is used as the first step in all analyses to identify changes in glycans, for example in a cancer



tissue, which can then be validated on a high-throughput instrument such as Bruker's rapifleX MALDI Tissue typer. The same glycan imaging run that would take between six and eight hours on the solariX can be completed in 45 minutes on the rapifleX, which has enabled the group to propose validation studies for their biomarkers. The group has recently received a \$3 million grant from the NCI to conduct glycan imaging on over a thousand cancer samples, which would not be possible without the throughput of the rapifleX.

Dr. Mehta comments on how MALDI Imaging has furthered his work on liver cancer: *"By coming to MUSC and using the solariX and rapifleX instruments, we've been able to confirm that, for the most part, the same glycan and glycoprotein modifications we see in circulation are directly associated with the tumor and not adjacent tissue, or a distally adjacent tumor. This has been very successful and we are leveraging the expertise of Dr. Drake and Dr. Angel to extend the imaging technology."*

Collaboration with Bruker

Dr. Drake, Dr. Mehta and Dr. Angel have varying degrees of experience with Bruker's instrumentation, MALDI Imaging and MS as a whole. Dr. Angel spent six years after graduate school at Vanderbilt University – where the Mass Spectrometry Research Center, led by Prof. Caprioli, has a longstanding relationship with Bruker – developing MALDI Imaging methods. "It was during my time at Vanderbilt University that I really began appreciating the collaboration between academia and instrument vendors that is essential for progressing the technology forward" Dr. Angel explains, adding: "It's the collaboration between Bruker, the scientists using the instruments and the clinicians that is really driving the research."

Dr. Mehta comments on how Bruker has assisted the group's research: *"Bruker has always been willing to collaborate and assist where they can, to help us move our research forward. We are always adapting to the results the instruments provide, and there is a continual high level of innovation from both sides, but particularly from Bruker. They are incredibly receptive to our new ideas."*

One of the most impactful developments in MALDI Imaging for the MUSC group was the decrease in laser spot size, which has been fundamental to Dr. Angel's research. In the past 10 years, the laser spot size has decreased from 150 μm to 5 μm , to enable better targeting of specific cells in tissue and report on these cell's activity in a particular disease status. Dr. Angel explains how collaborations such as that between MUSC and Bruker drives these innovations:

"It's critical for a lab, whether old or new, to foster a relationship with instrument vendors. MALDI Imaging wouldn't be in the place it is now, being used for advanced clinical studies, if it weren't for the close collaborations between vendors, academia and clinicians."

Translating research to the clinic

One of the primary goals of the MUSC group is to translate their findings into clinical biomarkers, which can help detect disease earlier – particularly cancer – and help inform treatment. Dr. Drake's laboratory works with industrial partners to develop their biomarkers for clinical use. The biomarkers of liver cancer currently being marketed require simple, plate-based assays that only analyze one protein at a time, and provide a binary 'yes/no' answer of whether the cancer is there. This is problematic because in general, one protein is not going to be found in all cancers. Dr. Mehta explains the issue: "Cancer is a very heterogeneous disease – one person's cancer is not the same as another's – therefore you need multiple biomarkers to really detect all cancers. The glycan imaging methods we have developed allow you do that. The first step is looking at the glycans on a thousand glycopeptides, and the second is combining this with the glycopathology, where we perform glycan tissue imaging to establish the aggressiveness of the cancer. I truly believe that glycan imaging is more than a research tool, it's a clinically viable tool that I think will have a tremendous impact in the diagnostic space."

These assays currently being developed, using the rapifleX, provide the potential to create signatures of the changes occurring on different proteins during disease progression. Dr. Drake explains the significance of this:

"I have a vision that you could have a single slide capturing 150 key glycoproteins from a patient blood sample, and this one slide could tell you whether the patient has breast cancer, prostate cancer, liver cancer or colorectal cancer, and differentiate the cancer stage and tumor aggressiveness based on the glycan signature. This liquid biopsy precision medicine assay is the dream for us, and we are almost there for liver cancer."

These blood assays will allow prognosis and diagnosis, but the group is also developing cell-based assays, where patient-specific cells can be analyzed to determine their sensitivity to certain therapies, based on the glycan signature. *"This is a really exciting area that draws on the entire group's research"* comments Dr. Angel.

Dr. Angel's research also focuses on classifying cancer using tissue microarrays, which contain many representative tissue samples from a large cohort of patients. Her group found that the ECM changes in disease and can differentiate between a benign status and a cancer status, providing an extra level of classification that can be added to different biomarker signatures.

The group is also working to link MALDI Imaging workflows to clinical imaging, such as magnetic resonance imaging (MRI) and positron emission tomography (PET) imaging. The aim is to translate the information obtained at the tissue level into probes that could be used in patients prior to surgery, in diagnostics, or for therapy monitoring. The 3D imaging capabilities of the solariX and rapifleX are crucial for this next project.

"We are not only asking very clinically-relevant questions, but new questions that I don't think Bruker envisioned or designed the instruments to do" comments Dr. Mehta, adding: *"We are opening up new avenues, such as imaging captured cells, tissue culture cells, captured proteins for their glycans, as well as tissues. I do not have a background in MS, so I have no preconceived ideas of what the instruments can or cannot achieve, and therefore push them to their limits."*

The rapifleX would be an example of excellent instrument innovation. It's designed to enhance and bring MALDI Imaging to the clinic."



Continuing biomarker development

One of the longstanding challenges of glycan imaging is the number of structural isomers. In glycobiology, how sugars are arranged on proteins dictates the impact on cancer growth and which cancer pathway has been activated. Currently, the solariX and rapifleX allow the group at MUSC to make a prediction on the arrangement of sugars, but further analysis is required to confirm the glycoforms. Ion mobility separation is an MS technique that separates molecules based on their conformation and can therefore detect isomers and glycoforms. The high resolution and sensitivity of the solariX and the speed of the rapifleX is now combined in Bruker's latest instrument, the timsTOF flexX, which utilizes trapped ion mobility spectrometry (TIMS) and is powered by parallel accumulation-serial fragmentation (PASEF) technology. Dr. Drake explains how this instrument could drive future glycan imaging at MUSC:

"Having ion mobility separation incorporated into the instrument would be an excellent way to help us identify glycoforms. The other challenge is that we are releasing glycans from protein carriers, but we don't know what these protein carriers are. We would like to be able to look at glycopeptides directly, so we can take our glycan maps and link them to the proteins themselves. Having a platform where we can actually get protein ID as well as glycan ID would take our research to another level. Bruker's timsTOF flexX has great potential to do all of this. There would have to be a lot of method development, but there's no reason why we can't look at glycopeptides."

The timsTOF flex will also provide the capabilities required to link MALDI Imaging with MRI and PET. Dr. Angel comments on where she sees the field developing:

"I expect that, in the next five years, the field of imaging is going to see the emergence of additional ancillary laboratory tests that use MALDI Imaging for the diagnosis of certain diseases. I think new tests will be developed to provide information on how disease progresses, and how it is diagnosed at an earlier stage."

The timsTOF flex combines the great range of sensitivity in looking at different analytes in complex biological matrices, with the rapid scanning capabilities of the rapifleX – we will be able to separate molecules and understand how they change in disease at a much deeper level."

For more information about Bruker's MALDI Imaging solutions, please visit <https://www.bruker.com/applications/life-sciences/maldi-imaging.html>

References

- [1] West CA, Wang M, Herrera H, Liang H, Black A, Angel PM, Drake RR, Mehta AS (2018) N-Linked Glycan Branching and Fucosylation Are Increased Directly in Hcc Tissue As Determined through in Situ Glycan Imaging, J Proteome Res; 5;17(10):3454-3462.
- [2] Angel PM, Comte-Walters S, Ball LE, Talbot K, Mehta A, Brockbank KGM, Drake RR. (2018) Mapping Extracellular Matrix Proteins in Formalin-Fixed, Paraffin-Embedded Tissues by MALDI Imaging Mass Spectrometry. J Proteome Res, 17(1):635.
- [3] Angel PM, Schwamborn K, Comte-Walters S, Clift CL, Ball LE, Mehta AS, Drake RR. (2019) Extracellular Matrix Imaging of Breast Tissue Pathologies by MALDI-Imaging Mass Spectrometry. Proteomics Clin Appl, 13(1):e1700152.



● High-resolution climate reconstruction using MRMS MALDI Imaging

Reconstruction of past climate conditions, e.g. sea surface temperature, with organic marker molecules archived in marine sediments is a well-established technique in paleoclimate research.

Abstract

Conventionally, biomarkers indicative of past climate conditions such as C_{37} -alkenones from haptophyte algae are chromatographically analyzed from lipid extracts generated from centimeter- and gram-sized sediment samples.

Consequently, the temporal resolution of the results is rather coarse and abrupt events or small-scale climate changes are averaged into a smoothed signal. Processes operating on these timescales are, however, the ones impacting modern ecosystems. Insights into these

paleoenvironments are crucial to assess their potential response to future climate change. This study shows how molecular imaging of these target molecules with MRMS MALDI Imaging enables paleoclimate research at unprecedented resolution.

Keywords:
Imaging, solarIX,
flexImaging,
climate proxies

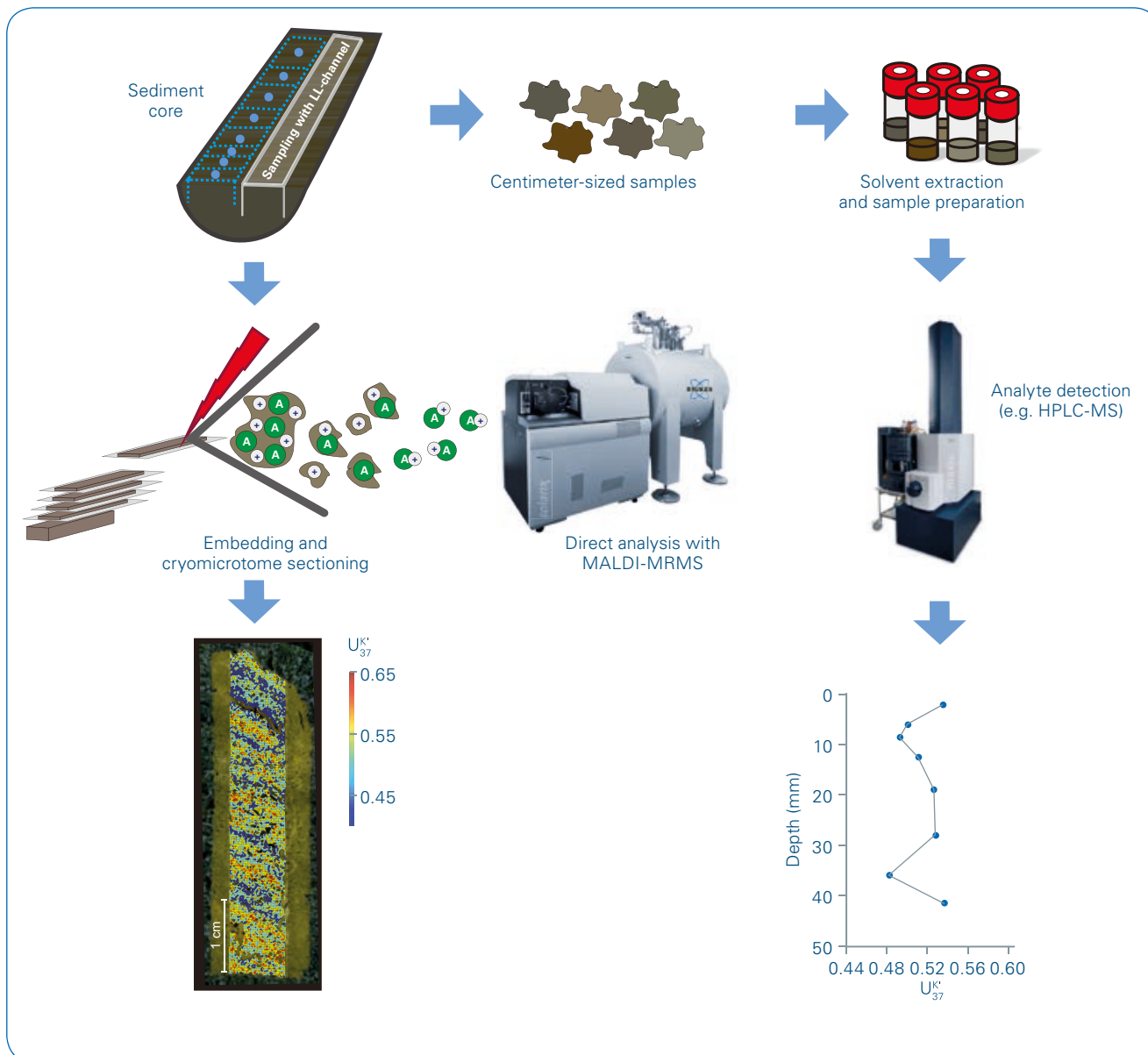


Figure 1: Schematic workflow of molecular imaging of marine sediments with MALDI-MRMS compared to conventional extraction based analysis by HPLC-MS.

Introduction

Gaining insights into past climate variability is essential to classify its current state and future trend. Marine sediments have shown to be valuable climate archives, as they can be accurately dated and record the prevailing environmental conditions under which they were formed. One approach of reconstructing paleoclimate uses molecular tracers originating from the lipid membrane of microorganisms that once inhabited

the water column. These biomarkers provide information on properties such as temperature, nutrient availability or pH in their biological producers' habitat. Conventionally, biomarker analysis uses gram-sized samples from a sediment core to account for the amount of material needed to generate a lipid extract using organic solvent-based extraction methods. The subsequent analysis is usually performed by gas- or liquid chromatographic methods coupled to mass spectrometry (Figure 1).

Besides the time-consuming procedure for the analysis, the extraction-based approach entails a loss of information as several millimeters to centimeters of the sediment are combined into one sample. Depending on the sedimentation rate, this method limits the temporal resolution of paleoclimate studies to decades or even centuries. Consequently, short-term climate oscillation operating on (sub)annual time oscillations remain inaccessible by this approach.

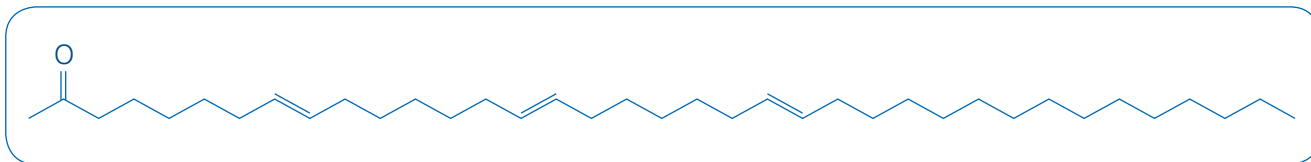


Figure 2: Structure of a $C_{37.3}$ alkenone.

Long-chain alkenones from haptophyte algae are widely applied biomarkers to assess past sea surface temperature (SST) changes. The degree of unsaturation in these compounds is correlated to the temperature in the haptophyte's habitat, i.e. higher (lower) degree of unsaturation with lower (higher) temperatures. This relation is expressed in the SST proxy U_{37}^K as formula (equation 1 and 2) [1,2].

Here we show how molecular imaging by mass spectrometry can be used to reveal the micrometer-scale distribution of this proxy, allowing for high-resolution reconstruction of past SST, and provide an example from varved (i.e. annually laminated) sediments recovered from the Santa Barbara Basin (CA, USA). Molecular imaging is ideally suited to overcome the limitations of the extraction-based method and has the potential to set the stage for paleoclimatology at unattained temporal resolution.



Figure 3: Scanning electron microscope picture (JEOL JSM-6330F) of the long-chain alkenone producing coccolithophore *Gephyrocapsa oceanica*. Colors are artificial. Scale bar = 1.0 μm . (source: <https://en.wikipedia.org/wiki/Coccolithophore>).

Methods

Sample preparation

Sediment cores recovered from areas with a strong preservation of the organic matter due to high-sedimentation rates and oxygen depleted bottom waters are ideally suited for high-resolution molecular imaging. To analyze sediments with MALDI MRMS, spatially intact sub-sections of the sediment core are sampled with double L-channels and further sectioned into 5 cm pieces. The following sample preparation of the 5 cm section from a sediment box core recovered from the center of the Santa Barbara Basin in 2009 includes freeze-drying of the sediment and a subsequent embedding in a mixture of gelatin (5%) and carboxymethyl cellulose (2%) (Figure 1) [3]. Composition of embedding media might be modified in densely packed material. A 60 μm slice was prepared from the embedded and frozen sediment block using a cryotome and placed onto the conductive indium tin oxide glass slide for imaging mass spectrometry. No MALDI matrix was added to the sample in accordance to Wörmer et al. [4] who proposed that the natural occurring NaCl in marine sediments as well as the organic matter in the sediment may facilitate ionization.

Additionally, 8 sediment samples covering ~ 4.5 cm adjacent to the intact section were extracted using a modified Bligh and Dyer protocol [5].

MS analysis

Molecular imaging of the 60 μm sediment slice was performed using a solarix XR MRMS system equipped with a 7T magnet and a MALDI source. Measurements were performed in the continuous accumulation of selective ions (CASI) mode in order to enhance sensitivity in the m/z range of targeted molecules (Wörmer et al. 2019). For the alkenone analysis, an isolation window for CASI with a mass to charge ratio (m/z) of 550 ± 30 Da was chosen. Mass spectra were acquired in positive ionization mode with a data size of one megaword and a data reduction of profile data of 95%. For the spatially resolved analysis a ~ 8 mm wide area covering the entire length of the sediment section was defined and scanned at a special resolution of 200 μm using a large laser focus. The number of laser shots per spot was set to 700 with a frequency of 1 kHz and a laser power of 35%. External mass calibration was performed in electrospray ionization mode with sodium trifluoroacetate prior to the MALDI Imaging experiment, followed by an internal lock mass calibration of each single spectrum in DataAnalysis (Bruker Daltonik GmbH, Bremen, Germany) using the highly abundant Na^+ -adduct of pyropheophorbide *a* at m/z 557.2523.

$$1. U_{37}^K = \frac{C_{37.2}}{C_{37.2} + C_{37.3}}$$

$$2. U_{37}^K = 0.033T + 0.044$$

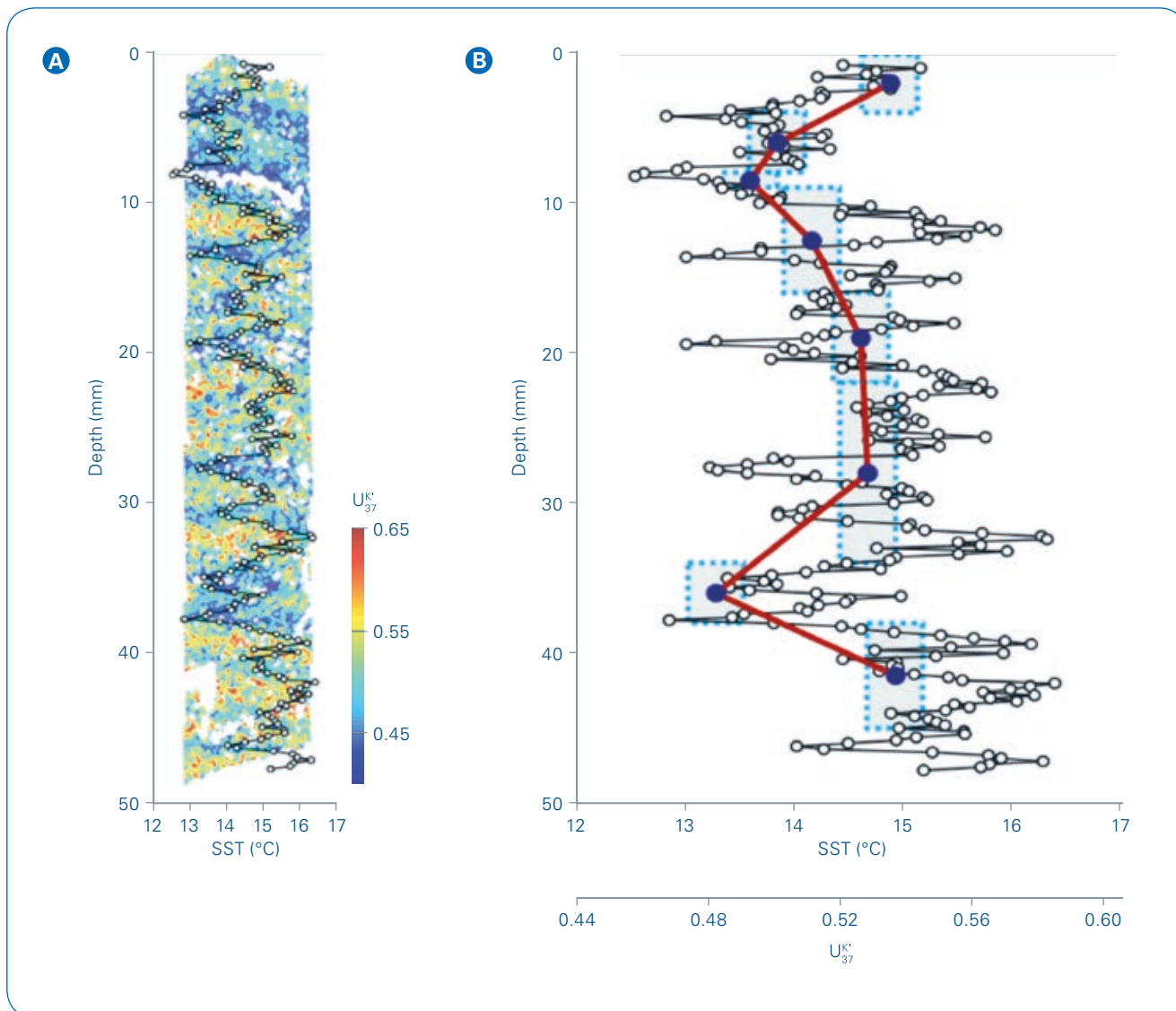


Figure 4: (A) Distribution of U_{37}^K corrected for inclined lamination and overlaid with 200 μm resolution averaged profile. (B) Comparison of conventional, extraction-based U_{37}^K values (blue dots, red line) with MALDI-MRMS-derived high-resolution profile. Dotted rectangles indicate sample amount used for extraction.

Data processing

The alkenone mass range of the calibrated profile spectra for each spot position were exported and further evaluated with Matlab R2016a (Natick, MA: The MathWorks Inc.). Proxy data of each individual spot were calculated using the intensities of the di- and tri-unsaturated C_{37} alkenones as Na^+ -adducts identified by accurate m/z values. To assess information of the proxy-derived recon-

structed temperature over time, the mapped data were averaged along each individual horizontal line resulting in a 200 μm spatial resolution profile. The goal was to pool data from coeval horizons, therefore correction for tilting or disturbance of laminae were required. In the present case, a simple correction for tilting was applied.

The alkenone unsaturation index U_{37}^K was calculated from the absolute

intensities of the detected $\text{C}_{37:2}$ and $\text{C}_{37:3}$ alkenones (Figure 2). In the SBB, these long-chain alkenones are produced, i.a., by the coccolithophore *Gephyrocapsa oceanica* (Figure 3). U_{37}^K is defined as described by Prahl et al. [2] with the transformation into SST according to Müller et al. [6].

Results

In total an area consisting of 9525 spots was measured with MALDI MRMS. Successful ionization of both alkenones defining the U_{37}^K index was achieved in 8759 spectra, resulting in a success rate of ~92%. Taking into account the small cracks in the sediment slice, it can be assumed that these biomarkers can be detected throughout the sediment. Alkenones predominantly ionized as Na^+ -adducts and successful ionization was achieved without the addition of artificial matrices, such as dihydroxy benzoic acid (DHB).

The visualization of the U_{37}^K reveals the alternating seasonal deposition of the sediment in the Santa Barbara Basin, i.e., colder SST during winter/

spring represented by lower U_{37}^K , and warm water temperatures in summer/autumn archived by higher U_{37}^K values (Figure 4A). This annual change of SST becomes also visible in the averaged 200 μm resolution downcore profile with reconstructed temperatures ranging from 12.5 to 16.4°C (Figure 4B).

The comparison of the 200 μm resolution MALDI-based analysis to the extraction-based approach shows an overall strong correspondence suggesting that no systematic bias is produced due to the different ionization. Additionally, this overlay emphasizes the strong advantage of the much higher spatial resolution produced by molecular imaging and consequently reveals the loss of information due to extraction-based analysis (Figure 4B).

Conclusion

- Molecular Imaging by MRMS reveals the so far undetectable small-scale distribution of organic geochemical proxies archived in marine sediments.
- Molecular imaging by MRMS paves the way for paleoclimate reconstruction at previous inaccessible resolution.



Learn More

You are looking for further Information?
Check out the link or scan the QR code for more details.

www.bruker.com/solarix



References

- [1] Brassell SC, Eglinton G, Marlowe IT, Pflaumann U, Sarnthein M (1986). *Molecular stratigraphy: a new tool for climatic assessment*. Nature **320** (6058), 129–133. DOI: 10.1038/320129a0
- [2] Prahl FG, Wakeham SG (1987). *Calibration of unsaturation patterns in long-chain ketone compositions for palaeotemperature assessment*. Nature **330** (6146), 367–369. DOI: 10.1038/330367a0
- [3] Alfken S, Wörmer L, Lipp JS, Wendt J, Taubner H, Schimmelmann A, Hinrichs K-U (2019). *Micrometer scale imaging of sedimentary climate archives—Sample preparation for combined elemental and lipid biomarker analysis*. Organic Geochemistry **127**, 81–91. DOI: 10.1016/j.orggeochem.2018.11.002
- [4] Wörmer L, Wendt J, Alfken S, Wang J-X, Elvert M, Heuer VB, Hinrichs K-U (2019). *Towards multiproxy, ultra-high resolution molecular stratigraphy: Enabling laser-induced mass spectrometry imaging of diverse molecular biomarkers in sediments*. Organic Geochemistry **127**, 136–145. DOI: 10.1016/j.orggeochem.2018.11.009
- [5] Sturt HF, Summons RE, Smith K, Elvert M, Hinrichs K-U (2004). *Intact polar membrane lipids in prokaryotes and sediments deciphered by high-performance liquid chromatography/electrospray ionization multistage mass spectrometry—new biomarkers for biogeochemistry and microbial ecology*. Rapid Communications in Mass Spectrometry **18** (6), 617–628. DOI: 10.1002/rcm.1378
- [6] Müller PJ, Kirst G, Ruhland G, Storch I von, Rosell-Melé A (1998). *Calibration of the alkenone paleotemperature index U_{37}^K based on core-tops from the eastern South Atlantic and the global ocean (60° N–60° S)*. Geochimica et Cosmochimica Acta **62** (10), 1757–1772. DOI: 10.1016/S0016-7037(98)00097-0

For Research Use Only. Not for Use in Clinical Diagnostic Procedures.



● Designer drug analysis by forensic MALDI techniques

The versatility of MRMS for forensic analysis.

Abstract

The phenethylamines derivatives, known as NBOMes, N-bomb or Smiles, are potent hallucinogens, which are often sold as blotter paper. Herein, matrix-assisted laser desorption/ionization mass spectrometry (MALDI MS) and MALDI mass spectrometry imaging (MALDI Imaging) were coupled to a Magnetic Resonance Mass Spectrometer (MRMS, classically known as FT-ICR MS), a high mass accuracy, high resolu-

tion mass spectrometer, and used to analyze seven blotter papers of NBOMes containing 25I-NBOH (m/z 414) and 25I-NBOMe (m/z 428).

Introduction

The term designer drug refers to a synthetic version of an illicit drug modified to potentialize or create new psychoactive effects. Some of the new psychoactive substances (NPS) are often sold impregnated on blotter paper,

where each small square is sold as a dose. They have colorful images printed on its surface, as shown in Figure 1 and are administered sublingually.

Mass spectrometry (MS) has been widely used in forensic investigations of NPS, being extremely versatile, due to the fact that it allows the use of different sources of ionization such as paper spray, direct sample analysis (DSA), electrospray ionization (ESI), desorption atmospheric

Keywords:
NBOMes, MALDI
Imaging, MRMS

Authors: Camila M. de Almeida¹, Wanderson Romão^{1,2,3};

¹Laboratório de Petroleômica e Forense, Universidade Federal do Espírito Santo (UFES), Avenida Fernando Ferrari, 514, Goiabeiras, Vitória, ES, CEP: 29075-910, Brazil; ²Instituto Nacional de Ciência e Tecnologia Forense (INCT Forense), Brazil; ³Instituto Federal do Espírito Santo (IFES), Av. Ministro Salgado Filho, Soteco, Vila Velha, 29106-010, Espírito Santo, Brazil.

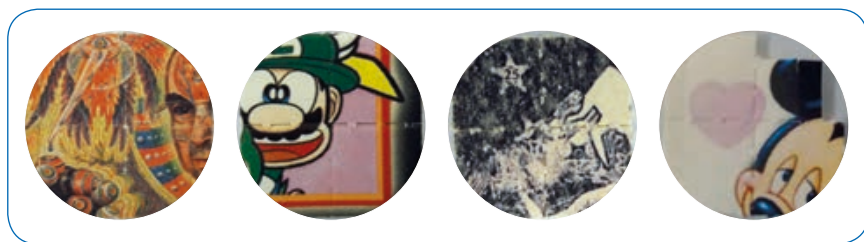


Figure 1: Blotter papers containing illicit substances.

pressure photoionization (DAPPI), easy ambient sonic-spray ionization (EASI) and matrix-assisted laser desorption/ionization (MALDI). Among the cited methods, MALDI MS can be considered a rapid analysis strategy for the identification of NPS as well as their metabolites. In the forensic context, mass spectrometry imaging has been used to investigate the chemical distribution on a surface of interest, mainly in the detection of drugs in hair, tissues, blood and fingerprints present on banknotes. The main challenge of the MALDI Imaging technique lies in the sample preparation, being the choice of the organic matrix, which is used in the desorption and ionization process of the analyte of interest, a crucial step in sample preparation that can have a significant effect on the outcome results of an imaging experiment.

In this study, analysis of blotter papers containing NBOMes was explored using the laser desorption ionization (LDI), MALDI and MALDI Imaging techniques combined with Magnetic Resonance Mass Spectrometry (MRMS), classically known as Fourier transform ion cyclotron resonance mass spectrometry (FT-ICR MS).

Experimental

Seven blotter papers were supplied by the Civil Police of the State of Espírito Santo (PC-ES), Brazil. They were cut and fixed on a stainless steel plate with the aid of double-sided tape. Matrix application was

evaluated, being performed in two ways: (i) small volumes (15 μ L) of matrix was directly spotted onto the surface of the blotter paper using an automatic pipette (Transferpette[®]); and (ii) with a sprayer assisted by an ESI probe (Bruker Daltonics, Bremen, Germany). In both cases, the process was optimized using the CHCA matrix at a concentration of 25 mg/mL. After optimization of the matrix application method, the ionization efficiency was evaluated in function of the four matrices studied (DHB), CHCA, sinapinic acid (SA and (TCNQ)) and their respective concentrations (from 5 to 25 mg/mL).

The LDI, MALDI and MALDI Imaging analyses were performed on a 9.4 T Solarix mass spectrometer (Bruker Daltonics, Bremen, Germany), equipped with a smart beam-II[™] laser (355 nm) and MALDI source. All analyses were performed in positive ionization mode in a spectral range between m/z 200 and 1500, and each analysis was the result of 100 laser shots per pixel, with laser focus setting small ($\sim 30 \mu$ m), laser frequency of 200 Hz and laser power of 33%. The LDI and MALDI images were acquired in a spatial resolution of 300 μ m and processed with FlexImaging 3.0 software (Bruker Scientific LLC).

Results and Discussion

LDI-MS analysis

Initially, blotter papers, samples S1-S7, seized by PC-ES, were analyzed by LDI-MS, and their respective

spectra are observed in Figures 2A-G. Blotter papers exhibited a similar spectral profile, with detection mainly of 25I-NBOMe (in samples S1-S6, Figures 2 A-F), that has m/z 428.07208 and 450.05406 (in protonated form, $[C_{18}H_{22}INO_3 + H]^+$, and as a sodium adduct $[C_{18}H_{22}INO_3 + Na]^+$, respectively) with mass errors of less than 2 ppm. The 25I-NBOH molecule, $[C_{17}H_{20}INO_3 + H]^+$, $[C_{17}H_{20}INO_3 + Na]^+$ and $[C_{17}H_{20}INO_3 + K]^+$ ions, of m/z 414.05731, 436.03944 and 452.01346, and error = 3.02, 3.28 and 3.36 ppm, respectively, on the other hand, was detected only on the blotter paper S7, Figure 2G.

MALDI MS and MALDI Imaging analyses

A crucial step in the sample preparation for a MALDI Imaging experiment is the application of the matrix, which must be deposited as a homogeneous layer on the surface of the sample, maintaining the natural arrangement of the analytes in the sample.

In the images generated by MALDI Imaging (Figure 3 A-C), the application of the matrix with sprayer assisted by an ESI probe proved to be more efficient in the ionization of ion of m/z 414 (Figure 3C), detecting a higher signal intensity of the compound of interest on the blotter paper surface when compared to the automatic pipette method (Figure 3B) as well as the LDI-MS technique, i.e., without the use of matrix (Figure 3A). Besides, a higher sensitivity, measured by the TIC values for the ion of m/z 414, was observed using the matrix sprayer in the MALDI mass spectrum (Figure 3F), which presented a higher value of TIC (8.0×10^7). This behavior indicates that the matrix sprayer had a higher ionization power when compared to the mass spectra obtained by

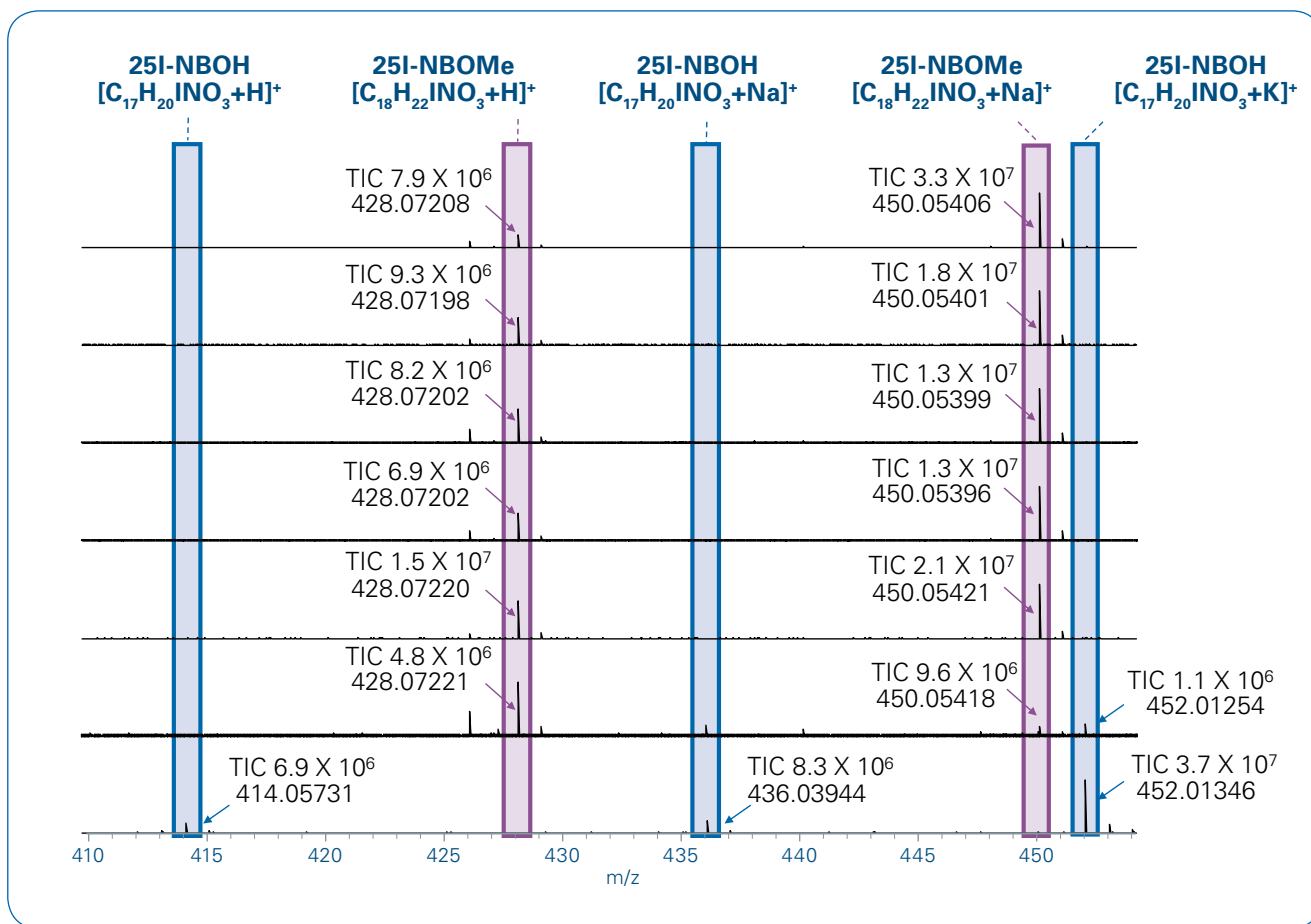


Figure 2: LDI mass spectra of seven blotter papers showing the presence of designer drugs: (A)-(F) 25I-NBOMe detected as $[C_{18}H_{22}INO_3 + H]^+$ and $[C_{18}H_{22}INO_3 + Na]^+$ ions at m/z 428 and 450, respectively, and (G) 25I-NBOH, detected as $[C_{17}H_{20}INO_3 + H]^+$, $[C_{17}H_{20}INO_3 + Na]^+$ and $[C_{17}H_{20}INO_3 + K]^+$ ions at m/z 414, 436 and 452, respectively.

the automatic pipette (TIC 5.7×10^7 , Figure 3E) and without the use of the matrix, which use is necessary to facilitate the ionization of the ion of interest (m/z 414) and decrease the suppression caused by the paper signal, m/z 575.07841 (TIC 3.0×10^7 , Figure 3D). One of the reasons for this efficiency may be related to the small droplets uniformly formed by the matrix on the surface of the sample during the process of deposition by the matrix sprayer.

To evaluate the best matrix and their concentration in the distribution study of 25I-NBOMe hallucinogen, m/z 428, the spatial distribution of this ion was measured on the surface of

the blotter paper by MALDI Imaging from the individual deposition of four matrices: DHB, CHCA, SA and TCNQ, in the concentrations of 5, 10, 15, 20 and 25 mg/mL in small pieces (0.2 x 0.5 cm) of sample S5, Figure 4 A-D. The matrices were applied with the matrix sprayer.

The CHCA matrix showed to be more efficient in the ionization of 25I-NBOMe (Figure 4D), evidenced by the higher abundance and uniform distribution of the compound on the surface of the blotter paper, especially at concentrations higher than 10 mg/mL. This higher efficiency in the ionization of 25I-NBOMe, provided using the CHCA matrix, may be

related to the interactions of the matrix with the analyte through hydrogen bonds. The CHCA matrix is generally applied in the ionization of compounds of lower m/z values, also commonly used in forensic analysis.

Ionization studies of psychoactive compounds intentionally added to absorption papers, which are illegally commercialized and seized by the local police, had their spatial distributions evaluated by MALDI Imaging methodology, that contemplated tests of matrix reagent application forms, varying their concentrations and chemical structures (four matrices were evaluated).

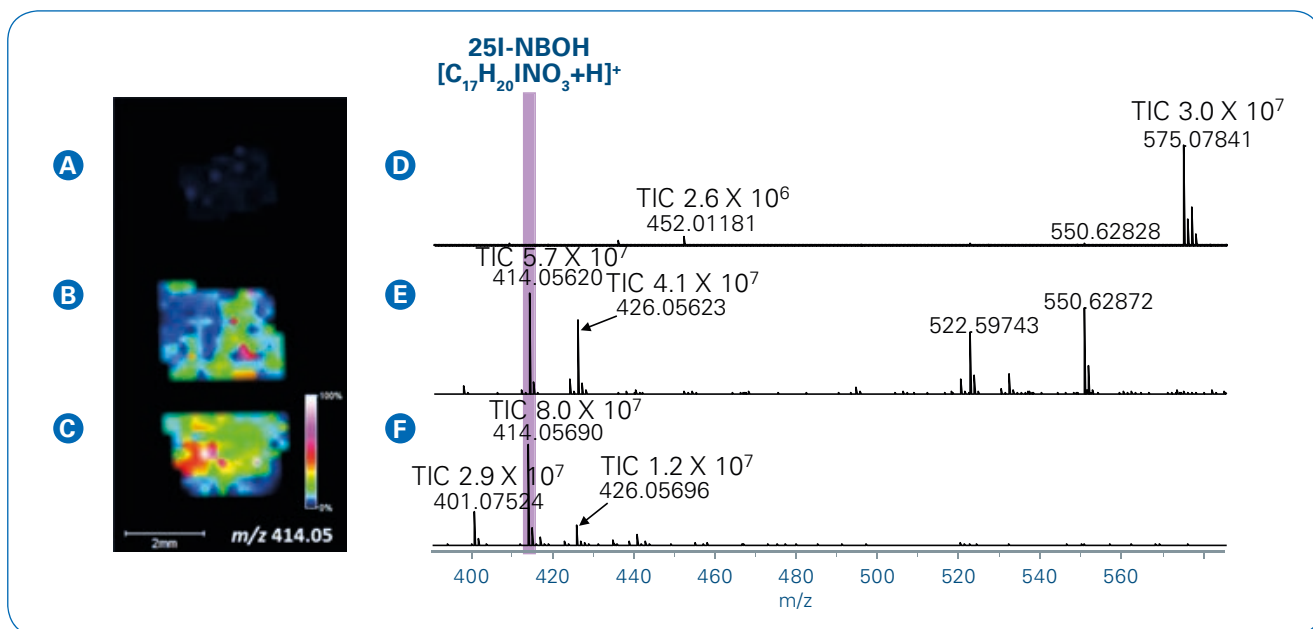


Figure 3: MS images showing the distribution of 25I-NBOH molecule at m/z 414 on the surface of sample S7: using **(A)** LDI, and **(B-C)** MALDI, **(B)** with CHCA matrix applied via automatic pipette and **(C)** with a sprayer assisted by an ESI probe. LDI **(D)** and MALDI **(E-F)** mass spectra of their respective MS images, Figure **(A)** and **(B-C)**, respectively.

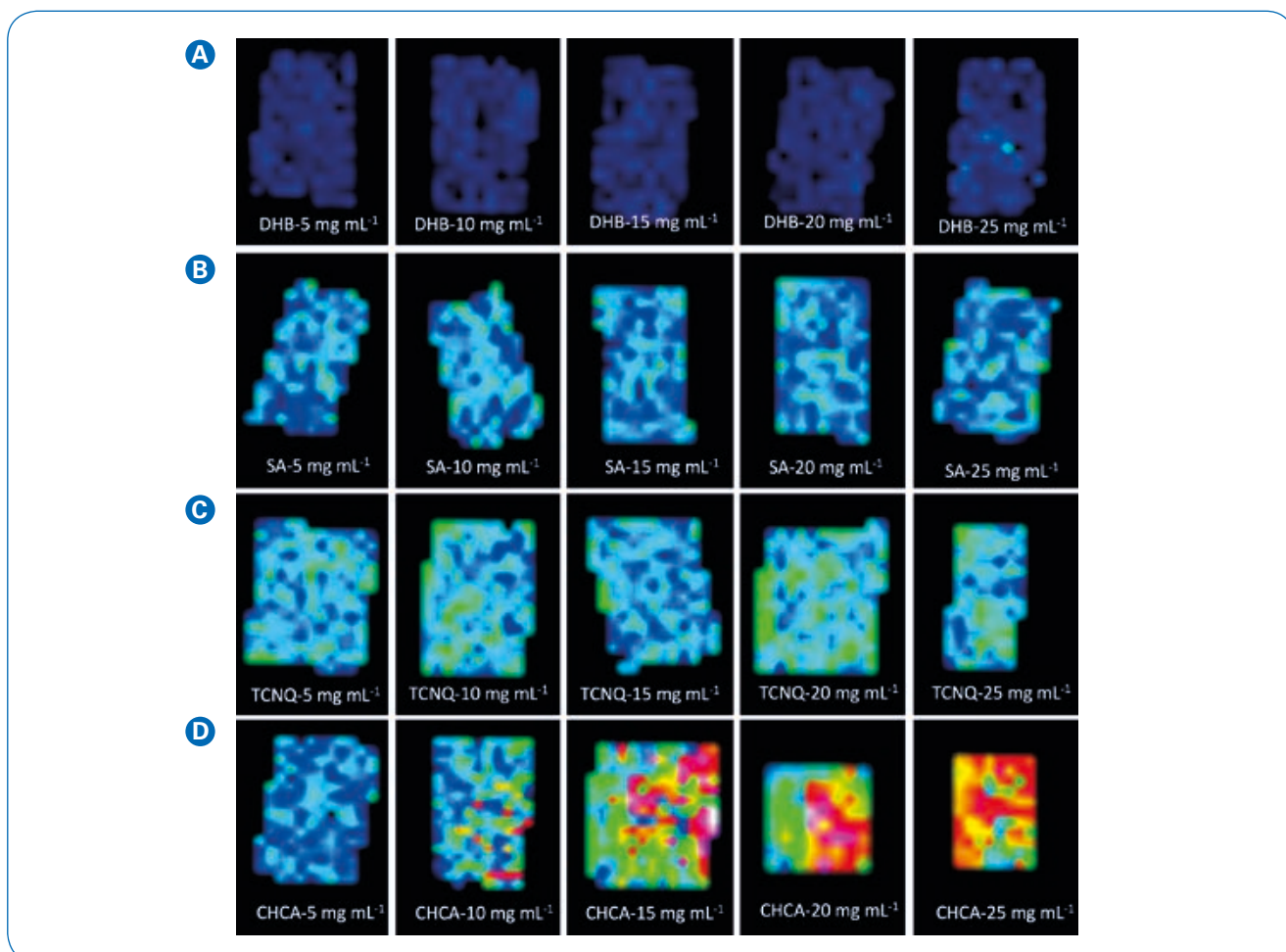


Figure 4: Positive MALDI MS images showing the distribution of 25I-NBOMe at m/z 428 on the surface of sample S5 coated with four different matrices: **(A)** DHB, **(B)** SA, **(C)** TCNQ and **(D)** CHCA in different concentrations (from 5 to 25 mg/mL).

Conclusions

- The initial characterization by the LDI-MS technique in the analysis of blotter papers seized by PC-ES provided the identification of the psychoactive compounds 25I-NBOH and 25I-NBOMe, having m/z values of 414 Da and 428 Da, respectively, and mass accuracy lower than 4 ppm. The experiments of MALDI MS and MALDI Imaging were optimized, where among the application forms studied, the matrix sprayer showed to be the best method, compared to the use of the automatic pipette, providing a greater surface homogeneity, resulting in the detection of the monitored ions with more excellent uniformity

and intensity. In the evaluation of the best matrix and concentration, the CHCA, in concentrations higher than 10 mg/mL, were more efficient in the ionization of compound 25I-NBOMe in comparison to the other matrices evaluated, presenting a uniform distribution of the drug throughout the blotter paper surface. These results have demonstrated the higher analytical power provided by the analyses of the MRMS due to its ability of determination of the elemental composition ($C_cH_hN_nO_o$) of the drugs compounds with high accuracy and resolving power.



Learn More

You are looking for further Information?
Check out the link or scan the QR code for more details.

www.bruker.com/solarix



This Application Note is a condensed and revised version of the Microchemical Journal article "Designer drugs analysis by LDI(+), MALDI(+) and MALDI(+) imaging coupled to FT-ICR MS".

References

- [1] Almeida CM, Pinto FE, Santos NA, Souza LM, Merlo BB, Thompson CJ, Romão W (2019) *Designer drugs analysis by LDI(+), MALDI(+) and MALDI(+) imaging coupled to FT-ICR MS*. *MicroChemical Journal*, **149**, 104002. <https://doi.org/10.1016/j.microc.2019.104002>.
- [2] See references within.

For Research Use Only. Not for Use in Clinical Diagnostic Procedures.



● Interrogation of the Spatial Metabolome of *Ginkgo biloba* with high-resolution MALDI and LDI Mass Spectrometry Imaging

MALDI Imaging was used to unravel distinct spatial metabolomics in leaf cross sections.

Introduction

Ginkgo biloba is the only extant species in the division Ginkgo-phyte, and so is called a "living fossil". Leaves of the *Ginkgo biloba* are a rich resource for bioactive products for treatment of diseases associated with peripheral circulation, memory dysfunction, etc. Numerous

modern techniques have been used to study *Ginkgo biloba*, trying to profile metabolites to help understand biosynthesis pathways from the ginkgo plant; ex., gas chromatography (GC), liquid chromatography (LC), capillary electrophoresis (CE), GC/LC coupled mass spectrometry (MS), and nuclear magnetic resonance (NMR) [1]. However,

little is known about the distribution of various types of metabolites due to tissue homogenization. There are at least ten basic tissue types and more than 15 cell types [2] that are heterogeneously distributed in the plant. Current plant imaging techniques, such as light or electron microscopy, have been used to study the distribution of chemical

Keywords:
MALDI Imaging, Lipid, MALDI-TOF, MRMS, Solarix, ultrafleXtreme, plant metabolites

Authors: Bin Li^{1,2}, Elizabeth K. Neumann², Ping Li¹, Jonathan V. Sweedler²;

¹School of Traditional Chinese Pharmacy, China Pharmaceutical University, Nanjing, 211198, China; ²Department of Chemistry and Beckman Institute for Advanced Science and Technology, University of Illinois at Urbana-Champaign, Urbana, Illinois, 61801, USA.

components in plant tissues, but these approaches require molecular labels and are ineffective at mapping unlabeled compounds.

MALDI imaging has been extensively used for imaging of proteins, peptides, lipids and metabolites with no labeling required[3]. In this study, adapted from our recent article in Plant, Cell and Environment [4], we have used two MALDI platforms to map constituent compounds in *Ginkgo biloba*: the ultrafleXtreme MALDI-TOF/TOF and solariX MRMS. The faster ultrafleXtreme was used as a screening tool to optimize the matrix, detection mass range, spatial resolution, etc. The solariX MRMS offers greater molecular specificity and was used to collect ginkgo leaf images and representative spectra from various ginkgo cross leaf sections. Numerous species including flavonoid aglycones, bi-flavonoids, flavonoid glycosides, biginkgosides, ginkgolides etc. were visualized in ginkgo leaf for the first time. High

mass accuracy and in situ MSMS measurements were used to identify metabolites.

Materials and Methods

Chemicals and plant samples

Formic acid, acetonitrile, trifluoroacetic acid (TFA), water (all LCMS grade) 2,5-dihydroxybenzoic acid (DHB), α -cyano-4-hydroxycinnamic acid (CHCA) and 9-aminoacridine (9-AA) were purchased from Sigma-Aldrich (St. Louis, MO, USA). *Ginkgo biloba* leaves were collected from the arboretum at the University of Illinois at Urbana-Champaign, USA.

Sample preparation for MALDI imaging

Fresh *Ginkgo biloba* leaves were immediately embedded in 10% gelatin (W/V) solutions. Tissues kept in the molds were transferred to a -80°C

freezer for 30 min before sectioning using a cryostat (Leica, Germany) with deionized water as the adhesive. 16- μ m thick tissues were obtained at -20°C and mounted on indium tin oxide (ITO)-coated glass slides, followed by a 10 min dehydration process using a vacuum desiccator. A Zeiss Axio M2 microscope (Zeiss, Germany) was used to obtain optical images of the sections.

Wet spraying

A home-built matrix application system was used to apply matrix by aerosol[5]. Briefly, 50 mg/mL DHB or 15 mg/mL CHCA dissolved in ACN: Water (0.1% TFA) (7:3, V/V) was applied for the positive ion mode MALDI experiments. For negative ion mode MALDI, 10 mg/mL 9-AA dissolved in methanol: water (9:1, V/V) was applied.

Dry spraying

Additionally, DHB was sublimed using a home-built apparatus.

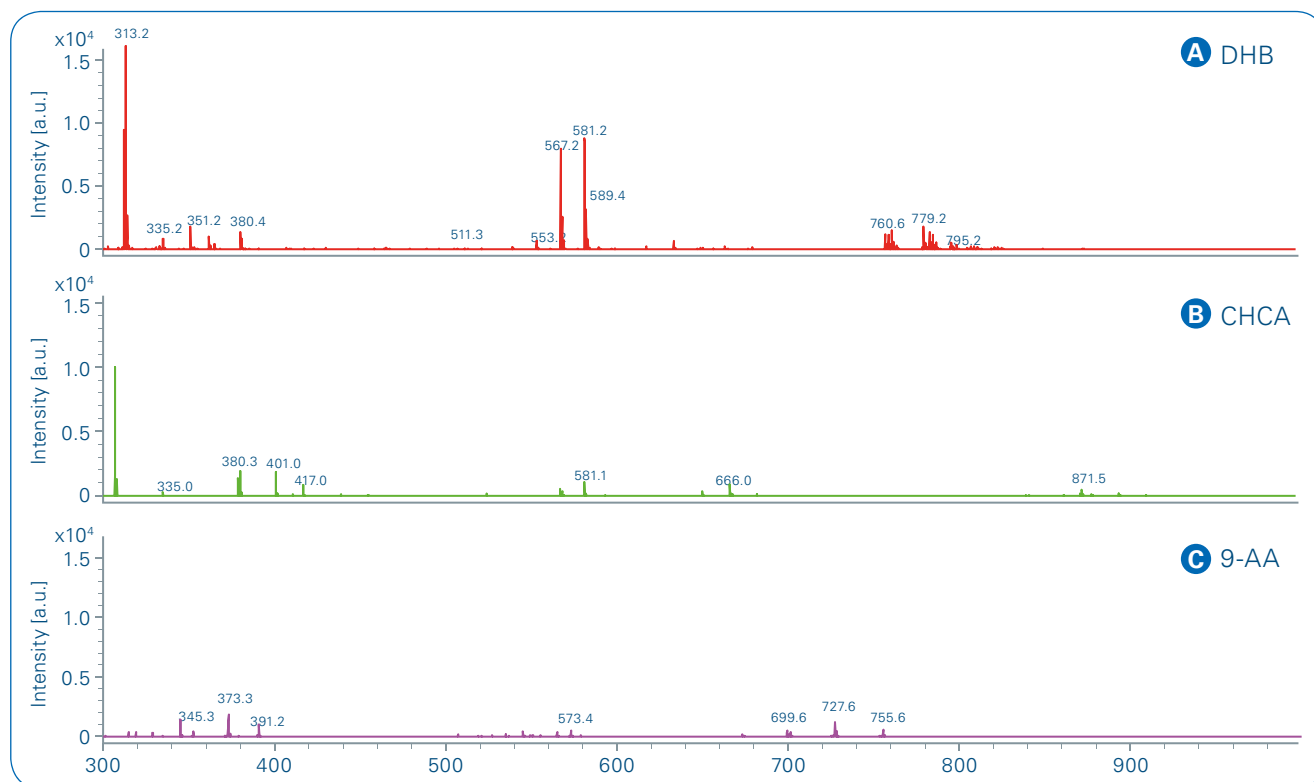


Figure 1: Matrix optimization. Representative single-pixel MALDI-TOF mass spectra acquired from a cross section of ginkgo leaf. (A) Positive ion mode with DHB as matrix. (B) Positive ion mode with CHCA as matrix. (C) Negative ion mode with 9-AA as matrix

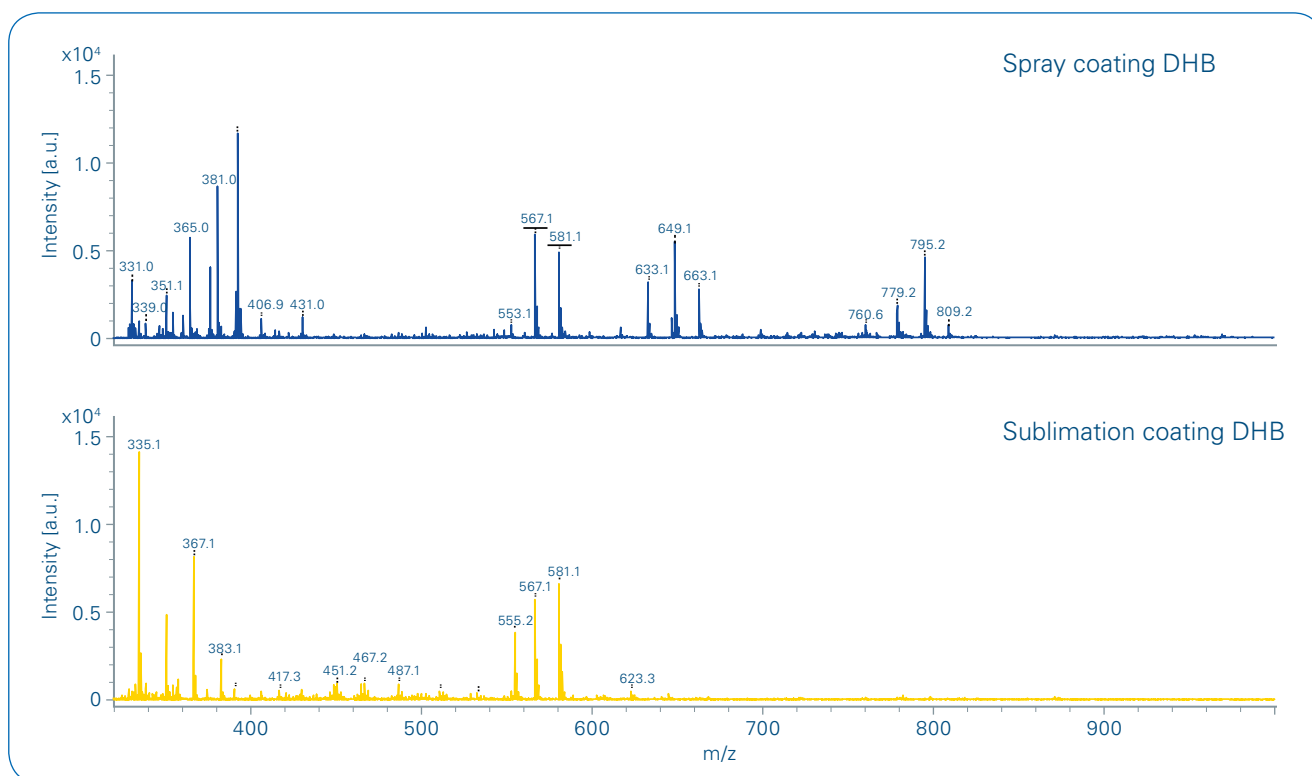


Figure 2: Matrix coating comparison between spray (wet) coating or sublimation (dry) coating

MALDI imaging instrumentation

MALDI imaging was performed using a 7T solariX MRMS mass spectrometer (Bruker Daltonik, Germany) equipped with a dual ESI/MALDI source and a Smartbeam II laser. An m/z range of 150–2000 was acquired with single-scan spectra consisting of 100 accumulated “Small” laser shots at 1 kHz. MALDI images were acquired at a 50 μm pitch.

An ultrafleXtreme MALDI TOF/TOF mass spectrometer was used to optimize the matrix selection and experimental design in MS and MS/MS mode. Data were analyzed using flexAnalysis 3.4, and Data Analysis 4.0. flexImaging 4.1 was used to produce a peak list linked to 2D tissue maps for visualization. (Bruker Daltonik, Germany).

Results

To choose the best matrix to detect metabolites in ginkgo leaves, three

matrices (DHB and CHCA for positive ion mode, and 9-AA for negative ion mode) were tested on tissue using the ultrafleXtreme and wet spraying technique. The total average spectra are shown in Figure 1. Figure 1a spectrum has the most signals, which were identified as biflavonoids, flavonoid glycosides, and lipids (data not shown). Therefore, DHB was selected for analyzing ginkgo leaf sections in positive ion mode.

Next, the two coating systems (wet and dry spraying) were also compared to determine which one produces the optimized signal intensity and most analyte signals, as well as the lowest metabolite delocalization. In Figure 2, more ion signals were detected using the wet spraying system than sublimation with DHB matrix in positive ion mode using the ultrafleXtreme. Most of the ion signals were later identified as biflavonoid-associated ions based on accurate mass using the solariX MALDI-MRMS and/or MALDI TOF/

TOF using the ultrafleXtreme (data not shown). Based on these observations, the wet spraying preparation using the home-built sprayer was used to collect all imaging data from leaf sections.

After the experimental conditions were optimized, the solariX was used to collect single pixel spectra from various leaf cross sections. In addition to delivering much higher mass resolving power, the MRMS ion source produces less interference from matrix ions in the lower molecular mass range. An optical image of one of the *Ginkgo biloba* sections analyzed is shown in Figure 3. Representative spectra in positive and negative ion modes taken from various locations on leaf sections from the upper epidermis, mesophyll and secretory cavity are shown in Figure 4. Compounds were identified based on accurate sub ppm mass accuracy. Flavonoid glycosides (Figure 4a) were easily resolved from the upper

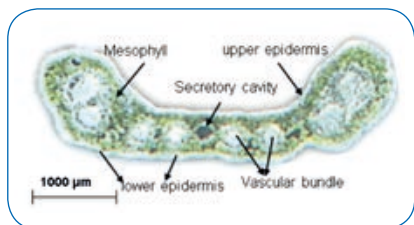


Figure 3: Optical images of Ginkgo biloba leaf

epidermis surface in protonated ions as well as in sodium- and potassium-adduct ions. Relatively large molecules were also detected at about m/z 1500 Da from the upper epidermis and these were identified as dimers of flavonoid aglycones in potassium ion form (Figure 4b). LDI was also

explored to detect UV-absorbing flavonoid aglycones in negative mode. Three pairs of flavonoid aglycone peaks were able to be observed from the upper epidermis at ~ 1 Da apart, ex., m/z 284.0331 and 285.0409, m/z 300.0279 and 301.0359, m/z 314.0437 and 315.0517 (Figure 4c).

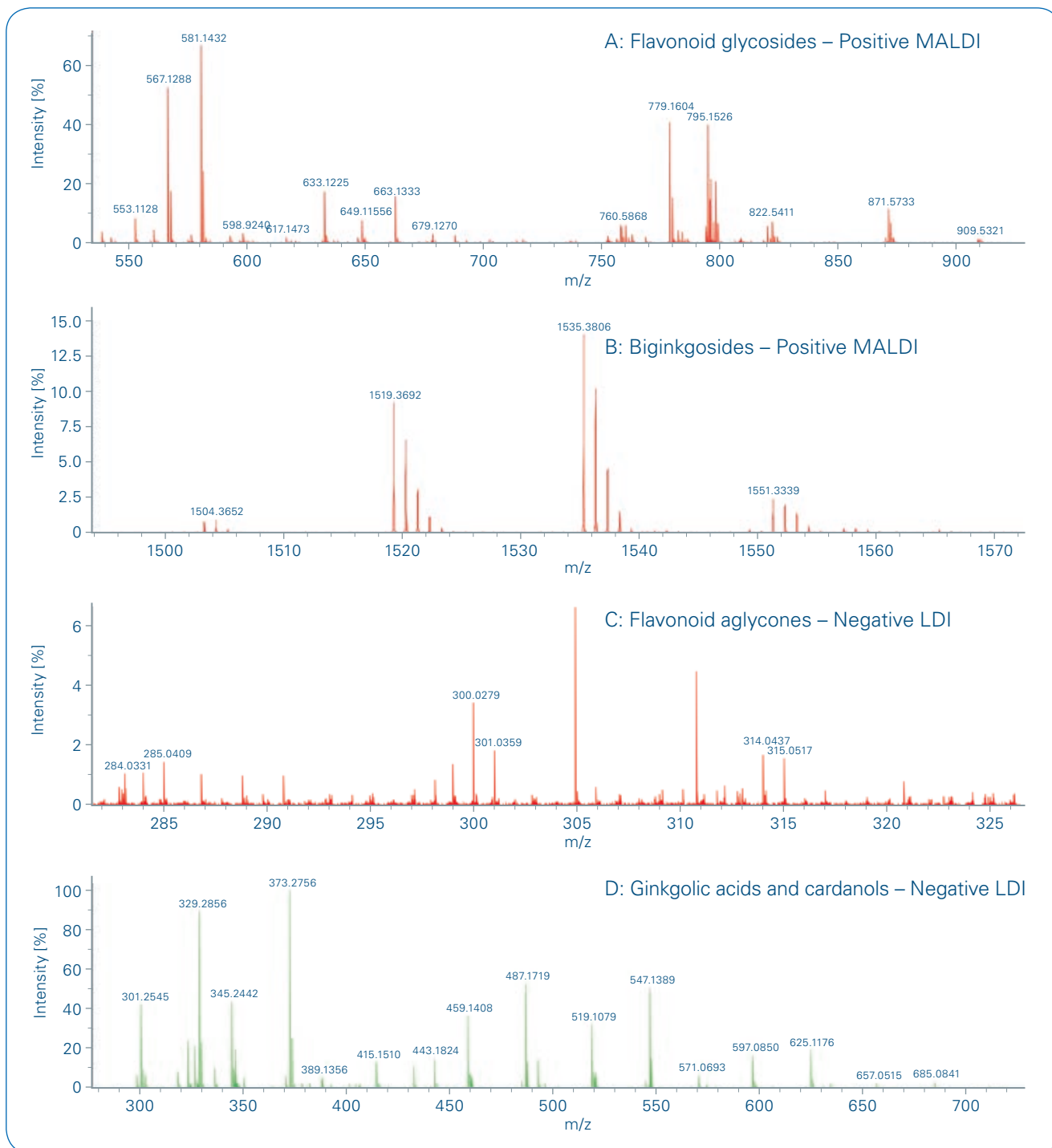


Figure 4: Representative single-pixel MALDI/LDI mass spectra. Identified compounds are labeled with measured mass

These were identified as deprotonated ions [M-H]⁻ and radical product ions [M-H-H]^{-•} due to the presence of a free 4'-OH group on the B-ring of some aglycones. A negative ion mode LDI mass spectrum of ginkgolic acids and cardanols obtained from the secretory cavity is shown in Figure 4d.

MALDI-TOF imaging technology has been used to reveal heterogeneous

distribution of metabolites in the ginkgo leaf. In Figure 5 several ion images (including flavonoid aglycones, bi-flavonoids, flavonoid glycosides, and biginkgosides) with different localizations were visualized using the flexImaging software. The majority of ions mainly accumulated in the upper and lower epidermis. Notably, flavonoids have only been reported very recently due to their

low abundance in plants. The reason is because typical LCMS needs to homogenize whole samples, and therefore, these compounds are usually not detected due to their low amounts in mixtures. MALDI imaging is well suited for acquiring very localized distributions from plant sections or other materials. Also observed in Figure 5, several ions were found to be localized in higher abundance on the upper epidermis than the lower side, such as *m/z* 1551.34 and *m/z* 1535.35 (biginkgosides). The data is consistent with the heterogeneous distribution of chalcone synthase bioactivity (a key enzyme in flavonoid biosynthesis), which is mainly present in the upper epidermis. Some phos-phocholines (PCs) were detected in mesophyll layers and secretory cavities (ex., *m/z* 796.52); these lipid-associated compounds have been reported to act as second messengers in plant cells [6] and were observed mainly in secretory cavities.

In this study, we have demonstrated the use of MALDI imaging technology to visualize metabolites in leaf cross sections.

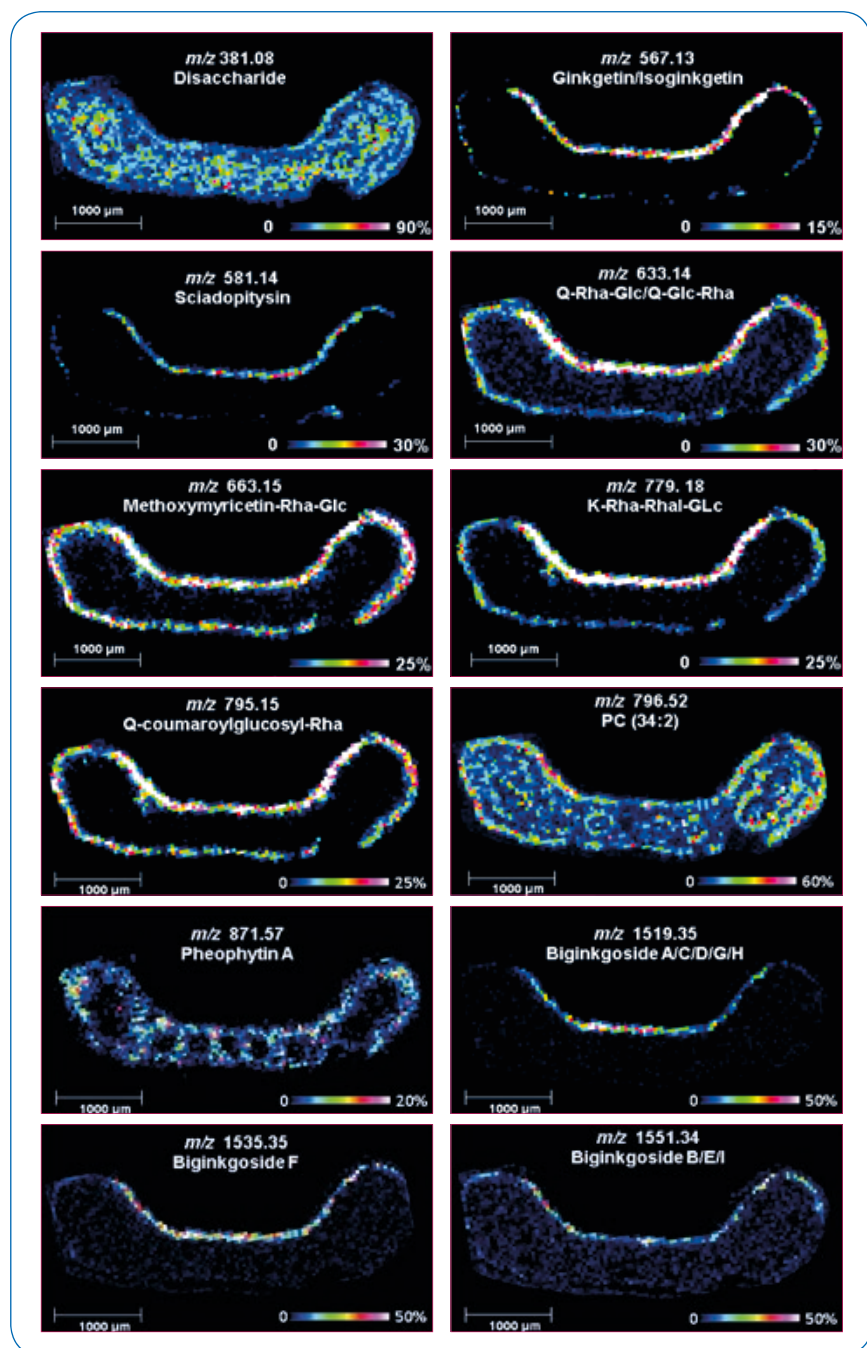


Figure 5: MALDI images of selected ions including flavonoid aglycones, biflavonoid, flavonoid glycosides, etc.

Conclusions

- MALDI Imaging is shown to be a powerful tool to visualize ginkgo leaf metabolites for the first time.
- These ion images could improve the understanding of the distinct functions of individual species, and their biofunctions in plant growth and development, as well as abiotic and biotic stress response.



Learn More

You are looking for further Information?
Check out the link or scan the QR code for more details.

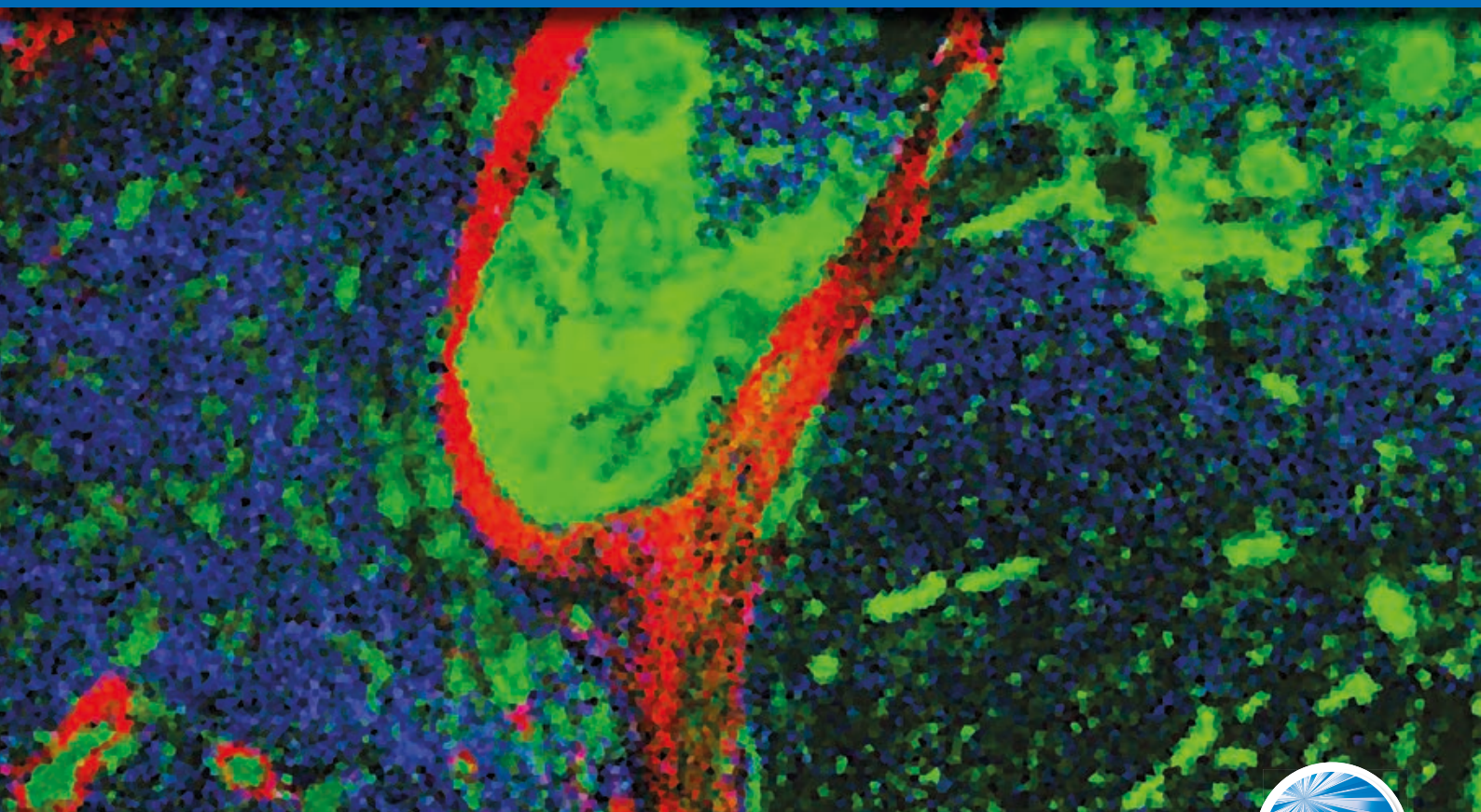
www.bruker.com/solarix



References

- [1] van Beek TA (2002). *Chemical analysis of Ginkgo biloba leaves and extracts*. Journal of Chromatography A, **967**, 21–55.
- [2] Goldberg RB (1988). *Plants: Novel developmental processes*. Science, **240**, 1460–1467.
- [3] Cornett DS, Reyzer ML, Chaurand P, Caprioli RM (2007). *MALDI imaging mass spectrometry: molecular snapshots of biochemical systems*. Nature Methods, **4**, 828–833.
- [4] Li B, Neumann EK, Ge J, Gao W, Yang H, Li P, Sweedler JV (2018). *Interrogation of spatial metabolome of Ginkgo biloba with high-resolution matrix-assisted laser desorption/ionization and laser desorption/ionization mass spectrometry imaging*. Plant, Cell and Environment, **41**, 2693.
- [5] Li B, Comi TJ, Si T, Dunham SJB, Sweedler JV (2016). *A onestep matrix application method for MALDI mass spectrometry imaging of bacterial colony biofilms*. Journal of Mass Spectrometry, **51**, 1030–1035.
- [6] Meijer HJG, Munnik T (2003). *Phospholipid-based signaling in plants*. Annual Review of Plant Biology, **54**, 265–306.

For Research Use Only. Not for Use in Clinical Diagnostic Procedures.



● Integrating Ultra-High Speed MALDI-TOF and MALDI MRMS Imaging For Spatial Proteomics

MALDI imaging is a powerful technology that allows the detection of analytes from tissue while preserving their spatial distribution

Introduction

Cystic fibrosis (CF) is inherited in an autosomal recessive manner, and caused by the presence of mutations in both copies of the gene for the cystic fibrosis transmembrane conductance regulator (CFTR) protein. Patients with CF

present difficulty breathing due to the blockage of airways by thick mucus, as well as bacterial colonization of the lungs [2,3]. Lung tissue from CF patients is highly heterogeneous, giving rise to numerous biologically relevant substructures. A greater understanding of these protein

substructures may lead to a greater understanding of the pathogenesis of CF.

Cancer diagnosis of the kidney have a ~23% mortality rate, with the vast majority being cases of ccRCC [4]. Visual (by CT and MRI) and histological

Keywords:
MALDI-TOF, MRMS,
imaging, rapifleX,
solarix

assessments of tumor margins have proven deficient at the time of surgical removal, leading to disease recurrence [5]. Determining molecular localization patterns in and around the tumor would aid in the determination of its molecular margins [6], aiding in removal of the diseased tissue and prevention of recurrence.

In both of these clinical cases, the ability to locate the presence of diagnostic proteins is of great importance to further understanding of the disease. MALDI imaging of intact proteins is of great relevance for biomedical research, since it provides spatial information of endogenous proteins, as well as their post-translational modifications. Previous work of the Caprioli group has recently shown the use of MALDI Magnetic Resonance Mass Spectrometry (MRMS) imaging to produce ion images of intact proteins [1].

However, intact protein imaging faces a number of inherent challenges related to low throughput, decreased sensitivity at high spatial resolution, and low molecular specificity and identification. Next-generation platforms such as ultra-high speed MALDI-TOF and high mass resolution MALDI MRMS mass spectrometers can overcome these limitations, improving protein acquisition rates by ten-fold, achieving high spatial resolution with high sensitivity, and resolving protein isotopes up to ~20 KDa.

Here we use imaging to examine protein expression in 1) human lung tissue of a patient with CF, and 2) human clear cell renal cell carcinoma, using ultra-high speed MALDI-TOF and MALDI MRMS imaging, respectively.

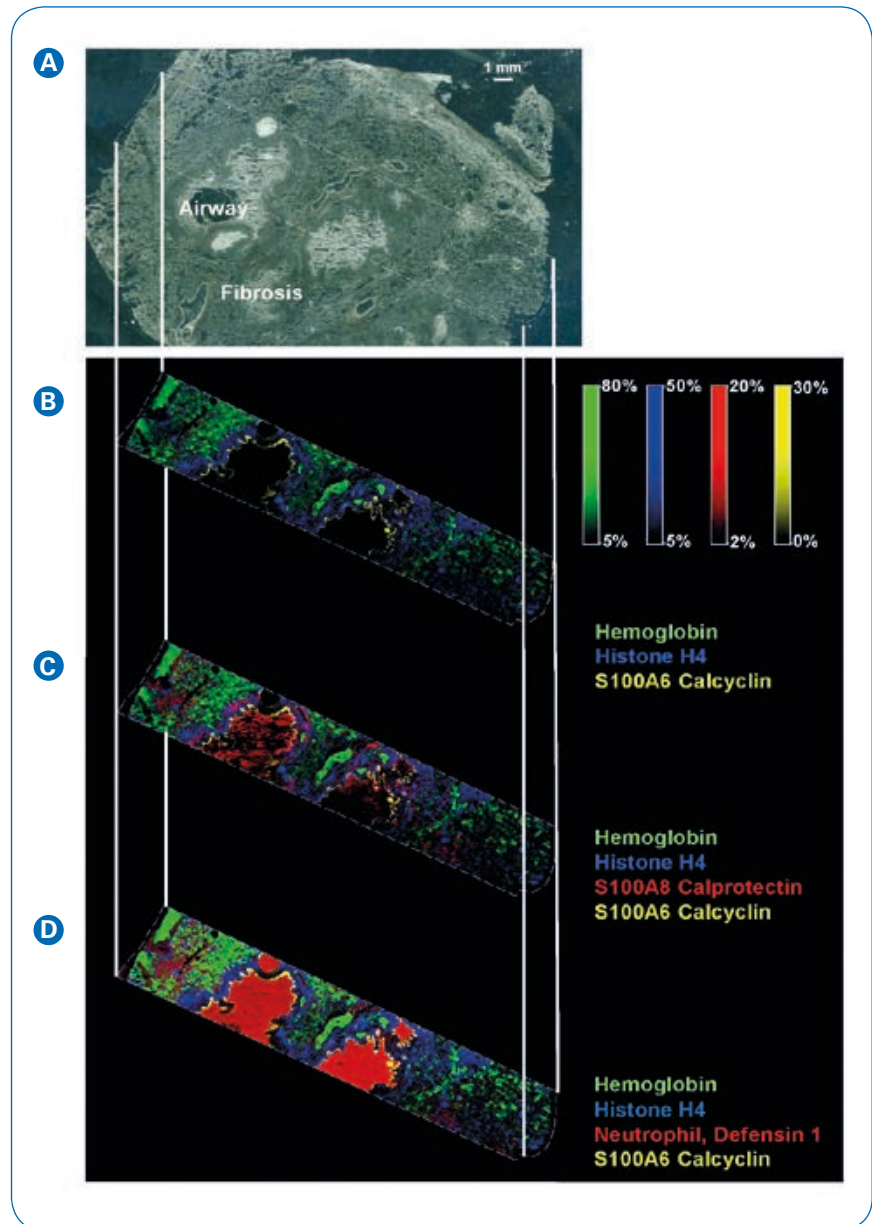


Figure 1. **A** Image of CF human lung with trichome staining prior to IMS acquisition. CF human lung at 30 μ M using the rapifleX MALDI Tissue Imager, on linear positive ion mode. **B** Overlay: m/z 15,125.74 (hemoglobin, green), m/z 11,305.05 (histone H4, blue), m/z 10,095.5 (calcyclin, yellow). **C** Overlay: m/z 15,125.74 (hemoglobin, green), m/z 11,305.05 (histone H4, blue), m/z 10834.93 (S100A8, red), m/z 10,095.5 (calcyclin, yellow). **D** Overlay: m/z 15,125.74 (hemoglobin, green), m/z 11,305.05 (histone H4, blue), m/z 3450 (neutrophil Defensin 1, red), m/z 10,095.5 (calcyclin, yellow). Pixels are beam scanned with a 30 x 30 pixel. 141,000 pixels were acquired in about 1.5 hrs. Scale bar 1 mm.

Imaging Workflow

10 μ m cryosections of human lung or kidney tissue were placed onto conductive ITO coated slides. Tissue was then washed with

70% EtOH for 30 sec, 100% EtOH for 30 sec, Carnoy fluid (6:3:1 EtOH:chloroform: acetic acid) for 2 min, 100% EtOH for 30 sec, H₂O with 0.2% TFA for 30 sec, and 100% EtOH for 30 sec, and stored

at -80°C until IMS analysis. Sections were coated with 4 passes of DHA (15 mg/mL in 9:1 ACN:H₂O) using an HTX TM-Sprayer (HTX Technologies).

For CF lung tissue, images were collected on the rapifleX in positive ion mode with a single-spot laser setting of $\sim 5\ \mu\text{m}$ and a pixel scan size of $30\ \mu\text{m}$ in both x and y axis, over a mass range of m/z 2,000 to 20,000. For kidney tissue, images were collected on the solariX with a small laser setting of $\sim 50\ \mu\text{m}$ and a pixel spacing of $100\ \mu\text{m}$ in both x and y axis, over a mass range of m/z 1,100 to 25,000.

Results

Figure 1A shows a representative image from human lung tissue from a CF patient. Selected protein ion images collected with ultra-high speed MALDI-TOF imaging are shown in Figures 1B-D.

Hemoglobin was detected throughout the tissue while histone H4 and S100A8 (a subunit of calprotectin) were found in abundance in the infected airways. The neutrophil antibacterial peptide Defensin 1 co-localized with the former. Calcyclin usually localizes in cells under mechanical strain. The high

spatial resolution MALDI-TOF imaging data presented in Figure 1 demonstrates the great spatial heterogeneity of the sample.

MALDI MRMS imaging data obtained from human ccRCC tissue is shown in Figure 2. Note the localization of hemoglobin is the highest close to the tumor regions, a direct reflection of significant carcinogenic angiogenesis taking place. Histone H4 was observed to co-localize with calcyclin (S100A6).

Acknowledgements

This Technical Note, including figures and illustrations, was produced by Maria J. Torres, East Carolina Diabetes and Obesity Institute, East Carolina University, based on a consultation with Jessica Moore, co-author of the study published in [7]. Tissue images and MS data were provided courtesy of Jessica Moore, and Jeff Spraggins, Mass Spectrometry Research Center, Department of Chemistry, Vanderbilt University School of Medicine, Nashville, TN, USA.

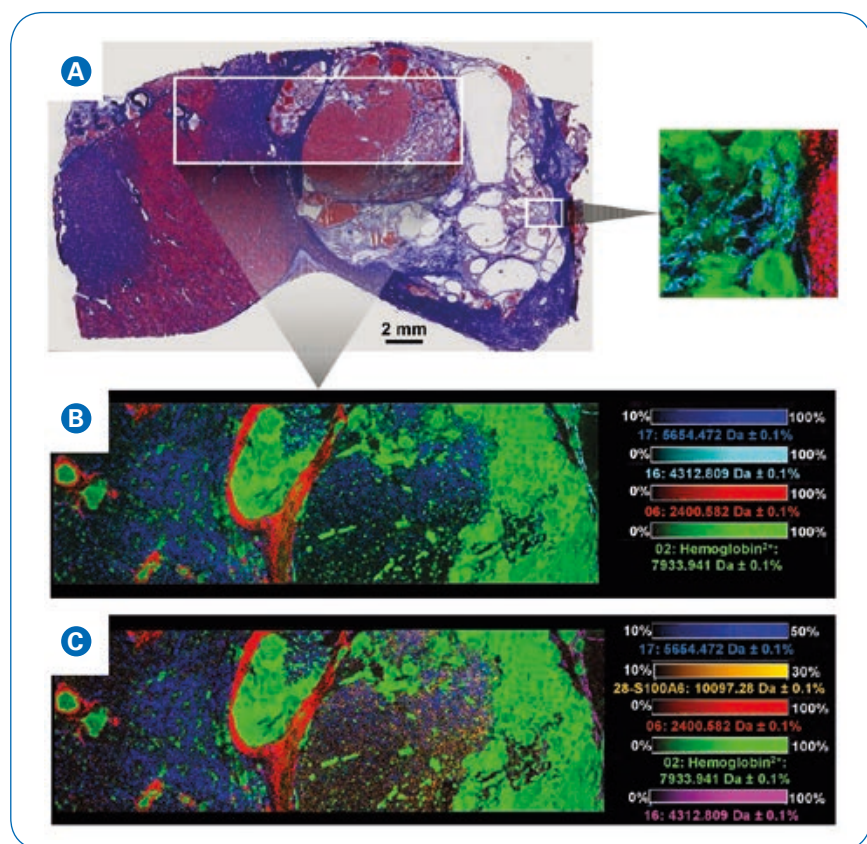


Figure 2. **A** Trichrome staining of a clear cell renal cell carcinoma human sample. **B** and **C** show MALDI MRMS protein imaging data collected with a 15T FTICR Bruker solariX, on positive ion mode, at $100\ \mu\text{m}$ spatial resolution. Overlay for **B**: m/z 5654.472 (histone H4 with an acetylation and demethylation, blue), m/z 4312.809 (turquoise), m/z 2400.582 (red), m/z 7933.941 (hemoglobin subunit, green). Overlay for **C**: m/z 5654.472 (histone H4 with an acetylation and demethylation, blue), m/z 10097.28 (orange), m/z 2400.582 (red), m/z 7933.941 (hemoglobin subunit, green), m/z 4312.809 (pink). Acquisition time $\sim 1.5\ \text{sec/pixel}$, total $\sim 6\ \text{hrs}$. Scale bar 2 mm.

Conclusions

- Ultra-high speed MALDI-TOF imaging and high-resolution MALDI MRMS imaging are the next-generation technologies for molecular histology. Ultra-high speed MALDI-TOF imaging provides high spatial resolution, while MALDI MRMS imaging excels at molecular specificity for protein imaging.



Learn More

For more information contact Bruker or visit:

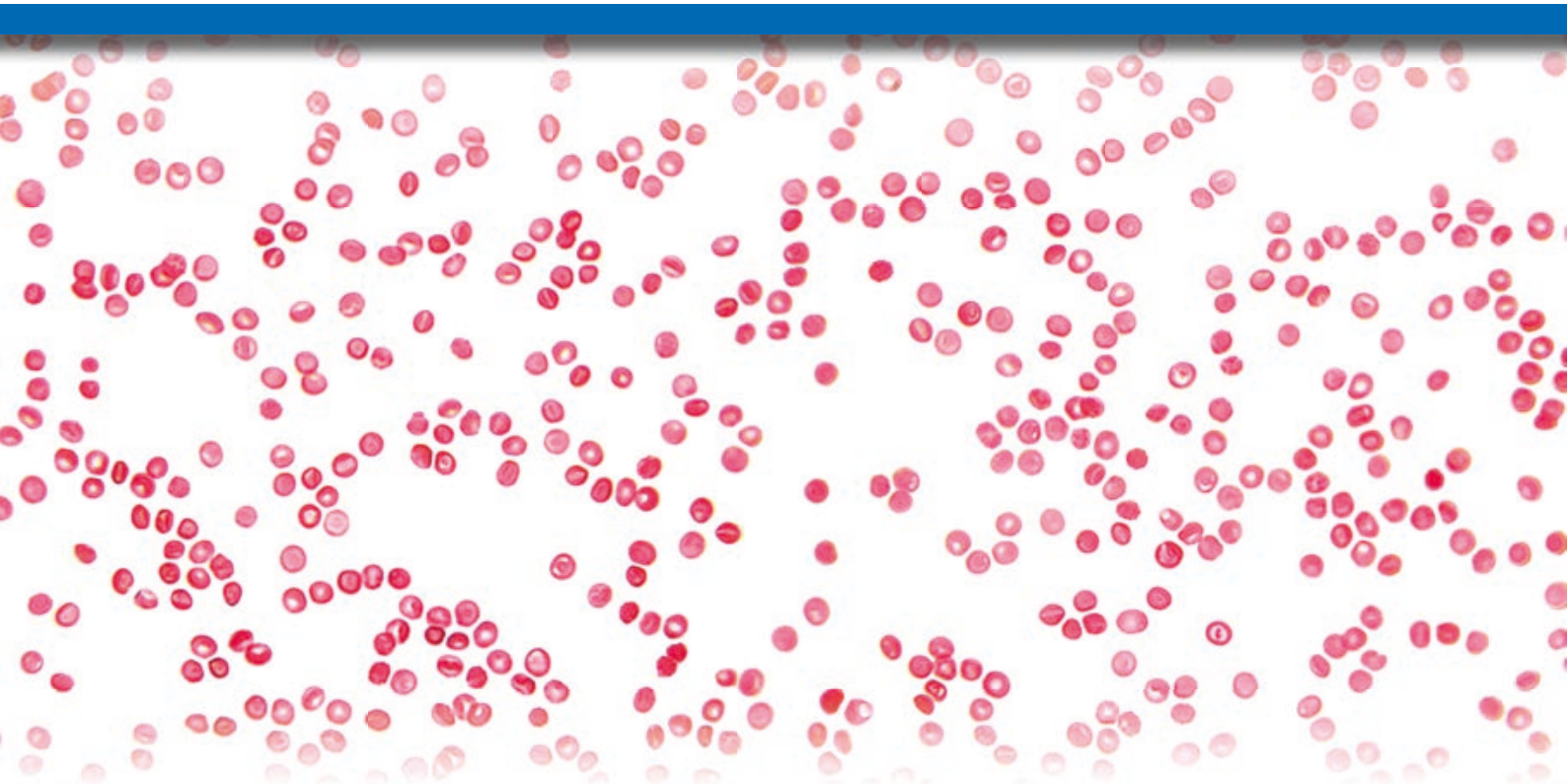
www.bruker.com/maldi-imaging



References

- [1] Spraggins, J. M., Rizzo, D. G., Moore, J. L., Rose, K. L. et al., *MALDI FTICR IMS of intact proteins: using mass accuracy to link protein images with proteomics data*. J. Am. Soc. Mass Spectrom. **2015**, 26, 974–985.
- [2] O'Sullivan, B. P., Freedman, S. D., *Cystic fibrosis*. Lancet **2009**, 373, 1891–1904.
- [3] Rowe, S. M., Miller, S., Sorscher, E. J., *Cystic fibrosis*. N. Engl. J. Med. **2005**, 352, 1992–2001.
- [4] Siegel, R. L., Miller, K. D., Jemal, A., *Cancer statistics, 2015*. CA Cancer J. Clin. **2015**, 65, 5–29.
- [5] Chow, W. H., Dong, L. M., Devesa, S. S., *Epidemiology and risk factors for kidney cancer*. Nature Reviews Urology **2010**, 7, 245–257.
- [6] Oppenheimer, S. R., Mi, D., Sanders, M. E., Caprioli, R. M., *Molecular analysis of tumor margins by MALDI mass spectrometry in renal carcinoma*. J. Proteome Res. **2010**, 9, 2182–2190.
- [7] Spraggins, J. M., Rizzo, D. G., Moore, J. L., Noto, M. J., Skaar, E. P., Caprioli, R. M., *Next-generation technologies for spatial proteomics: integrating ultra-high speed MALDI-TOF and high mass resolution MALDI FTICR imaging mass spectrometry for protein analysis*. Proteomics **2016**, 16, 1678–1689.

For research use only. Not for use in diagnostic procedures.



● Single Cell Lipid Analysis using the Bruker ultrafleXtreme TOF/TOF and the 7T solariX MRMS Mass Spectrometers

Matrix assisted laser desorption ionization (MALDI) mass spectrometry imaging (MSI) visualizes the distribution of a variety of molecules in biological systems, such as small metabolites, lipids, peptides, and proteins.

Introduction

Generally for MSI, mass spectra are acquired in a raster pattern, pixel by pixel, to build a chemical image of detected biomolecules. While this technique works well

for many samples and tissues, there are other approaches that are more efficient when probing dispersed cells on a slide. By performing an acquisition via a uniformly spaced grid, cells may

be split into multiple pixels, dividing the chemical information and complicating data analysis. Moreover, while imaging populations of dispersed or cultured cells, most of the analysis time

Keywords:
single cell analysis,
MALDI, multimodal
analysis, lipidomics

is spent acquiring spectra from empty spaces between cells rather than the cells themselves. This can lead to hours of imaging, with only a small fraction of the spectra containing cellular data. Accordingly, we have developed alternative approaches that are more efficient for examining thousands of individual cells dispersed on a slide (Figure 1).

To increase acquisition efficiency, we created the freely available microMS software [1], which automatically locates the spatial positions of fluorescently labelled cells or objects. Using these positions, microMS creates a geometry file that is compatible with Bruker MALDI mass spectrometers, allowing fast and efficient acquisition of individual cells randomly seeded on a sample substrate. Though developed for single cell analysis, this software can be used for many sample types that may require creation of non-standard geometry files with high precision and accuracy, such as bacterial colonies [2] and other objects. Further, microMS enables

multimodal analysis of the same individual cells (or samples) across multiple Bruker mass spectrometry (MS) platforms and stages, including orthogonal approaches such as immunochemistry [3] and capillary electrophoresis [4]. Here, we describe the use of microMS to study lipids within single rodent brain cells on the Bruker ultrafleXtreme and 7T solariX XR MALDI MS systems.

How to perform single cell measurements

Full experimental details have been described in detail [3], but are briefly outlined here. Dissected rodent cerebellar tissues were enzymatically and physically dissociated before being transferred onto indium-tin oxide glass slides with etched fiducials. Brightfield and fluorescence images were acquired on a Zeiss Axio M2 microscope. Cell locations were found using the high fluorescence from a nuclear dye and filtered by size, shape, and distance using the microMS software [1]. Slides were then coated with 0.1 to

0.2 mg/cm² of dihydroxybenzoic acid using an automatic sprayer described previously [5]. Single cell analysis was performed on a Bruker ultrafleXtreme TOF/TOF mass spectrometer with a mass window of 500–3000. The “Ultra” (~100 μm footprint) laser setting was used and 300 laser shots were accumulated at 1000 Hz and 60% laser energy for each cell. Additional experiments were performed on a Bruker 7T solariX XR Magnetic Resonance Mass Spectrometry (MRMS) system with a mass window of 150–3000, yielding a transient length of 2.94 s, and each MALDI spectrum was acquired with 20 laser shots at 1000 Hz and 60% laser energy with ~100 μm footprint. Cell coordinates were obtained using microMS and filtered with a 100 μm distance filter to prevent mixing of information from too closely located cells. Select slides were then immuno-stained with primary antibodies against glial fibrillary acidic protein and neurofilament-light chain and fluorescently labelled secondary antibodies.

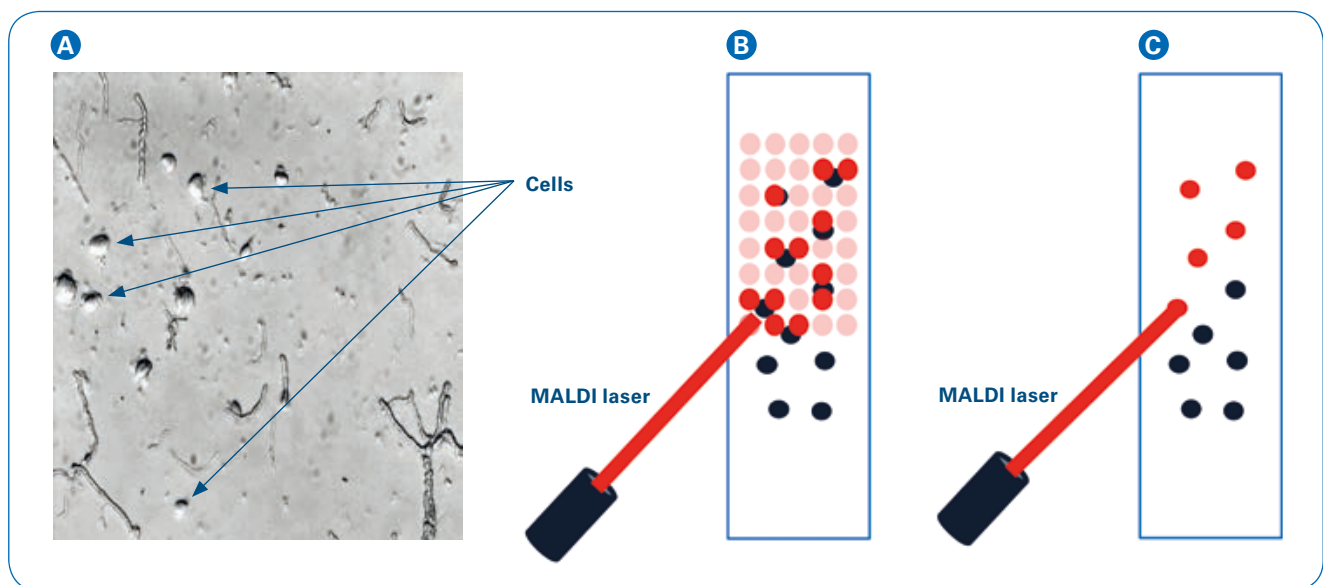


Figure 1: Characterizing a slide with dispersed cells. **A** A slide has a collection of cells mixed with non cellular objects where we only want to characterize the cells with MS. We optically image the slide, determine the locations of the cells we want to measure, and feed these target locations into the mass spectrometer. **B** Mass spectrometry imaging acquires data in a regularly spaced raster pattern and so spends valuable time on the empty spaces and does not center the laser onto the cells. **C** Instead of mass spectrometry imaging, here we acquire spectra from the positions of the cells of interest. Because MS data is only acquired from the cells, because the empty space on the slide is not interrogated and because the acquisitions are centered on the cells of interest, the approach is faster and produces more reproducible data. Using microMS, we expand this approach to slides with tens of thousands of cells.

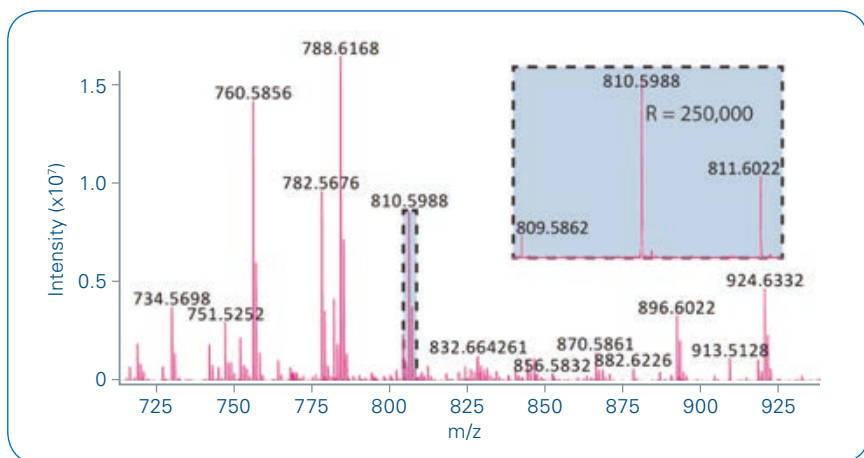


Figure 2: Single rodent cell spectrum taken on the Bruker 7T solariX XR system. Several lipids with a resolution of $\sim 250,000$ are labelled with high signal-to-noise ratios.

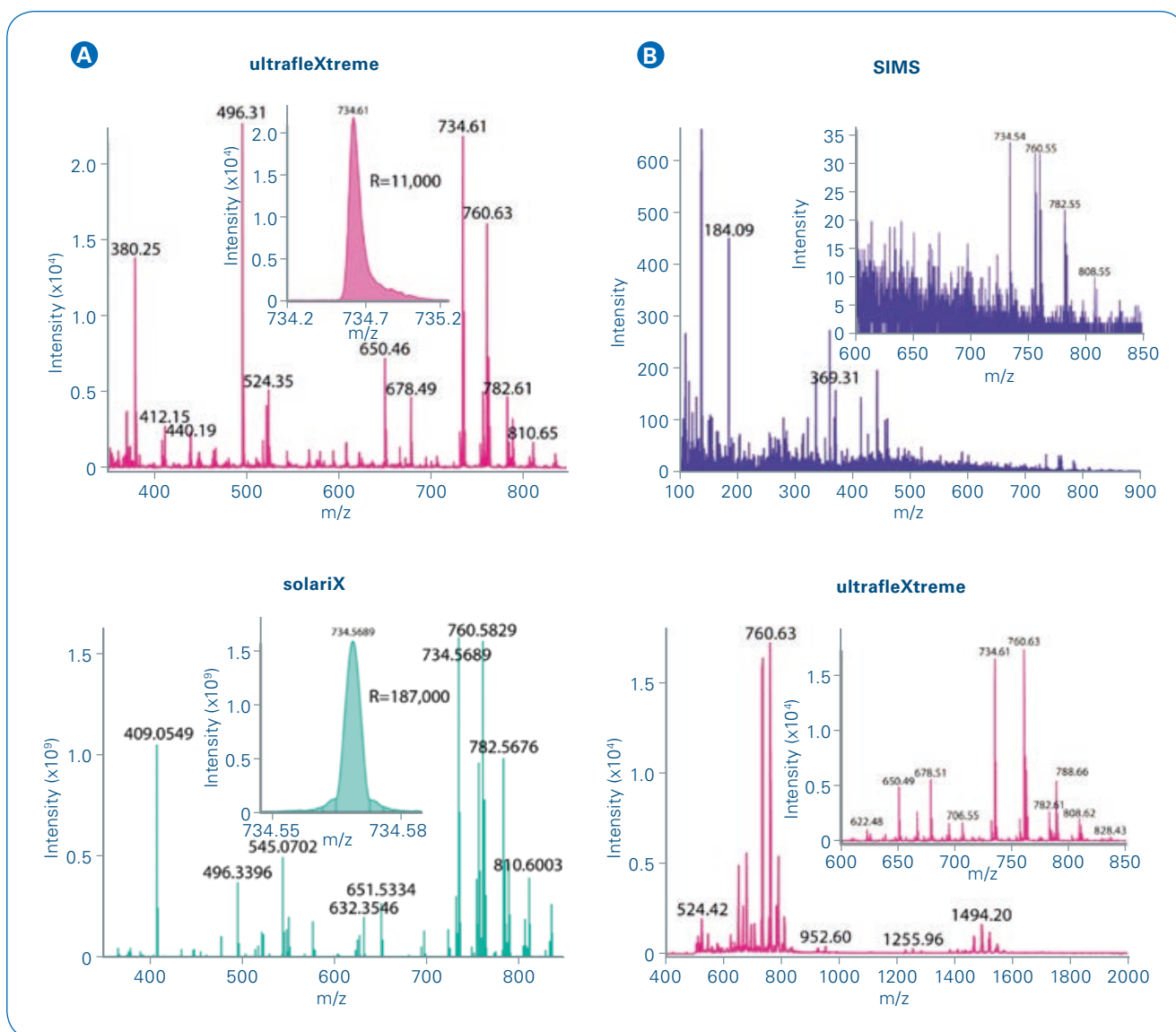


Figure 3: Spectra from the same single cell can be serially acquired on multiple MS systems to enhance the chemical information obtained from an individual cell or sample using microMS. **(A)** A Bruker ultrafleXtreme obtains single cell spectra at a rate of 1 cell per second and a resolution of 11,000 for the lipid mass range, and was used to screen cells for follow-up analysis by a Bruker 7T solariX XR system at a rate of 1 cell per 30 seconds and a resolution of $\sim 180,000$ for the lipid mass range. **(B)** A custom secondary ion mass spectrometer and a Bruker ultrafleXtreme system can also be used sequentially on a single cell for obtaining both metabolic and lipid/peptide chemical information.

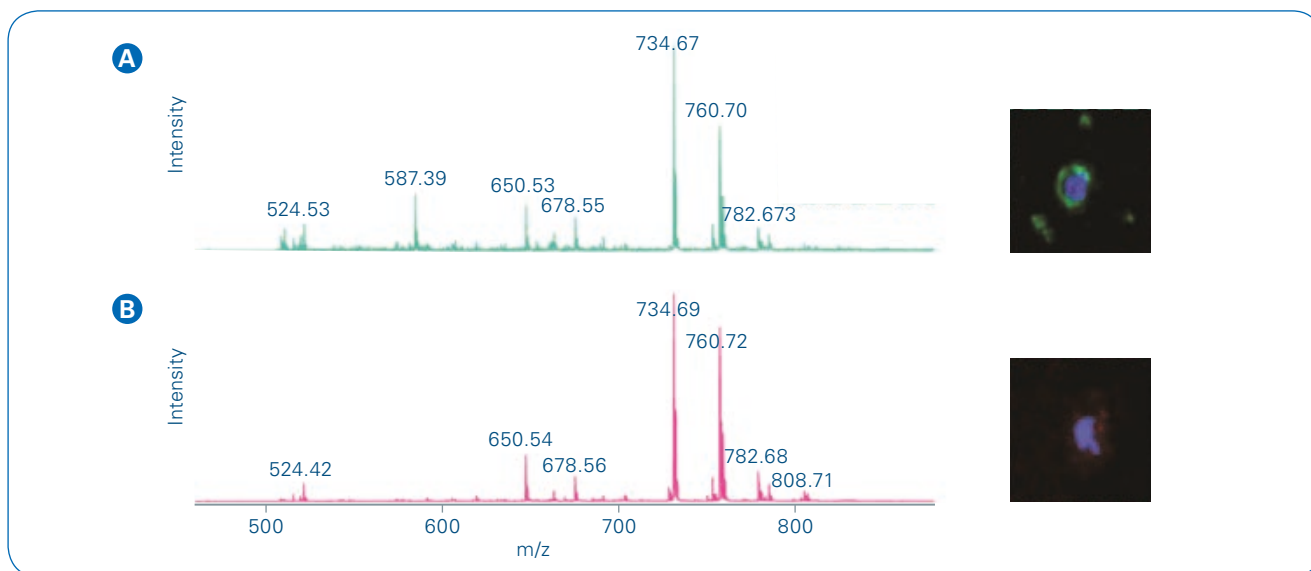


Figure 4: Single cell mass spectrometry lipid information can be directly correlated to immunocytochemical profiles for cell identification. Spectra were acquired on a Bruker ultrafleXtreme instrument. **A**) Single neuron mass spectra and immunocytochemical image. **B**) An astrocyte with its corresponding mass spectra. Green and red fluorescence corresponds to neurofilament- light chain (neuronal marker) and glial fibrillary acidic protein (astrocyte marker) respectively, while blue fluorescence corresponds to a nuclear dye.

Results and Discussion

By using a custom geometry file, we acquired single cell spectra from rodent brain cells using the Bruker ultrafleXtreme TOF/TOF mass spectrometer at a rate of ~ 1 cell/s and ~ 1 cell/30 s on the Bruker solariX MRMS MS system. This allowed us to profile thousands of cells in a reasonable time frame, making the technique applicable for studying systems of high complexity and diversity spread over large numbers of cells, such as the brain. We can target an individual cell with a spatial accuracy of $\sim 30 \mu\text{m}$. While the ultimate spatial accuracy depends on instrument stage movement accuracy, in practice we find that it is related to the number of training fiducials and the accuracy of the training set. While the accuracy is greater than the size of most mammalian cells, we compensate for the uncertainty of position by using a laser footprint that is large enough

($\sim 100 \mu\text{m}$) to assure that we sample the desired cells. Of course, we can improve our spatial resolution via an increase in the number of training fiducials. By only acquiring spectra for cells that are at least $100 \mu\text{m}$ apart, we limit cell-to-cell contamination within our single cell spectra.

An example single cell spectrum taken on the 7T solariX XR MRMS system is shown in Figure 2. Dozens of lipid species are detected between the m/z values of 700 to 925 with high mass resolution ($\sim 250,000$). For most single cell mass spectra, the spectral quality is generally high, with an average of 40 lipid features detected per cell, ranging between one and over a hundred lipid features within individual cells. We mostly detected phospholipids from the outer membrane of the cell, including phosphatidylcholines, phosphatidylethanolamines, sphingo-myelin, and many others. It is possible to produce similar spectra on the

ultrafleXtreme at a faster acquisition rates, although at a lower mass resolution and, therefore, a fewer number of lipids that are resolved.

Because microMS can be implemented on both MALDI instruments, the same microscopy image can be used without changing the pixel coordinate of any cells, greatly simplifying multimodal MS acquisition and subsequent data analysis. For instance, initial single cell profiling experiments can be performed on the ultrafleXtreme TOF to prescreen cells for subsequent solariX MRMS MS measurements (Figure 3a) [1]. By performing the faster TOF MS measurements first, we reduce the number of targets for the subsequent, slower MRMS MS analysis, thereby increasing the efficiency of our overall experiment. Similarly, MALDI MS can be used to re-assay cells for subsequent capillary electrophoresis analysis as well [4].

MicroMS and subsequent single cell analysis on the Bruker MALDI imaging systems is applicable to other chemical classes beyond lipids, such as small metabolites, peptides, and proteins; however, each chemical class requires optimization and different sample preparation approaches.

While MS produces rich chemical details, how do we link this information to cell type? For us, this has involved the introduction of orthogonal analytical approaches for comprehensive single cell analysis. Using microMS, we have correlated ultrafleXtreme spectra with immunocytochemical (ICC) classifications on the same cells [3]. By coupling these two approaches, we obtained reproducible lipid profiles for rodent astrocytes and neurons located within the cerebellum. Because the

position remains constant throughout both MALDI MS analysis and antibody staining, we directly correlate the mass spectral features and ICC-based fluorescence profiles from individual cells (Figure 4). For example, we determined that neurons (Figure 4a) have a higher abundance of phosphatidylcholine lipids compared to astrocytes (Figure 4b), which have a higher abundance of phosphatidylethanolamine lipids. Ultimately, the lipid differences between these two cell types were modest, requiring single cell MS analysis via microMS. While this example demonstrates our ability to distinguish two canonical cell types, astrocytes and neurons, using the ultrafleXtreme, the sampling procedure can be extended to other Bruker MALDI instruments, biological samples, and antibodies.

Conclusions

- Our single cell approaches, aided by microMS, enable sparse object locations and acquisitions that are compatible with many Bruker MALDI MS instruments. By creating a custom geometry file to obtain multiplexed chemical information from each cell, the methodology provides efficient analyses of thousands of randomly-seeded cells. The workflow is easily adaptable for multiple analyses being performed on the same cellular or non-cellular targets to extend the information that can be gained from a small sample.



Learn More

You are looking for further Information?
Check out the link or scan the QR code for more details.

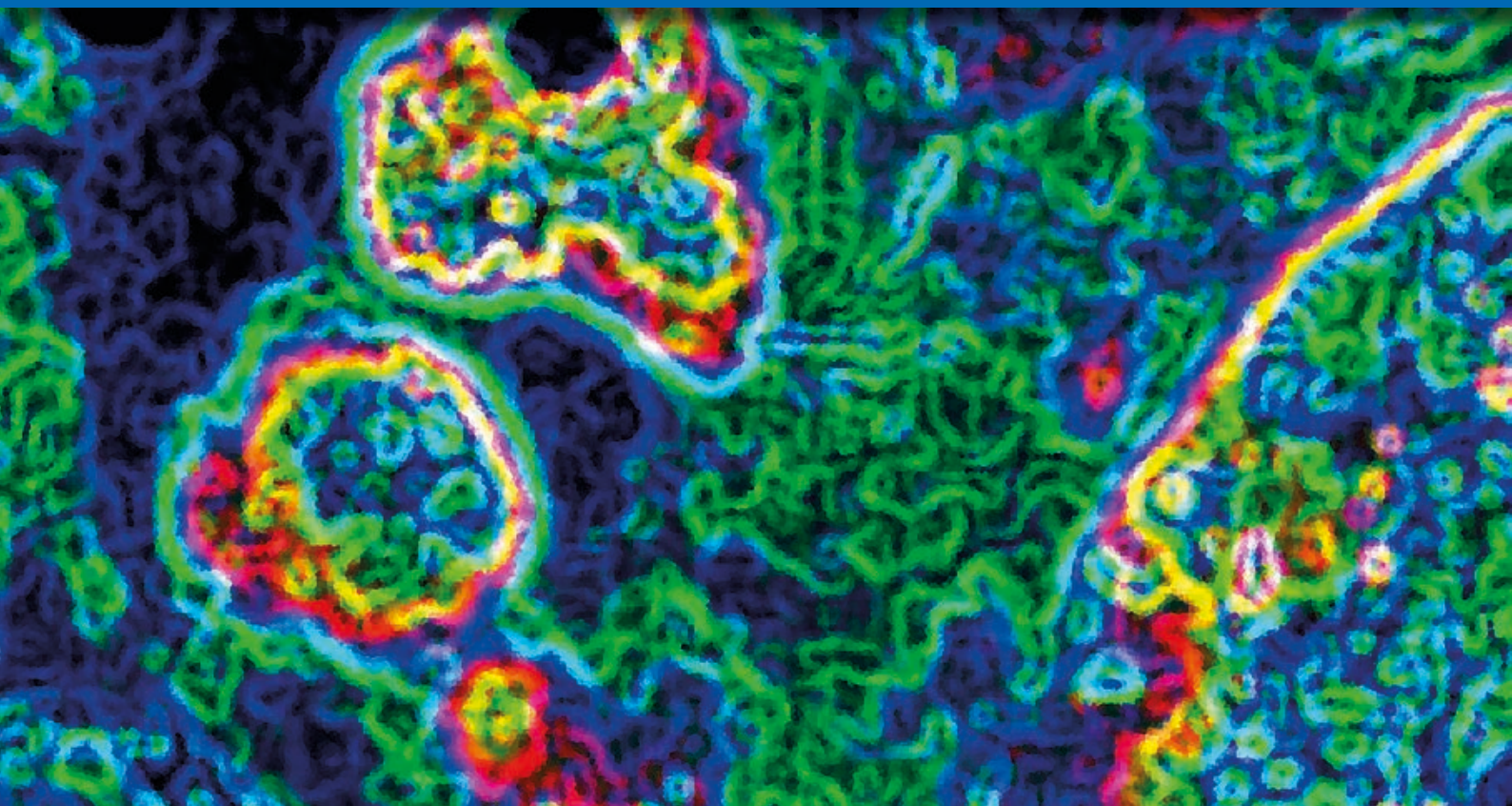
www.bruker.com/solarix



References

- [1] Comi TJ, Neumann EK, Do TD, Sweedler JV (2017). *microMS: A Python Platform for Image-Guided Mass Spectrometry Profiling*. J. Am. Soc. Mass Spectrom., **28**:1919-1928.
- [2] Si T, Li B, Comi TJ, Wu Y, Hu P, Wu Y, Min Y, Mitchell DA, Zhao H, Sweedler JV (2017). *Profiling of Microbial Colonies for High-Throughput Engineering of Multistep Enzymatic Reactions via Optically Guided Matrix-Assisted Laser Desorption/Ionization Mass Spectrometry*. J. Am. Chem. Soc., **139**:12466-12473.
- [3] Neumann EK, Comi TJ, Rubakhin SS, Sweedler JV (2019). *Lipid Heterogeneity between Astrocytes and Neurons Revealed by Single-Cell MALDI-MS Combined with Immunocytochemical Classification*. Angew. Chem. Int. Ed. Engl., **58**:5910-5914.
- [4] Comi TJ, Makurath MA, Philip MC, Rubakhin SS, Sweedler JV (2017). *MALDI MS Guided Liquid Microjunction Extraction for Capillary Electrophoresis-Electrospray Ionization MS Analysis of Single Pancreatic Islet Cells*. Anal. Chem., **89**:7765-7772.
- [5] Jansson ET, Comi TJ, Rubakhin SS, Sweedler JV (2016) *Single Cell Peptide Heterogeneity of Rat Islets of Langerhans*. ACS Chem. Biol., **11**:2588-2595.

For Research Use Only. Not for Use in Clinical Diagnostic Procedures.



● MALDI FTMS Imaging Mass Spectrometry of N-glycans as Tissue Biomarkers of Cancer

In this application note, we describe preparation and imaging analysis of N-glycans from formalin-fixed paraffin embedded (FFPE) tissues using the solarix MALDI FTMS.

N-glycosylation is a common post translational modification consisting of a carbohydrate moiety attached to the consensus sequence Asn-X-Ser/Thr, where X may be any amino acid residue other than proline, and a frequent modification of membrane associated proteins.

N-glycans are synthesized and processed in the ER and Golgi through the activity of over 300 enzymes that attach or trim sugar residues, resulting in thousands of different structural combinations (1). The large structural diversity of N-glycans plays a role in fine tuning protein

structure and function. Cellular activities that depend on N-glycosylation include protein folding, protein targeting, regulation of protease activity, cell migration and cell-cell recognition (2, 3).

Keywords:
glycans, MALDI,
Imaging, FTMS, solarix

In cancer, N-glycosylation plays a critical role in the tumor micro-environment, mediating inflammatory and immune response, altering extracellular matrix production, and modulating cell surface receptor and stroma-tumor interactions. N-glycosylation alterations thus serve

as important biomarkers and targets of therapy regulating the development and progression of cancer (4). Recently, methods for using MALDI imaging mass spectrometry to evaluate the N-glycome from FFPE thin tissue sections were reported (5, 6). The developed workflow is

amenable for evaluation of the vast numbers of stored FFPE clinical samples towards new studies in cancer diagnosis and prognosis (7). Although N-glycan imaging may be accomplished with any MALDI imaging mass spectrometry platform, there are certain advantages

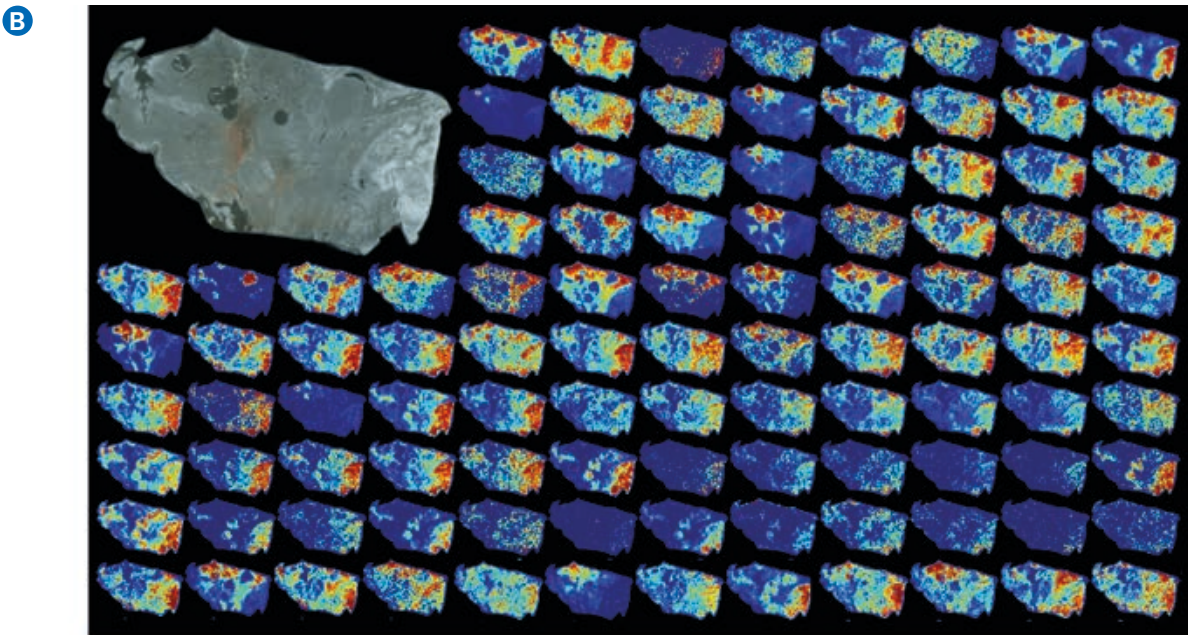
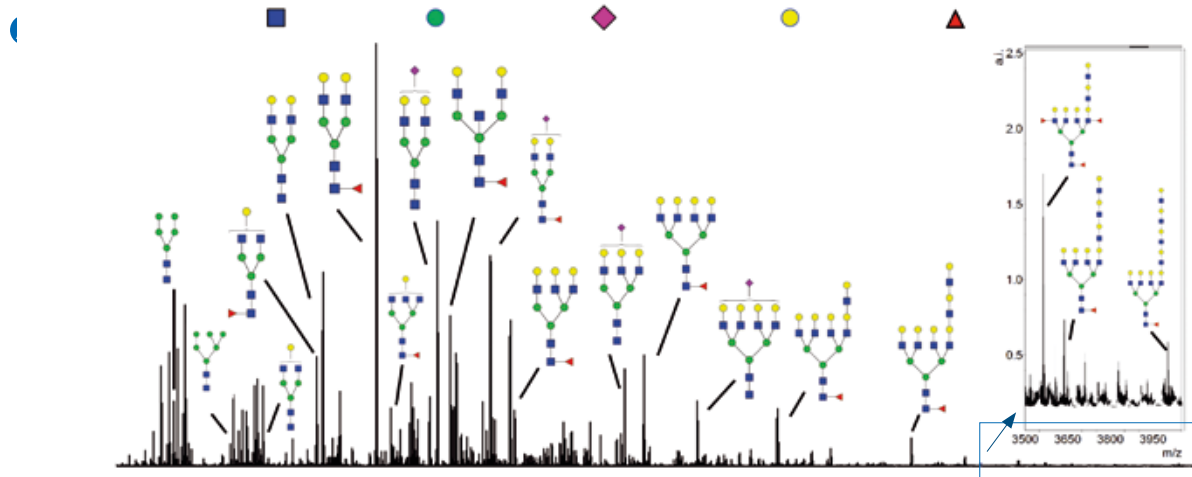


Figure 1. Example N-glycan signal from a single section of thyroid cancer. **A** Total average spectrum from the image with example glycoform structures per m/z; **B** Tile view of example images. Inset top right, photomicrograph of unstained tissue prior to imaging. Abbreviations: GlcNAc, N-acetylglucosamine

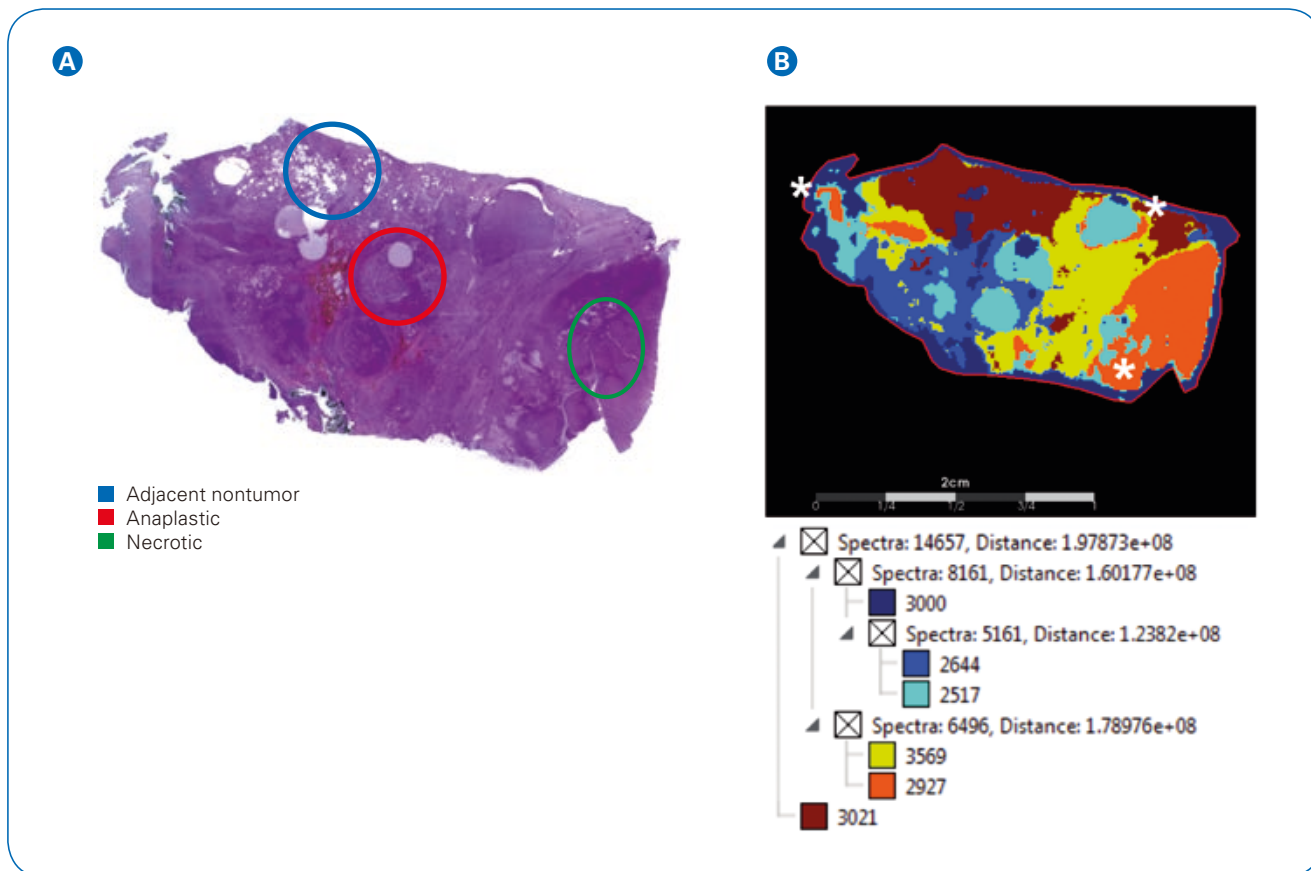


Figure 2. Image segmentation showing complexity of N-glycan signatures in a thyroid cancer tissue section. **A** Pathologist marked H&E stain of section highlighting adjacent nontumor, anaplastic, and necrotic regions. **B** SCiLS image segmentation of N-glycans from 2D mapping. White asterisks mark calculated overlaps of anaplastic and necrotic regions.

to using the solariX MALDI FTMS. In this note, we discuss high sensitivity mapping of the N-glycome as detected from the complex tissue environment of an FFPE thyroid cancer specimen.

Methods

Methods for releasing N-glycans from FFPE tissue have been described in detail (5). Use of de-identified tissue specimens to be discarded was approved by an Institutional Review Board. Briefly, a 5 μm thick FFPE tissue section of thyroid cancer was incubated for one hour at 60°C, dewaxed, and antigen retrieved under acidic conditions (10 mM citraconic buffer, pH 3). A robotic sprayer (TM-Sprayer™, HTXImaging) was used to apply

the enzyme and matrix in separate steps. First, recombinant PNGase F (Mehta Lab, Medical University of South Carolina) was sprayed onto tissue at 0.1 $\mu\text{g}/\mu\text{L}$. The sample was then incubated in a closed cell culture dish at 37°C under high humidity for two hours. Afterwards, α -cyano-4-hydroxycinnamic acid (CHCA) was sprayed onto tissue at 7 mg/mL in 50% acetonitrile, 0.1% trifluoroacetic acid. MALDI imaging analysis was performed in positive ion mode using a 7 T solariX equipped with a dual ESI/MALDI ion source and a Smartbeam II laser set to minimum focus. A total of 200 laser shots were collected at each pixel with a spacing of 150 μm between each pixel. Images were collected in broadband mode spanning m/z 500-5,000, with a

transient length of 1.2 seconds, resulting in an on-tissue resolving power of approximately 85,000 at m/z 1,850. FlexImaging software version 4.1 was used to produce a peak list linked to 2D tissue maps. N-glycans were putatively identified based on accurate mass within 5 ppm using GlycoWorkbench 2.0.(8) The 2D data and peak lists were uploaded to SCiLS Lab software (2016b, Version 4.01.8705, Bruker Daltonics) for analysis between pathologist marked tumor and nontumor regions. For image segmentation, SCiLS parameters used were weak denoising, bisecting K-means, and the Manhattan metric. Altered N-glycans were filtered by Wilcoxon rank sum hypothesis testing p value $\leq 1.0E-3$ and area under the receiver operating curve ≤ 0.8 .

Results and Discussion

In this work, we demonstrate N-glycan imaging analysis using a tissue section containing anaplastic thyroid cancer. Thyroid cancer is the most common malignancy of the endocrine system. Most thyroid cancers remain stable and indolent and patients have a good outcome when treated by surgical resection or therapies directed at inhibiting growth promoting kinases and angiogenesis (9). Anaplastic thyroid tumors are the least common but the most deadly form of thyroid cancer, and most patients die within a year. Prognosis is poor due to a lack of effective therapies and new molecular information is sought to develop therapies that stop tumor progression.

The example tissue section of an anaplastic thyroid cancer was prepared using our standard protocol for N-glycan release and analyzed by MALDI FTMS using a 7.0 Tesla solariX. Figure 1 shows total ion current and examples of 2D N-glycans mapped across the tissue. Detection of N-glycans is entirely dependent on the activity of the applied PNGase F. Here, over 111 N-glycans were detected as $[M+Na]^+$ or $[M-H+2Na]^+$, including high mannose, complex, hybrid, and sialylated structures. It is important to note that sialic acids are thermally labile and most MALDI sources result in loss of the sialic acid from the N-glycan. The solariX was designed specifically to minimize loss of sialic acids using high pressure collisional cooling gas (10). As a result, sialylated N-glycans are detected with equivalent intensity to N-glycans that do not contain this labile residue (Figure 1A). A second advantage using the solariX is that the source is decoupled from the mass measurement so that tissues mounted on standard microscope slides may be analyzed with negligible loss of mass resolution or mass

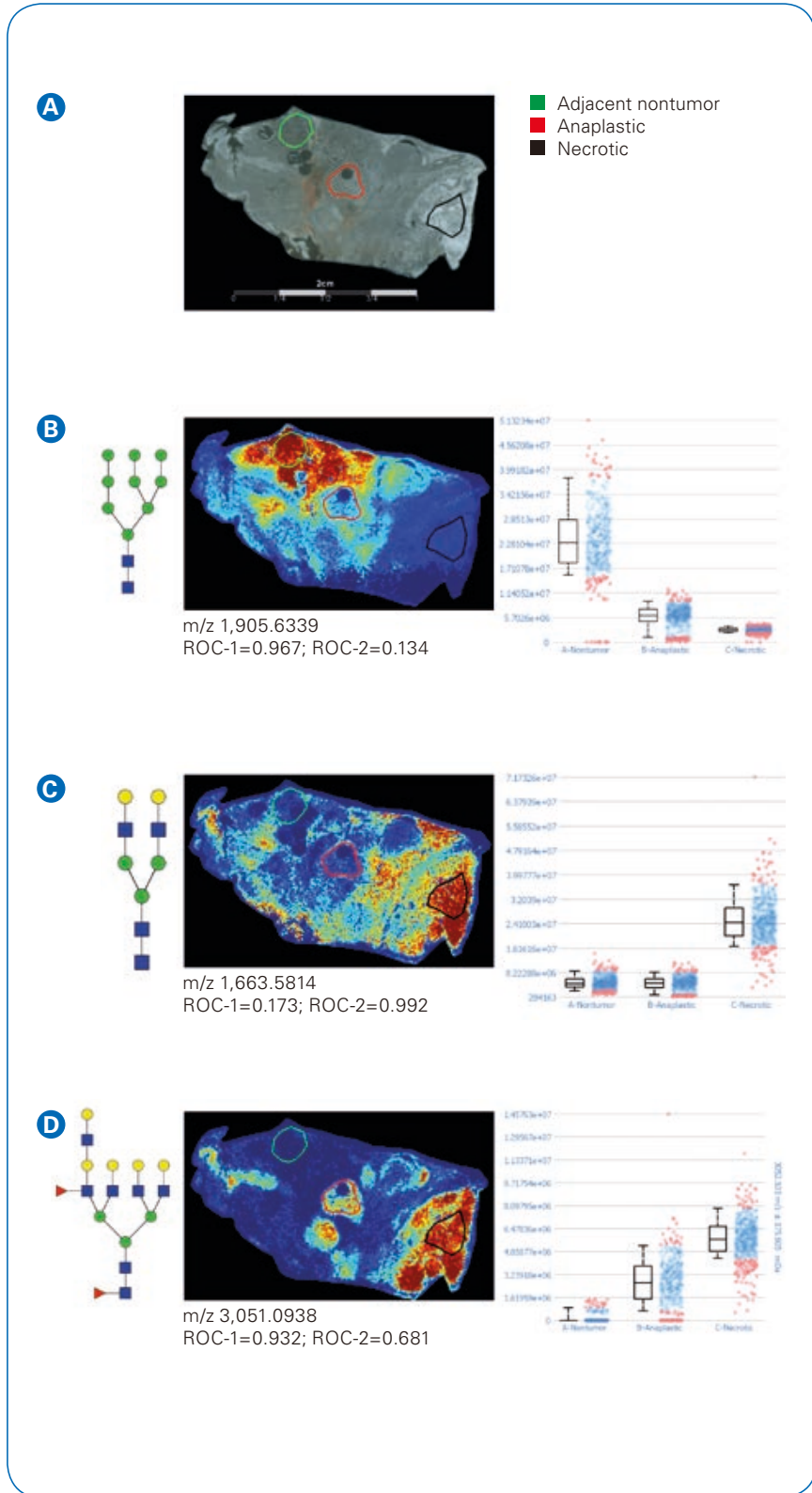


Figure 3. Quantification of N-glycan signatures from regional areas on tissue. Statistical testing was done comparing nontumor adjacent and anaplastic regions (ROC-1) or anaplastic versus necrotic (ROC-2). **A** Photomicrograph depicting areas selected for measuring relative abundance of N-glycan expression. **B** A high mannose (Man9) structure distinguishing nontumor adjacent compared to anaplastic tumor or necrotic regions. **C** A biantennary N-glycan defining necrotic regions with low expression in nontumor adjacent and anaplastic. **D** A tetrantennary fucosylated structure with low expression in adjacent nontumor and increasing expression in anaplastic and necrotic tissues regions.

accuracy. Here, the combined workflow and imaging platform yield high sensitivity detection of a broad m/z range of N-glycans, spanning from small pentamannose structures (Man5, m/z 1,257.4226) to fucosylated tetraantennary species with extended poly-N-acetylactosamine (polyLacNAc) series (m/z 4,000.4325). Overall, the N-glycan imaging workflow produces intense and comprehensive N-glycan signatures from FFPE tissue. In general, we have observed that the analysis of advanced tumors (like this example) have N-glycan signatures that allow mapping of well over 100 N-glycan species.

SCiLS image segmentation was used to evaluate the imaged tissue in comparison to the pathologist marked tissue. Figure 2 shows the pathologist marked hematoxylin and eosin stain of the thyroid tissue, with regions marked as adjacent nontumor, necrotic or anaplastic tumor. Segments were manually expanded to give equivalent numbers of spectra per region. Comparison of pathologist marked sections to SCiLS segmentation highlights the complexity of the tumor environment. Specifically, segments match to pathologist markings of normal adjacent (dark red) and necrotic (orange), but show increased

expansion of anaplastic tumor regions (aqua). However, N-glycan signatures mapping to the anaplastic region extend into the necrotic regions with some dispersion near adjacent non-tumor tissue. These data highlight that N-glycan signatures link to distinct tissue pathologies.

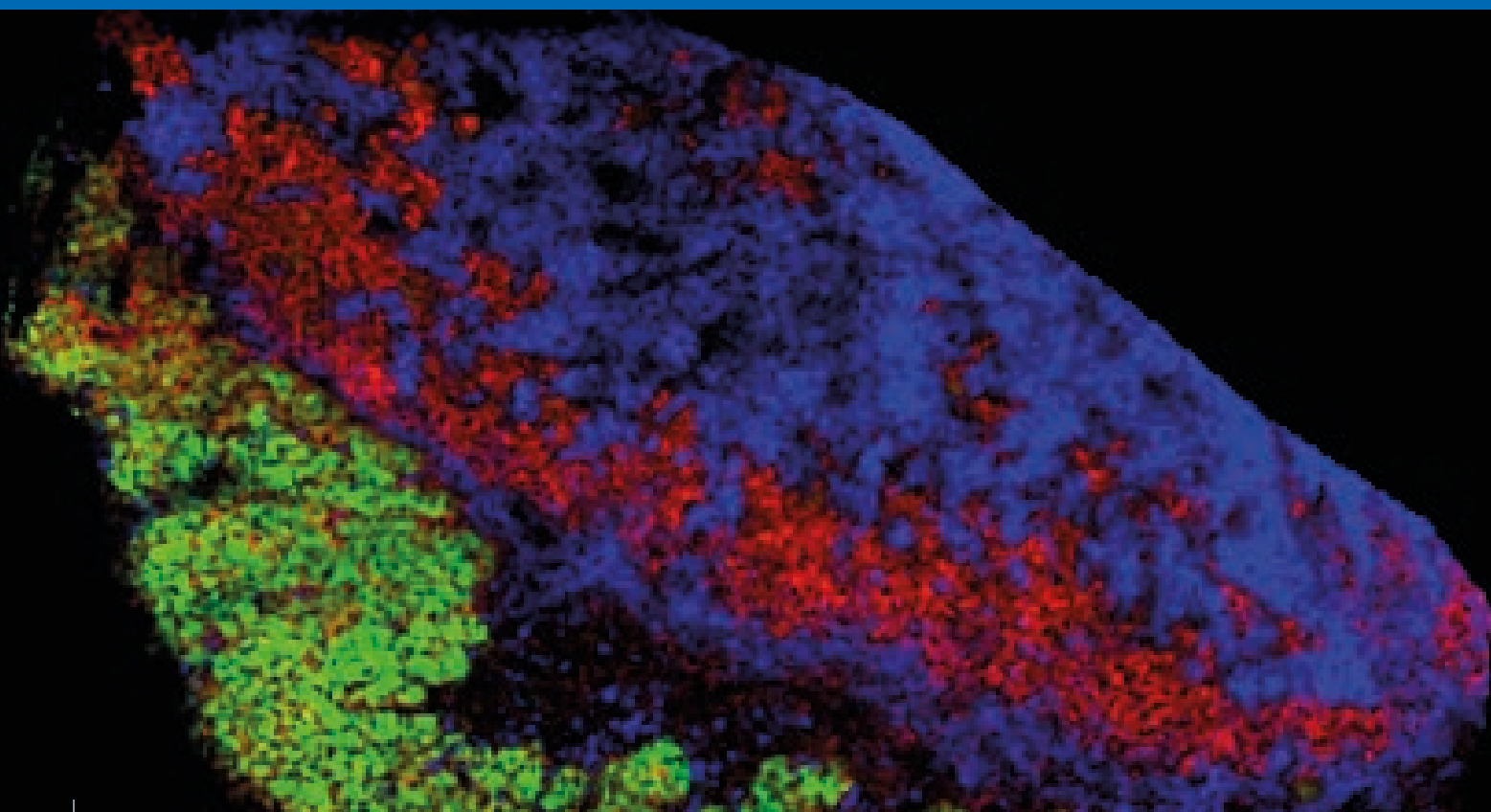
Tissue regions were selected from the pathologist marked regions to evaluate quantitative measurement of N-glycans (Figure 3). Regions were selected from within the pathologist marked areas for adjacent nontumor, necrotic, and anaplastic tumor. An example is shown of a high mannose structure (Man9) mapped to nonadjacent tissue areas with a ~ fourfold increase based on median value compared to anaplastic tumor regions. Necrotic regions showed unique signatures apart from both nonadjacent tumor and anaplastic tumor, shown here with an example biantennary structure. Interestingly, N-glycans found in anaplastic tumor regions were frequently also found in pathologist marked necrotic regions (see also Figure 1 B). These examples illustrate that N-glycan expression is uniquely regulated within the tumor micro-environment, and these alterations may be detected by the solariX MALDI FTMS imaging platform.

Conclusions

The N-glycan imaging workflow reveals complex carbohydrate interactions taking place within FFPE tumor tissues. An important component of the imaging workflow as illustrated here is the use of the solariX. The cooled source enables capturing biologically important but labile carbohydrate moieties, sialic acids, that would otherwise be lost in MALDI analysis. High sensitivity allows detection over a wide range of N-glycan structures. Analysis of this single piece of tissue section highlights the many unique N-glycosylation changes that can occur in anaplastic thyroid cancer. This workflow provides a valuable tool that allows deeper investigations into the molecular causes of disease, and can be applied to any FFPE tissue.

References

1. Moremen KW, Tiemeyer M, Nairn AV. 2012. *Nature Reviews Molecular Cell Biology* 13: 448-62
2. Stanley P, Schachter H, Taniguchi N. 2009. Chapter 8: N-Glycans. In *Essentials of Glycobiology*, ed. A Varki, RD Cummings, JD Esko, HH Freeze, P Stanley, et al. Cold Spring Harbor (NY): Cold Spring Harbor Laboratory Press
3. Varki A. 2017. *Glycobiology* 27: 3-49
4. Pinho SS, Reis CA. 2015. *Nature Reviews Cancer* 15: 540-55
5. Powers TW, Neely BA, Shao Y, Tang H, Troyer DA, et al. 2014. *PLoS One* 9: e106255, pp1-11. PMID: 25184632
6. Drake RR, Powers TW, Jones EE, Bruner E, Mehta AS, Angei PM. 2017. *Advances in Cancer Research* 134: 85-116
7. Gorzolka K, Walch A. 2014. *Histology and Histopathology* 29: 1365-76
8. Ceroni A, Maass K, Geyer H, Geyer R, Dell A, Haslam SM. 2008. *Journal of Proteome Research* 7: 1650-9
9. Lin R-Y. 2011. *Nature Reviews Endocrinology* 7: 609-16
10. O'Connor PB, Mirgorodskaya E, Costello CE. 2002. *Journal of the American Society for Mass Spectrometry* 13: 402-7



• MALDI Imaging Success Stories in Clinical Research – Mini Review

Abstract

MALDI Imaging is a technique that allows the direct detection of proteins, lipids, drugs and metabolites in tissue and when integrated with histology becomes a powerful tool for molecular histology. In contrast to other molecular histological techniques, it does not require a molecular probe and can therefore be used for the discovery of new biomarkers. In recent years, MALDI Imaging has been used successfully to identify biomarkers for a number of clinical cases. However, there has been discussion in the field whether the resulting protein markers are merely surrogate markers for disease states or if they also have functional implications.

Authors

Sören-Oliver Deininger
Bruker Daltonik GmbH, Bremen, Germany

Shannon Cornett
Bruker Daltonics, Billerica, MA, USA

This mini-review focuses on recent imaging studies that use validation strategies to demonstrate a functional role of identified markers within the respective disease pathways. We include also one example of a recently published drug-safety study with important implications for human safety.

MALDI Imaging reveals mechanism of neoadjuvant chemotherapy resistance in Barrets carcinoma

In oesophageal adenocarcinoma the patient is usually treated with a neoadjuvant chemotherapy consisting of Cis-Platin and 5-Fluorouracil to shrink the tumor prior to surgery. However, a large percentage of patients do not respond to this treatment. Aichler et al. [1] has used MALDI Imaging to compare protein profiles from tissue samples from 10 patients who responded to treatment and 13 patients who were non-responders. They found that 22 of the 150-250 proteins detected were differentially regulated between responders and non-responders. Four of the proteins down regulated in responders were identified as mitochondrial proteins, COX7A2, COX6B1, COX6C and complex I-MLRQ. From this observation it was hypothesized that mitochondria might be involved in the drug resistance. Using electron microscopy to examine the mitochondria of responders and non-responders it was found that the mitochondria of non-responders presented a normal phenotype while the mitochondria of the responders appeared abnormally large and with damaged cristae.

The authors further hypothesized that mitochondrial damage might lower the threshold of the cancer cells for cell death and consequently pre-dispose the cells to respond positively to the chemotherapy. The protein COX7A2 exhibited the strongest correlation between chemotherapy response and the MALDI Imaging and so COX7A2 knock-out cells were cultured and treated with the chemotherapeutic drugs. The knock-out tumor cells showed a distinct change in mitochondrial phenotypes to a “cup-shape” similar to that seen in the responder cohort after neoadjuvant chemotherapy, confirming the hypothesis. Moreover, these cells exhibited a significantly lower threshold to cell death which also confirmed the hypothesis on the role of mitochondria in the response to chemotherapy.

This study stands out because it linked the protein changes seen in MALDI Imaging to a functional understanding of a drug resistance. It is also a prime example for a “reverse-translational” study, where the initial findings were made in patients and the mechanism was confirmed by model experiments, and it shows how knowledge gene-rated by MALDI Imaging can have potential implications for personalized medicine.

MALDI Imaging reveals posttranslational changes in histones are linked to microvascular invasion in hepatocellular cancer

Hepatocellular carcinoma is a leading cause of cancer-related deaths. Long-term prognosis is poor due to high recurrence rates and microvascular invasion (MiVI) is a major risk factor for recurrence and mortality. Usually, MiVI cannot be assessed in pre-operative biopsies, because the sampled volume is too low for clinical assessment using known gene expression signatures. MiVI can only be determined after surgical resection and histological analysis of the complete tumor. There is a need for predictive proteomic markers that can be assessed with immunohistochemical staining of routine biopsies prior to resection to better direct therapeutic strategy. Poté et al [2] used a MALDI Imaging strategy to investigate a discovery set of hepatocellular carcinoma tissues that presented both with and without MiVI with the aim of finding diagnostic protein biomarkers. The discovery set consisted of 30 patient samples presenting MiVI and 26 patient samples without MiVI. Comparative analysis of image data from these patient groups identified 30 mass spectrometric peaks that were differentially expressed between the groups. Two of the signals were identified as modified forms of Histone H4: both acetylated at the N-terminus and dimethylated at Lysine 20 and one with an additional acetylation at Lysine 16. The modified histone markers were confirmed in an independent validation cohort of 23 samples by immunohistochemistry and western blot analysis.

Histones have a regulatory function in transcription, and post-translational modifications such as acetylation and methylation play a role in this regulation. Furthermore, the modification of histones leads to less tight wrapping of the DNA in the nucleus and therefore to an increased transcription of the regulated genes into RNA. To our knowledge, this is the first study that linked MALDI Imaging data of post-translationally modified proteins to a histological disease state.

This study stands out, because it shows for the first time functional implications of post-translationally modified proteins observed directly by MALDI Imaging. In doing so it underpins the potential of MALDI Imaging as a true top-down technique.

MALDI Imaging was used to find a new prognostic marker in HER2 positive breast cancer

The HER2 receptor status is a well studied property in breast cancer. The overexpression of this receptor leads to an increased proliferation of tumor cells and is linked to an unfavorable outcome. There is a targeted individualized therapy available; the monoclonal antibody Trastuzumab can be used to treat HER2 overexpressing breast cancer. Previously, Rauser et. al [3] used MALDI Imaging to compare HER2 positive and negative breast cancer specimens. Among the differences they found an up regulation of the protein CRIP1 (Cysteine rich intestinal protein 1) in HER2 positive samples. This was the first time that this protein was found in a proteomic experiment in breast cancer (although an increased gene expression was linked to HER2 positive breast cancer earlier). Another notable aspect of this publication was also the direct identification of the protein by a top-down fragmentation with electron transfer dissociation in a spherical ion trap; an instrument that is particularly suited for this purpose. The CRIP1 marker could be validated by MALDI Imaging in an independent cohort, but at the time of the publication there was no antibody available to do a more comprehensive validation.

In the meantime, an antibody became available and allowed the analysis of the CRIP1 status in several types of tumors. In a follow-up to their previous MALDI Imaging study, Lydiga et al. [4] analyzed the CRIP1 status in breast cancer by immunohistochemistry. This study revealed that CRIP1 expression is indeed correlated with HER2 expression in breast cancer, Figure 1. Even more interesting is the fact that CRIP1 is an independent prognostic factor in Her2 positive breast cancer: Low expression of CRIP1 in HER2 positive breast cancer is associated with an unfavorable outcome while high expression of CRIP1 is linked to a good prognosis, Figure 2.

The important implication of this study is the proof that MALDI Imaging can find protein changes in diseases that not only are surrogate markers for known tissue states (such as HER2 status in this case), but can also be new markers for other important parameters, such as prognosis.

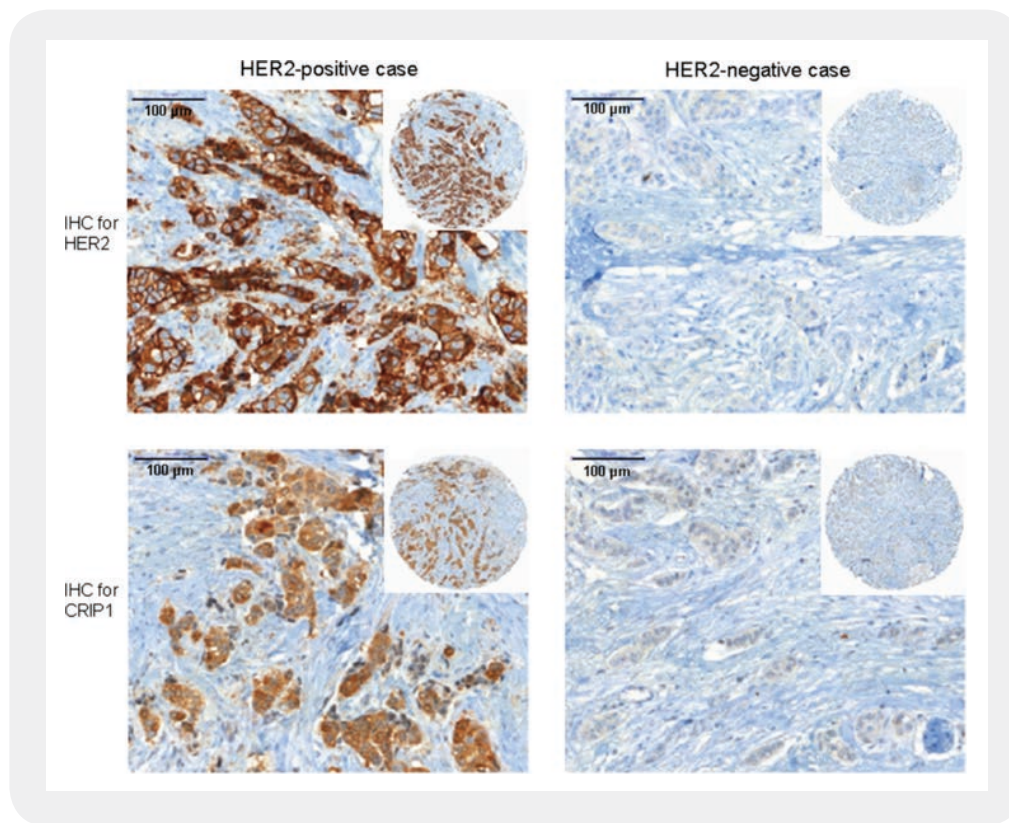


Figure 1: The co-expression of HER2 and CRIP1 in breast cancer tissue. Representative images of breast cancer tissues showing positive or negative immunohistochemical staining for HER2 and CRIP1, respectively. From [4], released under the terms of the Creative Commons Attribution License (<http://creativecommons.org/licenses/by/2.0>).

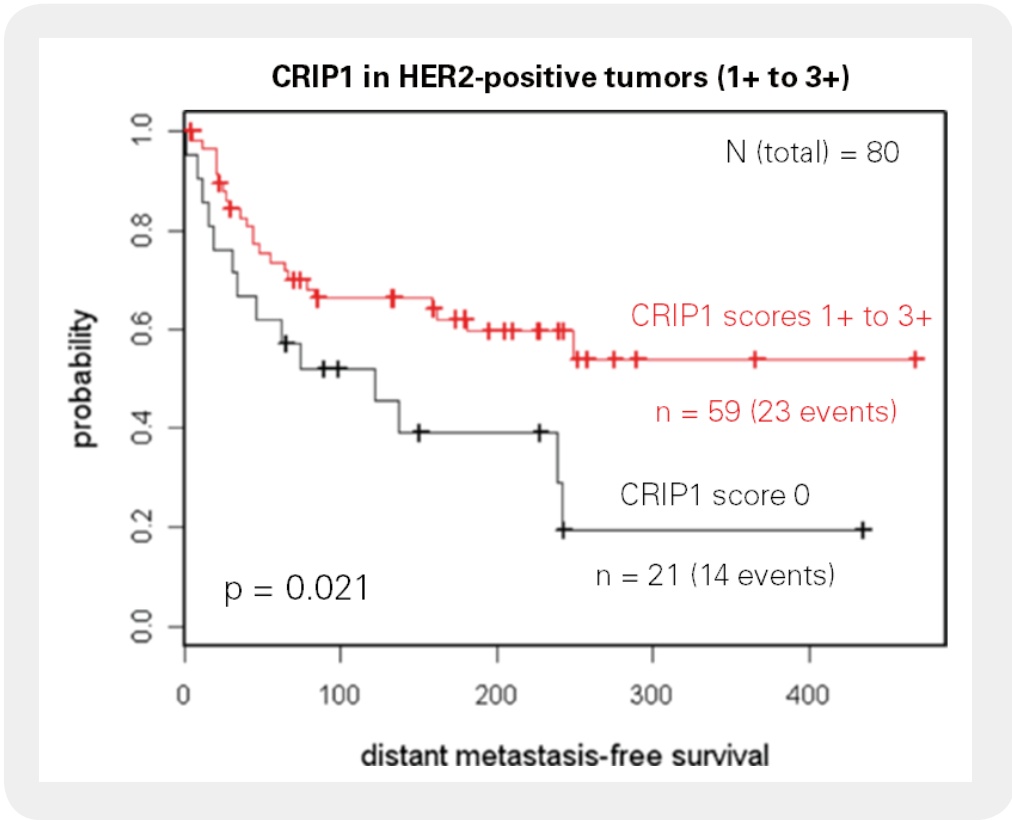


Figure 2: Kaplan Meier survival analysis of the distant metastases-free survival of patients. Patients with HER2-positive tumors were stratified according to their CRIP1 expression (negative vs. positive). Adapted from [4], released under the terms of the Creative Commons Attribution License (<http://creativecommons.org/licenses/by/2.0>).

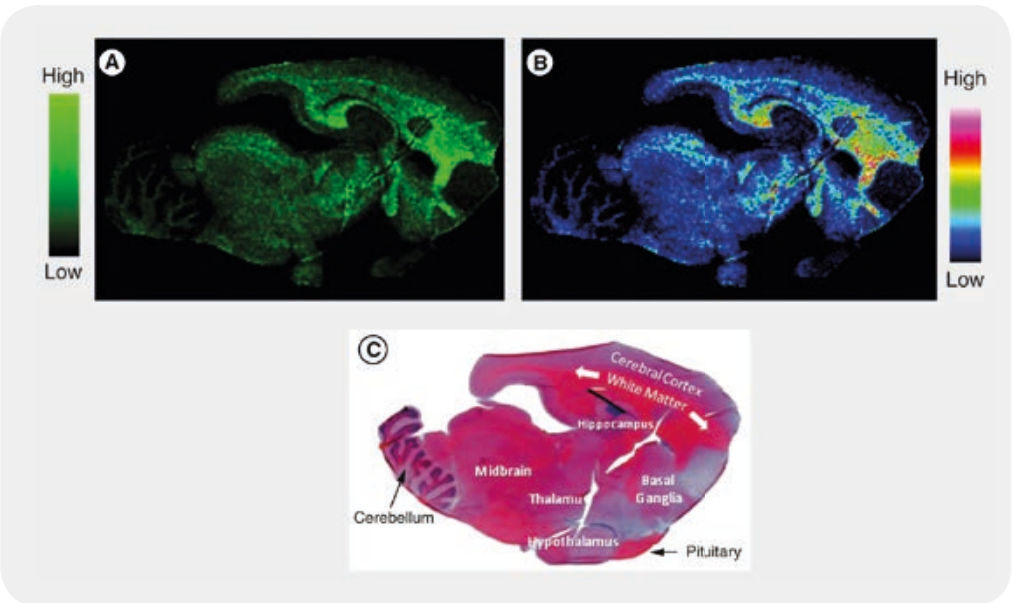


Figure 3: Drug Imaging / Histopharmacology: Sagittal rabbit brain section showing distribution of a cysteine conjugate metabolite. (A) Monochromatic ion image showing brain distribution of cysteine conjugate metabolite (170 μm spatial resolution). (B) Same ion image as (A) but shown in rainbow intensity format. (C) Hematoxylin and eosin histology slide showing regions of the rabbit brain. From: Castellino et al. (2011) *Bioanalysis* 3(21),2427-41 with kind permission of the authors.

MALDI Imaging contributed in the safety assessment of a drug that showed unexpected side effects in a clinical trial

Fosdevirine (FDV) is an antiretroviral drug that showed promising properties in early development. Pre-clinical toxicity studies on rodents and monkey showed no indication of risk of drug-related Central Nervous System (CNS) effects. One adverse reaction was observed in a test population of rabbit but this single example was later discounted. Results from a Phase I clinical study indicated that FDV was well tolerated and exhibited antiviral activity. During a Phase IIb clinical study a high number of seizures presented in a population of HIV patients who had previous antiretroviral therapy and the trial was placed on clinical hold. After which, results became available from a FDV study in minipigs in which a number of animals exhibited neurobehavioral signs, up to 25 days after final dose.

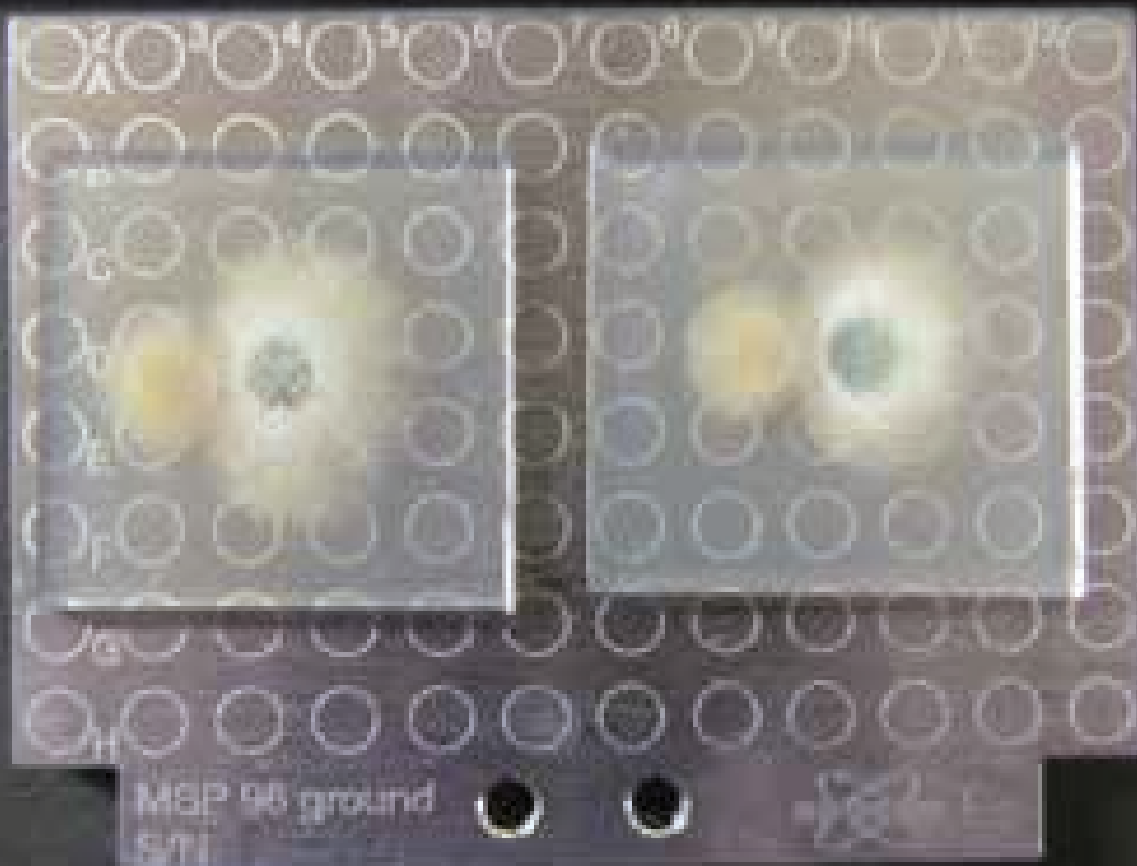
To gain better insight into a physiochemical cause for the adverse activity Castellino et. al [5] used LC-MS to characterize FDV and its metabolites in cerebrospinal fluid (CSF) from seizure patients, rabbit and monkey as

well as brain tissue from rabbit, minipig and monkey. The authors supplemented the LC-MS data with a MALDI Imaging study of brain tissue from rabbit, monkey and minipig to map the distribution of the parent drug and several metabolites. These data showed that in the monkey the predominant drug-related material was the intact FDV which was observed by MALDI Imaging to be localized to the grey matter of the brain. LC-MS analyses of CSF in seizure patients and MALDI Imaging in rabbit and minipig revealed the predominant drug-related compound to be a cysteine-addition metabolite found in high concentrations in the corpus callosum. Together with results from other techniques the MALDI Imaging data provides valuable insight into the mechanism of the adverse side effect (the authors speculate a role of an altered blood-brain barrier in HIV patients) as well as the applicability of the animal models.

This paper is particularly noteworthy because it shows the potential for MALDI Imaging data to support classical workflows while offering a unique analytical perspective that is not otherwise possible. The authors make a strong case for including MALDI Imaging in the drug development process where it offers direct imaging of a drug and its metabolites.

References

- [1] Aichler M, Elsner M, Ludyga N, Feuchtinger A, Zangen V, Maier SK, Balluff B, Schöne C, Hierber L, Braselmann H, Meding S, Rauser S, Zischka H, Aubele M, Schmitt M, Feith M, Hauck SM, Ueffing M, Langer R, Kuster B, Zitzelsberger H, Höfler H, Walch AK. Clinical response to chemotherapy in oesophageal adenocarcinoma patients is linked to defects in mitochondria. *J Pathol.* 2013 Aug;230(4):410-9.
- [2] Poté N, Alexandrov T, Le Faouder J, Laouirem S, Léger T, Mebarki M, Belghiti J, Camadro JM, Bedossa P, Paradis V. Imaging mass spectrometry reveals modified forms of histone H4 as new biomarkers of microvascular invasion in hepatocellular carcinomas. *Hepatology.* 2013 Apr 2. doi:10.1002/hep.26433.
- [3] Rauser S, Marquardt C, Balluff B, Deininger SO, Albers C, Belau E, Hartmer R, Suckau D, Specht K, Ebert MP, Schmitt M, Aubele M, Höfler H, Walch A. Classification of HER2 receptor status in breast cancer tissues by MALDI Imaging mass spectrometry. *J Proteome Res.* 2010 Apr5;9(4):1854-63
- [4] Ludyga N, Englert S, Pflieger K, Rauser S, Braselmann H, Walch A, Auer G, Höfler H, Aubele M. The impact of cysteine-rich intestinal protein 1 (CRIP1) in human breast cancer. *Mol Cancer.* 2013 Apr 9;12:28. doi: 10.1186/1476-4598-12-28
- [5] Castellino S, Groseclose MR, Sigafos J, Wagner D, de Serres M, Polli JW, Romach E, Myer J, Hamilton B. Central nervous system disposition and metabolism of Fosdevirine (GSK2248761), a non-nucleoside reverse transcriptase inhibitor: an LC-MS and Matrix-assisted laser desorption/ionization imaging MS investigation into central nervous system toxicity *Chem Res Toxicol.* 2013; 26(2):241-51



• Microbial Imaging Mass Spectrometry with Fourier Transform Ionization Mass Spectrometry

Abstract

In this application note we describe a straightforward approach for the preparation and molecular analysis of a bacterial-fungal interaction and the visualization of metabolic exchange factors using an FT-ICR high resolution mass spectrometer.

Introduction

Since the discovery of penicillin it has been widely recognized that microbes produce biologically active molecules, some of which have been found beneficial for treating infections (e.g. penicillin, vancomycin and daptomycin), enabling transplantations (e.g. rapamycin) and lowering cholesterol (e.g. lovastatin). Despite the

Authors

Vanessa Phelan¹, Pieter C. Dorrestein¹,
Shannon Cornett²
University of California San Diego¹, Bruker Daltonics²

Keywords	Instrumentation and Software
SmartFormula	solariX
Bacteria	
Microbiology	

importance of these molecules in agriculture, diagnostic and therapeutic areas, there are few methods that capture molecular information directly from microbial cultures.

In 2009, microbial imaging mass spectrometry was developed as a way to capture the molecular information from cultured microbes directly from agar surfaces¹. Microbial imaging mass spectrometry is an extension of the field of histological imaging mass spectrometry² and has resulted in the capture of otherwise hidden molecular microbial phenotypes and metabolic exchange of compounds that promise new therapeutic and biochemical activities^{1, 2-13}. Often however, these bioactive compounds can be small-molecules that are isobaric with intense matrix ions or other endogenous compounds. When imaging with MALDI-TOF systems it is often useful to supplement MALDI imaging analyses with other techniques such as TOF/TOF imaging or LC-MS in order to fully characterize molecular structures and/or molecular distributions. However these approaches are not without disadvantages. MALDI-TOF/TOF imaging provides high molecular specificity which lends itself quite well to verification of a suspected molecule but is limited for discovery experiments. On the other hand, LC-MS strategies provide access to a wide dynamic range of compounds but at the sacrifice of enriching specific molecules via extraction and the LC procedure itself, as many molecules are difficult to extract and/or chromatograph poorly, as well as missing the spatial information.

Although MALDI-TOF based imaging is incredibly useful for microbiology, Bruker's solariX high-performance mass spectrometer offers an enhanced strategy for MALDI imaging that is well suited to studying microbial metabolites and other small molecules¹². It's high mass-resolution capabilities in MS-mode facilitates discovery studies by separating metabolite images from the interferences presented by ions that are very close in mass. At the same time, solariX's high measurement accuracy can often provide unambiguous molecular formula assignment for each of these resolved images. The same resolution and accuracy capabilities are also present in MS/MS mode if more detailed structural confirmation is needed. In this note we show the power of solariX for metabolic imaging of a *Pseudomonas aeruginosa* and *Aspergillus fumigatus* interaction, two organisms found in cystic fibrosis lungs.³

Methods

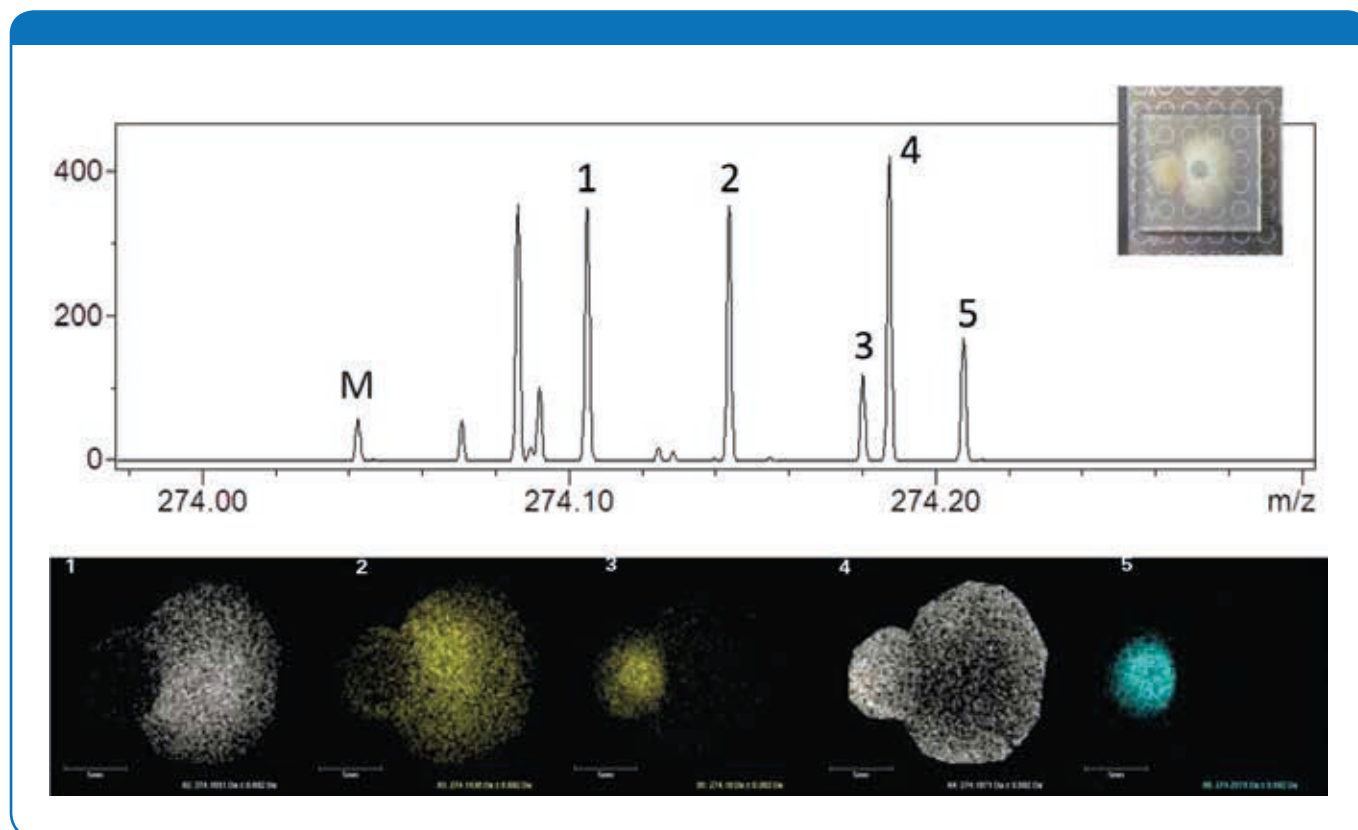
Detailed descriptions of the microbial sample preparation can be found in the references and several minor variations exist. Typically, 10-11 ml of 1-2% agar with necessary nutrients was poured into a Petri-dish to form a layer of agar ~1mm thick. *Pseudomonas aeruginosa* and *Aspergillus fumigatus* were subsequently added to the agar and incubated until colonies began to interact. During the

incubation period it is important to seal the Petri-dish in order to minimize evaporation. When the microbes reached the desired phenotype the agar was cut and peeled from the Petri-dish and placed on top of an unpolished MALDI target plate. A digital photo was taken of the sample before matrix was applied. While the sample was wet, it was 'dusted' with crushed crystals of 50:50 DHB:HCCA (Sigma-Aldrich #50149-1G-F) from a manually-agitated 53 μm sieve. After the sample became visibly saturated with matrix, it was dried at 37°C for 1-3 hours. As it dried the agar shrank from 1 mm to ~120 μm thick. Residual matrix was then removed using a gentle stream of compressed air. It is important to note that the plate can be analyzed immediately or stored in a desiccator. Although molecular decomposition during prolonged storage is possible, in our hands, samples stored in a desiccator for two weeks still produce strong ion signal with minimal degradation. A video of the sample preparation is available on youtube (<http://youtu.be/RIQ4BtjSCvI>) and the experimentalist wanting to perform these experiments should read ref 11.

MALDI imaging was performed using a 9.4T solariX equipped with dual ESI/MALDI ion source and Smartbeam II laser set to minimum focus. The m/z range acquired was 200 – 360 with a transient length of 700ms for a broad band resolving power of ~150,000. Single-scan spectra consisting of 500 accumulated laser shots were acquired at a rate of <1s/spectrum and calibrated using the DHB cluster ion at m/z 273.03936 as lock mass before saving. Data were post-processed using a proprietary data reduction algorithm which eliminates baseline data points but keeps intact full peak information. Fleximaging software was used to register the digital photo of the sample plate to the X-Y stage of the instrument so that measurement regions could be drawn around the colonies directly on the imported digital image of the sample. This enabled the direct correlation of the chemistry of microbes with the phenotypes of the microbes and surrounding agar. For the present study, high spatial resolution wasn't a requirement and so MALDI images were acquired at a spatial resolution of 300 μm .

Results and discussions

When two microbes interact, metabolic exchange factors are secreted as a means of chemical communication resulting in synergy, commensalism and antagonism. Key to identifying and characterizing compounds with high activity is to map relationships between compound distribution and any underlying microbial response. Figure 1 illustrates the performance benefits of microbial imaging with solariX. The example shows a narrow segment at m/z 274 from the microbial interaction in which at least 18 distinct ion images are resolved. Five of these ions present clear differentiation to either *P. aeruginosa* or *A.*



fumigatus as seen from the images shown in the figure. When investigating the activity of known target ions or discovering new compounds considerable molecular specificity is gained by separating isobaric ion images. The observation that some of the individual images are clearly specific to an individual microbial colony would otherwise go undetected in lower resolution systems. It is important to note here that ion desorption in solariX is decoupled from the mass measurement, unlike traditional MALDI-TOF, and we therefore observe minimal degradation of resolution or measurement accuracy from the non-conductive agar substrate.

Higher molecular specificity is accompanied by higher measurement accuracy which helps identify the molecular entity being imaged by allowing assignment of a molecular formula to each detected peak. For many metabolites, a measurement accuracy of 1 ppm or less is more than sufficient to determine a single molecular formula for an ion. An example of this is illustrated in Figure 1 using the ion images denoted as 1-5. Each of these five peaks was analyzed by SmartFormula to identify combinations of C, H, N and O would sum to within 5 ppm of the measured m/z and the results are presented in Table 1. With exception of ion 5, m/z 274.2075, a search window as large as 5 ppm returns a single molecular formula for each ion image. Enlarging the search window to 10 ppm

returned a single formula, listed in Table 1 as ion 5a, but on examination, the difference of 10 ppm observed between the calculated and measured m/z for 5a is out of line with differences for peaks 1-4. One must consider the possibility that peak 5 does not represent a monoisotopic ion but rather one that contains 1 or more heavy isotopes. Indeed, the peak labelled M was measured at m/z 274.04249, a difference of 0.80 ppm from the calculated mass of the A+1 peak of [DHB-H₂O]₂+H⁺. When we included heavy isotopes in the potential formulas peak 5 it matches very well to the A+2 peak of nitrohydroquinone (Row 5b, Table 1) a known molecular product of *Pseudomonas*. The difference between the calculated and measured m/z is consistent with peaks 1-4. Further, assignment to this compound is also supported by its image, with its distribution being localized to this colony.

peak	Meas. m/z	only formula in search win.	Calc m/z-meas m/z	Search window
1	274.1051	C ₁₁ H ₁₂ N ₇ O ₂	-1.57 ppm	5 ppm
2	274.1436	C ₁₆ H ₂₀ NO ₃	0.62 ppm	5 ppm
3	274.1800	C ₁₇ H ₂₄ NO ₂	0.53 ppm	5 ppm
4	274.1875	C ₁₁ H ₂₄ N ₅ O ₃	-0.34 ppm	5 ppm
5a	274.2075	C ₉ H ₂₄ N ₉ O	8.40 ppm	10 ppm
5b	274.2075	¹² C ₁₆ ¹³ C ₂ H ₂₆ NO	-0.36 ppm	5 ppm

Conclusion

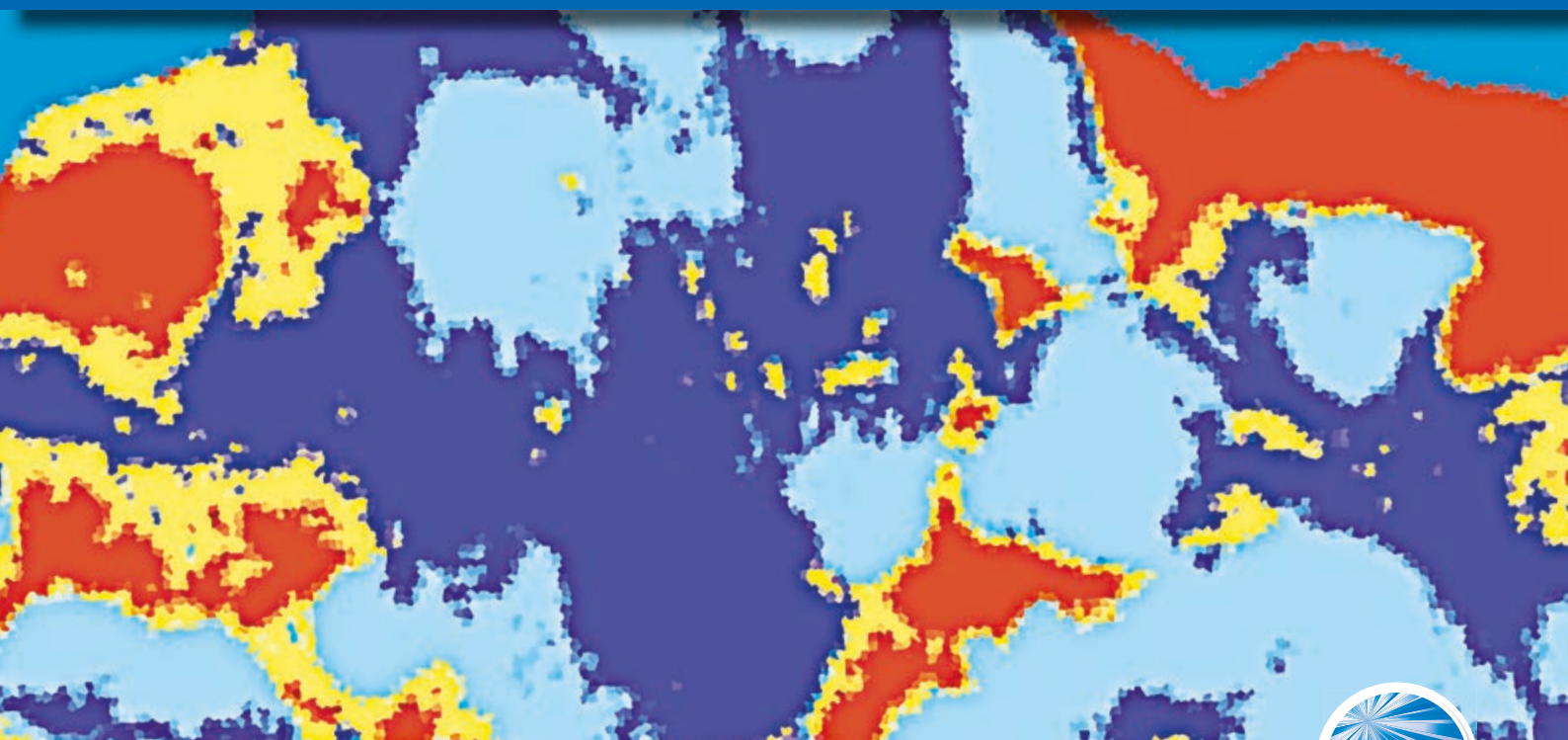
Microbial imaging is a strategy that enables the chemical analysis of microbes grown on agar surfaces under controlled conditions. Using solariX to carry out MALDI-MS imaging, one can utilize its high resolving power to differentiate these species, especially in the lower mass range where the matrix signals and many

of the relevant microbial metabolic exchange factors, virulence factors, and quorum sensors are found. In addition improving the specificity of images solariX can provide molecular formulas to ion images of interest. These capabilities can be invaluable tools for understanding the molecular discussions associated with microbial interactions.

References

- 1 Yang, Y.L., Xu, Y., Straight, P., Dorrestein, P.C., Translating metabolic exchange with imaging mass spectrometry. *Nature Chemical Biology*, 2009 Dec;5(12):885-7.
- 2 Schwamborn K., Caprioli, R.M., Molecular imaging by mass spectrometry — looking beyond classical histology, *Nature Rev Cancer* 10, 639-646 (September 2010).
- 3 Liu WT, Yang YL, Xu Y, Lamsa A, Haste NM, Yang JY, Ng J, Gonzalez D, Ellermeier CD, Straight PD, Pevzner PA, Pogliano J, Nizet V, Pogliano K, Dorrestein PC., Imaging mass spectrometry of intraspecies metabolic exchange revealed the cannibalistic factors of *Bacillus subtilis*., *Proc Natl Acad Sci U S A*. 2010 Sep 14;107(37):16286-90.
- 4 Yang YL, Xu Y, Kersten RD, Liu WT, Meehan MJ, Moore BS, Bandeira N, Dorrestein PC., Connecting chemotypes and phenotypes of cultured marine microbial assemblages by imaging mass spectrometry. *Angew Chem Int Ed Engl*. 2011 Jun 20;50(26):5839-42.
- 5 Gonzalez DJ, Haste NM, Hollands A, Fleming TC, Hamby M, Pogliano K, Nizet V, Dorrestein PC., Microbial competition between *Bacillus subtilis* and *Staphylococcus aureus* monitored by imaging mass spectrometry. *Microbiology*. 2011 Sep;157(Pt 9):2485-92.
- 6 Watrous JD, Dorrestein PC., Imaging mass spectrometry in microbiology., *Nat Rev Microbiol*. 2011 Aug 8;9(9):683-94.
- 7 Liu WT, Kersten RD, Yang YL, Moore BS, Dorrestein PC., Imaging Mass Spectrometry and Genome Mining via Short Sequence Tagging Identified the Anti-Infective Agent Arylomycin in *Streptomyces roseosporus*. *J Am Chem Soc*. 2011 Nov 16;133(45):18010-3.
- 8 Gonzalez DJ, Okumura CY, Hollands A, Kersten R, Akong-Moore K, Pence MA, Malone CL, Derieux J, Moore BS, Horswill AR, Dixon JE, Dorrestein PC, Nizet V., Novel phenol-soluble modulins derivatives in community-associated methicillin-resistant *Staphylococcus aureus* identified through imaging mass spectrometry. *J Biol Chem*. 2012 Apr 20;287(17):13889-98.
- 9 Xu Y, Kersten RD, Nam SJ, Lu L, Al-Suwailem AM, Zheng H, Fenical W, Dorrestein PC, Moore BS, Qian PY., Bacterial biosynthesis and maturation of the didemnin anti-cancer agents, *J Am Chem Soc*. 2012 May 23;134(20):8625-32.
- 10 Gonzalez DJ, Xu Y, Yang YL, Esquenazi E, Liu WT, Edlund A, Duong T, Du L, Molnár I, Gerwick WH, Jensen PR, Fischbach M, Liaw CC, Straight P, Nizet V, Dorrestein PC., Observing the invisible through imaging mass spectrometry, a window into the metabolic exchange patterns of microbes, *J Proteomics*. 2012 Aug 30;75(16):5069-76.
- 11 Yang JY, Phelan VV, Simkovsky R, Watrous JD, Trial RM, Fleming TC, Wenter R, Moore BS, Golden SS, Pogliano K, Dorrestein PC., Primer on agar-based microbial imaging mass spectrometry, *J. Bacteriol*. 2012 Nov;194(22):6023-8.
- 12 Moree WJ, Phelan VV, Wu CH, Bandeira N, Cornett DS, Duggan BM, Dorrestein PC., Interkingdom metabolic transformations captured by microbial imaging mass spectrometry. *Proc Natl Acad Sci U S A*. 2012 Aug 21;109(34):13811-6.
- 13 Rath CM, Alexandrov T, Higginbottom SK, Song J, Milla ME, Fischbach MA, Sonnenburg JL, Dorrestein PC., Molecular analysis of model gut microbiotas by imaging mass spectrometry and nanodesorption electrospray ionization reveals dietary metabolite transformations. *Anal Chem*. 2012 Nov 6;84(21):9259-67.
- 14 Watrous JD, Phelan VV, Hsu CC, Moree WJ, Duggan BM, Alexandrov T, Dorrestein PC., Microbial metabolic exchange in 3D, *ISME J*. 2013 Apr;7(4):770-80.
- 15 Hoefler BC, Gorzelnik KV, Yang JY, Hendricks N, Dorrestein PC, Straight PD., Enzymatic resistance to the lipopeptide surfactin as identified through imaging mass spectrometry of bacterial competition. *Proc Natl Acad Sci U S A*. 2012 Aug 7;109(32):13082-7.

For research use only. Not for use in diagnostic procedures.



- **High-performance MALDI imaging analysis of on-tissue digested proteins in mammalian FFPE tissues using the Bruker rapifleX MALDI-TOF/TOF**

In this application note, we describe a workflow for MALDI Mass Spectrometry Imaging (MSI) of proteins from a variety of FFPE tissues. The method comprises steps of paraffin removal and antigen retrieval followed by on-tissue digestion and deposition of MALDI matrix.

MALDI imaging of the resulting tryptic peptides is performed using the Bruker rapifleX MALDI-TOF/TOF instrument. SCiLS Lab statistical software was used to

highlight regionally specific peptides which can be subsequently identified by direct interrogation with MALDI-TOF/TOF and database searching. An added

dimension of molecular specificity is demonstrated by imaging the tissue using TOF/TOF mode and spatially mapping characteristic fragment ions of target peptides.

Keywords:
rapifleX, MALDI imaging, MALDI-MSI, FFPE tissue, proteins, digestion, TOF/TOF, MS/MS, peptide identification, bioinformatics, statistical data analysis, HTX TM-sprayer, SCiLS Lab

Introduction

Formalin-fixation followed by paraffin embedding (FFPE) is the standard for preserving tissue samples. Many institutions such as hospitals and universities have assembled extensive tissue libraries with corresponding patient information. Therefore, FFPE tissue represents a particularly important type of sample to be dealt with in mass spectrometric imaging (MSI).

Formalin cross-links primary amine groups of protein backbones while paraffin embedding allows for easier sectioning and infinite storage of samples at room temperature. Both processes, however, are inherently incompatible with MALDI, but additional sample processing can be carried out to make FFPE samples amenable for MALDI imaging analysis:

- Paraffin must be removed as it would otherwise interfere with subsequent steps in the sample prep workflow as well as the ionization.
- Antigen retrieval (AR) must be performed to disrupt a portion of the cross-linked protein network to open cleavage sites for endoproteases such as trypsin.

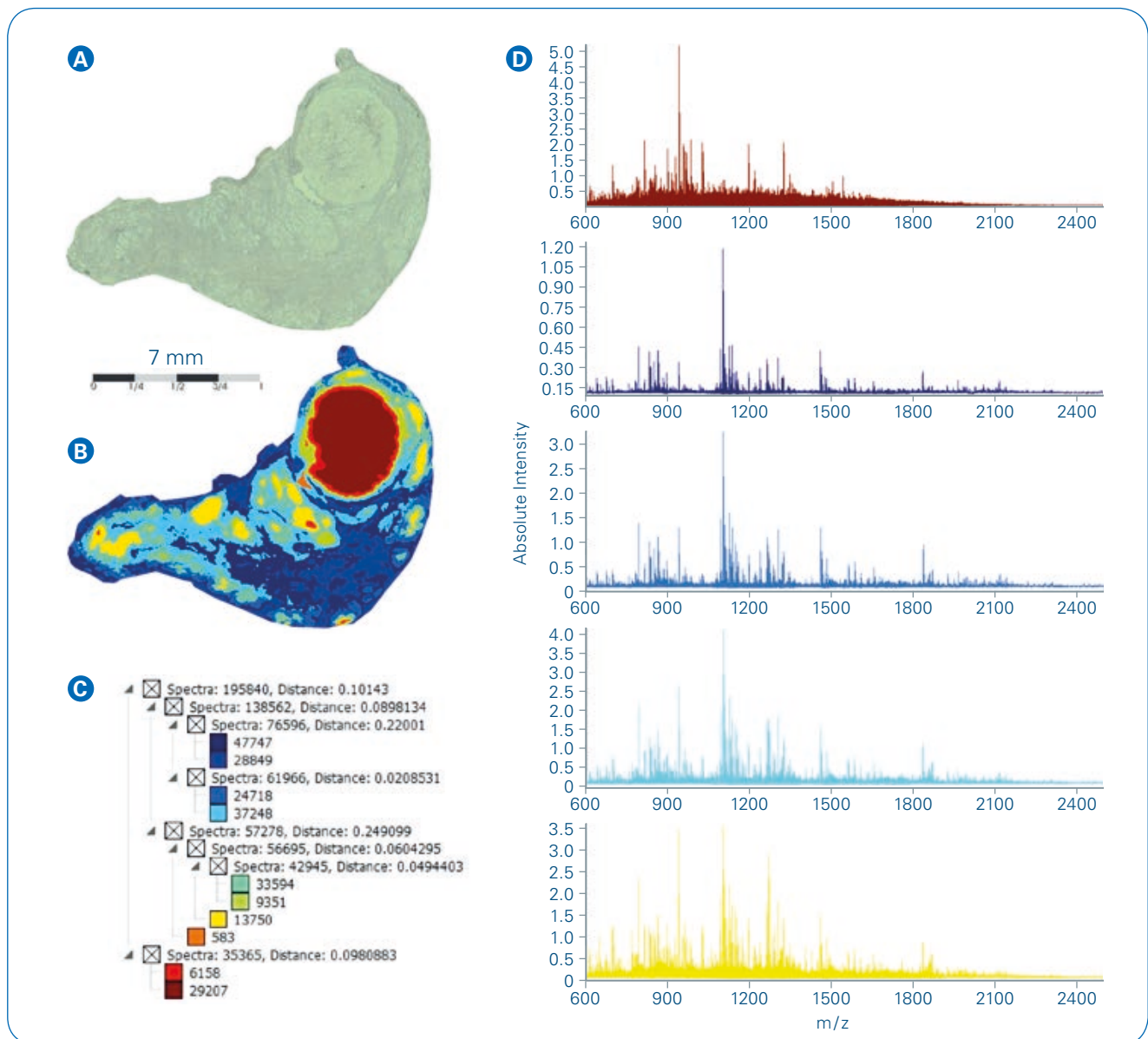


Figure 1: Spatial segmentation analysis of MALDI-MSI dataset from FFPE human thyroid tissue:

A Optical image **B** Segmentation map **C** Segmentation tree **D** Mean spectra of main regions extracted from segmentation result

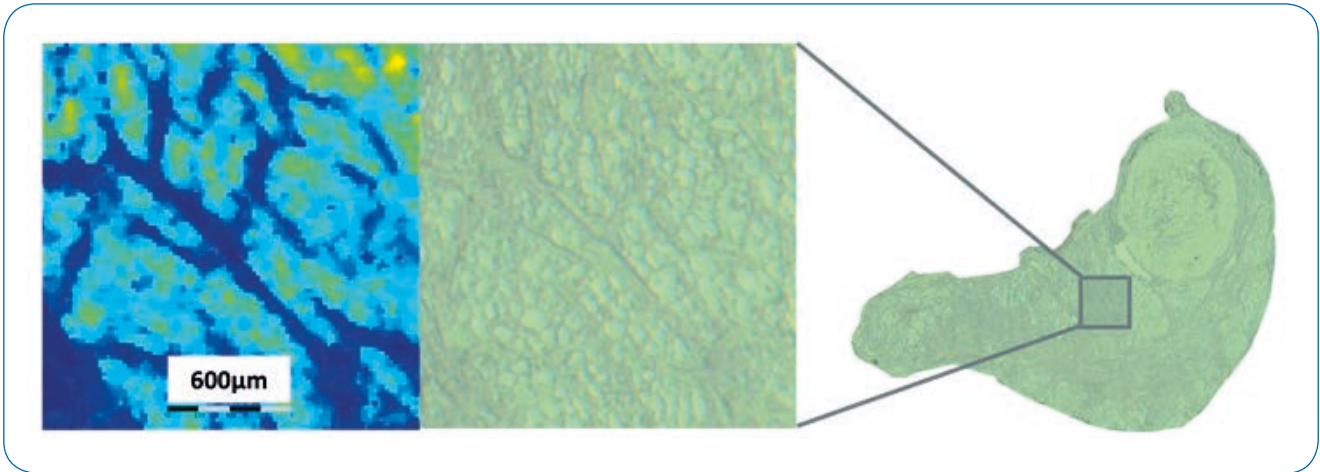


Figure 2: An expanded view of an ion image of m/z 644.4 from a region of human thyroid FFPE tissue to assess the MSI spatial resolution achieved using the sample analysis workflow described. Smallest structural features observed in the MSI dataset are approximately 40-50 μm , i.e. 2 pixels wide.

- Finally, enzymatic digestion is necessary to liberate peptides from the remaining cross-linked protein.

In this application note, we describe a protocol for preparing FFPE tissue

sections for MALDI imaging analysis and apply it to various tissues (human thyroid; human breast cancer; mouse brain) using the rapifleX MALDI-TOF/TOF.

Analyses of the MSI data using SciLS Lab reveals many of the dige-

sted peptides to have distributions specific to tissue pathology. Further, these peptides can be selected for fragmentation by TOF/TOF to identify the originating protein behind.

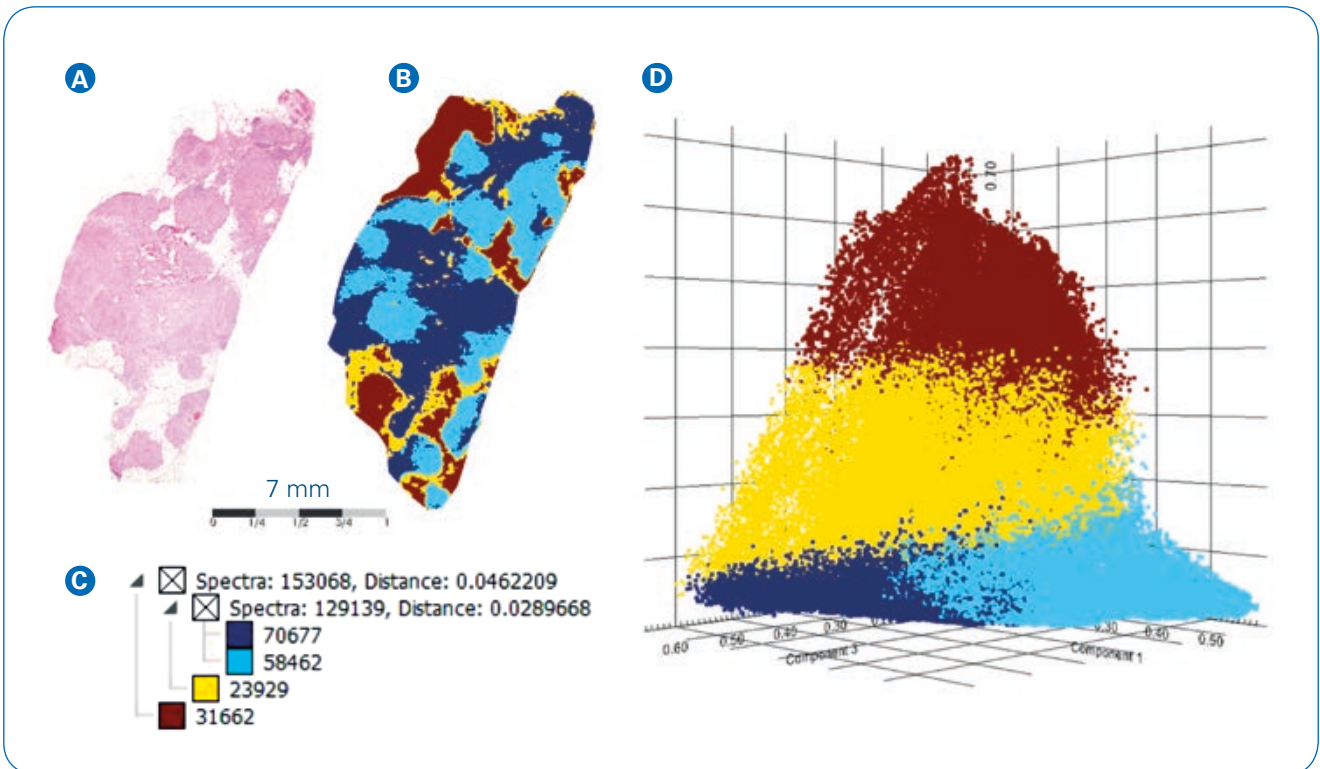


Figure 3: MALDI-MSI analysis of FFPE human breast cancer tissue:

A Co-registered H&E image of tissue section stained post-MALDI **B** Spatial segmentation map **C** Corresponding segmentation tree **D** PLSA Scores plot from the four main segmentation regions

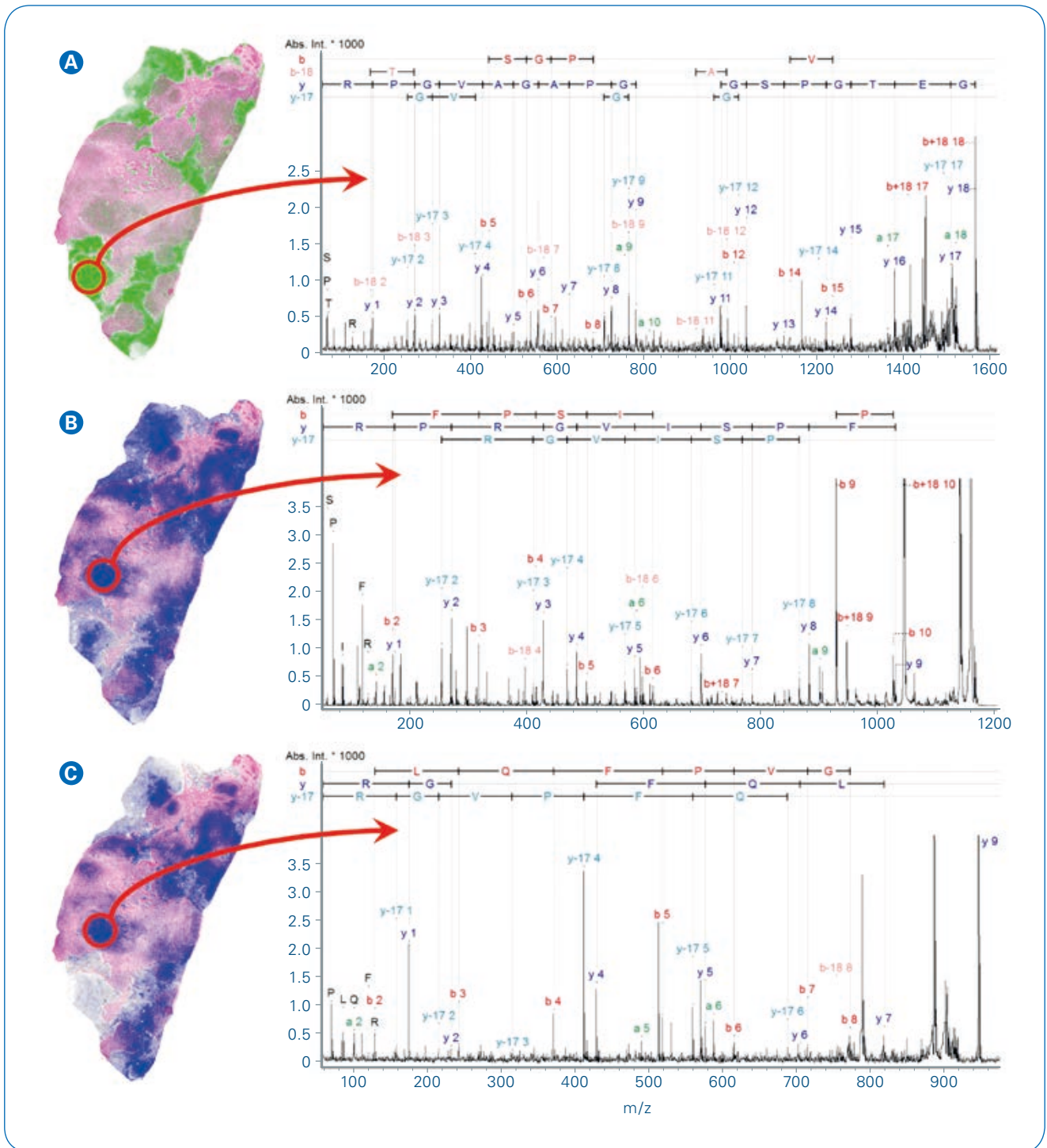


Figure 4: Selected MALDI ion images from FFPE human breast cancer tissue overlaid with co-registered H&E. Peptide identification was achieved by MALDI-MS/MS directly from tissue.

A m/z 1562.8; GETGPGVGPAGAVGPR from Collagen alpha 2 **B** m/z 1198.7; AVFPSIVGRPR from Actin, cytoplasmic 1 **C** m/z 944.5; AGLQFPVGR from Histone H2AV

Experimental

Samples

FFPE tissue sections were mounted on conductive slides precoated with polylysine. Thickness of tissue sections was as follows: human thyroid 6 μm ; human breast cancer 3 μm ; mouse brain 5 μm . Human thyroid sections were provided by Prof. Fulvio Magni, University of Milano-Bicocca, Italy. Human breast cancer sections were obtained from Dr. Zeljko Debeljak, KBC Osijek, Croatia.

Sample preparation

Paraffin removal was carried out applying the following protocol: Slides were vertically oriented and heated at 85 °C for 15 min; slides were rinsed in a succession of baths: xylene (5 min, 2x; first bath was performed immediately after removing slide from oven); isopropanol (5 min, 1x); ethanol gradient (100%, 96%, 70%, 50%, 5 min each); water (5 min, 1x).

Antigen retrieval was performed in a NXGEN decloaking chamber (Biocare Medical) at 110 °C for 20 min using only deionized water as bath. Processed slides were gently cooled down by stepwise partial exchange of the hot bath solvent and were dried under vacuum.

Deposition of trypsin (porcine sequencing grade; Promega) was performed using a HTX TM-sprayer connected to a syringe pump. The deposition method used the following parameters: trypsin solution 25 ng/ μl in 20 mM ammonium bicarbonate buffer; nozzle height 40 mm; nitro-

gen pressure 10 psi; nozzle temperature 30 °C; flow rate 0.03 ml/min; z-arm velocity 750 mm/min; number of passes 8; moving pattern CC; track spacing 2 mm; drying time 0 s.

Sections coated with trypsin were incubated for 2 hours at 50 °C under humidity-saturated atmosphere. After incubation, slides were dried under vacuum for 30 minutes.

Deposition of HCCA matrix was performed on a HTX TM-sprayer connected to an isocratic LC pump applying the following method parameters: HCCA solution 10 mg/ml in ACN:H₂O 70:30, 1% TFA; nozzle height 40 mm; nitrogen pressure 10 psi; nozzle temperature 75 °C; flow rate 0.12 ml/min; z-arm velocity 1200 mm/min; number of passes 4; moving pattern HH; track spacing 3 mm; drying time 0 s.

After MALDI data acquisition, sections were prepared for histological staining by removing the remaining MALDI matrix by washing in 70% ethanol for 2 min and subsequent dip-washing in deionized water. Haematoxylin and Eosin (H&E) staining was performed according to common protocols.

Data acquisition

Prior to deposition of MALDI matrix, slide-mounted tissue sections were scanned on a Reflecta MF-5000 medium format scanner at a resolution of 3200 dpi.

Additional high-resolution optical images of H&E stained tissue sections were acquired on a MIRAX DESK scanner (3DHISTECH) after finishing MALDI data acquisition.

All MALDI-MS imaging data were acquired on a Bruker rapifleX MALDI-TOF/TOF system in positive reflector mode. The following MS image acquisition parameters were applied:

- **Human thyroid:**
20 μm pixel size; 300 laser shots per pixel; m/z 600 – 2500 detection range
- **Human breast cancer:**
25 μm pixel size; 400 laser shots per pixel; m/z 700 – 3200 detection range
- **Mouse brain:**
20 μm pixel size; 400 laser shots per pixel; m/z 700 – 2400 detection range

MALDI-MS/MS spectra of selected peptides were acquired directly from tissue in positive MS/MS mode without the use of collision gas. The number of laser shots accumulated per spectrum varied depending on signal to noise ratio of each peptide. MS/MS imaging of selected precursor peptides was performed using 40 μm pixel size and 1000 laser shots per pixel.

Data analysis

Analyses of imaging data, including co-registration of H&E stained optical images, was performed in SCiLS Lab software. Calculations were performed on datasets normalized to Total Ion Count (TIC).

Results and Discussion

The FFPE sample processing workflow described above was applied to a variety of tissue samples and data analyzed for spatial resolution, correlation with tissue architecture and ability to identify proteins. [Figure 1](#) shows results obtained from MALDI-MSI of human thyroid FFPE tissue. The dataset was spatially segmented in SCiLS Lab using an unsupervised multivariate statistical analysis method. The segmentation map ([Figure 1B](#)) attributes similar digest spectra to a common color and the color mapping reveals tissue heterogeneity as function of protein fingerprint, i.e. as reflected in the individual peptide profiles resulting from on-tissue digestion. The segmentation tree shown in [Figure 1C](#), provides an overview over the hierarchical structure of pixel cohorts within the MSI dataset, i.e. describes the level of similarity/dissimilarity between various pixel cohorts. [Figure 1D](#) presents in a side-by-side comparison the mean spectra representing five main branches (i.e. proposed tissue subtypes) from the segmentation result.

The FFPE sample preparation workflow described here involves a number of steps e.g., incubation with the enzyme and matrix deposition, that bear a certain risk of artificial delocalization of peptides. To assess the spatial resolution that can be achieved using the workflow, [Figure 2](#) shows a zoomed view on the human thyroid tissue section along with the corresponding ion image of m/z feature 644.4. The architectural features visible in this ion image are highly consistent with the structures visible on the corresponding optical image. Further examination reveals that the minimum dimension of structural feature that can be resolved in the image is 40-50 μm , i.e. 2 pixels wide. In a second example, the workflow was used to image

a section of FFPE human breast cancer tissue and results are presented in [Figure 3](#). As before, spatial segmentation analysis of the breast cancer tissue produced the map given in [Figure 3B](#). Together with the corresponding hierarchical cluster tree ([Figure 3C](#)), and the overlaid H&E image ([Figure 3A](#)), the segmentation map indicates a clear differentiation between section areas that represent low density, i.e. fatty and connective tissue (yellow and brown colors) and the higher density tumor tissue (light and dark blue colors), respectively. To cross-validate the segmentation results, the dataset was subjected to Probabilistic Latent Semantic Analysis (PLSA), another method of unsupervised multivariate data analysis that deconvolutes pixel spectra into contributing molecular signatures. On the resulting PLSA scores plot, shown in [Figure 3D](#), the image pixels differentiate into virtually non-overlapping clusters that correspond to the four main branches of the segmentation tree (i.e. low density tissue colored yellow/brown vs. higher density tumor tissue colored light/dark blue). The striking consistency observed when comparing the results obtained from two independent statistical analysis methods illustrates the high level of confidence featured by the MALDI-MSI data.

Statistical analysis of MSI data can yield a number of putative tissue marker ions. The next step is to identify the putative peptide and the protein from which it derived. First choice for such task is tandem-mass spectrometry of the peptides directly from tissue. [Figure 4](#) shows MALDI-TOF/TOF fragment ion spectra of three peptides that were acquired directly from tissue regions of highest local appearance. Precursor m/z 1562.8 ([Figure 4A](#)) was selected for MS/MS analysis as an example of peptides showing high

relative intensity in the low density tissue regions, whereas the other two precursors (m/z 1198.7, m/z 944.5, [Figure 4B-C](#)) were detected at elevated relative peak intensities in the higher density tumor tissue. MASCOT ion searches identified all three peptides at highly significant ion score values.

With an estimated 10,000 proteins expressed in each cell, on-tissue digestion produces a highly complex mixture of analytes. We should expect cases in which multiple nominally-isobaric peptides will cause undesired interferences in MS ion images. To eliminate such interferences, the complete imaging experiment can be performed in MS/MS mode to confirm the results obtained from MS imaging. [Figure 5](#) shows TOF/TOF imaging results obtained from FFPE mouse brain tissue. [Figure 5B](#) shows the MS ion image of m/z feature 1198.7, which was identified using MALDI-MS/MS directly from tissue as peptide AVFPSIVGRPR from Actin, cytoplasmic 1 ([Figure 5C](#)). A subsequent MS/MS imaging experiment was made to confirm the distribution of this peptide. The peptide's most abundant fragment ion $[b+18]_{10}$ at m/z 1042.4 ([Figure 5E](#)) yields an ion image ([Figure 5D](#)) that is consistent with the MS image obtained for m/z 1198.7. The consistency observed between MS and MS/MS imaging results indicates the dominance of the identified actin peptide in its contribution to the MS ion image and excludes any significant interference from other isobaric peptides.

Acknowledgements

We would like to thank Prof. Fulvio Magni, University of Milano-Bicocca, Italy, and Dr. Zeljko Debeljak, KBC Osijek, Croatia, for providing human FFPE tissue sections.

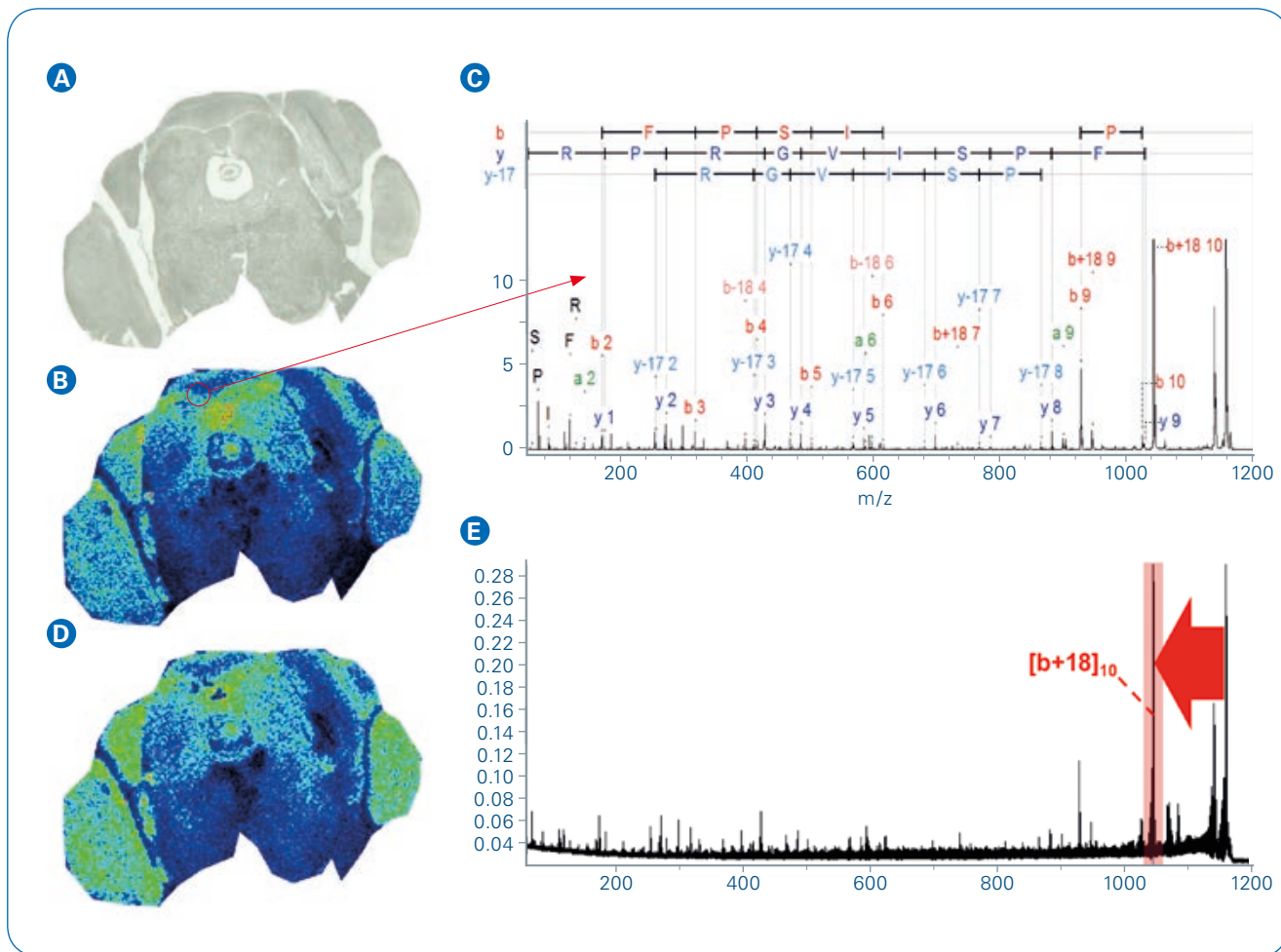


Figure 5: MALDI-MSI analysis of FFPE mouse brain tissue:
A Optical image **B** MALDI-MS ion image of m/z 1198.7 **C** Annotated MALDI-TOF/TOF spectrum of precursor m/z 1198.7 that was acquired directly from tissue and identified as peptide AVFPSIVGRPR from Actin, cytoplasmic 1 **D** MALDI-MS/MS ion image of m/z 1042.6, the most abundant fragment ion ($[b+18]_{10}$) from precursor m/z 1198.7 **E** The mean spectrum from dataset D, red arrow indicates the MS/MS transition used to generate the MS/MS ion image

Conclusions

- A dedicated workflow has been described for preparing samples for MALDI imaging and sophisticated data analysis of FFPE tissue samples, the most commonly found type of tissue sample. Using the protocol for deparaffinization, antigen retrieval and on-tissue digestion, FFPE tissue can be made compatible with both MALDI MS and MS/MS imaging facilitated by the new Bruker rapifleX MALDI-TOF/TOF instrument. Spatial feature resolution of 40-50 μm , limited by delocalization effects inherent in the upfront sample preparation workflow, can be achieved. RapifleX data acquisition is much faster than on any previously available MALDI-MS instrument and integration with SCiLS Lab software allows one to extract highly confident and detail-rich information from the dataset.
- The outstanding MS/MS capabilities of the rapifleX instrument enable straightforward identification of peptides from tissue directly. The instrument's ability to perform fast MS/MS imaging adds another dimension of specificity and allows one to investigate potential interferences that may be induced by the presence of multiple isobaric peptides.

• Metabolomics and Phenomics



Brochures

- Metabolomics
- MRMS aXelerate

Application Notes

- MRMS Powered Single Cell Metabolomics – Quantification of Picogram Amounts of a Biocatalytic Product from Few Living Cells
- Fast Profiling of Sphingolipids Alteration in Hypertension by MRMS
- MRMS aXelerate for Targeted Metabolomics Profiling of Myxobacterial Extracts
- Elucidation of Carotenoids in Microalgae Formulations by MRMS aXelerate
- IFS with Traditional Chinese Medicines on Alzheimer
- Analysis of Metabolic Changes in Murine Hair Follicles
- Rapidly Detected Micropollutants and Plant Response Metabolites in Poplar Leaves
- Automated MALDI MRMS for Biomarker Identification in Large Clinical Sample Sets
- Unambiguous Natural Product ID
- Electron Induced Dissociation for the Differentiation of Isomeric Metabolites of Diclofenac
- Ultrafast Statistical Profiling of Bacterial Metabolite Extracts
- Profiling of Wine Using Ultra-High Resolution Flow Injection MRMS and $^1\text{H-NMR}$ Spectroscopy
- Mapping of Greek Olive Oil Using MRMS Flow Injection Analysis and Multivariate Data Analysis

User Testimonials: Metabolomics



"The performance of our new solariX 7 Tesla MRMS system has met and exceeded all our expectations across a variety of high end metabolic phenotyping challenges in molecular profiling, structure elucidation and imaging- and it is highly user friendly - every laboratory should have one!!"

*Professor Jeremy Nicholson
Director of the Australian National Phenome Center
ProVice Chancellor for Health
Murdoch University*



"Virtually every metabolomics project we have going right now will benefit from this new instrumentation..."

*Arthur S. Edison
Professor and GRA Eminent Scholar, Departments of Biochemistry & Molecular Biology and Genetics Institute of Bioinformatics, Complex Carbohydrate Research Center, University of Georgia, Athens, GA*



"We set up new discovery approaches to describe the compositional space of any complex system in biology and geochemistry. MRMS eXtreme Resolution enables us to address next generation metabotyping, i.e. simultaneous rapid description of hundreds of known and thousands of new metabolites relevant for dynamic biological/chemical processes. MRMS in combination with MetaboScape will also enable other researchers to shed light to this new exciting research field of this yet dark metabolome."

Prof. Philippe Schmitt-Kopplin, Analytical BioGeoChemistry, Helmholtz Zentrum Munchen, Germany

Benefits for Metabolomics

Whether Metabolomics, Phenomics or any other complex sample analysis, large scale sample evaluation is now possible with scimaX and the MRMS aXelerate workflow. The eXtreme Resolution allows for direct sample analysis and enables true high sample throughput complementary to established NMR based solutions. From the largest unknown to the smallest, scimaX ensures confident molecular formula assignment at any level.





Metabolomics

- Novel solutions for Metabolomics, Lipidomics and high-throughput Phenomics

Powerful Yet Intuitive



The metabolome is the final manifestation of biochemical pathways. It shows an extremely large variety of structural classes as it includes the complete set of metabolites of all cellular processes.

Changes in the metabolite composition reflect the outcome (phenotype) of interactions at the genomic, transcriptomic and proteomic levels. Therefore, studying the phenome is a cornerstone to gain deeper insights related to e.g. diseases, therapeutic interventions or environmental influences.

MetaboScope helps to find regulated biomarkers in the global profiling of large sample cohorts and offers tools for automated and confident identification.

MetaboScope software delivers key advantages such as:

- Intuitive **T-ReX** algorithm (**T**ime aligned **R**egion complete **eX**traction) for fully automatic calibration, retention time alignment, adduct management and recursive feature extraction
- T-ReX offers universal processing skills:
New! T-ReX² for MALDI-QTOF-MS
T-ReX 2D for FIA-MRMS and MALDI-MRMS
T-ReX 3D LC-QTOF-MS and LC-MRMS
T-ReX 4D LC-TIMS-MS
- Processing of **large data sets** (> 1000 LC-MS injections) e.g. for ultra-fast chromatography-free FIA-MRMS workflows of > 200 samples/day
- **“Annotation Quality”** scoring boosts confidence in compound identification with up to five specific indicators of data quality
- Workflow integration with SCiLS Lab Pro for identification and spatial distribution mapping of specific metabolites and lipids. This data processing pipeline supports unique timsTOF fleX (MALDI-QTOF-MS) and MALDI-MRMS data

Confidently venture into the unknown

Metabolomics and high-throughput Phenomics

Flow Injection Analysis - MRMS provides high sample throughput for phenomics research with ~5 min cycle time per sample (including both polarities) - more than a factor of 10x faster than conventional LC-MS methods. FIA-MRMS can generate thousands of molecular formulae for metabolites in every sample and reveals additional compounds not detectable via LC-MS. scimaX and solariX platforms also provide complementary MALDI Imaging capabilities for SpatialOMx.



The Phenomics Workhorse

Complementary deep metabolomics by UHPLC-QTOF-MS/MS can 'detect' thousands of features and identify hundreds of metabolites by combining different LC methods and positive and negative ion runs. The impact II is perfectly suited to meet the demands of large profiling studies.



The Phenomics Workhorse featuring TIMS and MALDI Imaging

The technology of the impact II raised to the next dimension: The timsTOF instrument series offers **T**rapped **I**on **M**obility **S**pectrometry and gives access to the exact collisional cross section values for higher confidence in compound IDs. The combined ESI and MALDI source on the novel timsTOF fleX enables direct localization of lipids, metabolites, and drugs for an integrated spatial omics workflow that combines MALDI Imaging and ESI-based metabolomics and lipidomics on the same platform.



NMR based clinical research phenomics

Avance IVDr 600 MHz NMR can measure ~250 plasma or serum samples per day, and reliably identifies and quantitates the ~100+ most abundant metabolites in phenomics research, e.g., in the IPCN*.



For research use only

* IPCN = International Phenome Center Network (led by Prof. Jeremy Nicholson, ICL)

How robust is your data quality over a sequence of several weeks? –The “Phenomics workhorse”

Achieving a high data quality is mandatory for complex profiling experiments. Large batches of samples frequently bring along an increasing build-up of contamination. The larger the batch, the more important a steady data quality becomes for subsequent statistical calculations.

The impact II offers outstanding robustness and excellent long-term stability for long sample sequences typical of large cohort studies, making it truly a phenomics workhorse.

Figure 1 shows the development of data quality over > 1100 injections, covering a time span of more than 14 days [1]. The mass accuracy and the isotopic pattern quality (mSigma value) e.g., of uric acid did not degrade. As well, the peak areas showed no decreasing trends.

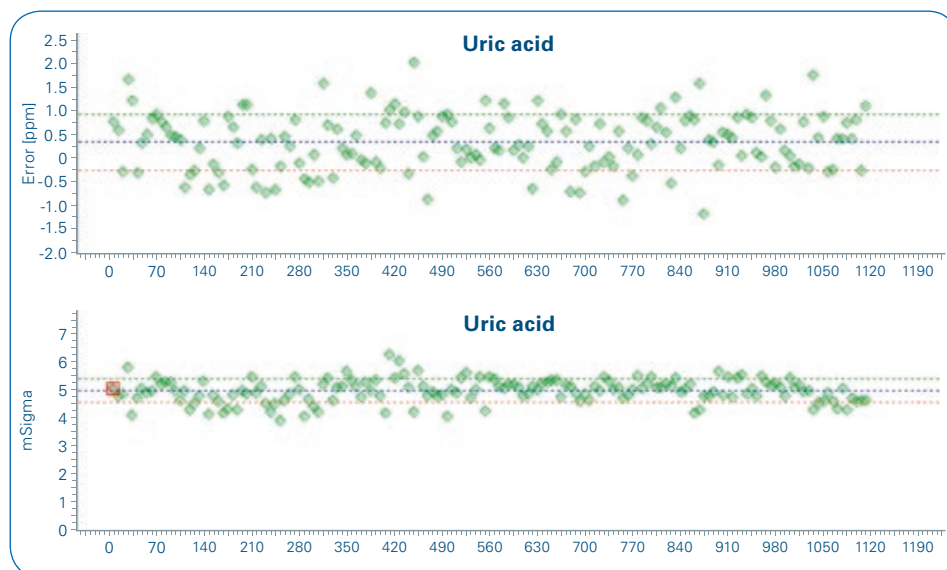


Figure 1: Development of mass accuracy and isotopic pattern quality over > 1100 injections. Every 7th data point is shown

The Phenomics workhorse delivers:

- Unmatched long-term stability of data quality
- No compromise Full Sensitivity Resolution
- InstantExpertise™ for simultaneous acquisition of MS and MS/MS information in “one shot”
- Isotopic pattern fidelity, facilitating molecular formula generation
- Dynamic range of > 4 orders of magnitude for quantitative performance without limitations



[1] The data was acquired following a fixed standard operating procedure: M.R. Lewis, J.T.M. Pearce, K. Spagou, M. Green, A.C. Dona, A.H.Y. Yuen, M. David, D.J. Berry, K. Chapell, V. Horneffer-van der Sluis, R. Shaw, S. Lovestone, P. Elliott, J. Shockcor, J.C. Lindon, O. Cloarec, Z. Takats, E. Holmes, J.K. Nicholson, *Analytical Chemistry* (2016), **88**, 9004-9013

Simplified T-ReX LC-QTOF solution for non-targeted Metabolomics

Confidently identifying compounds relevant for metabolic processes relies on several crucial steps, including sample preparation, data acquisition, data pre-processing and data evaluation. In order to simplify and harmonize this workflow, Bruker developed the **T-ReX LC-QTOF solution**:

1. Sample preparation

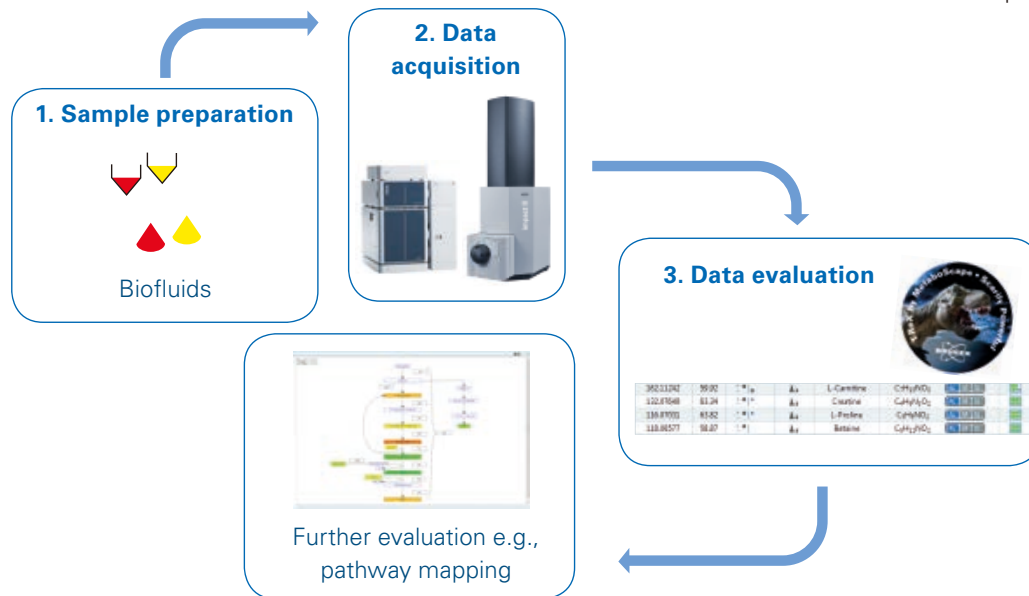
- Standard Operating Procedures (SOPs) for the preparation of typical clinical research samples, e.g., urine and plasma

2. Data acquisition

- ELUTE UHPLC for analyzing large sample cohorts with high retention time stability
- Metabolomics Reverse Phase column kit to enable matching of retention times to the Bruker HMDB Metabolite Library 2.0
- impact II QTOF-MS system, with a robust performance for large profiling studies of complex samples

3. Data evaluation

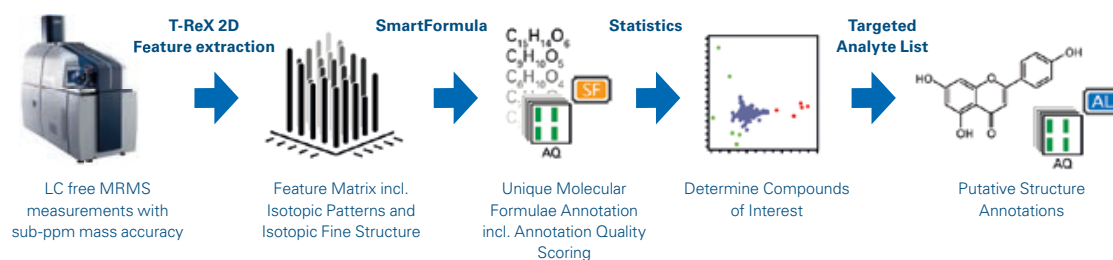
- MetaboScape software for automatic identification of known compounds, incl. the T-ReX 3D algorithm for a minimized false negative rate in statistical analysis
- Bruker HMDB Metabolite Library 2.0, providing MS/MS spectra for > 880, and retention time information for > 600 metabolites, as prerequisite for confident identification of relevant markers
- Bruker MetaboBASE Personal Library 3.0: MS/MS spectra from more than 100,000 compounds – endogenous metabolites, drugs, pesticides and other chemical entities
- Annotation Quality Scoring: A fast overview of the confidence of each annotation parameter



Dr. Liang Li, Professor of Chemistry, University of Alberta, Canada

"We are delighted to have collaborated with Bruker to produce the comprehensive T-ReX LC-QTOF solution. The complete out of the box solution provides the basis for high confidence identification of relevant known endogenous metabolites and enables to set these into a biological context using pathway mapping. This solution will provide researchers a head start in non-targeted metabolomics for typical research samples like urine or plasma."

Achieve high sample throughput with MRMS aXelerate ...



Perfect for Metabolomics, Phenomics or any other large-scale sample evaluation:

MRMS aXelerate is based on the extreme resolving power of the scimaX MRMS system and uses MetaboScape to enable a powerful chromatography-free solution.

The FIA-MRMS approach enables the measurement of > 200 samples per day in both, positive and negative ion modes.

The extreme resolution allows for direct sample analysis and enables true high sample throughput complementary to established NMR based solutions. From the largest unknown to the smallest, MRMS aXelerate utilizes a combination of ultra-high mass accuracy, True Isotope Pattern, and Isotopic Fine Structure to ensure confident assignments of molecular formulae at any level.

- **Accelerate** sample throughput enabling large cohort and longitudinal studies in phenomics research (> 200 samples/day)
- **Simultaneous analysis** of known and unknown metabolites
- **Access compounds** not readily detectable by LC-MS analysis



Prof. Philippe Schmitt-Kopplin, Analytical BioGeoChemistry, Helmholtz Zentrum München, Germany

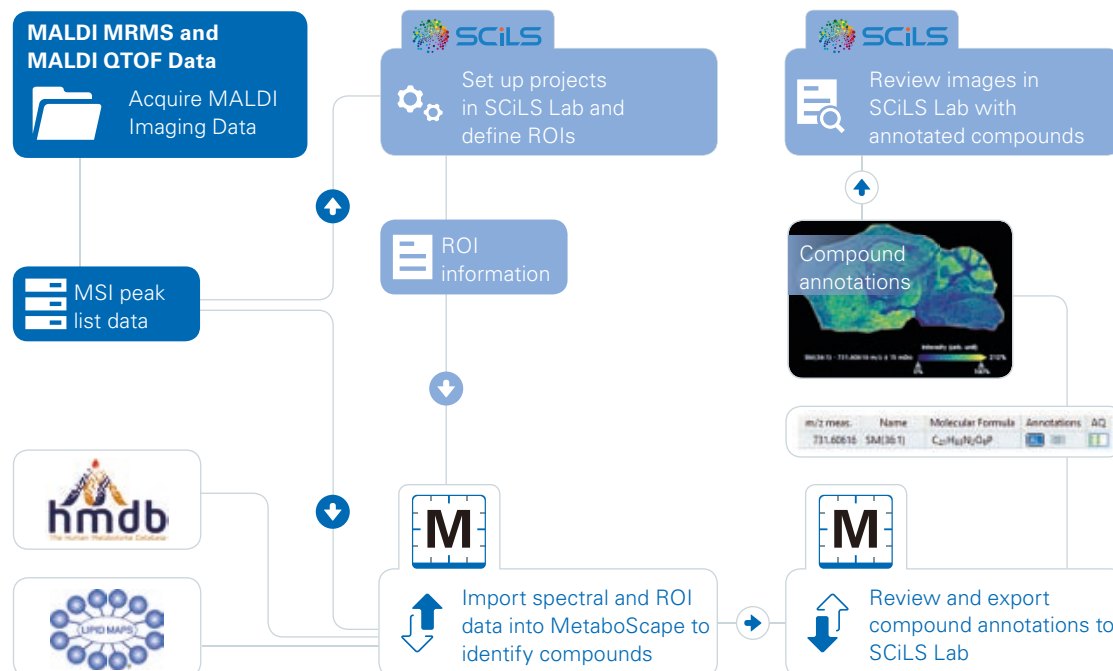
"We set up new discovery approaches to describe the compositional space of any complex system in biology and geochemistry. MRMS eXtreme Resolution enables us to address next generation metabolotyping, i.e. simultaneous rapid description of hundreds of known and thousands of new metabolites relevant for dynamic biological/chemical processes. MRMS in combination with MetaboScape will also enable other researchers to shed light to this new exiting research field of this yet dark metabolome."

Discover – Validate – Localize, Think Biology!

Spatial Metabolomics by MALDI Imaging

- Direct localization of lipids, metabolites, drugs, and peptides
- SCiLS Lab and MetaboScape featuring a novel mass spectrometry imaging bioinformatics pipeline for identification of metabolites and lipids from tissue making use of T-ReX²
- Supporting MALDI-MRMS for high selectivity using extreme resolution and providing Isotopic Fine Structure for unambiguous formula assignment
- Leveraging timsTOF fleX by enabling on the same platform:
 - MALDI Imaging for discovering relevant ions
 - Confident identification of targets in MetaboScape
 - Optional validation and improved annotation confidences by complementary chromatographic retention times- and ion mobility cross section and PASEF-MS/MS

Novel Mass Spectrometry Imaging Workflow



Novel mass spectrometry imaging workflow: Automated annotation of metabolites and lipids from tissue
*Lipid Maps and HMDB are not Bruker products.

Look Out!

MetaboScape will provide deeper insights and simplify your metabolomics and lipidomics data processing



The "Phenomics workhorse": the impact II LC-QTOF provides outstanding robustness for large cohort studies



scimaX MRMS aXelerate enables the measurement of > 200 samples per day with chromatography-free acquisitions for large-scale profiling studies



Confidence by powerful T-ReX feature extraction technology

timsTOF fleX provides MALDI Imaging and LC based metabolomics and lipidomics capabilities



For research use only. Not for use in clinical diagnostic procedures.

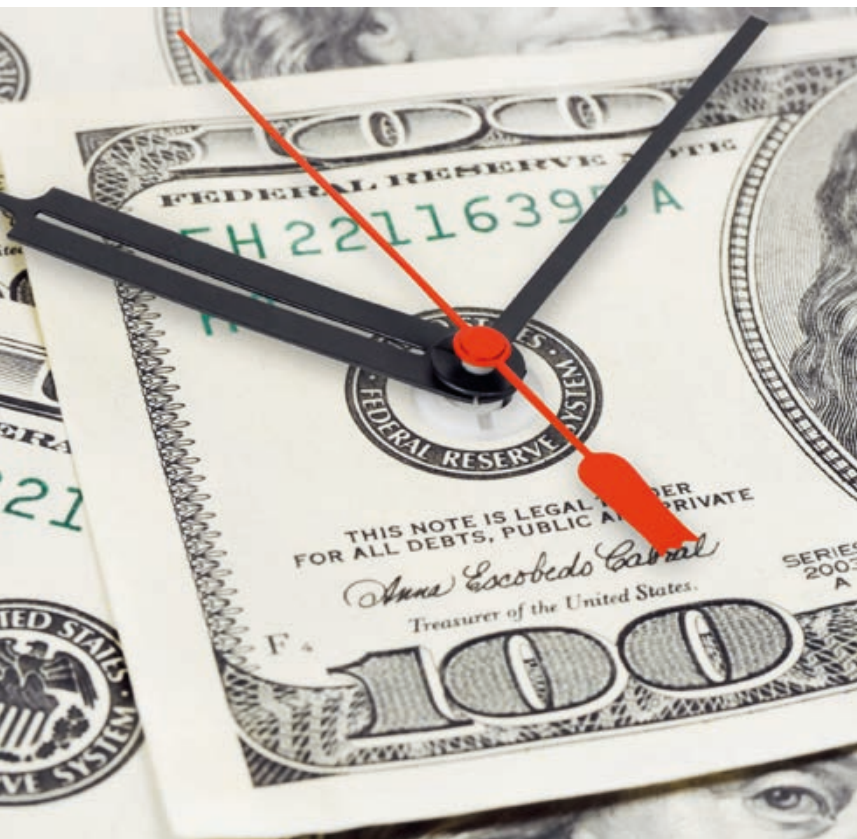


MRMS aXelerate

- Phenomics, Metabolomics and beyond

Answers in Minutes not Hours

Flow Injection Analysis



The chemical complexity of clinical samples is traditionally measured by GC- or LC-MS. While powerful, the performance is dependent on the time invested, limiting throughput and coverage.

What if we can eliminate the time consuming LC step and still provide the answers needed in minutes? Flow injection analysis (FIA), provides an additional and unique tool to Metabolomics and Phenomics labs.

MRMS, Magnetic Resonance Mass Spectrometry, is the pinnacle of MS for both resolving power and mass accuracy. This performance provides the foundation for the utility of the FIA-MRMS workflow, or simply MRMS aXelerate.

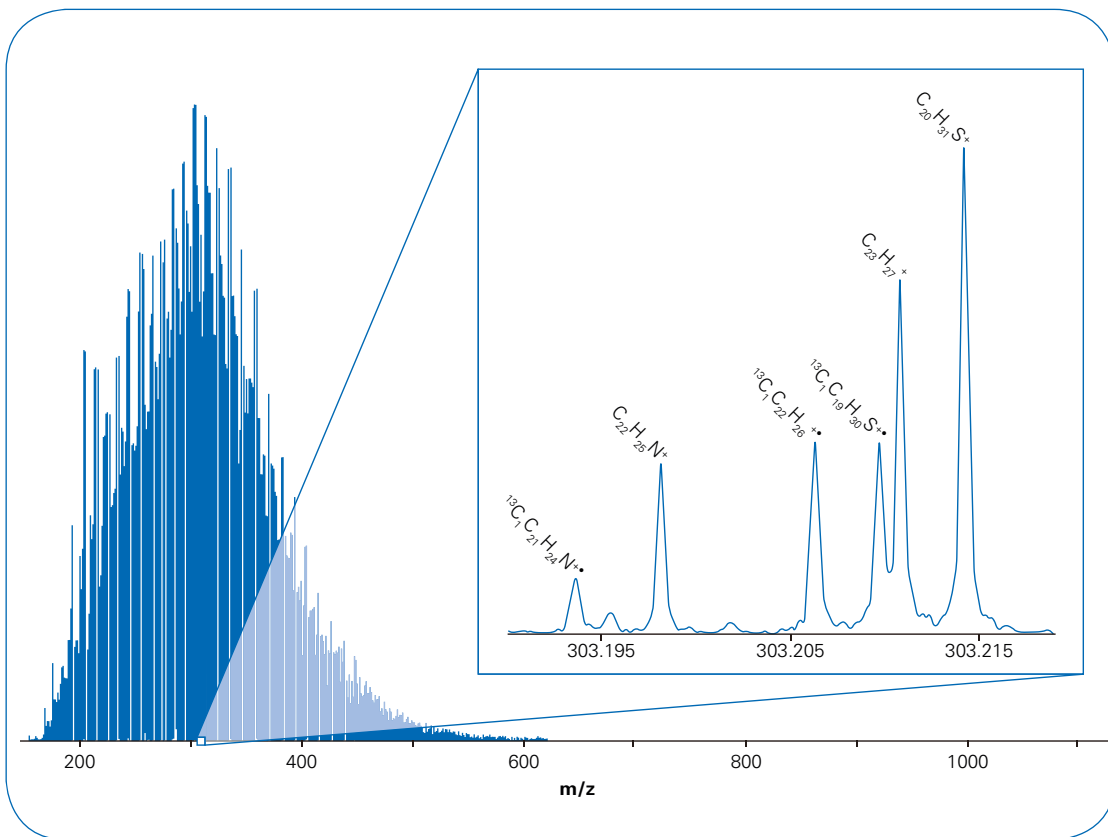
Knowing the value of the FIA-MRMS workflow allows researchers to move beyond the conventional concerns of dynamic range and ion suppression and apply this new information to solving real problems, as is being done in the oil industry. (see adjacent page)

Traditional Metabolomics and Phenomics labs are already discovering the many benefits of MRMS aXelerate.

Complex Mixture Analysis

FIA and Industry

FIA-MRMS is a proven workflow for major petrochemical companies as it provides real answers to real problems. Essentially ancient metabolites, crude oil serves as the worst case scenario for LC free analysis, especially when compared to clinical samples.



FIA

Provides Real Solutions For The Petroleum Industry

Corrosion Issues Prevention

Asphaltene Characterization

Biodegradation

Catalyst Poisoning

Environmental Monitoring

Reservoir Characterization

Process Optimization

Emulsion Stability

Waste Water Treatment

Dissolved Organic Matter

Finding a Needle in a Haystack

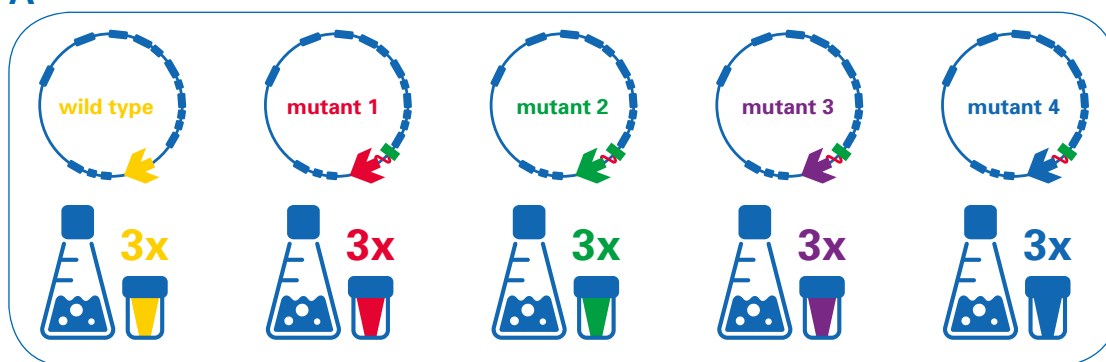
Rapid Statistical Analysis

M

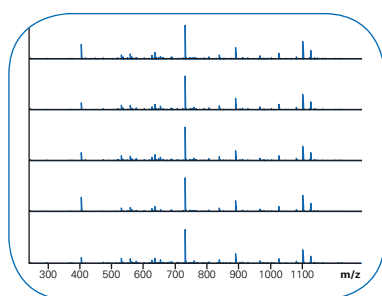
Rapid, LC-free MS followed by statistical analysis provides a sensitive, high-throughput workflow for modern phenotyping and metabolotyping.

Workflow: A: Generate a series of different samples B: Rapidly measure high resolution mass spectra C: Perform rapid statistical analysis D: Discover unique biomarkers

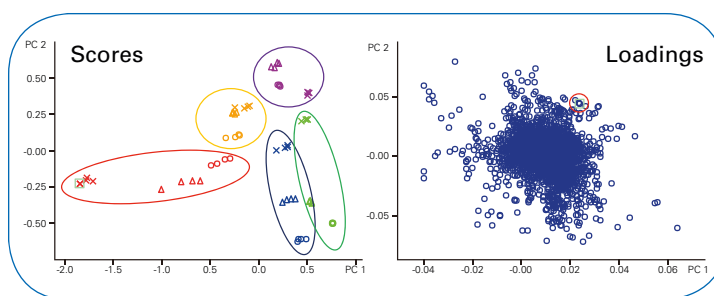
A



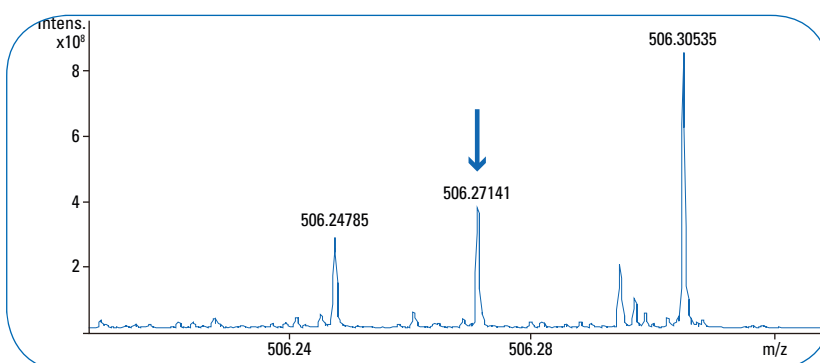
B



C



D

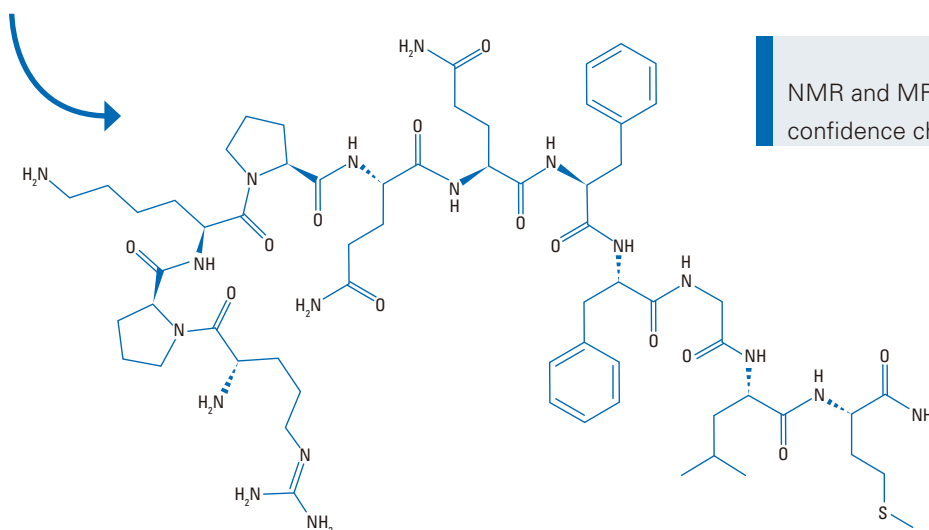
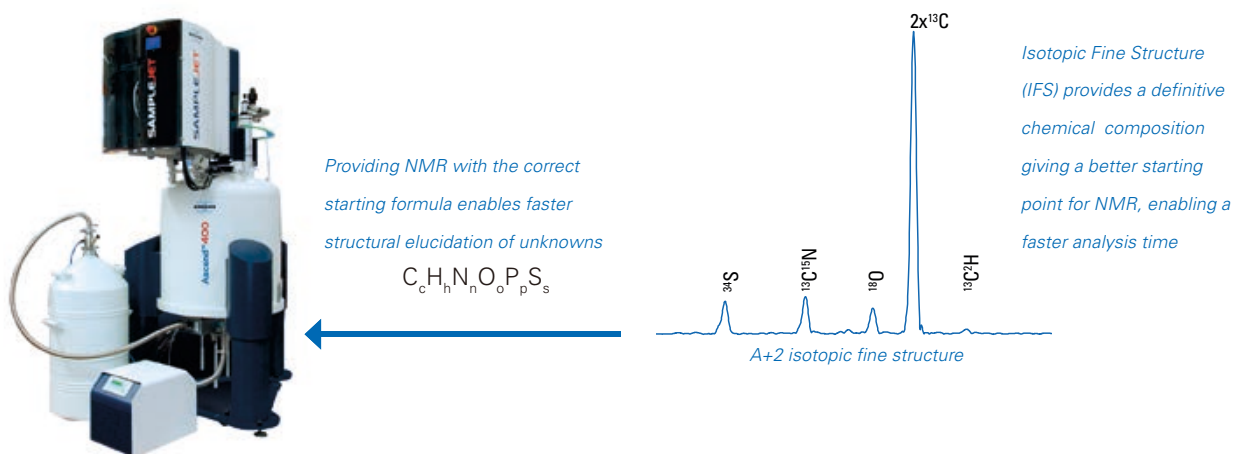


If required, additional analysis can be run for quantitation, MS/MS, or any further analysis.

Composition and Structure

Isotopic Fine Structure

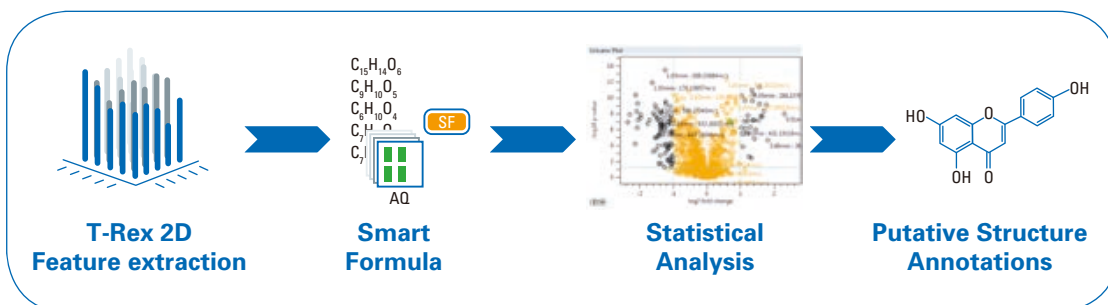
NMR is the gold standard for structural analysis and ID; however, it can be very time consuming if structural elucidation is done blindly. Providing the exact formula greatly improves the confidence in identification, and drastically increases the analysis time and overall throughput.



NMR and MRMS provide a high confidence chemical assignment

MRMS aXelerate

The Complete Solution



- Accelerate throughput (> 200 samples/day)
- Complementary to established NMR based solutions
- Simultaneous analysis of known and unknown metabolites
- Access compounds not readily detectable by LCMS analysis
- 3-tiered confidence in annotation



Prof. Philippe Schmitt-Kopplin Analytical BioGeoChemistry,
Helmholtz Zentrum München, Germany

"MRMS eXtreme Resolution enables us to address next generation metabotyping, i.e. simultaneous rapid description of hundreds of known and thousands of new metabolites relevant for dynamic biological/chemical processes."

Pushing the Frontiers

of Scientific Discovery

Systematic isolation and structure elucidation of urinary metabolites optimized for the analytical-scale molecular profiling laboratory.

Matt Lewis and co-workers

Anal. Chem. 2019, 91, 14, 8873-8882

A *de novo* strategy for the structural elucidation of urinary metabolites, where MRMS provides a high-confidence starting point for NMR analysis, increasing the efficiency and reducing the time required for complete structural elucidation.

A metabolomic study based on accurate mass and isotopic fine structures by dual mode combined-FT-ICR-MS to explore the effects of *Rhodiola crenulata* extract on Alzheimer disease in rats.

Fei Han and co-workers

J Pharm Biomed Anal. Vol 166, p347-356 (2019)

A dual mode MRMS strategy (HPLC & Fractionation) is applied to profile biochemically the metabolic pathways of plasma serum of Alzheimer disease rats affected by *Rhodiola crenulata* extract.

Potential of dynamically harmonized Fourier transform ion cyclotron resonance cell for high-throughput metabolomics fingerprinting: control of data quality

Estelle Rathahao-Paris and co-workers

Anal Bioanal Chem. 410 (2), 483-490 (2018)

Details the utility and robustness of the FIA-MRMS workflow for performing large-scale high-throughput metabolomic analyses under routine condition.

Coculture of Marine Invertebrate-Associated Bacteria and Interdisciplinary Technologies Enable Biosynthesis and Discovery of a New Antibiotic, Keyicin

Tim S. Bugni and co-workers

ACS Chem. Biol., 12 (12), pp 3093–3102 (2017)

As part of a larger complete antibiotic discovery process, Isotopic Fine Structure provides the exact molecular formula to identify the novel antibiotic.

Metabolomics reveals metabolic biomarkers of Crohn's disease

Philippe Schmitt-Kopplin and co-workers

PloS one, 4 (7), e6386 (2009)

Non-targeted metabolic profiling is used to determine the contribution of metabolites produced by the gut microbiota towards disease status of the host. MRMS is used to discern the masses of thousands of metabolites.

Molecular Profiling



Traditional Chinese Medicine



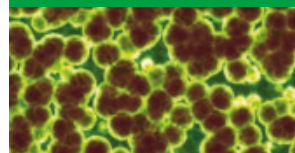
High Throughput



Natural Products



Biomarkers



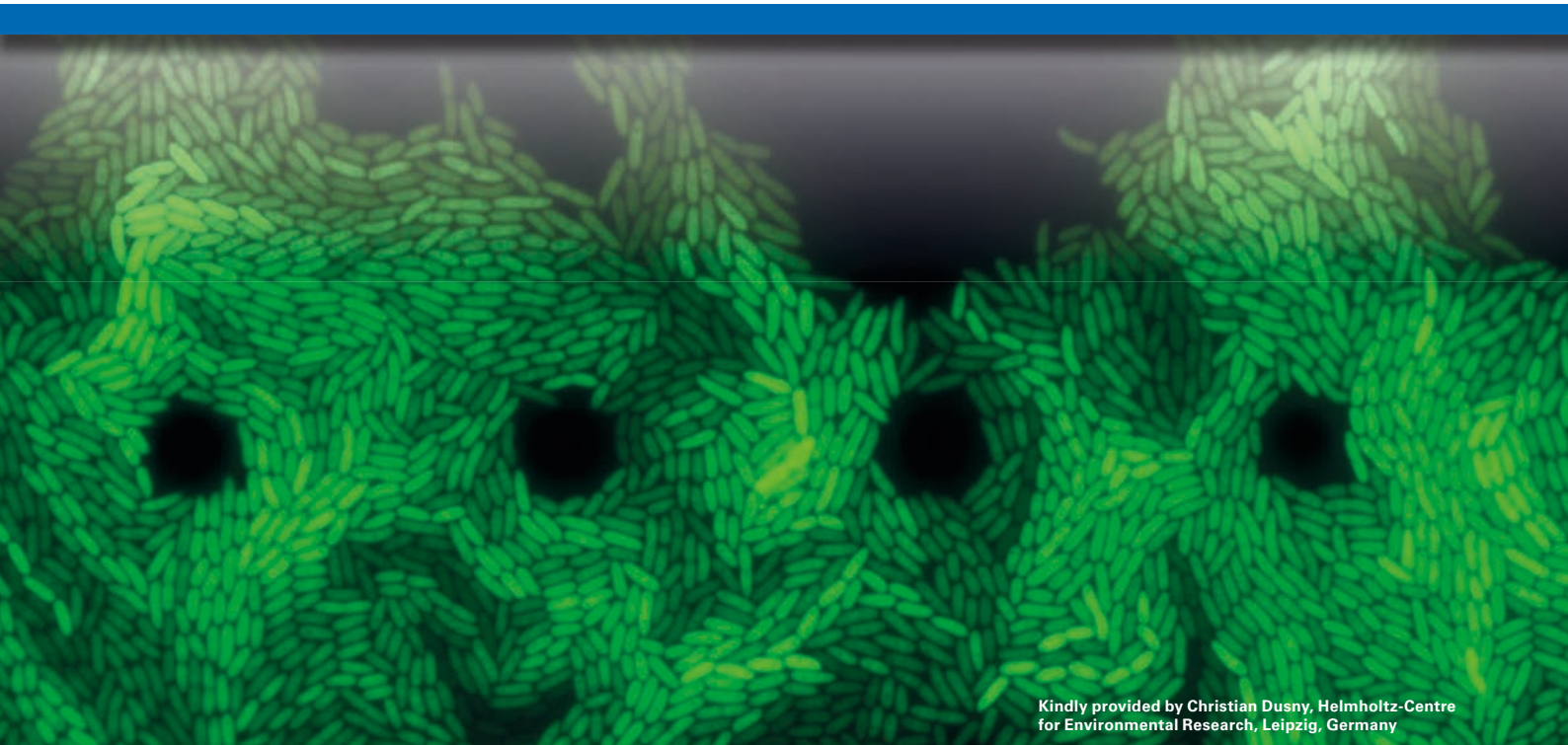
scimaX

Taking science to the max



Gone are the days of weekly or yearly liquid cryogen fills. Bruker's novel conduction-cooled Maxwell™ magnet technology essentially makes the magnet 'invisible'.

For research use only. Not for use in clinical diagnostic procedures.



Kindly provided by Christian Dusny, Helmholtz-Centre for Environmental Research, Leipzig, Germany

● MRMS powered single cell metabolomics – Quantification of picogram amounts of a biocatalytic product from few living cells

Single cell metabolomics via mass spectrometry can successfully cope with many related analytical requirements such as very small volumes and low analyte concentrations typically found in intra- and extracellular media.

Abstract

Probing the metabolic state of **living** microbial cells via their secreted metabolic products is highly challenging as it requires measures to maintain the

cellular integrity and to collect the analytes. This application note demonstrates how direct infusion magnetic resonance mass spectrometry (DI-MRMS) is able to quantify lysine produced by a few intact microbial

cells. The high mass resolution and sensitivity of MRMS in combination with a reliable sample introduction and transfer is a helpful tool for assessing cellular processes.

Keywords:
solariX, single cell analysis, metabolomics, MRMS

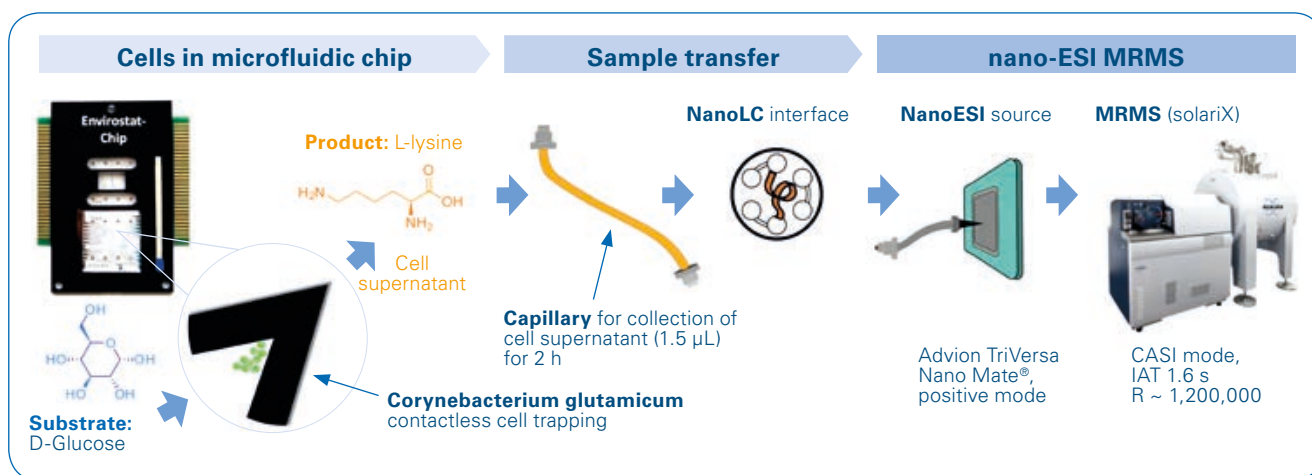


Figure 1: Workflow for the analysis of single cell secretome using MRMS [1].

Introduction

Information on the metabolic state of individual cells in a population can't be generated from a bulk analysis of the culture. Microfluidic systems are powerful tools to study living single cells. These miniaturized bioreactors enable the precise control, growth, and monitoring of single cells [1]. While optical methods to study single cells are well advanced, mass spectrometric applications are mostly limited to destructive imaging techniques such as MALDI. To better understand the metabolic activity and metabolite productivity of a living cell, label-free analytical concepts for the detection of minute amounts of secreted low molecular weight compounds are needed.

Here, we report an analytical framework that interfaces non-invasive microfluidic trapping and cultivation of a few bacterial single cells (*Corynebacterium glutamicum* DM1919 pSenLys) with the quantification of their catalytic products by DI-MRMS (Figure 1) [1].

The main challenges of this framework are:

- Transfer of a small sample volume (~1 μL) to the ion source
- Detection of secreted metabolites at low concentration ($\text{pg-ng cell}^{-1} \text{h}^{-1}$)

- Matrix effects caused by the buffer and possible isobaric/isomeric interferences.

Methods

Cell sampling and transfer of μL -sample volumes

Cell populations of *C. glutamicum* DM1919 were cultivated using CGXII medium, harvested, washed, and transferred to the microfluidic Envirostat chip [2]. Microfluidic cultivations with the Envirostat were performed in glucose-containing ammonium bicarbonate (ABC) buffer to facilitate subsequent direct infusion ESI analysis. Cell supernatants from Envirostat cultivations (i.e. medium with the secreted product lysine) were collected in 1.5 μL PEEK-capillaries (Waters Corporation, USA). After 12 h of incubation, the capillary was removed, sealed with PEEK-MicroTight adapters and immediately transferred to the MRMS for mass spectrometric analysis (Figure 2).

nanoESI-DI-MRMS measurements

All mass spectrometric measurements were performed with a 12 T solarix XR MRMS system. A nanoESI ion source (TriVersa Nanomate, Advion BioSciences) was used in positive ion mode (dry gas flow: 8 L/

min, dry temperature: 150°C, capillary voltage: 1.7 kV). An LC-coupler (20 cm fused silica capillary, Advion BioSciences) was connected to a six-way auto-sampler valve of a NanoLC system (Ultimate 3000 nanoRSLC, Thermo Fischer Scientific) via a nanoViper-capillary (ID: 20 μm , OD: 1/16", length: 750 mm, Thermo Fischer Scientific). LC-Coupler and nanoViper capillary were connected with a PEEK-MicroTight adapter (P-882, IDEX Health & Science LLC). The cell supernatant was transferred into a 1 μL nanoViper sample loop and subsequently transported to the nanoESI source with a flow rate of 150 nL/min. A solution of 1:1 (v/v) ultrapure water and methanol, supplemented with 0.1% (v/v) formic acid was used as eluent.

CASI mode (Continuous accumulation of selected ions) was used at m/z 147.5 with a window size of ± 2.5 Da centering the quasimolecular ion of lysine ($[\text{M}+\text{H}]^+$, m/z 147.112804) and its isotopologue. Mass spectra were recorded in the mass range m/z 73–1000 and time of flight of 0.6 ms using broadband mode detection. Data were processed in magnitude mode with data size 8 MW (transient length of 3.5 s). 64 single scans were co-added with an ion accumulation time (IAT) of 1.6 s per

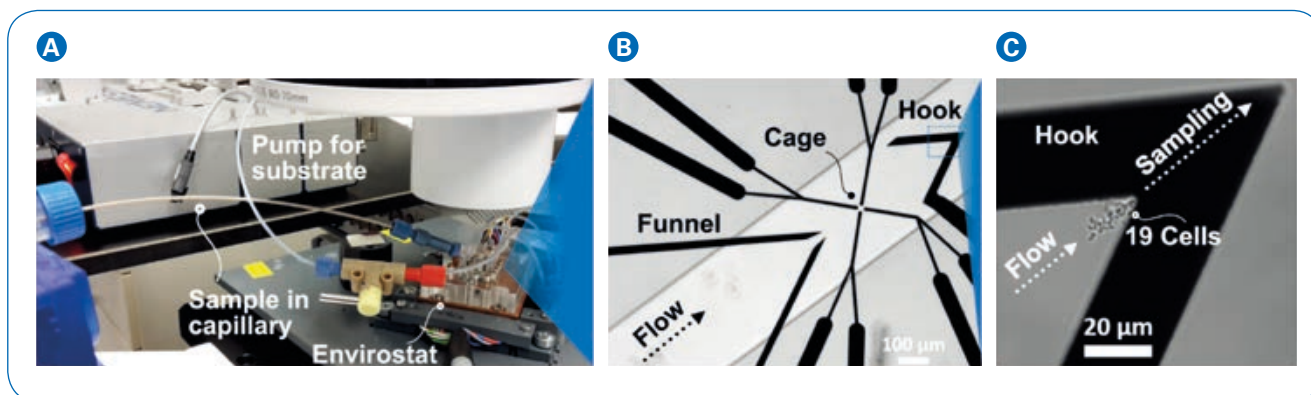


Figure 2: (A) Setup for sampling the secretome from a few microbial cells. (B) Flow path inside the Envirostat chip: in the microfluidic channel cells are focused in the funnel and can be captured either in the cage or in the hook. (C) Zoom into the region around the hook: 19 cells are captured contactlessly by negative dielectrophoresis while the secreted metabolites were sampled for 2 h [1].

scan. Peaks were picked when their signal-to-noise (S/N) ratio was greater than four. Peak intensities were used for quantification. Instrumental limits of detection and quantification were determined by taking mean peak intensities plus 3× and 9× the respective standard deviation of repeated blank measurements.

As internal standard, $^{15}\text{N}_2$ -labeled L-lysine (Sigma-Aldrich) was used. For method blank assessment, PEEK capillaries were filled at the outlet of the Envirostat under cultivation conditions (before cell transfer) and injected as described above.

Results

Transfer of μL -Volumes to MRMS

The transfer of μL sample volumes to a mass spectrometer is routinely performed with LC-systems and appropriate autosamplers and vials. However, this procedure is not feasible for small total available sample volumes of 1 μL and less. The injection-system would require more volume than a single cell sampling approach would deliver, thus wasting valuable sample. Sampling of a microfluidic bioreactor (Envirostat) in vials bears the risk of sample contamination, and solvent evaporation,

thus changing metabolite concentration. In contrast, the sampling of μL -volumes of secretome samples in PEEK-capillaries allows for a direct hyphenation to the Envirostat and storage of the sample overnight. Directly, connecting the capillary to a nanoLC injection valve is a functional setup for the lossless transfer of the 1.5 μL secretome samples (Figure 3). A reliable aliquotation and injection of 1 μL of the sample was possible using the autosampler valve and syringe.

Since the focus was on the analysis of a highly polar, basic amino acid (i.e. lysine) direct-infusion MRMS provided an “unbiased view” into the sample without altering the composition of the sample. However, the sensitivity of the analysis was limited by a background signal on the exact mass of lysine. To limit the effect of the blank, the application of a (nano)-LC-separation could be beneficial.

Since a volatile buffer was used for cell cultivation (ammonium bicarbonate) desalting of the sample before analysis was not necessary.

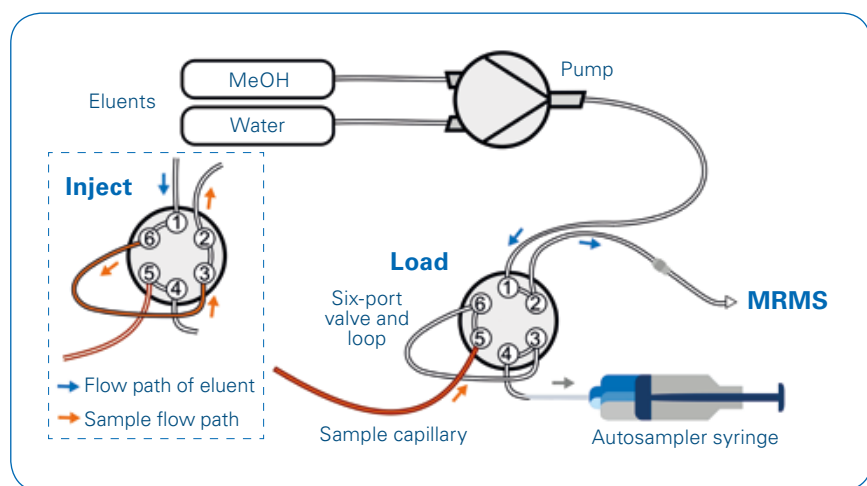


Figure 3: Setup for the injection of μL volumes via a nanoLC-system from a capillary

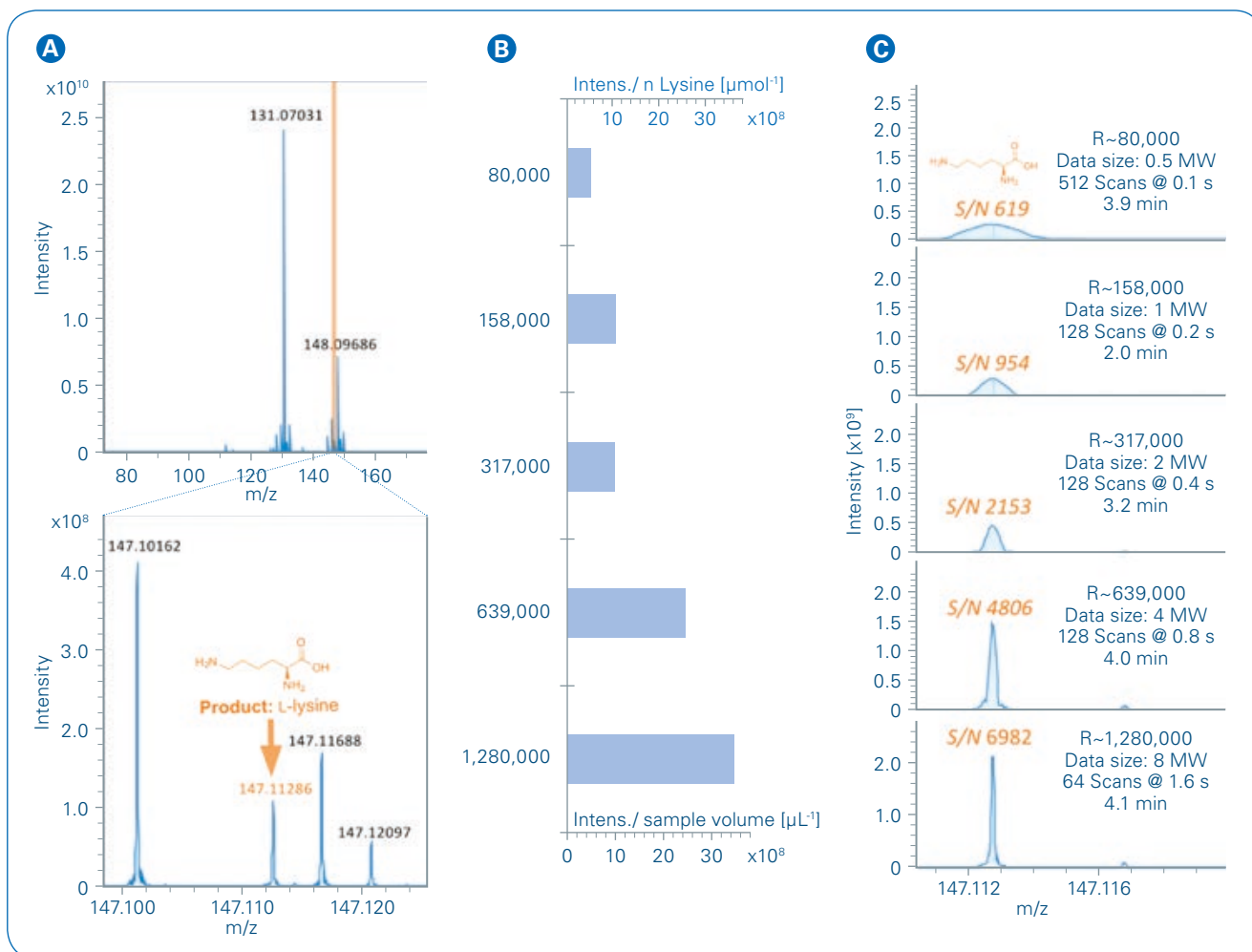


Figure 4: **A** Top: CASI spectrum of a secretome sample from 19 cells (m/z 147 ± 2.5 Da). Bottom: Zoom into the detected mass of lysine ($[M+H]^+$), mass error: 0.37 ppm). **B** The intensity of the signal of lysine normalized to the consumed sample volume and the amount of substance needed for generating the spectrum for different transient length. **C** CASI spectrum of a lysine standard (70 ng/mL, m/z 147.11280) for different transient length.

Effect of transient length and accumulation time on sensitivity

The benefit of ultra-high mass resolution MRMS can be observed on the nominal mass of lysine (Figure 4A).

The mass peak of lysine is fully resolved despite the complexity of the sample - laying the foundation of reliable quantification of this metabolite. Additional improvement in the sensitivity can be achieved by increasing the ion accumulation time (IAT) after CASI isolation and the co-addition of 64 single scans for a final mass spectrum. However,

this approach is often limited by ion-gas and ion-ion interactions (e.g. H_2O loss as observed in Figure 4A for some co-isolated masses) in either the collision cell or analyzer cell, reducing the number of ions for detection and deteriorating the mass peak shape. Also the available sample volume (max. $1.5 \mu\text{L}$) was limiting the total analysis time and the nanoESI source was chosen to maximize the time available for spectra acquisition. In order to increase the overall duty cycle of the instrument the software feature 'accumulate ion during detection' was used. For an optimal analysis of

a μL -sample volume, we compared different transient length and IAT settings for a given maximum time of analysis of 6.5 min ($1 \mu\text{L}$ sample volume @ 150 nL min^{-1} infusion rate). We found that the combination of a very narrow isolation window (m/z 147 ± 2.5 Da), high IAT (1.6 s) and long transients of 3.5 seconds (resulting in highest S/N) provided highest sensitivity for the analysis of individual metabolites in small sample volumes (Figure 4B and C). Instrumental limits of detection and quantification (from $1 \mu\text{L}$ sample volume) were determined as 0.5 and 1.1 ng/mL,

respectively. This limit of detection corresponds to just 1.1 pg or 7.5 fmol of lysine.

Quantification of a metabolic product from ca. 19-21 cells

With the developed setup of sample transfer and highly sensitive detection of lysine from microliter sample volumes, the application to single cell analysis is within reach. Since the overall time to generate a single replicate sample was in the order of 24h, we used an isotope labelled internal standard ($^{15}\text{N}_2$ -lysine) to compensate for day-to-day variability. The internal standard was added directly to the Envirostat medium.

Calibration of our MRMS method was done via injection of standards (plus internal standard) from vials and a full method blank was generated daily from Envirostat supernatants prior loading of the cells (Figure 2 and Figure 5).

We could successfully quantify the produced and secreted lysine from 19 (8.5 ng/mL) and 21 cells (38.8 ng/mL). This enabled us, for the first time, to assess the specific productivity of lysine between 2 and 10 $\text{fmol cell}^{-1} \text{h}^{-1}$ -calculated from just a few bacterial cells.

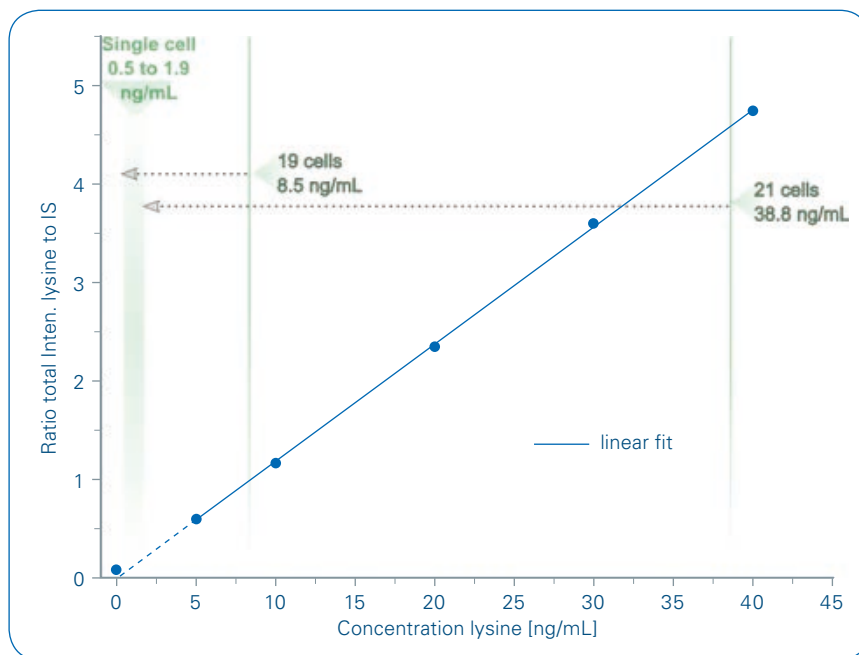


Figure 5: Calibration of lysine using the nanoLC-nanoESI-MRMS setup. Duplicated injection (mean values shown) of standards from vials with the respective linear fit are shown. Samples were prepared in 20 mM ABC buffer with 500 mM glucose. The internal standard (IS) concentration was 10 ng/mL and the lysine calibration range was adjusted to the expected concentrations from the experiments with cells [1].

Conclusion

- Direct infusion MRMS can be used for the analysis of metabolites in very small sample volumes.
- A stable sample flow and nano-electrospray is important for a reliable quantification of metabolites at the single cell level.
- MRMS provides benefits for complex metabolomic samples: high sensitivity and ultrahigh mass resolution for separation of isobaric signals.
- Detection and quantification of other, potentially more sensitive, low blank probes for cell metabolism are possible (by simply adjusting the CASI window).

References

- [1] Dusny C, Lohse M, Reemtsma T, Schmid A, Lechtenfeld OJ (2019). *Quantifying a Biocatalytic Product from a Few Living Microbial Cells Using Microfluidic Cultivation Coupled to FTICR-MS*. *Anal. Chem.*, **91**, 7012–7018.
- [2] Rosenthal K, Falke F, Frick O, Dusny C, Schmid A (2015). *Micromachines*, **6** (12), 1836–1855. <https://www.mdpi.com/2072-666X/6/12/1459>



- **Fast profiling of sphingolipids alteration in hypertension by MRMS**

Hypertension is characterized by endothelial dysfunction and vascular remodeling. Since lipids, and especially sphingolipids have been implicated in vascular tone and function, in this contribution we investigated the differences in plasma sphingolipids among hypertensive and normotensive patients by means of a fast and high-resolution magnetic resonance mass spectrometry (MRMS) approach using direct infusion electrospray (DI).

*Keywords:
MRMS, lipidomics,
hypertension,
sphingolipids, solarix*

*Authors: Eduardo Sommella¹, Fabrizio Merciai¹, Paola Di Pietro¹, Matthias Witt², Pietro Campiglia¹;
¹Università degli Studi di Salerno, Fisciano, Campania, Italy; ²Bruker Daltonik GmbH, Bremen, Germany*

Introduction

Hypertension is one of the major worldwide causes of death. Although the precise cause-effect relationship is controversial, many studies have proposed that endothelial dysfunction may contribute to emergence of hypertension [1]. Sphingolipids are involved in the regulation of both vascular growth and vascular tone. Several reports have shown that in hypertension, essentially sphingolipids levels are altered. The profiling of sphingolipids is usually carried out by liquid chromatography coupled to tandem mass spectrometry (LC-MS/MS). As an alternative to LC-MS/MS, which suffers from long analysis time and lack of reproducibility due to retention time drift, direct infusion magnetic resonance mass spectrometry (DI-MRMS) provides short analysis time for sample screening including high mass accuracy as well as isotopic fine structure for metabolite identification, allowing analysis without the front-end separation step and derivatization. This MRMS workflow

maximizes high throughput in metabolic profiling. In this study sphingolipid levels among healthy and hypertensive patients were investigated using DI-MRMS.

Methods

Extraction

Twenty-four patients with hypertension (defined as DBP \geq 90 mmHg and/or SBP \geq 140 mm Hg or on the basis of use of anti-hypertensive medication) and 9 healthy donor control subjects (non-smokers and non-diabetic) without previous cardiovascular events and not on statin therapy, belonging to the Campania Salute Network Registry, were studied. The database generation of the Campania Salute Network was approved by the Federico II University Hospital Ethic Committee. Signed informed consent was obtained from all the participants to use data for scientific purposes. Plasma samples were thawed and extracted with methanol (MeOH) and methyl-tert-butyl ether

(MTBE). Briefly, 225 μ L of MeOH was added to 20 μ L of plasma and the mixture was vortexed for 10 seconds.

Then 750 μ L of MTBE was added and the obtained solution was incubated at 300 rpm for six minutes at 4°C. Afterwards, 188 μ L of H₂O was added to induce phase separation and the mixture was vortexed for 20 seconds. After centrifuging for five minutes at 14,680 rpm, 650 μ L of the upper organic phase was transferred into a new vial and dried. For mass spectrometric analysis, the sample (organic phase) was solubilized in 200 μ L of 5 mM ammonium acetate 90%MeOH/DCM (2:1 v/v).

MS analysis

Analyses were performed by direct infusion using electrospray ionization following a previous protocol using flow injection with 250 μ L syringe at a flow rate of 2 μ L/min. Data were acquired on a solariX XR 7T (Bruker Daltonik GmbH, Bremen, Germany). The instrument was tuned and

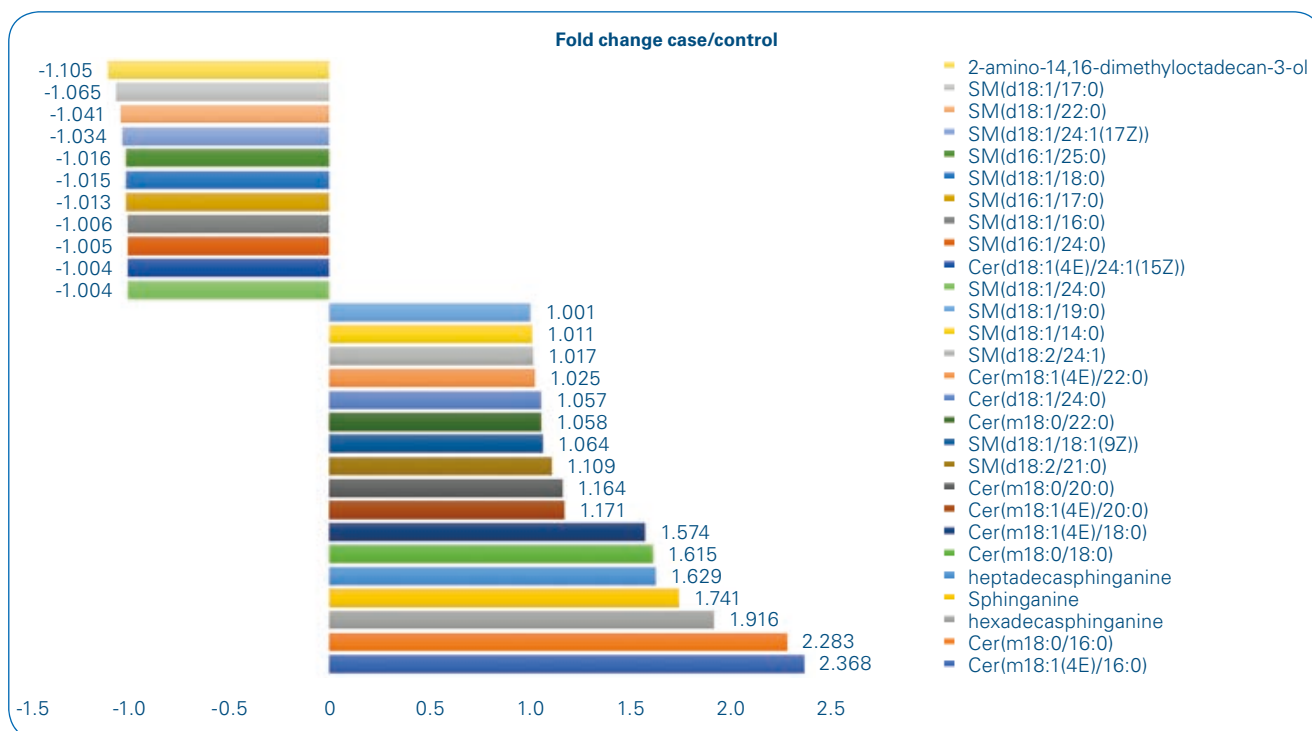


Figure 1: Ceramides as well as sphinganine levels are increased in hypertensive patients

calibrated with a standard solution of NaTFA (0.1 mg/mL in 50% acetonitrile). Mass spectra were acquired in broadband mode in the range 100-1200 m/z with an ion accumulation time of 10 ms. 32 single scans were added for the final mass spectrum using 2 million data points (2M). Nebulizing gas pressure was set to 1 bar. Drying gas pressure was set to 4 L/min at a temperature of 200°C. Both positive and negative ionization modes were employed. Five measurement replicates of each sample were performed.

Data processing

Peak alignment and putative annotation of compounds based on accurate MS measurements was performed in MetaboScape 4.0 (Bruker Daltonik GmbH, Bremen, Germany). LipidMAPS was used as the analyte list for compound identification. Comparisons and differences of samples and patient groups were analyzed by two-way Anova test and Bonferroni post tests analysis for statistical significance.

Results

Total lipid extracts from 33 human plasma samples were analysed in this study. The analysis of plasma lipid extracts showed a very complex profile. Roughly 200 lipids (considering both positive and negative ionization) were putatively annotated, with very good mass accuracy (average error ≤ 0.1 ppm) and detected lipids belonging to different classes. Among them, as shown in Figure 1, different sphingolipids showed alteration between healthy and hypertensive subjects (patients). This is shown in Figure 1 reporting

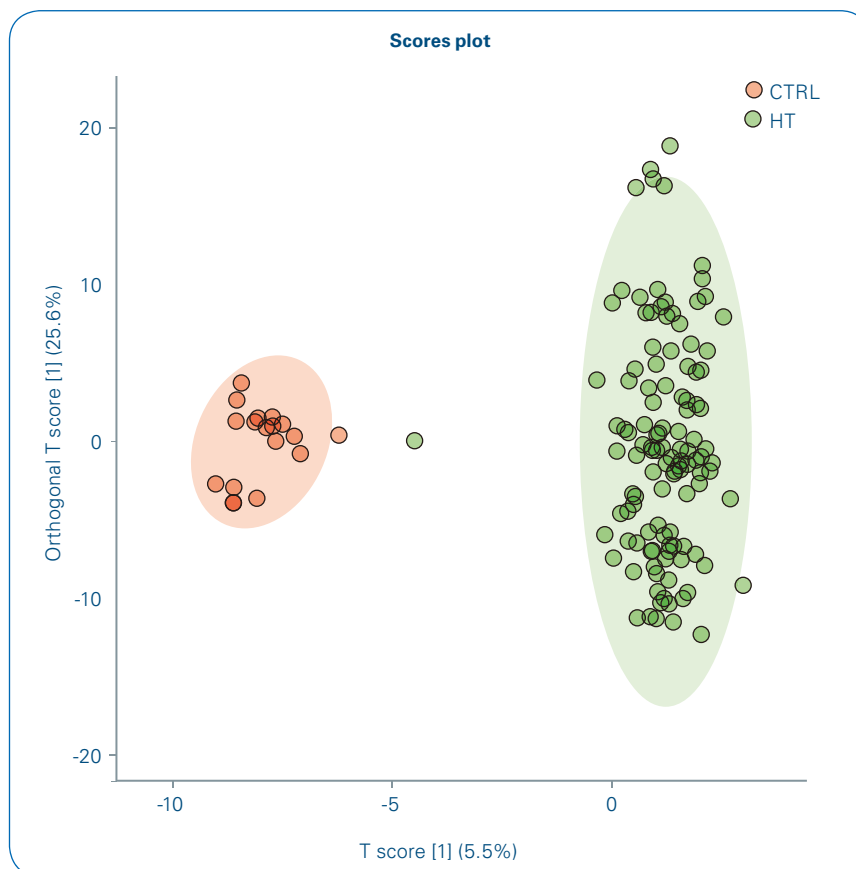


Figure 2: PLS-DA statistical plot (red: control, green: hypertensive)

the fold change of mainly sphingolipids. Both groups, healthy and hypertensive, could be clearly separated in the statistic plot shown in Figure 2. In particular the ceramide level, especially medium-length ceramides such as Cer (18:1(4E)/16:0) showed an increase of hypertensive patients. This data is supported by a growing number of publications of hypertensive studies [2].

Acknowledgements

The authors thank the Campania Salute Network for providing the plasma sample analysed in this study.

Conclusion

- DI-MRMS is a fast and reliable method for sphingolipids profiling.
- Several sphingolipids levels alter by hypertensive disease when comparing the healthy patients. In particular these are ceramides with medium length.
- This data further highlights the role of ceramides associated to endothelium dysfunction.

References

- [1] Oscar A. Carretero OA, Oparil S (2000). *Essential Hypertension Part I: Definition and Etiology*, Originally published 25 Jan 2000 <https://doi.org/10.1161/01.CIR.101.3.329> Circulation. **101**:329–335
- [2] Meeusen JW, Donato LJ, Bryant SC, Baudhuin LM, Berger PB, Jaffe AS (2018). *Plasma Ceramides A Novel Predictor of Major Adverse Cardiovascular Events After Coronary Angiography*, Originally published 14 Jun 2018 <https://doi.org/10.1161/ATVBAHA.118.311199> Arteriosclerosis, Thrombosis, and Vascular Biology. **38**:1933–1939

For Research Use Only. Not for Use in Clinical Diagnostic Procedures.



● MRMS aXelerate for targeted metabolomics profiling of myxobacterial extracts

Myxobacterial secondary metabolomics deals with highly complex samples to uncover novel natural products and is therefore one of the many analytical fields where increased sensitivity and resolution are crucial for a comprehensive analysis [1,2].

Introduction

Many related scientific questions can be answered with a combination of UHPLC and UHR-Q-TOF analysis, representing the current state-of-the-art technique for the analysis of myxobacterial extracts [3]. However,

genomic analysis of myxobacterial strains has shown that their enormous potential for the biosynthesis of secondary metabolites is far from exploited [4]. One plausible reason for the current discrepancy between genome encoded potential and analytically detected chemistry is that

growing myxobacteria in liquid culture fails to mimic all facets of their natural growth behavior as soil-dwelling bacteria. Another often overlooked limitation is related to the analytical methods applied: Combining high resolution mass spectrometry with liquid chromatography limits the

Keywords:
Myxobacteria, Targeted Metabolomics, Untargeted Metabolomics, Metabolic Profiling, Principle Component Analysis, FIA-MRMS

amount of compounds detectable, as not every chromatographic method is equally effective for all types of metabolites [5]. Therefore, there is demand for improving analytical methods and especially for workflows compatible with high-throughput screening to compare extracts from different cultivation scenarios.

Here we present a workflow coined MRMS aXelerate: a flow injection analysis - magnetic resonance mass spectrometry (FIA-MRMS) based analysis of myxobacterial metabolites, enabling the rapid and robust identification of known compounds in a non-targeted metabolomics workflow. Challenges regarding throughput, accuracy, sensitivity and reproducibility are discussed. Furthermore, statistical evaluation of known myxobacterial secondary metabolites in a non-targeted metabolomics workflow is implemented to highlight the differences between myxobacterial cultivation on plate and in liquid culture.

Experimental

The myxobacterial strain *Myxococcus xanthus* DK1622 was cultivated in liquid culture as well as on agar plates in biological triplicates, respectively. Cells from the agar plates were scraped off and the liquid cultures were centrifuged to separate cells and supernatant. The cells were lyophilized prior to extraction with methanol. Blank samples were generated by lyophilizing and extracting the cultivation medium. All samples were diluted 1:200 prior to measurement and two technical replicates were generated. ESI-MS measurements were performed using a scimaX MRMS system (Bruker Daltonics) in positive ion mode and quadrupolar phase detection. 28 single scans were added in 1.5 minutes for the final mass spectrum. The mass range for detection was set to m/z 107-3000 with a data size of 8 MW resulting in a 2 s transient and a mass resolution of 650,000 at m/z 400. The ion accumulation time was set to 20 ms. FIA was

performed with a Bruker Elute UHPLC (Bruker Daltonics). Identification of known target compounds was carried out with MetaboScape 4.0 (Bruker Daltonics), by matching ultra-high resolution m/z values and evaluating isotopic patterns. Statistical interpretation using PCA including all data preprocessing was performed with MetaboScape. The minimal intensity threshold for feature detection was set to 7×10^5 with a maximum charge state of 3. The minimal group size for creating batch features was set to 5. As standardized reference method the extracts were measured in 1:10 methanolic dilution on an Ultimate 3000™ RSLC (Dionex) system coupled to a maXis 4G UHR-Q-TOF-MS (Bruker Daltonics). Separation was achieved on a RP C18 column (100 x 2.1 mm, 1.7 μ m particle size) with a 5-95% gradient of acetonitrile (B) in water (A) each spiked with 0.1% formic acid. The gradient with a total runtime of 21 min was initiated by a 0.5 min isocratic step at 5% B and ended with a 2 min step at 95% B before returning

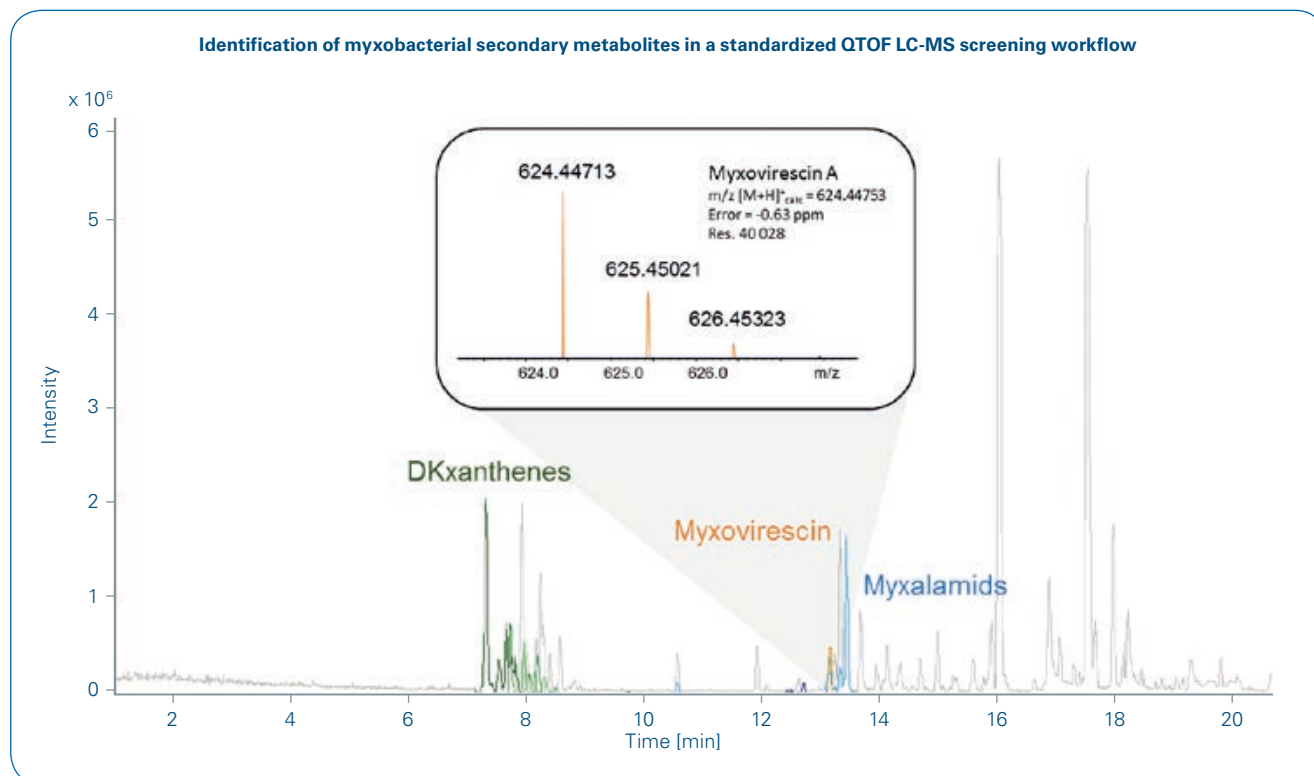


Figure 1A: Base peak chromatogram (BPC) of a *M. xanthus* DK1622 crude extract analyzed by LC-QTOF-MS with extraction ion chromatogram (EIC) traces of known secondary metabolites and zoomed in Myxovirescin A mass spectrum.

and equilibrating under initial conditions. Mass spectra were acquired in centroid mode with a scan range from m/z 150-2500 at 2 Hz scan rate.

Results

Throughput and mass accuracy

In a standard LC-MS screening workflow, myxobacterial secondary metabolites can reliably be identified by matching retention times, high resolution masses and isotope patterns (Figure 1A) [6]. While retention times offer a second dimension for increasing confidence in annotations it comes at the price of long measurement times. The typical method requires 21 minutes total runtime whereas FIA-MRMS measurements can be performed in 1.5 minutes [6]. This reduction in measurement time is especially interesting for high throughput screening. Even though the spectra generated in this manner come with increased complexity, myxobacterial metabolites can be assigned with mass accuracy below 1 ppm as demonstrated for Myxovirescin A in Figure 1B.

Sensitivity and resolution

When characterizing the secondary metabolome of a myxobacterial strain, sensitivity of the analytical

method of choice plays a crucial role as metabolites that are only produced in very small amounts need to be detected in an extremely complex sample. FIA-MRMS works without diluting the sample in an eluent/gradient and it also avoids the introduction of biases due to the chosen chromatographic conditions. As presented in Figure 2, FIA-MRMS is an extremely sensitive method that enabled the detection of Myxovirescin H, which is member of the Myxovirescin family not detectable in the UHPLC-Q-TOF workflow. The high mass resolution of more than 400,000 at m/z 648 allowed differentiation of neighboring signals, and the assignment of the potassium adduct of Myxovirescin H with an error of only 0.15 ppm. The additional detection of the sodium adduct of Myxovirescin H increased the confidence of this annotation.

Data reduction

The high complexity of mass spectra generated from bacterial crude extracts requires data reduction if more than a few metabolites are analyzed. After processing and generation of a feature table in MetaboScape, all blank features were subtracted from the analysis resulting in approximately 55% data

reduction. Blank subtraction is thus a key processing step for the analysis of myxobacterial extracts, because bacteria require particularly complex nutrition media to grow, resulting in a multiplicity of background signals interfering with metabolomics characterization. Annotation of the sample features with the Bruker Sumner MetaboBASE Plant Library, LMSD [7] and the Myxobase (in-house database [1]) enabled the annotation of about 14% of the filtered features in *M. xanthus* DK1622 extracts.

Targeted analysis of known metabolites in a non-targeted workflow using PCA

FIA-MRMS spectra can also be used to compare different cultivation systems in a non-targeted metabolomics workflow. Principal component analysis (PCA) was carried out with two different datasets generated by cultivating *M. xanthus* DK1622 in liquid cultures and on agar plates. The PCA results for the two cultivation systems are presented in Figure 4A, showing that the biological and technical replicates cluster close together, whereas blank, liquid and plate cultures show significant differences in the score plot. Figure 4B shows how PCA can help to identify a suitable cultivation system for known myxobacterial secondary metabolites when dealing with high numbers of annotations. Four different myxobacterial metabolites were analyzed in depth to exemplify the graphical representation of single metabolites with the aim to get an easy and fast overview of the production differences (see Figure 4B). DKxanthene-534 and Myxalamid A can be detected with similar intensity levels from the plate and from liquid cultures. On the contrary, Myxovirescin A shows better production in liquid culture and Cittilin A is enhanced on agar plates.

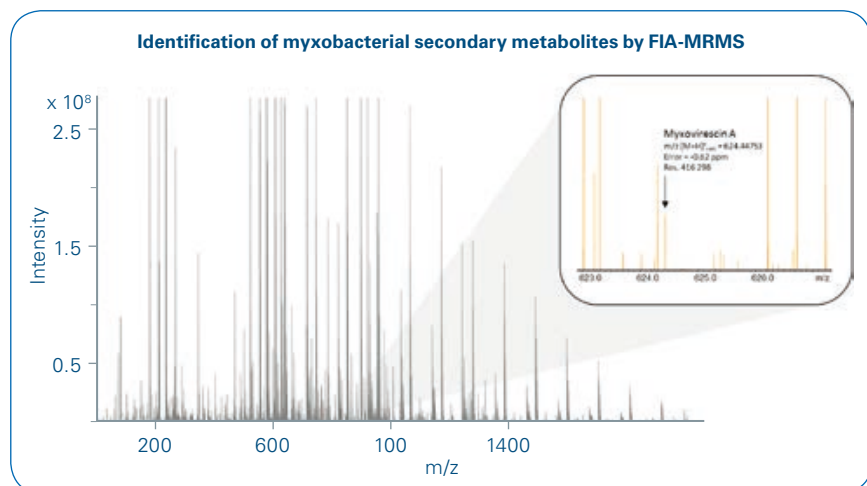


Figure 1B: Mass spectrum of a *M. xanthus* DK1622 crude extract acquired by FIA-MRMS with zoomed spectrum of detected Myxovirescin A.

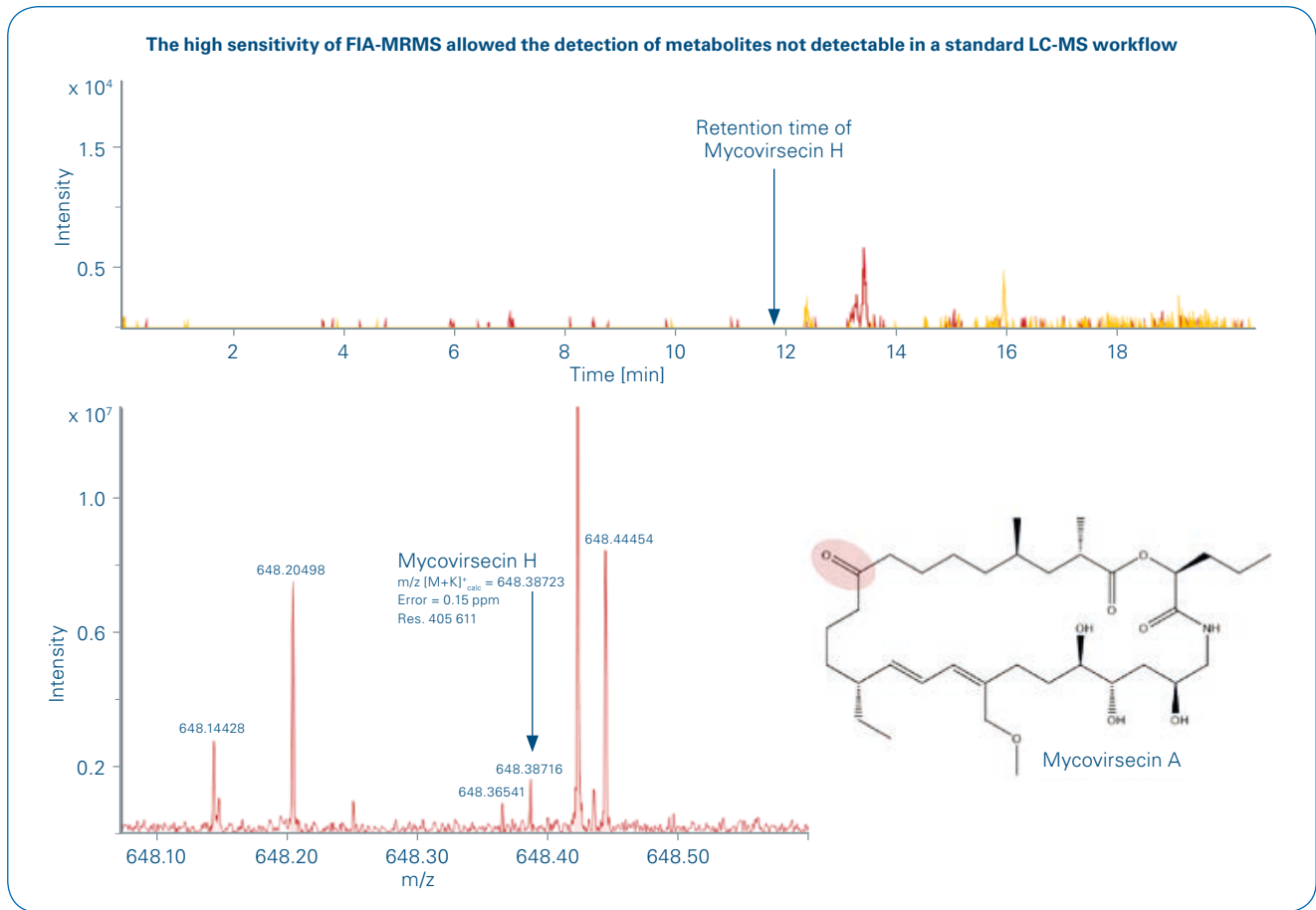


Figure 2: Extraction ion chromatogram (EIC) traces (upper part) showing that Mycovirescin H is not detectable by LC-MS. In contrast, Na⁺ and K⁺ adducts of Mycovirescin H could be detected by FIA-MRMS (lower part). Mycovirescin H only differs from Mycovirescin A (shown on right lower side) by the absence of one ketone moiety.

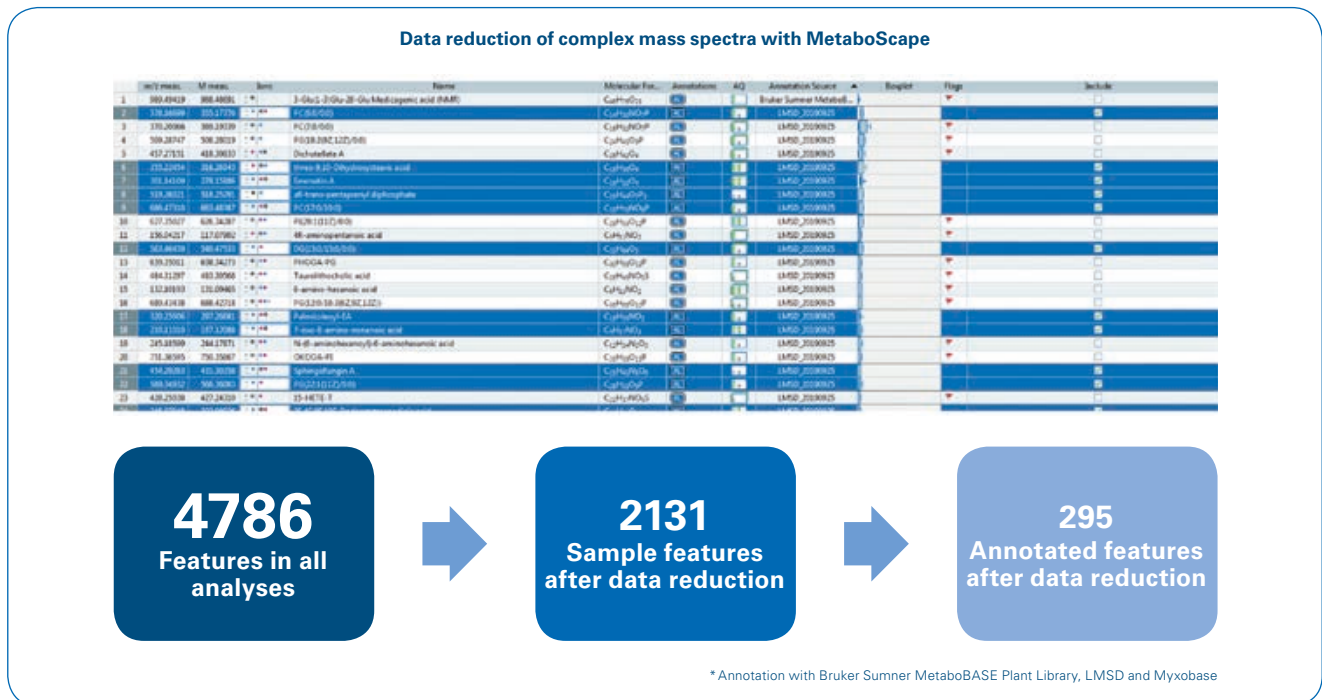


Figure 3: Highly complex mass spectra of *M. xanthus* DK1622 crude extracts require data reduction for interpretation. Detected features can be reduced by automated blank subtraction and library annotation.

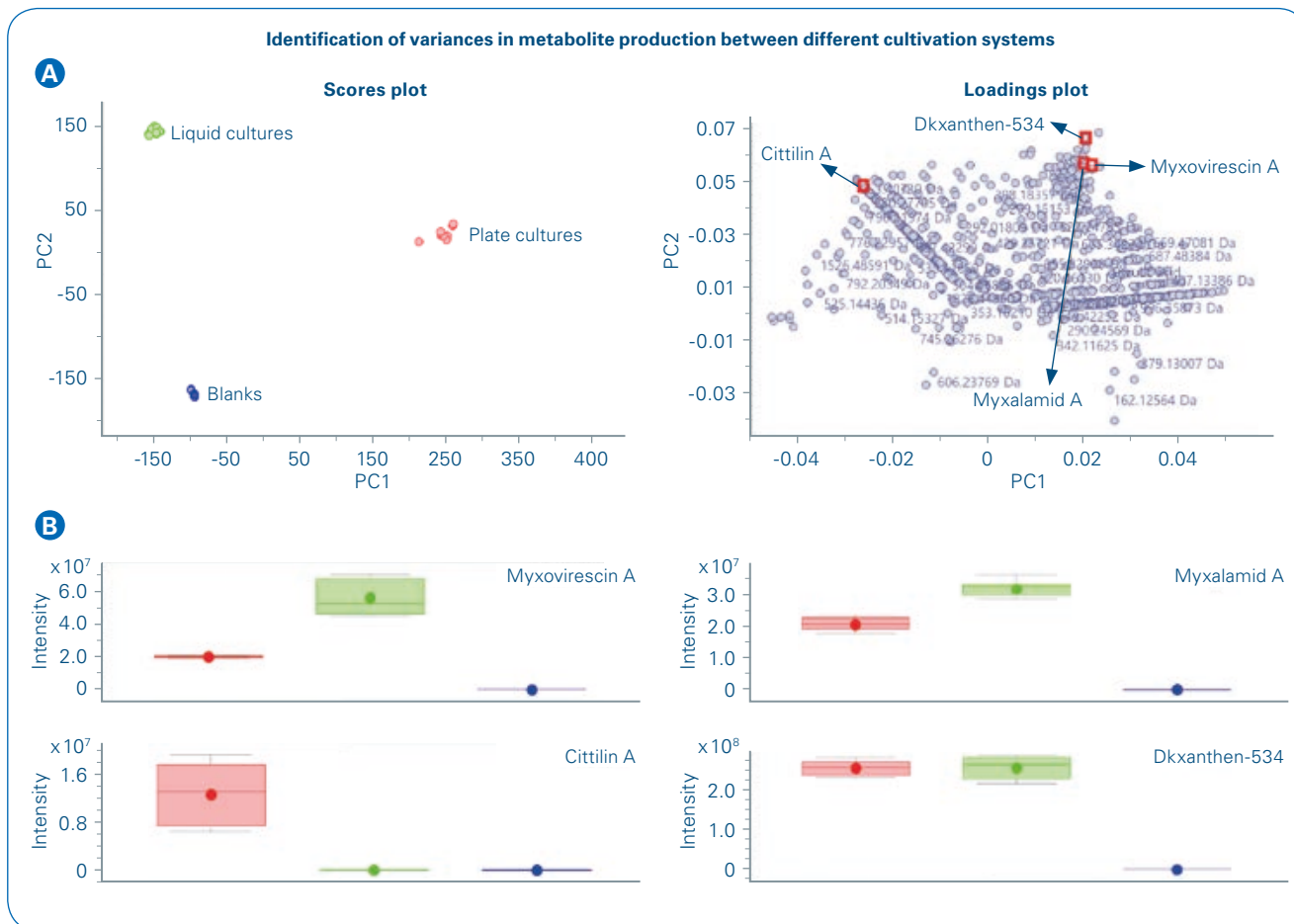


Figure 4: PCA of *M. xanthus* DK1622 cultivated on plate and in liquid culture. Liquid culture extracts are shown in green, plate culture extracts in red and medium blank extracts in green. **(A)** Scores and loadings plots PC1 vs PC2. Biological and technical replicates are shown in the same color. **(B)** Box plot of four myxobacterial metabolites, Myxovirescin A, Myxalamid A, Citterlin A and DKxanthen-534.

Conclusion

Myxobacterial secondary metabolites can be confidently detected by the MRMS aXelerate workflow using the Bruker scimaX MRMS system. The high sensitivity and ultra-high mass resolution were proven to enable detection of compounds missed in a standard LC-MS workflow. Very short measurement times of less than 2 minutes per sample facilitated high throughput screening. Subsequent data reduction and statistical profiling is required and can be performed with the MetaboScape software. Automated blank subtraction and annotation with pre-installed libraries as well as self-created analyte lists helped to scrutinize data sets with high complexity. PCA is a suitable tool to highlight similarities or discrepancies between different data sets. In this example of myxobacterial extract, PCA supported the prioritization of the cultivation system achieving sufficient production of metabolites of choice.



Learn More

You are looking for further Information?
Check out the link or scan the QR code for more details.

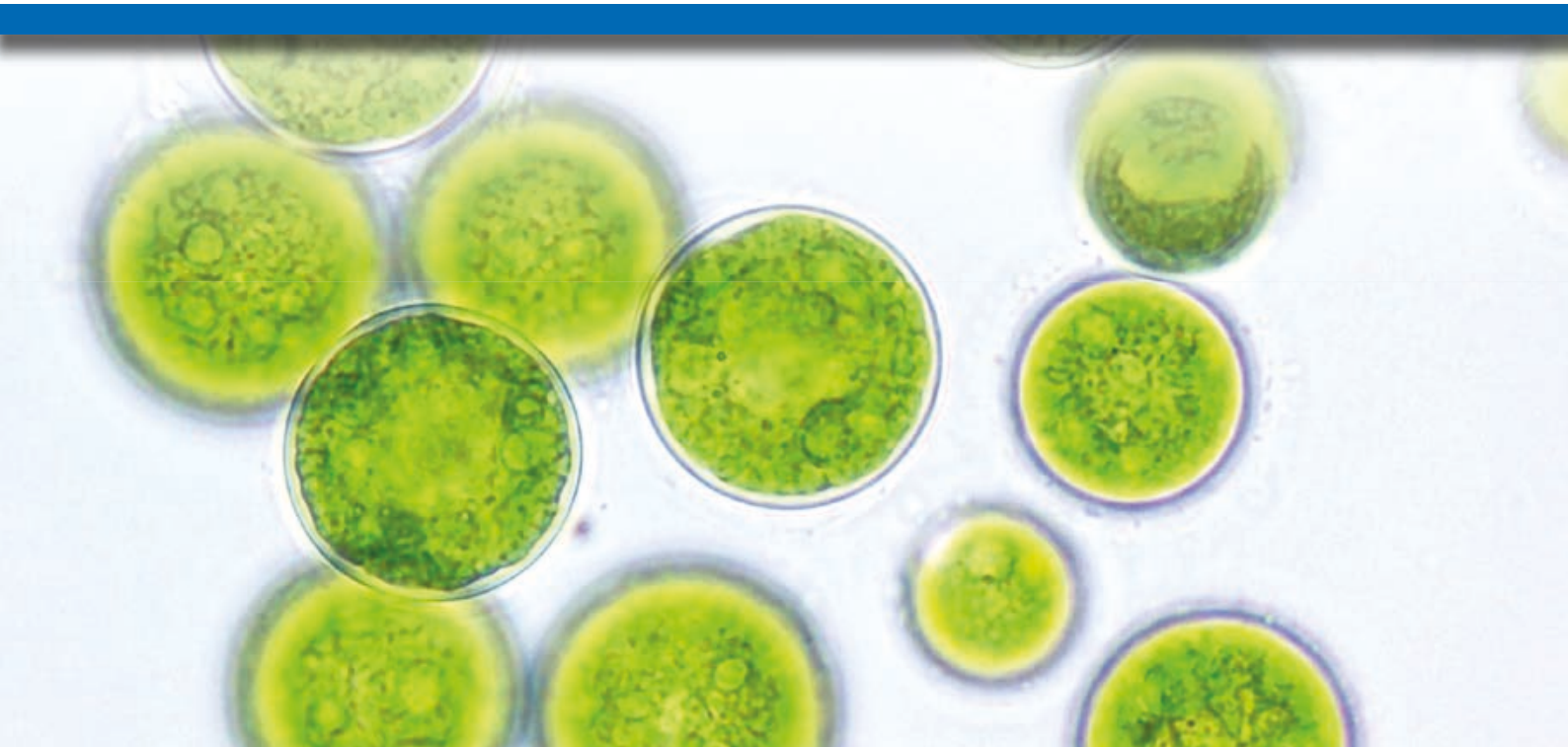
www.bruker.com/scimaX



References

- [1] Krug D, and Müller R (2014). *Secondary metabolomics: the impact of mass spectrometry-based approaches on the discovery and characterization of microbial natural products*, Nat. Prod. Rep. **31**, 768–783.
- [2] Hoffmann T, Krug D, Bozkurt N, Duddela S, Jansen R, Garcia R, Gerth K, Steinmetz H, Müller R. (2018). *Correlating chemical diversity with taxonomic distance for discovery of natural products in myxobacteria*, Nat. Commun. **9**, 803.
- [3] Barsch A, Zurek G, Krug D, Cortina NS, Müller R (2010). *Challenges in Metabolomics addressed by targeted and untargeted UHR-Q-TOF analysis*. Accessible at: https://www.bruker.com/fileadmin/user_upload/8-PDF-Docs/Separations_MassSpectrometry/Literature/literature/ApplicationNotes/ET-21%20Metabolomics_ebook.pdf.
- [4] Wenzel SC, Müller R (2009). *Myxobacteria—'microbial factories' for the production of bioactive secondary metabolites*, Mol. Biosyst. **5**, 567–574.
- [5] Hug JJ, Bader CD, Remškar M, Cirnski K, Müller R (2018). *Concepts and Methods to Access Novel Antibiotics from Actinomycetes*, Antibiotics **7**, 44.
- [6] Krug D, Zurek G, Schneider B, Bässmann C, Müller R (2007). *Analysis of secondary metabolites from myxobacteria using ESI-TOF-MS and PCA*. Accessible at: https://www.bruker.com/fileadmin/user_upload/8-PDF-Docs/Separations_MassSpectrometry/Literature/literature/ApplicationNotes/ET-29_Myxobacteria_eBook.pdf.
- [7] Fahy E, Subramaniam S, Murphy RC, Nishijima M, Raetz CRH, Shimizu T, Spener F, van Meer G, Wakelam MJO, Dennis EA (2009). *Update of the LIPID MAPS comprehensive classification system for lipids*, J. Lipid Res. **50** Suppl, S9-14.

For Research Use Only. Not for Use in Clinical Diagnostic Procedures.



● Rapid elucidation of carotenoids in microalgae formulations by MRMS aXelerate

Arthrospira platensis, better known as Spirulina, is one of the most important microalgae species. This cyanobacterium possesses a rich metabolite pattern including high amounts of natural pigments such as carotenoids.

Abstract

In this study, Spirulina pigments in three different commercial dietary supplements were characterized. Direct infusion (DI) Magnetic Resonance Mass Spectrometry (MRMS) was proven to be a fast (4 min) and

very accurate (mass accuracy ≤ 0.1 ppm) tool for these kinds of studies. In this experiment 49 pigments were tentatively detected. The profile revealed different classes of metabolites such as carotenes, xanthophylls and chlorophylls.

Introduction

Among the natural matrices rich in bioactive compounds, microalgae represent one of the most promising matrices [1]. These microorganisms are a source of various biologically active molecules, including amino acids,

Keywords:
MRMS, microalgae,
direct infusion,
metabolomics

polyunsaturated fatty acids, minerals, proteins and pigments. *Arthrospira platensis*, also known as Spirulina, is one of the most economically important species. Spirulina-based products are used by athletes as anti-fatigue and amino acid supply, and for their anti-aging detoxifying and antioxidant properties in cosmetics. The antioxidant potential of Spirulina is partially attributed to the high content of natural pigments, especially carotenoids, which are also recognized for having numerous healthy benefits. Despite the success of Spirulina in the market, the profiling of pigment in this species has been only partially described. The determination of carotenoids in Spirulina has been carried out mainly by liquid chromatography (LC) coupled with diode array detector (DAD) and mass spectrometry (MS) detection by employing a low-resolution mass analyzer [2]. Recently high-performance thin layer chromatography (HPTLC) was used for the identification of carotenoids in Spirulina [3]. Given

that the Spirulina pigment fraction is highly complex, conventional LC-MS based methods suffer from low separation efficiency of very complex mixtures as well as long analysis time and low mass accuracy, which can result in inaccurate and incorrect compound identification. In this regard, the objective of this study was the development of a combined platform for qualitative and quantitative characterization of Spirulina pigments in different dietary supplements. To tackle this task, we exploited the very accurate mass measurement and ultra-high mass resolution of Magnetic Resonance Mass Spectrometry (MRMS) for the qualitative profiling of the extract.

Methods

Chemicals

LC-MS grade acetonitrile, methanol, and standards of β -carotene, lutein, and zeaxanthin were purchased from Sigma-Aldrich (St. Louis, MO, USA).

Spirulina powders and tablets were purchased from FarmaLabor SRL (Canosa di Puglia, Barletta-Trani, Italy) and Dr. Giorgini (Bologna, Italy) respectively. Lab-made Spirulina powder was kindly donated by a local farmer.

Sample Extraction

Pigment extraction was carried out as follows. 350 mg of Spirulina powder (tablets were prior pulverized in a mortar) were treated with 50 mL of ethanol fortified with 20 μ g/mL of Butyl hydroxyl toluene (BHT) to prevent oxidation. The sample was subjected for 15 min in an ultrasonic bath, then the suspension was stirred for 30 min at room temperature and then centrifuged for 10 min at 6000 rpm at room temperature. The supernatant was removed, and the pellet was retreated following the same protocol another four times. Finally, the supernatants were pooled and lyophilized. The same conditions were employed for each sample of Spirulina.

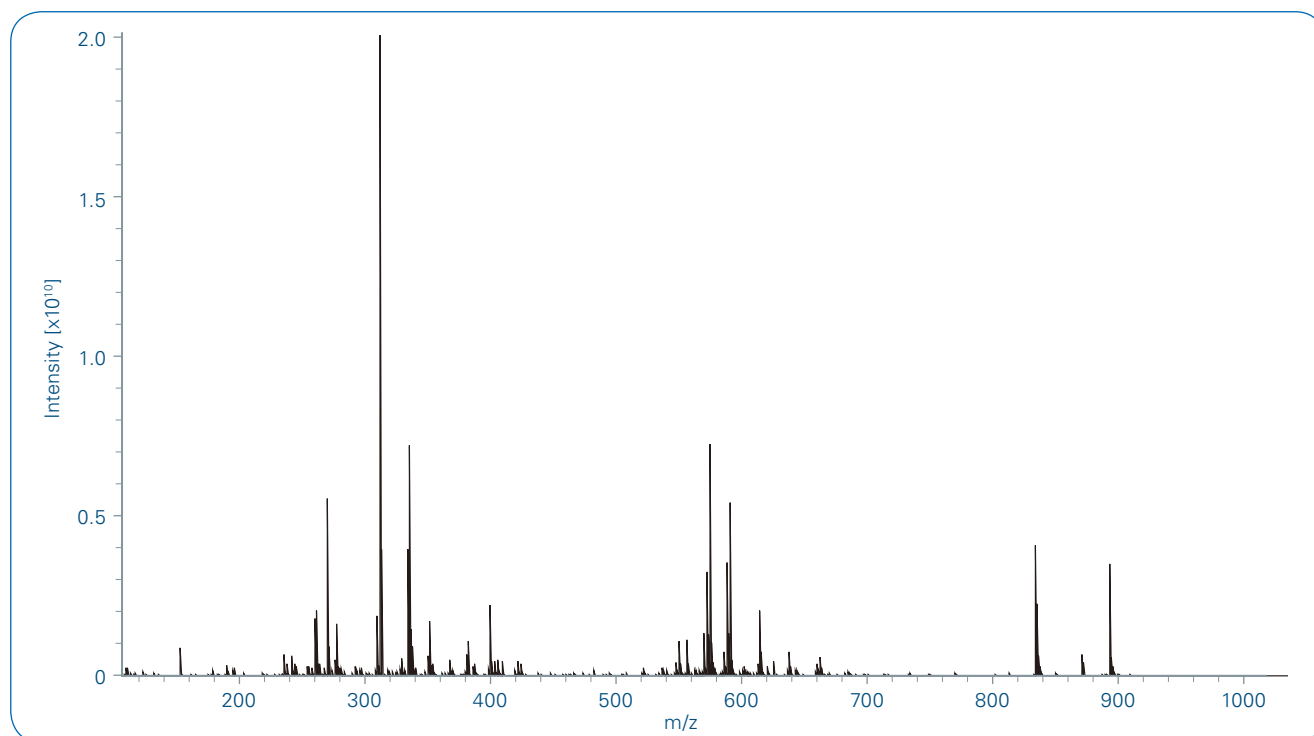


Figure 1: Broad band APCI-MRMS spectrum of a Spirulina powder extract

MS analysis

Data was acquired on a solarix XR 7T MRMS (Bruker Daltonik GmbH, Bremen, Germany) equipped with an Apollo II APCI ion source. The instrument was tuned and externally calibrated with a standard solution (100 µg/ml in 50% acetonitrile) of sodium trifluoro-acetate (NaTFA). Samples (10 µg/mL in methanol) were infused into the ion source at 50 µL/min. Mass spectra were recorded in broadband mode in the range 150–3000 m/z with an ion accumulation time of 20 ms. 200 single scans were added. Spectra were acquired with 8 million data points (8M) resulting in a mass resolution of 700,000 at m/z 400 with a transient length of 6 seconds. Nebulizing (N_2) and drying gases (N_2) were set at 1 and 4 L/min, respectively. Drying gas temperature was set to 200°C. Five measurement replicates were carried out of each sample.

Data processing

Peak alignment and tentative identification of compounds was based on accurate mass measurement. Spectra were loaded in MetaboScape 4.0 (Bruker Daltonik GmbH, Bremen, Germany) for feature extraction and database search.

Results

MRMS is characterized by unmatched ultra-high mass accuracy and mass resolution, which are ideal for the analysis of complex mixtures such as phytochemical samples. In this approach, we employed APCI ionization, which outperformed electrospray for almost all analytes classes (data not shown). Table 1 shows the detection and tentative identification of compounds in three formulations. A high number of tentatively identified compounds could be detected with respect to previous investigations of *Spirulina* [2].

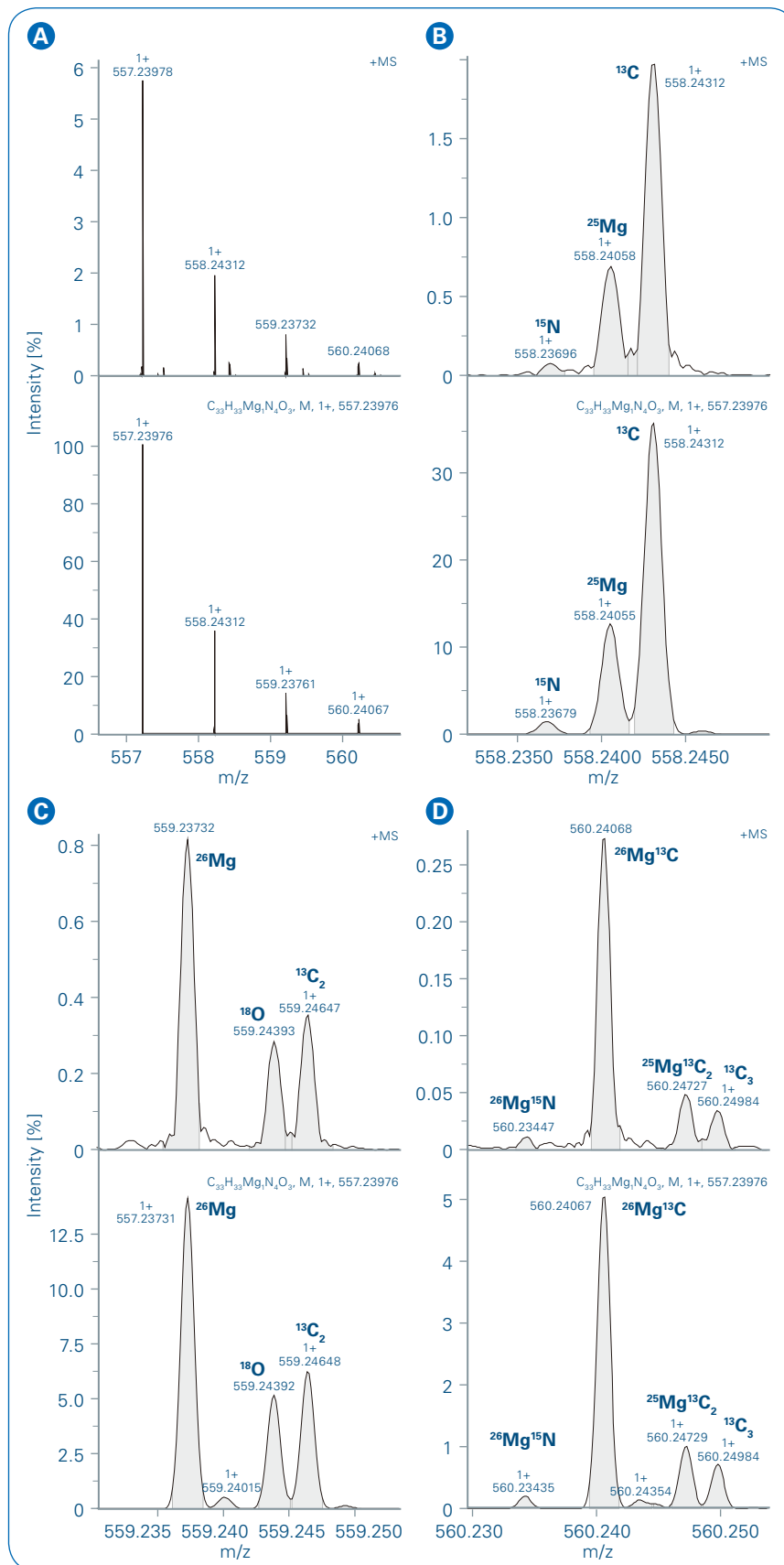


Figure 2: Zoom-in of broad band spectrum at m/z 557 of compound Pyro Chlorophyllide-a (Pyro Chld a) ($C_{33}H_{32}MgN_4O_3$) and IFS pattern. Measured spectrum in top and simulated spectrum in bottom, (A) zoom-in at m/z 557 of isotopic pattern, (B) A+1 pattern, (C) A+2 pattern, (D) A+3 pattern.

Figure 1 reports the full APCI spectrum of a Spirulina extract. Different carotenoid classes could be identified: hydroxyl, epoxy, keto-carotenoids, carotenes as well as chlorophylls and pyro chlorophylls. Several compounds are reported here for the first time present in Spirulina (Table 1). Ultra-high mass accuracy lead to

highly confident identification, such as for the Pyro Chlorophyllide-a, a chlorophyll derivative (Figure 2). The molecular formula could be confirmed by isotopic fine structure (IFS) of the A+1, A+2 and A+3 pattern shown in Figure 2 B-D. Based on the identified molecular formula possible structures of this molecule can

be found using CompoundCrawler (Figure 3). A further benefit of DI-MRMS is the analysis time. A mass spectrum could be acquired in only four minutes which is much faster than conventional LC-MS experiments for detection of carotenoids.

SmartFormula Manually

Lower formula: C₂₄
 Upper formula: MgH₁₀O₁₀
 C 24-n, Mg 0-1, N 0-10, O 0-10

Note: for m < 2000 the elements C, H, N, and O are considered implicitly.

Adducts, pos. M+H Collect adducts
 Adducts, neg. M-H

Measured m/z 557.23978 Tolerance: 1 ppm Charge: 1

Meas. m/z	#	Ion Formula	Score	m/z	err [ppm]	Mean err [ppm]	mSigma	rdb	e ⁻ Conf	N-Rule
557.23978	1	C ₃₃ H ₃₃ MgH ₄ O ₃	100.00	557.23976	-0.04	-0.66	18.7	20.0	even	ok
557.23978	2	C ₃₁ H ₃₃ N ₄ O ₆	21.89	557.23946	-0.58	-0.01	51.6	18.0	even	ok

Compound Crawler

Compound Crawler

C₃₃H₃₃MgH₄O₃ = M Search

Search for: Molecular Formula Name

Compound	Name
1	22376829 C33H3...
2	22376831 C33H3...
3	(3-[(35,45)-14-Ethyl-4,8,13,18-tetramethyl-20-cis-9-vinyl-3-p...
4	3-vinylbacteriochlorophyllide-d 65321431 C33H3...
5	magnesium;(1Z,3R,9Z,13Z,19Z,21S,22S)-22-ethyl-4-keto-11,12...
6	magnesium;(1Z,3R,9Z,13Z,19Z,21S,22S)-11,22-diethyl-4-keto-1...
7	magnesium;3-[(1Z,9Z,13Z,19Z,21S,22S)-11-ethyl-4-keto-12,17...
8	magnesium;(1Z,3R,4R,5Z,13Z,19Z,21S,22S)-11-ethyl-16-ethyny...
9	magnesium;(1Z,3R,9Z,13Z,19Z,21S,22S)-11-ethyl-4-keto-12,17...
10	magnesium;3-[(9Z,13Z,19Z,21S,22S)-11-ethyl-4-keto-12,17,21...
11	magnesium;3-[(21S,22S)-11-ethyl-4-keto-12,17,21,26-tetramet...

Figure 3: Accurate mass combined with isotopic fine structure (IFS) results in top score for molecular formula of C₃₃H₃₃MgH₄O₃. Possible structures have been found for this molecular formula by CompoundCrawler.

Table 1. Detected compounds found in three Spirulina formulation extracts

Compound	Molecular Formula	[M+H] ⁺ DI-APCI-MRMs	Mass accuracy
Apo-12-Violaxanthin ¹	C ₂₅ H ₃₄ O ₃	383.25809	-0.05
Vaucheriaxanthin ¹	C ₄₀ H ₅₆ O ₅	617.42010	-0.08
Diadinoxanthin ¹	C ₄₀ H ₅₄ O ₃	583.41458	-0.02
Canthaxanthin	C ₄₀ H ₅₂ O ₂	565.40402	-0.01
Ethyl β-apo-8'-carotenoate ¹	C ₃₂ H ₄₄ O ₂	461.34143	-0.04
Adonirubin ¹	C ₄₀ H ₅₂ O ₃	581.39892	0.01
Diatoxanthin ¹	C ₄₀ H ₅₄ O ₂	567.41967	-0.02
β-Apo-8'-carotenol ¹	C ₃₀ H ₄₀ O	417.3152	-0.01
Hexadehydro-β,β-caroten-3-ol ¹	C ₄₀ H ₅₀ O	547.39347	-0.06
Rhodoxanthina	C ₄₀ H ₅₀ O ₂	563.38838	-0.04
Astaxanthin	C ₄₀ H ₅₂ O ₄	597.39382	0.02
Antheraxanthin ¹	C ₄₀ H ₅₆ O ₃	585.43023	-0.02
Myxoxanthophyll	C ₄₆ H ₆₆ O ₇	731.48807	0.08
Zeaxanthin	C ₄₀ H ₅₆ O ₂	569.43529	0.02
10-Apo-β-carotenol ¹	C ₂₇ H ₃₆ O	377.28389	-0.06
α-tocopherol	C ₂₉ H ₅₀ O ₂	431.38835	0.01
Echinenone	C ₄₀ H ₅₄ O	551.42473	0.02
Pyro Chl <i>b</i>	C ₅₃ H ₆₈ MgN ₄ O ₄	849.51640	-0.03
Phy <i>a</i> derivate	C ₅₅ H ₇₂ N ₄ O ₅	869.55755	0.01
Chld <i>b</i>	C ₃₅ H ₃₂ MgN ₄ O ₆	629.24050	0.01
Chl <i>b</i>	C ₅₅ H ₇₀ MgN ₄ O ₆	907.55824	0.01
Pyro Chl <i>a</i>	C ₅₃ H ₇₀ MgN ₄ O ₃	835.53711	0.01
Pyro Chld <i>a</i>	C ₃₃ H ₃₂ MgN ₄ O ₃	557.23978	-0.04
Pyro Chld <i>b</i>	C ₃₃ H ₃₀ MgN ₄ O ₄	571.21901	0.02
OH-Chl <i>a</i>	C ₅₅ H ₇₂ MgN ₄ O ₆	909.53746	0.05
Protochld <i>a</i>	C ₃₅ H ₃₂ MgN ₄ O ₅	613.22959	-0.01
13-OH-Chld <i>a</i>	C ₃₅ H ₃₄ MgN ₄ O ₆	631.24015	0.01
Divinyl Chl <i>a</i>	C ₅₅ H ₇₀ MgN ₄ O ₅	891.52691	0.04
Chl <i>a</i>	C ₅₅ H ₇₂ MgN ₄ O ₅	893.54262	-0.03
Cryptoxanthin*	C ₄₀ H ₅₆ O	553.44040	0.01
Chld <i>a</i>	C ₃₅ H ₃₄ MgN ₄ O ₅	615.24526	-0.04
Phy <i>b</i>	C ₅₅ H ₇₂ N ₄ O ₆	885.55233	0.14
15-OH-Lactone-Chl <i>a</i>	C ₅₅ H ₇₃ MgN ₄ O ₇	925.53199	0.47
Pyro Pheo <i>b</i>	C ₃₃ H ₃₂ N ₄ O ₄	549.24967	-0.08
15-OH-Lactone-Phy <i>a</i>	C ₅₅ H ₇₃ N ₄ O ₇	903.56328	-0.28
Chlorobactene	C ₄₀ H ₅₂	533.41416	0.03
Chl <i>a</i> derivate I	C ₅₅ H ₆₈ MgN ₄ O ₅	889.51122	0.08
Phytoene	C ₄₀ H ₆₄	545.50810	-0.03
13-OH-Pheo <i>a</i>	C ₃₅ H ₃₆ N ₄ O ₆	609.27078	-0.02
OH-Phy <i>a</i>	C ₅₅ H ₇₃ N ₄ O ₆	887.56810	0.01
β-carotene	C ₄₀ H ₅₆	537.44547	0.01
Octadehydro-β,β-carotene	C ₄₀ H ₄₈	529.38288	0.03
Phy <i>a</i>	C ₅₅ H ₇₄ N ₄ O ₅	871.57318	0.02
Pheophorbide <i>a</i>	C ₃₅ H ₃₆ N ₄ O ₅	593.27583	0.02
Pyro Pheo <i>a</i>	C ₃₃ H ₃₄ N ₄ O ₃	535.27037	0.01
Pyro Phy <i>a</i>	C ₅₃ H ₇₂ N ₄ O ₃	813.56769	0.04
δ-tocopherol	C ₂₇ H ₄₆ O ₂	403.35706	0.01
γ-tocopherol	C ₂₈ H ₄₈ O ₂	417.37270	0.02
Phytofluene	C ₄₀ H ₆₂	543.49242	0.01

¹Detected for the first time in Spirulina (Arthrospira Platensis). Chld: chlorophyllide; Pheo: pheophorbide; Phy: Pheophytin; Chl: Chlorophyll.

Conclusion

The developed analytical strategy using APCI combined with DI-MRMS has been proven for analysis of carotenoids in Spirulina pigment fractions. This method based on ultra-high mass resolution and accurate mass as well as isotopic fine structure is a promising tool for in-depth profiling of microalgae pigments. Furthermore, this study confirms the high importance of DI-MRMS for bio-compound detection such as carotenoids in Spirulina, and its importance in the nutraceutical and pharmaceutical area.

Acknowledgement

We kindly would like to thank a local farmer for providing the Spirulina powder for this study.



Learn More

You are looking for further Information?
Check out the link or scan the QR code for more details.

www.bruker.com/solarix



References

- [1] Singh S, Kate BN, Banerjee UC (2005). *Bioactive Compounds from Cyanobacteria and Microalgae: An Overview*. Crit. Rev. Biotechnol., **25**, 73–95.
- [2] Mendiola JA, Marin FR, Hernández SF, Arredondo BO, Señoráns FJ, Ibañez E, Reglero G (2005). *Characterization via liquid chromatography coupled to diode array detector and tandem mass spectrometry of supercritical fluid antioxidant extracts of Spirulina platensis microalga*. J. Sep. Sci., **28**, 1031–1038.
- [3] Hynstova V, Sterbova D, Klejdus B, Hedbavny J, Huska D, Adam V (2018). *Separation, identification and quantification of carotenoids and chlorophylls in dietary supplements containing Chlorella vulgaris and Spirulina platensis using High Performance Thin Layer Chromatography*. J. Pharm. Biomed. Anal., **148**, 108–118.

For Research Use Only. Not for Use in Clinical Diagnostic Procedures.



● A strategy using isotopic fine structure to reveal potential biomarkers showing the effects of traditional Chinese medicines on Alzheimer disease in rats

Alzheimer disease (AD) is a progressive, unremitting, neurodegenerative disease characterized by progressive memory decline and subsequent loss of broader cognitive functions.

Introduction

As the pathogenesis and progression of AD remain unclear, no curative treatment is currently available to slow down or stop the degenerative effects of AD until now. *Rhodiola crenulata* has been widely served as antifatigue, antidepressant and health food for many years in

China. Recently, researches showed that not only the *Rhodiola crenulata* extract (RCE) but also its major component, salidroside, has ameliorative effects on the learning and memory deficits in the treatment of AD. However, the therapeutic mechanisms underlying the protective effects of RCE against

AD are still unclear. In this study, a metabolomic strategy based on accurate mass and isotopic fine structure (IFS) by Magnetic Resonance Mass Spectrometry (MRMS, traditionally known as FT-ICR MS), was established to explore the effects of *Rhodiola crenulata* extract (RCE) on Alzheimer disease (AD) in rats.

Keywords:
MRMS, traditional Chinese medicines, *Rhodiola crenulata*, metabolomic study, accurate mass, Isotopic fine structure

Experimental

Experimental AD model was induced in rats by bilateral hippocampal injection of $A\beta_{1-42}$, and Morris water maze task (MWM) was used to evaluate the effects of RCE on AD. The metabolomic study was performed using a solarix 7T MRMS system. The experimental workflow consisted of HPLC-MRMS, fraction collection and direct infusion (DI)-MRMS to screen and identify the potential biomarkers, Figure 1. Elemental compositions were determined using the following seven steps.

Step 1. Identify the monoisotopic peak, A+1, A+2 and A+3 isotopic peaks in the experimental data.

Step 2. Acquire the experimental IFS with the relative intensities of each isotopic peak.

Step 3. Assign the M+1 isotopic peaks originating from ^{15}N , ^{33}S and ^{13}C by calculating the mass difference between the monoisotopic mass and each peak and then estimate the carbon numbers based on the relative intensity of ^{13}C isotopic peak.

Step 4. Exclude enough candidates by relative intensities of ^{13}C isotopic peaks.

Step 5. Assign the A+2 isotopic peaks originating from $^{15}\text{N}^{13}\text{C}$, ^{18}O , ^{34}S and $^{13}\text{C}_2$ substitution and the A+3 isotopic peaks (if necessary) by calculating the mass difference between the monoisotopic mass and each peak.

Step 6. Acquire the theoretical IFS for candidate formulae and the relative intensities of isotopic peaks by Compass Isotope pattern Software.

Step 7. Determine the elemental

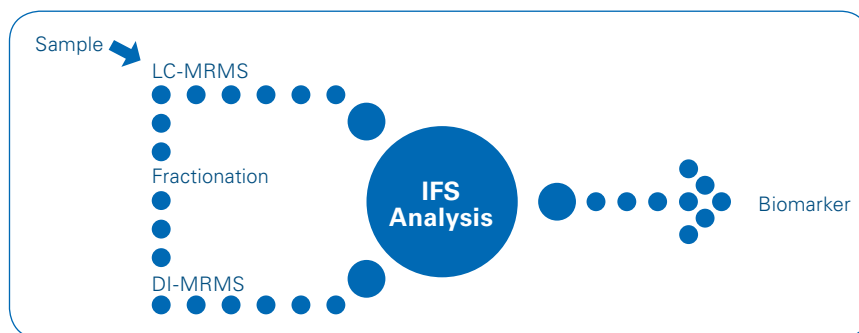


Figure 1: Workflow for identification of biomarkers based on accurate mass and isotopic fine structures by dual mode combined-MRMS.

composition by comparing the experimental and the theoretical data and assign a definite formula to each potential biomarker.

Results and Discussion

The initial HPLC profiling results were screened by statistical differentiation to reveal potential biomarkers with an experimental mass accuracy of less than 1 ppm. The samples are then fractionated, and the fractions of interest are remeasured using ultra-high resolution MRMS to reveal the experimental IFS. An example is shown for an unknown with a retention time of 16.24 minutes and m/z 524.37054. Using a mass accuracy of less than 1 ppm, there are 4 possible chemical formula, shown in Table 1. The proposed formulae contain 5 elements that have stable heavy isotopes: ^{13}C , ^2H , ^{15}N , ^{18}O and ^{34}S . The absence of the ^{34}S isotope clearly eliminates 2 candidates. The difference in the relative intensity of the experimental heavy isotopes to the simulated pattern is used to determine the correct formula. After IFS analysis, only one candidate remained, $\text{C}_{26}\text{H}_{55}\text{NO}_7\text{P}^+$. The simulated IFS mass spectrum of $\text{C}_{26}\text{H}_{55}\text{NO}_7\text{P}^+$ at $\text{RP}=1,000,000$ is given in Figure 2.

A total of 20 metabolites contributing to AD progress were decisively identified, and 17 metabolites of them were restored to the control-like levels after RCE treatment (daily

dose: 2.24 g/kg), shown in Table 2. The metabolic pathway analysis revealed that the disturbed pathways including tryptophan metabolism, sphingolipid metabolism and glycerophospholipid metabolism in AD model rats were regulated after high dose RCE application. It is the first time that the dual mode combined MRMS based metabolomic strategy was applied to biochemically profile the serum metabolic pathways of AD rats affected by RCE. These outcomes provide reliable evidence to illuminate the biochemical mechanisms of AD and facilitate investigation of the therapeutic benefits of RCE in AD treatment. Notably, it indicated that the developed method based on accurate mass and IFS has sufficient performance for decisive identification of biomarkers in metabolomic studies.

Table 1: Candidate molecular formula annotations for the unknown at m/z 524.37054 and retention time 16.24 minutes.

Proposed Annotation	Major IFS Peaks
$\text{C}_{26}\text{H}_{55}\text{NO}_7\text{P}^+$	$^{13}\text{C}_{26} \ ^{15}\text{N}_1 \ ^{18}\text{O}_7$
$\text{C}_{29}\text{H}_{46}\text{N}_7\text{O}_2^+$	$^{13}\text{C}_{29} \ ^{15}\text{N}_7 \ ^{18}\text{O}_2$
$\text{C}_{29}\text{H}_{54}\text{N}_3\text{OS}_2^+$	$^{13}\text{C}_{29} \ ^{15}\text{N}_3 \ ^{18}\text{O}_1 \ ^{34}\text{S}_2$
$\text{C}_{21}\text{H}_{50}\text{N}_9\text{O}_4\text{S}^+$	$^{13}\text{C}_{21} \ ^{15}\text{N}_9 \ ^{18}\text{O}_4 \ ^{34}\text{S}_1$

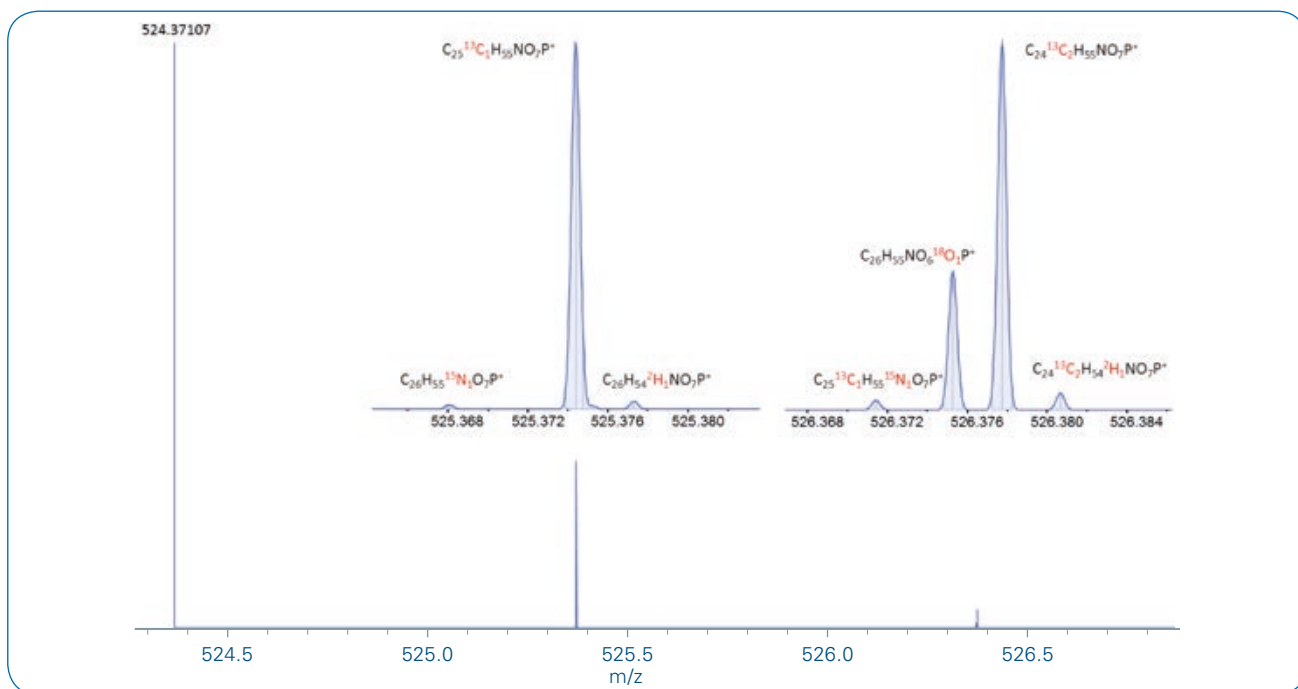


Figure 2: Simulated IFS mass spectrum for $C_{26}H_{55}NO_7P^+$ at a resolution of 1,000,000 for the monoisotopic mass.

Table 2: IFS Annotated Metabolites

Molecular Formula	Proposed Compound	Reversed
$C_{10}H_{19}NO_4$	Propionylcarnitine	Y
$C_{11}H_{21}NO_4$	Butyrylcarnitine	Y
$C_{11}H_{12}N_2O_2$	L-Tryptophan	Y
$C_{43}H_{83}O_{13}P$	PI (34:0)	--
$C_{18}H_{39}NO_2$	Sphinganine	Y
$C_{24}H_{48}NO_7P$	LysoPC (16:1(9Z))	Y
$C_{26}H_{48}NO_7P$	LysoPC (18:3)	Y
$C_{26}H_{50}NO_7P$	LysoPC (18:2(9Z,12Z))	Y
$C_{24}H_{50}NO_7P$	LysoPC (16:0)	Y
$C_{28}H_{50}NO_7P$	LysoPC (20:4)	Y
$C_{23}H_{45}NO_4$	L-Palmitoylcarnitine	--
$C_{25}H_{45}NO_4$	Linoleyl carnitine	Y
$C_{30}H_{50}NO_7P$	LysoPC (22:6(4Z,7Z,10Z,13Z,16Z,19Z))	Y
$C_{26}H_{52}NO_7P$	LysoPC (18:1)	Y
$C_{25}H_{52}NO_7P$	LysoPC (17:0)	Y
$C_{28}H_{54}NO_7P$	LysoPC (20:2(11Z,14Z))	Y
$C_{23}H_{48}NO_7P$	LysoPC (15:0)	Y
$C_{28}H_{52}NO_7P$	LysoPC (20:3)	Y
$C_{26}H_{54}NO_7P$	LysoPC (18:0)	Y
$C_{18}H_{30}O_2$	Alpha-Linolenic acid	--



Learn More

You are looking for further Information?
Check out the link or scan the QR code for more details.

www.bruker.com/solarix



This Application Note is a condensed and revised version of the Journal of Pharmaceutical and Biomedical Analysis article "A metabolomic study based on accurate mass and isotopic fine structures by dual mode combined-FT-ICR-MS to explore the effects of *Rhodiola crenulata* extract on Alzheimer disease in rats".

References

- [1] Zhang Xiaoxue, Jiang Xiwei, Wang Xue, et al. (2019) *A metabolomic study based on accurate mass and isotopic fine structures by dual mode combined-FT-ICR-MS to explore the effects of Rhodiola crenulata extract on Alzheimer disease in rats*. J Pharm Biomed Anal, **166**: 347-356.

For Research Use Only. Not for Use in Clinical Diagnostic Procedures.



● Analysis of metabolic changes in murine hair follicles treated with Procyanidin-B2 rich nutraceuticals by DI-MRMS

Known for anti-inflammatory and antioxidant properties, nutraceuticals enriched in Procyanidin-B2 promote hair growth both in vitro and in vivo. However, the metabolic changes associated with the treatment have not been elucidated.

Abstract

In this study, direct infusion magnetic resonance mass spectrometry (DI-MRMS) was employed to understand the metabolic shift produced by treatment with Procyanidin-B2

nutraceuticals (Anurca apple extract) in murine models. DI-MRMS allowed the identification of several metabolites using ultra-high mass accuracy and fast analysis time, glutaminolysis, pentose phosphate pathway, glutathione, citrulline and

nucleotide synthesis derived metabolite were detected. The metabolic profile revealed that the treatment with Procyanidin-B2 results in the early exit of hair follicles from telogen phase and increased keratin biosynthesis.

Keywords:
Metabolomics,
Metabolite,
MetaboScape, MRMS,
solarix

Introduction

Patterned hair loss affects around 50% of the adult population worldwide. Independent of age and gender, this condition exerts a profoundly negative impact on people's quality of life and is frequently associated with depression, especially when occurring at an early age. Among pharmacological treatments, Finasteride and Minoxidil are FDA approved drugs. However, Finasteride and Minoxidil activity reaches a plateau within two years of usage and both drugs produce adverse effects on patients. In the past decade an increasing number of reports have proven nutritional and antioxidant therapies to be an effective and safe treatment as an option for hair loss. Among these, nutraceuticals enriched in Procyanidin-B2 (Figure 1), a dimeric Procyanidin, such as Annurca apple extract (AAE), have been recently shown to promote hair growth and induce anagen phase in humans. This has resulted in the increased usage of these types of nutraceuticals for hair growth over the last several years. However, studies reveal this mechanism is far from being complete. Here, the metabolic profile of AAE treatment on mice hair follicles was studied to give new insights into the promotional growth effects of Procyanidin-B2.

Methods

Animals

Wild-type C57/BL6 mice (7 weeks old, postnatal day 42) were used in all experiments to test the effect of cosmetic foam containing AAE. All animals received humane care and were maintained in separate cages at 22°C – 24°C and fed a general rodent diet. Differently from other published protocols, here animals were left unshaved and topically treated with 2 cm³ of the indicated cosmetic foam for 4 weeks, twice a week. Only male animals were used in this study. All animal experiments were performed in compliance with ethical guidelines and approved by the University of Naples Federico II.

Extraction

Mice tissues were rinsed and kept in PBS immediately after tissue excision. Hair shafts were plucked out with sterile tweezers and immediately covered with a solution of PBS at room temperature. To allow detachment of hair follicle cells, plucked hair shafts were incubated for 15 minutes in PBS supplemented with 5 mM EDTA. Hair shafts were then removed and the remaining hair follicle cells centrifuged for 5 minu-

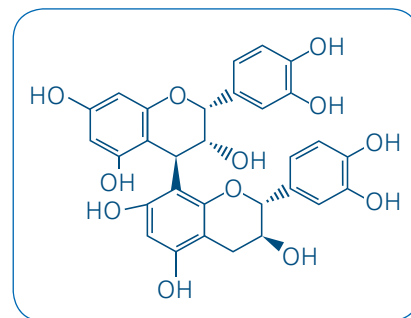


Figure 1: Structure of Procyanidin-B2

tes at 500 rpm. The cell pellets were washed twice in PBS and homogenized in 1 ml of pre-chilled methanol/water 80:20 solution and finally centrifuged at 10,000 g for 10 min at 4°C. The resulting supernatants were collected and transferred into new Eppendorf tubes and stored at -80°C.

MS analysis

Analyses were performed by direct infusion electrospray ionization using a Hamilton syringe (250 µL) at a flow rate of 2 µL/min. Data were acquired on a MRMS solariX XR 7T. The instrument was tuned and calibrated with a standard solution of NaTFA. Mass spectra were recorded in broadband mode in the range m/z 100-1500 with an ion accumulation time of 20 ms. 32 single scans were added for the final mass

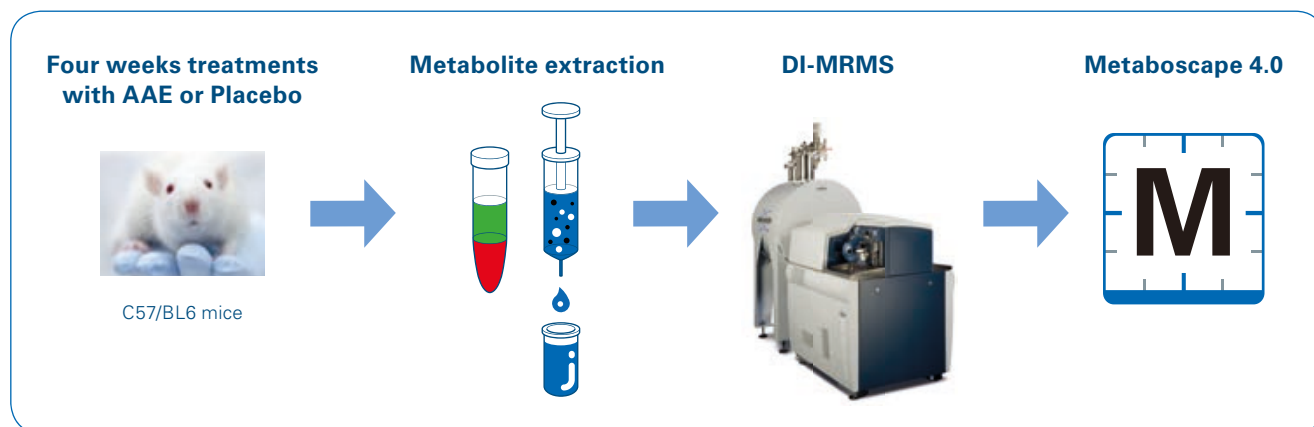


Figure 2: Workflow for analysis of the metabolite profile of mice hair follicles using DI-MRMS

spectrum. Data were acquired with 2 million data points. Nebulizing (N₂) and drying gases (N₂) were set at 1 and 4 L/min, respectively, using a drying gas temperature of 200°C. Spectra were acquired in positive and negative ion mode. The measurements were performed in five replicates (Figure 2).

Data processing

Peak alignment and tentative assignment of compounds was performed in MetaboScape 4.0 based on accurate mass measurements and a HMDB plasma analyte list. The feature calculation was performed with a mass resolution of 1 mDa. A bucket filter of 75% was used for replicate

measurements and the values of the calculated features were recalibrated with accurate masses of compounds known in plasma. The accuracy of the isotopic with a maximum mSigma value of 50 was used for feature assignment. Statistical analysis with significant results were performed with Statistica® using two-way Anova and Bonferroni post tests.

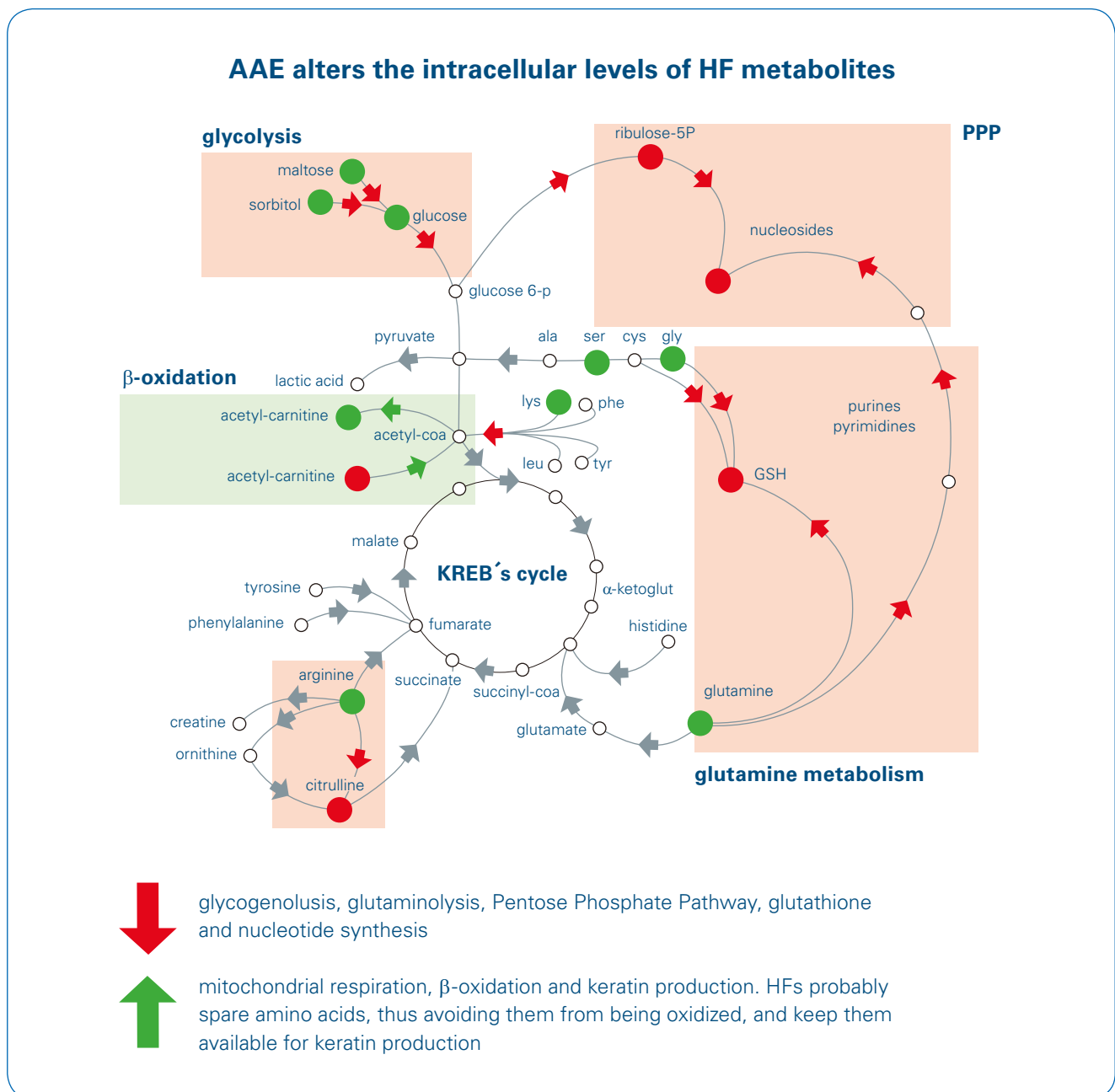


Figure 3: Modulation of mice hair follicles metabolites following treatment with apple Annurca foam

Metabolite	Pathway	m/z	Detected as	Mass error (ppm)
Glucose	Glycolysis	203.05265	[M+Na] ⁺	0.006
Lactic acid		113.02091	[M+Na] ⁺	-0.176
Maltose	Glycogenolysis	365.10543	[M+Na] ⁺	-0.012
Glutamine	Aminoacids	169.05836	[M+Na] ⁺	0.001
Arginine		197.10090	[M+Na] ⁺	0.029
Glutathione		306.07675	[M-H] ⁻	0.028
Citrulline		198.08495	[M+Na] ⁺	0.072
Adenosine	Nucleotides	290.08596	[M+Na] ⁺	0.028
Cytosine		266.07476	[M+Na] ⁺	0.015
Deoxy-Cytosine		250.07984	[M+Na] ⁺	0.044
Deoxy-Inosine		275.07507	[M+Na] ⁺	-0.091
Palmitoyl-carnitine	β-oxidation	422.32404	[M+Na] ⁺	0.148
Acetyl-carnitine		226.10501	[M+Na] ⁺	0.211

Table 1: List of relevant metabolites for treatment of hair follicles with apple Annurca foam detected by DI-MRMS

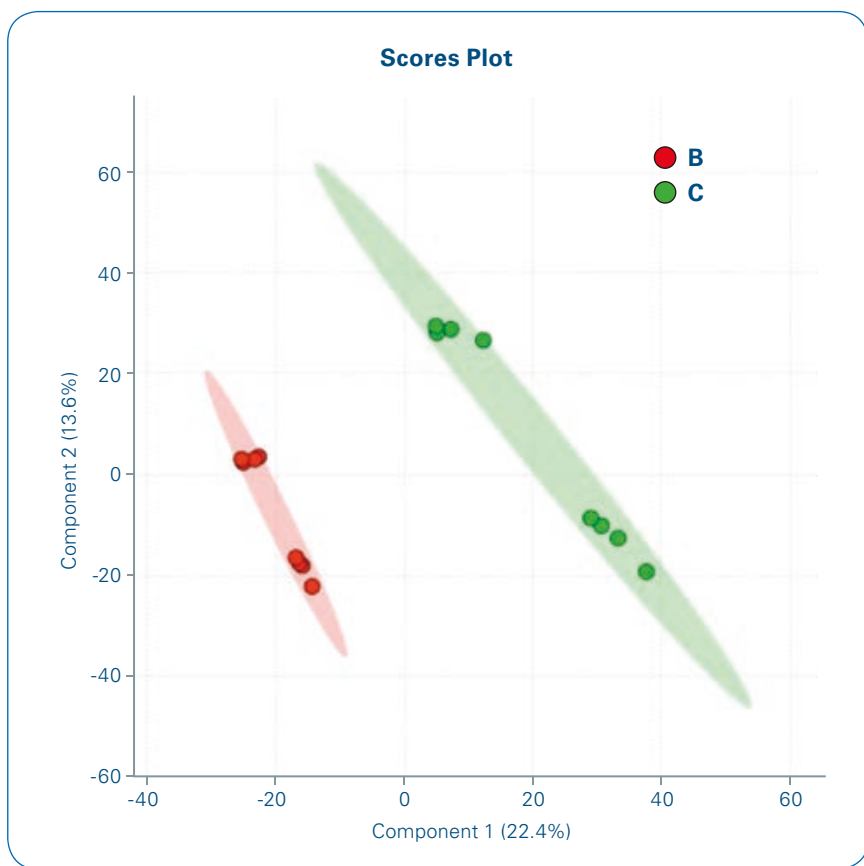


Figure 4: PLS-DA scores plot of control hair follicle (red) vs treated (green) with apple Annurca foam

Results

C57/BL6 mice were topically treated with a foam supplemented either with AAE or with a placebo. After 4 weeks of treatment, mice (11 weeks old) were sacrificed and their dorsal skin was excised. Skin biopsies were embedded in paraffin and prepared for histology. The metabolic content of hair follicle cells plucked out by mice were treated topically with AAE and analyzed by DI-MRMS mass spectrometry (workflow is shown in Figure 2). Complex profiles were obtained in positive and negative ion mode. The ultra-high mass accuracy (average mass error of only 0.166 ppm, Table 1), exact isotopic distribution and comparison with available standards ensured identification with high confidence. By screening intracellular metabolites with similar alteration tendency in all the AAE treated mice, glutaminolysis, pentose phosphate pathway (PPP), amino acid oxidation, mitochondrial β-oxidation as well as

Arginine metabolites became our focus. Significant elevation of glutamine and glycine as well as the increase in the intracellular level of the PPP intermediate Ribulose 5P together with the reduction of the intracellular level of nucleotides and deoxy-nucleotides suggest that AAE cause a reduction in the utilization of glucose and glutamine for PPP (Figure 3). This is a metabolic pathway that correlates with nucleotide biosynthesis in hair follicles. The reduced intracellular level of glutathione also confirmed that the catabolism of glutamine is halted in AAE treated hair

follicles. It can be concluded from PLS DA scores plot in Figure 4 that the hair follicles treated with AAE were well separated from the mice hair follicles treated with placebo. This verifies the observed results of the regulation of the metabolites shown in Table 1.

Overall, considering the results of SEM data (not shown here) and the metabolite profiles we could suggest that AAE diverts the intracellular metabolism of hair follicles from mainly set on PPP to a pool of selected amino acids to be used for keratin biosynthesis.

Conclusions

- Direct infusion MRMS can be used for fast and reliable metabolite profiling of hair follicle cells treated with Annurca apple extract.
- Several metabolites involved in different pathways could be detected and identified by DI-MRMS.
- A metabolic shift of hair follicle cells towards production of keratin was elucidated.
- A further test on a larger population is needed, as well as the employment of different Procyanidin rich extracts.



Learn More

You are looking for further Information?
Check out the link or scan the QR code for more details.

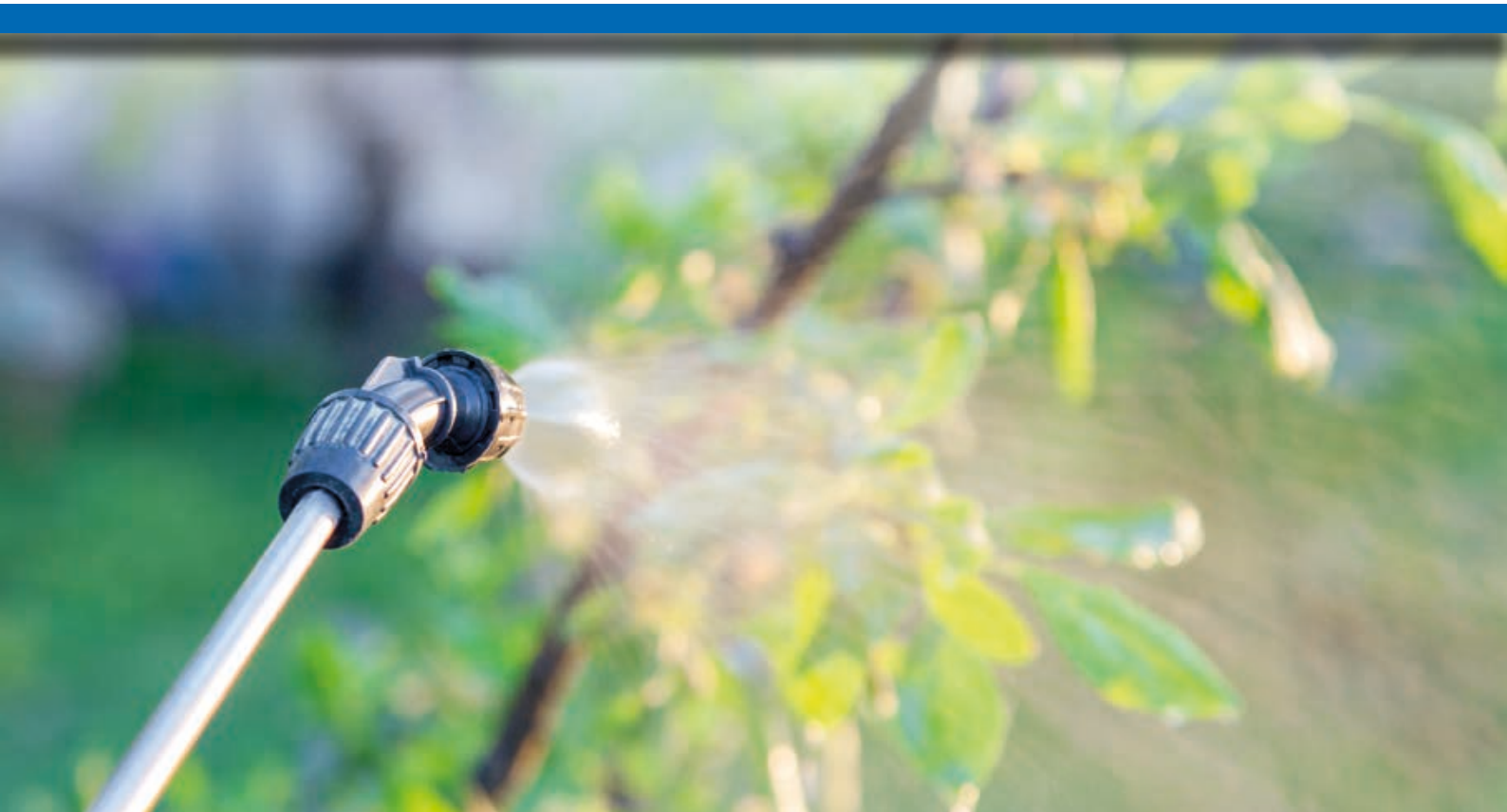
www.bruker.com/scimax



References

- [1] Sonthalia S, Daulatabad D, Tosti A (2016) *Hair Restoration in Androgenetic Alopecia: Looking Beyond Minoxidil, Finasteride and Hair Transplantation*. **2**, 1–13, doi:10.4172/2471-9323.1000105.

For Research Use Only. Not for Use in Clinical Diagnostic Procedures.



● MRMS aXelerate – rapidly detected micropollutants and plant response metabolites in poplar leaves

MRMS aXelerate is demonstrated to be a new and powerful workflow to rapidly profile plant extracts in a context of environmental pollution. This technique enables increased sample throughput by chromatography-free flow injection analysis (FIA) in combination with extreme mass resolution provided by the scimaX MRMS system complementary to deep profiling by LC-MS

MRMS aXelerate incorporates a 3-tier confidence engine provided by MetaboScape 4.0 allowing confident assignments of molecular formulae: a combination of ultra-high mass accuracy, True Isotopic Pattern and Isotopic Fine Structure to ensure confident

assignments at any level. Here it enabled the annotation of plant metabolites from several classes. Additionally, micropollutants (drugs and pesticides) which accumulated in poplar leaves could be detected. This accumulation reflected the growth

conditions of the analysed plants, either near polluted water or using only rain water. This study shows the straightforward workflow from plant crude extracts to detect drugs and pesticides using MRMS aXelerate.

Keywords:
plant metabolites, drugs, pesticides, FIA, MRMS, screening, metabolite profiling, metabolomics

Introduction

Wetlands are used for water depollution purposes in small towns. The waste water from houses is brought to a constructed wetland composed of several ponds planted with reeds (*Phragmites australis*), to be filtered. Before rejection to the natural environment (for example a river), the filtered water goes through a natural pond colonized by endemic species. The study presented here focuses on two poplars (*Populus nigra*) planted either on the natural pond riverbank (called "polluted" poplar), or several meters from the pond (called "control" poplar). FIA-MRMS and subsequent annotation with MetaboScape 4.0 using drug and pesticide databases were successfully used to analyse the plant metabolome and micropollutants.

Experimental

Sample preparation

Poplar leaf samples were collected from a wetland in Alsace (east of France). The differential analysis was permitted thanks to the build-up of the experiment: one poplar was planted on the riverbank of the natural

Table 1: Number of features and annotations using ESI(+), ESI(-) and combined data

Measurement	Features	Analytes FooDB*** plus drugs and pesticides	Mol. Formula with SF calc.**
ESI(+)	2,093	87/100*	1,801/1,876*
ESI(-)	1,444	277/306*	1,304/1,404*
ESI(+) and ESI(-) combined	3,452	326/383*	2,638/3,116*

Mass tolerance for Analyte List based search: 0.2/0.5 ppm

Mass tolerance for SmartFormula search: 0.2/0.5 ppm

Isotope accuracy for SmartFormula search: 0.2/0.5 ppm

* First value with mass tolerance of 0.2 ppm; second value with mass tolerance of 0.5 ppm

** Elements C₆N₂₀H_nO₄₀P₄S₄ have been considered for molecular formula calculations

pond of the wetland; a control poplar was planted several meters away from the pond to grow using only rain water. The poplars were planted approximately 2 years before the study occurred. For each condition, eight biological replicates were prepared using 300 mg (FW) of leaves, ground in liquid nitrogen and extracted three times with methanol. The supernatant was collected and dried, then resuspended in 1 ml MeOH. Deuterated abscisic acid was added (1 µg/ml ²H₆ ABA final) prior to extraction as an internal standard. A QC sample was prepared by mixing half part of control and half part of polluted extracts.

MS analysis

8 biological replicates of the "polluted" and the control samples and 2 QC samples were measured in 3 replicates in ESI(+) and ESI(-) modes using a scimaX 7T MRMS system. The stock solutions were diluted 1:1,000 with MeOH for the FIA-MRMS measurements. The detection mass range was set to m/z 107 – 3,000 with a mass resolving power of 1,350,000 at m/z 200 using quadrupolar detection. The measurements were performed with an UHPLC Elute HT system using a 20 µl sample loop. The sample loop was fully filled with sample solution

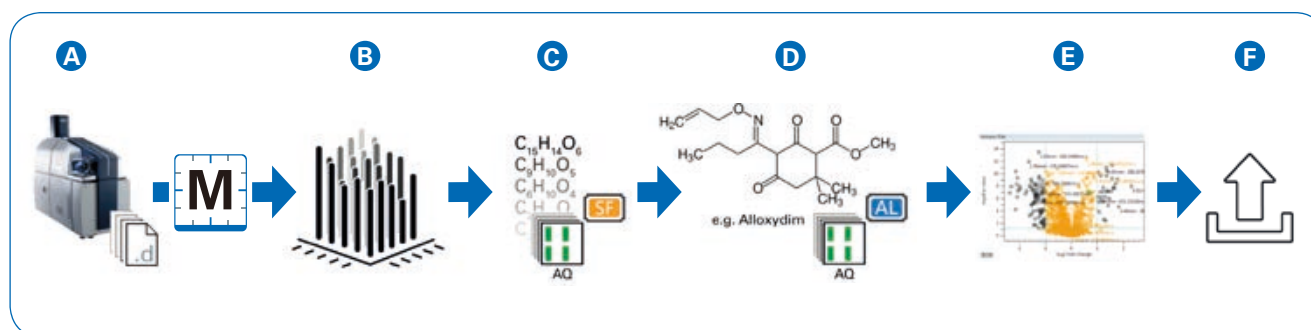


Figure 1: Schematic workflow: **A** FIA-MRMS acquisition using a scimaX MRMS **B** Data processing and evaluation using T-ReX 2D in MetaboScape 4.0 **C** Generate list of molecular formula annotations including annotation qualities **D** Putative compound annotations using AnalyteList of known and expected compounds **E** Statistical analysis to identify features of interest **F** Optional export for advanced statistical analyses

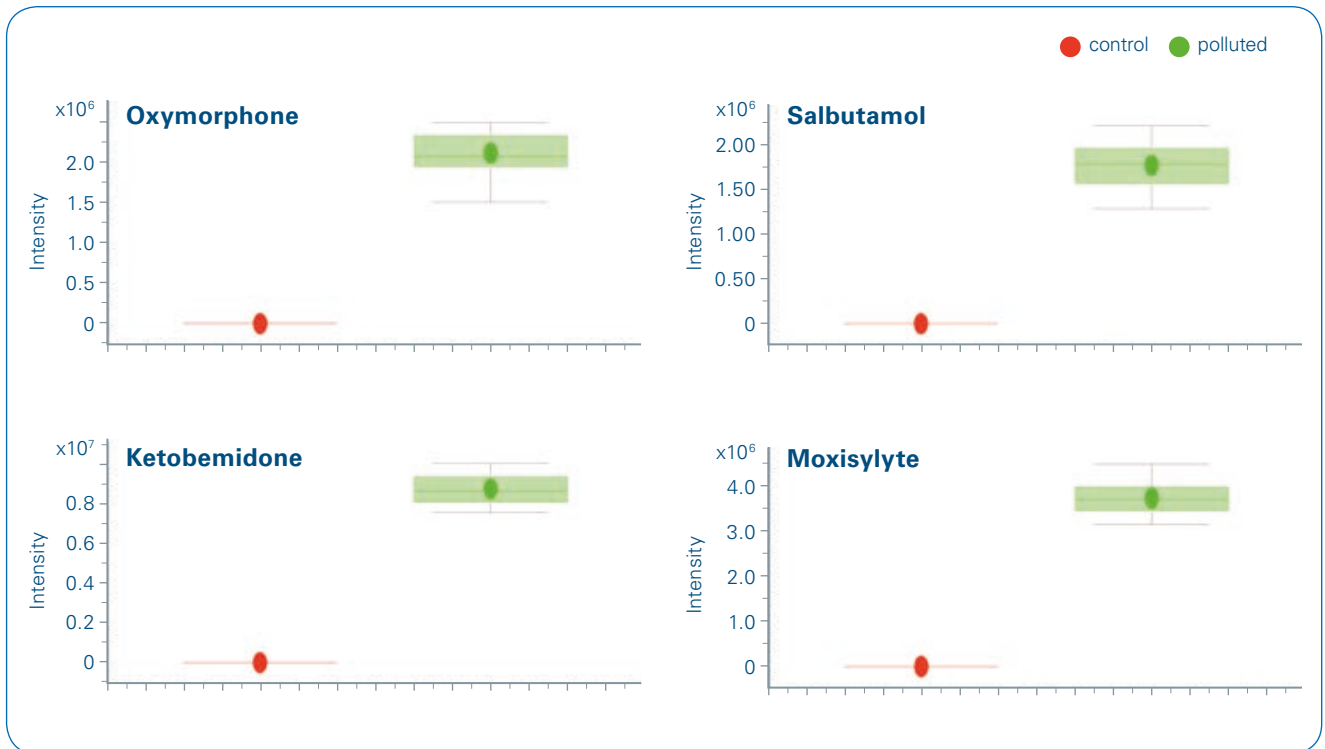


Figure 3a: Bucket statistic (box plots) of detected drugs in polluted poplar samples (green) and control poplar samples (red) detected in positive ion mode

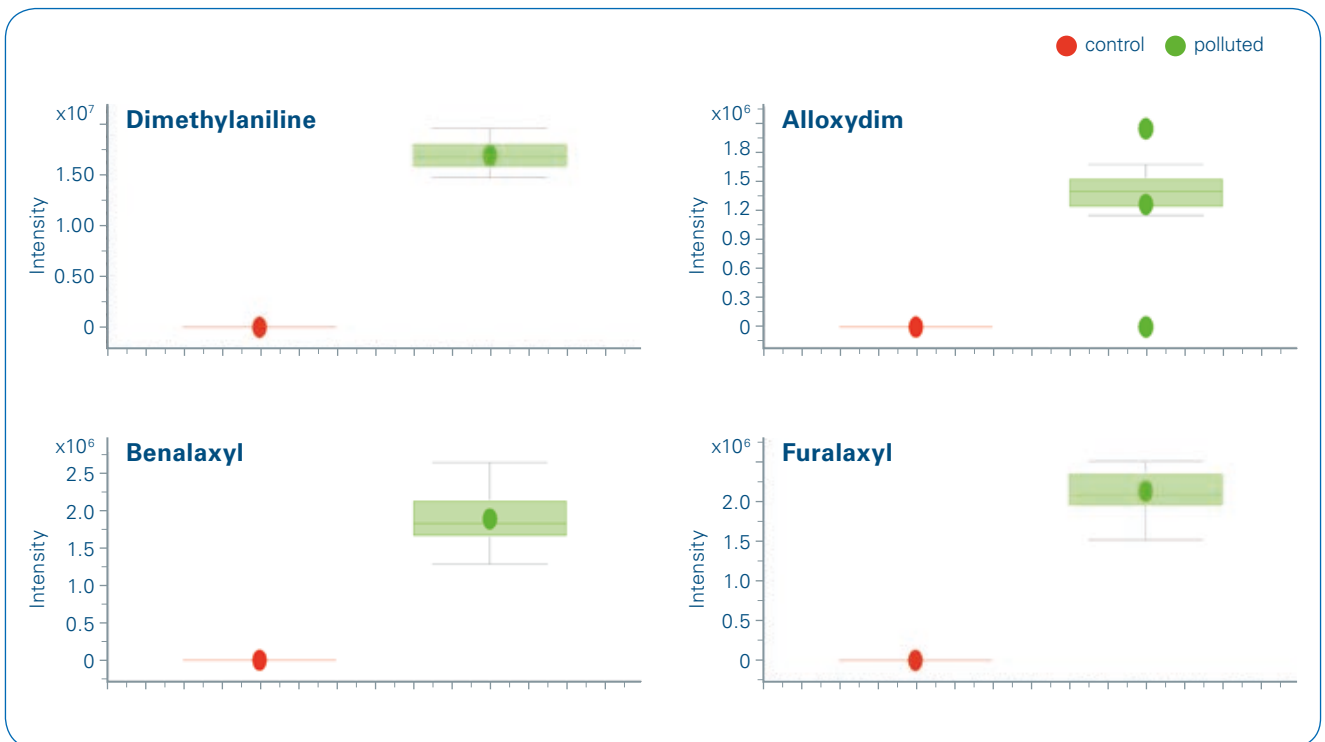


Figure 3b: Bucket statistic (box plots) of detected pesticides in polluted poplar samples (green) and control poplar samples (red) detected in positive ion mode

compounds with the Analyte List containing plant metabolites, drugs and pesticides. 2,638 (0.2 ppm) and 3,116 (0.5 ppm) molecular formulae were assigned with automatic Smart Formula based annotation. Several classes of plant metabolites could be detected and annotated: chlorophyll and derivatives, lipids, flavonoids, sugars, but also less abundant metabolites as hormones and derivatives. This experiment also showed the presence of micropollutants and drugs in poplar leaves, which were expected due to the growth conditions of the plants. T-test calculation of the T-ReX 2D extracted features in MetaboScape revealed several significant changes between the two different plants (see Figure 2). Investigating these in more detail by box plot displays in MetaboScape

revealed clear differential patterns for several micropollutants (drugs and pesticides) between control and polluted plants (Figure 3a and 3b).

This workflow proves that the assignment of metabolites and micropollutants in chromatography-free non-targeted profiling of crude plant extracts is possible. Additionally, MRMS aXelerate can increase sample throughput using the applied rapid flow injection analysis. Even in these conditions, low abundant metabolites could still be detected and annotated.

*** Note: FooDB is not a Bruker product.

Acknowledgements

We acknowledge the Agence de l'Eau Rhin Meuse (AERM) for access to the experimental field.

Conclusion

- MRMS aXelerate significantly reduces the sample analysis time by omitting time consuming chromatographic separation.
- Flow Injection Analysis increases sample throughput.
- Low abundant plant metabolites could be detected from crude extracts without dedicated purification.
- Metaboscape 4.0 allows the annotation of plant metabolites and micropollutants based on 3 tier confidence using specific databases.
- This technique enables non-targeted analysis of crude extracts, which could lead to detection of several different micropollutants accumulating in plant leaves.



Learn More

You are looking for further Information?
Check out the link or scan the QR code.

www.bruker.com/mrmsaxelerate



For research use only. Not for use in diagnostic procedures.



● Automated MALDI Magnetic Resonance Mass Spectrometry (MRMS) for biomarker identification in large clinical sample sets

The selection of a MALDI MS approach in conjunction with the high mass accuracy and resolving power of the MRMS platform has enabled increased sample throughput and the direct interrogation of complex clinical biofluids such as serum and urine without the need for any advanced sample preparation or purification after collection

In conjunction with advanced automated acquisition strategies, data has been acquired in a fraction of the time previously required to facilitate high quality data with the high sample throughput required for large clinical sample sets.

Introduction

Mass spectrometry has increasingly been applied in the clinical

setting due to the high and specific information content provided to researchers that enables a positive effect on patient outcomes. The foundation of this application is the high sensitivity, mass resolving power, and mass accuracy in combination with the multiplex detection advantage of MRMS when compared to other analytical approaches. A major drawback though is the

additional sample preparation required for biofluids prior to LC-MS or direction infusion ESI-MS. An alternative to this approach that eliminates the majority of sample preparation is MALDI-MS. Beyond mixing with a suitable ionization matrix, small amounts of sample (~ 1 μ L) can be analyzed with no prior preparation or purification after clinical collection and in a high throughput fashion via

*Keywords:
Metabolomics, Clinical,
MALDI, MRMS*

MALDI automation. A single spectrum can typically be collected per sample spot in less than a minute resulting in the ability to measure an entire 384 spot plate in several hours. Post-acquisition, MetaboScape 3.0 enables the analysis of complete sample sets for compound identification based on isotopic fine structure (ISF) and library searches in addition to multivariate statistical analysis.

Sample Preparation

Serum and urine were collected for clinical patients and stored at -80°C . After thawing at 4°C , samples were mixed 1:1 with DHB matrix and 1 μL spotted onto a 384 sample Anchor-Chip target. No additional preparatory steps were required before mass spectrometry analysis.

Mass spectrometry analysis

Urine and serum samples were analyzed on a Bruker MRMS system at either 9.4 T or 12 T using MALDI automation for increased throughput. For urine samples, a 4 M transient (1 s) with a low detection m/z of 75 was acquired. 12 scans were summed for each sample leading to an average of ~ 40 seconds to ana-

lyze each spot (including instrument overhead time). In selected cases (sp. serum), detection at twice the cyclotron frequency (2ω) and absorption mode processing were employed to increase the mass resolving power.

Data Analysis

Analysis was performed in Bruker DataAnalysis 5.0 for individual spectra and MetaboScape 3.0 for multivariate analysis of large sample sets.

Results

To date NMR data has been collected for over 300 clinical samples. Preliminary metabolic profiles have been established to determine relative differences in lipid, amino acid, and glucose levels. In our preliminary MS data, samples from three patient sub-groups have been examined in positive ion mode by MALDI-MRMS. Each acquisition required less than a minute and resulted in complex spectra. For example in serum, we have been able to identify molecular compositions that correspond to over 100 lipid species with a mass error less than 250 ppb shown in Figure 1 (A). Due to the

ionization mechanism during MALDI, most analytes are observed as singly charged species. Although MALDI reduces the spectral density of peaks when compared to ESI, these samples still benefit from the high resolving power due to the structural similarity of lipids. This intrinsic quality poses a limitation on the number of unique assignments when a mass spectrometer with insufficient mass resolving power is employed due to the over-lapping nature of isotopic envelopes in lipids where a difference of 2H can arise due to bond saturation. Seen in Figure 1 (B), a mass resolving power of approximately 325,000 is required to resolve the A+2 peak of a preceding phosphocholine/ phosphoethanolamine (PC/PE) lipid species from the A or monoisotopic peak of the following PC/PE with one less double bond. Without the mass resolution provided by MRMS, the presence of two species could not be confirmed with a high level of certainty.

In addition to serum, urine from the same sample pool have been analyzed by automated MALDI-MRMS. Due to the increased salt content, additional sample preparation and/or chromatographic methods are

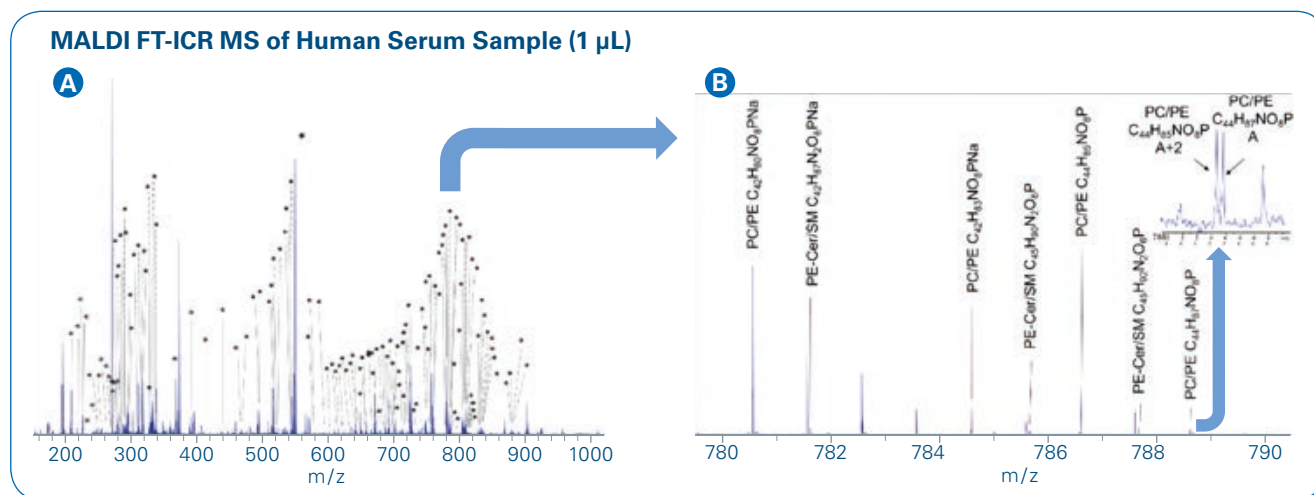


Figure 1: **A** 129 molecular compositions assigned for lipid species (*). Detected as either $[M+H]^+$ or $[M+Na]^+$ with mass error < 250 ppb. Molecular composition at m/z 203.05261 detected as $[M+Na]^+$ and assigned as $\text{C}_6\text{H}_{12}\text{O}_6\text{Na}$ (49 ppb). **B** Zoom of m/z 780-790 to indicate importance of resolving power to detect and assign lipid series that overlap due to variations in saturation (mass increases of 2H) resolving power $\sim 325,000$ required to make the split indicated in the inset.

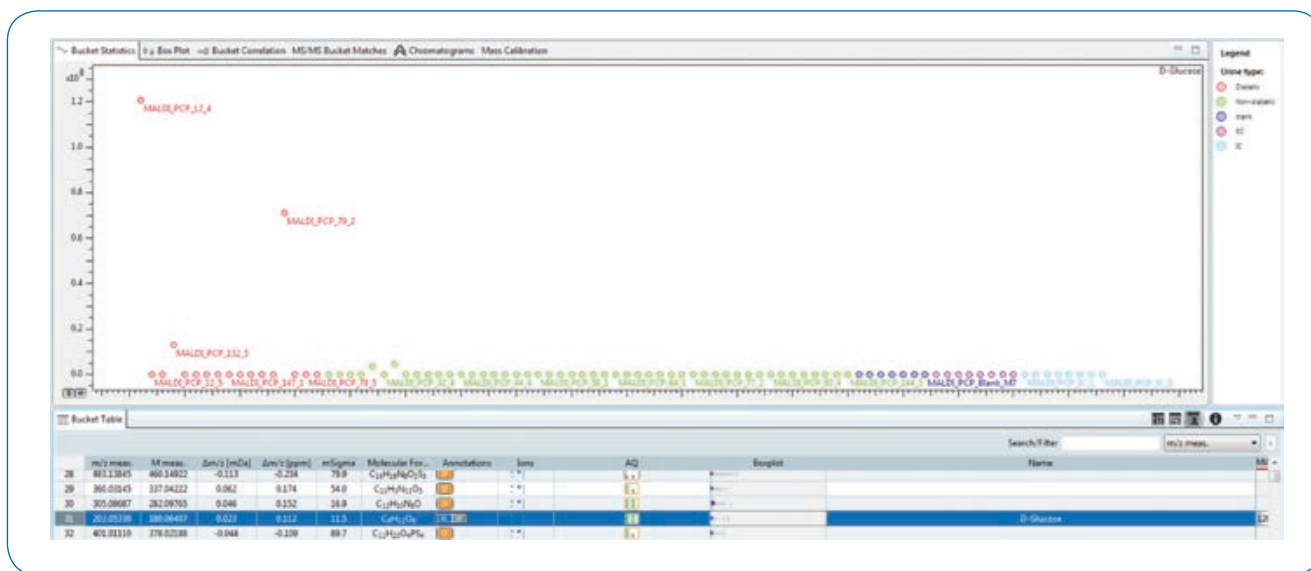


Figure 2: The bucket at m/z 203.05261 was detected as [M+Na]⁺ and assigned as D-Glucose (49 ppb). Bucket statistics for this metabolite shows that high intensities of D-Glucose can only be detected in samples of diabetic patients.

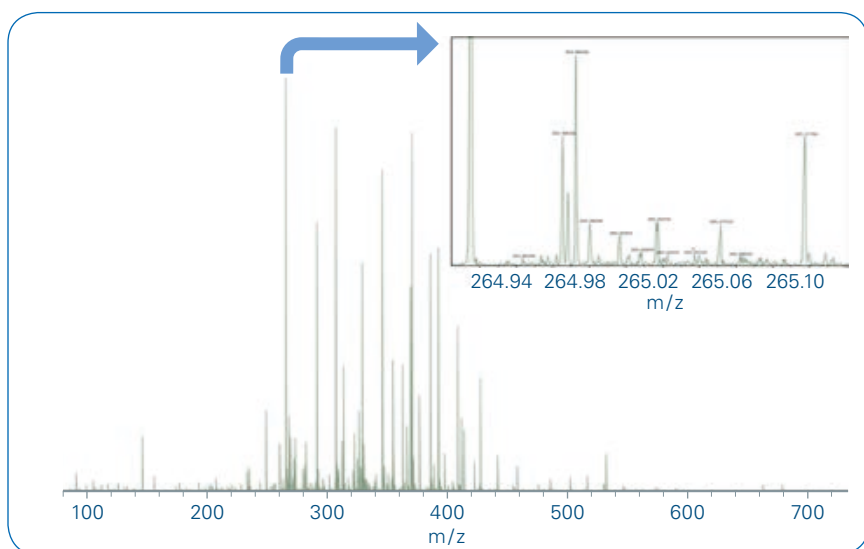
required prior to MS analysis. MALDI is more tolerant of the salt and presents a straightforward path for sample ionization. The MALDI automation approach has resulted in the ability to directly measure the chemical complexity of over 300 clinical urine samples plus internal/external controls and blanks (480 total spots) in less than 6 hours. For comparison, an LC-MS approach would have required approximately 120 hours

Figure 3: MALDI MRMS analysis of 355 clinical urine samples with no sample prep beyond the addition of DHB matrix and just under 6 hours of instrument time required.

based on 15 minute gradients alone and not including equilibration or washes. A typical spectrum is shown in Figure 2 and demonstrates the molecular complexity of this biofluid. Shown in the Figure 3 inset is a 0.10 Th wide excerpt of the spectrum illustrating the need for the increased mass resolving power afforded by MRMS in this experimental approach.

Detailed analysis of this large sample set was performed within MetaScape 3.0. Automatic assignment of elemental compositions and ana-

lyte identifications was performed for detected features using accurate mass and isotopic pattern information using a novel algorithm for mass recalibration, feature extraction, and de-isotoping. The generated Bucket Table was automatically annotated by assigning analyte names based on a list of known urine metabolites obtained from the Human Metabolome Database (<http://www.hmdb.ca/>). Additional databases can also be imported for further assignments. A key feature of the analysis is the identification of patients with elevated urine glucose levels shown in Figure 3.



For research use only. Not for use in diagnostic procedures.

Conclusion

- Automated MALDI MRMS provides the opportunity to obtain complementary information that support NMR findings on large clinical sample sets with minimal sample prep.
- MetaboScape 3.0 enabled processing of MALDI-MRMS data facilitating this higher throughput profiling workflow.



• Unambiguous Natural Product ID

Unambiguous molecular formula identification of natural products by analyzing Isotopic Fine Structures acquired from high resolution mass spectrometer

Introduction

Identification of an exact molecular formula for natural products represents one of the major goals and challenges in discovery of novel secondary

metabolites.^[1] Molecular formulas can be utilized as a golden standard for dereplication of known natural products from existing compound databases, which prevents unnecessary time and reduces labor cost. In

addition, the rapid confirmation of molecular formula would provide significant information for structural elucidation of unknown compounds and accelerate the whole discovery process of natural products.

Keywords:
Mass Spectrometry,
High Resolution, Iso-
topic Fine Structure,
Molecular Formula
Identification, Natural
Products

Authors: Jia-Xuan Yan; Dr. Fan Zhang, Dr. Navid Adnani, Dr. Tim S. Bugni
School of Pharmacy, University of Wisconsin, Madison, USA

Mass spectrometry is a well-established technique for measuring the accurate mass to charge (m/z) ratios of different ions. This technique has been widely used in determining the molecular formulas of natural products as well as synthetic compounds. In mass spectrometry, resolution could be defined as: [2]

$$\text{Resolution} = R = M/\Delta M$$

M is the m/z ratio of the selected peak and ΔM is usually defined as the peak width at its half-maximum peak height. The resolution of the measurement could be improved by increasing the resolving power of the mass spectrometers. Thus, the monoisotopic mass peak could be identified correctly and lead to an accurate molecular weight of the compound. However, the accurate mass alone is not sufficient for determining the unambiguous molecular formula of natural products due to combinatorial explosion. [3] It has been demonstrated that even with

Table 1: Mass defects and natural abundance of common isotopes in organic compounds

Element	Isotope	Atomic Mass (u)	Mass Defect (u)	Natural abundance (%)
Hydrogen	^1H	1.00783	0.00783	99.9885
	^2H (D)	2.01410	0.01410	0.0115
Carbon	^{12}C	12.00000	0.00000	98.93
	^{13}C	13.00335	0.00335	1.07
Nitrogen	^{14}N	14.00307	0.00307	99.632
	^{15}N	15.00011	0.00011	0.368
Oxygen	^{16}O	15.99491	-0.00509	99.757
	^{17}O	16.99913	-0.00087	0.038
	^{18}O	17.99916	-0.00084	0.205
Sulfur	^{32}S	31.97207	-0.02793	94.93
	^{33}S	32.97146	-0.02854	0.76
	^{34}S	33.96787	-0.03213	4.29
Chlorine	^{35}Cl	34.96885	-0.03115	75.78
	^{37}Cl	36.96590	-0.03410	24.22
Bromine	^{79}Br	78.91834	-0.08166	50.69
	^{81}Br	80.91629	-0.08371	49.31

0.1 ppm mass accuracy for the MS instrument, a unique molecular formula could not be determined when C, H, N, S, O, P atoms were included in the search list for molecules with molecular weight above 185.9760 Da. [3] Therefore, additional information, such as isotope abundance

ratio, would be required for the determination.

The concept of mass defect is the result of different nuclear binding energies of different elements and their nuclides. [4] Conventionally, ^{12}C was defined as the element with zero mass defect while other nuclides have different mass defect depending on their relative nuclear binding energy to ^{12}C . Additionally, each element would have a certain ratio of different isotopes based on their natural abundance. Therefore, compounds with different elemental composition would have different exact masses as well as unique Isotopic Fine Structure (IFS). Mass defects and natural abundance of common elements in organic compounds and their isotopes are displayed in Table 1. [4]

Here we demonstrate the unambiguous molecular formula determination of a natural product echinomycin A using the above mentioned IFS concept. This method would potentially be used as a powerful tool for rapid discovery of novel compounds and quick dereplication of known compounds in natural product libraries. We recently found that IFS was crucial for determining an exact molecular formula for the unambiguous molecular formula determination of keyicin, an antibiotic produced by marine bacterial co-culture. [5] The determination of the exact formula played a crucial role in the structural elucidation process of keyicin because an exact carbon count by NMR was unattainable without ^{13}C isotopic enrichment.

Experimental

The examined compound, echinomycin, was isolated from the marine *Streptomyces* sp. WMMC-592 following the typical include the natural product isolation and purification

process. [6] HPLC purification was performed using a Shimadzu LC-20AP system with a Luna 5 μm C18 100Å 250*10 mm column. Linear gradient from 25:75 MeCN/ H_2O (with 0.1% acetic acid) to 50:50 MeCN/ H_2O (with 0.1% acetic acid) over 35 minutes was used.

Mass spectrometry detection was performed using a Bruker 12T MRMS (Magnetic Resonance Mass Spectrometry) instrument and a Bruker QTOF MS instrument. The instruments were operated under ESI positive mode to acquire full scan MS spectra. Bruker ESI-MS tuning mix was used for the instrument calibrations. The compound was dissolved in LC/MS grade MeOH (2 $\mu\text{g}/\text{mL}$). The acquired data was analyzed by Bruker Compass DataAnalysis 4.4 SR1. Molecular formula determination was carried out using SmartFormula and the isotopic patterns were simulated by Simulate Pattern.

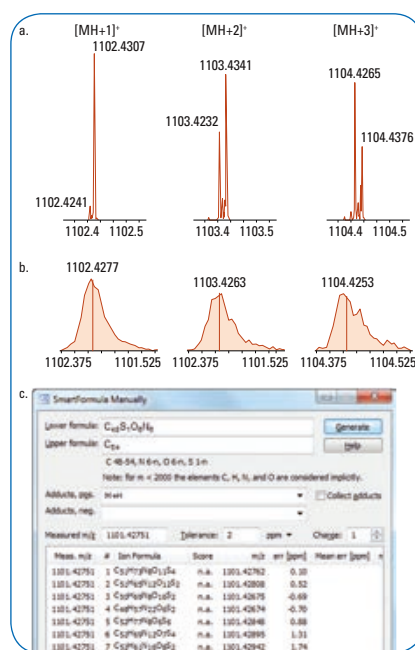


Figure 1: a.) Bruker 12T MRMS spectra and b.) Bruker QTOF MS spectra of tested compounds. [MH+1]⁺, [MH+2]⁺, [MH+3]⁺ ions were displayed. c.) SmartFormula analysis of possible adducts formulas.

Results and Discussion

Assignment of the molecular ion and SmartFormula prediction of possible molecular formulas

Direct infusion MRMS data collected under ESI (electrospray ionization) positive mode displayed an intense $[M+H]^+$ adduct peak with m/z ratio of 1101.4275. Isotopologues were fully resolved in the spectra for $[MH+1]^+$, $[MH+2]^+$ and $[MH+3]^+$ ions (Figure 1a). On the other hand, data acquired on a QTOF did not show resolved isotopologues (Figure 1b). SmartFormula was used to provide a range of reasonable formulas. The search was set to be C48S1N6O6 and the upper formula C54 based on preliminary NMR data. The MS error tolerance was set to be 2 ppm, and seven possible molecular formulas were given by SmartFormula analysis (Figure 1c): $[C_{51}H_{73}N_8O_{11}S_4]^+$, $[C_{51}H_{65}N_{12}O_{12}S_2]^+$, $[C_{50}H_{69}N_8O_{16}S_2]^+$, $[C_{48}H_{57}N_{22}O_6S_2]^+$, $[C_{52}H_{77}N_8O_6S_6]^+$, $[C_{52}H_{69}N_{12}O_7S_4]^+$ and $[C_{51}H_{61}N_{16}O_8S_2]^+$.

Determination of the exact molecular formula

Different element composition of the molecules would show their unique IFS and these fine structures could be observed with the improved resolution of the MRMS instrument (Figure 1a). For $[MH+1]^+$ ion, the difference between the two peaks

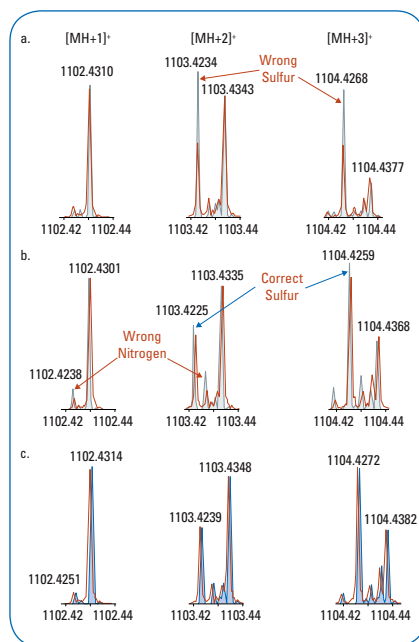


Figure 2: Overlaid IFS of the actual tested compound spectra and a.) $[C_{51}H_{73}N_8O_{11}S_4]^+$; b.) $[C_{48}H_{57}N_{22}O_6S_2]^+$; c.) $[C_{51}H_{65}N_{12}O_{12}S_2]^+$.

was 0.0066 u, which matched the mass defect difference of $^{15}N^{12}C$ and $^{14}N^{13}C$ (0.0063 u). Similar calculations were performed and the different peaks observed in $[MH+2]^+$ and $[MH+3]^+$ ions were assigned to the combinations of $^{34}S^{12}C_2^{32}S^{13}C_2$ and $^{34}S^{13}C^{12}C_2^{32}S^{13}C_3$ respectively. In contrast, the spectra collected from the QTOF instrument were not able to display similar fine structures (Fig. 1b). Therefore, the accurate molecular formula could be identified from various possibilities by matching its unique IFS to the collected spectra. The IFS of three possible species,

$[C_{51}H_{73}N_8O_{11}S_4]^+$, $[C_{48}H_{57}N_{22}O_6S_2]^+$ and $[C_{51}H_{65}N_{12}O_{12}S_2]^+$ were simulated by Simulate Pattern function and the simulated MS peaks were overlaid with the actual spectra (Figure 2). For $[MH+2]^+$ ion, the relative abundance of $[^{12}C_{51}H_{73}N_8O_{11}^{32}S_3^{34}S]^+$ was significantly higher than the actual molecule, (Figure 2a) which indicated the tested compound should have less sulfur atoms than $[C_{51}H_{73}N_8O_{11}S_4]^+$. Similar trend was found in the $[MH+3]^+$ ion overlaid spectra. The tested compound was suggested to contain 2 sulfur atoms since the sulfur related peaks in $[MH+2]^+$ and $[MH+3]^+$ overlaid spectra matched the simulated IFS of $[C_{48}H_{57}N_{22}O_6S_2]^+$ (Figure 2b). However, the simulated $[C_{48}H_{57}^{14}N_{21}^{15}NO_6S_2]^+$ ion abundance and $[^{12}C_{47}^{13}CH_{57}^{14}N_{21}^{15}NO_6S_2]^+$ ion abundance were higher than the corresponding ion abundance in the actual spectra, indicating this adduct formula was a mismatch. Similar evaluations were performed on $[C_{51}H_{65}N_{12}O_{12}S_2]^+$ and the simulated fine structure could match the actual spectra (Figure 2c), indicating the molecular formula of the tested compound was $C_{51}H_{64}N_{12}O_{12}S_2$. This compound was identified as echinomycin A by detailed NMR analysis.^[7]

Conclusion

The unambiguous identification of the tested compound molecular formula among various possibilities was achieved by acquiring data from Bruker 12T MRMS system and analyzing the IFS of the acquired MS spectra. This technique features efficient and rapid molecular formula identification for further dereplication and novel natural products discovery efforts.

The SmartFormula and Simulate Pattern functions of Bruker Compass DataAnalysis 4.4 SR1 software were crucial for this analysis. When setting up proper limitations in SmartFormula search, the possible molecular formulas of the tested sample could be narrowed down and simplify the Simulate Pattern process. The identified accurate molecular formula would potentially be used as one of the key elements for metabolites database analyses.



Learn More

You are looking for further Information? Check out the Link or scan the QR Code.

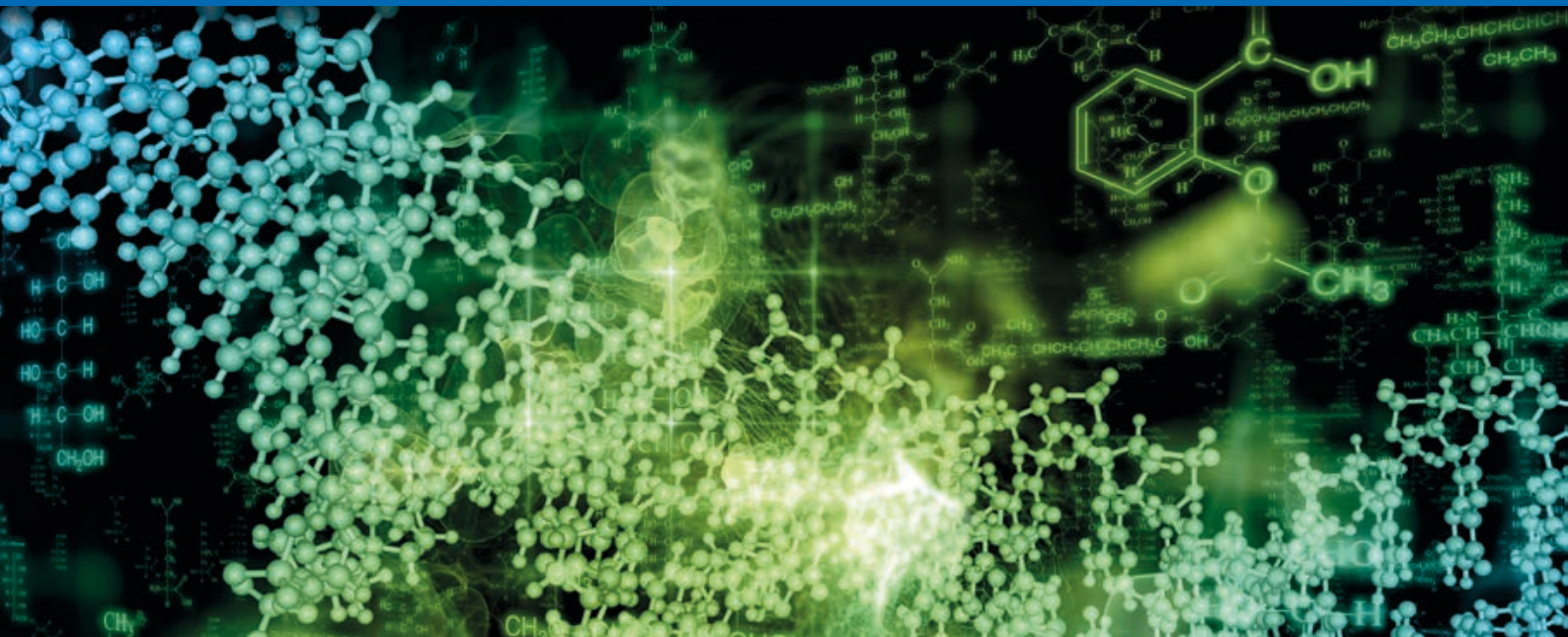
www.bruker.com/isotopic-fine-structure-webinar



References

- [1] Dührkop, K.; Hufsky, F.; Böcker, S., *Mass Spectrom (Tokyo) 2014*, 3(3): S0037; DOI: 10.5702/massspectrometry.S0037
- [2] Guan, S.; Marshall, A. G., *Anal. Chem.* 1996, 68(1), 46-71.
- [3] Kind, T.; Fiehn, O. *BMC Bioinformatics* 2006, 7:234.
- [4] Sleno, L., *J. Mass. Spectrom.* 2012, 47, 226-236.
- [5] Adnani, N.; Chevette, M. G.; Adibhatla, S. N.; Zhang, F.; Yu, Q.; Braun, D. R.; Nelson, J.; Simpkins, S. W.; McDonald, B. R.; Myers, C. L.; Piotrowski, J. S.; Thompson, C. J.; Currie, C. R.; Li, L.; Rajski, S. R.; Bugni, T. S. *ACS Chem. Biol.* 2017, 12, 3093-3102.
- [6] Zhang, F.; Adnani, N.; Vazquez-Rivera, E.; Braun, D.R.; Tonelli, M.; Andes, D.R.; Bugni, T.S. *J. Org. Chem.* 2015, 80, 8713-8719.
- [7] Dell, A.; Williams, D. H.; Morris, H. R.; Smith, G. A.; Feeney, J.; Roberts, G. C., *J. Am. Chem. Soc.* 1975, 97(9), 2497-2502.

For research use only. Not for use in diagnostic procedures.



● Electron Induced Dissociation for the Differentiation of Isomeric Metabolites of Diclofenac

Electron induced dissociation (EID) is applied for the differentiation of structural isomers of diclofenac metabolites. EID showed superior capability over collision induced dissociation (CID) by providing detailed structural information to locate the hydroxyl groups on different rings.

In the human body, metabolism of drugs is a detoxification process. In some cases, the metabolites formed are chemically or pharmacologically active and may play an important role in observed pharmacology and/or toxicology in humans¹. Diclofenac is a non-steroidal anti-inflammatory drug (NSAID) commonly used to reduce inflammation and pain. A major metabolic pathway for diclofenac

is phenyl hydroxylation, resulting in two major metabolites, 4'-OH-diclofenac (4'-OHD) and 5-OH-diclofenac (5-OHD), catalyzed by cytochrome CYP2C9 and 3A4, respectively². Determining the structures of these metabolites is critical for understanding the underlying biological activities and safety risk.

NMR is well-established as a powerful structural elucidation

technique³; however, it requires a relatively large amount of purified material that requires labor intensive and time-consuming purification steps. Alternatively, low energy CID, one of the most commonly used MS/MS techniques, provides detailed structural information for molecules of interest. Unfortunately, low energy CID is unable to differentiate the structural isomers due to the lack of specific bond cleavages.

Keywords:
EID, solarIX,
Metabolomics

Authors: Zhidan Liang¹, Zhoupeng Zhang², Jeremy J. Wolff³, Christopher J. Thompson³, Wendy Zhong¹ *

1. Analytical Research & Development, MRL, Merck & Co., Inc., Rahway, NJ 07065, USA

2. Department of Pharmacokinetics, Pharmacodynamics, & Drug Metabolism (PPDM), West Point, PA 19486, USA

3. Bruker Daltonics, Inc., Billerica, MA, 01821, USA

* Corresponding: Wendy Zhong, wendy.zhong@merck.com; Tel: +1 732-594-3431

Alternative fragmentation methods, including electron capture dissociation (ECD), have been developed and extensively studied in recent years⁴⁻⁶, but are limited to multiply charged ions. Consequently, ECD cannot be used for the structure elucidation of small molecules since they typically form singly charged molecules. Recently, electron induced dissociation (EID) has emerged as a technique that can be used to dissociate singly charged molecules^{5,7}. In this note, EID is used to differentiate isomeric diclofenac metabolites and the EID fragmentation behavior is compared with that generated via traditional CID.

Experimental

Sample Preparation

Diclofenac, 4'-OHD and 5-OHD were generously provided by Ian S. McIntosh (MRL). Each compound was directly infused into the mass spectrometer by a TriVersa NanoMate robot (Advion, Inc., Ithaca, NY, USA) at a concentration of 20 pmol/ μ L in a spray solution of 50:50 acetonitrile:water with 0.1% formic acid.

Mass Spectrometry

EID experiments were performed on a 9.4T Solarix qQq-Fourier transform ion cyclotron resonance (ICR) mass spectrometer (Bruker Daltonics, Billerica, MA, USA). Mass spectra were collected with 4 M data points, and summed over 100-200 scans depending on signal quality. The transient length was 0.84 s, and the estimated resolving power was \sim 150,000 at m/z 400. The signal-to-noise ratio (S/N) threshold was set to 3, and signals below that threshold were ignored. Data were analyzed using DataAnalysis 4.4 (Bruker Daltonics) with a mass accuracy of < 3 parts per million (ppm).

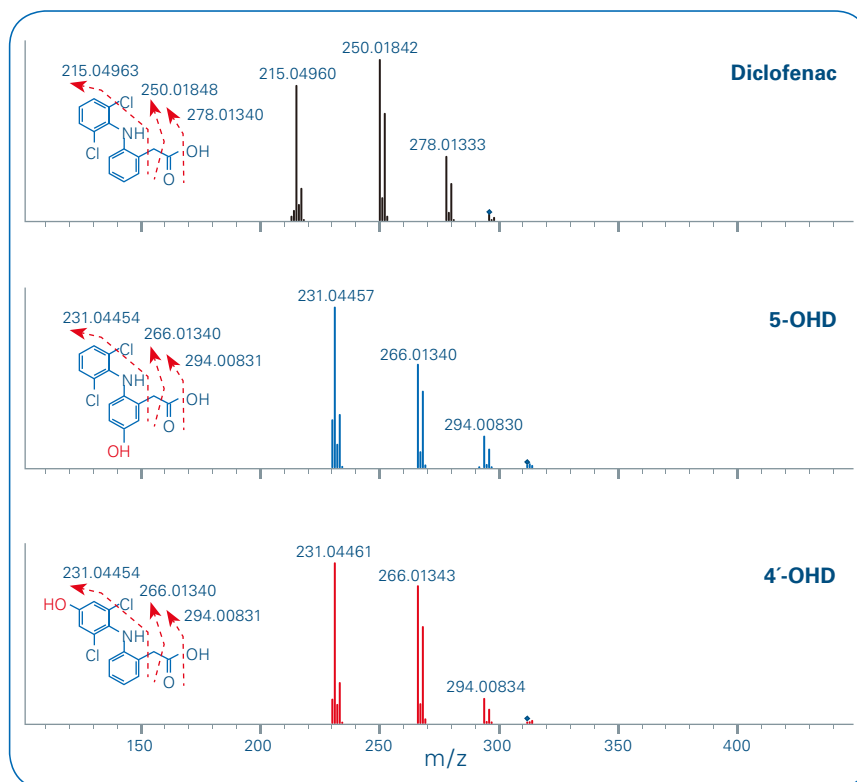


Figure 1: CID spectra of 4'-OHD and 5-OHD

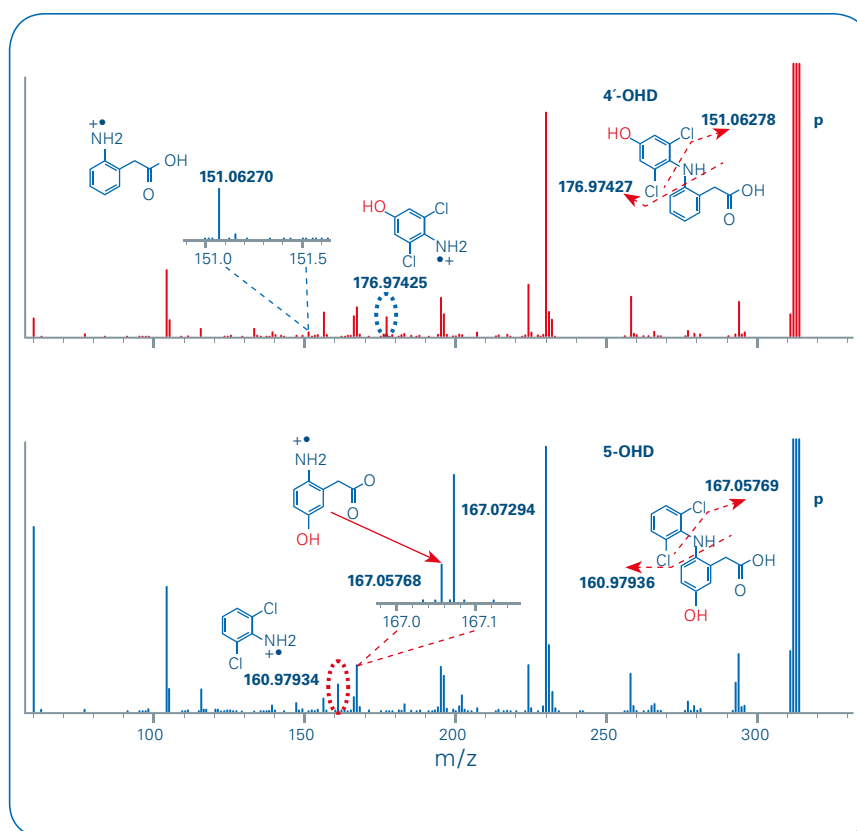


Figure 2: EID spectra of 4'-OHD and 5-OHD

Results and Discussion

CID Mass Spectrometry

Figure 1 shows the CID spectra of diclofenac, 4'-OHD, and 5-OHD. CID of all three compounds exhibited the same fragmentation behavior, always leading to chemical bond cleavage at identical locations. CID fragmentation of these compounds could not generate diagnostic fragments to differentiate which of the phenyl rings underwent hydroxylation.

EID Mass Spectrometry

The EID spectra of diclofenac, 4'-OHD and 5-OHD are shown in Figure 2. A greater number and

variety of fragments were detected under EID, especially fragment ions from the cleavage of the two aromatic ring systems. The most abundant fragments observed in the EID spectrum are summarized in Table 1. Diagnostic ions for the pair of isomers were at m/z 176.97425 and 151.06270 for 4'-OHD; m/z at 160.97934 and 167.0575 for 5-OHD under EID fragmentation. The resulting fragments preserved the substituents on the phenyl rings, including the chlorine and the hydroxyl. These fragments enabled the differentiation of the two structural isomers with hydroxyl groups on the two different phenyl rings. In particular, the

diagnostic ion at m/z 167.05756 for 5-OHD was very close to another fragment with m/z 167.07295, and was fully resolved by FT-ICR at the resolving power of $\sim 150,000$.

The CID technique tends to cleave the weakest bonds first. EID induces more cleavages while sparing the more labile chloro and the hydroxyl groups, which were predominantly cleaved under CID. A direct comparison of EID to CID fragmentation demonstrates the valuable application of EID technique in the structural characterization of isomers.

Table 1

Diclofenac	Measured m/z		Proposed formula
	4'-OHD	5-OHD	
	312.01899	312.01899	$[C_{14}H_{12}Cl_2NO_3]^+$
296.02412			$[C_{14}H_{12}Cl_2NO_2]^+$
	294.00840	294.00840	$[C_{14}H_9Cl_2NO_2]^{*+}$
278.01357			$[C_{14}H_{10}Cl_2NO]^+$
	277.05028	277.05012	$[C_{14}H_{12}ClNO_3]^{*+}$
	266.01345	266.01389	$[C_{13}H_{10}Cl_2NO]^+$
	258.03183	258.03169	$[C_{14}H_9ClNO_2]^+$
250.01862			$[C_{13}H_{11}Cl_2N]^{*+}$
242.03697			$[C_{14}H_9ClNO]^+$
	230.03672	230.03672	$[C_{13}H_9ClNO]^+$
214.04186	214.04174	214.04164	$[C_{13}H_9ClN]^+$
208.07578			$[C_{14}H_{10}NO]^{*+}$
	195.06789	195.06781	$[C_{13}H_9NO]^{*+}$
180.08059			$[C_{13}H_{10}N]^+$
	183.06782	183.06788	$[C_{12}H_9NO]^{*+}$
179.07298			$[C_{13}H_9N]^{*+}$
	176.97419		$[C_6H_5Cl_2NO]^{*+}$
	167.07289	167.07289	$[C_{12}H_9N]^{*+}$
		167.05756	$[C_8H_9NO_3]^{*+}$
160.97941		160.97930	$[C_6H_5Cl_2N]^{*+}$
151.06269	151.06265		$[C_8H_9NO_2]^{*+}$

Conclusions

The combination of high accuracy, high resolution FT-ICR mass spectrometry, and EID fragmentation has been successfully applied to distinguish a pair of structural isomers (4'-OHD and 5-OHD). By utilizing high electron energy (>10 eV), EID accessed more high energy fragmentation pathways than CID while retaining critical low energy bonds, thus providing complementary structural information and in some cases even additional information.

In general, an EID-based mass spectrometry method has shown great capability for structural characterization of small molecules carrying a single charge and exhibited great potential in differentiation of isomeric compounds.



Learn More

You are looking for further Information? Check out the link or scan the QR code for our latest webinar.

www.bruker.com/isotopic-fine-structure-webinar



References

1. Z. Zhang, M. Zhu and W. Tang, *Curr Pharm Des*, 2009, 15, 2220-2235.
2. W. Tang, R. A. Stearns, S. M. Bandiera, Y. Zhang, C. Raab, M. P. Braun, D. C. Dean, J. Pang, K. H. Leung, G. A. Doss, J. R. Strauss, G. Y. Kwei, T. H. Rushmore, S. H. Chiu and T. A. Baillie, *Drug Metab Dispos*, 1999, 27, 365-372.
3. M. D. G. Y. Liu, R. Marques, T. Pereira, R. Helmy, R. T. Williamson, W. Bermel, G. E. Martin., *Tetrahedron Letters*, 2014, 55, 5450-5453.
4. H. J. Cooper, K. Hakansson and A. G. Marshall, *Mass Spectrom Rev*, 2005, 24, 201-222.
5. H. Lioe and R. A. O'Hair, *Anal Bioanal Chem*, 2007, 389, 1429-1437.
6. K. O. Zhurov, L. Fornelli, M. D. Wodrich, U. A. Laskay and Y. O. Tsybin, *Chem Soc Rev*, 2013, 42, 5014-5030.
7. J. W. Jones, C. J. Thompson, C. L. Carter and M. A. Kane, *J Mass Spectrom*, 50, 1327-1339.

For research use only. Not for use in diagnostic procedures.



• Ultrafast Statistical Profiling of Bacterial Metabolite Extracts

Abstract

With modern statistical analysis of complex mixtures, the mining of complex natural products can be hampered more by mass spectrometry analysis time than statistical analysis time. In this work we present the “Ultrafast Statistic Profiling” (USP) workflow; a rapid method for distinguishing and identifying characteristic compounds in complex mixtures. Using USP, a series of metabolite extracts were analyzed by direct infusion Electrospray Fourier Transform Ion Cyclotron Resonance Mass Spectrometry (ESI-FT-ICR MS) without LC separation. Statistical analysis like principle component analysis (PCA) is used to determine compounds unique to each sample. Therefore, up- and down regulation of specific compounds can be recognized with this method. Ultra-high resolution mass spectra were acquired and used to calculate theoretical molecular formula. Because elemental composition calculation can return multiple hits even within 0.5 ppm mass accuracy, ultrahigh resolution mass spectrometry is used to determine isotopic fine structure of the unknown compounds. The isotopic fine structure of each molecular formula candidate is compared against the experimental iso-

Authors

Matthias Witt, Bruker Daltonik GmbH, Bremen, Germany
 Aiko Barsch, Bruker Daltonik GmbH, Bremen, Germany
 Jeremy Wolff, Bruker Daltonics Inc., Billerica, MA, USA
 Daniel Krug, Helmholtz Institute for Pharmaceutical Research Saarland (HIPS) and Saarland University, Saarbrücken, Germany
 Thomas Hoffmann, Helmholtz Institute for Pharmaceutical Research Saarland (HIPS) and Saarland University, Saarbrücken, Germany
 Rolf Müller, Helmholtz Institute for Pharmaceutical Research Saarland (HIPS) and Saarland University, Saarbrücken, Germany

Keywords	Instrumentation and Software
isotopic fine structure	DataAnalysis
metabolomics	SmartFormula
statistical analysis	ProfileAnalysis
CASI	

Four Mutants and Wild Type

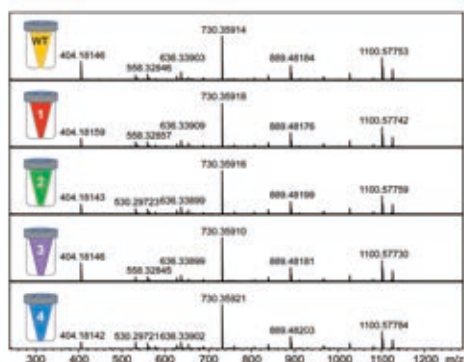


Figure 1: Broadband direct infusion FT-ICR mass spectra of wild type and mutant *Myxococcus xanthus* extracts appear very similar and show no visual differences.

topic fine structure. This enabled to literally “read out” the correct elemental composition for the target compounds. We have demonstrated for myxoprincomide, a recently discovered myxobacterial secondary metabolite, that this approach enables an unequivocal molecular formula generation for a compound with MW <1000 Da. With this USP workflow, we observe about a 20x decrease in sample analysis time combined with the unique capability to generate unambiguous molecular formula for compounds of interest by making use of isotopic fine structure information.

Introduction

Myxobacteria represent an important source of novel natural products exhibiting a wide range of biological activities. Some of these so-called secondary metabolites have been investigated as potential leads for novel drugs. Traditional approaches to discovering natural products mainly employ bioassays and activity-guided isolation from different myxobacterial isolates, but genomics-based strategies become increasingly successful to reveal additional compounds. These “metabolome-mining” approaches hold great promise for uncovering novel secondary metabolites from myxobacterial strains, as the number of known compounds identified to date is often significantly lower than expected from genome sequence information.[1]

Current, established methods are based on LC-QTOF-MS analysis requiring about 20 minutes of analysis time per sample. Facing several thousand myxobacterial strain isolates as well as numerous genetic knock-out mutant strains available to analyze for novel secondary metabolites, analysis time becomes the bottleneck of this workflow. In this work several metabolite extracts were analyzed from genetic knock-out mutants by Ultrafast Statistical

Statistical Data Treatment

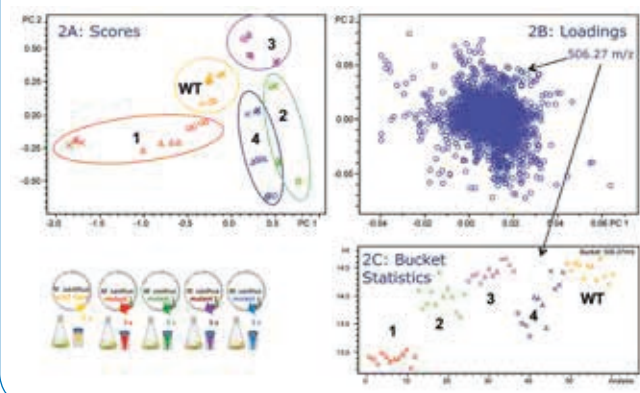


Figure 2: (A) PCA scores and (B) loadings plot of log transformed FT-ICR data reveals clustering of wild type (WT) and mutant samples (labeled 1 – 4). (C) Bucket statistics plot for selected loading m/z 506.27 shows this peak has decreased abundance in Sample 1.

Profiling (USP), a workflow designed to decrease sample analysis time by eliminating LC separation. For USP, each sample is analyzed by ultra-high resolution FTMS direct infusion measurements, requiring only about 1 minute per sample to measure. Statistical analysis is used to determine compounds characteristic to each metabolite sample, and possible molecular formulas are generated for each unique compound. Ultra-high resolution mass spectra, with resolving powers > 750,000 and the ability to observe isotopic fine structure, were acquired for each of the differentiating compounds, enabling unambiguous compound identification even for metabolites with MW > 1000 Da. The ultra-high resolution of an FT-ICR instrument enables for the first time an elemental composition determination for a molecular weight range where mass accuracy of existing mass spectrometers would be not enough for an unequivocal decision.

Experimental

Sample Preparation

Myxococcus xanthus wildtype DK1622 and 4 different gene knock out mutants were cultivated as 3 biological replicates each as described previously[1]. Mutant 1 was known to be impaired in the production of Myxoprincomid c506. [1] Mutants 2-4 contain deletions of a different gene each. All three genes are hypothetically encoding proteins within one biochemical pathway. Metabolic extracts were diluted 1:200 in 50% MeOH + 0.1% formic acid prior to analysis by mass spectrometry.

Mass Spectrometry Analysis

Samples were analyzed by direct infusion on a solariX 12T FT-ICR MS. Samples were ionized by ESI in positive ion mode at a flow rate of 2 μ L/min; data was acquired from m/z 200 – 1500. Sixty-four scans were averaged for each

High Resolution Differentiates Samples

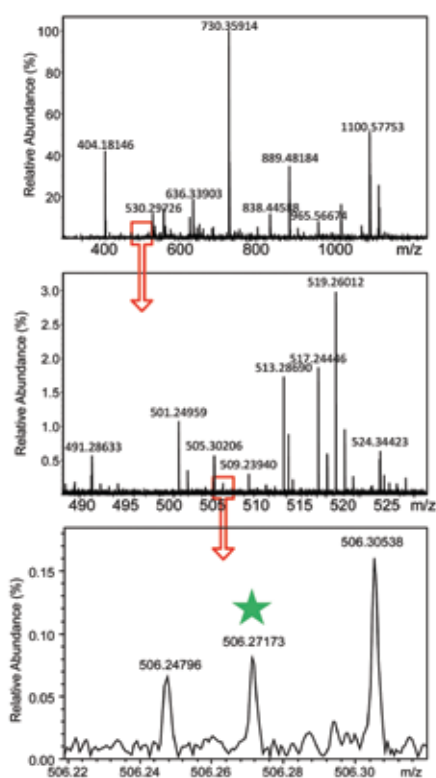


Figure 3: FT-ICR full scan mass spectrum of wild type sample showing zoomed region for the doubly charged compound at m/z 506.27 (marked with a green star), which differentiates the samples.

mass spectrum, with acquisition taking approximately 1 minute per sample. Each sample was analyzed 4 times (technical replicates) resulting in 60 FT-ICR MS spectra: 5 sample types x 3 biological replicates x 4 technical replicates. Statistical Analysis and Molecular Formula Generation ProfileAnalysis 2.1 was used for binning of MS peaks from ultra-high resolution FT-ICR MS single spectra acquired for all samples. The bucket table generated formed the basis for statistical data evaluation. The raw data was log transformed prior to PCA calculation. DataAnalysis 4.2 was used to generate molecular formula for peaks of interest generated from ProfileAnalysis, and to generate high resolution, simulated mass spectra of the predicted molecular formula.

Results

A visual comparison of the direct infusion high resolution FT-ICR MS spectra revealed no readily observable differences between the samples, as shown in Figure 1. Principal Component Analysis (PCA) of the normalized data using ProfileAnalysis clearly revealed a clustering of the samples according to their bacterial genetic background, e.g., wild type and mutants could be differentiated from each other with PCA (see Figure 2A). The second step in

CASI-enhanced Analysis

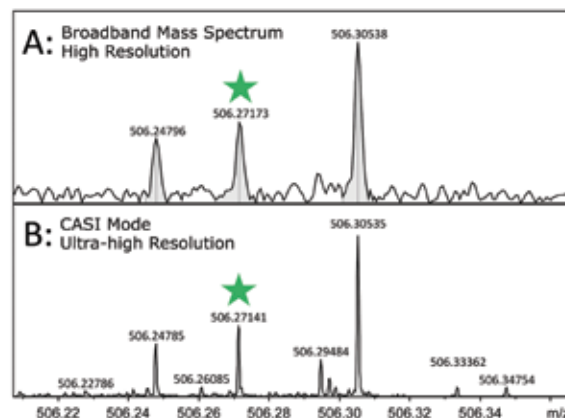


Figure 4: Zoom of mass spectrum around m/z 506 measured in (A) broadband and (B) CASI (continuous accumulation of selected ions) mode, which boosts the sensitivity. Resolving power was increased (RP = 780,00 for m/z 506) for CASI measurement. Peaks of interest are marked with a green star.

the USP workflow is to determine which compounds can be used to distinguish the samples. The PCA loadings plot, shown in Figure 2B, indicates one such compound responsible for this differentiation, the compound at m/z 506.27. The bucket statistics plot of the log normalized data for the doubly-charged compound at m/z 506.27 is shown in Figure 2C. This compound is responsible for differentiating Mutant 1 from all other samples, i.e. m/z 506.27 is present in all samples except Mutant 1. Closer analysis of wild type mass spectrum around m/z 506.27, Figure 3, confirms that very low abundance compound can be detected by statistical methods using ProfileAnalysis. In this example the target analyte had a relative intensity of 0.08% compared to the most intense MS peak in the same spectrum. The next step in the workflow is to determine the molecular formula of this unknown peak at m/z 506.27. Returning to the solariX, broad band, high resolution

Automated Isotopic Fine Structure Analysis

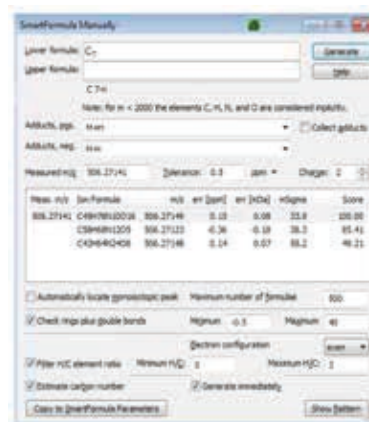


Figure 5: SmartFormula results for peak at m/z 507.27141. Three molecular formula hits were generated within a 0.5 ppm mass accuracy window

Isotopic Fine Structure—Ultimate Specificity

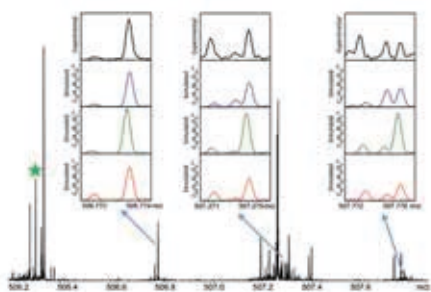


Figure 6: CASI spectrum of wild type sample with zoom-in of A+1, A+2 and A+3 region, highlighting experimental and simulated isotopic pattern for the three candidate molecular formulae. ^{12}C peak of compound of interest is marked with a green star.

CASI measurements (CASI = continuous accumulation of selected ions) were performed on the wild type sample for the mass range of $506 \pm 3 \text{ m/z}$. With CASI, only ions selected by quadrupole isolation are collected in the storage cell prior to detection in the ICR cell, increasing the S/N of the isolated ions. As shown in Figure 4, the combination of CASI and ultra-high resolution measurements ($\text{RP} = 780,000 @ \text{m/z } 500$) increased the S/N and resolving power of the peak at $\text{m/z } 506.27$. Predicted molecular formulae for the peak at $\text{m/z } 506.27 \pm 0.5 \text{ ppm}$ were determined with SmartFormula and generated 3 possible matches, as shown in Figure 5. In order to determine which of these elemental formulae is correct, the theoretical isotopic fine structure of the 3 predicted compositions were compared against the experimental fine structure of $\text{m/z } 506.27$, as shown in Figure 6. A comparison of the A+1 isotopic fine structure of the predicted formula $\text{C}_{43}\text{H}_{64}\text{N}_{24}\text{O}_{62}+$ (red spectrum) against the experimental isotopic fine structure (black spectrum), as shown in A+1 in Figure 7, reveals that the ^{15}N isotope peak in the A+1 region does not match the experimental data, eliminating this formula as a possibility. In the A+2 region of Figure 7, comparison of the $^{13}\text{C}_2$ and ^{18}O isotope peaks for the predicted formula $\text{C}_{58}\text{H}_{68}\text{N}_{12}\text{O}_{52}+$ (green spectrum) against the experimental fine structure shows a high abundance $^{13}\text{C}_2$ peak and a low abundance ^{18}O peak, eliminating this formula as a possibility. This leaves only $\text{C}_{45}\text{H}_{76}\text{N}_{10}\text{O}_{162}+$ (blue spectrum) as the possible molecular formula. Comparison of the isotopic fine structure for all the isotopes of $\text{C}_{45}\text{H}_{76}\text{N}_{10}\text{O}_{162}+$ against

Counting Hetroatoms with High Resolution

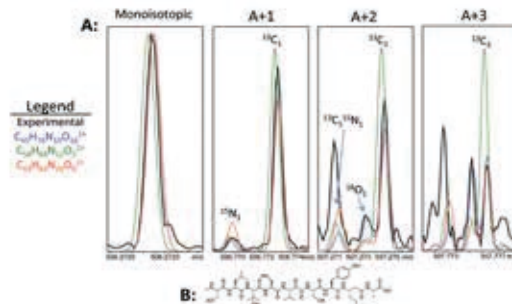


Figure 7: (A) Zoom of overlaid monoisotopic and A+1, A+2 and A+3 isotopic fine structures of experimental and simulated candidate formulae ($\text{RP} = 780,000$). (B) Structure of Myxoprincomide, $\text{C}_{45}\text{H}_{74}\text{N}_{10}\text{O}_{16}$, which is known to be absent in Mutant 1 [1] and is the only simulated molecular formula (blue line) which matches experimental (black line) isotopic fine structure.

the experimental data shows a very good match, as shown in A+1 to A+3 in Figure 7A. This formula fits perfectly to the structure of myxoprincomide (Figure 7B), known to be absent in Mutant 1 as recently published. [1] The newest DataAnalysis 4.2 version used in this study takes into account the isotopic fine structure information for calculating the mSigma value in SmartFormula. A low mSigma value indicates a good fit between measured and simulated isotopic pattern. Therefore, the visual isotopic fine structure comparison for candidate molecular formulae as outlined above is “automated” by SmartFormula. As shown in Figure 5 the mSigma value ranks the correct molecular formula candidate first.

Conclusion

The presented USP workflow enables rapid profiling of complex metabolite extracts by direct infusion FT-ICR MS measurements combined with statistical data evaluation. Unique identification capabilities of relevant and even minor abundant marker compounds are enabled by making use of the ultra-high resolution and the wide dynamic range provided by the FT-ICR MS technology—addressing several of the major requirements in metabolomics, sample throughput, sensitivity, and compound identification. The ultra-high resolution and high mass accuracy of the FT-ICR MS enabled observation of the isotopic fine structure allowing for an unambiguous molecular formula determination in SmartFormula for a compound with $\text{MW} < 1000 \text{ Da}$.

References

[1] Cortina et al., *Angew. Chem. Int. Ed.*, 2012, 51(3), 811-816



- **Profiling of Wine using ultra-high resolution Flow Injection Magnetic Resonance Mass Spectrometry (MRMS) and $^1\text{H-NMR}$ Spectroscopy**

The complexity of organic compounds in food products such as wine can be analyzed by LC free magnetic resonance mass spectrometry.

Introduction

Beside GCMS and LCMS, wine can be analyzed on the molecular level by Flow Injection Analysis (FIA) after solid phase

extraction (SPE) when combined with ultra-high resolution magnetic resonance mass spectrometry (MRMS). The mass spectra are a fingerprint of these complex mixtures of

organic compounds. Multivariate statistical analysis of FIA-MRMS and $^1\text{H-NMR}$ spectroscopy resulted in similar results.

Keywords:
MetaboScape 3.0,
Magnetic Resonance
Mass Spectrometry,
MRMS, NMR,
Metabolomics, Food
profiling, de-replication

Authors: Matthias Witt¹, Nikolas Kessler¹, Markus Godejohann², Michael L. Easterling³.

¹Bruker Daltonik GmbH, Bremen, Germany; ²Bruker BioSpin GmbH, Rheinstetten, Germany; ³Bruker Daltonics Inc., Billerica, MA, USA.

Methods

MS analysis: Wine samples were analyzed after solid phase extraction (SPE) using a Bruker solariX XR 7T mass spectrometer using ESI (-) mode with a resolving power of 300,000 at m/z 400. Raw spectra were subjected to deisotoping and adduct collation. Statistical analysis such as principal component analysis (PCA) as well as molecular formula calculation based on accurate mass, isotopic fine structure and filtering based on elemental composition were carried out automatically in MetaboScape 3.0. Annotated features were investigated using filters for mass defects and double bond equivalents (DBE). NMR analysis: SPE wine extracts were subjected to a Bruker FoodScreener™ (400 MHz Avance III NMR spectrometer). Automatic solvent suppression of the solvent resonances enabled the detection of organic constituents present in the extracts.

Data Preprocessing

The FIA-MRMS single spectral data from 145 analyses were processed within MetaboScape 3.0 using a novel algorithm (T-ReX 2D) for mass recalibration, feature extraction, deisotoping-, and pseudo spectra generation. Features were considered

red for further processing, if they could be recovered in at least 20 analyses.

The processing resulted in a feature matrix of 145 analyses \times 6436 putative molecular species. For each ion, isotopic patterns including isotopic fine structure if available, were all used to support compound annotation.

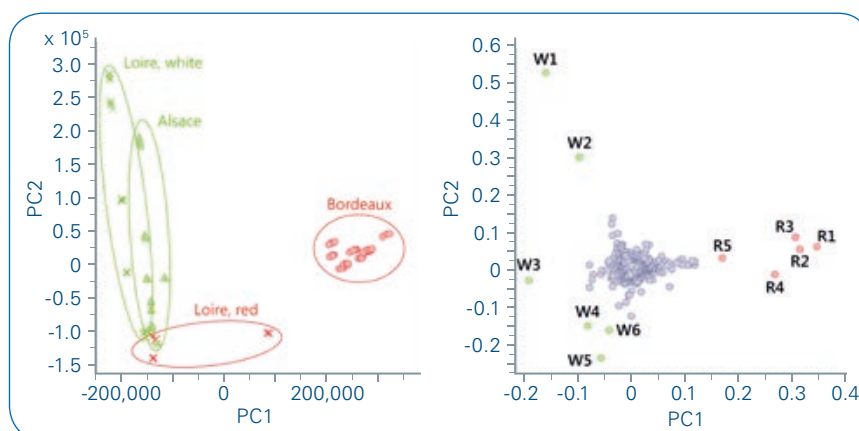


Figure 2: PCA scores plot (left) and loadings plot (right) of FIA-MRMS data of analyzed white and red wine from Bordeaux, Loire and Alsace. The red and the white wine as well as the wines from different regions were separated in the scores plot. Compounds mainly responsible for the separation/grouping are shown in Table 1 a) and b).

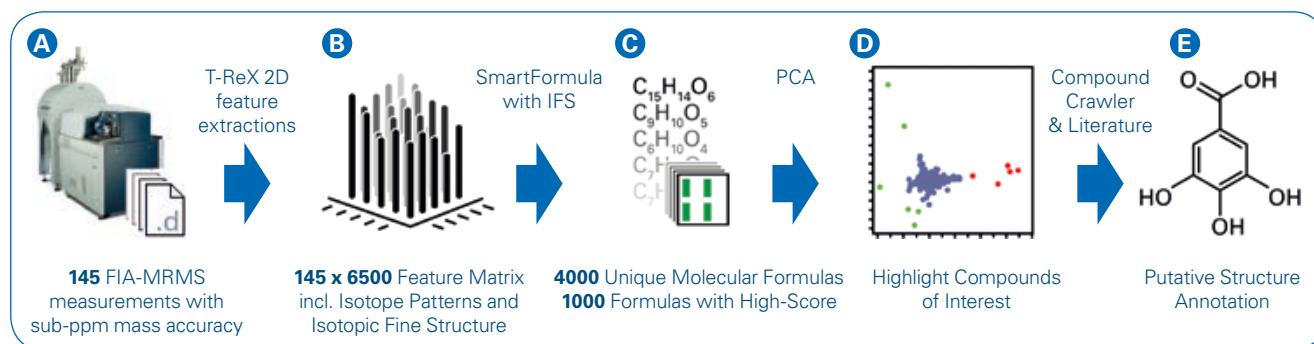


Figure 1: A schematic representation of the workflow performed in MetaboScape 3.0: The steps are (from left to right): **A** FIA-MRMS acquisition using a SolariX XR 7T; **B** Creation of a feature matrix, where a feature comprises the pseudo molecular ions and isotopologues of putative molecules; **C** A list of molecular formula annotations, including annotation qualities (first green bar means below 0.2 ppm mass deviation, second green bar reports a mSigma below 50); **D** Principal component analysis to identify features of interest; **E** Putative structure annotations for the interesting features.

Table 1a) High abundant compounds in red wine

Compound	Molecular formula	Name
R1	C ₁₅ H ₁₄ O ₆	Catechin
R2	C ₉ H ₁₀ O ₅	Syringic acid
R3	C ₆ H ₁₀ O ₄	Apidic acid/3-Methyl glutamic acid
R4	C ₇ H ₁₂ O ₅	Diacetin
R5	C ₇ H ₆ O ₅	Gallic acid

Table 1b) High abundant compounds in white wine

Compound	Molecular formula	Name
W1	C ₁₅ H ₁₈ O ₆	Methoxycoumarin
W2	C ₁₄ H ₁₆ O ₃	-
W3	C ₆ H ₁₀ O ₅	3-Hydroxy-3-methyl-glutaric acid
W4	C ₆ H ₈ O ₂	Sorbic acid
W5	C ₁₃ H ₁₂ O ₉	Caftaric acid
W6	C ₁₄ H ₁₄ O ₉	Fertaric acid

Automated Annotation

In a first step for compound annotation, molecular formulae were assigned to all detected ions using the SmartFormula algorithm, applying metabolomics- and wine-specific filters to elements and element ratios. 4097 compounds could be annotated with a putative molecular formula, 4071 of them uniquely within a 0.5 ppm mass accuracy window. 1177 molecular formulas matched within 0.2 ppm mass deviation and an isotopic pattern fit score below 50 mSigma and thus reached excellent annotation quality. When available, isotopic fine structure was automatically considered for assessing the fit.

Interactive Interpretation

PCA (pareto scaling) revealed ions that were most responsible for the separation of red and white wines. Using Compound Crawler, connected to public structure databases, molecular structures were retrieved to explain these compounds of interest. Literature research then helped to identify the most plausible molecules (see [Table 1a](#) and [1b](#)).

Results

Wine samples were measured in five replicates to check reproducibility of the mass spectrometric results for the multivariate statistical analysis using PCA. Very good reproducibility of FIA-MRMS results of the replicates of all wine samples was observed ([Figure 2](#)). Red wines and white wines could be well separated in the PCA scores plot. Bordeaux wines were separated from the wines from Loire and Alsace. However, even wines from Loire and Alsace were grouped by PCA. Compounds responsible to separate the wines by type (red or white) and origin (Bordeaux, Loire and Alsace) could be identified by high accurate mass detection and exact molecular

For research use only. Not for use in diagnostic procedures.

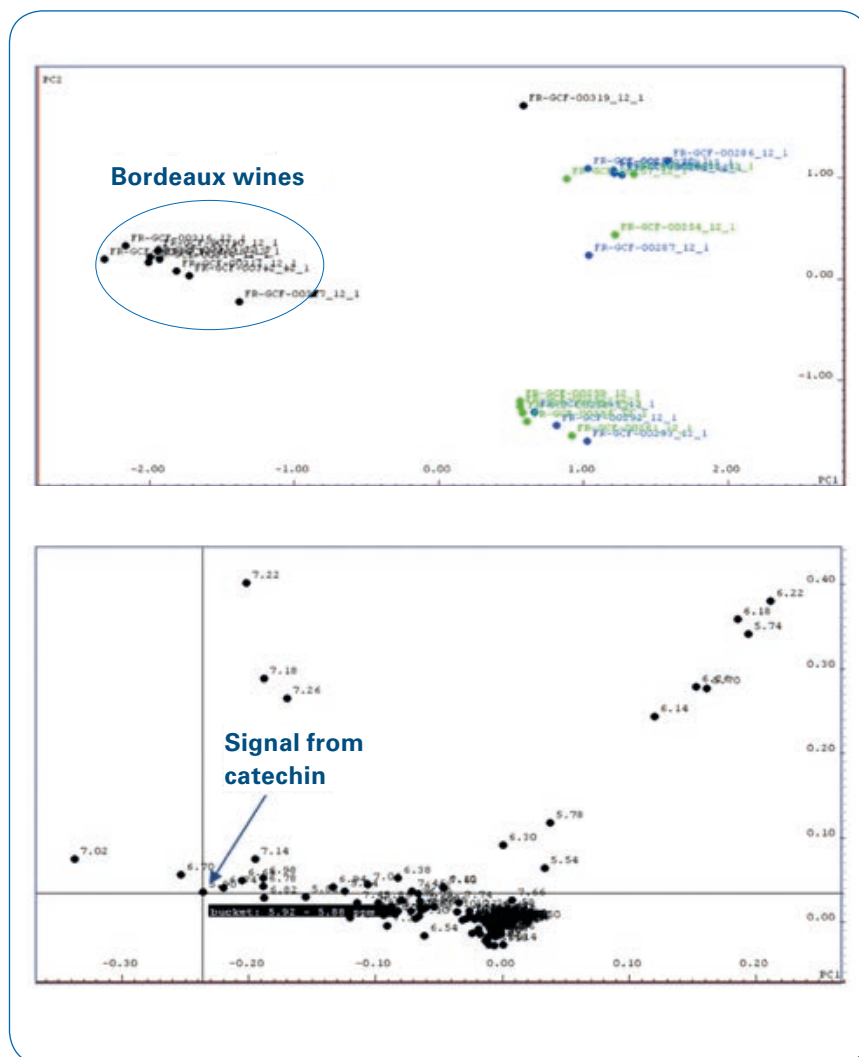


Figure 3: PCA scores plot (top) and loading plot (bottom) of ¹H-NMR data of analyzed white and red wine from Bordeaux, Loire and Alsace.

formula annotation. Most of these compounds could be identified by database search ([Table 1](#)). The results of multivariate statistical analysis of MRMS and ¹H-NMR analyses were very similar ([Figure 3](#)) – wines from Bordeaux were clearly separated from wines from Alsace and Loire. In the ¹H-NMR analyses mainly catechin was responsible for grouping of wines.

More than 3200 compounds of the O_x compound class were detected in the wine samples using MRMS negative ion mode. Even more than 450 compounds of the NO_x compound class were detected in these samples.

Conclusions

- Ultra-high resolution MRMS can be used to distinguish different wines on the molecular level.
- Molecular formulae were generated, assessed by mass accuracy, isotopic pattern fit and isotopic fine structure.
- Specific compounds could be identified responsible for separation of wines.
- Multivariate statistical analysis of MRMS and ¹H-NMR data were similar.



- **Mapping of Greek olive oil using magnetic resonance mass spectrometry flow injection analysis and multivariate data analysis**

In this study, LC free magnetic resonance mass spectrometry (MRMS) analysis was employed for mapping and quality control assessment of Greek extra virgin olive oil (EVOO) using a new and intuitive software workflow.

Introduction

The increasing popularity of EVOO over the last decade has provided the need for quality and authenticity control^[1]. Its chemical complexity impedes the

transaction of the typical analytical methodologies^[2]. In this study, a holistic approach to map Greek EVOO is presented. The workflow takes advantage of the rapid, LC free, flow injection analysis (FIA) based data acquisition

by ultra-high resolution MRMS. The obtained mass spectra were evaluated using the new MetaboScape[®] 3.0 software for deisotoping, as well as for identifying the most significant metabolites.

Keywords:
MetaboScape 3.0,
Magnetic Resonance
Mass Spectrometry,
MRMS, Olive Oil
profiling, Authenticity,
Metabolomics

Authors: Matthias Witt¹, Aiko Barsch¹, Theodora Nikou², Maria Halabalaki², Christopher J Thompson³.
¹ Bruker Daltonik GmbH, Bremen, Germany; ² Division of Pharmacognosy and Natural Products Chemistry, Department of Pharmacy, National and Kapodistrian University of Athens, Athens, Greece; ³ Bruker Daltonics Inc., Billerica, MA, USA.

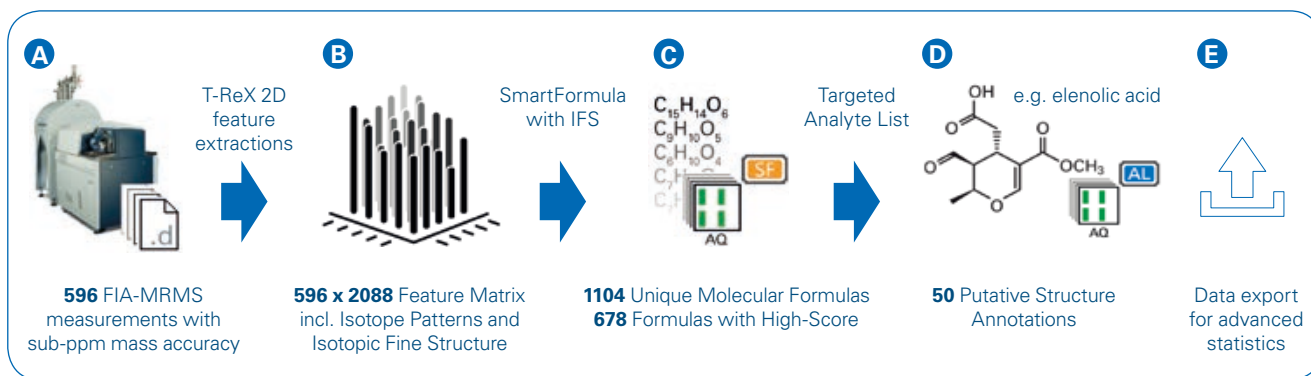


Figure 1: Schematic of the workflow performed in MetaboScape 3.0

Additionally, the data was subjected to multivariate data analysis (MDA), which revealed interesting clusters and trends according to significant discriminating factors of EVOO, such as geographical origin, cultivation practice and production procedure.

Methods

Sample collection: Samples were collected from the main Greek olive oil producing regions and stored at room temperature, in darkness, under nitrogen.

Sample Prep: Stock solutions were prepared by dissolving 10 μ L of samples in 500 μ L MeOH. The stock solutions were then diluted 1:20 in 50% MeOH + 10 mM Ammonium Acetate.

MS analysis: EVOO samples and their biphenolic extracts were analyzed using a Bruker solarix XR

7T mass spectrometer using ESI (-) mode by FIA.

Data Preprocessing

The complete experimental workflow is shown graphically in Figure 1. A detailed explanation for each step is as follows:

- A** Data was acquired via FIA-MRMS on a solarix XR 7T. Samples were run in five replicates, with a single mass spectrum acquired for each replicate.
- B** The 596 individual mass spectra were then loaded into MetaboScape 3.0, where the first step is the creation of a feature matrix (bucket table). Each feature is comprised of the molecular ion and its associated Isotopic Fine Structure (IFS), if available. Addi-

tionally, the features may include possible adduct peaks and the associated isotopologues.

- C** Features were then annotated with a molecular formula using SmartFormula™ (SF). Annotation qualities are provided for each result (the first green bar means below 0.2 ppm mass deviation, the second green bar reports a mSigma below 50).
- D** Features can also be matched with known databases for putative structure annotations of interesting features. Again, matching qualities are provided for each result.
- E** Finally, the data was exported for advanced statistical analysis (SIMCA 14.1, Umetrics, Sweden), in order to identify the features of interest.

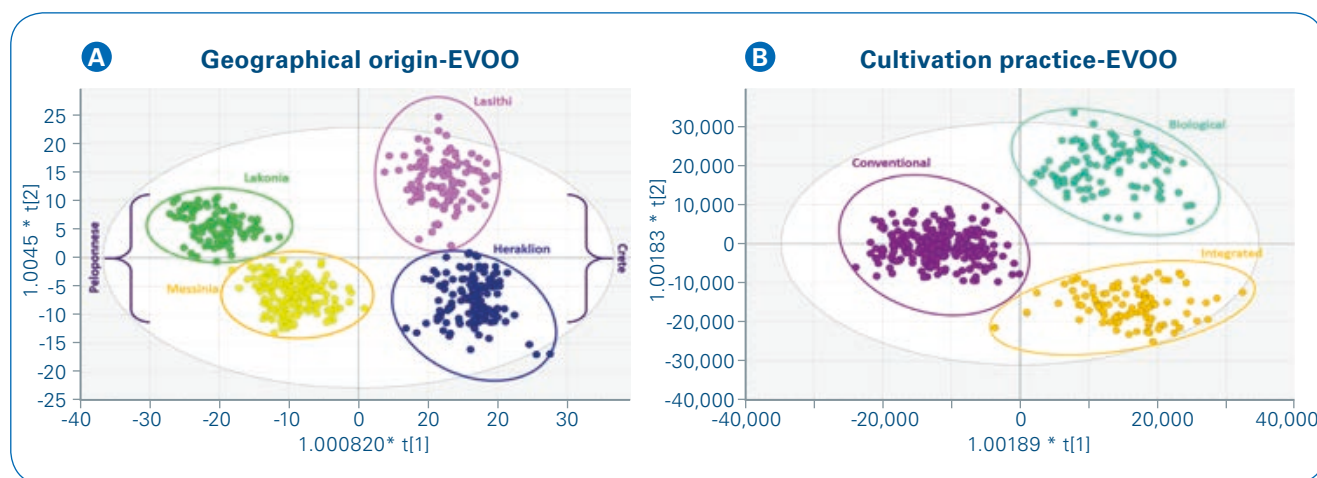


Figure 2: **A** OPLS-DA plot (scores plot-pareto scaling) of EVOO samples clustered according to geographical origin. Samples were separated in the first component according to the region and in the second component according to specific areas of each region. **B** OPLS-DA plot (scores plot-pareto scaling) of EVOO samples clustered according to cultivation practice.

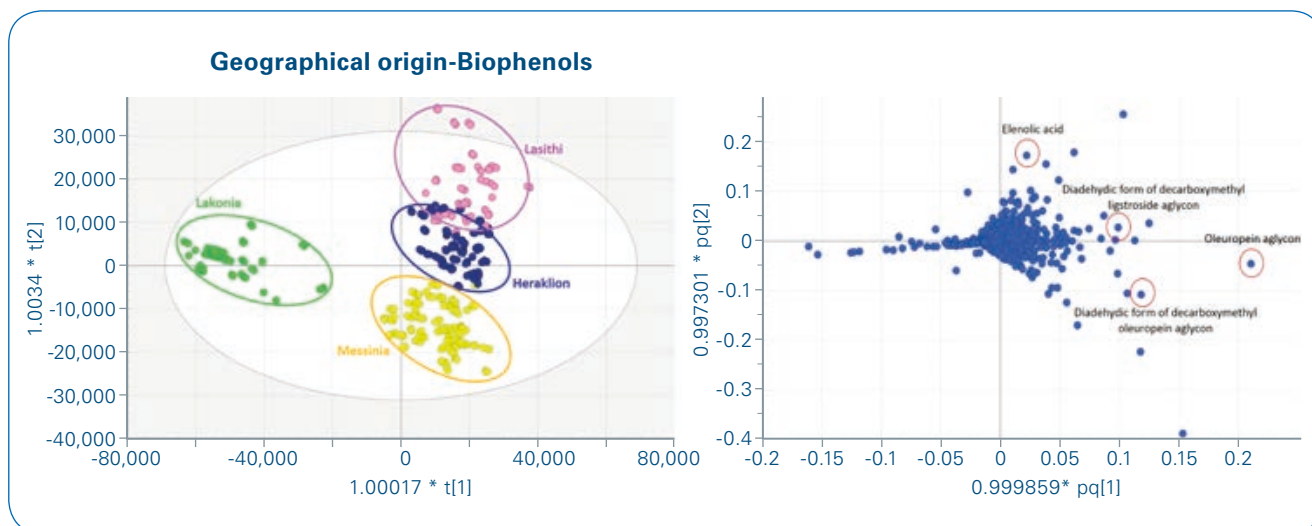


Figure 3: OPLS-DA plot (left scores plot-pareto scaling) of biophenolic extracts clustered according to geographical origin. The scores plot shows similar trend as Figure 2a. The dialdehdic forms of decarboxymethyl oleuropein and oleuropein could differentiate biophenolic EVOO extracts by region (right, loadings plot). Both compounds were significantly higher in extracts Heraklion and Lasithi (Crete) compared to the other regions.

Table 1: The most significant metabolites responsible for sample separation in biophenolic extracts. These were tentatively identified by exact molecular formula annotation making use of accurate mass and isotopic fidelity.

Sample	Molecular formula	Putative Name
Biophenolic extracts	$C_8H_{10}O_3$	Hydroxytyrosol
	$C_{11}H_{14}O_6$	Elenolic acid
	$C_{19}H_{22}O_8$	Oleuropein aglycon
	$C_{17}H_{20}O_5$	Dialdehdic form of decarboxymethyl ligstroside aglycon
	$C_{17}H_{20}O_6$	Dialdehdic form of decarboxymethyl oleuropein aglycon

Results

FIA-MRMS data acquired from EVOO samples enabled a clustering according to geographical origin, harvesting year, cultivation practice and the used oil production procedure using OPLS-DA multivariate data analysis methods. Target compounds responsible for differentiation could tentatively be identified based on ultra-high resolution accurate mass information.

References

- [1] Dion et al.; *Food Chemistry* **2008**, 107:897-911
 [2] Kalogeropoulos et al.; *Antioxidants* **2014**, 3:387-413

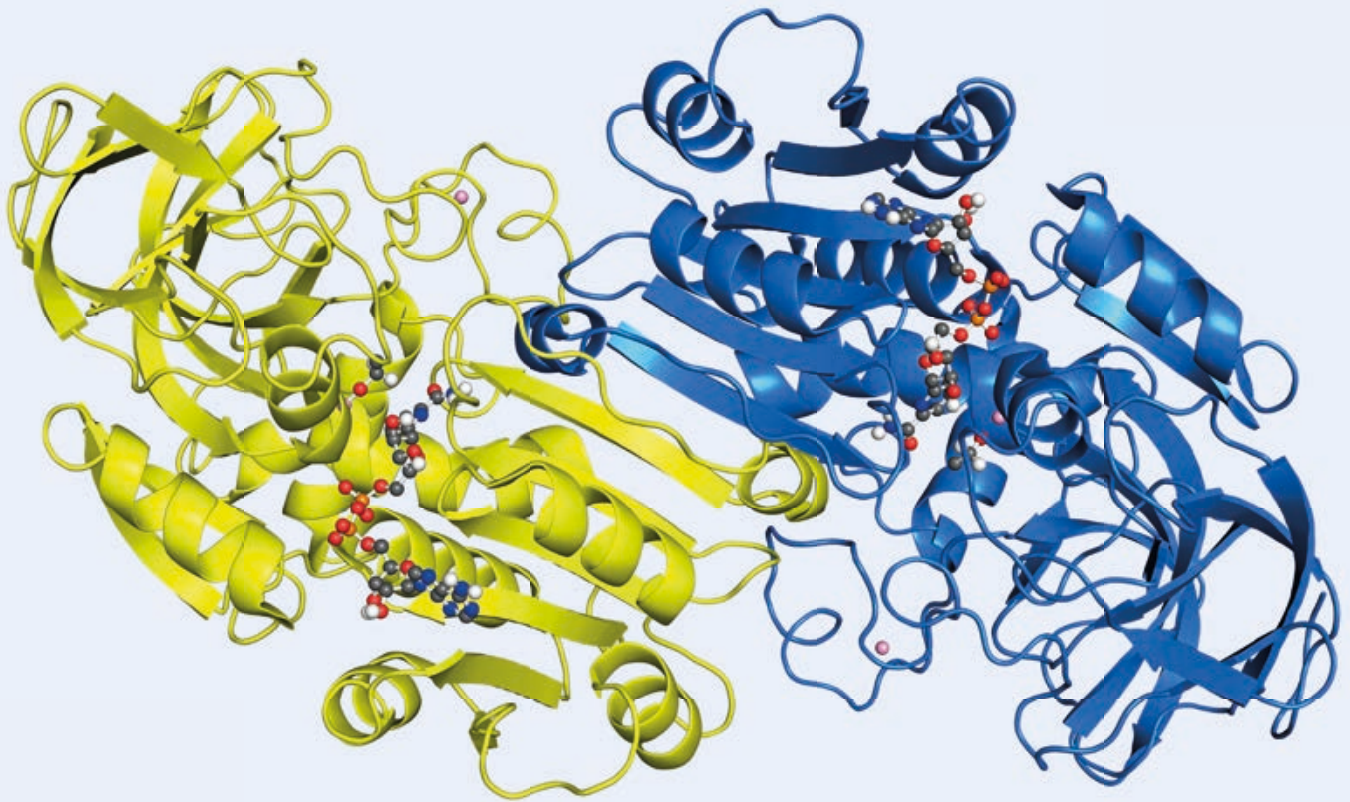
Acknowledgements

The present work is implemented with a State Scholarship Foundation (IKY). It is funded by the action "Strengthening Human Resources Research Potential via Doctorate Research." With additional funding from the operational program "Human Resources Development Program, Education and Lifelong Learning", 2014-2020, and co-funding from the European Social Fund (ESF) and Hellenic government. The authors would like also to thank Greek olive oil producers for their kind support.

Conclusions

- LC free, FIA-MRMS based profiling enabled to distinguish different Greek extra virgin olive oils (EVOO).
- FIA facilitates EVOO analysis, requiring limited sample preparation.
- Interesting clusterings were revealed according to geographical origin of EVOO and the used cultivation practice.
- The responsible metabolite biomarkers were identified.
- MetaboScape 3.0 provides an intuitive and powerful new workflow which enabled the profiling of FIA-MRMS data and confident assignment of molecular formula for metabolite markers.

• Native Proteomics



Brochure

- Native MS Solutions

Customer Insights

- Innovating in Medicinal Chemistry Using Fragment Based Drug Discovery combined with Native MS
- Top-Down Proteomics: An Emerging Technique Driven by Cutting-Edge Mass Spectrometry

Application Notes

- Glycan Sequencing by Electronic Excitation Dissociation Tandem Mass Spectrometry
- Comparison of CID and EID Mass Spectrum of Glycosides from solariX XR
- Top Down Analysis of Histone H4
- Expanded Collisional Energy Files for Automated Top Down and Bottom up Analysis on solariX
- MALDI In-Source Decay for Top-Down Analysis of Proteins

Bibliography

- Native MS Bibliography

User Testimonials: Native MS



“Native mass spectrometry and top-down proteomics are starting to impact studies in structural biology and medicine – and Bruker has all of the tools necessary for these growing technologies.”

Professor Joe Joo, University of California, Los Angeles, USA



“The MRMS method means you avoid wasting valuable time on compounds that will not advance drug discovery.”

Dr. Sally Ann Poulsen, Professor of Chemical Biology at the Griffith Institute for Drug Discovery (GRIDD), Griffith University, Brisbane, Queensland, Australia



“Our first experiments worked beautifully. Bruker MRMS retains weak non-covalent complexes and also easily handles screening of pools of compounds. The high resolution is perfect to resolve the complex mixtures.”

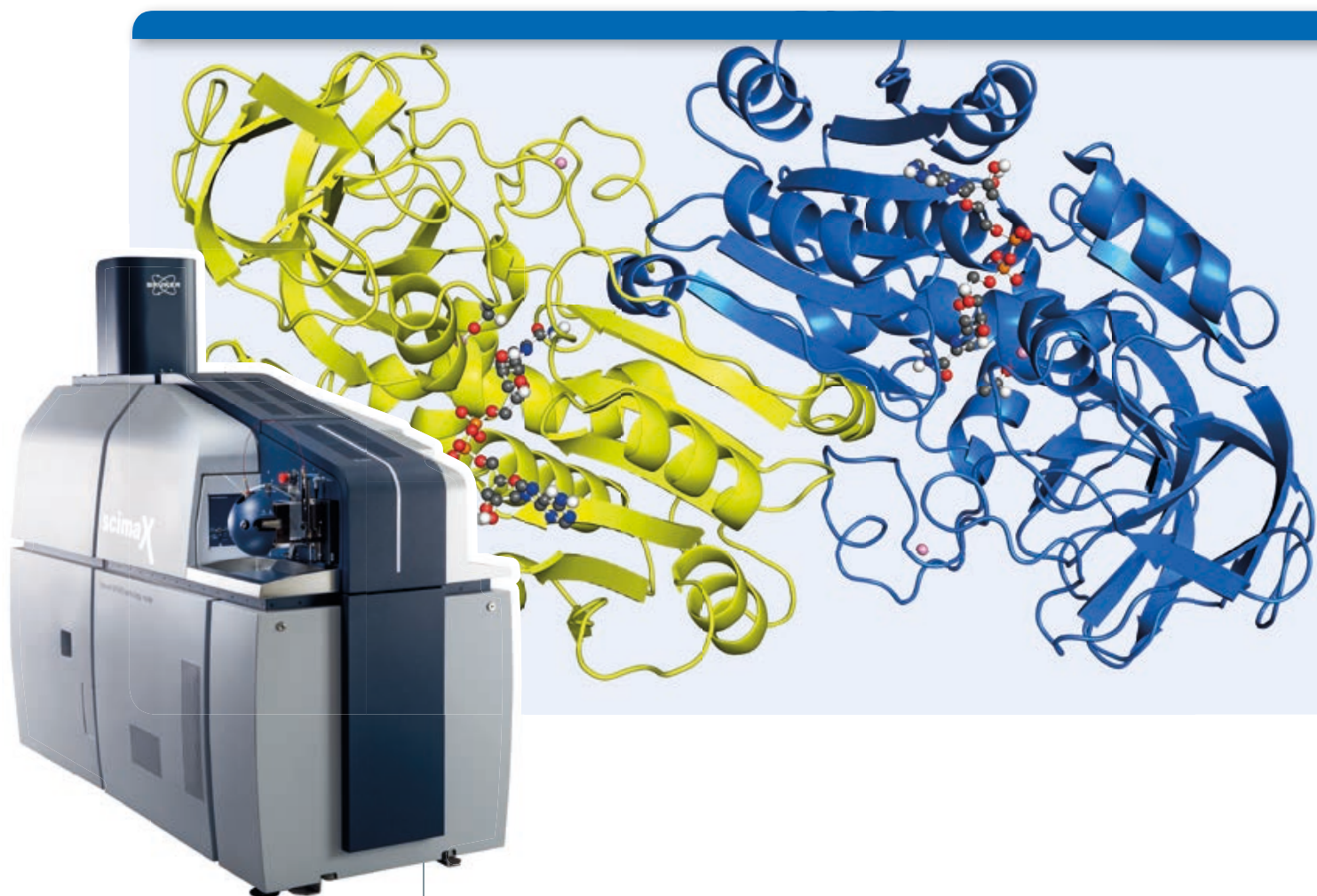
Professor Ronald Quinn, Griffith Institute for Drug Discovery, Brisbane, Australia

Benefits for Native MS

The critical requirement for native MS is an optimal pressure gradient between the electrospray source and the mass analyzer. The ion path on the scimaX MRMS enables the transmission of intact biomolecular complexes into the ParaCell, allowing for analysis of protein and protein complexes with isotopic resolution.



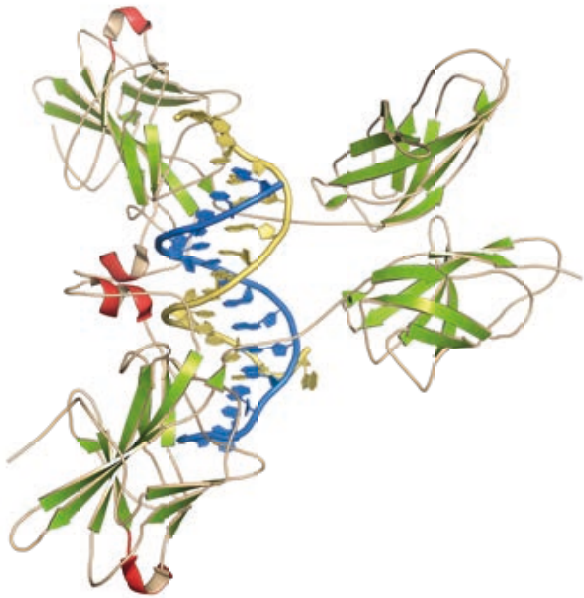
Now fragile fragment-protein, protein-substrate, multi-protein biomolecular complexes, membrane proteins with nanodiscs, mAbs, and native protein top-down analysis can all be analyzed on a standard (unmodified) scimaX.



Native MS Solutions

- scimaX MRMS: Perfectly designed for Native MS

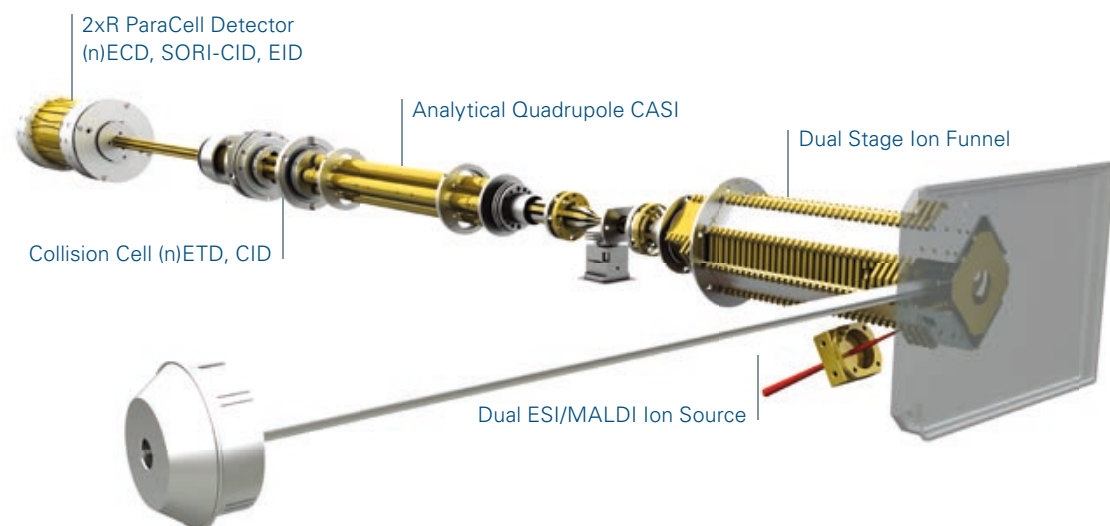
scimaX Ion Path – *Perfectly Balanced* for Native MS



The critical requirement for native MS is an optimal pressure gradient between the electrospray source and the mass analyzer. The ion path on the scimaX MRMS (magnetic resonance mass spectrometry) enables the transmission of intact biomolecular complexes into the ParaCell, allowing for extreme resolution analysis.

Now fragile fragment-protein, protein-substrate, multi-protein biomolecular complexes, membrane proteins with nanodiscs, mAbs, and native protein top-down analysis can all be analyzed on a standard (unmodified) scimaX.

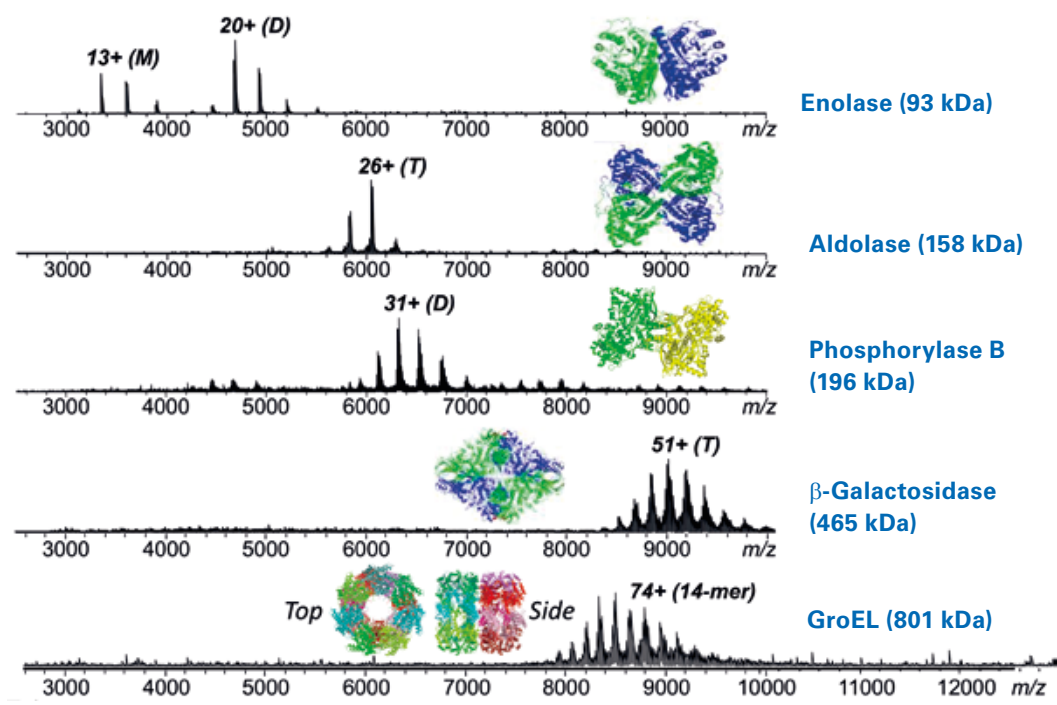
Standard features with scimaX



- CID: collision induced dissociation
- ECD: electron capture dissociation
- EID: electron induced dissociation
- ETD: electron-transfer dissociation
- SORI-CID: sustained off-resonance irradiation collision-induced dissociation
- CASI: continuous accumulation of selected ions

Native Mass Spectrometry: An Essential Tool for Modern Structural Biology

Native MS of Protein Complexes (15T MRMS)



Native Protein Complexes using MRMS - Courtesy Joe Loo, UCLA



Proprietary ParaCell detector with patented magnetron control technology. Superior trapping capacity for high m/z , highly charged ions.

Successful analysis of large proteins and their complexes requires three key conditions to be met. First, the proteins must be transmitted and detected without breaking intramolecular bonds. Secondly, the protein must be sufficiently desolvated to allow observation of the free protein ions. Finally, the extraordinary amount of charge on the molecules must not overwhelm the detector leading to space charge or coalescence issues. The scimaX and ParaCell technologies were designed with these goals in mind and are proven in labs worldwide for native MS experiments.

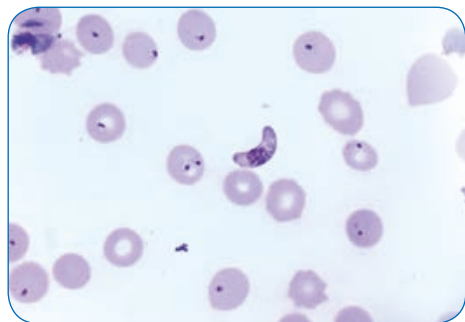


Professor Joe Loo, University of California, Los Angeles, USA

"Native mass spectrometry and top-down proteomics are starting to impact studies in structural biology and medicine – and Bruker has all of the tools necessary for these growing technologies."

Native MS Applications for Fragment Based Drug Discovery

MRMS takes on the challenge of discovering new drugs for Malaria



Malaria causing, crescent shaped *Plasmodium falciparum* gametocyte in blood smear

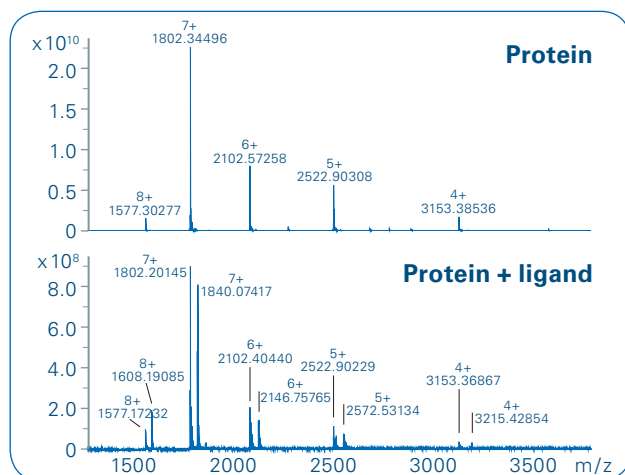
Advancing the frontiers of Fragment-Based Drug Design (FBDD), Professor Ron Quinn and co-workers of the Griffith Institute for Drug Discovery, analyzed a specially curated natural products fragment library of over 600 unique compounds against 62 separate potential malaria drug protein targets.[1] Using MRMS, 79 fragments were identified interacting with 31 proteins and later shown to have *in vitro* activity against *Plasmodium falciparum*, a parasite that induces severe malaria in humans. 13 of these compounds had IC_{50} values less than 45 μM , which is uncommon for leads from fragment libraries.



Professor Ronald Quinn, Griffith Institute for Drug Discovery, Brisbane, Australia

"Our first experiments worked beautifully. Bruker MRMS retains weak non-covalent complexes and also easily handles screening of pools of compounds. The high resolution is perfect to resolve the complex mixtures."

Observe free and bound protein target



Weak binding ($K_d > 10 \mu M$) interactions typical in FBDD are routinely preserved and observed by MRMS. The balanced ion optics require no special modifications for native MS.

[1] Fragment-Based Screening of a Natural Product Library against 62 Potential Malaria Drug Targets Employing Native Mass Spectrometry. Vu H, Pedro L, Mak T, McCormick B, Rowley J, Liu M, Di Capua A, Williams-Noonan B, Pham NB, Pouwer R, Nguyen B, Andrews KT, Skinner-Adams T, Kim J, Hol WGJ, Hui R, Crowther GJ, Van Voorhis WC, and Quinn RJ. *ACS Infectious Diseases* 2018 **4** (4), 431-444. DOI: 10.1021/acscinfecdis.7b00197.

Six Proven Reasons for Using the scimaX MRMS for Native MS

1 Ion path leaves fragile non-covalent interactions intact

Bruker's perfectly balanced MRMS ion optics have always been the most efficient in the industry for native MS – no changes to vacuum or a separate, special instrument needed. Complexes are desolvated but not disrupted.

2 Only instrument to offer broadband extreme resolution

Only Bruker MRMS offers the ability to detect molecules at 200 m/z at 20 million resolution and ppb mass accuracy while also providing resolving power in the hundreds of thousands at 5000 m/z.

3 Extreme Sensitivity

Protein concentrations ranging from 100 μ M to 10 nM have been observed, enabling a wide range of ligand affinities to be studied and compared (> 100 μ M often results in aggregation).

4 scimaX easily interfaces to multiple ion sources including cIEF

Bruker's sources are at ground allowing easy interface of most custom ion sources.

5 The ultimate companion for HTS and FBDD – eliminate your false positives

Native MS on scimaX is the best tool for distinguishing specific and non-specific interactions as well as determining stoichiometry of binding.

6 scimaX is the most flexible instrument in the industry with native MS capabilities

scimaX not only excels at native MS, but also MALDI Imaging, isotopic fine structure, metabolomics, petroleomics, and more.



The scimaX MRMS is built on conduction cooling technology. It does not require liquid cryogenics or a vent line for operation.

Proven MS technology for routine analysis of native protein complexes

- Wongkongkathep P, Han JY, Choi TS, Yin S, Kim HI, Loo JA. (2018) **Native Top-Down Mass Spectrometry and Ion Mobility MS for Characterizing the Cobalt and Manganese Metal Binding of α -Synuclein Protein**, Journal of the American Society for Mass Spectrometry, 10.1007/s13361-018-2002-2, **29** (9), 1870–1880
- Vu H, Pedro L, Mak T, McCormick B, Rowley J, Liu M, Quinn RJ (2018) **Fragment-Based Screening of a Natural Product Library against 62 Potential Malaria Drug Targets Employing Native Mass Spectrometry**, ACS Infectious Diseases, 0.1021/acsinfecdis.7b00197, **4** (4), 431-444
- Lin Z, Guo F, Gregorich ZR, Sun R, Zhang H, Hu Y, Shanmuganayagam D, Ge Y (2018) **Comprehensive Characterization of Swine Cardiac Troponin T Proteoforms by Top-Down Mass Spectrometry**, Journal of the American Society for Mass Spectrometry, 10.1007/s13361-018-1925-y, **29** (6), 1284–1294
- Li H, Nguyen HH, Ogorzalek LRR, Campuzano IDG, Loo JA (2018) **An Integrated Native Mass Spectrometry and Top-Down Proteomics Method that Connects Sequence to Structure and Function of Macromolecular Complexes**, Nature Chemistry, 10.1038/nchem.2908, **10** (2), 139–148
- Chen B, Lin Z, Alpert AJ, Fu C, Zhang Q, Pritts WA, Ge Y (2018) **Online Hydrophobic Interaction Chromatography-Mass Spectrometry for the Analysis of Intact Monoclonal Antibodies**, Analytical chemistry, 10.1021/acs.analchem.8b01865, **90** (12), 7135–7138
- Campuzano ID, Netirijanukul C, Nshanian M, Lippens JL, Kilgour DP, Orden SL, Loo JA (2018) **Native-MS Analysis of Monoclonal Antibody Conjugates by Fourier Transform Ion Cyclotron Resonance Mass Spectrometry**, Analytical Chemistry, 10.1021/acs.analchem.7b03021, **90** (1), 745-751
- Zhang J, Ogorzalek LRR, Loo JA (2017) **Structural Characterization of a Thrombin-Aptamer Complex by High Resolution Native Top-Down Mass Spectrometry**, Journal of the American Society for Mass Spectrometry, 10.1007/s13361-017-1751-7, **28** (9), 1815–1822
- Teruya K, Rankin G., Chrysanthopoulos PK, Tonissen KF, Poulsen S-A (2017) **Characterisation of Photoaffinity-Based Chemical Probes by Fluorescence Imaging and Native-State Mass Spectrometry**, Chembiochem: a European journal of chemical biology, 10.1002/cbic.201600598 **18** (8), 739–754
- Li H, Sheng Y, McGee W, Cammarata M, Holden D, Loo JA (2017) **Structural Characterization of Native Proteins and Protein Complexes by Electron Ionization Dissociation-Mass Spectrometry**, Analytical chemistry, 10.1021/acs.analchem.6b02377, **89** (5), 2731–2738
- Chrysanthopoulos PK, Mujumdar P, Woods LA, Dolezal O, Ren B, Peat TS, Poulsen S-A (2017) **Identification of a New Zinc Binding Chemotype by Fragment Screening**, Journal of medicinal chemistry, 10.1021/acs.jmedchem.7b00606, **60** (17), 7333–7349
- Cai W, Tucholski T, Chen B, Alpert AJ, Mcllwain S, Kohmoto T, Jin S, Ge Y (2017) **Top-Down Proteomics of Large Proteins up to 223 kDa Enabled by Serial Size Exclusion Chromatography Strategy**, Analytical chemistry, 10.1021/acs.analchem.7b00380, **89** (10), 5467–5475

For Research Use Only. Not for Use in Clinical Diagnostic Procedures.



Customer Insights

- Innovating in medicinal chemistry using Fragment Based Drug Discovery combined with Native Mass Spectrometry

Innovating in medicinal chemistry using Fragment Based Drug Discovery combined with Native Mass Spectrometry

Extreme resolution MRMS technology enables scientists to see “hidden gems” of information in fragment based drug discovery research at the Griffith Institute for Drug Discovery



Working with Bruker

Sally-Ann Poulsen's laboratory at the Griffith Institute for Drug Discovery (GRIDD) uses advanced MRMS technology to support their research in small molecule drug discovery.

“The instrument from Bruker brings high performance and flexibility for faster analysis, saving time and money while producing richer datasets for small molecule analysis.”

Strategically investing in drug discovery

Griffith University is located in Brisbane, Queensland, Australia and was founded over 40 years ago. The university is ranked among the top 3% of universities globally with over 50,000 students and 4,000 staff across its five campuses. The university has a large focus on research with an extensive network of research centers and institutes across a range of disciplines, including drug discovery. Sally-Ann Poulsen, Professor of Chemical Biology at Griffith Institute for Drug Discovery (GRIDD), at Griffith University, explains further:

“Griffith University is committed to areas of strategic investment to help facilitate research excellence and drive positive solutions. Drug discovery was identified as one area of interest and this is where the Griffith Institute for Drug Discovery (GRIDD) originated from. The institute was formerly known as Eskitis and was renamed to GRIDD two years ago.”

Internal work

At GRIDD, there are over 120 members of staff and students focusing on drug discovery across four main areas of interest: cancer; infectious diseases; neurodegenerative diseases and spinal cord injury repair. Cancer is Sally-Ann's laboratory's main area of focus.

Chemistry and biology – A collaborative approach

The institute is distinctive in its collaborative approach between chemists and biologists. This is particularly unusual in Australia, as the country has a large number of medical research institutes with few or no chemists on site. GRIDD is among only a handful of such institutes that operate with chemistry and biology under the same roof.

Furthermore, GRIDD uses High Throughput Screening (HTS) robotics for both phenotypic screening, where the drug target is unknown, and target based screening, where the protein of interest is known and the user is trying to affect

how it behaves, either by inhibiting or activating it.

GRIDD is unique in Australia for its NatureBank facility, a drug discovery platform based on natural product extracts and fractions that have been derived from Australian plants, fungi and marine invertebrates, from Australia to Papua New Guinea. These samples have been processed into two libraries (a 10,000 natural product extract library and a 50,000 natural product fraction library), which are ready for HTS against any disease. NatureBank also holds more than 30,000 archived biota samples.

Compounds Australia, of which Sally-Ann was academic lead from 2013 – 2016, located at GRIDD, is the premier compound management facility in the Southern Hemisphere. The facility provides access to critical infrastructure and expertise to ensure flexible, efficient, reproducible and cost-effective compound management. Compounds Australia makes compounds available in sophisticated assay-ready formats to researchers worldwide, addressing the demands

of bioactive compound discovery throughout the drug discovery pipeline.

Sally-Ann has three main research areas. The first is medicinal chemistry, for making bioactive compounds, completing the assays and elucidating structure activity relationships. Her flagship discovery in this area is compounds that reverse drug resistance in glioblastoma, the most common and lethal adult primary brain tumor.

The second research area is making chemical probes – molecules for biologists to use as tools to better understand their biological systems. Examples include molecules made for diseases such as Leishmaniasis, caused by the Leishmania parasite which lives inside cells. Sally-Ann describes how scientists are looking under the microscope to stain for DNA, but are struggling to confirm if the DNA is from the parasite or the host cell. Her team is making compounds to help biologists improve how they work in this area, alongside the commercial tools they can purchase.



The final research area is mass spectrometry (MS), and Sally-Ann describes her journey in how she came to be an advocate of this technique:

"I completed my PhD in Australia before completing my postdoctoral research in the UK. After a year in Big Pharma I moved to the University of Cambridge Chemistry Department, which is where I first started using Magnetic Resonance Mass Spectrometry (MRMS), formerly known as Fourier Transform Mass Spectrometry (FTMS). Following a talk from Prof Dame Carol Robinson, renowned for pioneering the use of mass spectrometry as an analytical tool and for her ground-breaking research into the 3D structure of proteins, I felt I could do this for a different application and at Cambridge I had the opportunity of working with an early 4.7 Tesla Bruker APEX MRMS system."

Introducing mass spectrometry to GRIDD

Following her return to Australia and with MS identified as a technique for use, Sally-Ann successfully applied for funding from the Australian Research Council and had the first system installed in 2003, only the 6th to be installed in Australia.

The primary focus for this was to study proteins in their native state, where they are folded as they would be in a cell, and so have the required 3D shape they need to bind to a small molecule. The key reason behind this was to use proteins as a template to help develop dynamic combinatorial libraries (1). These are mixtures of compounds that promised to improve aspects of drug discovery. Historically, however, scientists would complete the library synthesis, screen it and then have to go back to deconvolute, which was difficult and circumvented the benefits of working with the libraries, as Sally-Ann explains:



“As there were no available tools on the market, by using MS, I was able to observe the small molecule protein interactions and avoid the need to deconvolute, as well as confirm the quality of the analysis.”

This original system (decommissioned in 2017) was replaced by the Bruker solariX XR MRMS in 2014. The team at GRIDD led the application that secured funding through the highly competitive Australian Research Council for infrastructure.

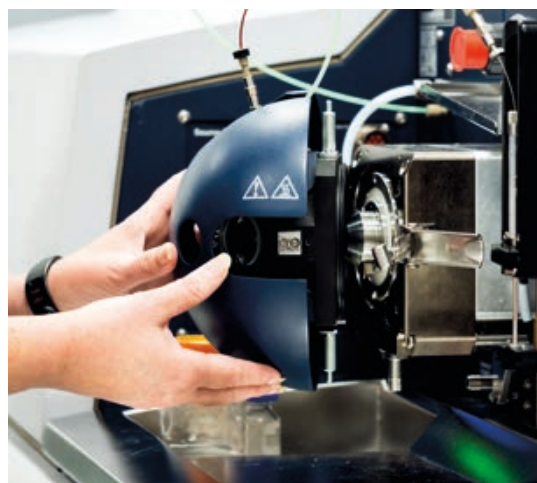
The team at GRIDD successfully presented the need for the new MRMS for its improved screening capabilities, as the solariX XR mass spectrometer has an increased upper size limit of proteins. This is due to the magnets being further developed – from 4.7 Tesla to the solariX XR's 12 Tesla magnet. The upper size limit for the proteins Sally-Ann and her team at GRIDD can study has increased from 50 kilodaltons (kDa) to 150 kDa. The difference has meant that the gap between 50 – 150 kDa, which includes a high proportion of proteins that are of interest for drug discovery, would be accessible and this advanced capability provided a compelling case on its own. More specifically, within drug discovery, is the tool of fragment based drug discovery (FBDD). FBDD has emerged as a powerful tool for discovering drug leads. The approach first identifies very small molecules (fragments) that are about half the size of standard drugs, and these fragments are expanded or linked together to generate drug leads.

Another key benefit of the new system is its lower running cost. The previous system required cryogen (liquid nitrogen and liquid helium) to maintain the super conducting magnet, which is a very expensive process for refilling. The old system required refilling liquid helium five times a year at a

cost of \$3,000 per refill. The new system recycles the helium and, therefore, it only requires refilling once a year, a key selling point for the solariX XR.

Additionally, ease of use for those operating the instrument has proven a key benefit, as Sally-Ann explains:

“We had originally intended to use both the old and new systems but as the new system performed so well, the old system was no longer the 'go to' instrument.



“The capabilities and ease of use of the solariX XR were so much greater, we retired the original instrument after 14 years of tremendous service that put GRIDD at the forefront of study drug-protein interactions.”

The solariX XR is equipped with extreme resolution and gives an extra layer of confidence in screening for weak interactions of very small molecules. Therefore, accurate identification of the binding and molecule mass for fragments is very important as a starting point in drug discovery.

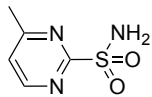
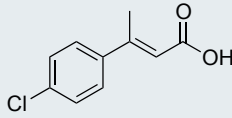
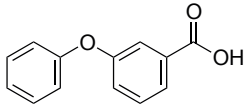
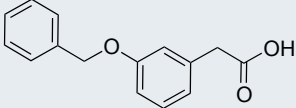
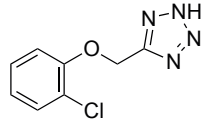
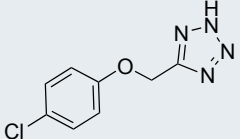
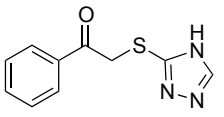
Compound No.	Fragment/Chemotype	SPR [Ⓐ] K _d (μM)	ESI-MS	nanoESI-MS [Ⓑ]	X-ray
1	 primary sulfonamide	1.35	✓	✓ (1:7.1)	✓
2	 cinnamic acid	905	✓	✓ (1:0.9)	✓
3	 benzoic acid	1280	✓	✓ (1:1.4)	✓
4	 phenylacetic acid	1080	✓	✓ (1:0.9)	✓
5	 5-substituted tetrazole	631	✓	✓ (1:1.7)	✓
6	 5-substituted tetrazole	709	n/a	✓ (1:1.4)	✓
7	 1,2,4-triazole	194	n/a	✓ (1:0.5)	✗

Table 1: Correlation of screening results for fragment hit chemotypes with surface plasmon resonance (SPR), electrospray ionization-mass spectrometry (ESI-MS), nanoESI-MS, and X-ray crystallography (green tick = hit, red cross = not a hit, n/a fragment not tested). **A** Dose-response experiment performed at 25 °C with a 5-point fragment concentration series range. **B** nanoESI-MS hit with ratio of unbound CA II:fragment bound CA II peak intensities in brackets.

As well as the MRMS system installed, GRIDD also has a Bruker quadrupole time-of-flight (QTOF) maXis II. Sally-Ann and her team have plans to use this instrument on future projects as another filter of obtaining data and ruling out ineffective compounds quickly. Sally-Ann's team would then take those compounds with binding potential across to the MRMS for higher resolution analysis.

Reducing false positives

A huge advantage of the MRMS system is its minimal false positive results. Other techniques suffer from producing high false positives but this is not an issue with the solariX XR, as Sally-Ann explains:

"Fragments at high concentrations can aggregate, or stick together, and do not behave as they should. Other fragment screening techniques may suffer from high false positives as they are having to deal with the fragments at higher concentrations. In our method, the fragment is at the same concentration as the protein, therefore we do not have these aggregation issues so false hits are much less likely to occur. This is a huge advantage, because if you have 1000 compounds screening in the library, you might only filter to 200-300 if the false positives are high in number rather than 10-30 true hits.

The MRMS method means you avoid wasting valuable time on compounds that will not advance drug discovery."

Lowering attrition with fragment based drug discovery

Sally-Ann is specifically focused on the area of FBDD. It is getting harder to progress new drugs through the drug development process, and the rate of acceptance is declining. The investment by the pharmaceutical industry in small molecules to get them to phase I, II and III clinical trials, before failing late in the process, is referred to as

attrition, and is extremely costly. The mantra in the pharmaceutical industry is if you are going to fail, fail early. Therefore, the industry has to look at how to avoid attrition and make the process less costly, leading to more attention for FBDD.

The difference between fragment and traditional HTS is the size of the molecule. A fragment, or small molecule, is typically under 200 Da in molecular weight, whereas a HTS compound is between 400-500 Da. The ability of the fragment to interact with a protein is less and the binding affinity is weaker, but if they do interact this indicates they fit perfectly. This is why it is an area of great interest for drug discovery, as it is less likely to be one of those compounds with high attrition later down the pipeline.

Sally-Ann explains the challenges associated with screening hits:

"If you identify a HTS screening hit, it can be very difficult to develop into a drug, as its potency can be made up of both good and bad interactions, which can compensate for each other. Therefore, as chemists try to improve the hit compound, the data can often lead them to change into a larger molecule with worsened drug-like properties and with a higher chance of failure. This is because as they get to the stage where they enter the human body, toxicity levels or associated off-target effects become visible.

Fragment screening offers a potentially much better starting point for drug discovery and better overall prospects that a compound will move along the drug discovery pipeline towards FDA approval or exit early to limit the investment knock as much as possible."

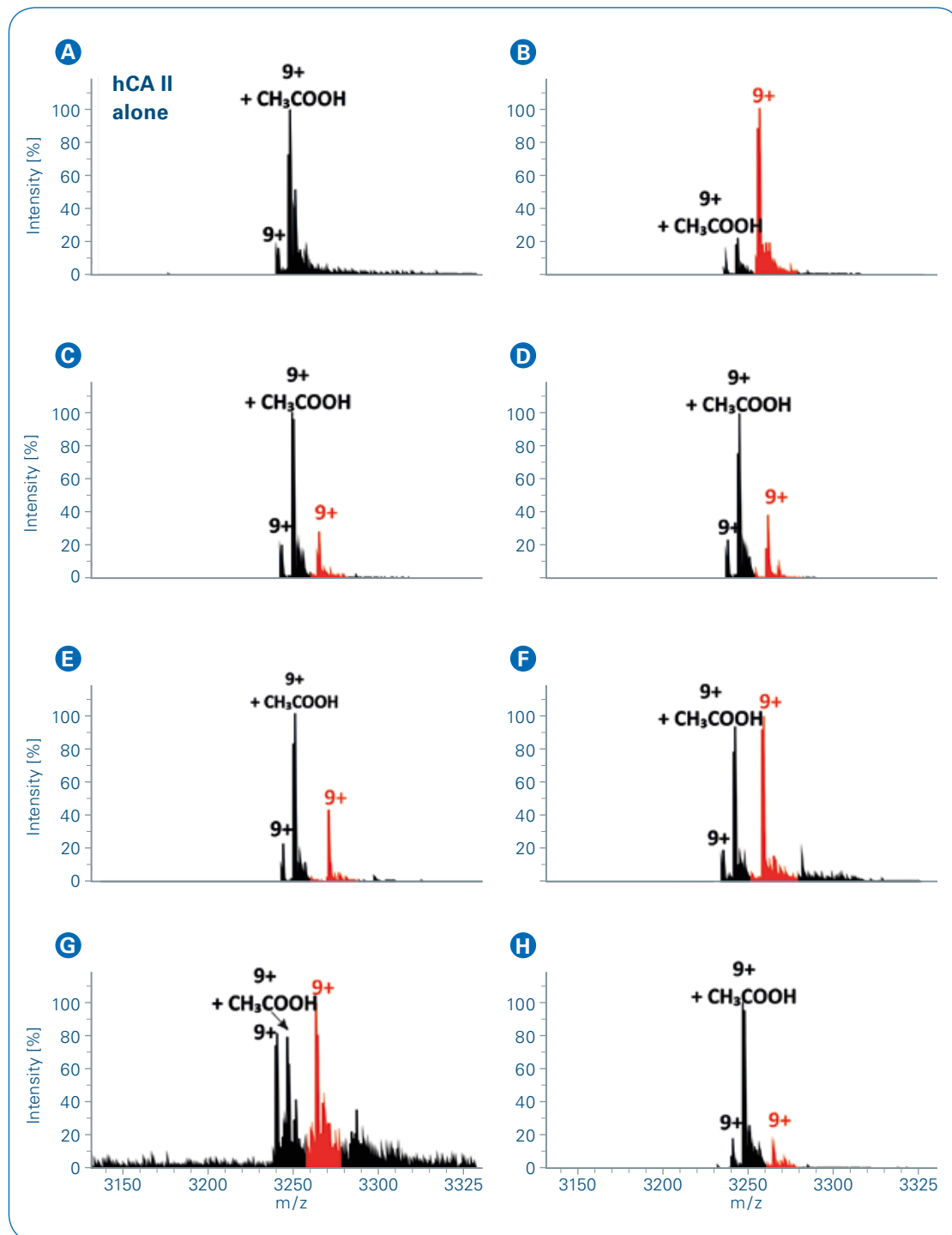


Figure 1: NanoESI mass spectra of hit fragments with carbonic anhydrase II (CA II). The 9+ charge state is shown, with [protein + fragment] 9+ peaks in red. **A** human CA II protein only **B** primary sulfonamide chemotype **C** cinnamic acid chemotype **D** benzoic acid chemotype **E** phenylacetic acid chemotype **F** tetrazole chemotype **G** tetrazole chemotype **H** 1,2,4-triazole chemotype.



Fragment screening combinations

Fragment screening has been a successful approach for FBDD researchers as there have been two FDA approved drugs from the process. It is proving an area of great and growing interest for the pharmaceutical industry and in academic research. FBDD is, however, contingent on the development of analytical methods such as MS to be able to identify the weak binding fragments. As such, researchers at GRIDD are optimizing their workflows and combining techniques together with collaborators in order to give the best chance of accelerating drug discovery. Techniques for FBDD, in addition to MS, include Surface Plasmon Resonance (SPR), X-ray Crystallography, Nuclear Magnetic Resonance (NMR) and Isothermal Titration Calorimetry (ITC). Each method has pros and cons but there is a need for multiple (orthogonal) methods, in order to be confident that a hit is a true hit.

Sally-Ann and her team have combined native state MS with two proven and popular fragment screening methods, SPR and X-ray crystallography, in a fragment screening campaign against human carbonic anhydrase II (CA II). (2)

The research recognized native state MS as a rapid, sensitive, high throughput, and label-free method to directly investigate protein–ligand interactions. However, there were few studies using this approach as a screening method to identify relevant protein–fragment interactions in FBDD. The results showed the first fragment screening analysis of electrospray ionisation (ESI)-MS and NanoESI-MS using a high resolution Fourier-transform ion cyclotron resonance (FTICR) instrument (Bruker solarix XR 12.0T MRMS) in parallel with SPR as shown in figure 1 and table 1.

MS has a huge number of advantages over other techniques as Sally-Ann explains:

“The advantages of MS are due in part to the speed, and it doesn’t use too much sample. Therefore, in a workflow, I envisage this technique as the front end of the fragment screening cascade of methods to try. I see MS as the starting point and the other methods can come in later as you bring the compounds screened down from, for example, 1000 to 50.”

It is almost a pre-filtering tool in the process but can be used as a standalone in the workflow.”

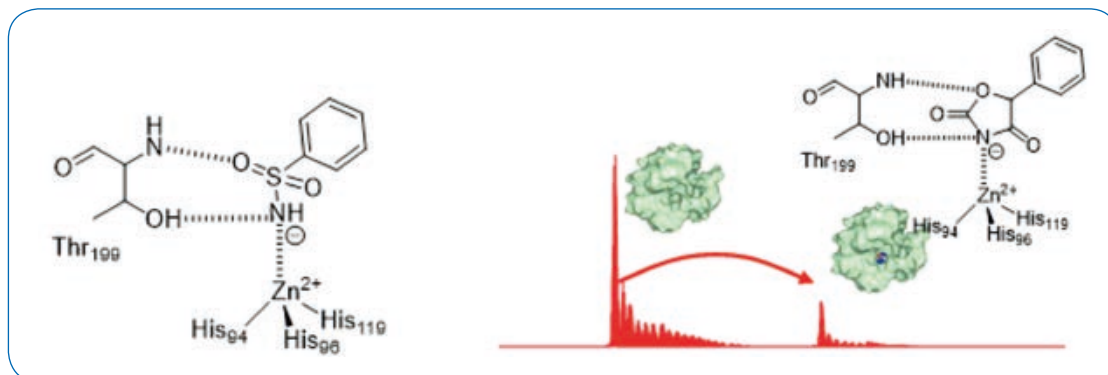


Figure 2: Binding interactions of the classic primary sulfonamide chemotype **A** with carbonic anhydrase II (CA II) are emulated by the oxazolidindione chemotype, compound 10 **B** discovered by fragment screening using magnetic resonance mass spectrometry (MRMS).

Identifying a new zinc binder by quantitative native MS

Another piece of published research by Sally-Ann and collaborators at Commonwealth Scientific and Industrial Research Organisation (CSIRO) reports the identification of a new zinc-binding fragment. (3) The researchers reveal an additional fragment that is both a novel and potent inhibitor of CA II. SPR and native ESI-MS identified compound 10, an oxazolidindione, which has an affinity and ligand efficiency approaching that of sulfonamides, a well-known class of zinc binder for CA II. The researchers were so astonished by the findings that upon first reflection, it was thought that the samples had been mixed up.

The researchers determined the crystal structure of compound 10 bound to CA II, confirming the binding pose of the new fragment to CA II, which

included a primary interaction with the zinc and a couple hydrogen bonds with the protein, helping to explain the high affinity, as seen in figure 2.

The research used a series of 18 analogues of compound 10 to assess the structure–activity relationship (SAR) using both SPR and MS. The researchers were able to obtain quantitative MS data by holding protein concentration constant (at 14.5 μ M) and varying the fragment concentration from 0.5 to 120 μ M. Plotting the percentage of protein bound and curve-fitting revealed dissociation constants remarkably similar to those determined using SPR. Nine of the new fragments showed at least some activity, though none were significantly more potent than compound 10. Crystal soaking experiments led to seven new structures, with all the fragments binding in a similar manner as compound 10.



FBDD in the future

Sally-Ann is looking to further collaborate with industry for FBDD in the future, as there is a growing interest from the pharmaceutical sector to aid drug discovery.

“The research landscape in Australia is changing, with the impact on working in industry really encouraged. This has timed well with the pharmaceutical industry growing its interest in FBDD, so I hope to work more with industry to use these applications for industry drug targets. This is possible as our method is unbiased, therefore, we can screen for different proteins.”

Sally-Ann has a passion for designing PhD research projects and supporting PhD candidates toward a rewarding future career. She hopes to recruit new talented PhD students to work on a range of projects leading to further innovation in the application of MS in drug discovery, a field in which diverse and satisfying post-PhD careers are in abundance.

For more information on the Griffith Institute for Drug Discovery, please visit <https://www.griffith.edu.au/institute-drug-discovery> or follow on twitter @GRIDD_GU or @sa_poulsen. For more information on the solariX XR, please visit <https://www.bruker.com/products/mass-spectrometry-and-separations/ftms/solarix/overview.html>.

Hanne’s images by courtesy of Desley Pitcher.

References

- [1]. Poulsen S. (2006) *Direct screening of a dynamic combinatorial library using mass spectrometry*. Journal of the American Society for Mass Spectrometry, **17** (8) 1074 -1080
- [2]. Woods L, Dolezal O, Ren B, Ryan J, Peat T, Poulsen S. (2016) *Native State Mass Spectrometry, Surface Plasmon Resonance, and X-ray Crystallography Correlate Strongly as a Fragment Screening Combination*, Journal for Medical Chemistry, **59**, 5, 2192-2204
- [3]. Chrysanthopoulos P, Mujumdar P, Woods L, Dolezal O, Ren B, Peat T and Poulsen S. (2017) *Identification of a New Zinc Binding Chemotype by Fragment Screening*, Journal for Medical Chemistry, **60**, 7333–7349



Customer Insights

- Top-Down Proteomics: An Emerging Technique Driven By Cutting-Edge Mass Spectrometry

Top-Down Proteomics: An Emerging Technique Driven by Cutting-Edge Mass Spectrometry

High resolution and extreme resolution mass spectrometry instrumentation facilitates multidisciplinary research by the Ge lab, University of Wisconsin Madison, a leader in the field of top-down proteomics



Professor Ying Ge's Ge Lab at the University of Wisconsin benefits from three key instruments for their capabilities for high resolution data acquisition.

The University of Wisconsin, Madison

Based in Madison, Wisconsin, The University of Wisconsin (UW) is a top 10 research university, with over \$1 billion in annual research expenditure, making it 6th in the United States for volume of research undertaken. UW has a highly collaborative approach on campus, with faculties from various departments sharing knowledge and expertise across numerous disciplines. The Chemistry Department is the largest, comprising approximately 30-40 separate faculties with 300-400 students. Biological and chemical research also spans the medical and vet schools, priming researchers for cutting-edge discoveries and forming a good position for translational and clinical research.

Professor Ying Ge is an Associate Professor in the Department of Cell Regenerative Biology, and the Department of Chemistry, as well as the Director of Mass Spectrometry in the Human Proteomics Program of the School of Medicine and Public Health at UW-Madison. Her research in cardiac systems biology is multidisciplinary, which utilizes the collaborative ethos of the university. Her group consists of one postdoctoral associate, 11 graduate students, five undergraduate students, and three visiting scholars. With over 70 peer-reviewed publications to her name, Professor Ge is an established leader in the field of proteomics with a special focus on cardiovascular systems biology, and her group relies on the most sophisticated equipment to push the field of top-down proteomics into the realm of mainstream science.

The Research

The Ge lab aims to understand the molecular and cellular mechanisms underlying cardiovascular diseases, using cutting-edge technology such as high-resolution mass spectrometry to study comparative proteomics and metabolomics together with biochemical and physiological studies. Professor Ge's research focus on top-down mass spectrometry-based proteomics with the goal to better understand heart diseases is unparalleled by any other group. The more conventional bottom-up approach to proteomics is arguably less powerful, as it involves digesting the protein into many smaller peptides, thereby complicating the proteome and reducing the level of obtainable information, as only a small fraction of peptides are recovered. Top-down proteomics allows more powerful, reliable data to be obtained, as it directly analyzes intact proteins before fragmentation and allow analysis of unique proteoforms using mass spectrometry. Mass spectrometry-based top-down proteomics has unique advantages for unraveling the molecular complexity, quantifying proteoforms, deep sequencing of intact proteins, mapping modification sites with full sequence coverage, discovering unexpected modifications, identifying and quantifying positional isomers and determining the order of multiple modifications. Many proteins are affected by post-translational modifications (PTMs), such as glycosylation and phosphorylation. PTMs can modulate protein activity and could therefore crucially link to many human diseases: their identification is greatly improved through top-down proteomics as the



analytical processes involved preserve protein modifications, making the technique useful in probing modified proteins as potential disease biomarkers. Innovative integrated top-down proteomics can enable researchers to examine biomarkers in healthy and diseased models, to characterize any protein modifications present.

Despite top-down proteomics emerging as an increasingly popular technique, there are still some important challenges to overcome before the method becomes fully robust. One such challenge, protein solubility, is being tackled by Professor Ge's group by the development of novel top-down mass spectrometry-compatible surfactants, which can solubilize all protein categories effectively. The group is also developing novel strategies for high-resolution multi-dimensional liquid chromatography, to address the present issue of protein separation. Sample preparation, detection of large-sized proteins and a lack of software integration are additional challenges. Most routine labs are yet to adopt the approach because of this, but Professor Ge is positive that "we are in the best position right now to integrate these technologies with biology and medicine. At the moment, top-down proteomics is still challenging, but we can present solutions to address the challenges to help the community adapt to the top-down methods."

Funding and Investment

Professor Ge's research spans multiple disciplines, which cuts across the traditional boundaries of chemistry, biology, and medicine, with the aim to further the understanding of the molecular basis of cardiovascular diseases.

Her group's focus on proteomics stems from the requirement for better understanding of how molecules interact as a system, in order to elucidate cellular system functions in health and disease. Professor Ge describes the process of selecting an instrument capable of accomplishing these goals:

"We wrote an application for a National Institute of Health (NIH) high-end instrument grant that was fortunately awarded. This award gave us the chance to purchase high resolution FTMS instruments, which are extremely beneficial to top-down mass spectrometry-based proteomics. When we got the funding we then carefully evaluated all of the high-end high-resolution instruments available on the market. Bruker instruments gave us a pleasant surprise in terms of the resolution and ease of use. They really captured the hearts of my students who operated the instruments during the demo, especially the TOF instruments! ..."

".. The amount of data they got just from the two-week demo trip was incredible."

As a result of the successful demonstration, Professor Ge decided to purchase the high-end extreme resolution solarix XR™ (FTMS) together with the two ultra-high resolution (UHR) Q-TOF (impact II and Maxis II) instruments, which are now central to the strength of proteomics and mass spectrometry on campus. The nature of the group's work demands extreme and ultra-high resolution mass spectrometry techniques, which



Professor Ge accesses through her collaboration with Bruker. The Q-TOF has surprisingly sophisticated capabilities for proteoform profiling, which allows intact protein masses to be measured to facilitate disease biomarker discovery, whilst the FT-ICR-MS provides the eXtreme Resolution (XR) necessary to resolve large proteins to ensure the success in top-down proteomics.

Instruments

Professor Ge's lab use three key instruments for top-down proteomics: the solarix XR™ (FTMS), Maxis II and Impact II Q-TOF, each of which provides different benefits for her work. Since the beginning of her academic career, Professor Ge used Fourier Transfer mass spectrometry (FTMS), and the ultra-high resolution and high sensitivity still makes it the best instrument for characterizing large proteins through a top-down approach, and differentiates it from other mass spectrometers currently in use on the UW-Madison campus. Professor Ge uses this instrument for translational and clinical research to understand the basis of human diseases, as well as identifying potential molecular biomarkers for treatment of disease. The FTMS instrument is housed in the Human Proteomics Program (HPP) Mass Spectrometry Core Facility, and is shared by users across the UW campus.

Technology across the field has improved dramatically: In comparison to the mass spectrometry instruments ten years ago, those available today are phenomenal. There's a day and night difference between their capabilities for high-resolution data acquisition ..."

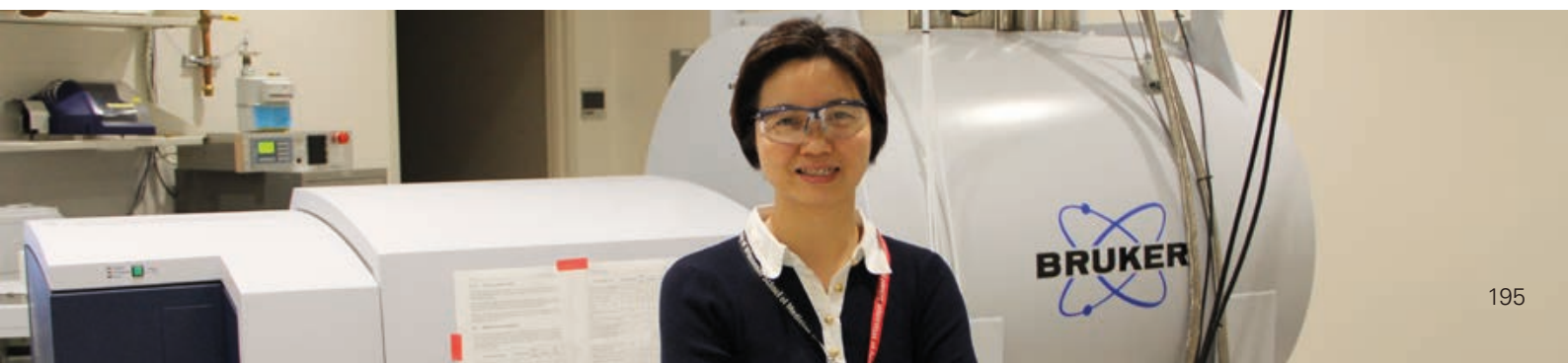
"It is now very likely that more and more proteomics labs will adapt the top-down approach soon, as the advanced instruments make it so much easier."

Campus-Wide Collaboration

The overarching aim of Professor Ge's research is to advance the understanding of the molecular basis of diseases and nurture the development of new methods for early diagnosis, prevention and better treatment of cardiovascular diseases. The group extracts intact proteins and metabolites from tissues and cells to identify, characterize and quantify them for proteoform profiling. Their studies uncover changes in the proteome and metabolome in response to external and internal stress factors, which would be lost using traditional bottom-up approaches.

Currently the group's research is split in two main directions: 1) studying cardiac myofilaments through top-down comparative proteomics, to establish a protein modification map in normal and disease models, and 2) studying cardiac regenerative biology using integrated proteomic and metabolomic approaches to evaluate the efficacy of stem cell therapies for heart failure treatment.

Professor Ge's research group enjoys collaborations widely spanning academia and industry. As director of the Human Proteomics Program at UW-Madison, Professor Ge is a strong advocate for a user-friendly facility that offer users training and access to the instruments so the instrumentation her lab uses is shared



with the whole campus. The high-end solariX XR™, Bruker's FTMS instrument, in particular is well-utilized across the campus including School of Medicine and Public Health, College of Letter and Sciences, School of Engineering, School of Pharmacy, College of Agriculture and Life Sciences, and School of Veterinary Medicine. The extreme resolution provided by the solariX XR™ enables accurate, high quality mass measurements.

In addition to academia, Professor Ge's lab collaborates with industry partners, particularly in the pharmaceutical field. Scientists from this industry visit the university to use the instruments for a broad range of applications, but most commonly for large protein (top-down proteomics) and small molecule (metabolites, natural products) experiments, and antibody-drug conjugates research. Professor Ge describes how this partnership is mutually beneficial:

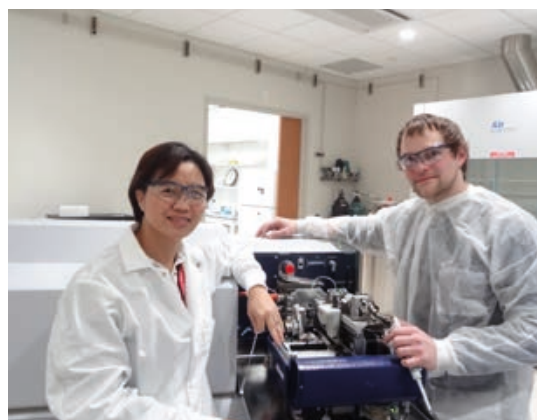
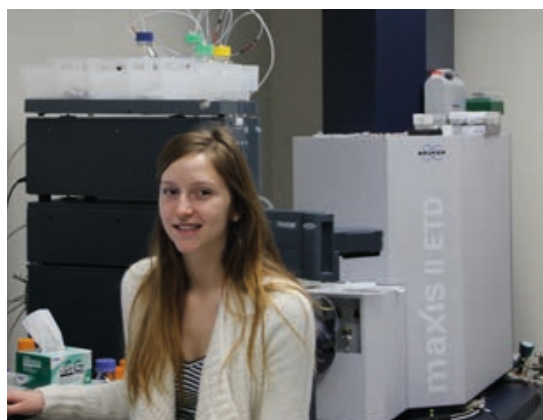
"The university is really the place for disseminating new ideas and technologies to the broad users in the community. We have achieved isotopic resolution for antibodies using the solariX XR™, and our industry collaborators are very impressed with the data. For natural product and small molecule characterization, ...

"... we showed that the extreme resolution capabilities with Bruker solariX XR™ are beyond what can be achieved by other instruments."

Access to superior mass spectrometry instrumentation is vital for the pharmaceutical industry. From Professor Ge's perspective, she can share her knowledge and expertise with the community, and importantly these collaborations generate revenue and bring business to the facility, which is essential for its continued research excellence.

The Research Challenges

Top-down proteomics is poised to move from academic curiosity to routine adoption: the key challenges which previously made the approach too difficult for most labs are now being addressed by advanced research groups such as that of Professor Ge. Specifically, her research group is employing a multi-pronged approach to address these challenges in a comprehensive manner by developing new MS-compatible surfactants for protein solubilisation (Chang et al. J. Proteome Res., 2015, 14, 1587-1599), new strategies for multi-dimensional chromatography separation of proteins (Valeja et al. Anal. Chem. 2015, 87, 5363-5371), novel nanomaterials for enrichment of low-abundance proteins (Hwang et al. J. Am. Chem. Soc., 2015, 137, 2432-2435), and a new comprehensive software package for top-down proteomics (Cai et al., Mol. Cell. Proteomics, 2016, 15, 703-14). Front end sample preparation and back end data analysis challenges are being overcome. But another industry-wide challenge facing proteomics and metabolomics research is the high degree of complexity and dynamic nature of the proteome and metabolome. High resolution and extreme resolution mass spectrometry instrumentation can address this issue; optimized for top-down



comparative proteomics and metabolomics, the instrumentation capabilities are now being tackled as sophisticated packages are brought to the market:

"Companies like Bruker are doing an excellent job of optimizing their instruments for top-down proteomics ..."

"... One of the previous challenges with the top-down approach was the instrument capabilities. Most mass spectrometers are designed for bottom-up. With the availability of these new instruments specially tailored for top-down, it's really an exciting era for top-down researchers, or those keen to enter the field." Professor Ge explains.

Current Performance

Bruker is optimizing its instruments in line with the needs of Professor Ge's lab for top-down proteomics development. In addition to data quality and quantity, instrument up-time is a dominating factor for considering an instrument's quality. When equipment breaks down or has to be switched off frequently or for long periods of time for maintenance and cleaning, the productivity of the lab dramatically decreases, affecting research output. So using instruments with minimal downtime has a positive impact on academic workload. Professor Ge explains how Bruker's zero-downtime instruments benefit her work:

"The new generation of mass spectrometers are amazing. We are lucky to have both Q-TOF instruments (Impact II and Maxis II) and FTMS (solariX XR™); we use TOF for more routine analysis and high throughput proteomics, which you can do on a daily basis – unimaginable compared to 10 years ago! During the past year of owning the impact II, Maxis II and solariX XR™ we have barely had any downtime, the

instrument essentially works 24/7. Indeed, we have already obtained enormous amount of data for publications."

In collaborations such as the one between Bruker and Professor Ge's lab, feedback is essential for Bruker to continue optimizing their instruments for Ge's increasingly complex needs: "We as a community usually shout out to companies like Bruker to inform them of our innovative new approaches to a problem, and rely on them to provide us with an instrument with the correct capabilities and compatibility for intact protein detection. Bruker heard our needs and came up with a solution incredibly quickly, giving leverage to the top-down consortium." Professor Ge explains,

"With the rapid advancements in technology, the major bottlenecks are now being overcome"

Training and Support

Staff employed by the UW-Madison Human Proteomics Program's mass spectrometry facility are dedicated to training users across the university. This forms a highly diverse collaboration:

"The impact we have generated at UW-Madison with these instruments is huge. In the past years, our facility has trained many 'super-users', meaning they can operate the instruments independently. This works really well, the instruments are so robust they can be used around the clock!" explains Professor Ge. "All these newly trained scientists now have the experience using excellent equipment, and could go on to purchase similar instruments in their future job positions."

The solariX XR™ is more sophisticated than the other instruments, so more time is required to learn how to use it:

"We are lucky to have a facility for training mass spectrometry users. The TOF instruments typically take one to two weeks for students with no previous experience to learn to operate, which is amazingly quick. The students really love this instrument. The solariX XR™ takes a little longer to grasp, but one user with no prior mass spectrometry experience can now independently operate this sophisticated instrument."

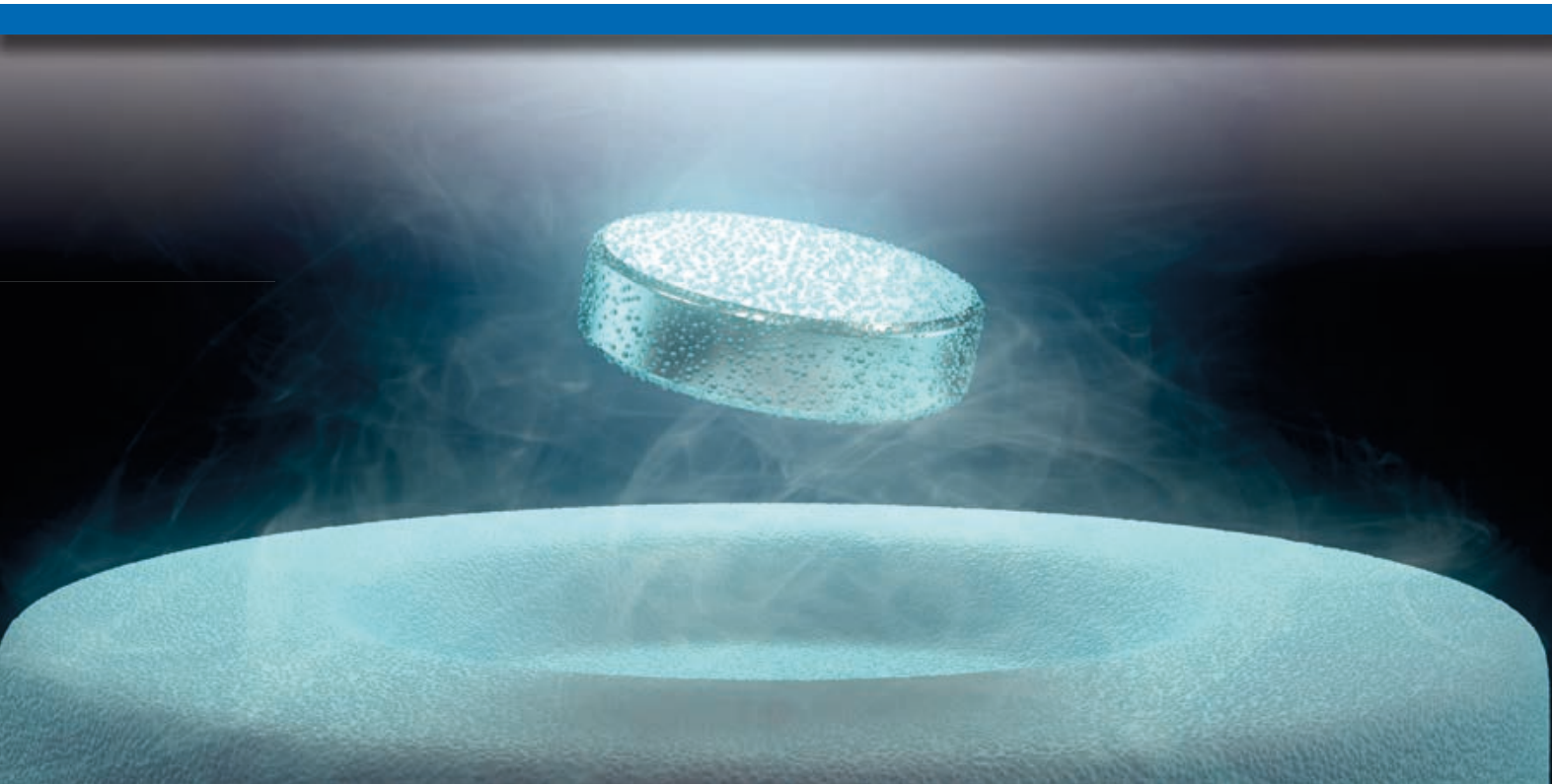
Future

"This year we expect to publish a number of papers using data acquired with Bruker instruments. The data output is incredible, and the quality is unmatched." Professor Ge predicts, with emphasis on the fact that this degree of lab productivity would not be possible without the highly advanced equipment they use. Professor Ge's work sets a precedent for the nature of the research to come: through her innovative solutions to top-down challenges and her passion for communicating to the community, top-down proteomics will soon break into the mainstream.

"Researchers in proteomics and mass spectrometry heavily rely on the quality of the instruments..."

"...The role that instrument capabilities play in academic life is so important -- excellent instruments can boost the productivity and ultimately, accelerate the success of our career! From the bottom of our hearts, we're so happy with our instruments and really want to thank Bruker."





● Glycan Sequencing by Electronic Excitation Dissociation Tandem Mass Spectrometry

Glycoconjugate glycans play vital roles in a wide range of physiological and pathological processes, such as embryogenesis, host-pathogen interactions, inflammation, and tumorigenesis. In the pharmaceutical industry, glycosylation is a key determinant for the solubility, stability, efficacy, and immunogenicity of recombinant monoclonal antibody therapeutics.

Introduction

Understanding the diverse functions of glycans requires determination of many structural variables, including their sequences, branching patterns,

linkages, and stereochemical configurations. This presents an analytical challenge that is further exacerbated by the presence of numerous glycoforms, including isomers, in naturally occurring glycan mixtures. Unlike pro-

teins, biosynthesis of glycans is not template-driven. There is no genome-predicted glycan structural database, and novel glycan structures can only be determined through *de novo* approaches.

Keywords:
Glycan Sequencing, MRMS (magnetic resonance mass spectrometry), ExD, Electron Induced Dissociation, MS/MS, tandem MS

Authors: Yang Tang¹, Juan Wei², Pengyu Hong³, Cheng Lin²;

¹Department of Chemistry, Boston University, Boston, MA 02215, USA; ²Department of Biochemistry, Boston University School of Medicine, Boston, MA 02118, USA; ³Department of Computer Science, Brandeis University, Waltham, MA 02454, USA

Tandem mass spectrometry (MS/MS) is a powerful structural characterization tool that has found many applications in biopolymer sequencing. For glycans, however, conventional collision-induced dissociation (CID)-based methods often fail to produce a sufficient amount of structural information for sequence and linkage elucidation. Therefore, sequential tandem mass spectrometry, or MSⁿ (n>2), is typically required to delineate the glycan structure, yet the MSⁿ approach suffers from its low throughput, lack of sensitivity, and difficulty in automation. Furthermore, MSⁿ analysis is usually performed on ion trap MS, and its limited mass accuracy and fragment ion co-isolation can adversely affect spectral interpretation.

A number of electron activated dissociation (ExD) methods were recently developed and applied to glycan analysis. In particular, we showed that irradiation of electrons with energy exceeding the ionization potential of the precursor ions led to a new fragmentation pathway, electronic excitation dissociation

(EED), providing rich structural information in a single stage of MS/MS analysis [1-4]. Unlike MSⁿ, EED MS/MS may be efficiently coupled to on-line liquid chromatography (LC) or ion mobility (IM) separation for facile characterization of glycan mixtures [5-6]. A novel bioinformatics algorithm was also developed for accurate reconstruction of the glycan topology from its complex EED tandem mass spectrum [7]. In this application note, we will introduce an integrated workflow that combines EED with on-line glycan separation and automatic spectral interpretation for detailed glycan structural characterization.

Experimental

Materials

Sialyl Lewis A (SLe^A) and sialyl Lewis X (SLe^X) were acquired from Dextra Laboratories (Reading, UK). Lacto-*N*-fucopentaose V (LNFP V) was obtained from Carbosynth Limited (Berkshire, UK). All other chemicals were purchased from Sigma-Aldrich (St. Louis, MO).

Sample preparation

Deutero reduction and permethylation were performed according to the method described previously [6]. Briefly, 2 μg of native glycans were dissolved in 200 μL of 0.1 M NH₄OH/0.25 M NaBD₄ solution for 2 h at room temperature, followed by addition of acetic acid (10%) until bubbling ceased. Reduced glycans were dried and resuspended in 100 μL of NaOH/DMSO mixture and vortexed for 1 h at room temperature, followed by addition of 50 μL of methyl iodide and 1 h of gentle vortexing in the dark. Additional NaOH/DMSO (100 μL) and methyl iodide (50 μL) were added followed by 1 hour of vortexing, and repeated 4 times to ensure complete methylation before the addition of 200 μL of chloroform and 200 μL of water to quench the reaction. Deutero-reduced and permethylated glycans were extracted by liquid-liquid fractionation in water and chloroform, and desalted using the Pierce PepClean C18 spin columns.

Tandem mass spectrometry analysis

All MS analyses were performed on a solariX™ Magnetic Resonance mass spectrometer (MRMS) equipped with a 12T magnet (Bruker Daltonik GmbH, Bremen, Germany). Permethylation glycans were introduced into the mass spectrometer either via static nanoelectrospray (2 μM in 50:50, v:v, methanol:water), or through LC (2 pmol per injection). Up to 2 s external ion accumulation time was used for on-line EED analysis. CID analysis was conducted with the collision energy set at 47 eV. EED analysis was performed with the cathode bias set at 16 V, and an electron irradiation time of 0.5 s. A 0.5 s transient was acquired for each mass spectrum.

Liquid chromatography

Instrument	Waters nanoACQUITY™ UPLC	
Trapping column	Waters nanoACQUITY UPLC 2G-VM, C18, 5 μm, 180 μm ID × 20 mm	
Analytical column	Waters nanoACQUITY UPLC Peptide BEH, C18, 1.7 μm, 150 μm ID × 100 mm	
Mobile phase A	99% water, 1% acetonitrile, 0.1% formic acid	
Mobile phase B	1% water, 99% acetonitrile, 0.1% formic acid	
Gradient:	0 – 2 min	38% B
	2 – 48 min	to 42% B
	48 – 50 min	to 80% B
	50 – 54 min	80% B
	54 – 56 min	to 2% B
Flow rate	500 μL/min	
Injection volume	1 μL (approximately 2 pmol)	
Column temperature	60°C	

Data analysis

Tandem mass spectra were processed using the DataAnalysis™ (Bruker Daltonik GmbH). Peak picking was performed with the SNAP™ algorithm using a quality factor threshold of 0.1 and S/N cutoff at 5. Peak assignment was achieved with the assistance of a custom VBA (Visual Basic for Applications) program, and ChemDraw 16.0. Automatic topology elucidation was achieved using the GlycoDeNovo software [7].

Results and Discussion

Glycans have relatively homologous elemental compositions and can generate many different types of fragments. This results in the common occurrence of isomeric and isobaric fragments that complicates tandem MS-based glycan sequencing. Peak assignment accuracies may be improved through the use of high-performance MS instruments, stable isotope labeling, and machine learning. Here, all glycans were deuterio-reduced and permethylated, and analyzed in their sodiated forms. Reduction eliminates anomers that can lead to undesirable chromatographic peak splitting; deuterium incorporation enables differentiation of non-reducing-end and reducing-end fragments; permethylation improves the glycan stability, ionization efficiency, and facilitates differentiation of internal and terminal fragment ions; and finally, sodium adduction promotes cross-ring cleavages and prevents proton-mediated gas-phase structural rearrangement.

EED provides greater structural details than CID

Figure 1 shows the CID and EED tandem mass spectra of LNFP V with their respective glycosidic cleavage maps. Although it is possible to deduce the sequence of this

Table 1: Topology reconstruction by GlycoDeNovo. The number inside the parenthesis indicates the number of co-ranked candidates with the true topology. The SPN and IC scores of the top three ranked candidates are given, with the values for the true topology underscored.

Glycan	Reducing End Modification	# Candidates	Rank by SPN	SPN of the top three candidates	Rank by IonClassifier	IC score of the top three candidates
LNFP V	D-reduced	9	1 (0)	<u>8</u> , 7, 7	1 (0)	<u>26</u> , 17, 14
SLe ^A	D-reduced	19	1 (0)	<u>6</u> , 5, 5	1 (0)	<u>23</u> , 15, 14
SLe ^X	D-reduced	12	1 (0)	<u>7</u> , 6, 6	1 (0)	<u>21</u> , 15, 14
SLe ^A	none	14	1 (2)	<u>7</u> , 7, 7	1 (0)	<u>20</u> , 15, 15
SLe ^X	none	22	1 (2)	<u>8</u> , 8, 8	1 (0)	<u>20</u> , 18, 18

glycan from its CID spectrum based on the presence of the Y-ion series, no linkage configuration can be determined due to a lack of cross-ring fragments. In contrast, EED generated many linkage-diagnostic cross-ring and secondary fragments. For example, the presence of ^{1,3}A_{2α} and C_{2α}/Z_{3α} ions is indicative of the Gal1→3GlcNAc linkage at the non-reducing end, and the observation of Z_{1β}•-CHDOCH₃ ion is characteristic of the Fuc1→3Glc linkage at the reducing end. The C_{2α}/Z_{3α} and Z_{1β}•-CHDOCH₃ ions likely resulted from the primary Z_{3α}• and Z_{1β}• ions, respectively, where the location of the initial radical site dictates the type of secondary fragments that can be generated via subsequent alpha cleavages. A detailed discussion of the utility of secondary fragments in linkage elucidation can be found in a recently published article [6].

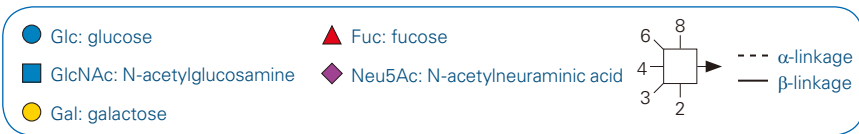
Reversed-phase liquid chromatography (RPLC)-EED analysis of isomeric glycans

For glycan mixtures containing isomeric structures, isomer separation is necessary prior to tandem MS analysis. EED MS/MS can be efficiently coupled to on-line RPLC for separation and characterization of isomeric glycans. Figure 2 shows a RPLC-EED MS/MS analysis of a

mixture of SLe^A and SLe^X. These two linkage isomers were baseline resolved by RPLC, as evident from the extracted ion chromatogram of the singly sodiated precursor (insets A1 and B1), where the arrows mark the retention times when the single-scan EED spectra shown in Figures 2A and 2B were acquired. EED generated complete series of glycosidic fragments for unambiguous determination of the glycan topology. Determination of the linkage configurations at the reducing-end for either isomer can be readily achieved based on the three pairs of secondary fragments labeled in red. Insets A2 and B2 show the zoomed-in regions containing the linkage-diagnostic Z_{1β}•-CH₂OCH₃ and Z_{1β}•-CHDOCH₃ fragments, respectively. Scheme 1 shows the proposed mechanisms for the formation of these linkage-diagnostic secondary fragments.

Automatic topology elucidation from EED spectra

De novo glycan sequencing requires the presence of at least one glycosidic fragment, or sequence ion, at each glycosidic linkage site. Identification of all sequence ions allows the construction of an interpretation-graph for glycan topology inference. However, by chance, a non-sequence fragment can have



Abbreviations and Symbol Nomenclature for Glycans

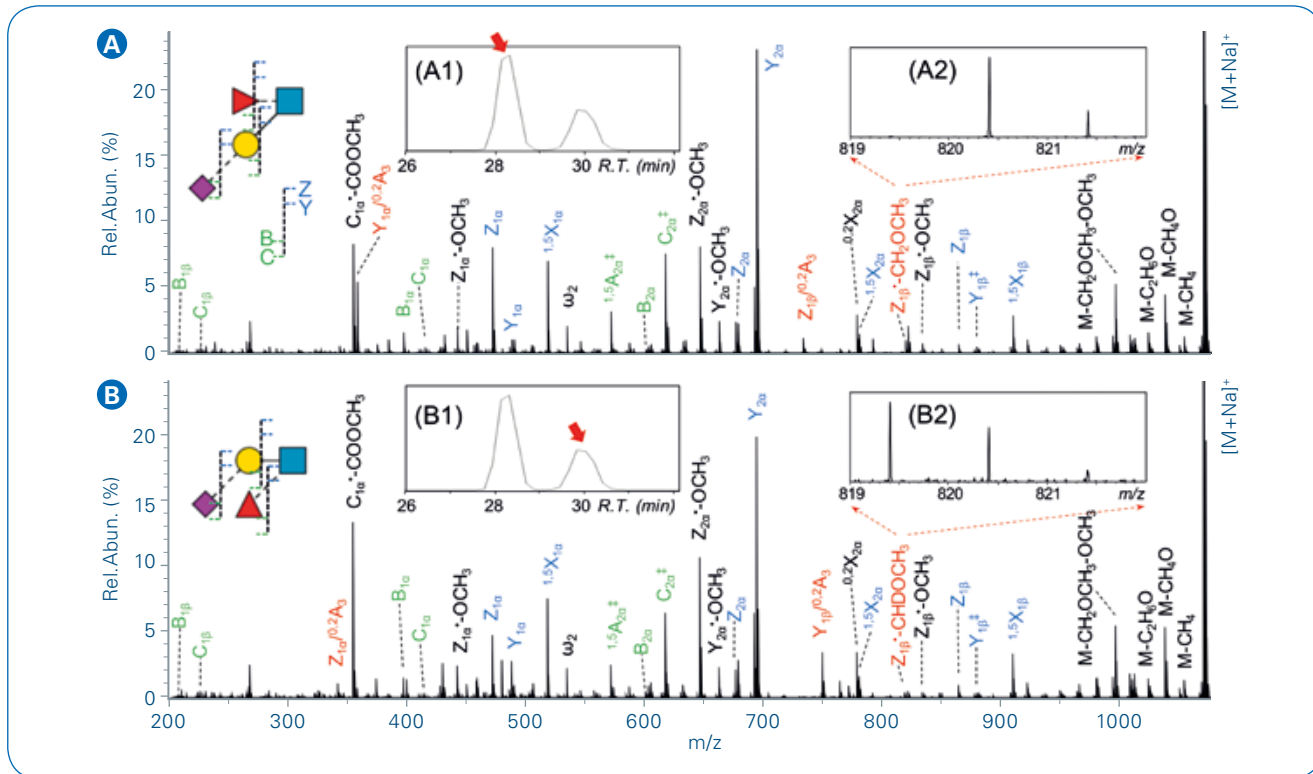


Figure 1: CID **A** and EED **B** tandem mass spectra of singly sodiated, deuterio-reduced and permethylated LNFP V

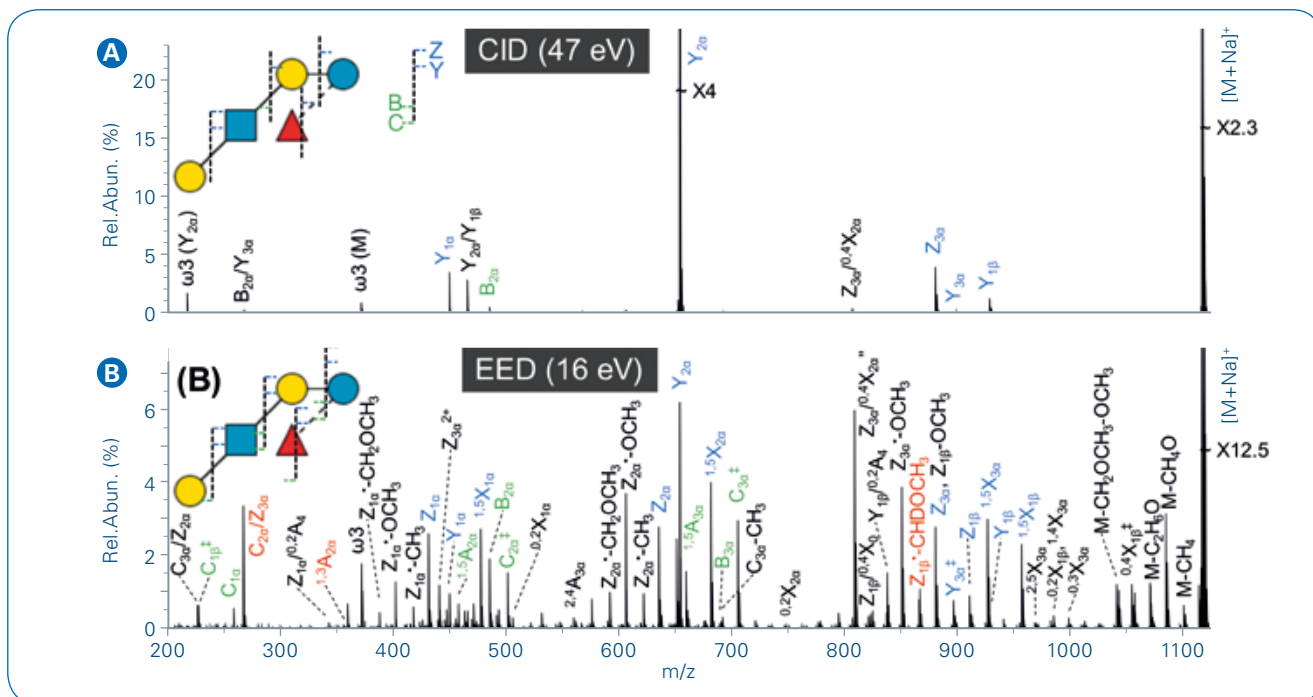
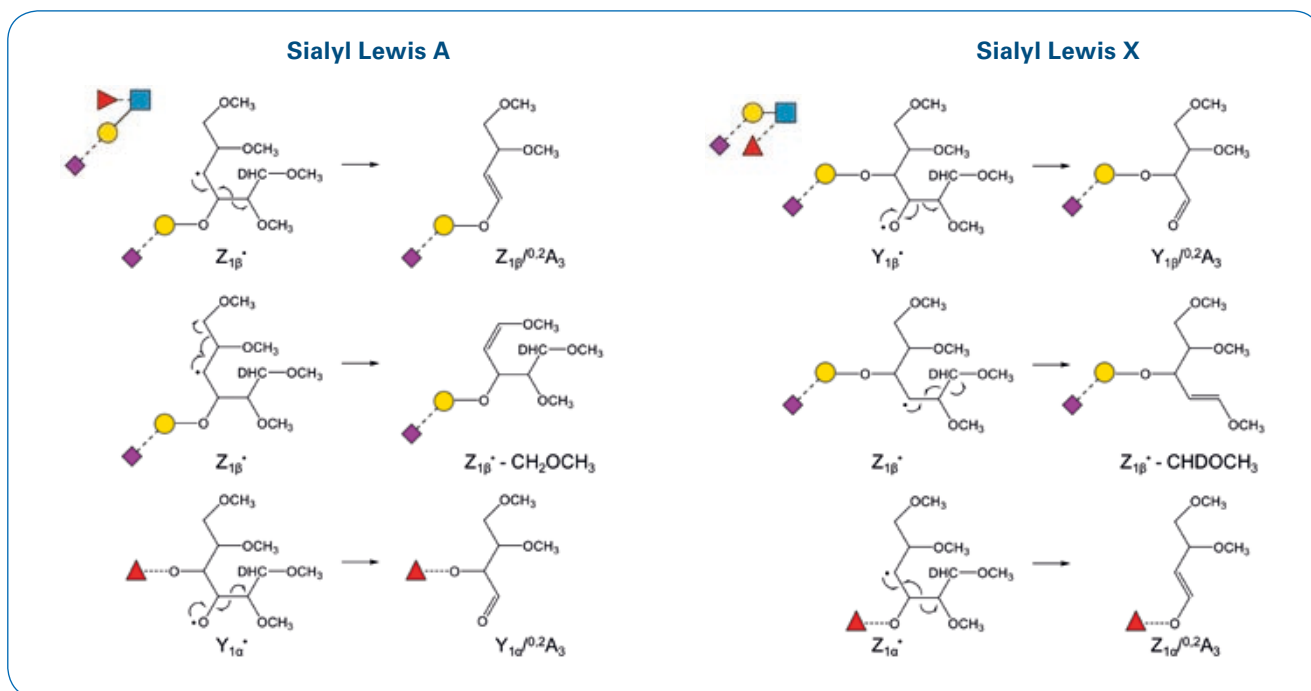


Figure 2: RPLC-EED MS/MS analysis of a mixture of deuterio-reduced and permethylated sialyl Lewis A and X



Scheme 1: Proposed mechanisms for the formation of linkage-specific secondary fragments highlighted in Figure 2

the same mass as a combination of several monosaccharide residue masses, and may be misinterpreted as a sequence ion. Although experimental measures, such as permethylation and selective isotope labeling, can be taken to reduce peak assignment ambiguity, they do not eliminate misidentification due to fortuitous matches. Candidate ranking by their supporting peak numbers (SPN) is also ineffective as revealed by a recent study [7].

We recently introduced an improved scoring algorithm in which the peak context is utilized to estimate the peak assignment accuracy. The context of a fragment is a collection of its neighboring peaks within a pre-determined mass window, expressed as mass shifts from the peak of interest. For example, a Y-ion is often accompanied by a Z-ion with a -18 Da mass shift, and a ^{1,5}X ion with a +28 Da mass shift (+86 Da for sialic acid residues), forming a characteristic triplet (labeled in blue in Figures 1 and 2). Given a set of EED spectra of glycan standards, it is possible to identify contextual features for

each type of fragments via machine learning, allowing construction of an IonClassifier that computes the likelihood of a peak assignment being right based on its peak context. Candidate structures can then be ranked by the cumulative IonClassifier scores of all their supporting peaks. Table 1 illustrates the performance of GlycoDeNovo on topology reconstruction from the EED spectra of the glycan standards shown here. With the reducing-end isotope labeling, the true topology was correctly ranked as the top

candidate in each case by either SPN or the IonClassifier. However, the IC score provides much better differentiating power than SPN. For SLe^A and SLe^X without the reducing-end modification, SPN failed to differentiate the correct topology from two co-ranked structures, whereas the IC score still ranked the true topology as the highest ranked candidate by itself. A detailed discussion of the GlycoDeNovo algorithm, the IonClassifier, and its performance on glycans with more complex structures, can be found in a recent publication [7].

Conclusions

- In this application note, we show that EED can generate far richer structural information than CID for elucidation of the glycan sequence (topology) and linkage configurations. Presently, EED of glycans has only been demonstrated on MRMS instruments, whose high mass resolving power and mass accuracy are critical for accurate peak assignments. Coupling of EED MS/MS with on-line LC separation allows characterization of glycan mixtures with isomeric structures. Finally, one can take advantage of the complexity of the glycan EED spectra to improve the confidence in fragment assignments by considering the contextual features of the peak of interest. The workflow presented here provides a powerful tool for facile and rapid characterization of complex glycan samples.



Learn More

You are looking for further Information?
Check out the link or scan the QR code for more details.

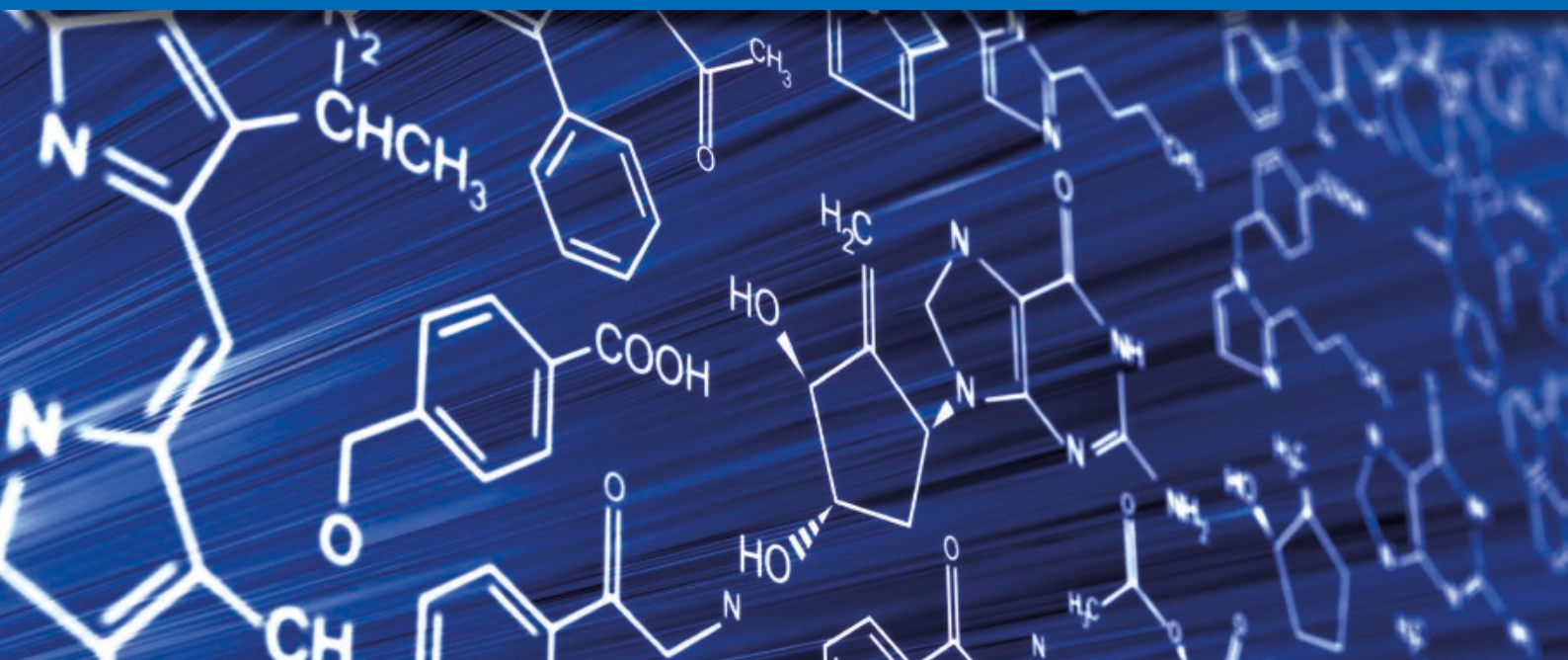
www.bruker.com/scimaX



References

- [1] Yu X, Huang Y, Lin C, Costello CE (2012) *Energy-dependent electron activated dissociation of metal-adducted permethylated oligosaccharides*. Anal. Chem., **84**, 7487-7494. PMC3568493
- [2] Yu X, Jiang Y, Chen Y, Huang Y, Costello CE, Lin C (2013) *Detailed glycan structural characterization by electronic excitation dissociation*. Anal. Chem., **85**, 10017-10021. PMC3851312
- [3] Huang Y, Pu Y, Yu X, Costello CE, Lin C (2016) *Mechanistic study on electronic excitation dissociation of the cellobiose-Na⁺ complex*. J. Am. Soc. Mass. Spectrom., **27**, 319-328. PMC4724539
- [4] Tang Y, Pu Y, Gao J, Hong P, Costello CE, Lin C (2018) *De novo glycan sequencing by electronic excitation dissociation and fixed-charge derivatization*. Anal. Chem., **90**, 3793-3801. PMID29443510
- [5] Pu Y, Ridgeway ME, Glaskin RS, Park MA, Costello CE, Lin C (2016) *Separation and identification of isomeric glycans by selected accumulation-trapped ion mobility spectrometry-electron activated dissociation tandem mass spectrometry*. Anal. Chem., **88**, 3440-3443. PMC4821751
- [6] Tang Y, Wei J, Costello CE, Lin C (2018) *Characterization of Isomeric Glycans by Reversed Phase Liquid Chromatography-Electronic Excitation Dissociation Tandem Mass Spectrometry*. J. Am. Soc. Mass. Spectrom., **29**, 1295-1307. PMC6004250
- [7] Hong P, Sun H, Sha L, Pu Y, Khatri K, Yu X, Tang Y, Lin C (2017) *GlycoDeNovo—an Efficient Algorithm for Accurate de novo Glycan Topology Reconstruction from Tandem Mass Spectra*. J. Am. Soc. Mass. Spectrom., **28**, 2288-2301. PMC5647224

For Research Use Only. Not for Use in Clinical Diagnostic Procedures.



● Comparison of CID and EID Mass Spectrum of Glycosides from solarix XR

Tandem mass spectrometry (MS/MS) is an important tool for structural determination and molecular identification. Collision-induced dissociation (CID) is the most commonly used ion activation method; however, it only gives limited fragments for some classes of compounds. Electron-induced dissociation (EID) provides an alternative ion activation mechanism for fragment generation, which can gain more wealthy information. Here, CID and EID were applied to potatoes glycoalkaloids and flavonoid glycosides for comparison.

Mass spectrometry is now an indispensable analytical technique for molecular characterization because of its high sensitivity and precision. Tandem mass spectrometry (MS/MS) breaks down molecular ions into fragment pieces which allows in-depth structural determination and elucidation. Collision-induced dissociation (CID)¹ is the most commonly used ion activation method for MS/MS. In

conventional CID, precursor ion is vibrationally activated through collisions with inert gas atoms/molecules. Bond cleavage occurs preferentially at weak linkage(s) and hence, gives limited structural information. Electron-induced dissociation (EID)¹ is an alternative ion activation approach that is based on electron-ion interaction. Different from CID, EID activates precursor ions by impacting

them with high energy electrons. EID produces more cleavages and provides important structural information that cannot be obtained from the traditional CID techniques. In addition, EID can be applied on both singly and multiply charged ions. In this study, two types of glycoconjugates, potatoes glycoalkaloids and flavonoid glycosides, have been analyzed by both CID and EID for comparison.

Keywords:
Tandem mass spectrometry; glycoside; glycoalkaloid; collision induced dissociation (CID); electron induced dissociation (EID); structural elucidation

Authors: Y.L. Elaine Wong¹, H. S. Yeung² and T.-W. Dominic Chan^{1*}.
¹ Department of Chemistry, The Chinese University of Hong Kong, HKSAR
² Bruker Scientific Instruments Hong Kong Co. Limited

Sample Preparation

α -solanine and α -chaconine were extracted from the sprout of a potato using 50% methanol. Hesperidin was purchased from Sigma Aldrich. All these compounds were diluted to 0.1 μ M for analysis.

Mass Spectrometry Analysis

All the experiments were performed on a Bruker solarix XR MRMS equipped with a 9.4T actively shielded refrigerated magnet. Samples were directly infused and ionized in positive ESI mode at 2 μ L/min. All mass spectra were acquired in broadband mode over a mass range of m/z 80 – 1500 using 1 MW data size. For the EID experiments, the precursor ions were isolated in the quadrupole and were accumulated in the collision cell before being transferred into the ParaCell™. The ions were then irradiated with electrons from a heated hollow cathode dispenser operated at a heating current of 1.4 A. The bias voltage was set at 26 V and the ECD lens voltage was set to 0 – 5 V. The electron irradiation time was 30 – 60 ms. For CID, the precursor ions were isolated in the first quadrupole and were fragmented in the collision cell with collision energies of 15 V for Hesperidin and 50 – 55 V for α -Solanine and α -Chaconine. The mass spectra were externally calibrated by cluster ions of sodium formate and were then internally calibrated using confidently assigned fragment peaks. Data was processed by Data-Analysis™ software (Version 4.4) and product ions were assigned through accurate mass measurements using SmartFormula.

Results

Figure 1 and Figure 2 show the CID and EID spectra of α -solanine, α -chaconine and hesperidin. Product ions were assigned with a mass

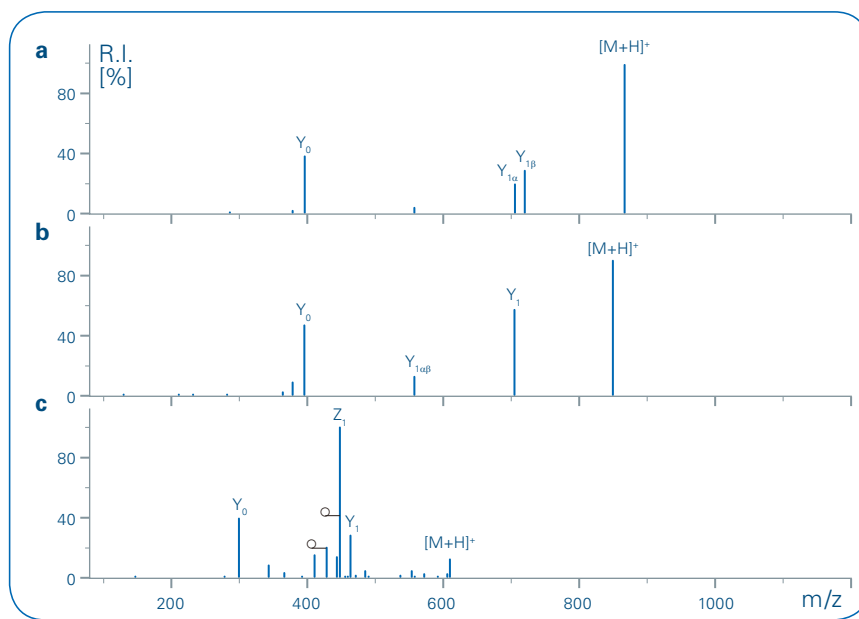


Figure 1. CID spectrum of a) α -solanine, b) α -chaconine and c) hesperidin; -o indicates the loss of water

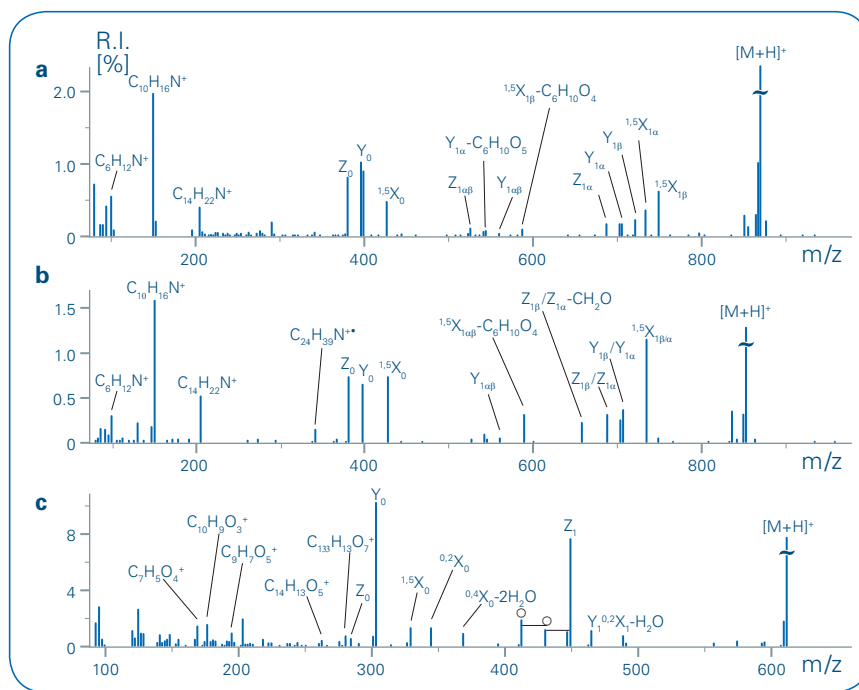
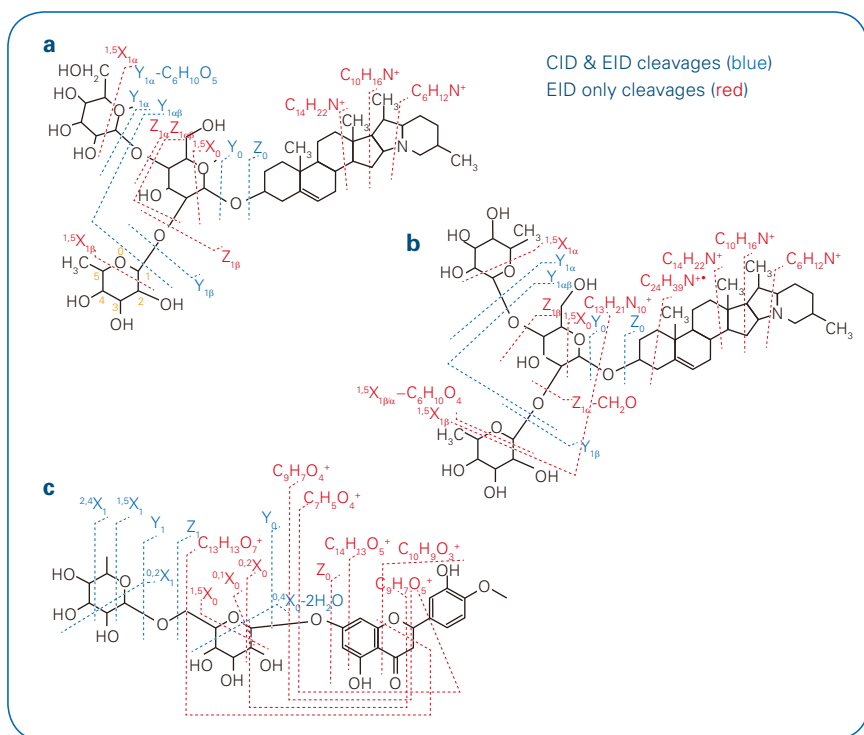


Figure 2. EID spectrum of a) α -solanine, b) α -chaconine and c) hesperidin

accuracy of less than 200 ppb (table 1 for α -chaconine). This high accuracy allows relatively easy and confident assignment.

Generally, EID, which is driven by radical fragmentation, produces more fruitful fragments than CID by comparisons. For α -solanine and α -chaconine, CID results show a preferential cleavage on glycosidic bonds, giving Y and Z ions and loss

of small neutral molecule such as water. Whereas, in EID, it includes all cleavages induced in CID and additionally generates extra multiple cleavages. Examples such as cross-ring fragmentation of the sugar parts to give X ions, and produces characteristic ions of steroidal aglycone moieties, $C_{14}H_{22}N^+$, $C_{10}H_{16}N^+$ and $C_6H_{12}N^+$ for both α -solanine and α -chaconine (Fig.1a, b and Fig.3).



The CID result of hesperidin shows relatively more fragments, including a certain extent of cross-ring cleavages in rhamnose ring. Compared to that, EID generates a higher degree of cross-ring cleavages in both rhamnose ring and glucose ring. It also gives more fragments in lower mass, $C_{14}H_{13}O_5^+$, $C_{10}H_9O_3^+$, $C_{10}H_{16}N^+$ and $C_6H_{12}N^+$, which arose from the cleavages of the flavonoid aglycone moiety (Fig.1c and Fig.3). This gives more useful information in the structural elucidations of different types of glycosides.

Figure 3. CID and EID cleavage of
a) α -solanine, b) α -chaconine and c) hesperidin

Table 1. Summary of CID and EID product ions of α -chaconine

CID of [M+H]⁺

Expt. m/z	Assigned Molecular formula	Theo. m/z	Error(ppb)	Assignments
852,510291	$C_{45}H_{74}NO_{14}^+$	852,510382	-107	[M+H] ⁺
706,452486	$C_{39}H_{64}NO_{10}^+$	706,452474	17	$Y_{1\beta}/Y_{1\alpha}$
560,394626	$C_{33}H_{54}NO_6^+$	560,394565	109	$Y_{1\alpha\beta}$
398,341726	$C_{27}H_{44}NO^+$	398,341741	-38	Y_0

EID of [M+H]⁺

Expt. m/z	Assigned Molecular formula	Theo. m/z	Error(ppb)	Assignments
852,510487	$C_{45}H_{74}NO_{14}^+$	852,510382	123	[M+H] ⁺
734,447479	$C_{40}H_{64}NO_{11}^+$	734,447388	124	$^{1.5}X_{1\beta}$
706,452385	$C_{39}H_{64}NO_{10}^+$	706,452474	-126	$Y_{1\beta}/Y_{1\alpha}$
688,441823	$C_{39}H_{62}NO_9^+$	688,441909	-125	$Z_{1\beta}/Y_{1\alpha}$
658,431279	$C_{38}H_{60}NO_8^+$	658,431344	-99	$Z_{1\beta}/Y_{1\alpha}-CH_2O$
588,389541	$C_{34}H_{54}NO_7^+$	588,389479	105	$^{1.5}X_{1\beta}-C_6H_{10}O_4$
560,394623	$C_{33}H_{54}NO_6^+$	560,394565	103	$Y_{1\alpha\beta}$
426,336617	$C_{28}H_{44}NO_2^+$	426,336656	-91	$^{1.5}X_0$
398,341707	$C_{27}H_{44}NO^+$	398,341741	-85	Y_0
380,331147	$C_{27}H_{42}N^+$	380,331177	-79	Z_0
341,307717	$C_{24}H_{39}N^+$	341,307702	44	$C_{24}H_{39}N^+$
337,112934	$C_{13}H_{21}O_{10}^+$	337,112923	33	$C_{13}H_{21}O_{10}^+$
204,174669	$C_{14}H_{22}N^+$	204,174676	-34	$C_{14}H_{22}N^+$
150,127729	$C_{10}H_{16}N^+$	150,127726	20	$C_{10}H_{16}N^+$
98,096425	$C_6H_{12}N^+$	98,096426	-10	$C_6H_{12}N^+$

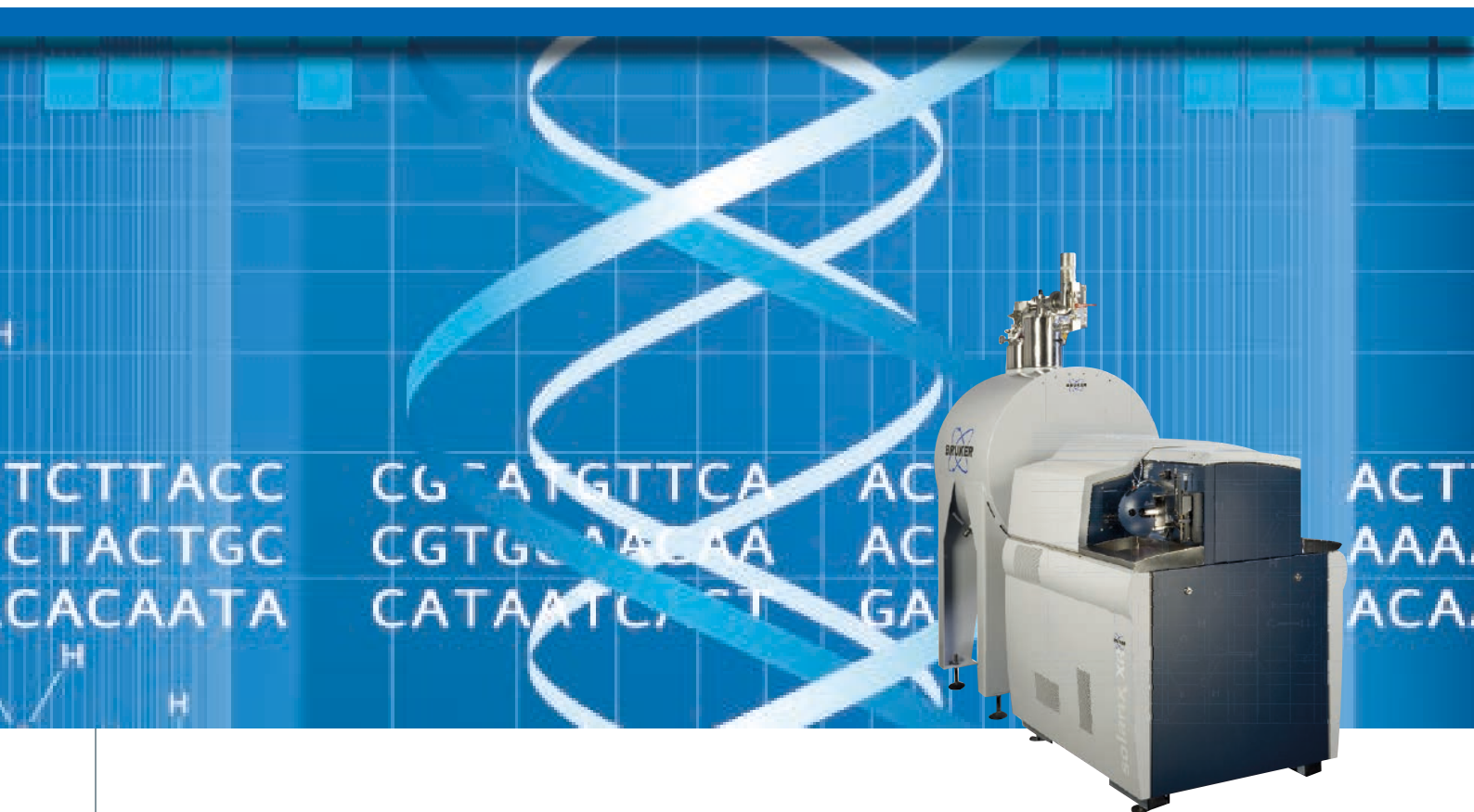
Conclusions

To conclude, EID is found to generate structurally informative fragments on the glycan sequence and linkage sites in glycoalkaloids and flavonoids glycosides. It also produces cleavages in their aglycone moieties, which are absent in CID. This enables more detailed analysis of different classes of glycoside. The supplementary information provided by EID greatly facilitates the structure elucidation of complex glycoconjugates.

References

1. R. B. Cody, R. C. Burnier, B. S. Freiser, *Anal. Chem.*, 1982, 54, 96-101.
2. H. Lioe., R.A. O'Hair, *Anal. Bioanal. Chem.*, 2007, 389, 1429-1437.

For research use only. Not for use in diagnostic procedures.



• Top Down Analysis of Histone H4

Abstract

Characterization of proteins by top-down mass spectrometry is often necessary when many post translational modifications are present. Histones are an example of this type of challenge due to their abundant and varying modifications. We demonstrate top-down dissociation of two intact human histone H4 proteins with ECD, ETD, CID and MALDI-ISD on the Bruker solarix FTMS platform. These dissociation techniques were used to determine the presence of both acetylation and dimethylation on the proteins.

Introduction

Mass spectrometry and tandem mass spectrometry have found wide application to the analysis of proteins and proteomes. However, some proteins cannot be identified by bottom-up mass spectrometry techniques for various

Authors

Jeremy J. Wolff, Christopher J. Thompson
Bruker Daltonics

Keywords	Instrumentation and Software
FTMS	solarix
Top Down	ECD
ETD	ETD
CID	ISD
MALDI-ISD	
Histone	

reasons. For example, the organisms genome may not be sequenced, modifications to the protein may have occurred, or there may be errors in either the genome or protein database. All of these examples alter the mass of the protein and may cause errors using bottom-up protein identification techniques. Top-Down proteomics is ideally suited to identify these proteins because the sequence of the protein is derived directly from the tandem mass spectra. In top-down mass spectrometry, a protein is dissociated by one of a variety of ion-activation methods in order to decipher the sequence and modifications of the protein. These dissociation techniques include electron capture dissociation (ECD), electron transfer dissociation (ETD), collision induced dissociation (CID) and matrix assisted laser desorption ionization in source decay (MALDI-ISD). Here, we use each of these fragmentation techniques to determine the type and location of various histone H4 modifications. Histones offer a good example of a complex problem that can be solved with top-down mass spectrometry. The protein sequence of histone H4 is known, but it has the potential for more than 20 post translational modifications. Because some of these modifications are labile, dissociation techniques which preserve the labile modification are necessary. The solariX offers both collisional- and electron-dissociation techniques to probe protein sequence, and thus is ideally suited to analyze the histone fraction.

Experimental

Sample Preparation

The H4 histone fraction is from human HeLa S3 suspension cells grown in Prof. Neil Kelleher's lab at Northwestern University. The histone was extracted from isolated nuclei by sulfuric acid extraction, followed by TCA precipitation, and then purified by RPLC. The dried sample was reconstituted in water to create a stock solution (~8 pmol/ μ L). For ESI experiments, the stock solution was diluted to a final concentration of 200 fmol/ μ L in 50:50:0.1 acetonitrile:water:formic acid. For MALDI-ISD experiments, a saturated solution of 1,5-diaminonaphthalene (DAN) was made using acetonitrile with 0.1% TFA. The DAN matrix and histone stock solutions were mixed 2:1 and then 0.5 μ L of the mixture was spotted on the target and allowed to dry at room temperature.

Mass Spectrometry Analysis

All experiments were performed on a Bruker solariX FTMS equipped with a 12T actively shielded refrigerated magnet. The instrument is fitted with a dual ion source which allows for rapid switching between ESI and MALDI, an indirectly heated hollow cathode for ECD, and a chemical ionization source for ETD. For qCID, ECD, and ETD experiments, the histone solution was directly infused at 2 μ L/min in positive ion mode. Precursor ions were isolated in the external quadrupole and stored in adjacent hexapole for 200 ms. For

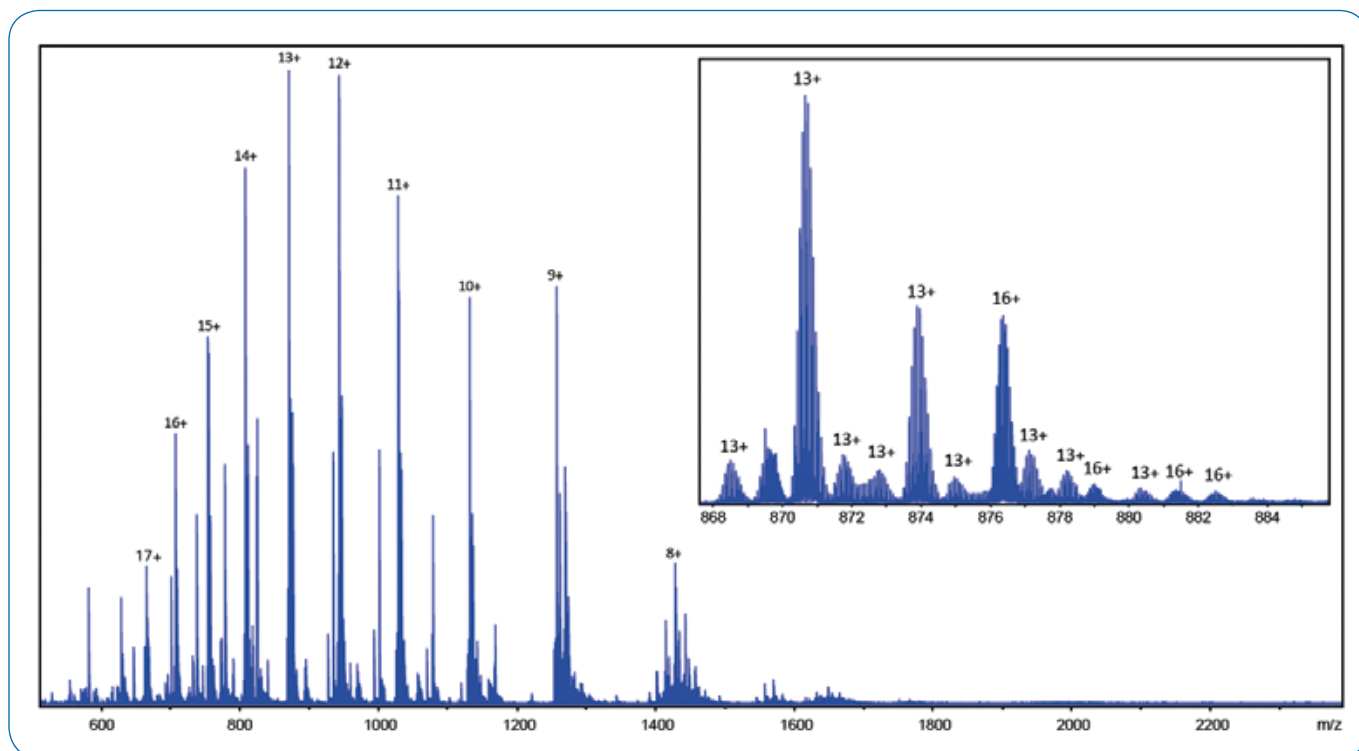


Figure 1. Broadband +ESI mass spectrum of the histone H4 fraction. The complexity of histone H4 is highlighted in the insert, showing the various species within the 13+ charge state.

qCID, ions were dissociated inside the external collision cell adjacent to the quadrupole. For ECD, q-isolated precursor ions were transferred to the ICR cell and irradiated with 0.8 eV electrons for <50 msec. For ETD, q-isolated precursor ions were reacted with the ETD reagent for 60 ms in the collision cell. For MALDI-ISD, the sample was irradiated with light from the Nd:YAG laser to produce product ions. ESI experiments were externally calibrated with NaTFA clusters, and MALDI-ISD experiments were externally calibrated with PFHA clusters.

Results

Positive mode ESI of the histone sample, shown in Figure 1, shows the complexity of the histone H4 fraction. A zoom in of the 13+ charge state of the most abundant species (Figure 1, inset) shows the many different species present in the sample. Initial sequencing efforts were focused on the 13+ ion at m/z 871. Comparison of the MS data (MH+mono = 11300.4232 Da) against the known human histone H4 sequence (MH+mono = 11230.3485 Da) showed a mass difference of 70.0747 Da. This mass difference is not a common mass difference, so multiple protein modifications are suspected. ECD of this 13+ species, shown in Figure 2, produced abundant product ions (Figure 2, inset) that are typical for top-down mass spectrometry with ECD. Monoisotopic m/z values and charge-states were determined using the SNAP II peak picking algorithm in DataAnalysis, and peak lists were transferred

to BioTools for further analysis. Using BioTools, fragment ions were searched using Mascot with a custom database with the histone sequence and predicted modifications using a 5 ppm search tolerance (from SwissProt, P62805). The search determined the histone contained two modifications: an N-terminal acetylation and a dimethylation at K20, as shown in the top of Figure 3, with a total sequence coverage of 78%. ETD and qCID of the peak at m/z 870 (Figure 3, middle and bottom) also confirmed the protein sequence and modifications, as shown in Figure 3. Because the modifications are not “labile”, the acetylation and dimethylation remain on the protein during collisional dissociation. Using an automated script to combine the three dissociation methods, the combined sequence coverage for the three dissociation techniques was 93%.

A second precursor ion at m/z 874 (MH+mono = 11342.4361 Da) was also selected for dissociation. The mass of this ion differs from the mass of the peak at m/z 870 ion by 42.0129 Da, indicating a possible acetylation. ECD and ETD were performed on this precursor ion, followed by SNAP II peak picking in DataAnalysis. The ECD and ETD peak lists were automatically combined and analysis of this combined peak list with BioTools and Mascot confirms a second acetylation is present on K16 as shown in Figure 4, with a combined sequence coverage of 64%.

MALDI-ISD of the histone mixture produces abundant product ions from m/z 1000 to 6000, as shown in Figure 5. For

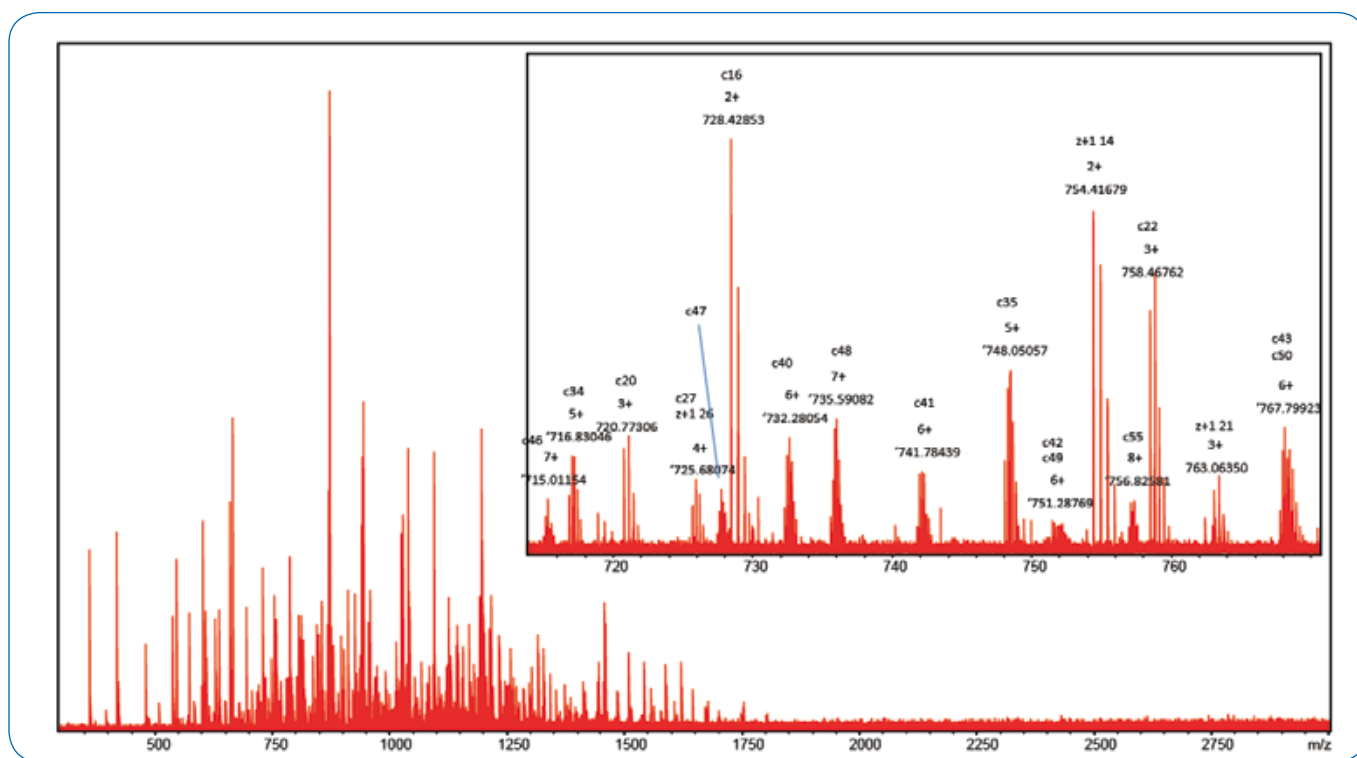


Figure 2. ECD spectrum of the isolated m/z 870 species. Inset show highly charged product ions typically observed in top-down ECD experiments.

Acetylation Dimethylation

ECD SGRGKGGKGL GKGGAKRHRK VLRDNIQGIT
KPAIRRLARR GGVKRISGLI YEETRGVLKV
FLENVIRDAV TYTEHAKRKT VTAMDVVYAL
KRQGR TLYGF GG

ETD SGRGKGGKGL GKGGAKRHRK VLRDNIQGIT
KPAIRRLARR GGVKRISGLI YEETRGVLKV
FLENVIRDAV TYTEHAKRKT VTAMDVVYAL
KRQGR TLYGF GG

CID SGRGKGGKGL GKGGAKRHRK VLRDNIQGIT
KPAIRRLARR GGVKRISGLI YEETRGVLKV
FLENVIRDAV TYTEHAKRKT VTAMDVVYAL
KRQGR TLYGF GG

Figure 3. Production ions observed from ECD, ETD, and CID fragmentation of 13+ ion at m/z 870. Fragmentation coverage is 78%, 60%, and 62%, respectively. The combined sequence coverage is 93%.

Acetylation Dimethylation

SGRGKGGKGL GKGGAKRHRK VLRDNIQGIT
KPAIRRLARR GGVKRISGLI YEETRGVLKV
FLENVIRDAV TYTEHAKRKT VTAMDVVYAL
KRQGR TLYGF GG

Figure 4. Combined sequence coverage for the ECD and ETD mass spectra of the isolated m/z 874 species. The combined total sequence coverage is 64%

Acetylation Dimethylation

SGRGKGGKGL GKGGAKRHRK VLRDNIQGIT
KPAIRRLARR GGVKRISGLI YEETRGVLKV
FLENVIRDAV TYTEHAKRKT VTAMDVVYAL
KRQGR TLYGF GG

Figure 6. Protein fragmentation of the MALDI-MS spectrum of entire Histone H4 sample, with a sequence coverage is 70%.

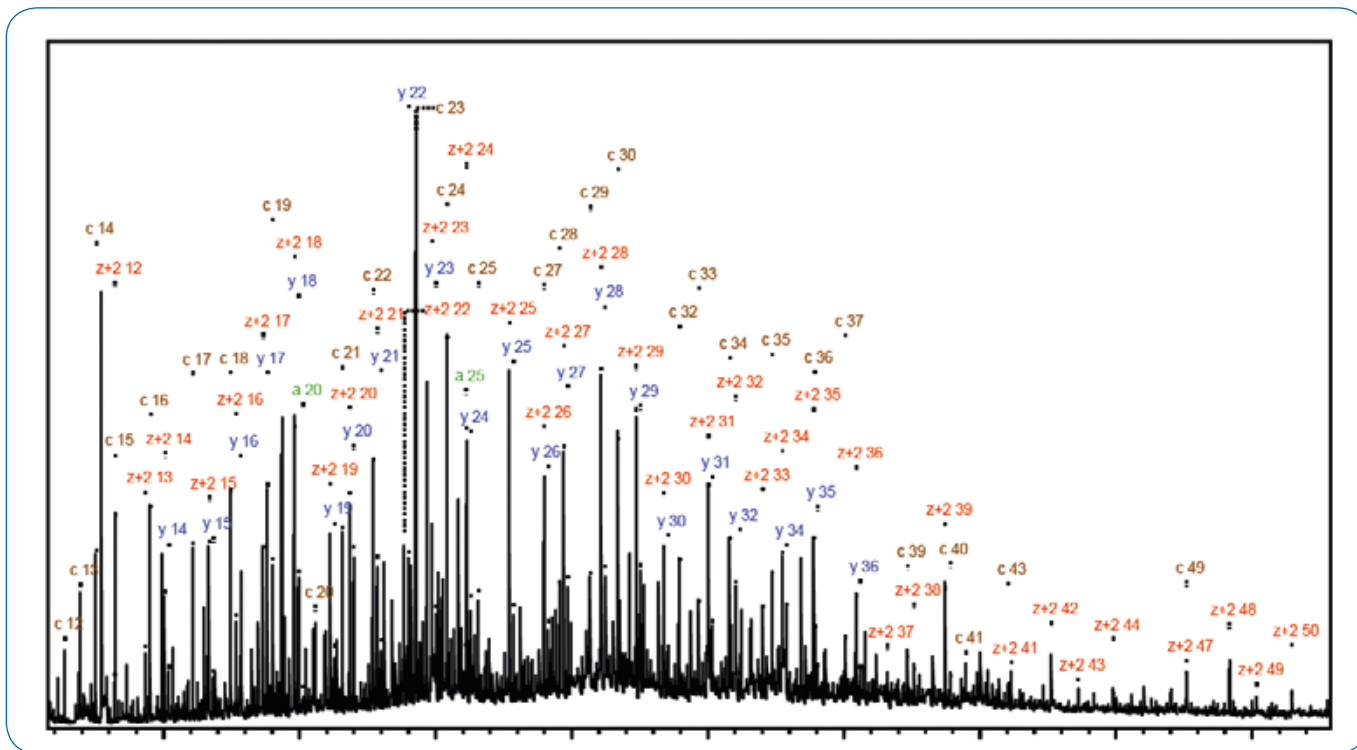


Figure 5. MALDI-MS/MS spectrum of entire Histone H4 envelope. Fragments correspond to the most abundant protein, containing an N-terminal acetylation and dimethylation at K20.

MALDI-MS/MS on protein mixtures, only fragmentation of the most abundant protein is typically observed. For the histone H4 sample, analysis of the data (Figure 6) shows only fragmentation of the most abundant species which contains an N-terminal acetylation and a dimethylation and K20 (70% sequence coverage), further validating the sequence and PTMs present on this protein.

Conclusion

Top-down mass spectrometry using a combination of ECD, ETD, CID and MALDI-MS/MS was able to rapidly determine the presence of an N-terminal acetylation and K20 dimethylation on both H4 proteins. The protein at MW 11342 also contains a second acetylation at K16.

References

- [1] Pesavento, J.J., Bullock, C.R., LeDuc, R.D., Mizzen, C.A., Kelleher, N.L.: Combinatorial Modification of Human Histone H4 Quantitated by Two-dimensional Liquid Chromatography Coupled with Top Down Mass Spectrometry. *J Biol Chem.* 22, 14927-14937 (2008).
- [2] Tian, Z., Tolic, N., Zhao, R., Moore, R.J., Hengel, S.M., Robinson, E.W., Stenoien, D.L., Wu, S., Smith, R.D., Paša-Tolic, L.: Enhanced top-down characterization of histone post-translational modifications. *Genome Biology.* 13, R86 (2012).

Acknowledgements

The authors would like to thank David Goodlett, Jenna Scotcher, Nicolas L. Young, Neil Kelleher and the "Consortium for Top-Down Proteomics" for providing the histone H4 sample.

For research use only. Not for use in diagnostic procedures.



• Expanded Collisional Energy Files for Automated Top Down and Bottom up Analysis on solariX

Abstract

Collisionally Induced Dissociation (qCID) energies are optimized on solariX for both peptide and protein species. To avoid over estimating the energies, only assignable fragment ions (b- and y-type) are included within the efficiency calculations. A single collisional energy file (cef) is created for LC-MS/MS applications that can be easily expanded via the procedures outlined within.

Introduction

The power of Top-down and Bottom-up analysis in the modern laboratory relies on automation. For qCID MS/MS, the energy required to dissociate a given ion is a function of both m/z and charge state, which varies greatly between proteins and peptides. This work examines the optimal collisional energy as a function of

distinct chemical classes: peptides and protein. Additionally, several methods for the determination of the optimized fragmentation voltages are evaluated and a procedure is outlined to easily expand the collisional energy file used for automated peptide and protein sequencing.

Experimental

All measurements were performed on a solariX FTMS (7T & 12T). Samples were infused via ESI at a flow rate of 2 $\mu\text{L}/\text{min}$ in positive ion mode. Peptides were infused at a concentration of 200 – 500 fmol/ μL , proteins were infused at a concentration of 200 fmol/ μL to 1 pmol/ μL . For qCID experiments, individual protein or peptide ions were isolated in the front end quadrupole. qCID was performed in the adjacent RF-only hexapole by the application of different DC voltages, which allow variable amounts of energy to be

Determination of optimized fragmentation energy

	Precursor ion	All products	Real products
23V	2.55	5.89	1.62
27V	0.55	4.97	2.48
29V	0.16	4.61	2.35

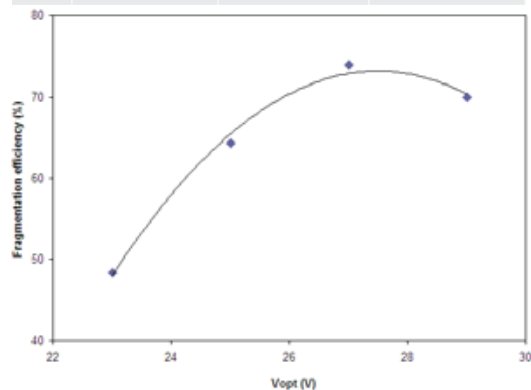


Figure 1: Determination of optimized fragmentation energy based upon known fragment ions. A maximum of 73% efficiency was found at 27V, which is more energy than if all products were used.

applied during the dissociation event. After qCID, product ions and any remaining precursor ion were transferred to the ICR cell for detection. 1 MW data sets were acquired for each spectrum and 100 spectra were averaged for each data point.

Results

Peptides generated from tryptic digestion and peptide standards were used for this study, allowing a broader peptide sample class to be examined. Peptide ions were isolated and dissociated via qCID. Product ion monoisotopic mass and abundance from the resulting MS/MS spectrum was determined using DataAnalysis 4.0. It is possible for fragmentation of product ions to occur (e.g. secondary fragmentation) during qCID. Therefore, only product ions (b- and y-type ions) that could be confidently assigned to the known peptide sequence were used to determine fragmentation efficiency. Efficiency calculations are performed by summing the intensity of the assigned product ions. The importance of using only known product ions is shown in Figure 1. If the sum of all product intensities were used, 23 V is found to be the optimum fragmentation voltage. If only the intensities of the identifiable product ions are used, then the optimum fragmentation voltage is determined to be 27.5 V.

The optimal fragmentation voltage is determined for a single charge state (CS) over a wide m/z range. For a single charge state, the optimal fragmentation voltage is plotted against the precursor ion m/z, as shown in Figure 2 for charge state 2+. A linear regression fit of the optimal fragmentation voltage versus precursor ion m/z for a single charge state

produces a fit that can be used to calculate the optimal fragmentation voltage for a precursor ion during an LC-MS/MS run. A similar graph is produced for other charge states. Due to the recent interest in Top-down protein analysis, this work was extended to LC-MS/MS of proteins. Individual protein charge states were isolated and dissociated in the same manner as for the peptide ions. Optimal fragmentation energies were determined and plotted against precursor ion m/z. Plotting the optimal fragmentation voltage for all charge states (CS 11-20) against precursor ion m/z is shown in Figure 3.

Linear dependence of fragmentation of voltage

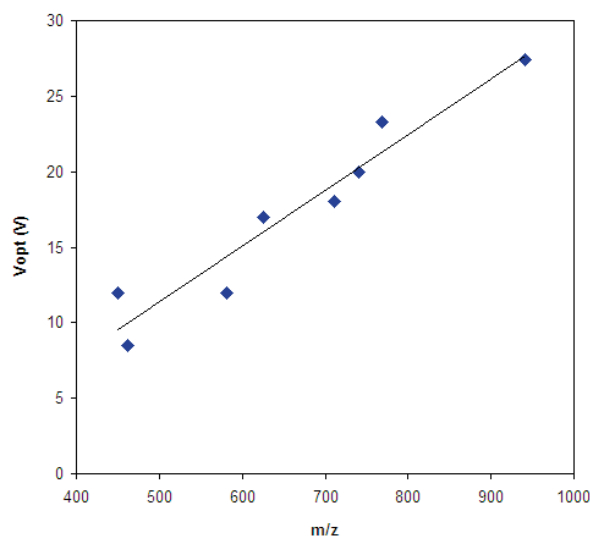


Figure 2: Linear dependence of fragmentation voltage versus m/z for all of the 2+ peptide ions.

Protein dependence

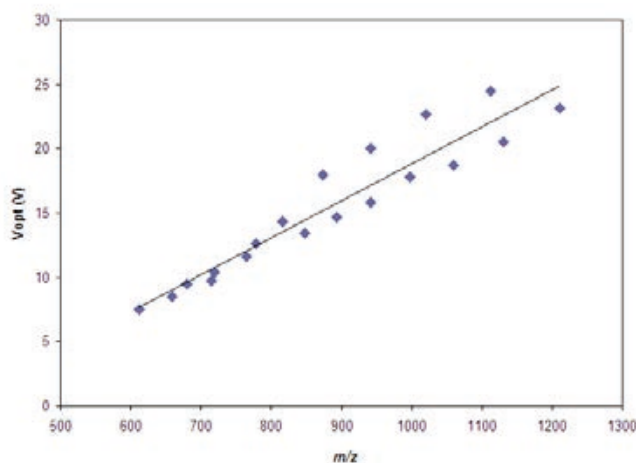
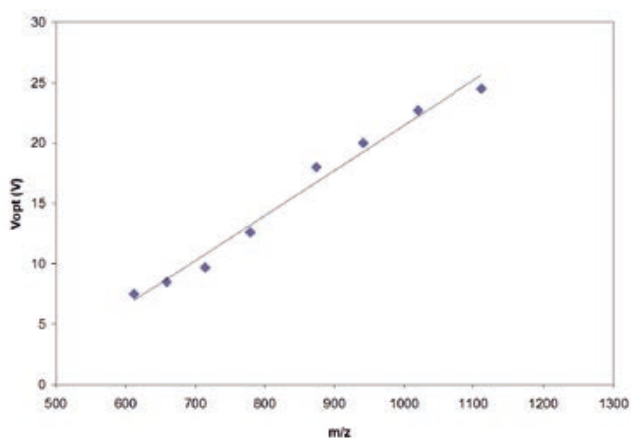
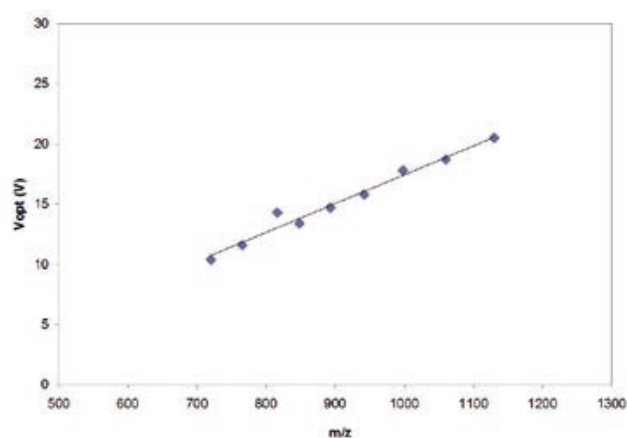


Figure 3: Protein dependence including all charge states (11-20). A reasonable correlation is found ($R^2=0.898$) with this wide range of charge.

Separated protein charge states



Charge States 11+ thru 14+



Charge States 15+ thru 20+

Figure 4: An improved fit is found when splitting up the charge states in to two groups. The left graph groups CS 11-14, with $R^2=0.983$ and the right shows CS 15-20, with $R^2=0.975$.

Interestingly, a good linear fit can be calculated for all protein charge states regardless of molecular weight or charge, as shown in Figure 3. This indicates that fragmentation conditions for proteins are not as critical as for peptides. However, the linear regression fit can be improved if the protein fragmentation data is divided into two distinct regions (CS 11-14 and 15-20), as shown in Figure 4. With the linear relationship determined for all of the various charge states, a simple collision energy file (.cef) is created. This file contains the optimized slope and intercept for each of the charge states studied and is editable via solariXcontrol. During auto MS/MS experiments, solariXcontrol determines an ions' m/z and charge state and then uses the file to set the optimised dissociation energy. Following the procedure outlined above, new energy correlation files can easily be created for other classes of analytes (glycans, carbohydrates, MALDI ions, etc...).

References

- [1] Haller, Mirza and Chait, Collision Induced Decomposition of Peptides. Choice of Collision Parameters, JASMS, 1996, 7, 677– 681.
- [2] Neta, Simon-Manson, Yang and Stein, Collisional Energy Dependence of Peptide Ion Fragmentation, JASMS, 2009, 20, 469-476.

Authors

Aaron Behr, Jeremy Wolff, Christopher Thompson
The Rivers School, Weston MA USA
Bruker Daltonics, Inc., Billerica MA USA

For research use only. Not for use in diagnostic procedures.

Conclusions

Using only assignable fragmentation products, qCID energies were optimized for peptides (CS 2&3) and proteins (CS 11-14 & 15-20) on solariX. The optimized cef file will lead to enhance sequence coverage of the parent species and thus better bioinformatic search results of LC-MS/MS data.

Keywords

FTMS
AutoMS
qCID

Instrumentation & Software

solariX
qCID



- **MALDI In-Source Decay for Top-Down Analysis of Proteins using Fourier Transform Mass Spectrometry**

MALDI – in-source decay (ISD) Fourier Transform Mass Spectrometry (FTMS) is used for fast and accurate assignment of protein termini. The sub ppm mass measurement accuracy of the Bruker FTMS system provides the specificity needed for the unambiguous assignment of the respective sequences. Results are analyzed using BioTools™, a comprehensive software package which manages database searches and sequence annotation.

Introduction

Fast and reliable assignment of N- as well as C-terminal protein sequences is an increasingly important task in protein biochemistry, for example in the quality control of

recombinant proteins, and within the field of proteomics. MALDI-ISD has been shown to efficiently produce c- and z+2-type ions [1],[2] for rapid analysis of both termini of a protein. Here we demonstrate the utility of MALDI-ISD-FTMS for protein identification.

The high resolving power and mass accuracy of FTMS enable unambiguous sequence assignment including the differentiation of Q and K.

Experimental

An important consideration for MALDI-ISD is the optimal choice for the matrix. Medium pressure MALDI, using DAN (1,5-Diaminonaphthalene) as matrix resulted in superior spectra compared to DHB. The protein analyzed was

Intact Protein MALDI-MS Analysis

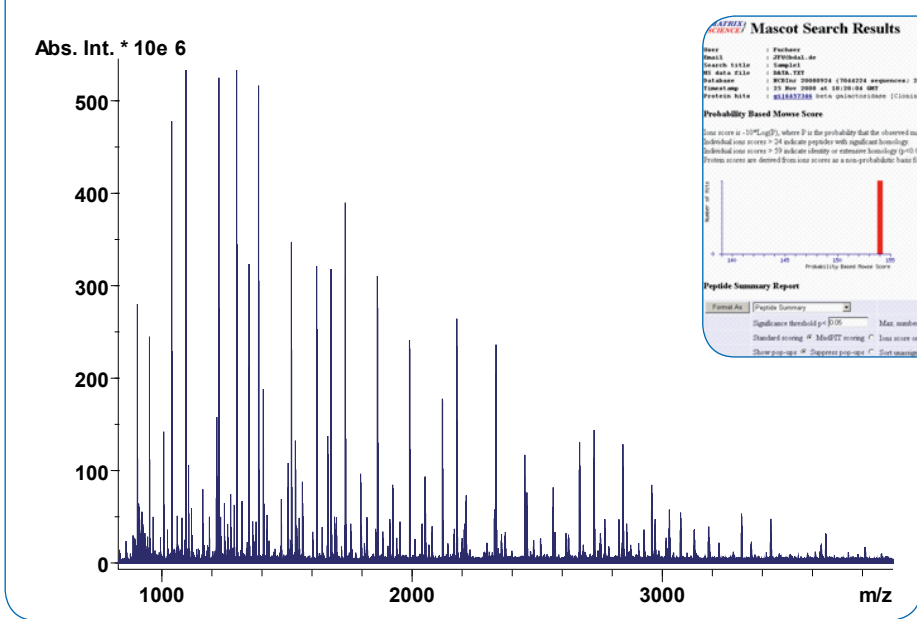


Fig. 1: MALDI-MS-FTMS spectrum of the intact protein of ABRF-ESRG 2009 (Sample 1)

N-terminal His-tag β -Gal Sequence

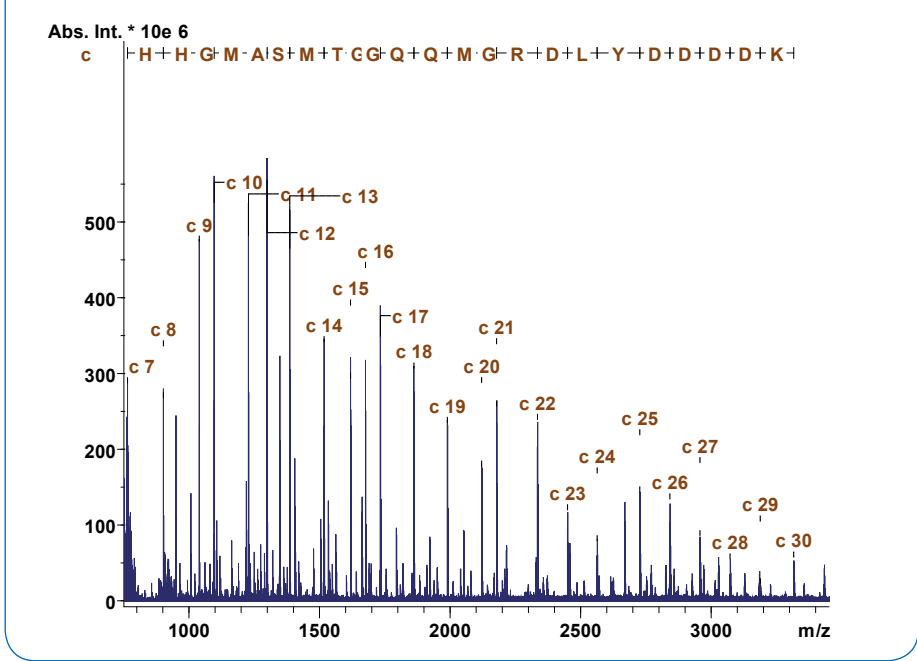


Fig. 2: Annotated MALDI-MS-FTMS spectrum of the intact protein of ABRF-ESRG 2009 (Sample 1).

“Sample 1” from the ABRF-ESRG 2009 study. The sample was dissolved in 20 μ L 0.1 % TFA. This solution was diluted 1/10 with acetonitrile/water = 3/7 (incl. 0.1 % TFA). Matrix solution: saturated DAN in 30 % acetonitrile 0.1 % TFA. 1 μ L of sample solution and 3 μ L of matrix solution were mixed and 1 μ L was applied on a stainless steel target. MALDI spectra were acquired using a apex ultra™ 70 (7.0 tesla) equipped with a DualSource including smartbeam laser optics and external ion accumulation. All data were

externally calibrated providing a mass accuracy of \sim 1ppm over the m/z range of interest, 500-4000 Da. Laser power was increased until fragments appeared in the spectrum, typically an increase of 20 % power relative to the standard setting was used. Data analysis was carried out using BioTools™ 3.2 (Bruker Daltonik GmbH) in combination with Mascot™ (Matrix Science).

Results

Unambiguous identification of y-ions

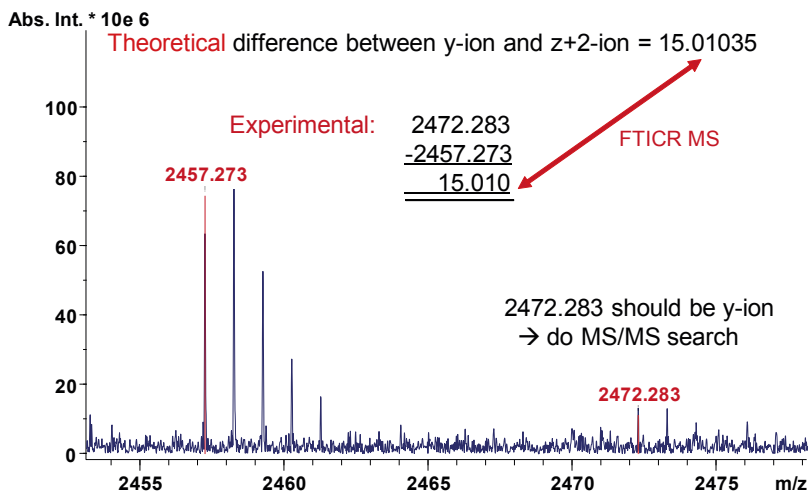


Fig. 3: Zoom of MALDI-MS/MS spectrum of the intact protein in ABRF-ESRG 2009 (Sample 1)

Annotation for c- and y-ions

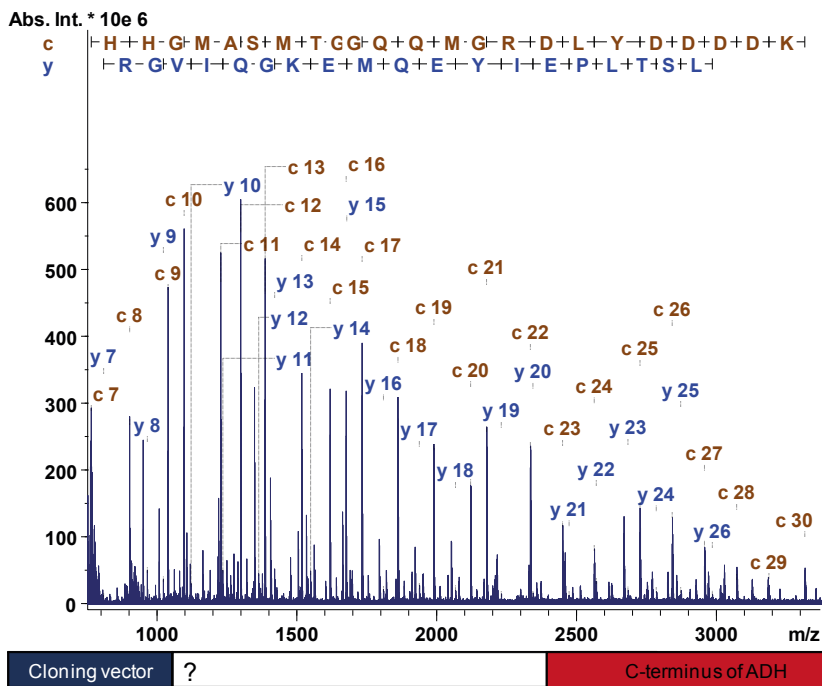


Fig. 4: Assignment of C- and N-terminal sequences after database search, alcoholdehydrogenase (EC 1.1.1.1) is identified.

MALDI-MS/MS predominantly yields c and z+2 ions, however, low-abundant y-ions are also observed. Searching the MS/MS derived spectrum against NCBI database reveals a His-tag β-Gal Sequence at the N-terminus (MS/MS search of the c-ion at 3313.388, Figure 1 & 2).

To further evaluate the protein sequence, a detailed analysis of the data is performed. The accurate mass measurement leads to the unambiguous identification of y-ions which are subsequently used for MS/MS searches (Figure 3 & 4).

To demonstrate the advantage of the mass accuracy of a MALDI FT-MS measurement, figure 5 and 6 show the annotation of the spectrum with two sequences: a) The correct, database derived sequence and b) an edited version of this sequence with two modifications: In position 337 Q has been changed to K and in position 332 K has been exchanged for a Q, i.e. the amino acids at position 332 and 337 have been swapped.

Uniquely, due to the low ppm mass tolerances used in

Mass accuracy advantages of the FT

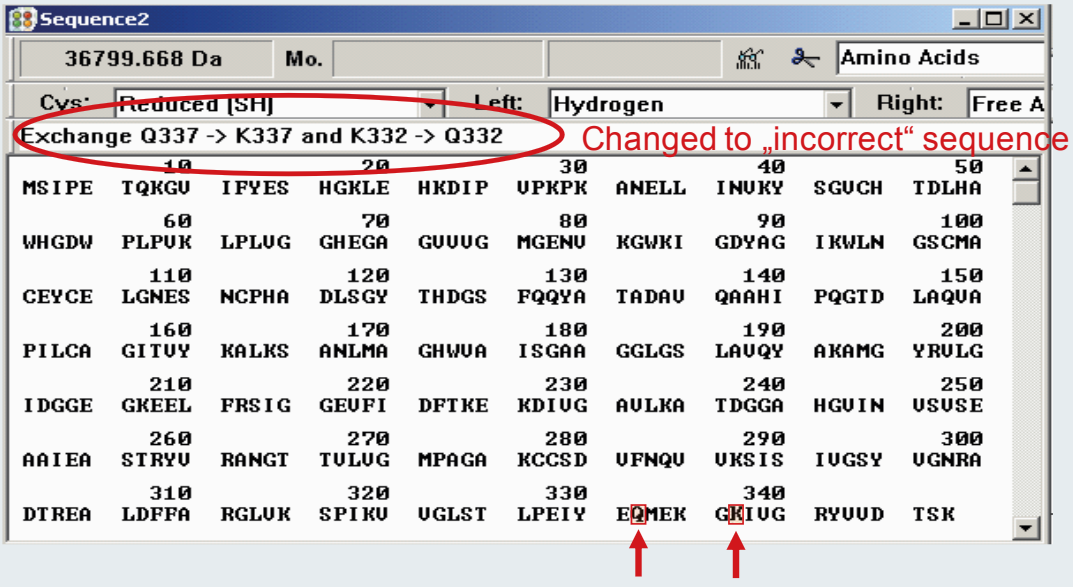


Fig. 5: Edited sequence with shifts for Q and K

Correct and modified sequence annotations

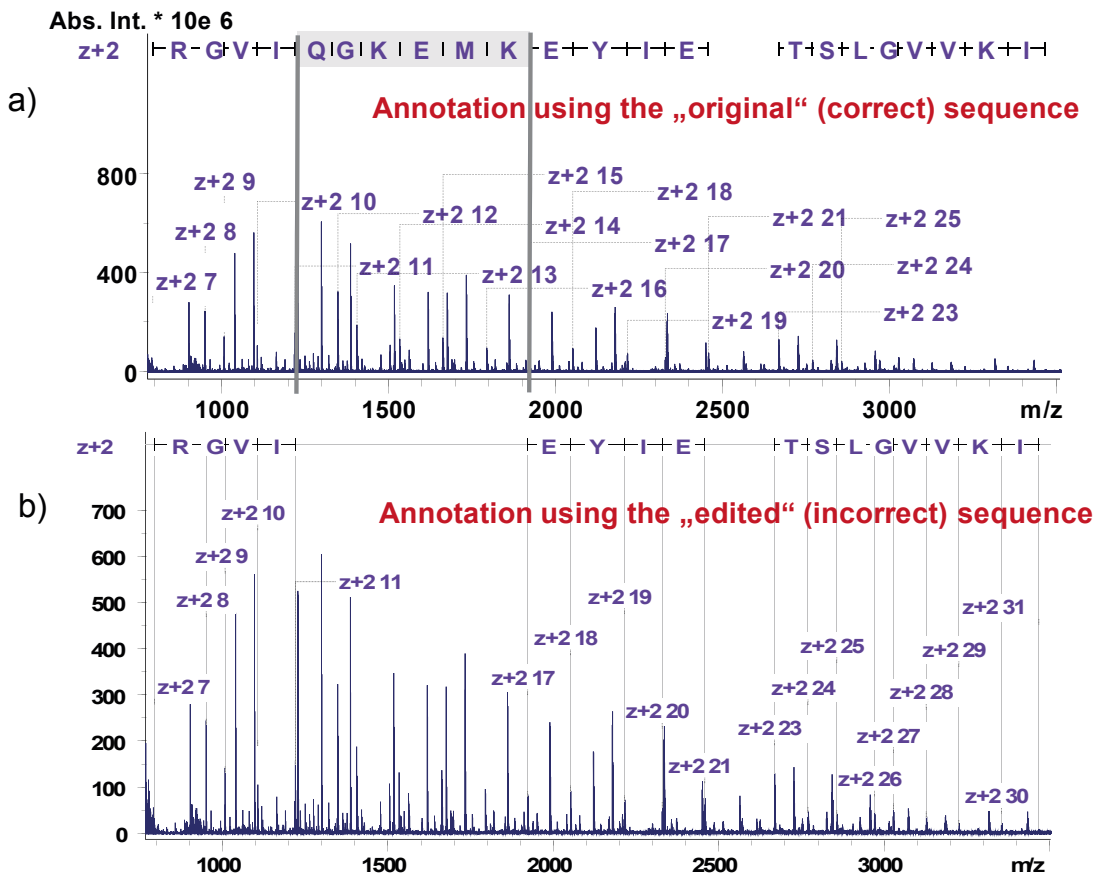


Fig. 6: Annotation using the correct (a) and the edited (b) sequence

RMS error below 1 ppm for the correct sequence

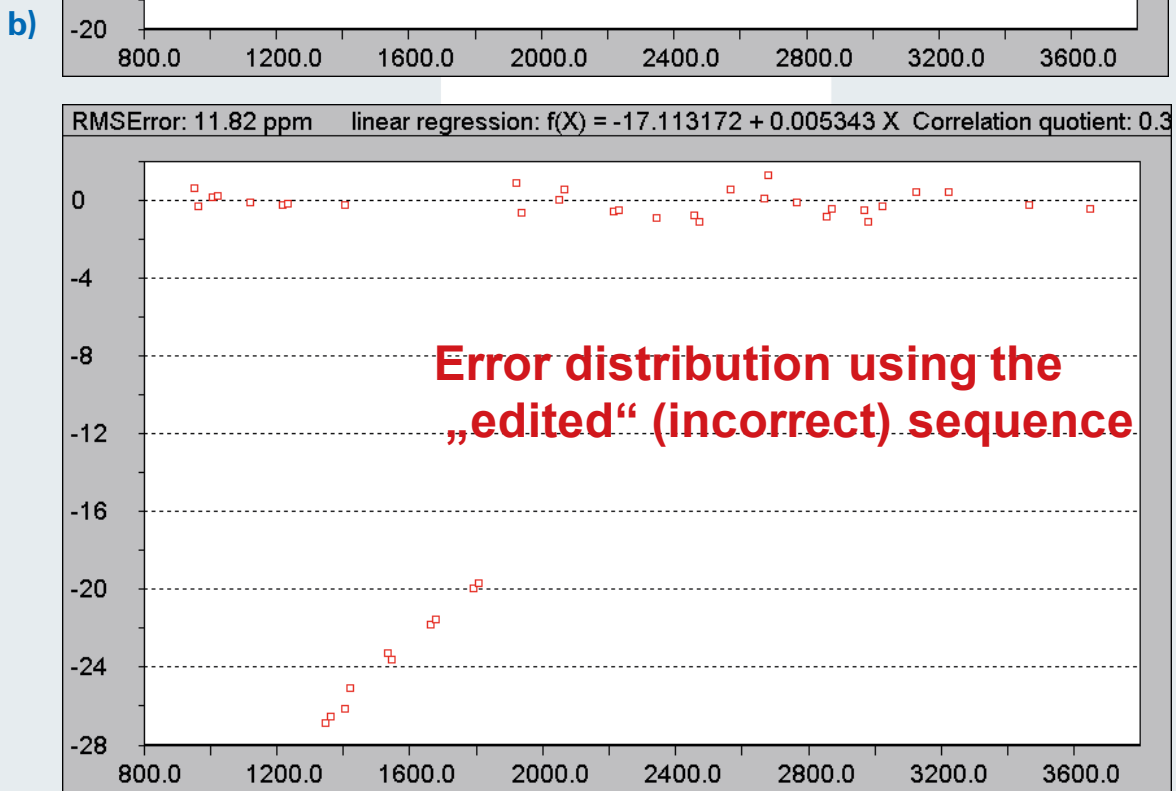
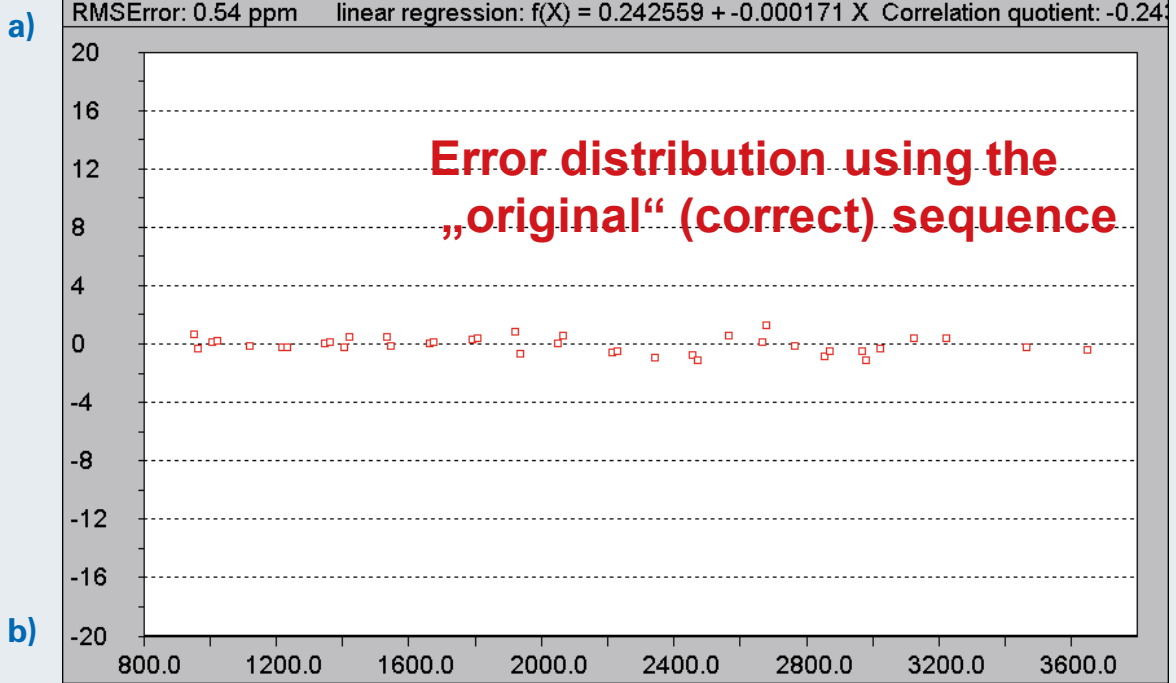


Fig. 7: Error distributions for the correct (a) and the edited (b) sequence

this approach, even Q. vs. K are confidently assigned from undigested proteins (Figure 6): The spectrum on top shows the (correct) annotation for the database derived sequence, the annotation in the bottom spectrum is achieved by exchanges of Q337 vs. K337 and K332 vs. Q332.

Figure 7 displays the error distributions for the two sequences. The correct sequence (a) shows a RMS error below 1 ppm whereas the wrong sequence (b) has a step in the error plot which points to the wrong assignment within this sequence.

Conclusion

MALDI-ISD using FT-MS is a new top-down sequencing (TDS) technique that is complementary to classical ESI-ECD, providing rapid sequencing of protein termini with high confidence. Furthermore, this technique enables the terminal sequencing of proteins as large as 40 kDa and higher. The preparation of the MALDI targets is a straightforward well established procedure. No further cleaning steps such as laborious desalting is needed thus making the entire TDS analysis very quick.

The high mass accuracy of FT-ICR MS allows for a rapid and unambiguous identification of proteins and the differentiation of amino acids that are closely spaced in mass (e.g. K and Q).

References

- [1] J. Hardouin, Protein sequence information by matrix-assisted Laser desorption/ionization in-source decay mass spectrometry, *Mass Spectrometry Reviews*, 2007, 26, 672–682.
- [2] D. Suckau and A. Resemann, T3-Sequencing: Targeted Characterization of the N- and C-Termini of Undigested Proteins by Mass Spectrometry, *Anal. Chem.* 2003, 75, 5817-5824.

Authors

Jens Fuchser, Matthias Witt, Anja Resemann
Bruker Daltonik GmbH, Fahrenheitstr. 4, D-28359 Bremen, Germany

For research use only. Not for use in diagnostic procedures.

Keywords
terminal sequencing
Top-Down
QC
MALDI-TDS

Instrumentation & Software
apex ultra

Bruker Native MS References

- Wu, Zhijie; Tiambeng, Timothy N.; Cai, Wenxuan; Chen, Bifan; Lin, Ziqing; Gregorich, Zachery R.; Ge, Ying (2018) *Impact of Phosphorylation on the Mass Spectrometry Quantification of Intact Phosphoproteins*, Analytical chemistry, 10.1021/acs.analchem.7b05246, **90** (8), 4935–4939
- Wongkongkathep, Piriya; Han, Jong Yoon; Choi, Tae Su; Yin, Sheng; Kim, Hugh I.; Loo, Joseph A. (2018) *Native Top-Down Mass Spectrometry and Ion Mobility MS for Characterizing the Cobalt and Manganese Metal Binding of α -Synuclein Protein*, Journal of the American Society for Mass Spectrometry, 10.1007/s13361-018-2002-2, **29** (9), 1870–1880
- Vu, H., Pedro, L., Mak, T., McCormick, B., Rowley, J., Liu, M., Quinn, R. J. (2018) *Fragment-Based Screening of a Natural Product Library against 62 Potential Malaria Drug Targets Employing Native Mass Spectrometry*, ACS Infectious Diseases, 10.1021/acscinfed.7b00197, **4** (4), 431–444
- Lin, Ziqing; Guo, Fang; Gregorich, Zachery R.; Sun, Ruixiang; Zhang, Han; Hu, Yang; Shanmuganayagam, Dhanansayan; Ge, Ying (2018) *Comprehensive Characterization of Swine Cardiac Troponin T Proteoforms by Top-Down Mass Spectrometry*, Journal of the American Society for Mass Spectrometry, 10.1007/s13361-018-1925-y, **29** (6), 1284–1294
- Li, H., Nguyen, H. H., Ogorzalek Loo, R. R., Campuzano, I. D. G., & Loo, J. A. (2018) *An Integrated Native Mass Spectrometry and Top-Down Proteomics Method that Connects Sequence to Structure and Function of Macromolecular Complexes*, Nature Chemistry, 10.1038/nchem.2908, **10** (2), 139–148
- Chen, Bifan; Lin, Ziqing; Alpert, Andrew J.; Fu, Cexiong; Zhang, Qunying; Pritts, Wayne A.; Ge, Ying (2018) *Online Hydrophobic Interaction Chromatography-Mass Spectrometry for the Analysis of Intact Monoclonal Antibodies*, Analytical chemistry, 10.1021/acs.analchem.8b01865, **90** (12), 7135–7138
- Campuzano, I.D., Netirajanakul, C., Nshanian, M., Lippens, J.L., Kilgour, D.P., Orden, S.L., & Loo, J.A. (2018) *Native-MS Analysis of Monoclonal Antibody Conjugates by Fourier Transform Ion Cyclotron Resonance Mass Spectrometry*, Analytical Chemistry, 10.1021/acs.analchem.7b03021, **90** (1), 745–751
- Zhang, Jiang; Loo, Rachel R Ogorzalek; Loo, Joseph A. (2017) *Structural Characterization of a Thrombin-Aptamer Complex by High Resolution Native Top-Down Mass Spectrometry*, Journal of the American Society for Mass Spectrometry, 10.1007/s13361-017-1751-7, **28** (9), 1815–1822
- Teruya, Kanae; Rankin, Gregory M.; Chrysanthopoulos, Panagiotis K.; Tonissen, Kathryn F.; Poulsen, Sally-Ann (2017) *Characterisation of Photoaffinity-Based Chemical Probes by Fluorescence Imaging and Native-State Mass Spectrometry*, Chembiochem: a European journal of chemical biology, 10.1002/cbic.201600598 **18** (8), 739–754
- Li, HuiLin; Sheng, Yuewei; McGee, William; Cammarata, Michael; Holden, Dustin; Loo, Joseph A. (2017) *Structural Characterization of Native Proteins and Protein Complexes by Electron Ionization Dissociation-Mass Spectrometry*, Analytical chemistry, 10.1021/acs.analchem.6b02377, **89** (5), 2731–2738
- Gahoual, Rabah; Heidenreich, Anna-Katharina; Somsen, Govert W.; Bulau, Patrick; Reusch, Dietmar; Wuhrer, Manfred; Habegger, Markus (2017) *Detailed Characterization of Monoclonal Antibody Receptor Interaction Using Affinity Liquid Chromatography Hyphenated to Native Mass Spectrometry*, Analytical chemistry, 10.1021/acs.analchem.7b00211, **89** (10), 5404–5412
- Chrysanthopoulos, Panagiotis K.; Mujumdar, Prashant; Woods, Lucy A.; Dolezal, Olan; Ren, Bin; Peat, Thomas S.; Poulsen, Sally-Ann (2017) *Identification of a New Zinc Binding Chemotype by Fragment Screening*, Journal of medicinal chemistry, 10.1021/acs.jmedchem.7b00606, **60** (17), 7333–7349
- Cai, Wenxuan; Tucholski, Trisha; Chen, Bifan; Alpert, Andrew J.; McIlwain, Sean; Kohmoto, Takushi; Jin, Song; Ge, Ying (2017) *Top-Down Proteomics of Large Proteins up to 223 kDa Enabled by Serial Size Exclusion Chromatography Strategy*, Analytical chemistry, 10.1021/acs.analchem.7b00380, **89** (10), 5467–5475
- Zhang, Ying; Cui, Weidong; Weckler, Aaron T.; Zhang, Hao; Molina, Patricia; Deperalta, Galahad; Gross, Michael L. (2016) *Native MS and ECD Characterization of a Fab-Antigen Complex May Facilitate Crystallization for X-ray Diffraction*, Journal of the American Society for Mass Spectrometry, 10.1007/s13361-016-1398-9, **27** (7), 1139–1142
- Woods, Lucy A.; Dolezal, Olan; Ren, Bin; Ryan, John H.; Peat, Thomas S.; Poulsen, Sally-Ann (2016) *Native State Mass Spectrometry, Surface Plasmon Resonance, and X-ray Crystallography Correlate Strongly as a Fragment Screening Combination*, Journal of medicinal chemistry, 10.1021/acs.jmedchem.5b01940, **59** 5, 2192–2204
- Chen, Bifan; Peng, Ying; Valeja, Santosh G.; Xiu, Lichen; Alpert, Andrew J.; Ge, Ying (2016) *Online Hydrophobic Interaction Chromatography-Mass Spectrometry for Top-Down Proteomics*, Analytical chemistry, 10.1021/acs.analchem.5b04285, **88** (3), 1885–1891
- Zhang, Jiang; Reza Malmirchegini, G.; Clubb, Robert T Clubb T; Loo, Joseph A. (2015) *Native top-down mass spectrometry for the structural characterization of human hemoglobin*, European journal of mass spectrometry (Chichester, England), 10.1255/ejms.1340, **21** (3), 221–231
- Cui, Weidong; Zhang, Hao; Blankenship, Robert E.; Gross, Michael L. (2015) *Electron-capture dissociation and ion mobility mass spectrometry for characterization of the hemoglobin protein assembly*, Protein science : a publication of the Protein Society, 10.1002/pro.2712, **24** (8), 1325–1332
- Li, HuiLin; Wongkongkathep, Piriya; Van Orden, Steve L.; Ogorzalek Loo, Rachel R; Loo, Joseph A. (2014) *Revealing ligand binding sites and quantifying subunit variants of noncovalent protein complexes in a single native top-down FTICR MS experiment*, Journal of the American Society for Mass Spectrometry, 10.1007/s13361-014-0928-6, **25** (12), 2060–2068
- Li, HuiLin; Wolff, Jeremy J.; Van Orden, Steve L.; Loo, Joseph A. (2014) *Native top-down electrospray ionization-mass spectrometry of 158 kDa protein complex by high-resolution Fourier transform ion cyclotron resonance mass spectrometry*, Analytical chemistry, 10.1021/ac4033214, **86** (1), 317–320
- Behnen, Henning N.; Ruthenbeck, Alexandra; Schulz, Jan-Mirco; Meyer, Bernd (2014) *Glycan analysis of Prostate Specific Antigen (PSA) directly from the intact glycoprotein by HR-ESI/TOF-MS*, Journal of proteome research, 10.1021/pr400999y, **13** (2), 997–1001
- Zhang, Hao; Cui, Weidong; Gross, Michael L. (2013) *Native electrospray ionization and electron-capture dissociation for comparison of protein structure in solution and the gas phase*, International journal of mass spectrometry, 10.1016/j.ijms.2013.06.019, 354–355
- Marty, Michael T.; Zhang, Hao; Cui, Weidong; Blankenship, Robert E.; Gross, Michael L.; Sligar, Stephen G. (2012) *Native mass spectrometry characterization of intact nanodisc lipoprotein complexes*, Analytical chemistry, 10.1021/ac302663f, **84** (21), 8957–8960
- Zhang, Hao; Cui, Weidong; Wen, Jianzhong; Blankenship, Robert E.; Gross, Michael L. (2011) *Native electrospray and electron-capture dissociation FTICR mass spectrometry for top-down studies of protein assemblies*, Analytical chemistry, 10.1021/ac200695d, **83** (14), 5598–5606
- Yin, Sheng; Loo, Joseph A. (2011) *Top-Down Mass Spectrometry of Supercharged Native Protein-Ligand Complexes*, International journal of mass spectrometry, 10.1016/j.ijms.2010.06.032, **300** (2-3), 118–122
- Drinkwater, Nyssa; Vu, Hoan; Lovell, Kimberly M.; Criscione, Kevin R.; Collins, Brett M.; Prisinzano, Thomas E.; Poulsen, Sally-Ann; McLeish, Michael J.; Grunewald, Gary L.; Martin, Jennifer L. (2010) *Fragment-based screening by X-ray crystallography, MS and isothermal titration calorimetry to identify PNMT (phenylethanolamine N-methyltransferase) inhibitors*, The Biochemical journal, 10.1042/BJ20100651, **431** (1), 51–61
- Poulsen, Sally-Ann (2006) *Direct screening of a dynamic combinatorial library using mass spectrometry*, Journal of the American Society for Mass Spectrometry, 10.1016/j.jasms.2006.03.017, **17** (8), 1074–1080

• **Petroleomics and Complex Mixtures**

Application Notes

- Characterization of Petroleum Samples via Thermal Analysis Coupled to APCI FTMS
- Reproducibility of Crude Oil Characterization by FlowInjection APPI-FT-ICR MS
- Laser/Desorption Ionization FT-ICR MS as a Tool for Statistical Analysis of Crude Oils
- Analysis of Peat Bog after Solid Phase Extraction by FTMS
- solarIX XR: Analysis of Complex Mixtures
- Analysis of Sulfur-Rich Crude Oil and Bitumen by FTMS
- Analysis of Gas Oil by GC/APCI FTMS

User Testimonials: Petroleomics



"With our Bruker MRMS in Rouen the analysis of highly Complex Mixtures has been pushed further than ever and could also be made on a routine basis in the framework of the C2MC joint lab".



*C2MC – Complex Matrices Molecular Characterization, Joint Laboratory
Carlos Afonso, University of Rouen
Pierre Giusti, TOTAL*



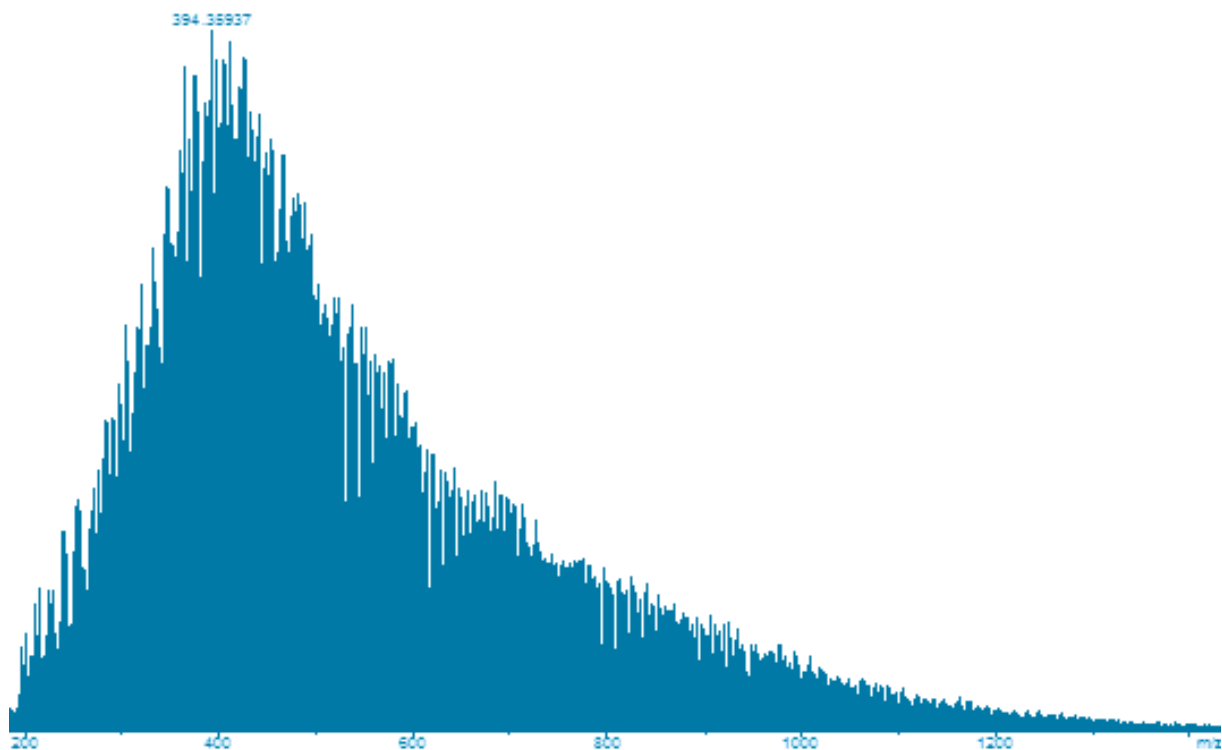
"Most of our research at UEF heavily relies on the use of Bruker MRMS technology to dig deep into chemistry of bio-oils, natural extracts and highly complex environmental samples"

*Janne Jänis
Professor of Organic Chemistry and Mass Spectrometry
University of Eastern Finland*

Benefits for Petroleomics

When knowing every molecule matters, scimaX empowers 7T systems with high field performance for any complex mixture.

scimaX powered by 2xR technology is easily matching or surpassing the resolving power of many conventional high field MRMS systems. Now such high field systems are no longer mandatory for crude oils, bio-fuels, DOM/NOM or any complex mixture





• Characterization of petroleum samples via thermal analysis coupled to APCI FTMS

Abstract

Thermal analysis, by means of a thermo balance (TG), was coupled to an atmospheric pressure chemical ionization source especially designed for gas phase analysis (Bruker GC-APCI II). Ultra-high resolution mass spectrometric analyses were done by a FT-ICR MS

(apex II Qe). Besides a fatty acid standard mixture (FAME) different petroleum samples were analyzed, such as a diesel fuel, a heavy fuel oil (HFO) and a crude oil. The petroleum samples revealed a high complex evolved gas mixture. Coupling of thermal analysis enables the analysis of heavy petroleum fractions, which are difficult to measure by gas

chromatography. After thermo desorption at a certain temperature of roughly 300 - 350 °C, pyrolysis start to occur and the sample decompose. Decomposition products can be used for structural elucidation. Furthermore, a simulated distillation pattern can be recorded. Ultra-high resolution mass spectrometric detection enables the calculation

Keywords:
thermal analysis,
atmospheric pressure
chemical ionisation
(APCI), ultra-high
resolution mass
spectrometry,
Petroleomics,
complex mixtures,
small molecules

of temperature profiles of individual molecular species as well as of chemical classes or double bond equivalent (DBE) groups. Key advantages of the thermal analysis are the minimal sample amount needed (less than 2 mg), no sample preparation steps as well as the opportunity to analyze high viscous and solid samples directly. Compared to the direct inlet probe (DIP, from Bruker available for the direct infusion APCI source) higher temperatures can be accessed up to 1000 °C (600 °C with aluminum crucible).

Introduction

The detailed chemical characterization of petroleum fractions is still an analytical challenge. Besides spray based sample delivery and ionization techniques, such as direct infusion ESI, APPI and APCI, evolved gas analysis (EGA) is a complementary approach. In thermal analysis a specific phys-

ical property, such as heat flux or mass, is measured, while a defined temperature program is applied. The sample heating will lead to vaporization and decomposition processes. The released evolved gas mixture can be analyzed, e.g. by mass spectrometry, which offers an analytical tool to identify the molecular composition. With thermal analysis, employing a thermo balance, high temperatures are accessible, e.g. the pyrolysis regime above 300-350 °C. At lower temperatures in the desorption phase the vaporizable compounds of the mixture are evaporated and can be analyzed as intact molecules. In the pyrolysis phase complex molecular structures decompose and fragment characteristically providing access to structural information. The ultra-high resolving power, mass accuracy and high dynamic range of Fourier Transform Mass Spectrometry (FT-ICR MS) allow a sensitive detection and the assignment of elemental

composition of individual species in a complex mixture. In this respect atmospheric pressure chemical ionization (APCI), which is highly sensitive towards polar species, allows the detection of certain compound classes, which cannot be ionized by ESI, such as polycyclic aromatic hydrocarbons (PAH) and their sulphur and nitrogen containing derivatives. In this study, we show the capabilities of thermal analysis coupled to FT-ICR MS equipped with a gas phase APCI source for the analysis of petroleum samples.

Method and Material

A thermo balance (TG 209, Netzsch Gerätebau GmbH, Selb, Germany) was coupled to the GC-APCI II source (Bruker) via a heated transfer line (Figure 1) as described elsewhere (1). Mass spectra were acquired using an Apex Qe 7 T FT-ICR mass spectrometer (Bruker) in positive ion mode. A

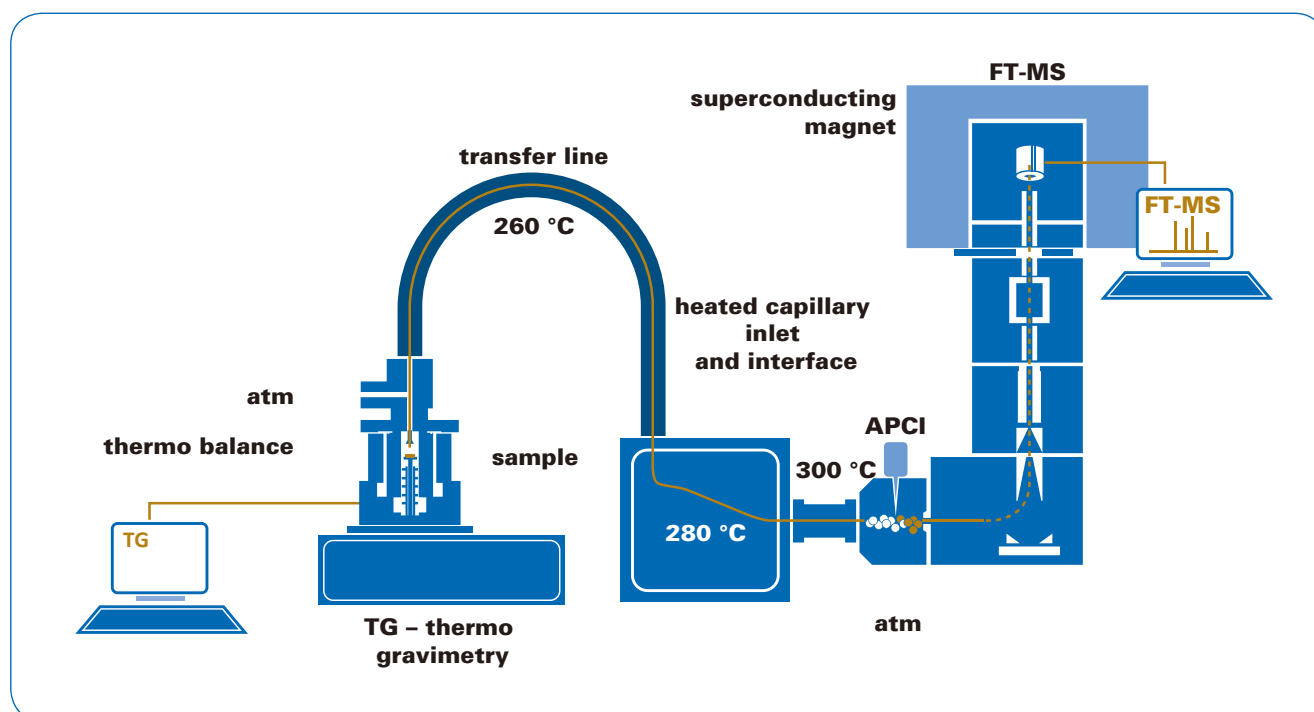


Fig. 1: Schematic representation of a TG coupled to a 7 T apex II ultra FT-MS system using a GC-APCI II source.

temperature program from 20 to 600 °C with a 10 K/min gradient was used (~ 1 h). The samples were directly placed in an aluminum crucible and the mass loss curve was recorded from the TG. The oil samples were diluted in dichloromethane for easier handling. Roughly, 1 mg petroleomic sample material was used. Spectra were acquired from m/z 100-1000 with 2 MW data points and five spectra averaging resulting in an acquisition frequency of approximately 0.4 Hz and a resolving power of about 260,000 at m/z 200. A fatty acid methyl ester standard mixture (FAME Mix, Sigma-Aldrich), a diesel fuel (DIN EN 590), a heavy fuel oil (HFO) and a crude oil (Greek crude) were investigated. Data were pre-processed (peak picking and m/z calibration) and exported using Data Analysis software (DA 4.0, Bruker) and processed utilizing self-written Matlab (MATLAB R2016a) scripts. Elemental compositions were assigned within a 2 ppm error range and the following restrictions: $C_{6-100}H_{6-200}N_{0-2}O_{0-10}S_{0-2}$. A comparable data processing approach was utilized in literature for GC-APCI data (2,3).

Results and Discussion

Evolved gas analysis, by means of thermal analysis coupled to mass spectrometry, is a powerful tool for insights into complex samples. The general application of TG-FT-MS utilizing a GC-APCI II source for ionization in the framework of petroleum analysis is shown. The unbeaten resolving power and mass accuracy enables a characterization at the molecular level. Figure 2, the survey view (a plot of temperature versus m/z using a color coding for the intensity) represent the complexity of the

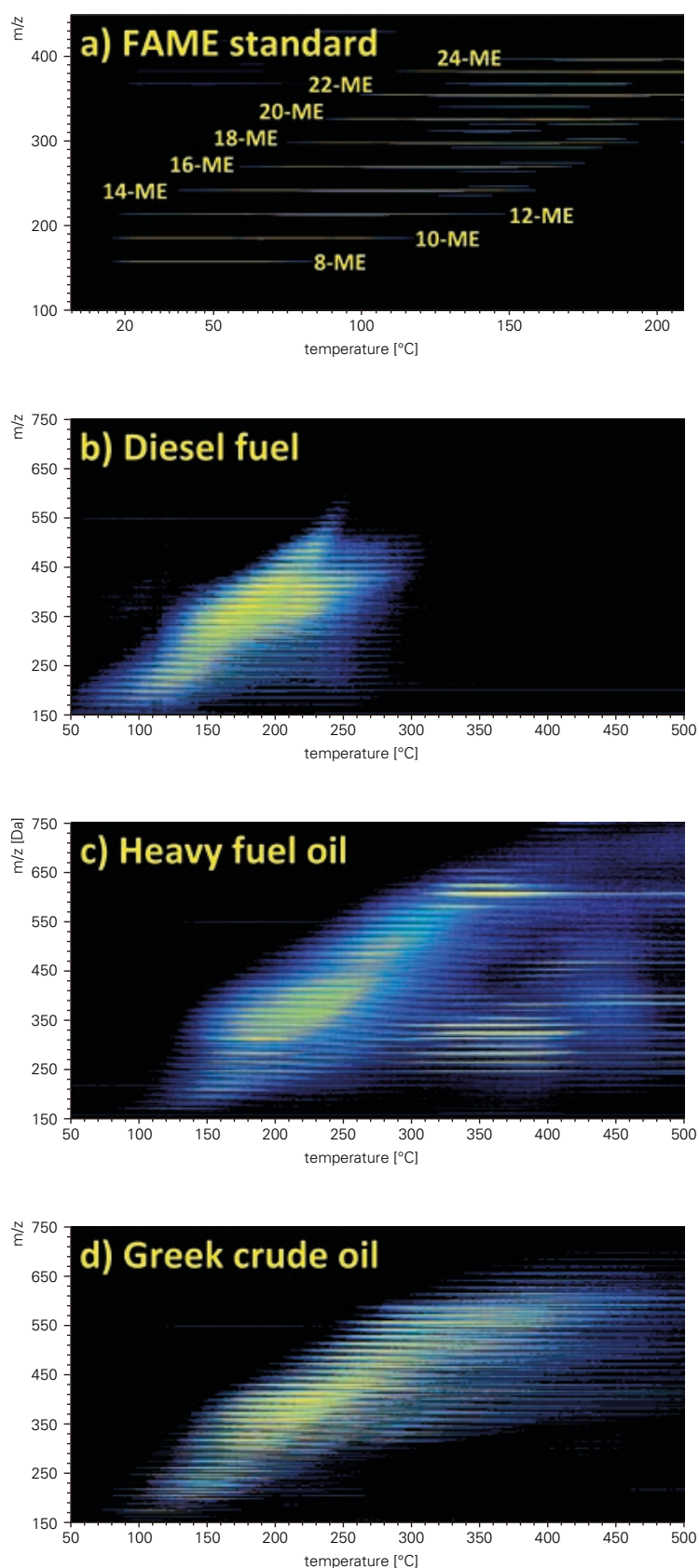


Fig. 2: Survey view of a) FAME standard, b) diesel fuel, c) heavy fuel oil and d) Greek crude oil measured by TG-APCI FT-MS. The high complexity and mass range of the petroleum samples is shown.

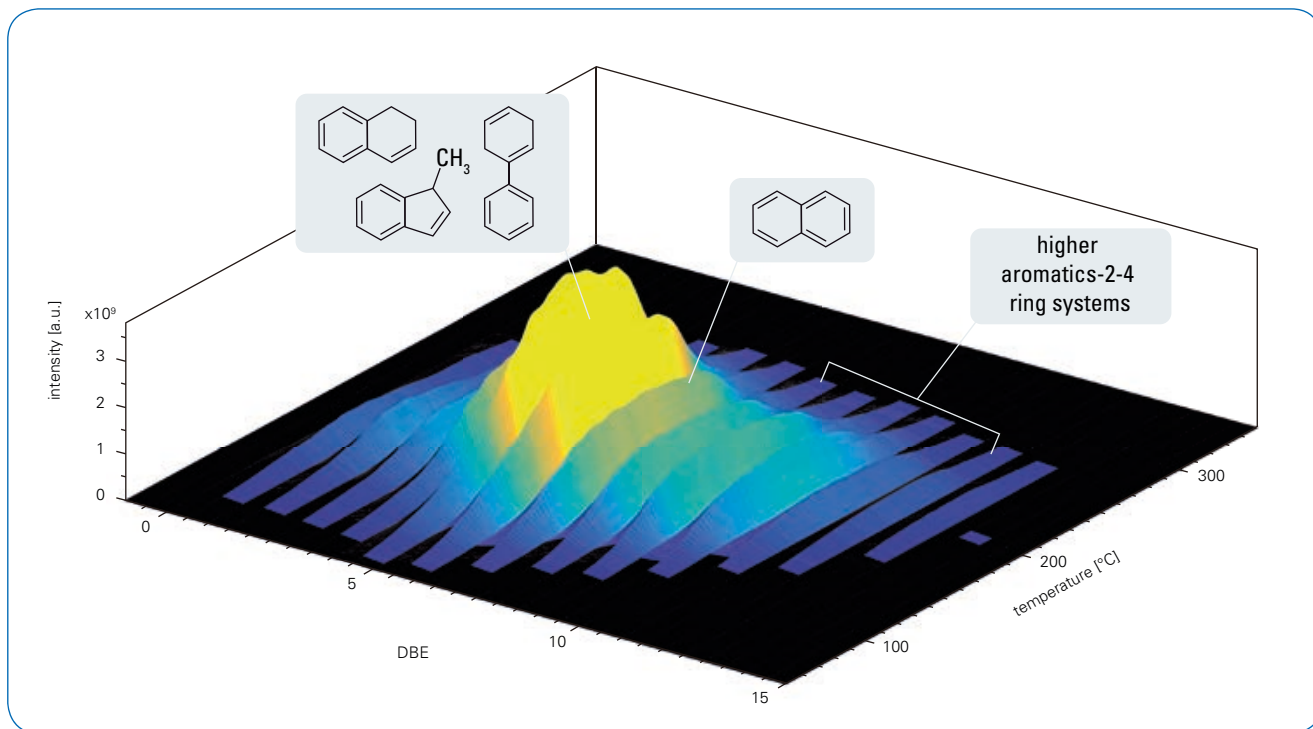


Fig. 3: Three dimensional visualization of the double bond distribution evolved over temperature for a diesel TG-FT-MS measurement. Intensity is color coded and a selection of potential structures is given.

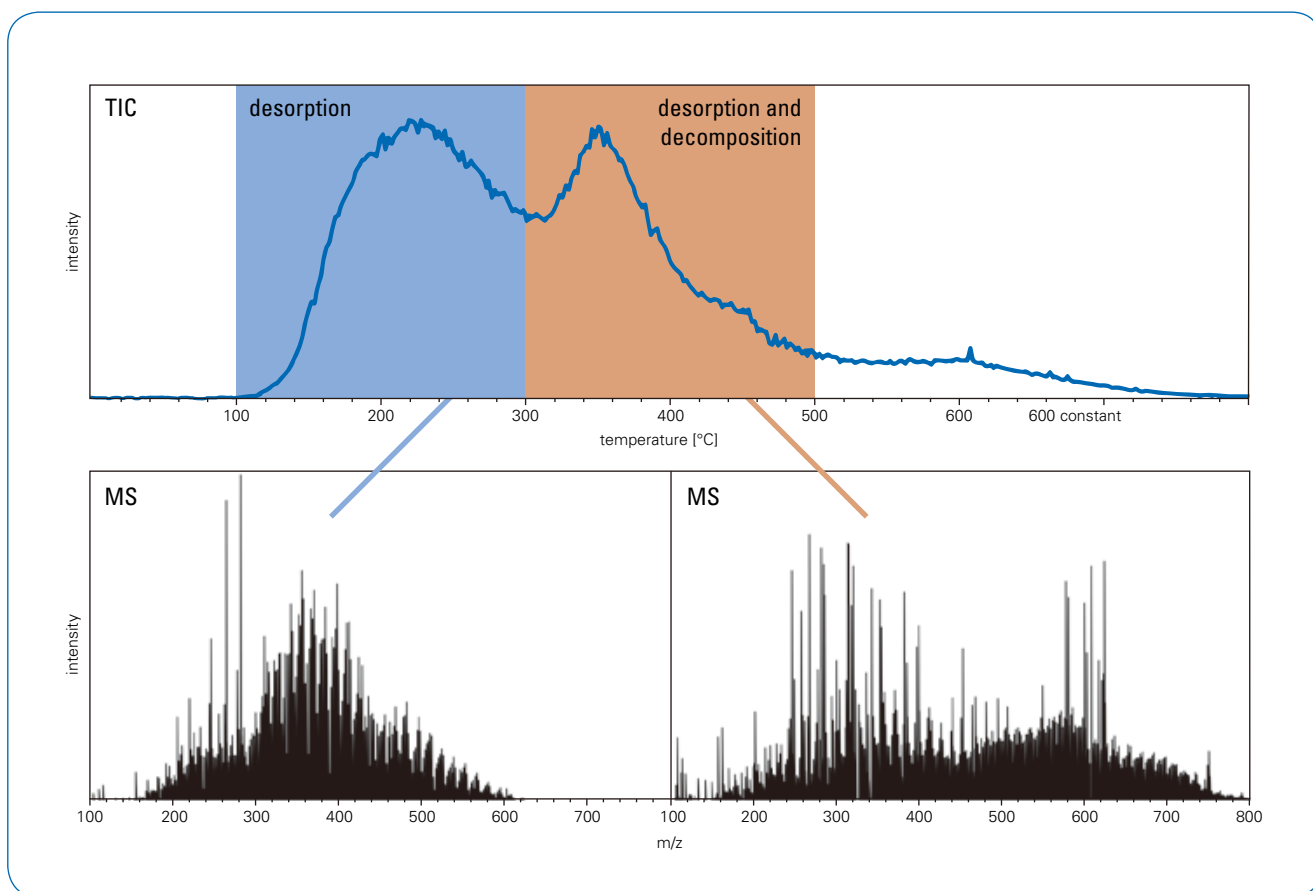


Fig. 4: Total ion count chromatogram with marked area of the desorption and desorption/pyrolysis phase for the heavy fuel oil TG-FT-MS measurement. Averaged mass spectra of the marked areas are given below.

investigated oil samples.

Several hundred features (elemental compositions with an individual temperature evolution profile) were detected for the diesel fuel and thousands for the HFO and crude oil, respectively. The evolved mixture spans a mass range from the lower acquired m/z boundary at 100 (for the diesel fuel) and up to 750 m/z for the crude oil and the HFO. The high resolution mass spectrometer allows an assignment of elemental compositions to the evolved mixture.

The diesel fuel reveals a high abundance of CH-, CHO₁- and CHO₂-class species, whereas the heavy fuel oil exhibit mainly CH and CHS-class species. The double bond equivalent (DBE) can be used for molecular interpretation of the results. In figure 3 a temperature resolved visualization of the DBE pattern evolved from the diesel fuel sample is shown.

As common thermal behavior of high boiling fuels with some non volatile residues thermal analysis revealed a desorption and pyrolysis phase (Figure 4). The pyrolysis phase is

characterized by a shift in molecular pattern towards smaller m/z, which is caused by decomposition products from larger molecular structures. In Figure 4 the shift in pattern can be seen in the averaged mass spectra for the 300 - 500 °C temperature range. A high proportion of CHO_x-class compounds is detected during pyrolysis. The decomposition pattern is overlaid with the desorption of heavier species, extending the upper m/z. Due to the complex mixture, both phases are not completely separated.

Conclusion

Thermal analysis coupled to ultra-high resolution mass spectrometry enables the detailed temperature resolved chemical characterization of the evolved gas mixtures on the molecular level. It can be used as complementary technique to direct infusion experiments or GC-APCI. Additional information is gained due to higher temperatures feasible with the thermo balance, e.g. pyrolysis fragments can give structural information about larger molecular entities. APCI is a sensitive technique for detecting the polar and medium-polar species released during the heating process. We have shown that TG-APCI FT-MS can be applied for various petroleum samples from different distillation ranges. Ultra-high resolution was needed to differentiate between the chemical species in the complex evolved mixture.



Learn More

You are looking for further Information? Check out the Link or scan the QR Code.

www.bruker.com/petroleomics



References

- [1] Ruger, C. P.; Miersch, T.; Schwemer, T.; Sklorz, M.; Zimmermann, R. Hyphenation of Thermal Analysis to Ultrahigh-Resolution Mass Spectrometry (Fourier Transform Ion Cyclotron Resonance Mass Spectrometry) Using Atmospheric Pressure Chemical Ionization For Studying Composition and Thermal Degradation of Complex Materials. *Analytical chemistry* 2015, 87 (13), 6493–6499. DOI: 10.1021/acs.analchem.5b00785.
- [2] Schwemer, T.; Ruger, C. P.; Sklorz, M.; Zimmermann, R. Gas Chromatography Coupled to Atmospheric Pressure Chemical Ionization FT-ICR Mass Spectrometry for Improvement of Data Reliability. *Analytical chemistry* 2015. DOI: 10.1021/acs.analchem.5b02114.
- [3] Smit, E.; Ruger, C. P.; Sklorz, M.; Goede, S. de; Zimmermann, R.; Rohwer, E. R. Investigating the trace polar species present in diesel using high resolution mass spectrometry and selective ionization techniques. *Energy Fuels* 2015, 150827122347008. DOI: 10.1021/acs.energyfuels.5b00831.

For research use only. Not for use in diagnostic procedures.



- # Reproducibility of Crude Oil Characterization by Flow Injection APPI-FT-ICR Mass Spectrometry

Introduction

The oil industry requires detailed information on the composition of crude oil for refinery and catalytic processes. The term used to describe the analysis of this extremely complex mixture at the molecular level is petroleomics. Due to the high chemical complexity of crude oil, the mass spectra of petroleum samples are also very complex, and ultrahigh resolution of $> 500,000$ is essential to resolve all peaks in the mass spectrum. Fourier Transform Ion Cyclotron Resonance (FT-ICR MS) mass spectrometry is a well-established method in petroleomics. FT-ICR MS is capable of achieving ultrahigh resolution as well as extremely high mass accuracy, enabling assignment of all peaks in the

Authors

Matthias Witt
Bruker Daltonik GmbH, Bremen, Germany

Keywords	Instrumentation and Software
Petroleomics	solariX XR
FTMS	APPI II source
APPI	Composer 1.0.6

mass spectrum with their correct molecular formula, even at masses up to m/z 800 [1-3].

Ionization methods such as electrospray ionization (ESI), atmospheric pressure chemical ionization (APCI), atmospheric pressure photo ionization (APPI) or laser desorption ionization (LDI) are typically combined with FT-ICR MS to determine the molecular composition of crude oils using positive- and negative-ion mode. Depending on the ionization method, compound classes such as hydrocarbons, O_x , S_x , SO_x , N_x , and NO_x are ionized with differing efficiencies. Therefore, the mass spectrum of a crude oil using a specific ionization method can be used as a “fingerprint” for crude oil characterization [4].

High reproducibility of mass spectrometric results is essential to enable use of these data for reliable characterization of crude oil at the molecular level or identification using statistical methods such as principle component analysis or unsupervised clustering. In addition, highly stable ionization conditions are crucial for reproducibility in the detection of relative abundances of compound classes and the ratio of radical cations to protonated species [5]. This ratio is mainly influenced by the dopant used for the photoionization process [6].

Flow injection analysis is a proven method for increasing the reproducibility of chemical analyses. In this study, flow injection analysis was combined with APPI-FT-ICR mass spectrometry for characterization of crude oil samples. Forty-five replicate measurements were performed on the same crude oil sample over 8 hours. Each measurement required around 9 minutes and samples were introduced by flow injection using an autosampler and a 100 μ L sample loop. To enable detection of polar compounds and non-polar compounds (such as hydrocarbons and S_1 compounds with a low proton affinity), APPI was used as the ionization method in positive-ion mode. Using this ionization method, radical cations and protonated species were principally detected. However, detection of both protonated species and radical cations resulted in very complex spectra.

Experimental

Sample preparation: A North Sea crude oil sample (light crude oil with a API gravity of 32.9° API, asphaltene content 1.9%) was measured without any purification by flow injection using APPI-FT-ICR MS. The sample was kindly provided by the Norwegian Petroleum Directorate, Stavanger, Norway. Crude oil (10 mg) was dissolved in 990 μ L dichloromethane. This stock solution was diluted 1:100 in 50% toluene / 50% methanol + 0.1% formic acid to give a final concentration of 100 ppm. Five vials were each filled with 1.5 mL of the sample solution. The five vials were used in rotation for sample injection (1st injection

from vial 1, 2nd injection from vial 2, 3rd injection from vial 3, 4th injection from vial 4, 5th injection from vial 5, 6th injection from vial 1, 7th injection from vial 2 and so on) to minimize the aging effect of the sample during the measurements. In total, 900 μ L sample solution was injected from each vial.

Mass analysis: Mass spectra were acquired with a Bruker solariX XR™ Fourier transform ion cyclotron resonance mass spectrometer (Bruker Daltonik GmbH, Bremen, Germany) equipped with a 12 T refrigerated actively shielded superconducting magnet (Bruker Biospin, Wissembourg, France) and the new dynamically harmonized analyzer cell (ParaCell™). The samples were ionized in positive-ion mode using the APPI ion source (Bruker Daltonik GmbH, Bremen, Germany) equipped with a krypton lamp at 10.6 eV. The sample was introduced to the mass spectrometer by flow injection using a G1367A well plate autosampler (Agilent, Santa Clara, CA, USA) with a 100 μ L sample loop and a G1311A pump (Agilent, Santa Clara, CA, USA). The flow was set to 100 μ L/min during the injection and 0.2 min after injection the flow was reduced to 10 μ L/min over 0.6 min. The flow of 10 μ L/min was maintained for 7.2 min and then increased over 1 min to 100 μ L/min. The final mass spectrum was acquired in 7.7 min by adding 128 single scans. The mass range was set to m/z 150 – 2000 using 8M data points with a transient length of 3.3 s resulting in a resolving power of 900,000 at m/z 400 in magnitude mode. The ion accumulation time was set to 30 ms. Ramped excitation (20% at m/z 147 to 35% at m/z 3000) was used for ion excitation before detection.

Mass calibration: The mass spectra were calibrated externally with arginine clusters in positive-ion mode using a linear calibration. A 10 μ g mL⁻¹ solution of arginine in 50% methanol was used to generate the arginine clusters. Single scans were aligned during the measurement with a single mass online calibration using mass m/z 500.437653 ($C_{37}H_{56}$) to align single scans to this mass. Spectra were recalibrated internally with the N_1 series in DataAnalysis™ 4.2 (Bruker Daltonik GmbH, Bremen, Germany). The RMS mass error of the internal calibration was better than 150 ppb for all measurements.

Molecular formula calculation: The mass formula calculation was performed using Composer 1.0.6 (Sierra Analytics, Modesto, CA, USA) with a maximum formula of $C_nH_nN_3O_3S_3$, electron configurations odd and even (due to the formation and detection of radical cations and protonated species), and a mass tolerance of 500 ppb. The relative abundances of all compound classes were calculated using the Composer software.

Results and Discussion

The mass spectra obtained in positive-ion mode of the 5th, 15th, and 25th injections are shown in Figure 1. Identical mass distributions were observed for the different measurements with a maximum abundance of the mass distribution at m/z 390. No additional peaks (siloxanes or silicones) from the septum of the vial were observed in any of the injections. Masses up to m/z 1100 were detected.

After internal calibration of the mass spectra, molecular formulas of all peaks in the spectra were calculated using the Composer software. Based on this data, relative abundances of compound classes were calculated for all 45 replicate measurements (see Table 1).

The relative standard deviations of abundant (> 5%) compound classes such as HC, N₁, O₁ and S₁ were very low (< 2%). This demonstrates not only the reproducibility of flow injection analysis but also the reproducibility of the APPI FT-ICR mass spectrometric results. Slightly higher standard deviations were observed for low-abundance compound classes such as N₁O₁ and O₁S₁. The presence of these oxygen-containing compound classes could partly be due to chemical reactions of highly reactive species in the APPI ion source. The higher standard deviation of such species could therefore be attributed to ionization effects of APPI as well as their low abundance.

Mass spectra of different crude oil injections

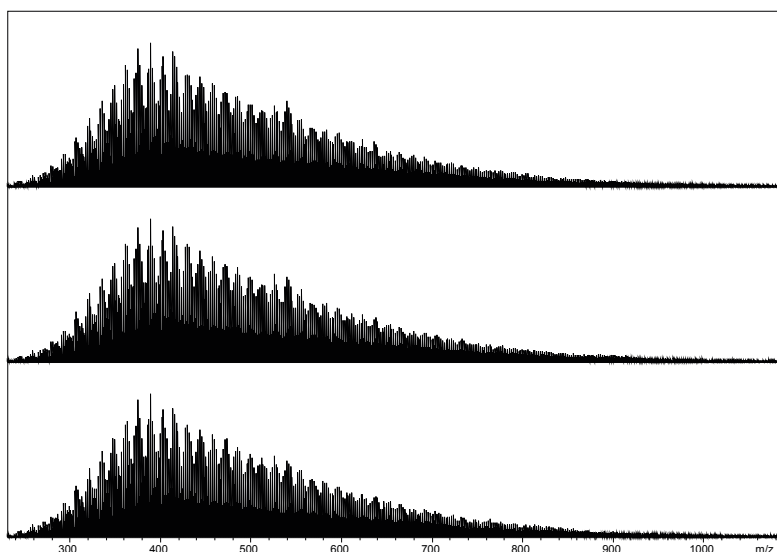


Figure 1: Mass spectra of the 5th, 15th and 25th injection of the North Sea crude oil using APPI in positive-ion mode.

Relative abundance of compound classes of all injections

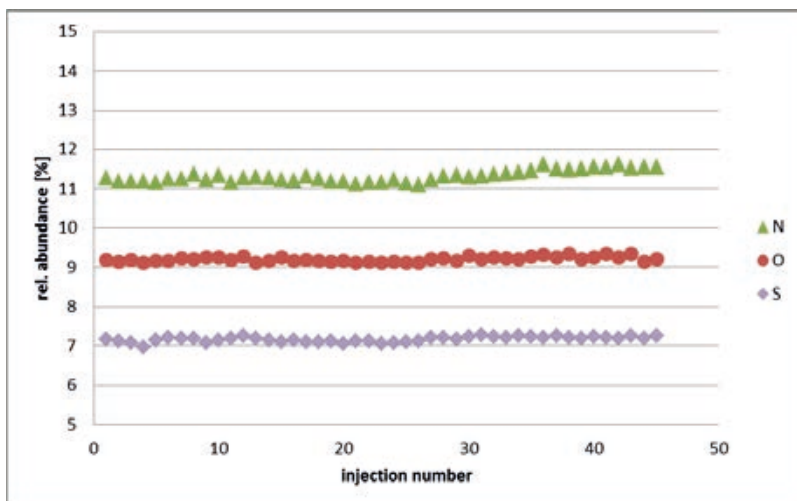


Figure 2: Relative abundance of compound classes N₁, O₁ and S₁ as radical cations.

Ratio of radical cations to protonated species

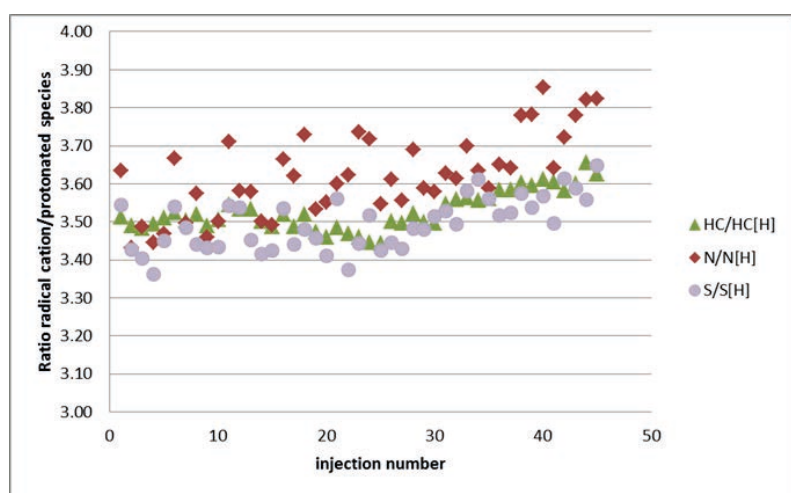


Figure 3: Ratio of radical cations to protonated species of compound classes HC, N_i and S_i.

Table 1: Average values and absolute and relative standard deviations of detected compound classes' relative abundances.

Relative abundance of compound classes and standard deviations

Class	Injection 1	Injection 2	Injection 3	...	Injection 43	Injection 44	Injection 45	Average	Standard deviation	Standard deviation [%]
HC	44.45	43.44	43.52	...	44.45	45.33	45.22	44.05	0.57	1.3
HC [H]	12.66	12.45	12.5	...	12.35	12.4	12.47	12.49	0.17	1.3
N	11.27	11.19	11.19	...	11.53	11.54	11.55	11.32	0.14	1.3
N [H]	3.1	3.26	3.21	...	3.05	3.02	3.02	3.13	0.08	2.5
NO	1.23	1.38	1.37	...	1.22	1.02	1.07	1.28	0.12	9.0
NO [H]	1.74	2.01	1.98	...	1.82	1.62	1.62	1.84	0.12	6.7
O	9.18	9.15	9.19	...	9.34	9.15	9.2	9.21	0.06	0.7
O [H]	1.3	1.43	1.45	...	1.25	1.15	1.2	1.35	0.09	6.7
OS [H]	1.11	1.2	1.19	...	1.08	1.07	1.05	1.13	0.04	3.5
S	7.16	7.13	7.08	...	7.25	7.19	7.26	7.17	0.07	1.0
S [H]	2.02	2.08	2.08	...	2.02	2.02	1.99	2.05	0.03	1.4

Table 2: Average values and absolute and relative standard deviations of the ratio of radical cations to protonated species for compound classes HC, N_i and S_i.

Ratio of radical cations to protonated species and standard deviations

Ratio	Injection 1	Injection 2	Injection 3	...	Injection 43	Injection 44	Injection 45	Average	Standard deviation	Standard deviation [%]
HC/HC[H]	3.51	3.49	3.48	...	3.60	3.66	3.63	3.53	0.05	1.5
N/N[H]	3.64	3.43	3.49	...	3.78	3.82	3.82	3.62	0.11	3.0
S/S[H]	3.54	3.43	3.40	...	3.59	3.56	3.65	3.50	0.07	1.9

The relative abundances of compound classes N_1 , O_1 and S_1 as radical cations for all injections are plotted in Figure 2. A small increase (< 3%) in the relative abundance of compound class N_1 was observed after 25 injections. This could be due to aging effects on the sample.

The reproducibility of the APPI method was also studied on the basis of the ratio of radical cations to protonated species. This ratio is very sensitive to ionization conditions in the APPI source, which must be kept constant for reproducible results from one injection to the next [6]. The results for the compound classes HC, N_1 and S_1 are shown in Table 2 and plotted in Figure 3. The higher fluctuation of the class N and S relative to the HC class indicates that the protonation is a first order reaction.

Conclusion

Mass spectra of crude oil can be measured with high reproducibility using flow injection APPI-FT-ICR mass spectrometry. Abundant (> 5% relative abundance) compound classes are detected with relative standard deviations of less than 2%. Low-abundance (< 2% relative abundance) compound classes have relative standard deviations below 10%. Therefore, these results can be used to get a semi-quantitative overview of the chemical composition of crude oils.

The low relative standard deviation (< 3%) in the ratio of radical cations to protonated species for the compound classes HC, N_1 and S_1 indicates that the ionization conditions in the APPI source are very reproducible.

This high-level of reproducibility could be used for quality control processes at refineries or to establish the origin of unknown samples.

References

- [1] Rodgers, R. P.; Schaub, T. M.; Marshall, A. G. *Anal. Chem.* 2005, 21A.
- [2] Marshall, A. G.; Rodgers, R. P. *Acc. Chem. Res.* 2004, 37, 53-59.
- [3] Cho, Y.; Ahmed, A.; Islam, A., Kim, S. *Mass Spectrom. Rev.* 2014, doi: 10.1002/mas.21438
- [4] Lobodin, V.V.; Nyadong, L.; Ruddy, B.M.; Quinn, J.P.; Hendrickson, C.L.; Rodgers, R.P. and Marshall, A.G., Ambient Ionization Fourier Transform Ion Cyclotron Resonance Mass Spectrometry for Comprehensive Chemical Fingerprinting of Petroleum and Deposits, Gulf of Mexico Oil Spill and Ecosystem Science Conf., New Orleans, LA, January 19-23 (2013).
- [5] Cai, S. S.; Hanold, K. A.; Syage, J. A. *Anal. Chem.* 2007, 79, 2491-2498.
- [6] Robb, D. B.; Covey, T. R.; Bruins, A. P. *Anal. Chem.* 2000, 72, 3653-3659.

For research use only. Not for use in diagnostic procedures.



• Laser/Desorption Ionization FT-ICR Mass Spectrometry as a Tool for Statistical Analysis of Crude Oils

Introduction

Crude oil is an extremely complex mixture of hydrocarbons and heteroatom-containing chemicals such as thiophenes, phenols, pyrrols, and pyridines. The composition can vary widely, depending on the origin of the oil and how the petroleum was formed. The maturity of each crude oil has a huge influence on its molecular composition. Each raw petroleum or crude oil has a characteristic composition and properties. Therefore, chemical analysis can be used to “fingerprint” the source of the petroleum. High-boiling–point hydrocarbons and highly polar compounds cannot be characterized by GC/MS analysis. However, these compounds can be analyzed at the molecular level by Fourier Transform Ion Cyclotron Resonance (FT-ICR) mass spectrometry, which is a well-established method

Authors

Matthias Witt
Bruker Daltonik GmbH, Bremen, Germany

Kolbjørn Zahlse, Anders Brunsvik
SINTEF Materials and Chemistry, Trondheim, Norway

Keywords	Instrumentation and Software
Petroleomics	solariX XR, 12 T
FTMS	ProfileAnalysis 2.1
LDI	MTP II MALDI source
	Composer 1.0.6

in petroleomics [1-3]. On the basis of the detected compounds, the relative abundance of different compound classes can be calculated and compared between different crude oils. The chemical composition of crude oil can also be correlated with the chemical properties of the oil. Such analyses complement characterization using standard crude oil parameters such as API gravity, TAN acidity, sulfur and nitrogen content.

It should be noted that the abundance of the detected compound classes depends heavily on the ionization method used. Therefore, crude oils can be compared by FT-ICR mass spectrometry, but this method is only semi-quantitative [4]. The types of compound classes that are detected are also influenced by the presence of salts and additives used to provide better ionization efficiencies. In this study, laser desorption/ionization (LDI) was coupled to a Fourier Transform Ion Cyclotron Resonance (FT-ICR) mass spectrometer for the analysis of crude oil [5]. A thin film of crude oil was applied onto a stainless steel target and analyzed by LDI using a UV laser at 355 nm. No matrix was added to the sample for these measurements.

Nine different crude oils were analyzed and compared at the molecular level. The relative abundances of compound classes with different numbers of heteroatoms were compared. In some cases, the relative abundances of the compounds classes were quite low. Therefore, high reproducibility of the LDI measurements is a prerequisite for reliable characterization of crude oils. Each crude oil sample was measured several times to calculate the standard deviation of the detected compound classes. Additionally, the results were analyzed using the statistical method principle component analysis (PCA). The results showed that the oils were well-separated in the PCA scoring plot, with low variation between the replicate measurements.

The statistical analysis also indicated that extremely high resolution mass spectra are required to distinguish between oils. Therefore, LDI coupled to FT-ICR mass spectrometry is a perfect tool for distinguishing between crude oils using statistical methods such as PCA. In addition, LDI is independent of solvent effects observed in atmospheric pressure ionization methods such as ESI or APPI, and sample preparation is extremely simple.

Experimental

Sample preparation: Samples were kindly provided by SINTEF, Department of Materials and Chemistry, Trondheim, Norway. The crude oil samples were measured by LDI without the addition of matrix and without any purification. Crude oil (10 mg) was dissolved in 990 μL toluene and 1 μL of this solution was spotted onto a stainless steel target and dried for 15 min at room

temperature. The samples were placed in the source chamber for 30 minutes at around 3 mbar before mass analysis by laser/desorption ionization.

Mass analysis: Mass spectra were acquired using a Bruker solariX XR Fourier transform ion cyclotron resonance mass spectrometer (Bruker Daltonik GmbH, Bremen, Germany) equipped with a 12 T refrigerated actively-shielded superconducting magnet (Bruker Biospin, Wissembourg, France) and the new dynamically harmonized analyzer cell (ParaCell™). The samples were ionized in positive ion mode using the MALDI ion source (Bruker Daltonik GmbH, Bremen, Germany). The mass range was set to m/z 150 – 2000 using 4M data points with a transient length of 1.6 s resulting in a resolving power of 450,000 at m/z 400 in magnitude mode. One hundred single scans were averaged for a final mass spectrum. The laser power was lowered to 12% to reduce fragmentation during the ionization process. The laser focus was set to a diameter of 30 μm and 4 laser shots were used for each scan. Five replicate measurements were performed for each sample for meaningful statistical analysis. Spectra were zero-filled to processing size of 8M data points before sine apodization.

Mass calibration: The mass spectra were calibrated externally using arginine clusters in electrospray ionization positive ion mode. A linear calibration was applied. A 10 μg ml^{-1} solution of arginine in 50% methanol was used to generate the clusters. To improve the mass accuracy, the crude oil spectra were recalibrated internally with the N_1 series. The RMS mass error of the recalibration of all acquired spectra was better than 150 ppb using a linear calibration.

Molecular formula calculation: The molecular formula calculation was performed in Composer 1.0.6 (Sierra Analytics, Modesto, CA, USA) using a maximum formula of $\text{C}_n\text{H}_n\text{N}_3\text{O}_3\text{S}_3$. Due to the formation and detection of radical cations and protonated species, the electron configuration was set to odd and even, and a mass tolerance of 500 ppb was used. The relative abundances of the compound classes were calculated with the Composer software. The statistical analysis was performed with the software ProfileAnalysis 2.1 (Bruker Daltonik GmbH, Bremen, Germany).

Results and Discussion

The mass spectra of three different crude oil samples measured in LDI positive ion mode are shown in Figure 1. The mass distribution of the samples is very similar, with an average mass of around m/z 300. Masses of up to m/z 800 were detected.

The average number of carbons in compounds detected

Mass spectra of three different crude oil samples

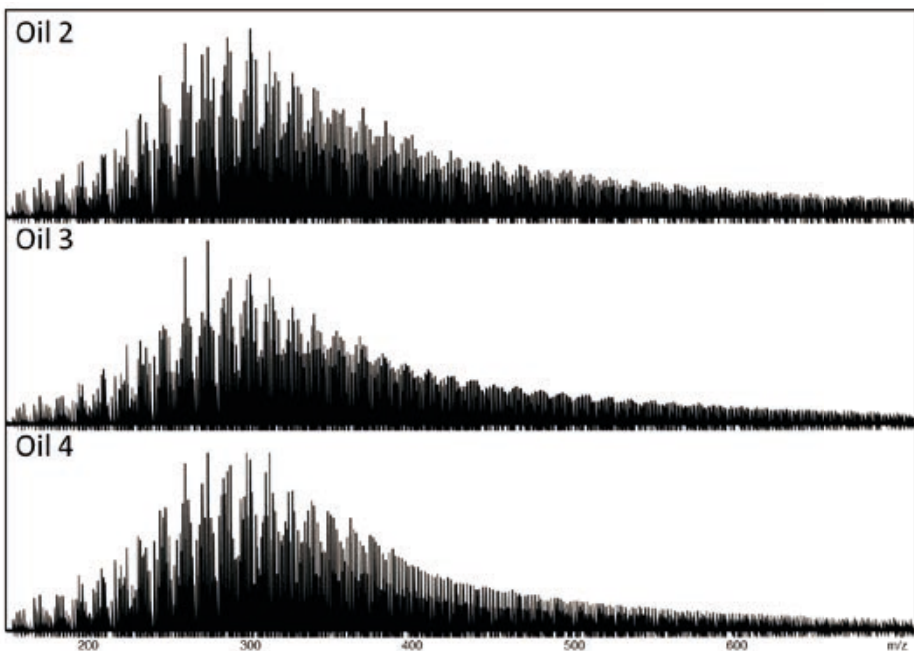


Figure 1: Mass spectra of three different crude oil samples measured in LDI positive ion mode.

Magnified view of crude oil mass spectra

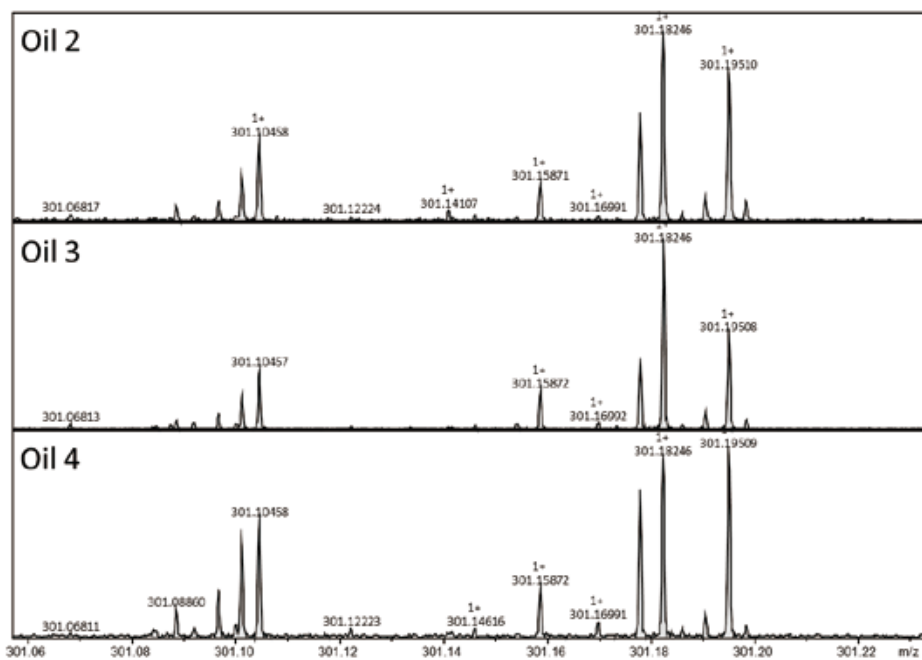


Figure 2: Magnified view of mass spectra of crude oils 2, 3, and 4 at m/z 301. Significant differences are only apparent using ultrahigh resolution.

by LDI can be estimated by mass distribution. Therefore, LDI-TOF-MS can be used as a general tool to measure the average mass and the mass distribution analysis of crude oil, lubricants, bitumen, and asphaltenes. However, ultrahigh-resolution mass spectrometry is required to analyze these samples at the molecular level. Only ultra-high-resolution FT-ICR is capable of resolving all mass peaks in the extremely complex mass spectrum, thereby enabling calculation the correct molecular formula of each peak based on highly accurate mass measurements (Figure 2).

The molecular formulas of mass peaks were calculated with a mass tolerance of 500 ppb. Using a maximum formula of $C_nH_nN_3O_3S_3$, single-candidate molecular formulas were obtained in the mass range up to m/z 500. Higher molecular formulas were obtained by extending the homologous series obtained in the lower mass region. This calculation

was performed using the Composer software. The mass spectra showed significant differences in ion abundance (Figure 2) resulting in different relative abundances of compound classes (Figure 3). Oil 8 and oil 8a are identical oils from different batches. Oil 9a corresponds to a sample of oil 9 that was stored in the source vacuum chamber for one day at 3 mbar, which resulted in the evaporation of volatile compounds.

Distinguishing between crude oils on the basis of compound class abundances alone only provides approximate and sometimes even inaccurate results. Therefore, our approach for distinguishing between crude oils was performed at the molecular level using all mass peaks detected by LDI-FT-ICR mass spectrometry. The mass spectra of the different oil samples were first

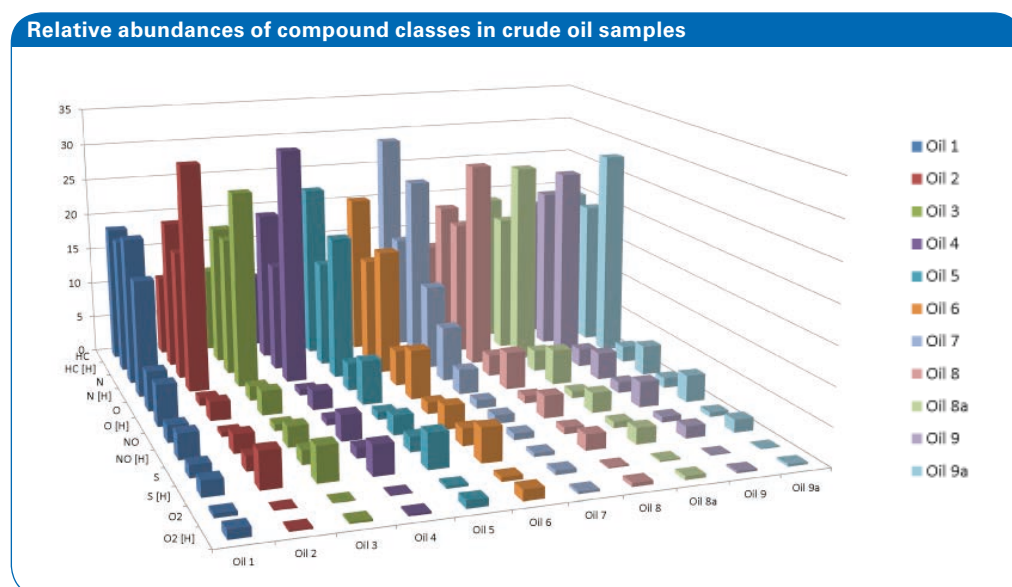


Figure 3: Three-dimensional column diagram showing relative abundances of compound classes detected as protonated species and radical cations by LDI-FT-ICR mass spectrometry. Class of protonated species is marked as [H].

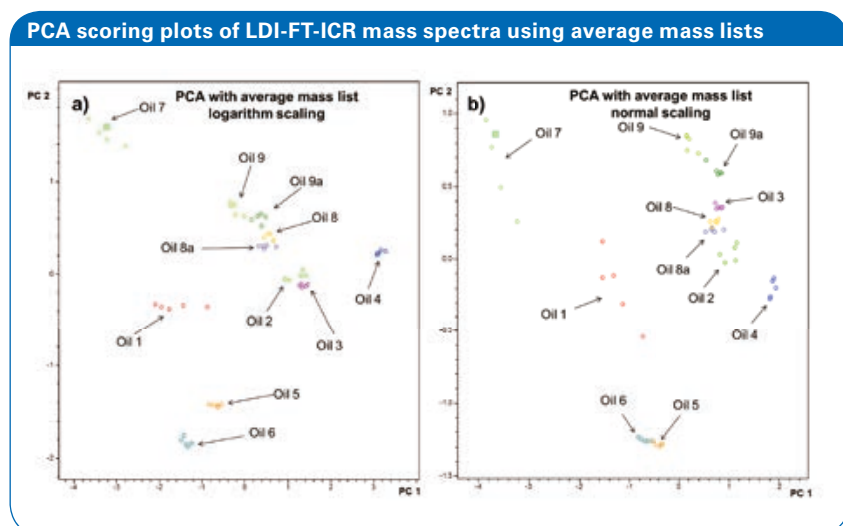


Figure 4: PCA scoring plots of LDI-FT-ICR mass spectra of all oil samples using average mass lists with a) logarithmic scaling and b) linear scaling. Oil 8 and oil 8a are identical oils from different batches. Oil 9a corresponds to a sample of oil 9 that was stored in the source vacuum chamber for one day at 3 mbar.

analyzed on the basis of relative abundance of compound classes (Figure 3) for an approximate characterization of the crude oils. For a more precise characterization, the mass spectra of the crude oils were analyzed using the statistical method principle component analysis (PCA). To obtain statistically meaningful results, five replicate measurements were performed on each sample. The results of the PCA calculated using the average mass list show that the oils are well-separated in the PCA scoring plot, with low variation between the replicate measurements (Figure 4).

Improved separation of the oils in the PCA scoring plot was observed using logarithmic scaling (Figure 4a) instead of linear scaling (Figure 4b). However, statistical analysis

indicated that extremely high resolution mass spectra were required for efficient separation of the oils by PCA (Figure 5). Using bucketing with a mass resolution of 2 mDa for PCA calculation instead of average mass lists resulted in inefficient separation of crude oils (Figure 5a). No separation of the crude oils was observed with low mass resolution of 20 mDa bucketing (Figure 5b). A bucketing mass resolution of 20 mDa corresponds to a mass spectrum with resolving power of only 20,000, as typically obtained using a MALDI-TOF instrument.

Therefore, the ultra-high resolution provided by FT-ICR MS is required to distinguish between the crude oils using LDI and PCA.

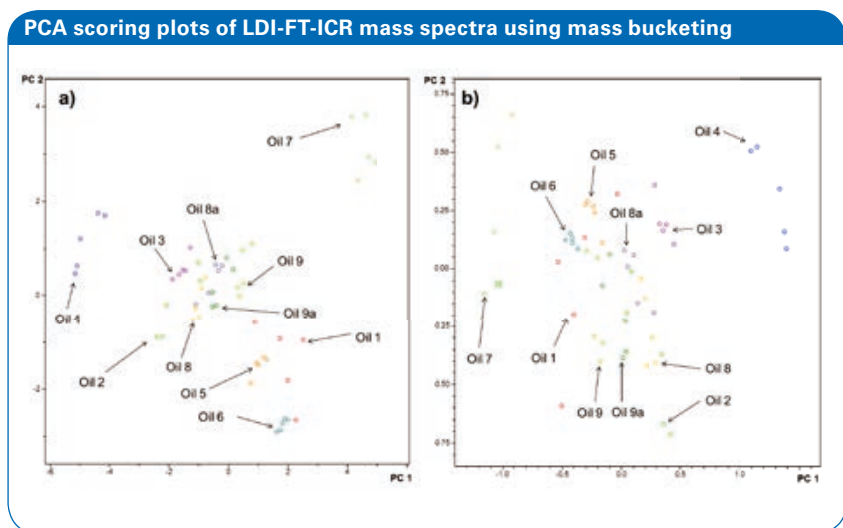


Figure 5: PCA scoring plots of LDI-FT-ICR mass spectra of all oil samples using logarithmic scaling and a) 2 mDa or b) 20 mDa mass bucketing. Oil 8 and oil 8a are identical oils from different batches. Oil 9a corresponds to a sample of oil 9 that was stored in the source vacuum chamber for one day at 3 mbar.

Table 1: Relative abundances of compound classes found in five replicate measurements of oil 8.

LDI-FT-ICR mass spectra						
Class	Oil 8 rep1	Oil 8 rep2	Oil 8 rep3	Oil 8 rep4	Oil 8 rep5	Std. deviation [%]
HC	12.97	12.17	12.83	13.04	12.25	3.3
HC [H]	20.24	19.67	20.36	20.44	19.87	1.6
N	18.62	18.28	18.25	18.21	18.22	0.9
N [H]	27.27	28.74	27.47	27.24	28.56	2.6
N ₂	0.47	0.46	0.46	0.47	0.46	1.2
N ₂ [H]	1.13	1.26	1.17	1.14	1.25	5.1
NO	0.93	0.88	1.01	0.97	0.91	5.4
NO [H]	2.64	2.83	2.7	2.76	2.89	3.6
O	2.82	2.62	2.76	2.71	2.61	3.3
O [H]	4.72	4.86	4.72	4.71	4.83	1.5
O ₂	0.21	0.18	0.19	0.2	0.18	6.8
O ₂ [H]	0.49	0.5	0.5	0.47	0.5	2.7
OS [H]	0.3	0.26	0.29	0.28	0.27	5.6
S	0.83	0.73	0.85	0.93	0.77	9.4

The high reproducibility of LDI mass spectra was demonstrated by the standard deviation of the relative abundances of the compound classes (Table 1). Low relative standard deviations of less than 4% were observed for highly abundant compound classes such as hydrocarbons or N₁. Relatively low standard deviations (< 10%) were observed for very low-abundance classes. Therefore, LDI-FT-ICR mass measurements are highly reproducible, a factor that is crucial for the efficient characterization of crude oil using this technique.

Conclusion

Crude oil samples can be distinguished at the molecular level by LDI ultra-high resolution mass spectrometry. LDI-FT-ICR mass spectrometry is capable of classifying crude oils by principle component analysis (PCA).

LDI-FT-ICR measurements provide the reproducibility required for efficient PCA characterization. Crude oils are best separated in PCA scoring plots using average mass lists and logarithmic *scaling*.

References

- [1] Rodgers, R. P.; Schaub, T. M.; Marshall, A. G. *Anal. Chem.* 2005, 21A.
- [2] Marshall, A. G.; Rodgers, R. P. *Acc. Chem. Res.* 2004, 37, 59-59.
- [3] Cho, Y.; Ahmed, A.; Islam, A., Kim, S. *Mass Spectrom. Rev.* 2014, doi: 10.1002/mas.21438
- [4] Witt, M. Comparison of LDI and APPI for correlation studies between physical and chemical properties of crude oil and FT-ICR mass spectra, Poster at Petrophase 2013.
- [5] Cho, Y.; Witt M.; Kim, Y. H.; Kim S. *Energy & Fuels* 2012, 84, 8587.

For research use only. Not for use in diagnostic procedures.



• Analysis of peat bog after solid phase extraction by FTMS

Introduction

Natural Organic Matter (NOM) is a very complex and polydisperse mixture of highly degraded organic compounds present in surface and ground water [1]. NOM is an important pool in the global carbon cycle. Therefore, structures and chemistry of these compounds are of high interest. The number of compounds is still unknown but exceeds several thousands in each sample. NOM is abundant in terrestrial, limnic and marine environments. Major contributors are humic substances, sedimentary and dissolved organic matter (DOM). A major part of humic substances are humic and fulvic acids, which differ in the solubility at low pH. DOM varies in the O/C and H/C ratios from 0.1-0.9 and 0.3-1.8, respectively [2]. Masses range

from 150 to 1,000 Da measured by Fourier transform ion cyclotron resonance (FTICR) mass spectrometry [3]. Structural information of organic molecules of NOM is difficult to gain from the molecular formula only. A huge variety of chemical isomers is possible even at small masses with different structures and functional groups. However, relative abundance of functional groups like hydroxyl or carboxyl groups can be determined by plotting double bond equivalents (DBE) vs. number of oxygen atoms [4].

The molecular formula of organic compounds in DOM can be determined by ultra-high resolution mass spectrometry. Due to the very high complexity of these samples extremely high resolving power of >300,000 is required and can only be achieved by FTICR mass spectrometry. Moreover,

Maximum of mass distribution at m/z 270

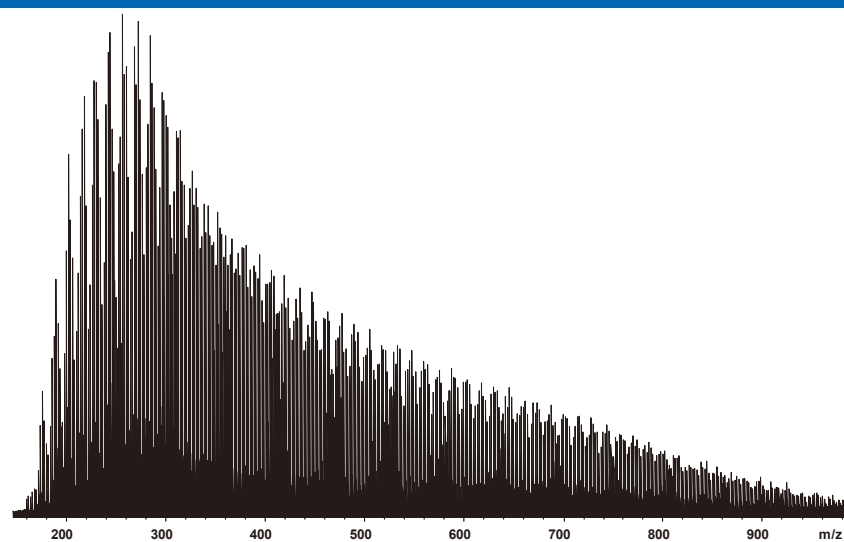


Figure 1: Electrospray mass spectrum of the peat bog sample in negative ion mode

Well separated mass peaks

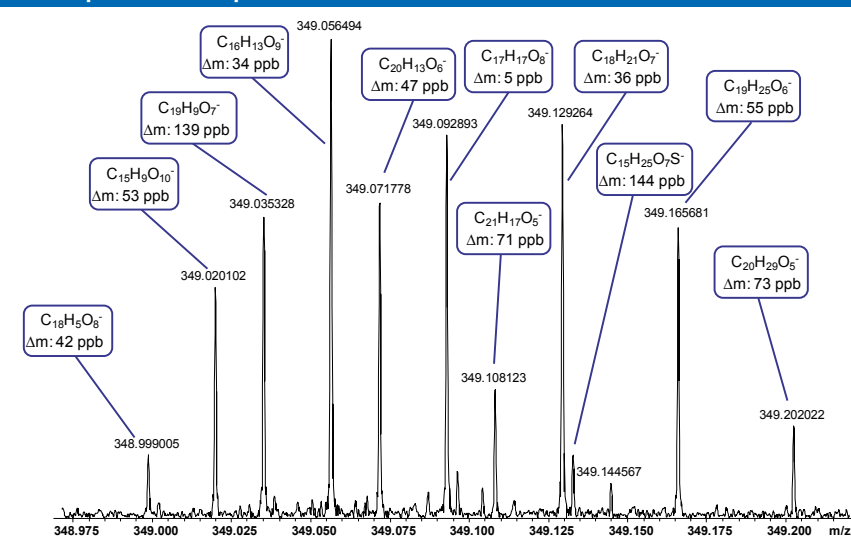


Figure 2: Zoom of the electrospray mass spectrum of the peat bog sample (negative ion mode) with molecular formula and mass error annotation of most abundant mass peaks

extremely high mass accuracy is provided by FTICR mass spectrometry which is essential for the exact determination of the molecular formula from one mass peak when several different heteroatoms are present in the molecule. In this study, a sample from peat bog treated by solid phase extraction was analyzed by FTICR mass spectrometry (MS). After molecular formula assignment of all mass peaks Van Krevelen plots were created for the compound classes O_x, NO_x and SO_x. Additionally, class distribution plots were created for these three compound classes as well as DBE distribution plots.

Experimentals

Sample preparation

40 ml of interstitial water of ombrotrophic and oligotrophic peat bog located in Stader Geest (Germany) was sampled

from 20 cm soil depth. The water was acidified to pH 2 and the DOM was extracted by solid phase extraction (200 mg, Bond-Elut-PPL, Varian) and eluted with 1 ml methanol. Prior to the FT-ICR mass spectrometric analysis 200 μl of the extract were diluted with water (50:50 v/v). The DOC concentration of the interstitial water was 10.5 mM. Total dissolved nitrogen (TDN) was 285 μM.

Mass Analysis

Mass spectra were acquired with a solarix Fourier transform mass spectrometer (Bruker Daltonik GmbH, Bremen, Germany) equipped with a 12 T refrigerated actively shielded superconducting magnet (Bruker Biospin, Wissembourg, France) and Infinity ICR analyzer cell [5]. The samples were ionized using a dual ion source in electrospray negative ion mode (Bruker Daltonik GmbH, Bremen, Germany). Sample solutions were continuously infused using a syringe at a

High mass accuracy of FT-ICR results

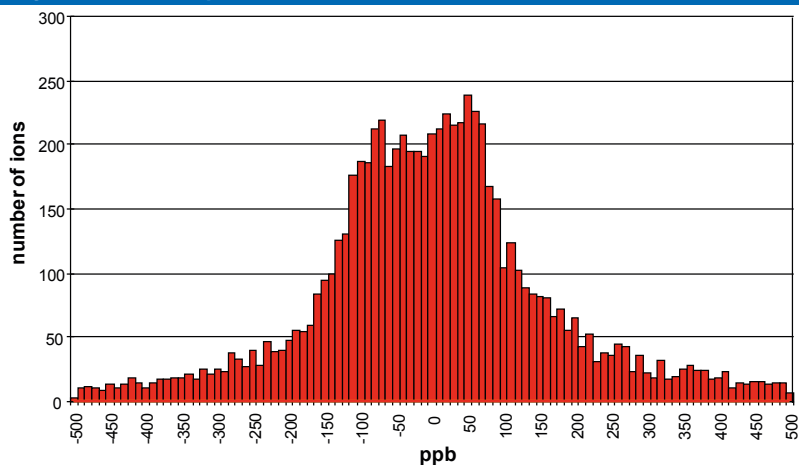


Figure 3: Error distribution of all mass peaks with molecular formula assignment. 7068 peaks were assigned with exactly one molecular formula. Average error was 2 ppb with an rms error of 159 ppb.

Van Krevelen plots for detailed analysis of data

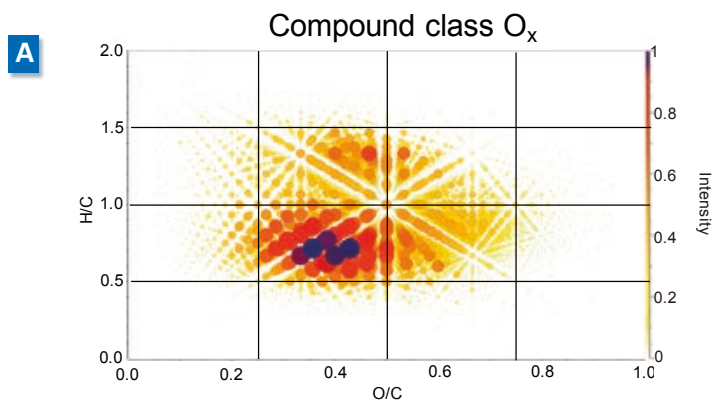


Figure 4a: Van Krevelen plot of compound class O_x . The intensity of the peaks in the mass spectrum is marked with the colour and size of the dots.

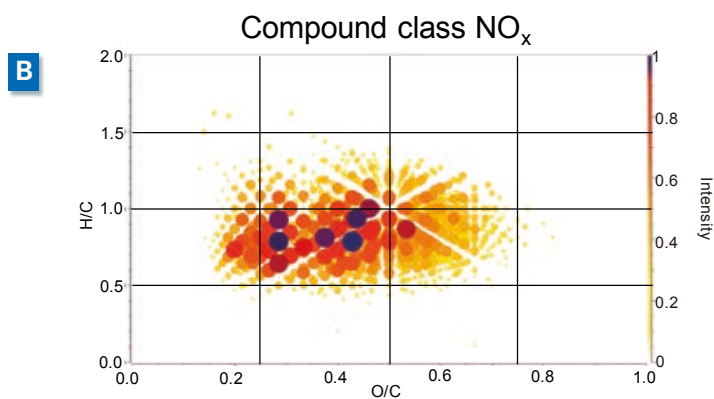


Figure 4b: Van Krevelen plot of compound class NO_x . The intensity of the peaks in the mass spectrum is marked with the colour and size of the dots.

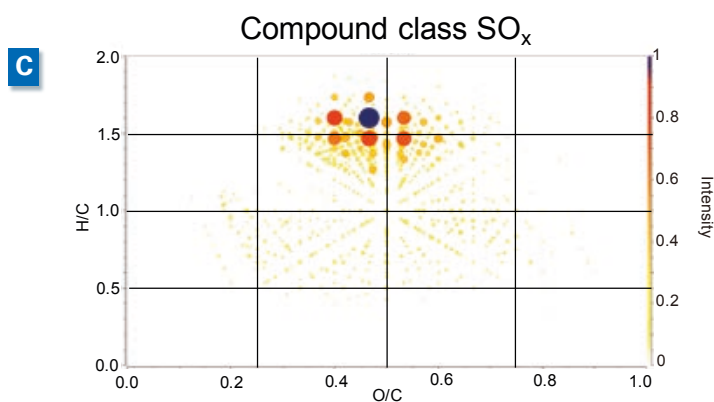


Figure 4c: Van Krevelen plot of compound class SO_x . The intensity of the peaks in the mass spectrum is marked with the colour and size of the dots.

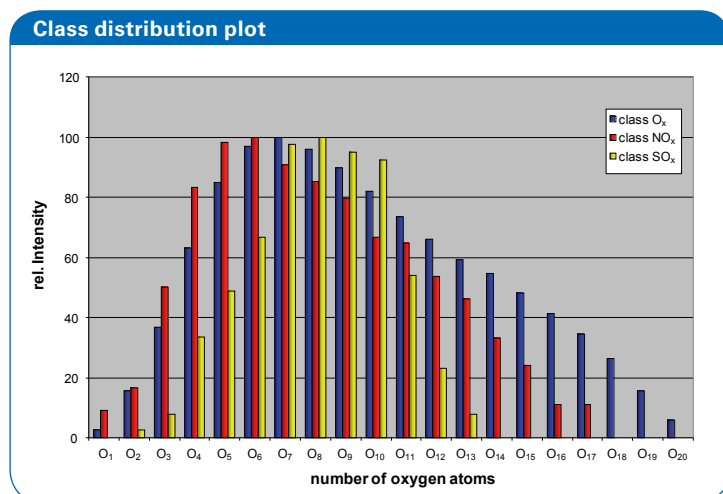


Figure 5: Relative class distribution of compound classes O_x, NO_x and SO_x.

flow rate of 120 $\mu\text{L h}^{-1}$. The detection mass range was set to m/z 150 – 3,000. Ion accumulation time was set to 0.1 s. Data sets were acquired with 4 MW data points resulting in a resolving power of 480,000 at m/z 400. 500 scans were added for each mass spectrum. Spectra were zero-filled to processing size of 8M data points before sine apodization.

Mass calibration

The mass spectra were calibrated externally with arginine clusters in negative ion mode using a linear calibration. A 10 $\mu\text{g ml}^{-1}$ solution of arginine in 50% methanol was used to generate the clusters. Mass spectra were recalibrated internally with typical C_nH_nO_n peaks to improve the mass accuracy.

Molecular formula calculation

The molecular formula calculation was done in DataAnalysis 4.0 (Bruker Daltonik GmbH, Bremen) and Composer 1.0.2 (Sierra Analytics, Modesto, CA, USA) using a maximum formula of C_nH_nN₂O₃₀S₁. Electron configuration was set to even electron species due to the formation and detection of deprotonated species. A mass tolerance of 0.5 ppm was used for the molecular formula calculation. The Van Krevelen plots were generated with the Composer software. Class distribution, DBE distribution and DBE vs. oxygen atom plots were generated with Windows Excel 2003 using the tables generated with the Composer software.

Results and Discussion

The mass spectrum of the peat bog sample is shown in figure 1. Mass peaks ranged from m/z 150 to about 1,000 with the maximum of the mass distribution at m/z 270. In figure 2, only the mass peaks at nominal mass m/z 349 are shown. The most abundant peaks were annotated with their molecular formula and mass error (difference between experimental and theoretical mass) which on average were below 100 ppb. Due to the very high resolving power

of FTICR-MS all mass peaks were well separated. The mass error distribution is shown in figure 3. An average error of only 2 ppb was calculated with an rms (root mean square) error of only 159 ppb using more than 7000 mass peaks. More than 70% of the mass peaks showed relative intensities below 10%. The mass peaks with relative intensities above 10% had only an rms error of 79 ppb. The errors were calculated with 10 ppb bins and about 75% of the mass peaks had errors below 150 ppb. Due to the high mass accuracy of FT-ICR results, peaks were unambiguously assigned with their molecular formula up to masses above m/z 800 using the following restrictions: maximum formula of C_nH_nN₂O₃₀S, maximum of double bond equivalents of 40, ratio H/C between 0.2 and 2.0 and ratio O/C between 0.0 and 1.0.

For a detailed analysis of the data, Van Krevelen plots were generated for the compound classes O_x, NO_x and SO_x (figure 4a-4c). More than 5000 compounds were found for compound class O_x compared to nearly 1000 compounds for compound class NO_x and about 600 compounds for compound class SO_x. The intensity weighted average values for class O_x were 0.49 for the O/C ratio and 0.91 for the H/C ratio. On average, the compounds of class NO_x were more aromatic with values of only 0.45 for O/C and 0.87 for H/C, respectively. The compound class SO_x was dominated by low aromatic species. This was reflected in the high intensity weighted average values of 0.61 and 1.26 for the ratios O/C and H/C, respectively. The most abundant compounds had H/C ratios of about 1.5 with O/C ratios between 0.4 and 0.6. Therefore, these compounds probably had a different core structure than compounds of class O_x and NO_x. A detailed analysis of the classes O_x, NO_x and SO_x is shown by the class distribution plot in figure 5. Class O_x showed a broad distribution from 1 to 20 oxygen atoms. The distribution of class NO_x was shifted to a lower number of oxygen atoms which was also reflected in the average number of oxygen of this class of only 8.1 compared to 9.6 oxygen atoms of class O_x. Class SO_x had the smallest

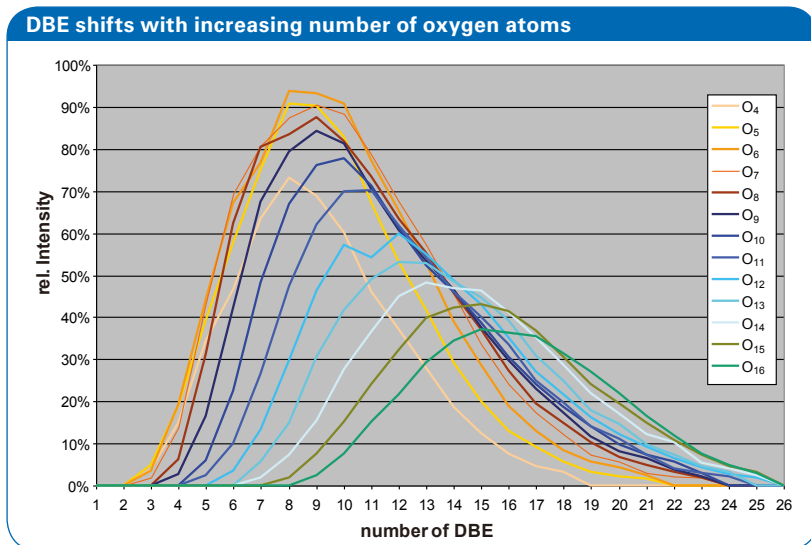


Figure 6: Relative distribution of double bond equivalents (DBE) of compound classes O_4 to O_{16} .

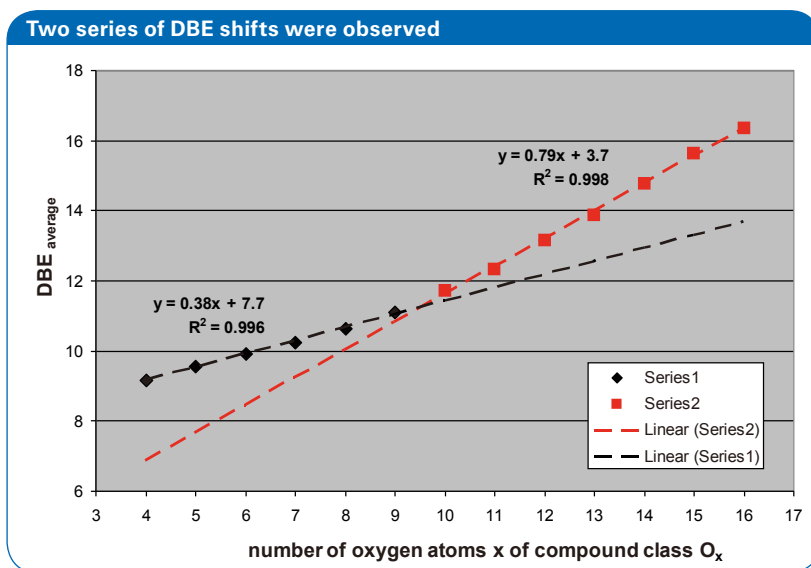


Figure 7: Average DBE vs. number of oxygen atoms including linear fit for both series (series 1: $O_4 - O_9$ and series 2: $O_{10} - O_{16}$).

oxygen atom distribution with oxygen atoms between 2 and 13. Even if the maximum of this distribution was higher with 8 oxygen atoms than class O_x with 7 oxygen atoms, the average number of oxygen atoms of the molecules of this compound class was only 8.0 and, therefore, the lowest of these three classes. It is very interesting to note that the relative distribution of double bond equivalents (DBE) of class O_x ranged from low to high numbers of oxygen atoms. DBE is defined as the number of rings and double bonds of a molecule and is calculated for $C_cH_hN_nO_oS_s$ with the following formula:

$$DBE = c - h/2 + n/2 + 1$$

DBE shifted to higher values with increasing number of oxygen atoms (figure 6) as expected. However, the DBE shift was not equal for compounds with low and high number of oxygen atoms. This can be directly observed by

plotting the average DBE value vs. the number of oxygen atoms x of class O_x (figure 7). Two series were observed, one series with a slope of 0.38 for compounds containing between 4 and 9 oxygen atoms and another series for the oxygen rich compounds ($O_{10} - O_{16}$) with a slope of about 0.8. For both series good linear regression factors of 0.996 and 0.998 were observed, respectively. Observation of two series could be correlated to the existence of more or less hydroxyl, carboxyl and carbonyl groups of these series. An addition of a hydroxyl group results in a slope of 0, a carboxyl group in a slope of 0.5 and a carbonyl group in slope of 1. Therefore, series 1 seems to be dominated by carboxyl groups, whereas series 2 seems to be dominated by carboxyl as well as carbonyl groups. However, the higher aromaticity in higher aromatic core structures resulted in more double bonds and rings. The intercept calculated for series 1 was 7.7. Therefore, the core structures of the

molecules with low number of oxygen atoms contain about eight double bonds or rings. So, these compounds are highly aromatic. The intercept of the other series was calculated as 3.7. Thus, molecules with high number of oxygen atoms contain only in average four double bonds or rings. They are less aromatic than compounds of series 1. These results were consistent with collision induced fragmentation experiments which revealed direct analytical evidence for NOM molecular structures [6].

Conclusions

Natural organic matter like NOM can be analyzed in detail on the molecular level by FT-ICR mass spectrometry. Van Krevelen plots can be used to compare compound classes like O_x , NO_x and SO_x . Intensity weighted average values for the H/C and O/C ratios of each compound class can be used to compare classes and also samples. Also, double bond distributions can be used to get insight into the average core structures of low oxidized and high oxidized DOM material. Based on the DBE average vs. oxygen atom plots, the results suggest that most of the oxygen in low oxidized DOM exists mainly in carboxyl groups, whereas oxygen is bound as carboxyl and carbonyl groups in highly oxidized DOM.

References

- [1] Hertkorn, N.; Kettrup, A. In Earth and Environmental Sciences, vol. 52, Perminova, I. V.; Hatfield, K.; Hertkorn, N. (eds). Springer, Heidelberg, 2005, 391-435.
- [2] Koch, B. P.; Witt, M.; Engbrodt, R.; Dittmar, T.; Kattner, G. Geochim. Cosmochim. Acta 2005, 69, 3299-3308.
- [3] Stenson, A. C.; Marshall, A. G.; Cooper, W. T. Anal. Chem. 2003, 75, 1275-1284.
- [4] Bae, E.; Yeo, I. J.; Jeong, B.; Shin, Y.; Shin, K.-H.; Kim, S. Anal. Chem. 2011, 83, 4193-4199.
- [5] Caravatti, P.; Allemann, M. Org. Mass Spectrom. 1991 26, 514-518.
- [6] Witt, M.; Fuchser, J.; Koch, B. P. Anal. Chem. 2009, 81, 2688-2694.

Authors

Dr. Matthias Witt, Bruker Daltonik GmbH, Fahrenheitstr. 4, D-28359 Bremen, Germany

Dr. Frauke Schmidt, MARUM, Leobener Str., D-28359 Bremen

Prof. Dr. Boris Koch, Alfred-Wegener Institut für Polar- und Meeresforschung, Am Handelshafen 12, D-27570 Bremerhaven

Keywords	Instrumentation & Software
Complex Mixture	solariX 12T
NOM	DataAnalysis 4.0
FTMS	Composer

For research use only. Not for use in diagnostic procedures.



• solarix XR: Analysis of Complex Mixtures

Introduction

Natural organic matter (NOM) as well as crude oil and crude oil fractions are very complex mixtures of organic compounds consisting of various elemental compositions and chemical structures. These mixtures can vary extremely depending on their origin and complexity. Natural organic matter consists mainly of oxygen containing compounds. However, also nitrogen and sulfur are presented in low amounts in NOM.

Therefore, high dynamic range and mass accuracy is needed to detect and identify these compounds. Beside the roughly 90% of hydrocarbon compounds in crude oil, the remaining polar mainly polar compounds are of major interest which are mainly in the resin and asphaltene fractions. These compounds contain different amount of

Authors

Dr. Matthias Witt
Bruker Daltonik GmbH, Bremen, Germany

Keywords	Instrumentation and Software
Complex Mixture	solarix XR
Petroleomics	DataAnalysis 4.0
Crude Oil	ESI Source
NOM	APPI II Source
FTMS	Composer

sulfur, nitrogen and oxygen which results in an extremely complex mixture difficult to analyze. Due to the complexity of oil, chromatography can be used to separate compound classes. However, separation of compounds by liquid chromatography is only of limited use. Therefore, mass spectrometers providing extremely high resolving power and mass accuracy like Fourier transform ion cyclotron resonance (FT-ICR) mass spectrometers are needed to analyze these samples [1-2].

Still, for FTMS the resolving power is limited by a) analyzer pressure, b) peak coalescence effects and c) non-perfect trapping potential resulting in a de-phasing of the ion cyclotron motion. The solarix XR has been developed to be able to study these kind of mixtures using only a 7T magnet. The non-perfect trapping has been overcome by the development of a new cell with parabolic trapping potentials, called dynamically harmonized analyzer cell (Fig. 1) [3-5]. It has been shown that extremely high resolving power of more than 20.000.000 can be achieved with this new analyzer cell, however, these measurements were performed with a limited number of ions using quadrupole isolation. Nevertheless, very high resolving power of 800.000 at m/z 400 have been achieved in magnitude mode in full broad band detection of very complex mixtures like crude oil and NOM without any quadrupole isolation using a solarix XR system.

Even higher mass resolution of more than 1.200.000 can be achieved of complex mixtures using the absorption mode processing (AMP) [6]. NOM as well as oil samples have been used to test the performance of the new solarix XR FTMS system with the new dynamically harmonized analyzer cell. Suwannee river fulvic acid (SRFA) as a NOM standard has been measured by electrospray ionization. The mixture consists mainly of oxygen containing compounds with different number of carboxyl, carbonyl and hydroxyl

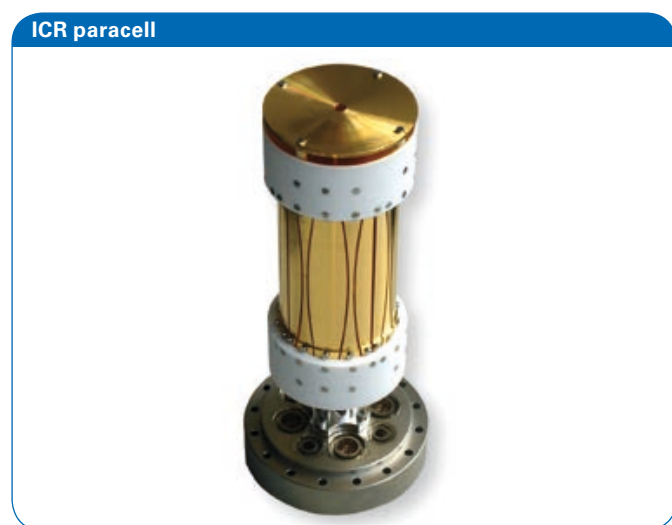


Figure 1: New dynamically harmonized analyzer cell with parabolic trapping plates.

functional groups. However, due to the origin of the sample sodium is present in the sample.

Therefore, sodium adducts beside protonated species are detected resulting in more than 5000 mass peaks in the spectrum. Different crude oil samples and bitumen as well as a residual fuel oil have been measured by APPI to test the performance of the new FT-ICR system concerning sample complexity. The APPI spectra in positive ion mode are extremely rich in content of peaks due to the formation of radical cations and protonated species. Hence, these spectra represent one of the most complex ones of small molecule mixtures. The spectra have been mainly analyzed concerning achieved mass resolving power and mass accuracy. Additionally, CASI measurements of complex mixtures have been carried out to compare CASI and full broad band results.

Experimental

Sample preparation

The NOM standard SRFA has been purchased by the International Humic Substance Society (IHSS order No. 2S101). SRFA has been measured without any further purification. 20 $\mu\text{g ml}^{-1}$ solution of SRFA in 50% methanol/50% water was directly sprayed into the electrospray ion source using a syringe pump.

One residual fuel oil purchased from TCI (TCI order number S0250) as well as two crude oils and one bitumen sample kindly provided by the company SINOPEC, China, were analyzed. Solutions of the oils were prepared without any further purification. 10 mg of the oil were dissolved in 200 μL dichloromethane. These sample stock solutions were diluted 1:500 with 50% methanol, 50% toluene for atmospheric pressure photoionization (APPI) measurements.

Mass analysis

Mass spectra were acquired with a Bruker solarix XR Fourier transform mass spectrometer (Bruker Daltonik GmbH, Bremen, Germany) equipped with a 7T refrigerated actively shielded superconducting magnet (Bruker Biospin, Wissembourg, France) and the new dynamically harmonized analyzer cell. The samples were ionized in positive ion mode using ESI and APPI (Bruker Daltonik GmbH, Bremen, Germany).

Sample solutions were continuously infused using a syringe pump. A flow rate of 120 $\mu\text{L h}^{-1}$ and 600 $\mu\text{L h}^{-1}$ were used for ESI and APPI, respectively. The size of the acquired data sets was 8 MW resulting in a resolving power of 800 000 at m/z 400. The detection mass range was set to m/z 150 – 3000. 300 scans were acquired for each mass spectrum. A sine apodization was performed before Fourier transformation.

Mass calibration

The mass spectra were calibrated externally with arginine clusters in positive ion mode using a linear calibration. A 10 $\mu\text{g ml}^{-1}$ solution of arginine in 50% methanol was used to generate the clusters. To improve the mass accuracy the spectra were recalibrated internally with a known homologous series.

Molecular formula calculation

The mass formula calculation of the SRFA spectrum was done in DataAnalysis 4.0 (Bruker Daltonik GmbH, Bremen, Germany) using a maximum formula of $\text{C}_n\text{H}_h\text{O}_{30}\text{Na}$, electron configurations even and a mass tolerance of 0.5 ppm.

The calculation of molecular formulae of the oil samples was done in DataAnalysis 4.0 using a maximum formula of $\text{C}_n\text{H}_h\text{N}_3\text{O}_3\text{S}_3$ and electron configurations odd and even due to the formation and detection of radical cations and protonated species. The mass tolerance was set to 0.5 ppm. Compound classes were calculated with the Composer software (Sierra Analytics, Modesto, CA, USA).

Results and Discussion

The performance of the solarix XR system has been demonstrated by measurement of different very complex samples. The mass spectrum of SRFA measured in positive ion mode using electrospray ionization is shown in Figure 2. The mass spectrum has more than 5000 mass peaks. More than 2700 molecular formulae containing only carbon, hydrogen, oxygen and maximum of one sodium could be calculated with a root mean square (RMS) mass error less than 50 ppb.

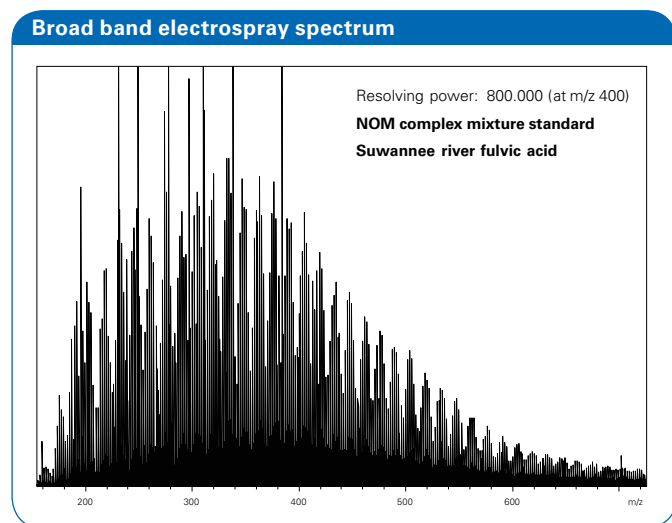


Figure 2: Broad band electrospray spectrum of Suwannee river fulvic acid from the IHSS measured in positive ion mode. More than 5000 mass peaks could be detected.

The mass error plot is shown in Figure 3. A residual fuel oil was measured to show the performance of the solarix XR for the petroleomics applications. The mass error plot of the ESI spectrum of the residual fuel oil is shown in Figure 4. Mainly compound class N and NO have been detected resulting in low number of peaks detected by electrospray ionization. Roughly 3000 molecular formulae have been calculated with a RMS error of 65 ppb. An even low RMS error of only 13 ppb could be achieved of the compound class N1 considering only mass peaks above with a relative abundance of more than 1%.

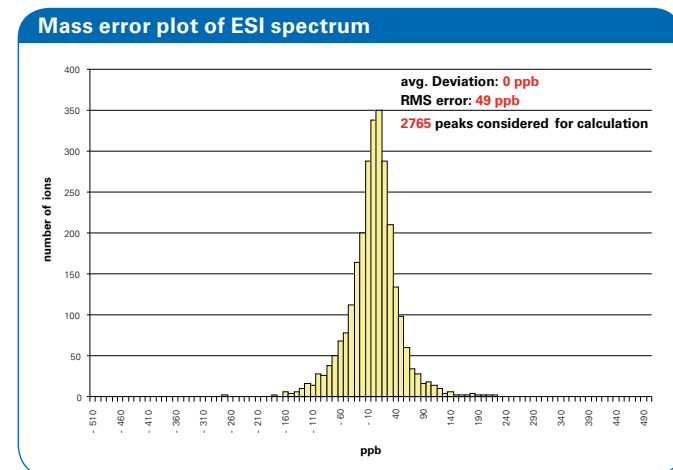


Figure 3: Mass error plot of ESI spectrum of SRFA in positive ion mode. 2765 peaks were considered for the calculation (^{13}C peaks were excluded). A RMS mass error of only 49 ppb was calculated.

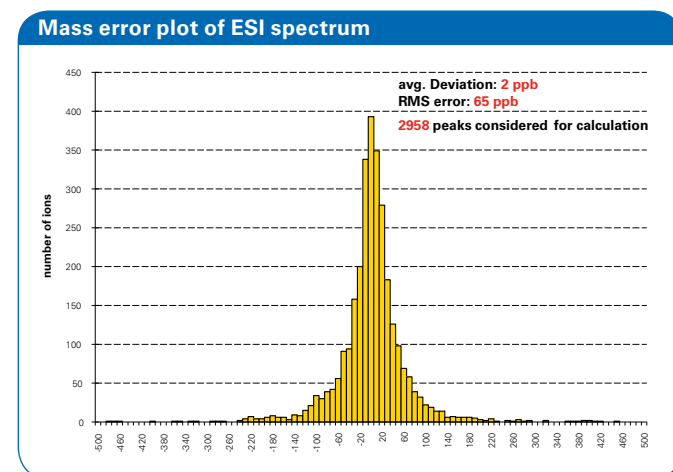


Figure 4: Mass error plot of ESI spectrum of a residual fuel oil in positive ion mode. Nearly 3000 peaks were considered for the calculation (^{13}C peaks were excluded). A RMS mass error of only 65 ppb was calculated.

More challenging samples are crude oils with high amount of sulfur when analyzed by APPI. These samples are extremely complex and APPI can detect sulfur containing compound with one, two or even three sulfur atoms. Additionally, radical cations as well as protonated species are formed resulting in spectra with much more peaks than detected by ESI. Two crude oil and a bitumen sample have been analyzed by APPI in positive ion mode. The APPI spectra are shown in Figure 5.

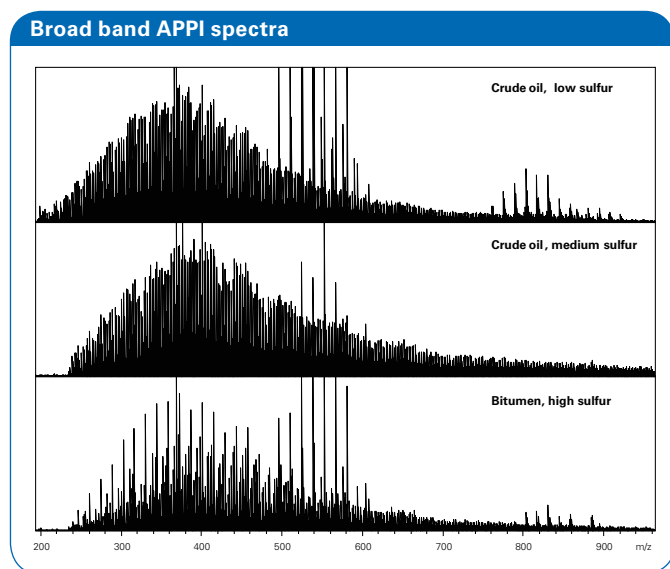


Figure 5: Broad band APPI spectra of two crude oil and one bitumen sample with different amount of sulfur in positive ion mode.

The average mass is shifting to higher mass with increase of the sulfur content. However, also the complexity is increasing resulting in a higher mass error. The error plots of the three samples are shown in Figure 6. The number of unambiguously assigned molecular formulae is increasing from roughly 5000 to nearly 8000 with the amount of sulfur in the complex sample. The RMS mass error shows the expected trend with an increase from 120 to 139 ppb based on the complexity of the sample. The difference of the RMS mass error of peaks with a relative abundance of more than 10% is even more significant. The error increases from 20 ppb to 40 ppb with higher sulfur content in crude oil and nearly doubles for the extremely complex bitumen sample. Nevertheless, a resolving power of 800.000 at m/z 400 could still be achieved even of the most complex bitumen sample. The mass spectra of extremely complex mixtures can be further improved by CASI (continuous accumulation of selected ions). Ions only of a limited mass range (typically 100 Da isolation mass window) are selected with a quadrupole. These selected ions are accumulated in the storage cell for detection. The dynamic range of the mass spectrum can be improved with this technique. Also mass errors are lowered due to the reduced number of detected peaks compared to the broad mass spectrum. The mass error plots of the broad band and CASI measurements are shown in Figure 7.

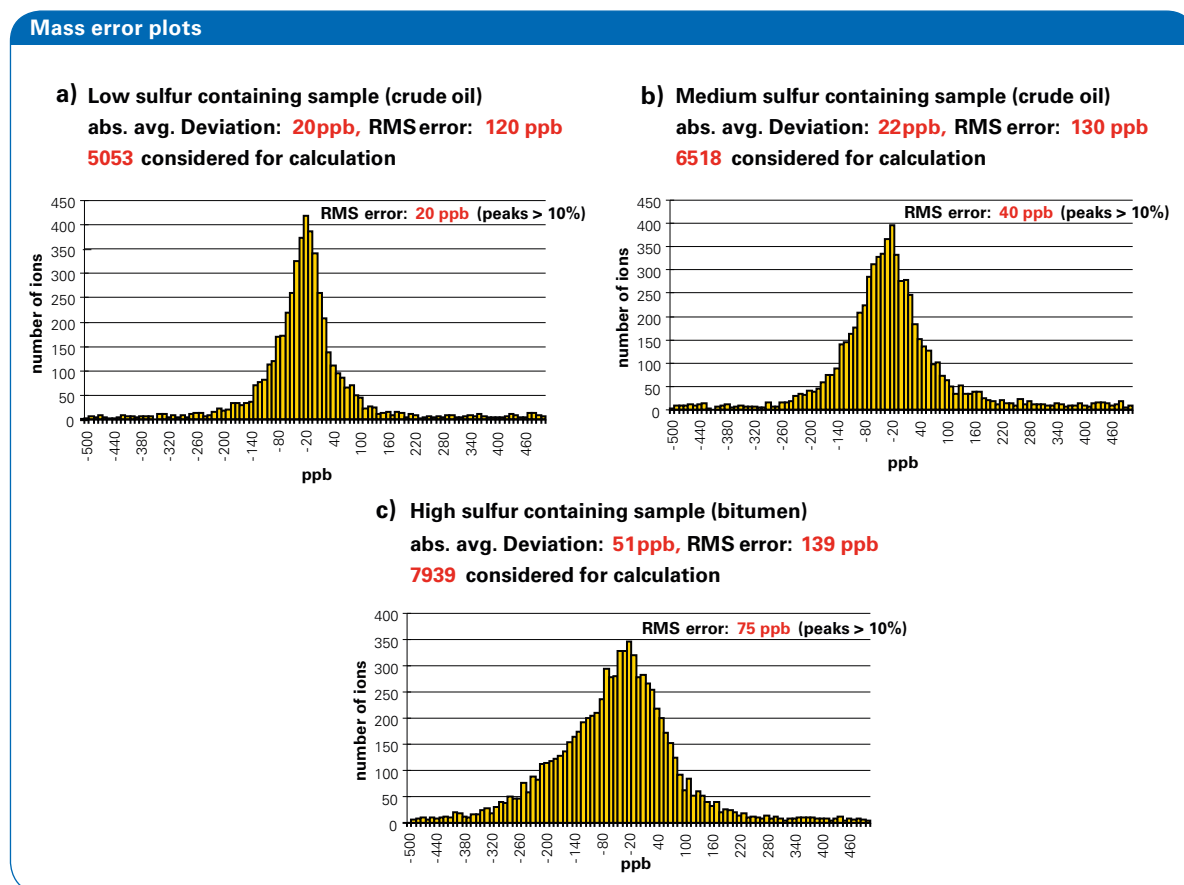
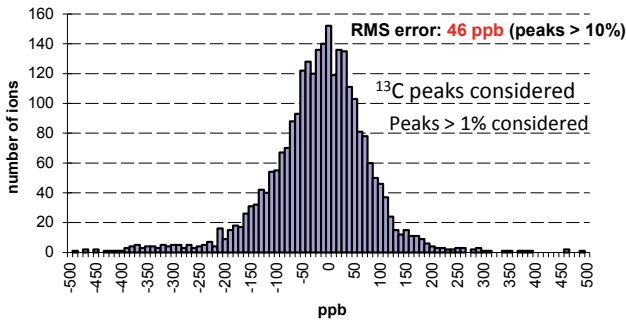


Figure 6: Mass error plots of a) crude oil with low amount of sulfur, b) crude oil with medium amount of sulfur and c) bitumen with high amount of sulfur. Complexity of mass spectra increases with amount of sulfur resulting in a) detection of more mass peaks for error calculation and b) increase of mass error.

Mass error plots of bitumen sample

a) Broad band, masses m/z 380 - 480

abs. avg. Deviation: **18 ppb**, RMS error: **99 ppb**
2650 considered for calculation



b) Broad band, masses m/z 380 - 480

abs. avg. Deviation: **4 ppb**, RMS error: **67 ppb**
3086 considered for calculation

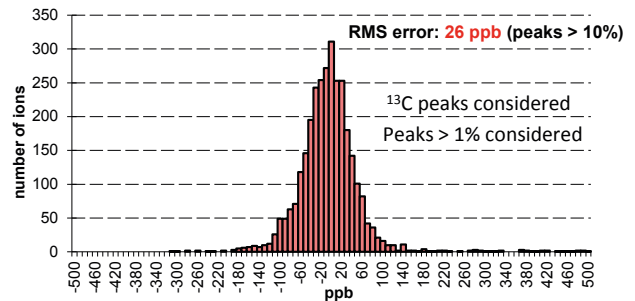


Figure 7: Mass error plots of bitumen sample with high amount of sulfur considering masses between m/z 380 and m/z 480 of a) broad band and b) CASI measurement. RMS mass error is further reduced from 99 to 67 ppb using CASI instead of broad band detection.

The mass error is further reduced from 99 to 67 ppb considering only peaks between m/z 380 and m/z 480 using CASI instead of broad band mass detection. Only unambiguously assigned mass peaks with a relative abundance of more than 1% have been considered for the error plot calculation to compare similar peaks in the mass spectrum. Therefore, the number of peaks used for the error plots increases only by about 20% and the

improvement in the dynamic range is not really visible here.

The effect of improved dynamic range by CASI is shown in Figure 8. Peaks not visible in broad band have been observed by CASI marked with the red arrows. Therefore, this technique can be used to detect very low abundant species in extremely complex mixtures not detectable in broad band mode.

Zoom in of CASI spectrum

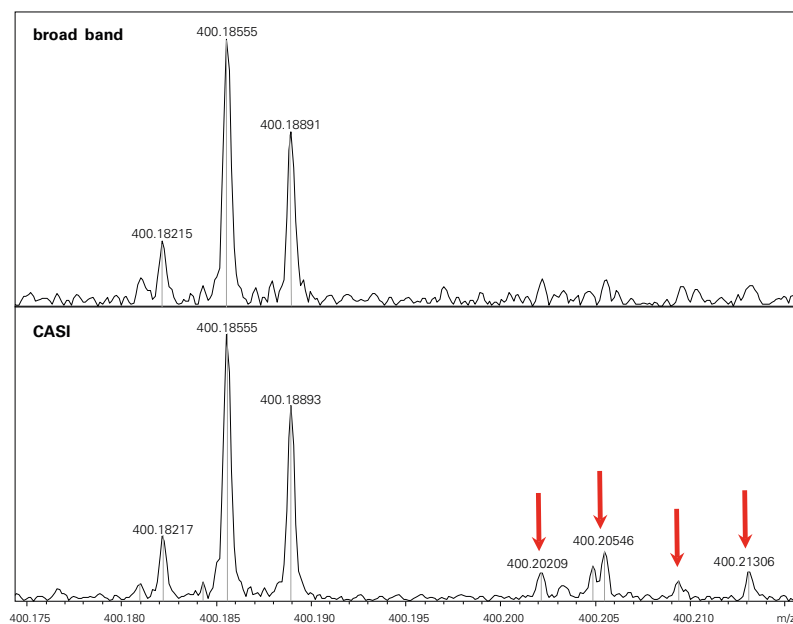


Figure 8: Zoom in of a) broad band and b) CASI spectrum to show the improvement of dynamic range using CASI. Peaks marked with arrows could only be detected with the CASI technique.

Conclusion

Complex mixtures like NOM and crude oil have been successfully analyzed on the molecular level with the new solarix 7T XR system.

Signal transients of more than 6 seconds could be achieved resulting in a resolving power of about 800.000 at m/z 400 in magnitude mode. RMS mass errors of less than 50 ppb could be obtained for SRFA. Low RMS mass errors below 150 ppb were observed for extremely complex mixtures like crude oil and bitumen. A resolving power of 800.000 could be achieved for very complex APPI spectra of these samples in broad band detection mode.

Acknowledgments

The author would like to thank Dr. Maowen Li from the company SINOPEC, China, for providing the crude oil and bitumen samples. Many thanks to Roland Jertz, Jochen Friedrich and Claudia Kriete from Bruker Daltonik GmbH (Bremen) for their support during sample measurements and generating mass error plots.

References

- [1] Marshall, A. G.; Rodgers, R. P. *Acc. Chem. Res.* 2004, 37, 59-59
- [2] Purcell, J. M.; Hendrickson, C. L.; Rodgers, R. P.; Marshall, A. G. *Anal. Chem.* 2006, 78, 5906-5912
- [3] Boldin, I.A., Nikolaev, E.N. *Rapid Commun. Mass Spectrom.* 2011, 25, 122-126
- [4] Nikolaev, E.N., Boldin, I.A., Jertz, R., Baykut, G. A. *J. Am. Soc. Mass Spectrom.* 2011, 22, 1125-1133
- [5] Nikolaev, E.N., Jertz, R., Grigoryev, A., Baykut, G. A. *Anal. Chem.* 2012, 84, 2275-2283
- [6] Qi, Y., Witt, M., Jertz, R. Baykut, G., Barrow, M.P., Nikolaev, E.N., O'Connor, P.B. *Rapid Commun. Mass Spectrom.* 2012, 26, 2021-2026

For research use only. Not for use in diagnostic procedures.



• Analysis of sulfur-rich crude oil and bitumen by FTMS

Introduction

Crude oil is a very complex mixture of organic compounds consisting of various elemental compositions and chemical structures. The composition of many compounds is not exactly known. Mixtures vary widely depending on the origin of the oil. Crude oil consists mostly (>90%) of hydrocarbons. Remaining compounds in oil mainly contain hetero atom classes with oxygen, sulfur and nitrogen. Commercial oils vary in the composition of the type and amount of compounds as well as compound classes. Crude oil and bitumen can be analyzed by analytical methods like nuclear magnetic resonance (NMR) [1], infrared (IR) [2] spectroscopy or X-ray fluorescence spectroscopy (XRF) [3]. Nevertheless, these methods are limited concerning the information of the elemental composition of compounds in oil. Also GC/LC separations of complex mixtures are difficult

and at least time consuming. Polar compounds in crude oil can be detected easily by atmospheric pressure ionization (API) mass spectrometry [4]. Direct infusion experiments of crude oil samples can be carried out by ultra-high resolving power mass spectrometry to achieve mass peak separation and correct annotation of the molecular formula of all peaks in the mass spectrum. Extremely high resolving power is needed to separate isobaric mass peaks which differ only by a few mDa. An important mass difference which has to be resolved in a mass spectrum is 3.4 mDa (difference between C_3 and SH_4). If radical cations of hydrocarbons are present also the mass differences of 4.4 mDa (difference between CH and ^{13}C) is observed. The composition of the hetero atomic compounds is a fingerprint for each crude oil. However, compounds containing only sulfur and no other hetero atoms are difficult to detect by electrospray ionization (ESI) or atmospheric pressure chemical ionization

(APCI) due to the fact that these compounds are difficult to be protonated or deprotonated. Therefore, atmospheric pressure photoionization (APPI) [5], which is able to generate radical cations using multi-photon ionization, is used to detect these compounds. Another method for the detection of compound classes C_xH_yS and $C_xH_yS_2$ is the chemical modification using methylation reagents. Speciation of heteroatomic compounds like compound class S_1 or S_2 with specific double bond equivalents (DBE) is necessary for crude oil and bitumen classification on the molecular level. Sulfur containing compound classes like benzothiophenes (DBE 6) or dibenzothiophene (DBE

9) can be identified based on the number of double bond equivalents. Several studies of crude oil and bitumen have been made in positive ion mode by Fourier transform mass spectrometry (FTMS) using APPI. More than 95% of all mass peaks can be assigned with exactly one molecular formula with a resolving power of 600,000 at m/z 400 and a mass accuracy better than 0.5 ppm using internal calibration calculated by Composer software.

Experimentals

Sample preparation

Four crude oils and two bitumen samples from the company SINOPEC, China, were analyzed. The spray solutions of the crude oils were prepared without any further purification. 10 mg of the crude oil were dissolved in 200 μ L dichloromethane. These sample stock solutions were diluted 1:300 with 50% methanol, 50% toluene for atmospheric pressure photoionization (APPI) measurements.

Mass Analysis

Mass spectra were acquired with a Bruker solariX Fourier transform mass spectrometer (Bruker Daltonik GmbH, Bremen, Germany) equipped with a 12 T refrigerated actively shielded superconducting magnet (Bruker Biospin, Wissembourg, France). The samples were ionized in positive ion mode using the APPI ion source (Bruker Daltonik GmbH, Bremen, Germany). Sample solutions were continuously infused using a syringe at a flow rate of 600 μ L h^{-1} . The size of the acquired data sets was 4 MW resulting in a resolving power of 600 000 at m/z 400. The detection mass

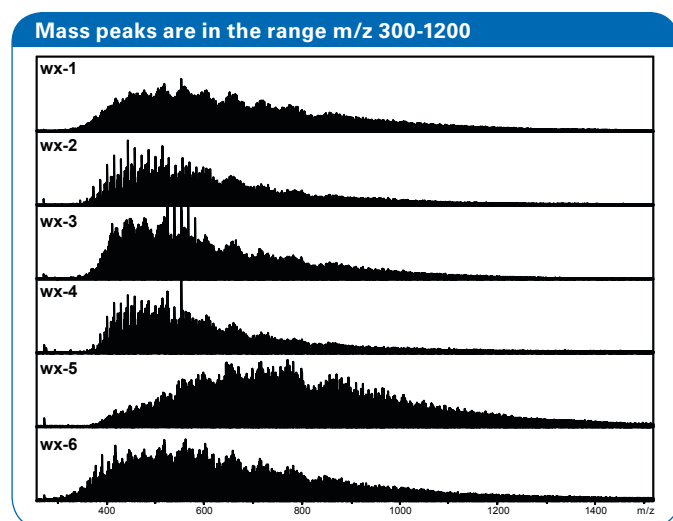


Figure 1: Mass spectra of crude oil and bitumen samples measured in APPI positive ion mode.

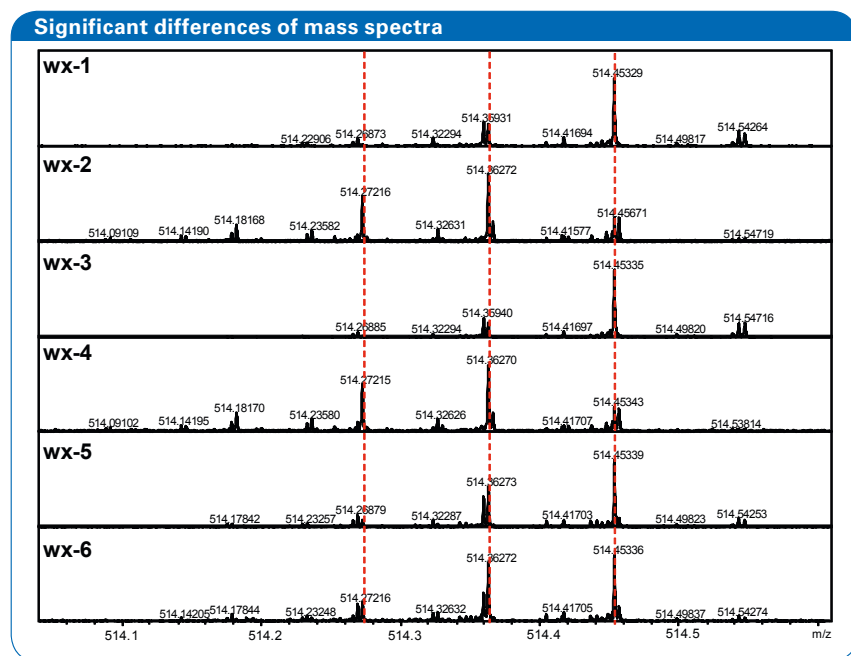


Figure 2: Zoom of all mass spectra at nominal mass m/z 514 to see fine structure of mass spectra.

Authors

Dr. Matthias Witt, Bruker Daltonik GmbH, Fahrenheitstr. 4, D-28359 Bremen, Germany

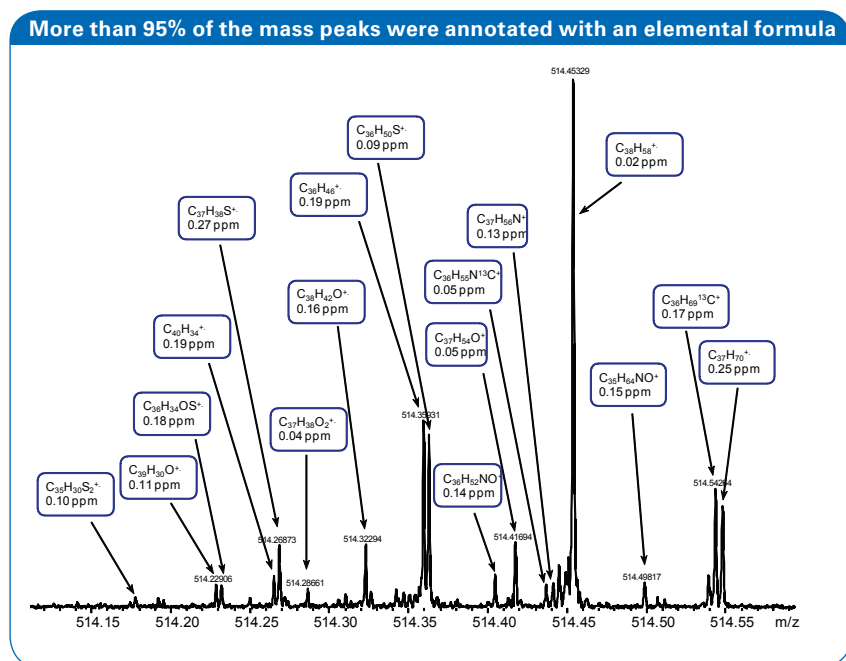


Figure 3: Zoom of mass spectrum of sample wx-1 at nominal mass m/z 514 with elemental formulae annotation of the most abundant peaks (30 peaks could be annotated in total for nominal mass m/z 514).

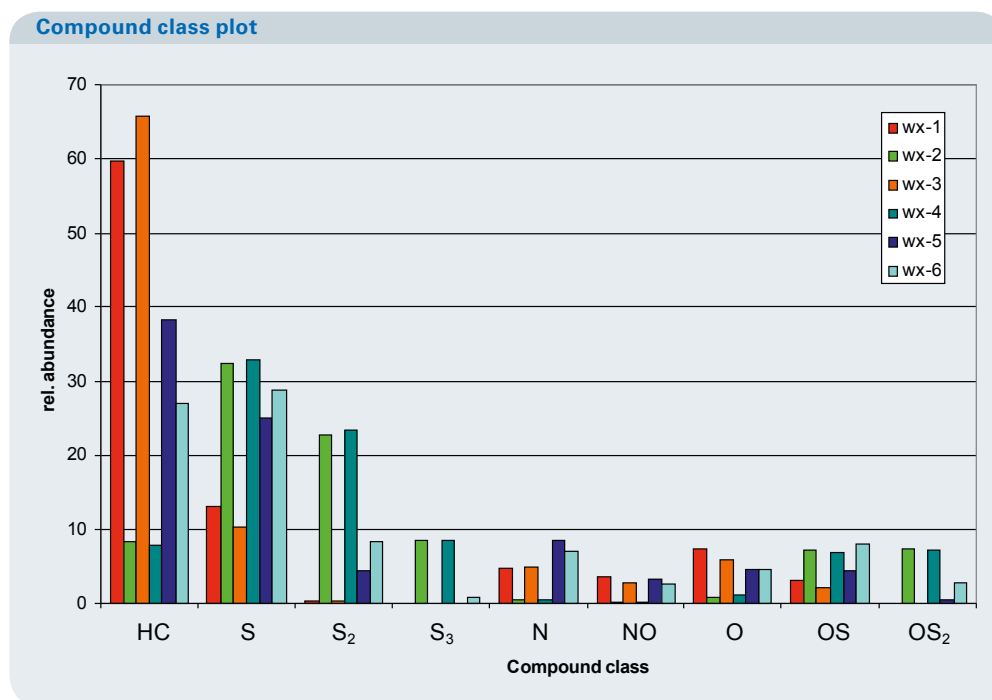


Figure 4: Relative abundances of compound classes of all samples (wx-1, wx-3, wx-5 and wx-6 are crude oil samples, wx-2 and wx-4 are bitumen samples).

range was set to m/z 250 – 3000. 300 scans were acquired for each mass spectrum. Spectra were zero-filled to processing size of 8M data points before sine apodization.

Mass calibration

The mass spectra were calibrated externally with arginine clusters in positive ion mode using a linear calibration. A $10 \mu\text{g ml}^{-1}$ solution of arginine in 50% methanol was used to generate the clusters. The crude oil spectra were recalibrated internally with the homologous series C_nH_{2n-16} and the bitumen samples with the homologous series $C_nH_{2n-16}S$

to improve the mass accuracy.

Molecular formula calculation

The mass formula calculation was done in Composer 1.0.2 (Sierra Analytics, Modesto, CA, USA) using a maximum formula of $C_nH_nN_3O_3S_3$, electron configurations odd and even due to the formation and detection of radical cations and protonated species and a mass tolerance of 0.5 ppm. The double bond equivalents (DBE) vs. carbon number plots as well as the compound class and Van Krevelen plots were also generated with the Composer software.

Relative abundances of the compound classes

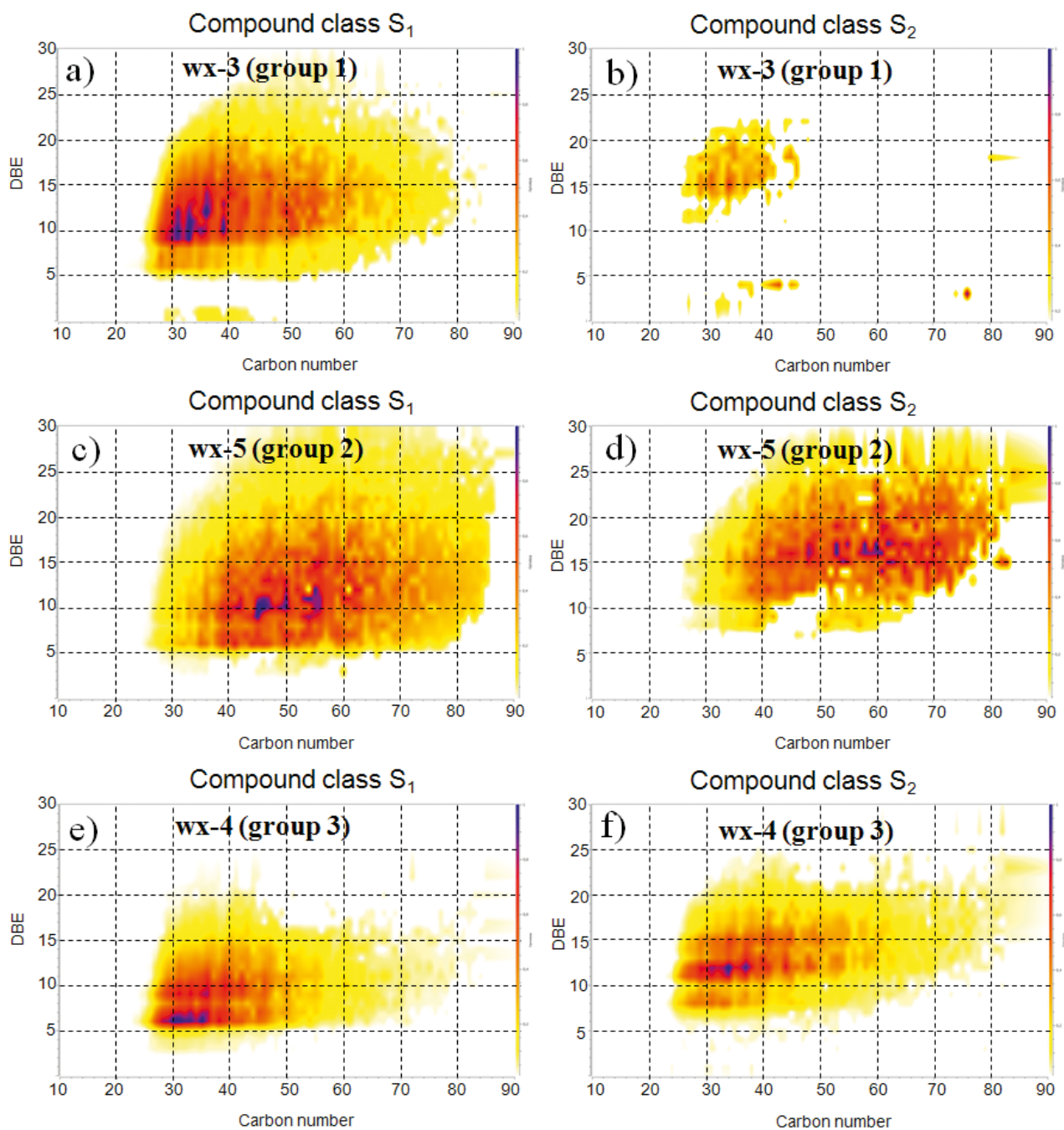


Figure 5: Plots of double bond equivalent (DBE) vs. carbon atom number of compound classes S_1 and S_2 of a) and b) sample wx-3 (crude oil, group 1), c) and d) of sample wx-5 (crude oil, group 2) and e) and f) of sample wx-4 (bitumen, group 3).

Results and Discussion

The mass spectra of the crude oil (wx-1, wx-3, wx-5 and wx-6) and bitumen (wx-2 and wx-4) samples measured in APPI positive ion mode are shown in Figure 1. The mass distribution of all six samples look similar except sample wx-5 which is shifted to higher mass. The mass peaks are in the mass range m/z 300-1200.

However, the full mass spectrum gives you only an estimation of the average number of carbons of the detected compounds. A detailed analysis of the single mass peaks is needed to analyze the sample on the molecular level (see Figure 2). The mass spectra have significant differences. However, several peaks are identical but with different peak ratios and intensities. More than 95% of the mass peaks could be annotated

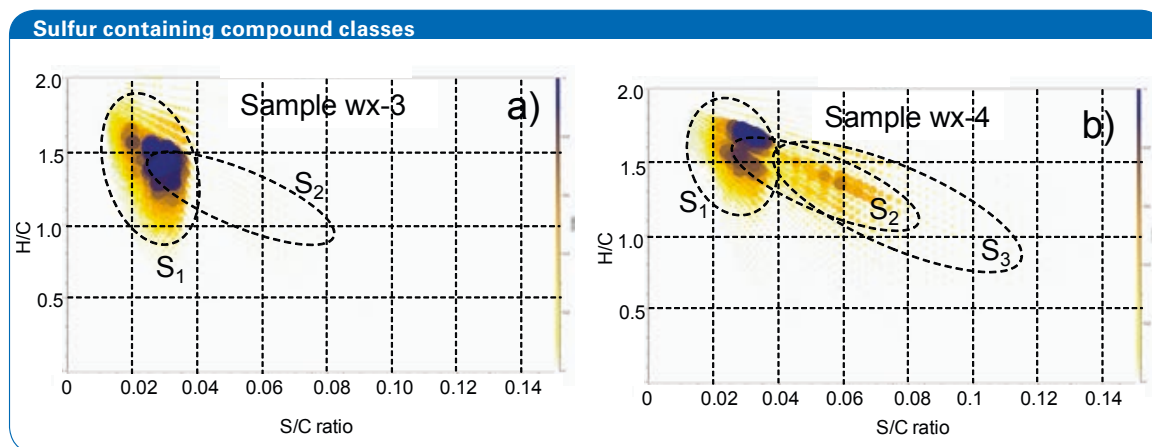


Figure 6: Van Krevelen plot S/C vs. H/C of a) sample wx-3 (group 1) and b) sample wx-4 (group 3) for visualization of aromaticity and relative ratios of sulfur containing compound simultaneously.

with an elemental formula. As an example the annotation of peaks with molecular formulae are shown in figure 3 for sample wx-1 for the nominal mass m/z 514.

The relative intensities of compound classes in all samples are shown in Figure 4. The six samples can be separated in three groups: group 1 with sample wx-1 and wx-3 (crude oil) containing low amount of sulfur, group 2 with sample wx-5 and wx-6 (crude oil) containing medium amount of sulfur and group 3 with sample wx-2 and wx-4 (bitumen) containing high amount of sulfur. Even compound class S_3 with a relative abundance of about 8% is present in samples wx-2 and wx-4.

Detailed analyses can be done on the molecular level by plotting the double bond equivalents (DBE) vs. the carbon number (Figure 5). The plots can be done for each compound class. Here, these plots have been generated for sample wx-3, wx-4 and wx-5 for the compound classes S_1 and S_2 which represent data of each group (group 1: low sulfur, group 2: medium sulfur and group 3: high sulfur). The DBE value is an indication for the aromaticity of the compound and the core structure. For instance dibenzothiophene can be identified in these plots with $DBE=9$. In group 1 and 2 the average DBE of compound class S_1 is mainly between 9 and 15. However, DBE is mainly DBE 6 and 9 in group 3 which indicates high amounts of benzothiophenes (DBE 6) and dibenzothiophenes (DBE 9) in samples of group 3. For all three groups DBE is shifted up to higher DBE values for compound class S_2 .

Another way beside the compound class plot (Fig. 4) to show the aromaticity and the relative amount of sulfur containing compound classes is the Van Krevelen plot (Figure 6). In addition the relative ratios of compounds of each class displayed with the size and color of the dots, the H/C ratio indicates the degree of unsaturation and indirectly the DBE of the core structure. For instance, the average H/C ratio of class S_1 of sample wx-3 (Fig. 5a) is about 1.4 in contrast to sample wx-4 with an average H/C of nearly 1.6 indicating the higher average DBE of sample wx-3.

Conclusions

Ultra-high resolution mass spectrometry can be used to characterize high mass sulfur containing compounds in crude oil and bitumen. These compounds are not accessible by GC due to their low volatility. The relative abundances of the compound classes S_1 , S_2 and S_3 in crude oil and bitumen can be measured. DBE vs. carbon number plots can be used to analyze the relative ratios of specific core structures like benzo- or dibenzo thiophenes of these compound classes.

Acknowledgement

The author would like to thank Dr. Maowen Li from the company SINOPEC, China, for providing the crude oil and bitumen samples.

References

- [1] Tomczyk, N. A.; Winans, R. E.; Shinn, J. H.; Robinson, R. C. *Energy Fuels* 2001, 15, 1498-1504.
- [2] Saab, J.; Mokbel, I.; Razouk, A. C.; Ainous, N.; Zydowicz, N.; Jose, J. *Energy Fuels* 2005, 19, 525-531.
- [3] Barker, L. R.; Kelly, W. R.; Gurthrie, W. F. *Energy Fuels* 2008, 22, 2488-2490.
- [4] Marshall, A. G.; Rodgers, R. P. *Acc. Chem. Res.* 2004, 37, 59-59.
- [5] Purcell, J. M.; Hendrickson, C. L.; Rodgers, R. P.; Marshall, A. G. *Anal. Chem.* 2006, 78, 5906-5912.

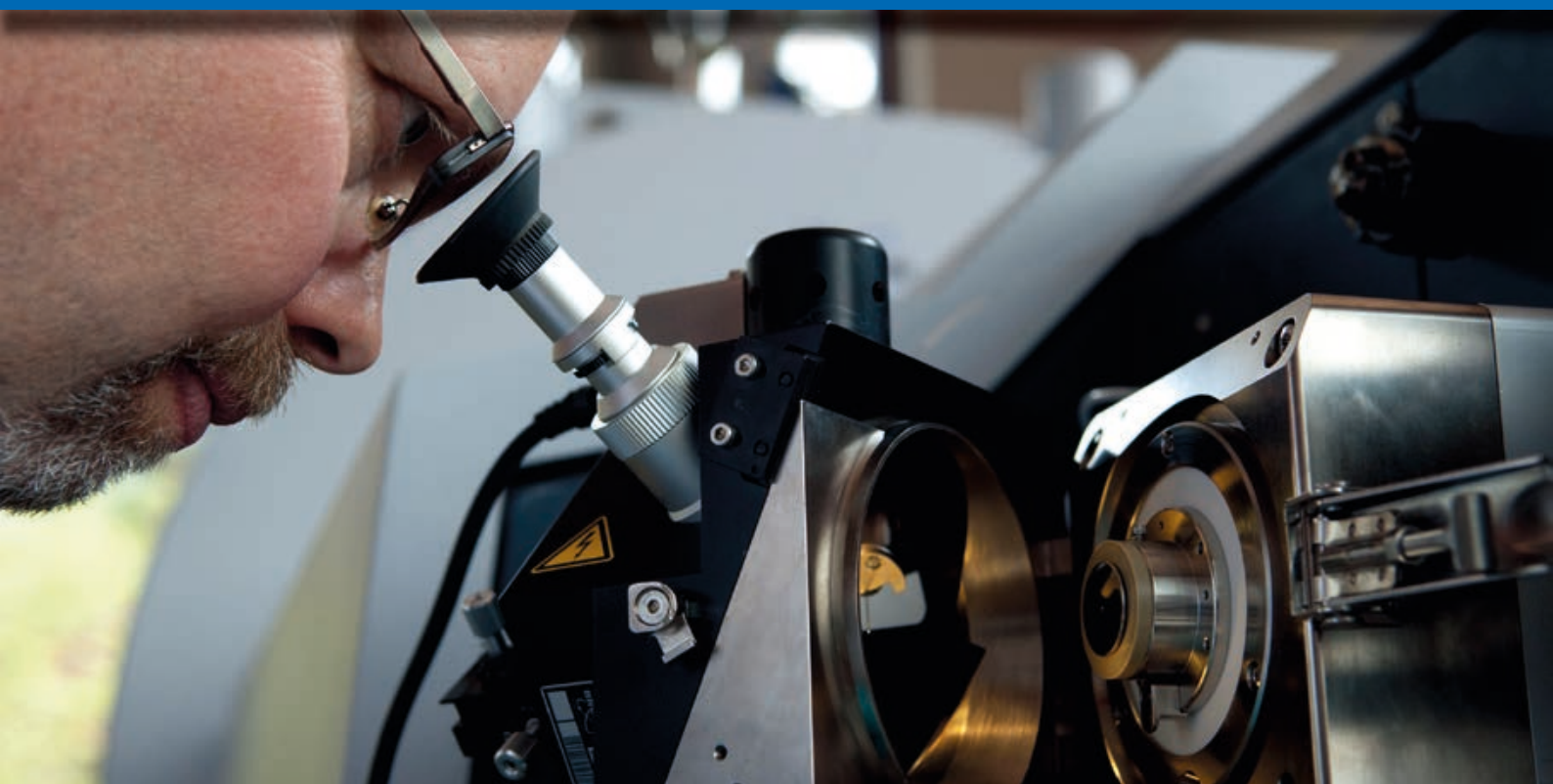
Keywords

Petroleomics
FTMS
APPI

Instrumentation & Software

solarix 12T
DataAnalysis 4.0
APPI II source
Composer

For research use only. Not for use in diagnostic procedures.



• Analysis of Gas Oil by GC/APCI FTMS

Introduction

Fuel oil is a fraction obtained from petroleum distillation, either as a distillate or a residue. It is made up of long hydrocarbon chains, and contains alkanes, cycloalkanes and aromatics. Different types of fuel oil are classified according to their boiling point, composition and purpose (e.g. gas oil) and vary in their alkyl chain length by 50 carbon atoms. Mass spectrometry is one of the major analytical tools to identify hydrocarbons and characterize impurities. These impurities contain hetero atoms such as nitrogen or sulfur. Due to environmental regulations of impurities (especially sulfur containing compounds) in gas and fuel oil, the detection and identification of these compounds is becoming more and more important. The ultra-high resolving power, mass accuracy and high dynamic range of Fourier Transform Mass Spectrometry (FTMS) improved the identification and detection of low-abundance impurities in these kind of samples.

Techniques such as gas chromatography (GC) or liquid chromatography (LC) can be used to separate isomers which cannot be distinguished only by mass using direct infusion measurements. In this study, GC was coupled to an FTMS instrument using a GC/APCI source to separate and detect isomers and quantify impurities in gas oil.

Experimentals

Mass spectra were acquired using a solariX 12 T FT-ICR mass spectrometer (Bruker) equipped with a GC/APCI source (Bruker) in positive ion mode (Figure 1) and coupled to a GC system. To separate compounds of this extremely complex mixture, 1 μL of a 1:100 dilution of gas oil in dichloromethane was injected splittless. A temperature gradient between 5 and 10 $^{\circ}\text{C}/\text{min}$ was used with a HP-5 ms, 30 m, 0.25 mm ID, 0.25 μm film thickness column. Spectra were acquired at 1 Hz using 2 MW data points with a mass range m/z 73-1000, resulting in a resolving power of about

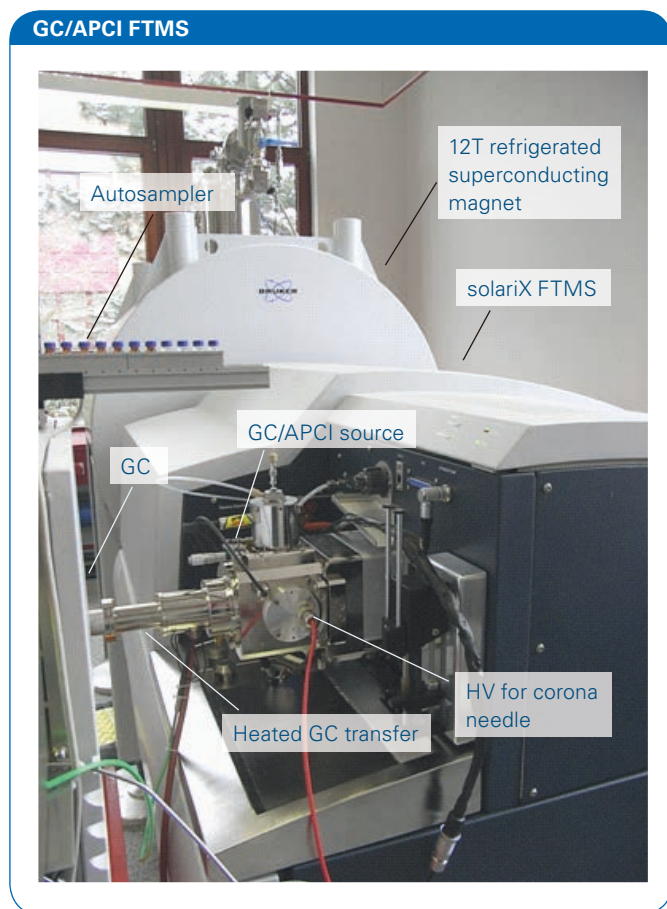


Figure 1: GC with autosampler coupled to a 12T solarix FTMS system using a GC/APCI source.

300,000 at m/z 200 with mass accuracies in the ppb range. Extracted ion chromatograms (EICs) with 1 mDa mass tolerance were calculated to identify isomers of a homologous series of alkylated benzothiophenes and dibenzothiophenes.

Results

APCI in combination with GC is an effective method for analysing substituted hydrocarbons, polycyclic aromatic hydrocarbons (PAH), and nitrogen and sulfur containing compounds. We focused in this study on sulfur containing compounds, especially thiophenes. A large number of isomers from a homologous series of alkylated benzothiophenes and dibenzothiophenes were detected in gas oil using GC/APCI-FTMS. The complexity of the sample is indicated in Figure 2, which shows the base peak chromatogram (BPC) (Figure 2a) and the survey view (a plot of RT vs. m/z using a color coding for the intensity) (Figure 2b). The complexity of the compounds of higher mass is due to the rise in the number of possible chemical isomers due to the increase of the length and number of alkyl residues (Figure 3a and 3b).

The carbon number distributions of the homologous

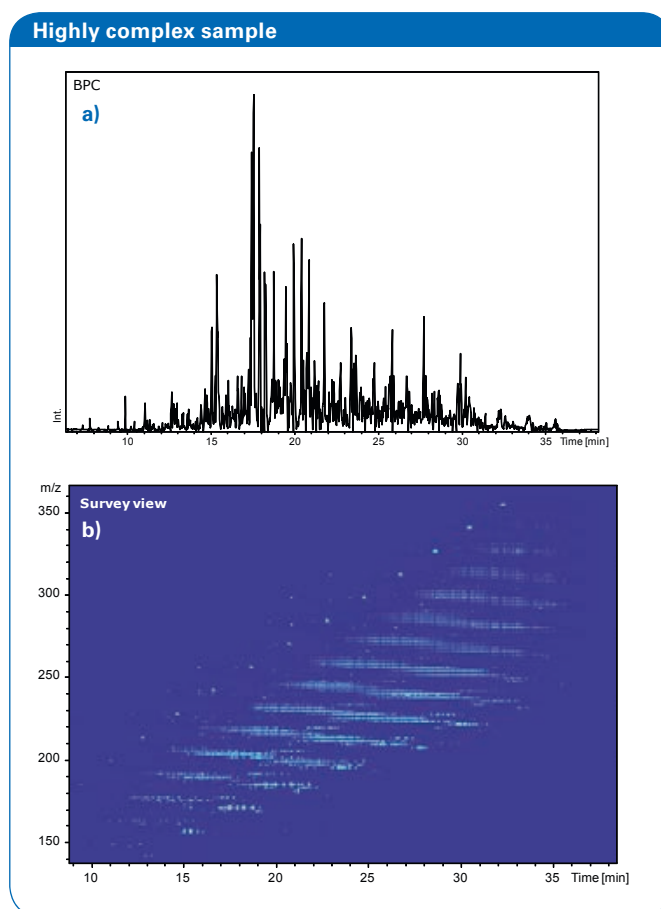


Figure 2: a) Base peak chromatogram and b) survey view of gas oil measured by GC/APCI showing the high complexity of this sample.

series of benzothiophenes and dibenzothiophenes were also compared with direct infusion APCI measurements (Figure 3c and 3d) of the same sample. We observed that GC/APCI and infusion APCI measurements result in different carbon distribution pattern due to (a) GC/APCI detecting compounds with lower boiling points than those detecting by APCI direct infusion and (b) ion suppression effects in direct infusion measurements caused by the high complexity of the sample (various isomers, isobars and compound classes). Co-eluting species with a mass difference of only 3.4 mDa were separated by the high resolving power of the FTMS technique (Figure 4). Thanks to the ability of GC to separate isomers, the intensities obtained from members of a homologous series can be used for a quantification approach of sulfur compounds in gas oil.

Carbon number distributions

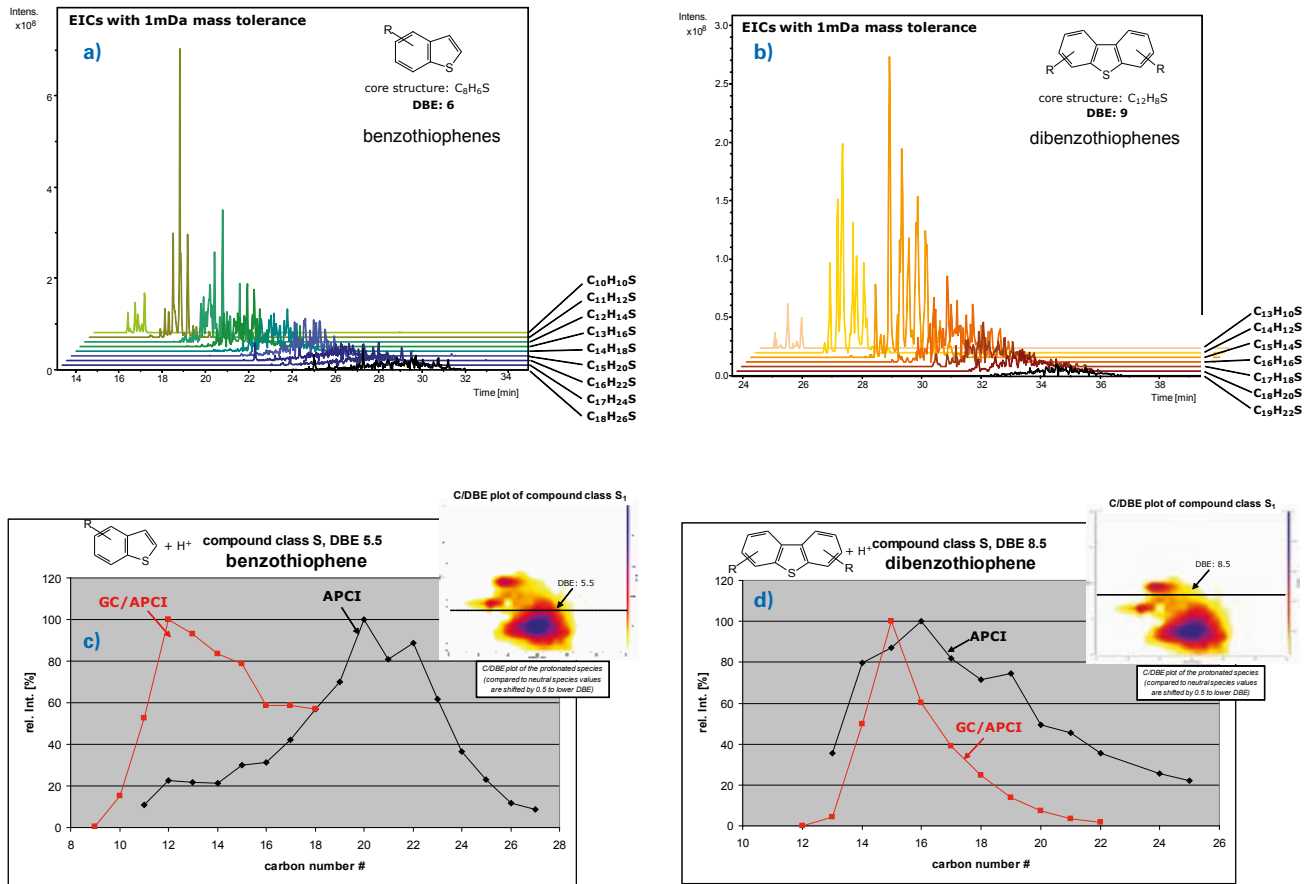


Figure 3: EICs of the homologous series of a) benzothiophenes and b) dibenzothiophenes. Comparison of GC/APCI and direct infusion APCI results of the carbon number distribution of the homologous series of c) benzothiophenes and d) dibenzothiophenes C/DBE plot of the compound class S_1 of the direct infusion APCI results.

High separation power

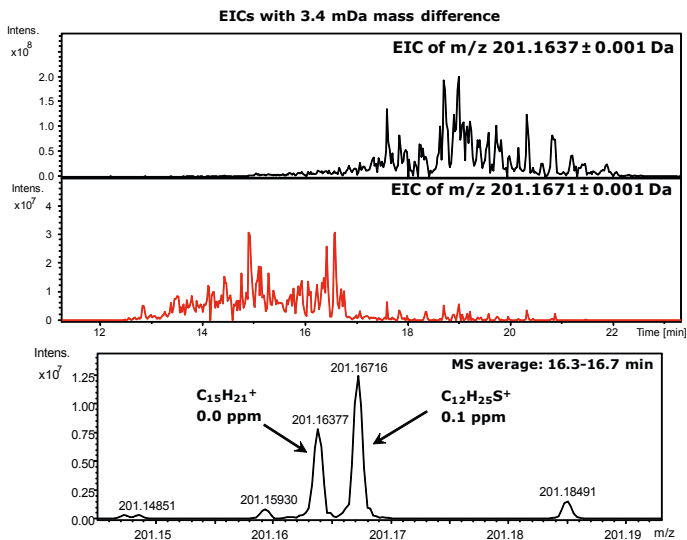


Figure 4: Example of EICs with a mass difference of only 3.4 mDa. Averaging mass spectra between retention time 16.3 min and 16.7 min results in the mass spectrum containing both compounds ($C_{15}H_{21}^+$ and $C_{12}H_{25}S^+$).

Summary

GC/APCI is a sensitive technique for detecting small volatile compounds with very accurate mass measurement. We have shown that sulfur containing compounds such as benzothiophenes and dibenzothiophenes can be detected and quantified in gas oil samples. Chemical isomers of these compound classes can be separated by gas chromatography and detected using ultra-high resolving power and the mass accuracy of FTMS. Ultra high resolving power is needed in very complex samples to separate isobars with a mass difference of only 3.4 mDa, which corresponds to the exact mass difference between C₃ and SH₄.

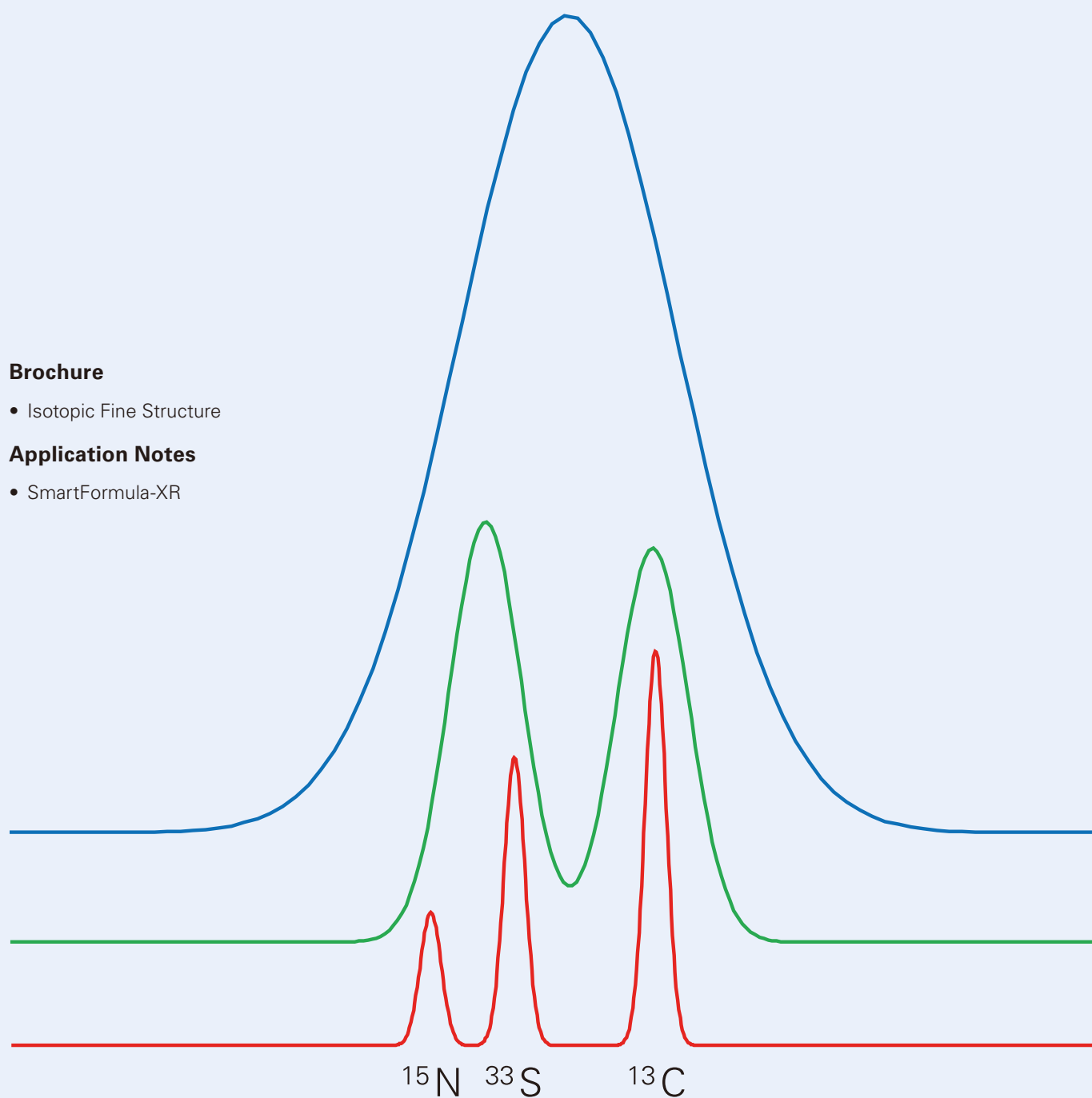
Authors

Matthias Witt, Thomas Arthen-Engeland, Bruker Daltonik GmbH.

Keywords	Instrumentation & Software
Petroleomics	solarix 12T
Complex mixture	DataAnalysis 4.0
GC	GC/APCI source
APCI	
Small molecules	

For research use only. Not for use in diagnostic procedures.

• Isotopic Fine Structure



Brochure

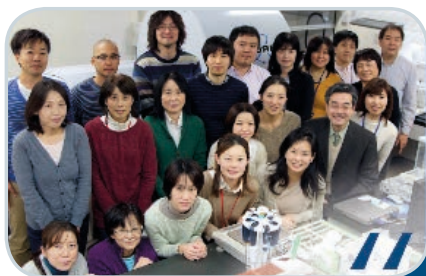
- Isotopic Fine Structure

Application Notes

- SmartFormula-XR

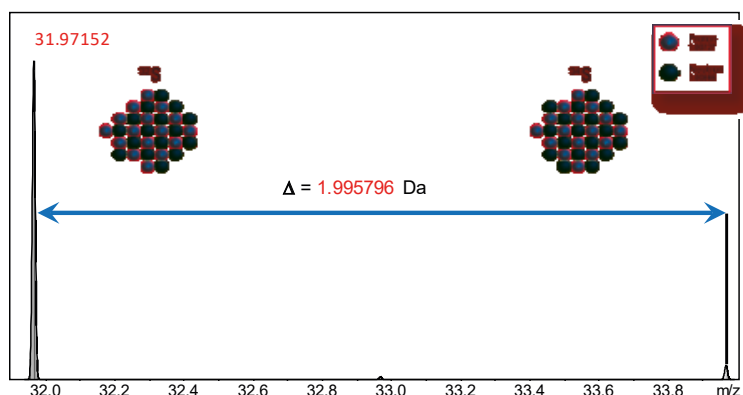
User Testimonials: Isotopic Fine Structure

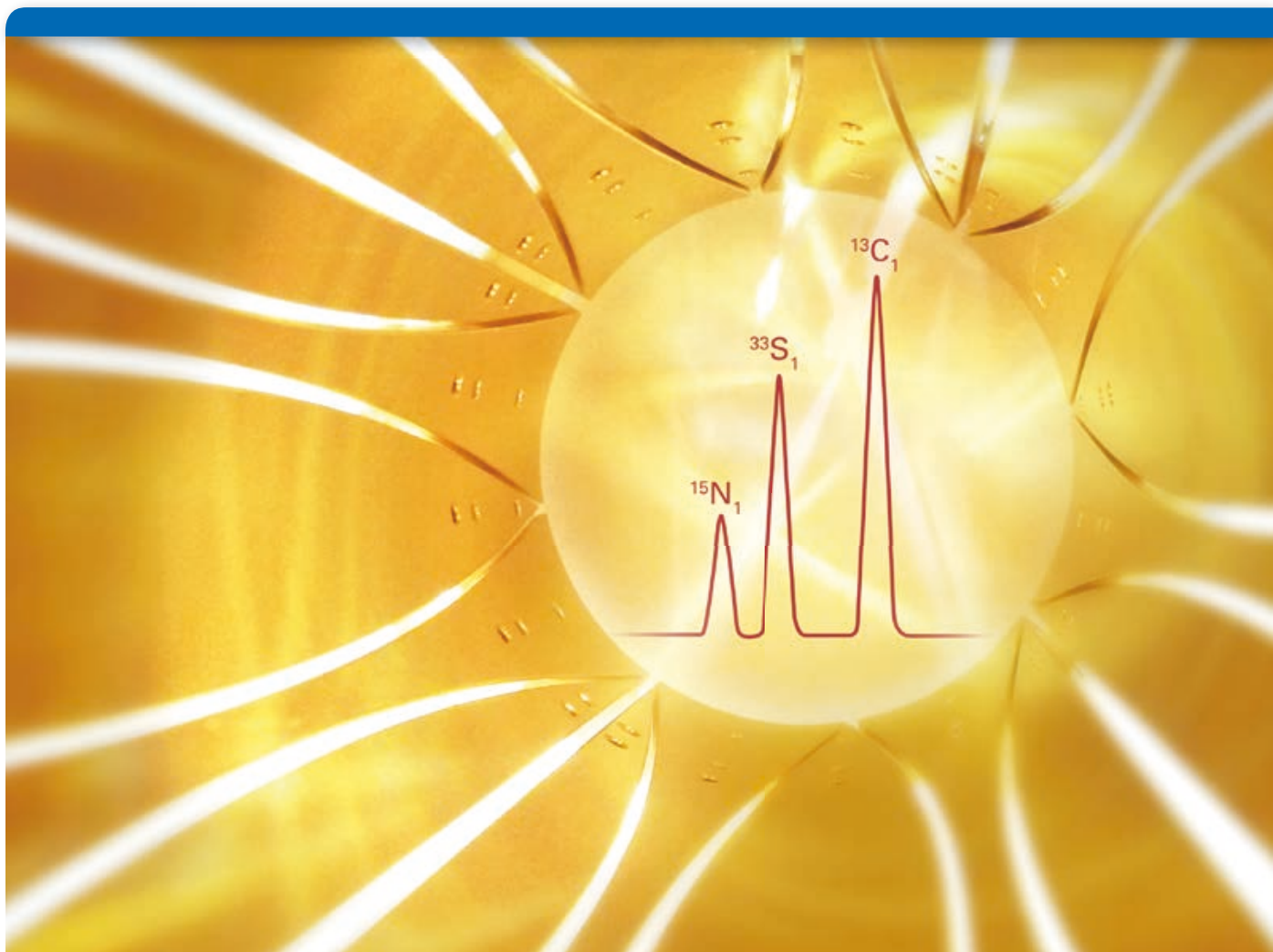
The IFS approach enables the ability to rapidly identify sulfur containing metabolites and calculate single sum formulas for each, increasing both the speed and accuracy of the workflow. The incredible power of this workflow is that with extreme resolving power and sum formula determination, rapid screening for other heteroatom (N & O) containing metabolites is also possible.



“This S-atom-driven approach afforded an efficient chemical assignment of S-containing metabolites, suggesting its potential application for screening not only S but also other heteroatom-containing metabolites in MS-based metabolomics.”

In 2013, Prof. Kazuki Saito of the RIKEN Plant Science Center (group photo shown), was acknowledged with an award for one of the top downloaded papers. Prof. Kazuki Saito has been selected as a highly cited Researcher in 2014 and 2015 by Thomson Reuters in the Plant and Animal Science field and won the 2016 Japanese Society of Plant Physiologists award.

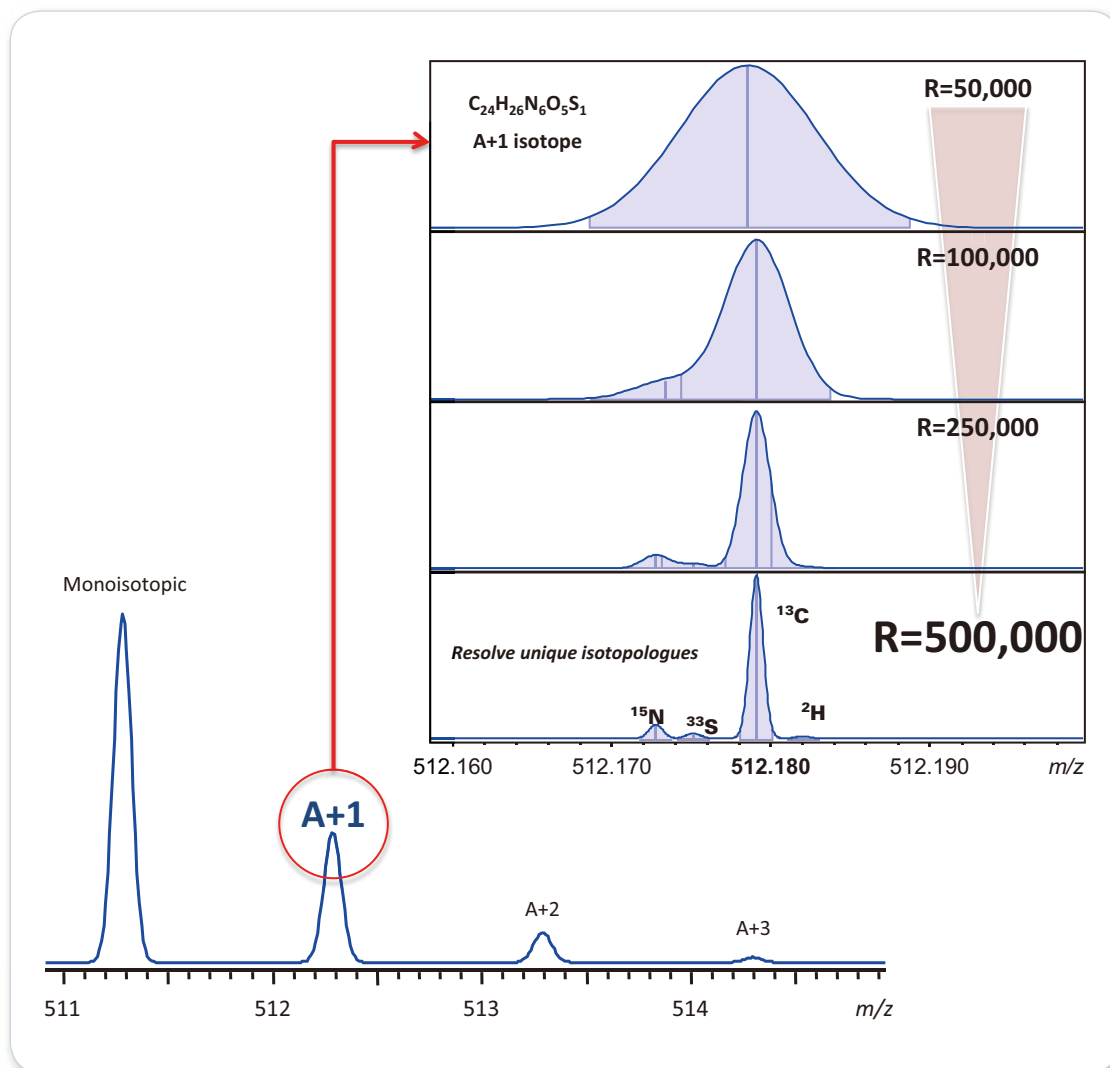




Isotopic Fine Structure

- Beyond the Molecular Realm:
Unambiguous Elemental Formula Determination

Resolve Beyond the Molecular Realm



View Natures Signatures

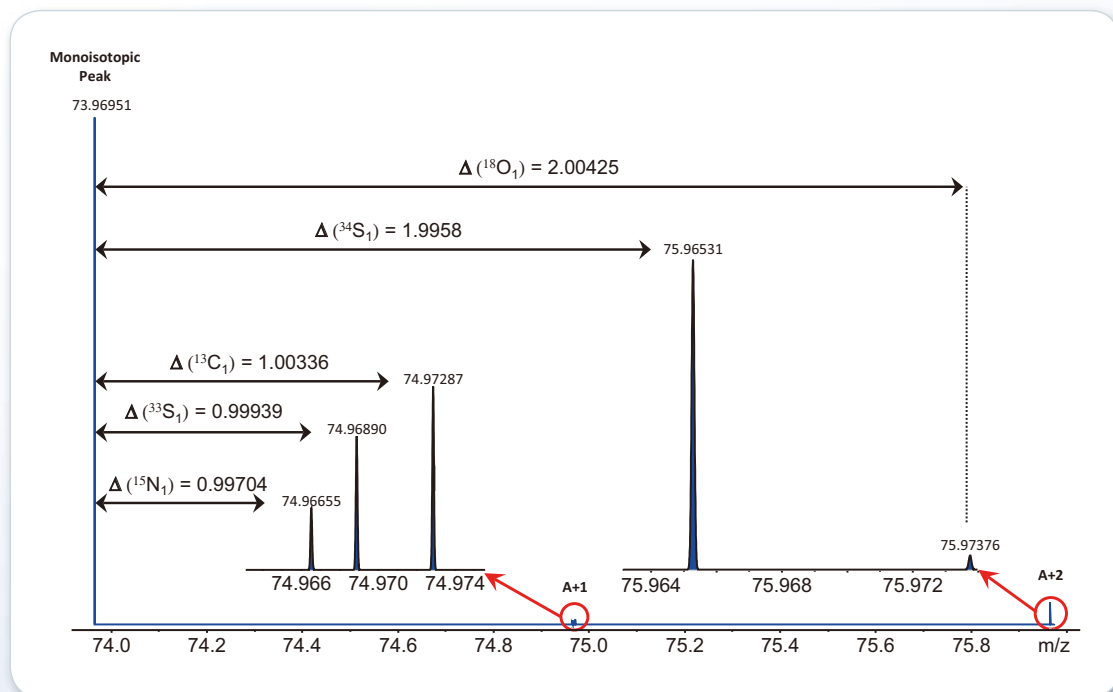
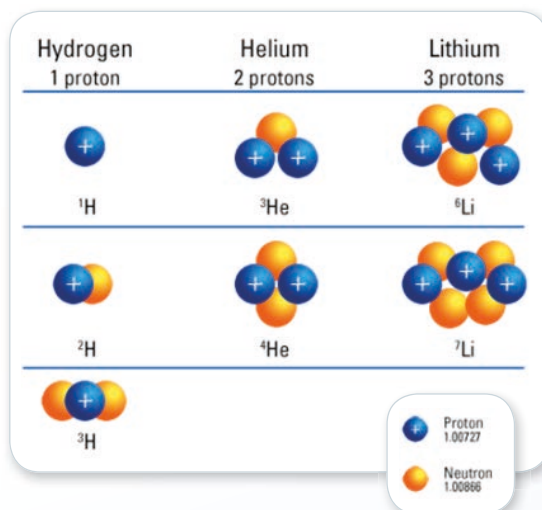
- Discover new chemical information by resolving unique isotopologues
- Confirm fundamental nuclear signatures to reveal the 'true molecular formula', by routinely working at resolving powers (RP) above RP=500,000, having easy access to RP > 1,000,000 when needed
- The exceptional capability of ParaCell™ technology enables you to work beyond the molecular realm*

* Boldin, I. A.; Nikolaev, E. N., Rapid Commun. Mass Spectrom., 2011, 25, 122-126.
Marshall, A.G.; Hendrickson, C.L.; Shi, S.D-H., Anal. Chem., 2002, 74, 252A-259A.

Isotopic Fine Structure (IFS)

The value of fundamental nuclear signatures

- Isotopic Fine Structure (IFS) is the unique mass spectral signature arising from naturally occurring isotopes within the molecule being measured
- Classically, the isotopic pattern was described using the isotopes of carbon ($^{13}\text{C}_1$, $^{13}\text{C}_2$), or more generally A+1, A+2, (see figure on opposite page)
- The A+1 IFS pattern consists of ^{15}N , ^{33}S , ^{13}C and ^2H isotopes, while IFS in the A+2 pattern has ^{18}O and ^{34}S isotopes. Combinations of these elements create unique patterns thanks to different mass defects of the isotopic contributions

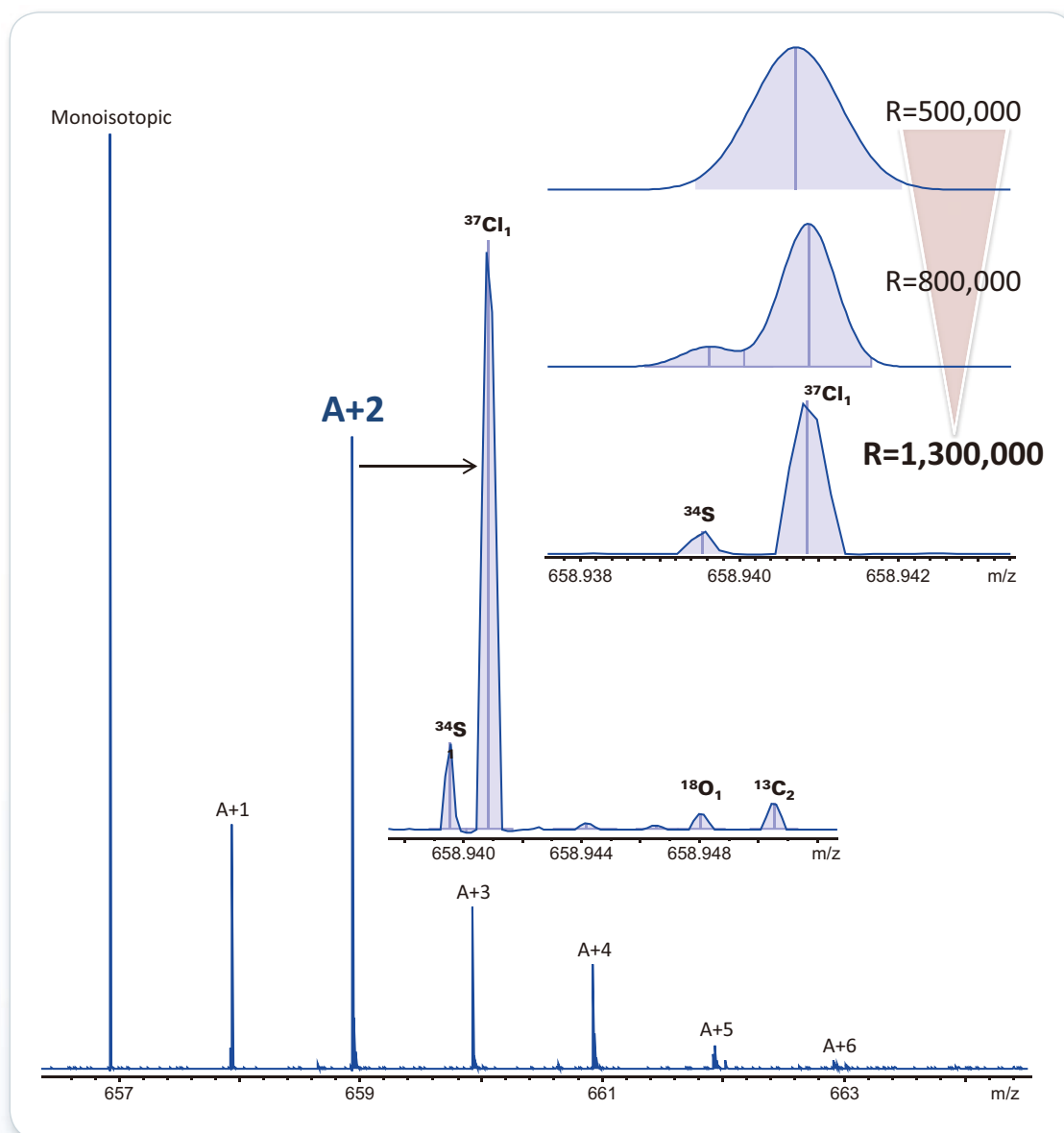


Isotopic fine structure is an EXACT fingerprint for every possible molecular configuration

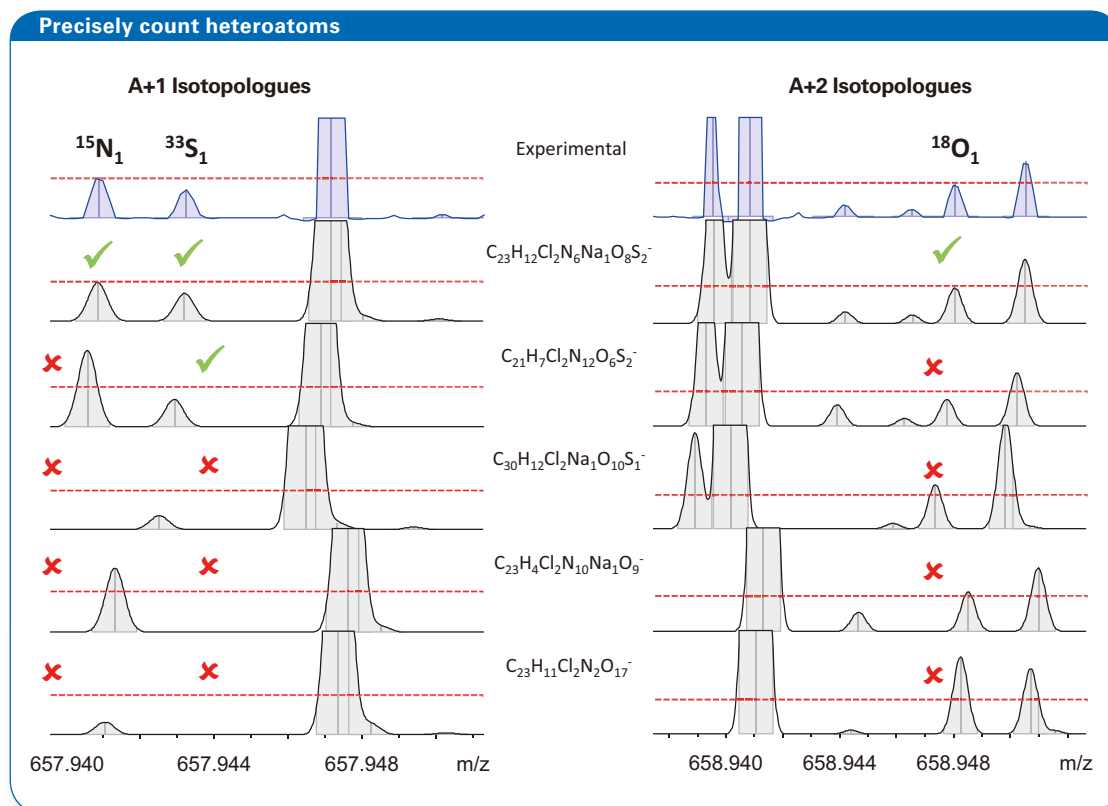
>1 Million Resolving Power

IFS unravels molecular formulae of unknown species

- The strong A+2 isotope suggests Chlorine.
- Sulfur-34 is hidden even at RP = 500,000, so we need the ability to access higher resolution to resolve peaks that are not of equal intensities.
- At eXtreme Resolving powers, isotopologues yield true qualitative molecular information on our unknown



IFS Powered Quantitative Information



Unknown sample is Reactive Blue 4 ($\text{C}_{23}\text{H}_{14}\text{Cl}_2\text{N}_6\text{O}_8\text{S}_2^-$)

Eliminate Errors Using Heteroatom Mass Spectrometry

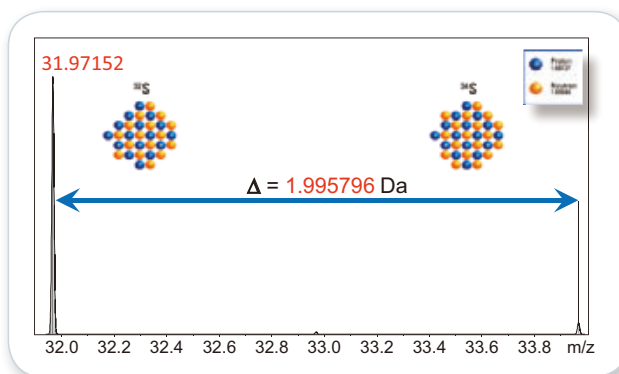
- Requires >500,000 RP to do it routinely
- Able to acquire full mass spectrum, not only a subset
- Perfect for quantitation of neutron labelled (^2H , ^{15}N) tags



Sulfur and S-omics

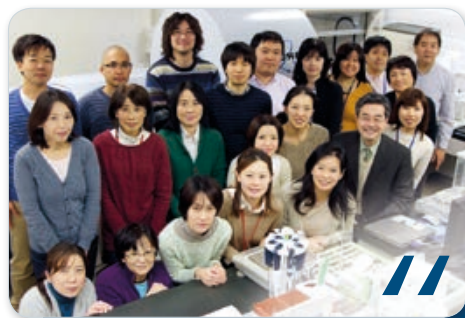
IFS allows discovery of completely new Sulfur containing metabolites with health promoting properties

The IFS approach enables the ability to rapidly identify sulfur containing metabolites and calculate single sum formulas for each, increasing both the speed and accuracy of the workflow. The incredible power of this workflow is that with extreme resolving power and sum formula determination, rapid screening for other heteroatom (N & O) containing metabolites is also possible.



Highlight:

In 2013, Prof. Kazuki Saito, of the RIKEN Plant Science Center (group photo below), was acknowledged with an award for one of the top downloaded papers. Prof. Kazuki Saito has been selected as a highly cited Researcher in 2014 & 2015 by Thomson Reuters in the Plant & Animal Science field and won the 2016 Japanese Society of Plant Physiologists award.



*This S-atom-driven approach afforded an efficient chemical assignment of S-containing metabolites, suggesting its potential application for screening not only S but also other heteroatom-containing metabolites in MS-based metabolomics.**

Breakthrough discoveries by accessing information from fundamental nuclear signatures

References

 *Ultra-high resolution metabolomics for S-containing metabolites. Current Opinion in Biotechnology (available online, print 2017)*

Chemical Assignment of Structural Isomers of Sulfur-Containing Metabolites in Garlic by Liquid Chromatography–Fourier Transform Ion Cyclotron Resonance–Mass Spectrometry. *The Journal of Nutrition* (2016)

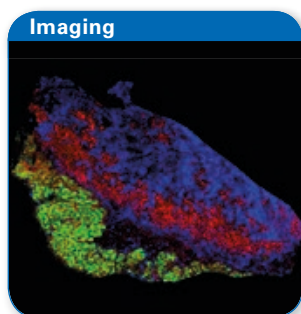
Top-down Targeted Metabolomics Reveals a Sulfur-Containing Metabolite with Inhibitory Activity against Angiotensin-Converting Enzyme in *Asparagus officinalis*. *The Journal of Natural Products* (2015)

Revisiting anabasine biosynthesis in tobacco hairy roots expressing plant lysine decarboxylase gene by using ^{15}N -labeled lysine. *Plant Biotechnology* (2014)

Metabolomics for unknown plant metabolites. *Analytical and Bioanalytical Chemistry* (2013)

*Combination of Liquid Chromatography–Fourier Transform Ion Cyclotron Resonance–Mass Spectrometry with ^{13}C -Labeling for Chemical Assignment of Sulfur-Containing Metabolites in Onion Bulbs. *Analytical Chemistry* (2013)

An Invitation to Push the Frontiers of Scientific Discovery



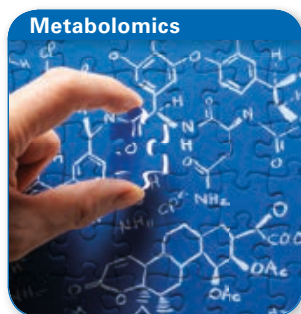
Imaging

In situ label-free imaging for visualizing the biotransformation of a bioactive polyphenol

Kim, Fujimura, Hagihara, Sasaki, Yukihiro, Nagao, Miura, Yamaguchi, Saito, Tanaka, Wariishi, Yamada and Tachibanad

Scientific Reports, 3, 2805 (2014)

IFS analysis allows for the visualization of spatially-resolved biotransformation based on simultaneous mapping of EGCG and its phase II metabolites. Complements conventional molecular imaging techniques, and can contribute to biological discovery.



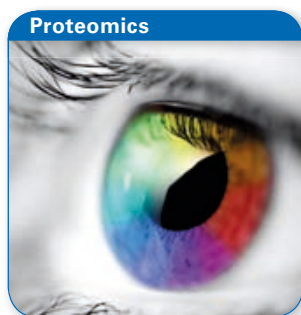
Metabolomics

Pyruvate carboxylase is critical for non-small-cell lung cancer proliferation

Sellers, Fox, Bousamra, Slone, Higashi, Miller, Wang, Yan, Yuneva, Deshpande, Lane and Fan

The Journal of Clinical Investigation, 125(2):687-698 (2015)

IFS enables the ability to trace biosynthetic pathways. ^{13}C labeled glucose is used to determine fluxomics. High resolution mass spectrometry is used to resolve isotopomers and properly determine the amount of ^{13}C enrichment in various lipids.



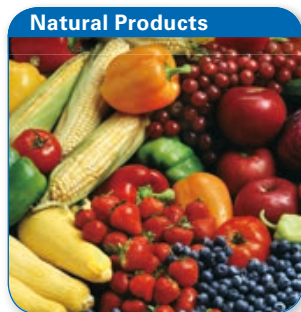
Proteomics

Resolving Isotopic Fine Structure to Detect and Quantify Natural Abundance- and Hydrogen/Deuterium Exchange-Derived Isotopomers

Liu, Easterling, and Agar

Analytical Chemistry, 86, 820–825 (2014)

Applies IFS to the HDX workflow. It overcomes a past limitation by using IFS (a real solution). Using ISF, one can simply count the number of deuterons in each one of the peptides, eliminating the need to make any guesses or utilize complex math. A very simple solution to a complex problem.



Natural Products

Synthesis of $7\text{-}^{15}\text{N}$ -Oroidin and Evaluation of Utility for Biosynthetic Studies of Pyrrole-Imidazole Alkaloids by Microscale ^1H - ^{15}N HSQC and FTMS

Wang, Morinaka, Reyes, Wolff, Romo and Molinski

Journal of Natural Products, 73 (3), pp 428–434 (2010)

Isotope labelling is used to follow biosynthetic pathways. IFS allows for an easy calculation of the amount of ^{15}N enrichment as compared to the natural abundance of Oroidin. By feeding live sponges ^{15}N foods, various biosynthetic pathways can be identified.

Isotopic Fine Structure

Breakthrough discoveries by accessing information from fundamental nuclear signatures



^{15}N ^{33}S ^{13}C

For research use only. Not for use in diagnostic procedures.

Bruker Daltonics is continually improving its products and reserves the right to change specifications without notice. © BDAL 09-2016, 1847374



• Definitive Elemental Formula Determination Debuts with SmartFormula-HR™

Introduction

The determination of elemental composition is a key step in drug discovery and metabolite studies. High performance mass spectrometry provides an extremely sensitive and accurate means for precisely determining the monoisotopic mass of an unknown, even when analyzing complex mixtures. In many cases sub-ppm mass accuracy is not sufficient for elemental sum formula determination due to the large number of possible atomic configurations for a given nominal mass. An additional dimension of information can be obtained for the heteroatom content of a molecule through evaluating nominally spaced isotopic intensities and positions (Bruker's sigmaFit™).

While this workflow fully utilizes the capabilities of faithful reproduction of isotopic profiles at low resolving powers, the additional data obtained by detection of individual contributions of the heteroatom peaks in high resolution experiments is not utilized. In this case, low abundant peaks from the non-carbon atoms are not sufficiently represented. This

capability which would allow a direct and quantitative determination of the molecular formula if it could be realized.

The solarix™ FTMS provides not only the highest mass accuracy, but also the highest resolving power of any modern mass spectrometer. For the isotopic profile of an unknown, the high RP experiment reveals the underlying isotopic fine structure. The peak intensities of the low abundant isotopes are now revealed with the solarix and the elements can be "counted" based upon their natural abundance. Automated elemental formula determination utilizing isotopic fine structure is now becomes possible using Bruker's SmartFormula-HR™.

Experimental

In the following example, SmartFormula-HR is applied to a mixture of pesticides. The mixture is first separated via HPLC, and then detected with high resolution mass spectrometry using the solarix (Figure 1).

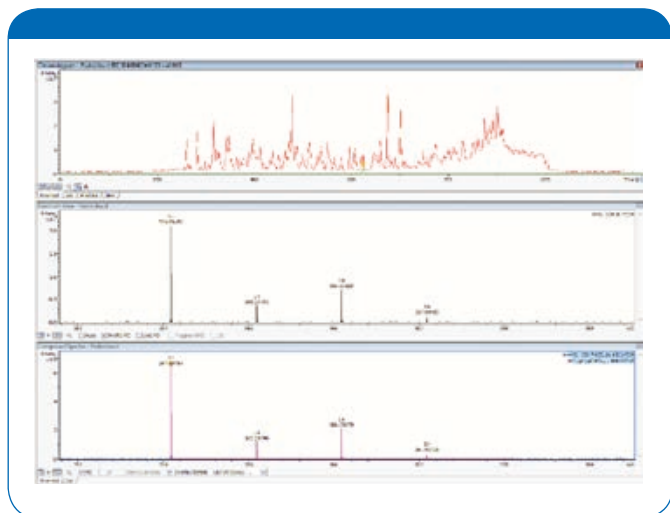


Figure 1: Total ion chromatogram (TIC), top in red, along with the compound mass spectrum.

Rank	#	Ion Formula	sigma	Score	MS	# Hk	mean Fit	File Structure	mean Fit	# State	en [Da]	en [amu]	Info	4 th Conf	Formula	Abund
34.094627	81	C ₁₈ H ₁₈ Cl ₁ N ₁ O ₅	145.7	5.46	346.094627	1	0.1	36	0.06	-0.21	8.8	mean	ok	Mean		
	89	C ₁₈ H ₁₈ Cl ₁ N ₁ O ₅	134.4	0.87	346.09228	2	0.1	46	0.29	4.29	0.0	mean	ok	Mean		
	75	C ₁₈ H ₁₈ Cl ₁ N ₁ O ₅	105.8	0.00	346.09181	3	0.1	88	-0.52	-4.87	4.0	mean	ok	Mean		
	36	C ₁₈ H ₁₈ Cl ₁ N ₁ O ₅	88.8	0.00	346.08794	4	0.1	23	2.89	7.84	9.3	mean	ok	Mean		
	72	C ₁₈ H ₁₈ Cl ₁ N ₁ O ₅	88.8	0.00	346.09227	5	0.2	80	4.72	12.97	4.3	mean	ok	Mean		
	76	C ₁₈ H ₁₈ Cl ₁ N ₁ O ₅	171.0	0.00	346.09062	6	0.2	75	-0.94	-10.82	5.3	mean	ok	Mean		
	65	C ₁₈ H ₁₈ Cl ₁ N ₁ O ₅	154.6	0.00	346.08858	7	0.2	63	6.87	-16.46	10.3	mean	ok	Mean		
	27	C ₁₈ H ₁₈ Cl ₁ N ₁ O ₅	81.7	0.33	346.09089	8	0.2	27	-0.70	-10.31	4.9	mean	ok	Mean		
	20	C ₁₈ H ₁₈ Cl ₁ N ₁ O ₅	81.7	0.38	346.09098	9	0.2	36	4.03	12.49	4.8	mean	ok	Mean		
	19	C ₁₈ H ₁₈ Cl ₁ N ₁ O ₅	81.2	0.01	346.09081	10	0.2	94	6.26	17.20	4.0	mean	ok	Mean		
	75	C ₁₈ H ₁₈ Cl ₁ N ₁ O ₅	88.8	0.01	346.09182	11	0.2	65	3.87	6.42	9.3	mean	ok	Mean		
	46	C ₁₈ H ₁₈ Cl ₁ N ₁ O ₅	80.3	0.00	346.09105	12	0.2	76	6.80	16.67	15.0	mean	ok	Mean		
	12	C ₁₈ H ₁₈ Cl ₁ N ₁ O ₅	43.7	12.22	346.09180	13	0.2	107	0.89	2.86	-0.9	mean	ok	Mean		
	88	C ₁₈ H ₁₈ Cl ₁ N ₁ O ₅	105.1	0.00	346.09158	14	0.2	49	2.04	5.99	5.8	mean	ok	Mean		
	17	C ₁₈ H ₁₈ Cl ₁ N ₁ O ₅	77.2	0.00	346.08794	15	0.2	72	-7.11	-19.52	5.9	mean	ok	Mean		
	11	C ₁₈ H ₁₈ Cl ₁ N ₁ O ₅	47.3	14.91	346.09109	16	0.2	11	-0.90	-0.62	5.9	mean	ok	Mean		
	79	C ₁₈ H ₁₈ Cl ₁ N ₁ O ₅	171.9	0.04	346.09086	17	0.2	62	1.42	3.86	14.0	mean	ok	Mean		
	87	C ₁₈ H ₁₈ Cl ₁ N ₁ O ₅	187.7	0.00	346.08990	18	0.2	90	6.44	17.69	9.8	mean	ok	Mean		
	13	C ₁₈ H ₁₈ Cl ₁ N ₁ O ₅	70.7	0.00	346.09186	19	0.3	89	7.11	19.33	5.0	mean	ok	Mean		
	46	C ₁₈ H ₁₈ Cl ₁ N ₁ O ₅	105.4	0.01	346.09103	20	0.2	52	-0.30	-14.69	4.0	mean	ok	Mean		
	75	C ₁₈ H ₁₈ Cl ₁ N ₁ O ₅	88.8	0.00	346.09050	21	0.2	85	5.95	16.25	0.3	mean	ok	Mean		
	93	C ₁₈ H ₁₈ Cl ₁ N ₁ O ₅	128.4	0.33	346.09080	22	0.2	35	2.27	6.24	18.9	mean	ok	Mean		

Figure 2: SmartFormula-HR results list. The standard sigma fit scoring ranks Benzoximate as 30, whereas SF-HR correctly ranks it as first.

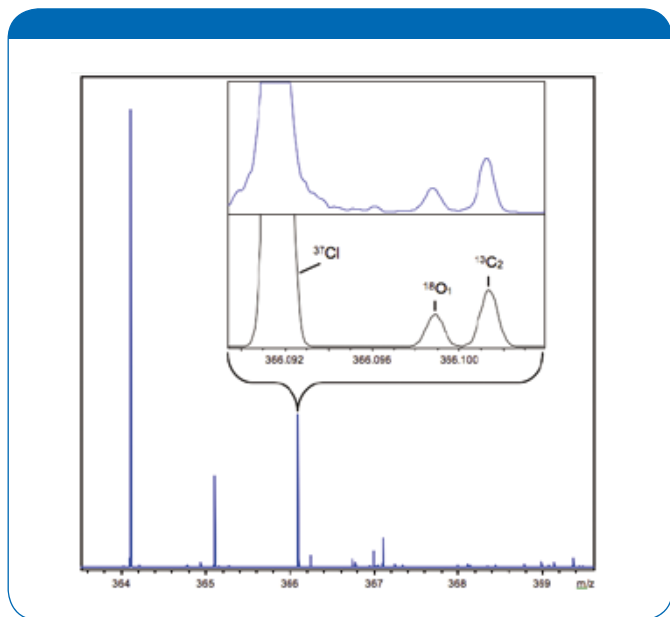


Figure 3: Mass spectrum of Benzoximate. The inset, 20x zoom, shows the experimental M+2 peak (top) along with the simulated isotopic pattern (bottom). A resolving power of 500k reveals the fine structure beneath the nominal M+2 peak.

Samples: Pesticide Mixture

MS system: solariX FT-ICR MS platform with 12T refrigerated cryo magnet and standard ESI source.

LC Conditions: Standard 20 minute gradient

Calibration: External linear calibration.

Results

The chromatographic compound at 10.4 minutes is taken as an example. The monoisotopic peak is found at m/z 346.094627. For the elemental formula calculation, a wide range of elements are allowed: Cl6 P6 Br6 S6. The elements C H N and O are considered implicitly. Under the standard sigmaFit scoring, the correct formula of Benzoximate (C₁₈H₁₈Cl₁N₁O₅ + H+) has a Sigma score of 145.7 and is ranked 30. A more restricted search space will result in a narrower distribution of elemental formula, but will not result in a confident assignment, especially if the chemistry of the species is unknown.

A new approach to scoring the possible elemental formulas is to use isotopic fine structure information. The scoring procedure is as follows:

- The theoretical isotopic fine structure distribution is generated based on monoisotopic peak width and is folded in with the line shape of the monoisotopic peak
- The theoretical patterns are shifted such that the monoisotopic peaks have the same m/z (independent from mass accuracy).
- A linear fit of M+1 and M+2 isotopic patterns is performed against the experimental data
- The normalized residuals for the M+1 and M+2 distributions (equally weighted) are used for scoring

Using this technique, the formula for Benzoximate (C₁₈H₁₈Cl₁N₁O₅ + H+) is now ranked as the number one result, up from 30th. All of the other possible formulas are ruled out based upon the correct isotopic fine structure. Neither a target approach, nor MS/MS was required to correctly and confidently determine the elemental formula. This is ideal for samples where there is no database information to search.

Conclusions

Using SmartFormulaHR, a user is enabled for the first time ever in mass spectrometry with the powerful ability to “read” molecular formula directly from a mass spectrum by combining the power of the solarix FTMS with a specialized algorithm for evaluating individual heteroatom contributions to the isotopic profile. This capability is extremely useful for the analysis of complex mixtures where multiple stages of MS/MS might not be allowed for discrete components or nominal isotopic pattern algorithms break down.

References

- [1]: BMC Bioinformatics 2006, 7:234
[2]: Anal. Chem. 2010, 82, 5887-5891, Miura, et. al.

Authors

Michael Easterling and Darwin Asa

Keywords
molecular formula
drug discovery
metabolite studies

Instrumentation & Software
solarix 12T
DataAnalysis 4.0
SmartFormula XR
SigmaFit

About Bruker Corporation

Bruker is enabling scientists to make breakthrough discoveries and develop new applications that improve the quality of human life. Bruker's high-performance scientific instruments and high-value analytical and diagnostic solutions enable scientists to explore life and materials at molecular, cellular and microscopic levels. In close cooperation with our customers, Bruker is enabling innovation, improved productivity and customer success in life science molecular research, in applied and pharma applications, in microscopy and nanoanalysis, and in industrial applications, as well as in cell biology, preclinical imaging, clinical phenomics and proteomics research and clinical microbiology.

For more information, please visit: www.bruker.com

● **Bruker Daltonik GmbH**

Bremen · Germany
Phone +49 (0)421-2205-0

Bruker Daltonics Inc.

Billerica, MA · USA
Phone +1 (978) 663-3660

ms.sales.bdal@bruker.com - www.bruker.com